THE UNIVERSITY OF CHICAGO

THE DEVELOPMENT AND APPLICATION OF THIOSQUARAMIDES AND BISPYRIDINIUMS AS HYDROGEN-BOND DONOR CATALYSTS

A DISSERTATION SUBMITTED TO

THE FACULTY OF THE DIVISION OF THE PHYSICAL SCIENCES

IN CANDIDACY FOR THE DEGREE OF

DOCTOR OF PHILOSOPHY

DEPARTMENT OF CHEMISTRY

BY

MICHAEL GREGORIO ROMBOLA

CHICAGO, ILLINOIS

JUNE 2018

For my family

TABLE OF CONTENTS

LIST OF SCHEMES

LIST OF TABLES

LIST OF FIGURES

LIST OF ABBREVIATIONS

Å	ångström
Ac	acetyl
acac	acetylacetonate
BINOL	1,1'-bi-2-naphthol
Bn	benzyl
brsm	based on recovered starting material
Bu	butyl
CPME	cyclopentyl methyl ether
DA	Diels-Alder
dba	dibenzylideneacetone
DBU	1,8-diazabicyclo[5.4.0]undec-7-ene
DCM	dichloromethane
DMF	*N*,*N*-dimethylformamide
DMS	dimethyl sulfide
DMSO	dimethylsulfoxide
DNA	deoxyribonucleic acid

dr	diastereomeric ratio
ee	enantiomeric excess
Et	ethyl
EWG	electron withdrawing group
GAA	glacial acetic acid
h	hours
H-bond	hydrogen bond
HIV	human immunodeficiency virus
HOMO	highest occupied molecular orbital
HPLC	high pressure liquid chromatography
HRMS	high resolution mass spectrometry
Hz	Hertz
*i*Pr	*iso*-propyl
IR	infrared
kcal	kilocalorie
LDA	lithium diisopropylamide
LUMO	lowest unoccupied molecular orbital

MA	Michael addition
Me	methyl
min	minutes
mol	mole
MS	molecular sieves
MVK	methyl vinyl ketone
NCS	*N*-chlorosuccinimide
NMR	nuclear magnetic resonance
Ph	phenyl
Pr	propyl
rt	room temperature
t	temperature
TADDOL	α,α,α,α-tetraaryl-1,3-dioxolane-4,5-dimethanol
TBAF	tetrabutylammonium fluoride
*t*Bu	*tert*-butyl
TBHP	*tert*-butyl hydroperoxide
TBS	*tert*-butyldimethylsilyl

Tf	trifluoromethanesulfonyl
TFAA	trifluoroacetic anhydride
THF	tetrahydrofuran
TIPS	triisopropylsilyl
TLC	thin layer chromatography
TMS	trimethylsilyl
Tr	trityl

Acknowledgements

My time as a graduate student at the University of Chicago has been fantastic, and I owe that to the many incredible people I've had the pleasure of working with. I would like to first thank Professor Viresh Rawal for letting me join his research group in early 2013 and having supported me since then. His mastery of synthesis and kindness have both shaped my experience here, and it has been a privilege to have him as an advisor.

I owe a special thanks to Dr. Julius Reyes, whose friendship has been genuinely invaluable. Thank you Dr. Chintan Sumaria for having been an awesome lab partner and friend. Other Rawal group members, particularly Jiasu Xu, Ferdinand Taenzler, Dr. Lan Luo, Dr. Yen-Ku Wu, Dr. Maciej Serda, Pavel Elkin, Lingbowei Hu, Dr. Antoinette Nibbs, Dr. Kin Yang, Dr. Thomas Montgomery, Dr. Aditya Unni, Dr. Natsuko Kagawa, Peter Ryffel, and Hannah Zinky are all thanked as well.

Other people in the Department of Chemistry who I would like to thank for their meaningful involvement in my graduate studies are Dr. Antoni Jurkiewicz, Michael Reedy, Laura Luburich, Dr. Irene Hsu, Dr. Alexander Filatov, Dr. Jin Qin, Dr. Valerie Keller, Dr. Vera Dragisich, Melinda Moore, and members of the Yamamoto, Snyder, Dong, Lewis, and Kozmin groups.

Dr. Chintan Sumaria and Dr. Thomas Montgomery were contributors to the thiosquaramide project, and I thank them for that. Similarly, Dr. Yunus Türkmen and Dr. Julius Reyes were contributors to the bispyridinium project, and I thank them for that.

I would like to thank Professor Scott Snyder and Professor Guangbin Dong for their willingness to serve on my defense committee and for their engagement during our weekly literature meetings.

Finally, I owe everything I have to my family.

– May 3, 2018 –

Chapter 1

Hydrogen-Bonding Catalysis by Small Molecules

I.1 Introduction

The earliest description of the hydrogen bond comes from Moore and Winmill in 1912.[1] The authors used the below wording and structural representations to depict what is now known as a hydrogen bond: “The following formulae, where thick strokes mean strong unions and thin strokes weak unions, show roughly the difference between trimethylammonium hydroxide and tetramethylammonium hydroxide:”

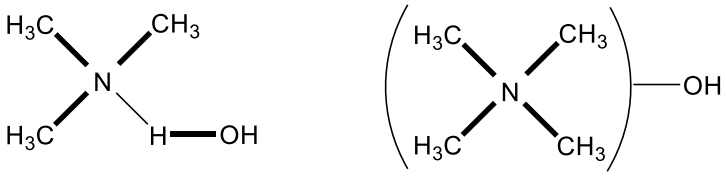

Figure 1. Earliest depiction of the hydrogen bond.

Less than ten years later, Latimer and Rodebush used the word “bond” for the first time in describing the intermolecular attraction between adjacent molecules of water: "In terms of the Lewis theory, a free pair of electrons on one water molecule might be able to exert sufficient force on a hydrogen held by a pair of electrons on another water molecule to bind the two molecules together.... Such an explanation amounts to saying that the hydrogen nucleus held between 2 octets constitutes a weak 'bond'.”[2]

[1] Moore, T. S.; Winmill, T. F. *J. Chem. Soc.* **1912**, *101*, 1635.
[2] Latimer, W. M.; Rodebush, W. H. *J. Am. Chem. Soc.* **1920**, *42*, 1419.

This principle was later generalized by Linus Pauling in 1939: "Under certain conditions an atom of hydrogen is attracted by rather strong forces to two atoms, instead of only one, so that it may be considered to be acting as a bond between them. This is called the hydrogen bond."[3]

Little has changed in the last 80 years regarding intuitive understanding of the hydrogen bond. A modern definition is given by the International Union of Pure and Applied Chemists: "The hydrogen bond is an attractive interaction between a hydrogen atom from a molecule or a molecular fragment X–H in which X is more electronegative than H, and an atom or a group of atoms in the same or a different molecule, in which there is evidence of bond formation."[4]

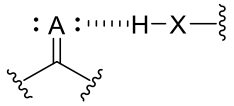

Figure 2. General representation of a hydrogen bond.

Hydrogen bonds (also known as H-bonds) can vary widely in strength, from 0.2 - 40 kcal mol^{-1}.[5] Consequently, classifying these interactions as strong, medium, or weak can be useful. Bond energies above 14 kcal mol^{-1} (bond length: 1.2 - 1.5 Å) are generally considered to be strong, while those below 4 kcal mol^{-1} (bond length: 2.2 - 3.2 Å) are considered to be weak.[6] Hydrogen bonds are also directional, and bond angles approach linearity with increasing H-bond strength.[6]

---

[3] Pauling, L. *The Nature of the Chemical Bond and the Structure of Molecules and Crystals: An Introduction to Modern Structural Chemistry*, 3rd ed., Cornell University Press, Ithaca, NY, 1960.
[4] Arunan, E.; Desiraju, G. R.; Klein, R. A.; Sadlej, J.; Scheiner, S.; Alkorta, I.; Clary, D. C.; Crabtree, R. H.; Dannenberg, J. J.; Hobza, P.; Kjaergaard, H. G.; Legon, A. C.; Mennucci, B.; Nesbitt, D. J. *Pure Appl. Chem.* **2011**, *83*, 1637.
[5] Steiner, T. *Angew. Chem. Int. Ed.* **2002**, *41*, 48.
[6] Jeffrey, G. A. *An Introduction to Hydrogen Bonding*, Oxford University Press, New York, NY, 1997.

The implications of hydrogen bonding have become particularly well-appreciated in biological systems: DNA base pairing (Figure 3), protein folding and secondary structure, and enzyme function are all manifestations of hydrogen bonding in a biological context.[7]

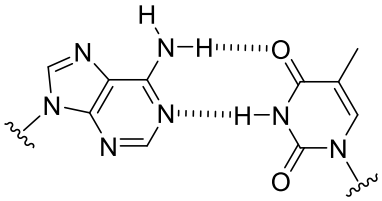

Figure 3. Adenine-thymine Watson-Crick base pair.

Hydrogen bonding can reduce the barriers of chemical transformations by lowering the energy of an electrophile's LUMO (lowest unoccupied molecular orbital) and stabilizing the transition states and intermediates of a given reaction.[8] In this way, H-bond donor molecules are capable of catalysis.

The utilization of hydrogen bonding for synthetic utility in catalysis is only a relatively recent phenomenon. Since the late 1990s, catalysis with chiral hydrogen bond donor small molecules has emerged as a powerful tool for asymmetric synthesis. Seminal contributions to the field predate the recent and ongoing flurry of research into H-bonding catalysis and are detailed below.

[7] Nelson, D. L.; Cox, M. M. *Lehninger Principles of Biochemistry,* 5th ed., W. H. Freeman and Company, New York, NY, 2008.
[8] Pihko, P. M., Ed. *Hydrogen Bonding in Organic Synthesis* Wiley-VCH: Weinheim, 2009.

I.2 Pioneering Studies of Hydrogen-Bonding Catalysis by Small Molecules

In 1942, Wassermann observed that the Diels-Alder reaction between cyclopentadiene and benzoquinone was accelerated in the presence of phenols and carboxylic acids.[9] Brønsted acid catalysis via proton transfer was already known. The catalytic function of phenol, being only weakly acidic, apparently raised questions to the authors about the nature of the catalysis. In concluding their work, they ask whether the catalysis "is dependent on proton-transfer processes or whether an essentially different mechanism is operative." These results would not be advanced for another 40 years.

In 1984, Hines characterized two cocrystals of 1,8-biphenylenediol (Figure 4).[10]

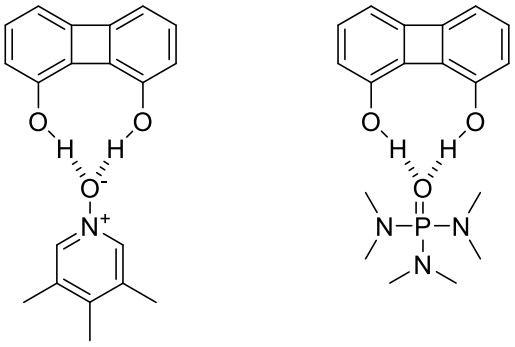

Figure 4. Structures of diol cocrystals.

Noting that the crystal forms of the adducts contain two strong hydrogen bonds between diol and carbonyl, the authors decided to study "the catalytic activity of such diols in reactions subject to catalysis by hydrogen bonding." The following year, they reported that 1,8-

[9] Wassermann, A. *J. Chem. Soc.* **1942**, 618.
[10] Hine, J.; Ahn, K.; Gallucci, J. C.; Linden, S. M. *J. Am. Chem. Soc*. **1984**, *106*, 7980.

biphenylenediol is an effective hydrogen bond catalyst for the nucleophilic epoxide opening of phenyl glycidyl ether with diethylamine (Scheme 1).[11]

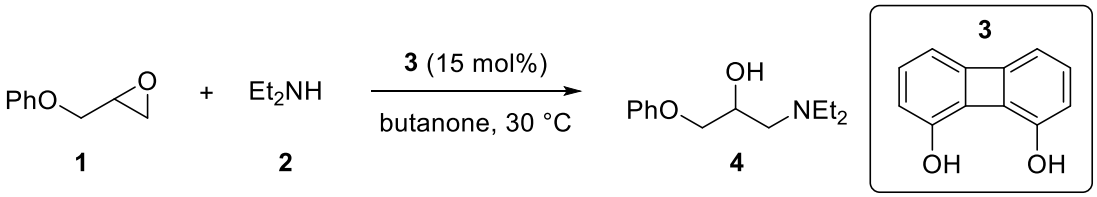

Scheme 1. Hydrogen bonding catalyzed epoxide ring opening.

Two key features of the hydrogen bond catalyst affecting rate enhancements of the reaction were mentioned. First was the correlation of the acidity of the phenol with the epoxide opening, a relationship which had been previously described.[12] Second was the significance of two hydrogen bond donors in the catalyst architecture: the authors found that the rate enhancements afforded by the diol were 600 times greater than what would have been predicted based on its acidity. Other diols incapable of forming effective two-point hydrogen bonds did not experience the same type of rate enhancements. The two-point hydrogen bond donor paradigm for electrophilic activation was thus uncovered.

Not long after, research in the hydrogen bonding potential of ureas began to accelerate, which is significant since these scaffolds (and their thiourea derivatives) have since made their way to the privileged class of modern day hydrogen bond donor catalysts. In 1988, Etter found evidence for a two-point hydrogen bond in the solid state between *m*-substituted ureas and hydrogen bond acceptor compounds (Figure 5).[13]

[11] Hine, J.; Linden, S.; Kanagasabapathy, V. M. *J. Am. Chem. Soc.* **1985**, *107*, 1082.
[12] Partansky, A. M. *Adv. Chem. Ser.* **1970**, *92*, 29.
[13] Etter, M. C.; Panunto, T. W. *J. Am. Chem. Soc*. **1988**, *110*, 5896.

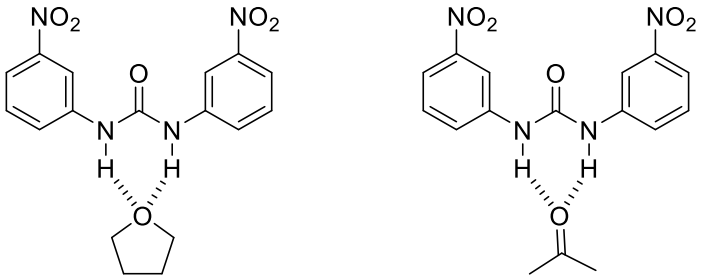

Figure 5. Structures of urea cocrystals.

Curran was the first to report catalysis with ureas,[14] and in 1995 showed that diaryl ureas were capable of catalyzing a Claisen rearrangement (Scheme 2).[15] The rate enhancements were attributed to the urea's ability to form a two-point H-bond to the vinyl ether oxygen. These experiments were likely guided by their recognition a number of years earlier that solvent H-bonding facilitated the Claisen rearrangement of polarized substrates.[16]

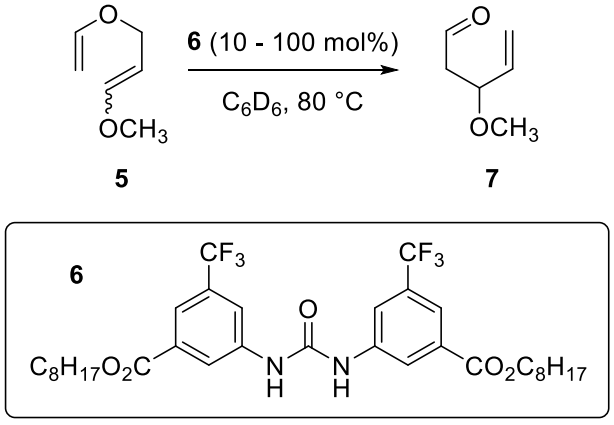

Scheme 2. Urea catalyzed Claisen rearrangement.

[14] Curran, D. P.; Kuo, L. H. *J. Org. Chem*. **1994**, *59*, 3259.
[15] Curran, D. P.; Kuo, L. H. *Tetrahedron Lett*. **1995**, *36*, 6647.
[16] Coates, R. M.; Rogers, B. D.; Hobbs, S. I.; Peck, D. R.; Curran, D. P. *J. Am. Chem. Soc*. **1987**, *109*, 1160.

Although asymmetric H-bonding catalysis would not take off until several years after Curran's work, a very limited number of pioneering studies exist prior to then, and those examples are included below.

I.3 Emergence of Asymmetric Hydrogen-Bond Donor Catalysis

In the early 1970s, researchers at Schering AG and Hoffman-La Roche discovered L-proline can catalyze enantioselective aldol reactions.[17] Results from Hajos and Parish are shown in Scheme 3.

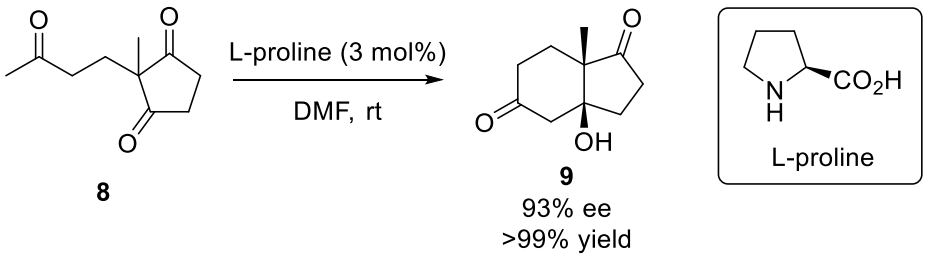

Scheme 3. Proline catalyzed aldol reaction.

The mechanism of catalysis was not understood at the time, particularly the role of the carboxylic acid. Later studies would establish proline's mode of catalysis to be bifunctional. In the above aldol reaction, proline condenses with the methyl ketone to form a reactive enamine, and the carboxylic acid activates another ketone through hydrogen bonding/Brønsted acid catalysis. As hydrogen bonding and Brønsted acid catalysis fall along a continuum with no clear

[17] (a) Eder, U.; Sauer, G.; Wiechert, R. *Angew. Chem. Int. Ed.* **1971**, *10*, 496. (d) Hajos, Z. G.; Parrish, D. R. *J. Org. Chem.* **1974**, *39*, 1615.

boundary, both will be included in this introduction as appropriate. Proline and its derivatives have since developed into a privileged class of organocatalysts.[18]

One of the earliest examples in small molecule catalysis to ascribe a role for hydrogen bonding comes from Wynberg in 1981.[19] The authors reported an asymmetric conjugate addition of thiophenol **11** to cyclic enone **10** with cinchonidine to deliver the Michael addition product in 75% ee (Scheme 4). In their paper, hydrogen bonding is invoked as a stabilizing transition state interaction responsible for the relatively high enantioselectivies: catalysts without the free hydroxyl group gave lower ee's.

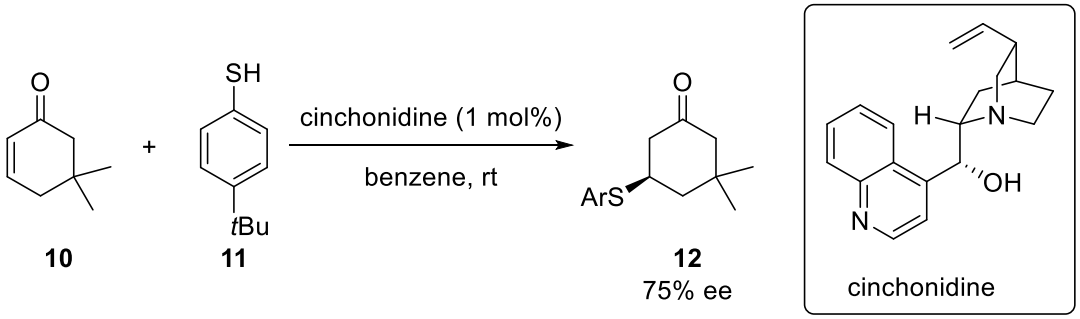

Scheme 4. Cinchonidine catalyzed thiol addition.

Remarkable about this paper is that it contains the basic premise for bifunctional hydrogen bonding catalysis: the combination of electrophilic activation through hydrogen bonding and nucleophilic activation through deprotonation. This general strategy has since proven to be extremely effective, although widespread adoption of this type of dual catalysis would not be seen for another 20 years.

[18] For a review on proline catalysis, see: List, B. *Tetrahedron* **2002**, *58*, 5573.
[19] Hiemstra, H.; Wynberg, H. *J. Am. Chem. Soc*. **1981**, *103*, 417.

In 1998, Jacobsen synthesized a library of catalysts using combinatorial chemistry for screening an enantioselective Strecker reaction (Scheme 5).[20] This approach led to the identification of thiourea-tethered Schiff base **15** as an active catalyst for the asymmetric Strecker reaction. Four years later, insight gained from mechanistic studies revealed the role of the thiourea to be one of hydrogen bonding.[21]

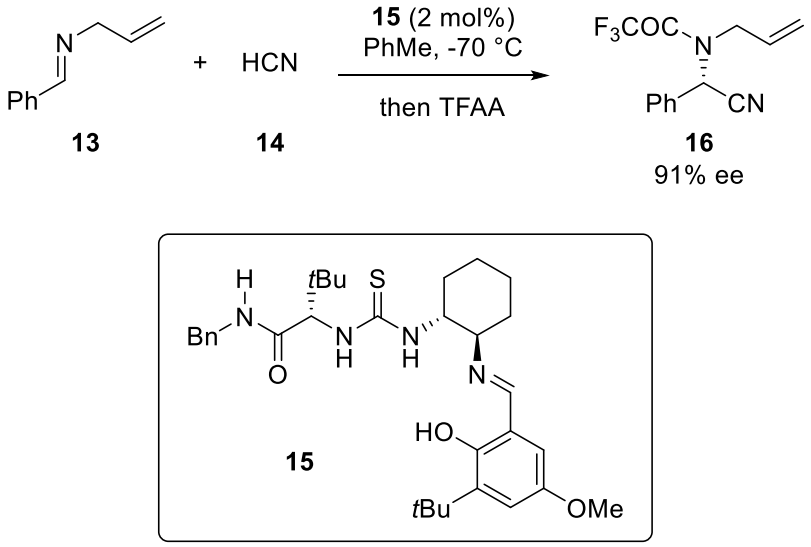

Scheme 5. Thiourea catalyzed Strecker reaction.

It is roughly around this time that research into the design of the hydrogen bond donor core began to take shape. In 1999, Corey reported on the use of a C2-symmetric (after protonation) guanidium catalyst **18** as a hydrogen bond donor catalyst for an enantioselective Strecker reaction (Scheme 6).[22]

[20] Sigman, M. S.; Jacobsen, E. N. *J. Am. Chem. Soc.* **1998**, *120*, 4901.
[21] Vachal, P.; Jacobsen, E. N. *J. Am. Chem. Soc*. **2002**, *124*, 10012.
[22] Corey, E. J.; Grogan, M. J. *Org. Lett*. **1999**, *1*, 157.

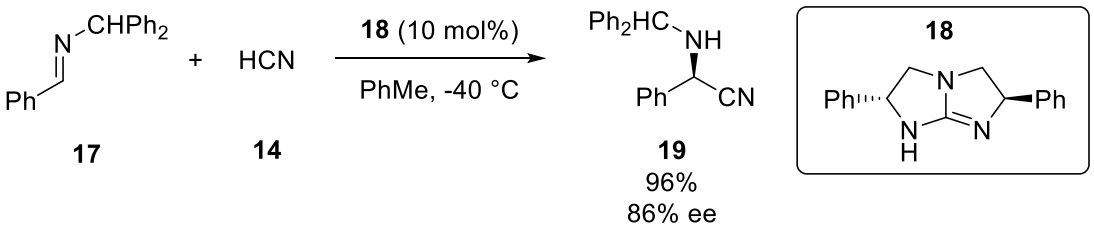

Scheme 6. Guanidinium catalyzed Strecker reaction.

In 2003, Rawal reported the use of chiral TADDOL derivatives as catalysts for the highly enantioselective hetero-Diels-Alder reaction between 1-amino-2-siloxy diene **20** and aldehydes (Scheme 7).[23] This finding closed the gap between the first report by Hine of diols being active hydrogen bond donor catalysts and the application of a chiral diol to an asymmetric transformation. Activation of the aldehyde in this example likely arises through a single hydrogen bond between catalyst and substrate, as shown in Figure 6.[24]

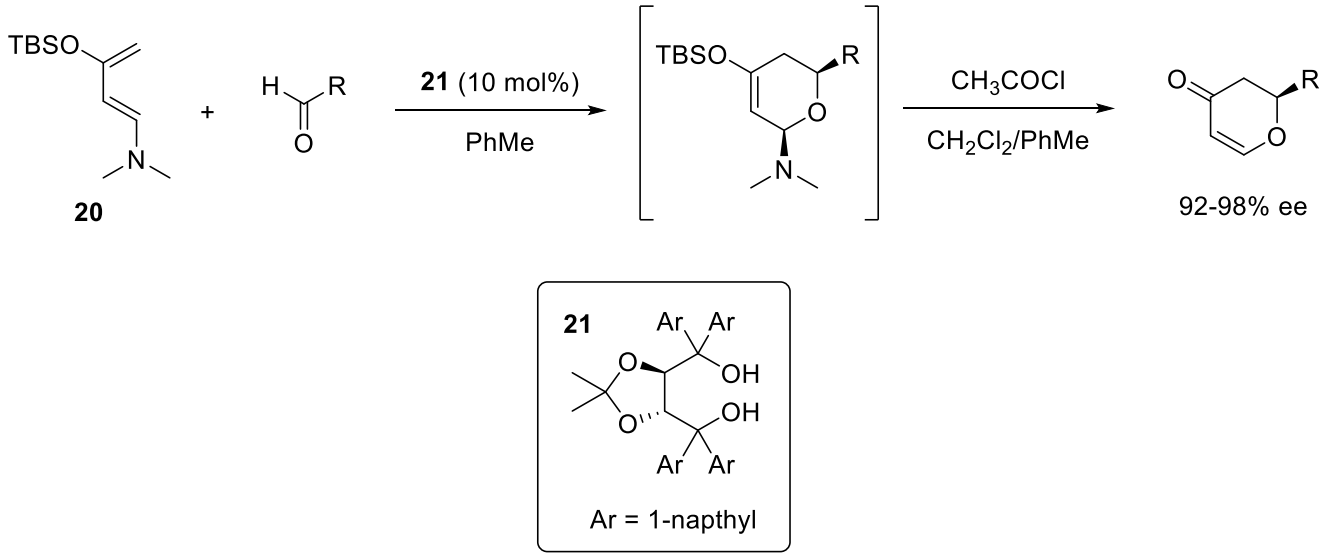

Scheme 7. TADDOL catalyzed hetero-Diels-Alder reaction.

[23] Huang, Y.; Unni, A. K.; Thadani, A. N.; Rawal, V. H. *Nature* **2003**, *424*, 146.
[24] McGilvra, J. D.; Unni, A. K.; Modi, K.; Rawal, V. H. *Angew. Chem. Int. Ed.* **2006**, *45*, 6130.

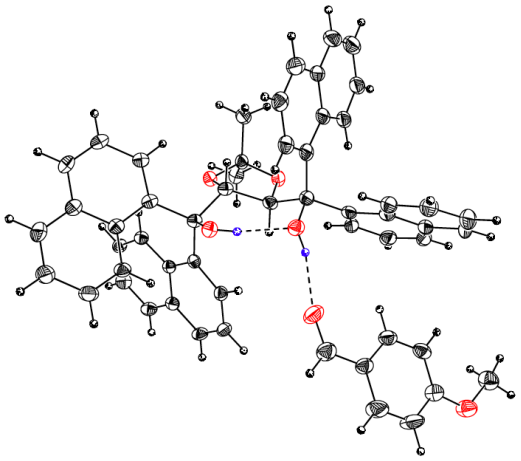

Figure 6. X-ray structure of a TADDOL-anisaldehyde complex.

In the same year, Takemoto incorporated the thiourea scaffold into a bifunctional catalyst based on a chiral 1,2-diaminocyclohexane (Scheme 8).[25] The catalyst was applied to an asymmetric conjugate addition of diethyl malonate to β-nitrostyrene and marked the first time the thiourea unit was used for activation of an electrophile other than an imine. Since then, chiral thioureas have been applied as catalysts in numerous transformations, and are one of the most commonly used H-bond donor scaffolds today.[26]

[25] Okino, T.; Hoashi, Y.; Takemoto, Y. *J. Am. Chem. Soc*. **2003**, *125*, 12672.
[26] For reviews on bifunctional thiourea catalysis, see: (a) Takemoto, Y. *Chem. Pharm. Bull*. **2010**, *58*, 593. (b) Siau, W.; Wang, J. *Catal. Sci. Technol*. **2011**, *1*, 1298. (c) Serdyuk, O. V.; Heckel, C. M.; Tsogoeva, S. B. *Org. Biomol. Chem.* **2013**, *11*, 7051.

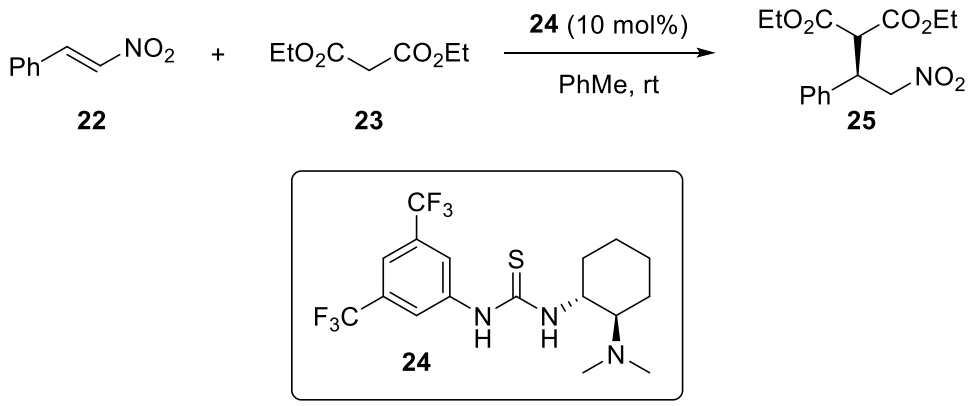

Scheme 8. Thiourea catalyzed Michael addition of diethyl malonate to β-nitrostyrene.

In 2004, Akiyama and coworkers reported an enantioselective Mannich reaction catalyzed by a chiral phosphoric acid (Scheme 9).[27] This represented the first example of chiral phosphoric acid catalysis, and the BINOL-type scaffolding would continue to be the preferred architecture for asymmetric phosphoric acid catalysis in the many asymmetric processes reported since Akiyama's original disclosure.[28]

[27] Akiyama, T.; Itoh, J.; Yokota, K.; Fuchibe, K. *Angew. Chem. Int. Ed*. **2004**, *43*, 1566.
[28] For a review on asymmetric BINOL-phosphate derived Brønsted acid and metal catalysis, see: Parmar, D.; Sugiono, E.; Raja, S.; Rueping, M. *Chem. Rev.* **2014**, *114*, 9047.

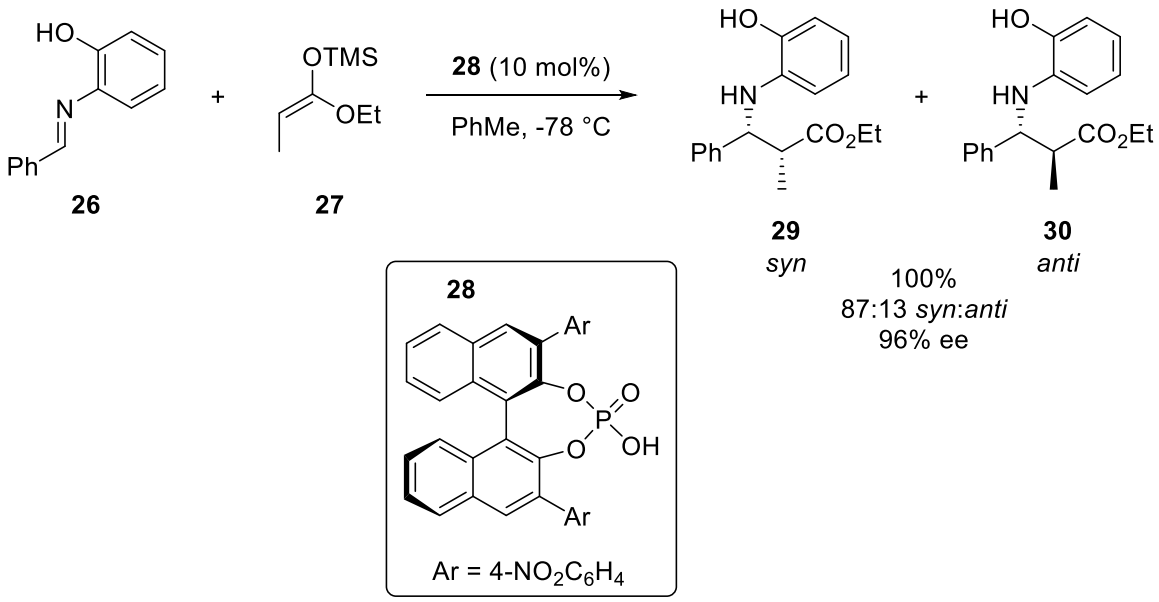

Scheme 9. Phosphoric acid catalyzed Mannich reaction.

Several years later, Rawal discovered that chiral squaramides are excellent H-bond donors for asymmetric catalysis.[29] The catalysts were found to be capable of delivering high enantioselectivities at exceptionally low catalyst loadings (Scheme 10).

[29] Malerich, J. P.; Hagihara, K.; Rawal, V. H. *J. Am. Chem. Soc*. **2008**, *130*, 14416.

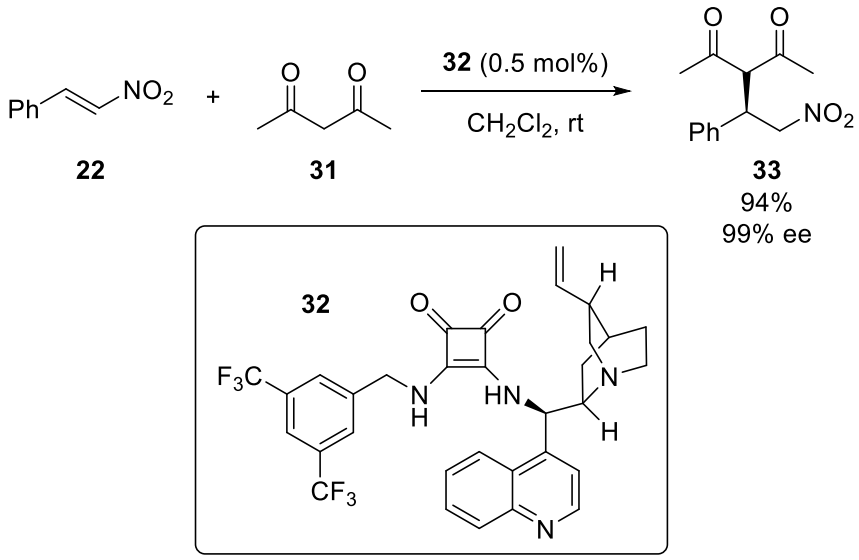

Scheme 10. Squaramide catalyzed Michael addition of acetylacetone to β-nitrostyrene.

Since the seminal report by Rawal in 2008, chiral squaramide catalysis has exploded in popularity, with a great variety of catalysts having been made and applied to countless asymmetric reactions.[30] The superb catalytic activity of squaramides and ease of preparation have resulted in squaramides being one of the most widely used scaffolds today in asymmetric H-bonding catalysis.

As new H-bond donor molecules have evolved for catalysis, so too has their catalytic activity and expansiveness of the reactivity enabled by them. The design and demonstration of new catalophores for H-bond donor catalysis endowed with further capability and performance is the subject of the following chapters.

[30] For reviews on bifunctional squaramide catalysis, see: (a) Alemán, J.; Parra, A.; Jiang, H.; Jørgensen, K. A. *Chem. - Eur. J.* **2011**, *17*, 6890. (b) Chauhan, P.; Mahajan, S.; Kaya, U.; Hack, D.; Enders, D. *Adv. Synth. Catal*. **2015**, *357*, 253.

Chapter 2

Synthesis and Properties of (Bifunctional) Thiosquaramides

II.1 Introduction

As discussed in Chapter 1, small molecule hydrogen bond donors can act as effective catalysts for asymmetric transformations. Of the many different types of scaffolds that have been explored in this context, the thiourea[1] and squaramide[2] core have dominated and emerged as the preferred platforms for hydrogen bonding catalysis. This is a consequence of both their high catalytic performance and the ease with which thiourea and squaramide catalysts can be prepared.

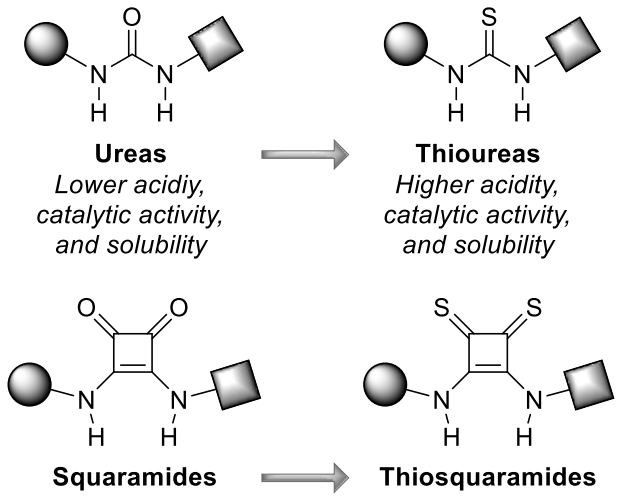

Figure 7. Relevant H-bond donor scaffolds.

Despite ureas being competent hydrogen bond donor molecules, they are rarely used when compared with thioureas. The more acidic thiourea core, and hence the strengthened

[1] For reviews on bifunctional thiourea catalysis, see: (a) Takemoto, Y. *Chem. Pharm. Bull*. **2010**, *58*, 593. (b) Siau, W.; Wang, J. *Catal. Sci. Technol*. **2011**, *1*, 1298.

[2] For reviews on bifunctional squaramide catalysis, see: Alemán, J.; Parra, A.; Jiang, H.; Jørgensen, K. *A. Chem. - Eur. J*. **2011**, *17*, 6890. Chauhan, P.; Mahajan, S.; Kaya, U.; Hack, D.; Enders, D. *Adv. Synth. Catal*. **2015**, *357*, 253.

hydrogen bonding capability of the thiourea, imparts superior performance to the thiourea scaffold for many catalytic applications.[3] This manifests itself in both faster reactions and improved enantioselectivities when compared to the urea core. Significantly, thioureas are also generally more soluble than the corresponding urea.

	O	S
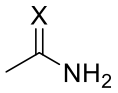 **34a**,**b**	25.5	18.5
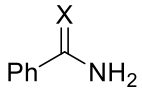 **35a**,**b**	23.4	16.9
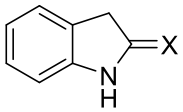 **36a**,**b**	18.5	10.0
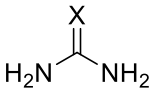 **37a**,**b**	26.9	21.0
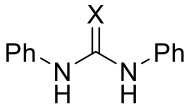 **38a**,**b**	19.5	13.5

Table 1. *p*K_a values of analogous oxo- and thioamides in DMSO.[4]

On the basis of these observations, it would be expected that thiosquaramides provide improved catalytic performance when compared to squaramides. Since the original disclosure of

[3] Increased acidity of a catalyst has been found to correlate with increased activity and capability. See, inter alia: (a) Wittkopp, A.; Schreiner, P. R. *Chem. - Eur. J.* **2003**, *9*, 407. (b) Jensen, K. H.; Sigman, M. S. *Angew. Chem. Int. Ed*. **2007**, *46*, 4748. (c) Jensen, K. H.; Sigman, M. S. *J. Org. Chem*. **2010**, *75*, 7194.

[4] Bordwell, F. G.; Algrim, D. J.; Jarrelson, J. A. *J. Am. Chem. Soc.* **1988**, *110*, 5903.

squaramides as hydrogen bond donor catalysts in 2008, almost 10 years went by during which not a single example of thiosquaramide catalysis was reported (although a computational study was published which predicted superior performance of thiosquaramides).[5] This in contrast to the hundreds of examples of squaramide catalyzed processes that were reported in the same interval. The conspicuous absence of thiosquaramide catalysis in the literature is an artifact of the surprising complexity of thiosquaramide chemistry. The synthesis, isolation, and characterization of (bifunctional) thiosquaramides are described in this chapter.

II.2 Initial Thionationation Studies of Squaramides and Squarates

At the start of this project, there existed no reported method for the synthesis of bifunctional thiosquaramides. Within our group, a method was discovered for their construction,[6] but reproducibility problems rendered the process unusable. This necessitated the invention of an alternative and more robust method of bifunctional thiosquaramide synthesis.

Previous studies on the thionation of squaramides and squarates[7] suggested that room temperature dithionation of a dialkyl squaramide should be possible with Lawesson's reagent. Since direct dithionation of a bifunctional squaramide would be the most straightforward method of synthesis, this was attempted first. Treatment of bifunctional squaramide **39** with 1.1 equivalents of Lawesson's reagent led to bifunctional thiosquaramide **40** after 1 hour at room temperature. The desired product was observed by crude ^{1}H NMR. Efforts to purify this compound from Lawesson's reagent byproduct failed. However, several important observations

[5] Lu, T.; Wheeler, S. E. *Chem. - Eur. J.* **2013**, *19*, 15141.
[6] Montgomery, T. D. Ph.D. Thesis, The University of Chicago, 2015.
[7] (a) Müller, M.; Heileman, M. J.; Moore, H. W.; Schaumann, E.; Adiwidjaja, G. *Synthesis* **1997**, *1997*, 50. For other examples of thionation of squaramides and squarates, see: (b) Eggerding, D.; West, R. *J. Org. Chem.* **1976**, *41*, 3904. (c) Frauenhoff, G. R.; Takusagawa, F.; Busch, D. H. *Inorg. Chem.* **1992**, *31*, 4002.

were made at this stage. One was that the purity of the bifunctional alkyl thiosquaramide degraded after silica gel chromatography. Another was the presence of rotameric forms of the catalyst in DMSO, which was expected due to the highly restricted rotation about the vinylogous thioamide bond.

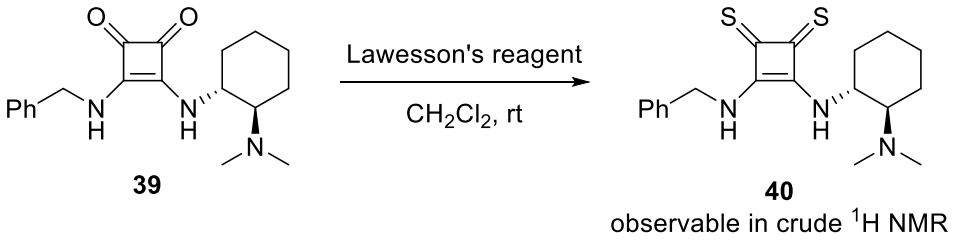

Scheme 11. Dithionation of a bifunctional squaramide.

Directed by these observations, a different route to access bifunctional thiosquaramides was conceptualized. If a vinylogous ester-amide could be dithionated and purified, it should be possible for the resulting product to undergo addition-elimination reactions with amines, in an analogous fashion to how squaramides are typically made. To test this strategy, vinylogous ester-amide **42** was chosen as the model substrate, due to the *tert*-butyl group serving as a useful ^{1}H-NMR handle to simplify characterization.

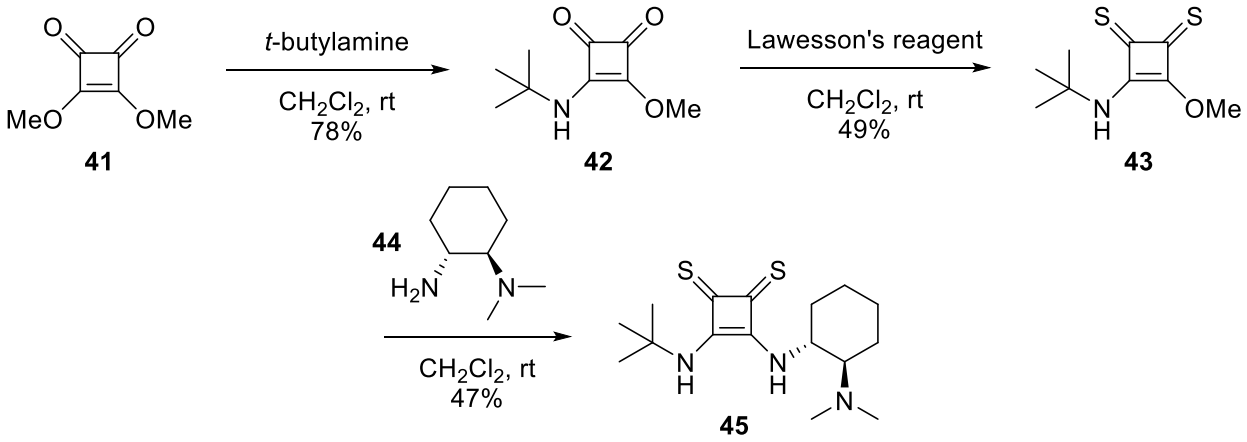

Scheme 12. Thiosquaramide synthesis from the vinylogous methyl thionoester.

Using 1.0 equivalents of Lawesson's reagent, dithionation of **42** proceeded at room temperature to deliver the desired dithiosquarate **43**. Importantly, this compound was stable to silica gel chromatography, enabling it to be isolated pure in 49% yield. Treatment of dithiosquarate **43** with chiral diamine **44** at room temperature led to bifunctional thiosquaramide **45**. Since the addition-elimination reaction proceeded so cleanly, and the only byproduct formed in the reaction was methanol, silica gel chromatography was avoidable, and the product was isolated by trituration in 47% yield.

Problems arose when dithionation was attempted on other substrates (Scheme 13). Dithionation of vinylogous ester-amide **46**, which differs with **42** only in the benzyl substitution, led to no desired product despite consumption of starting material. Since the principle difference between these two substrates was the steric bulk at the squarate nitrogen, it was reasoned that the steric environment around the squarate core heavily impacted the stability of corresponding dithio-derivatives. This prompted the examination of the dithionation of bulkier squarates, as detailed in the next section.

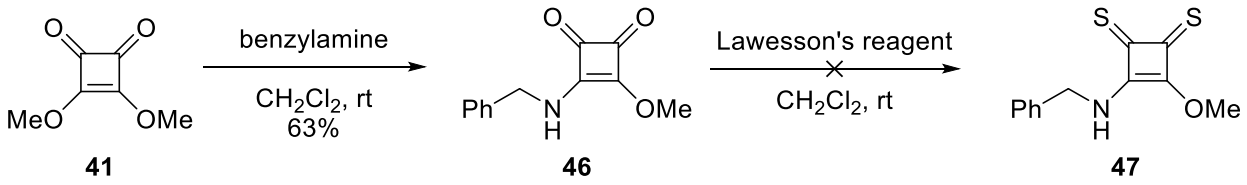

Scheme 13. Attempted dithionation of vinylogous ester-amide **46**.

II.3 Thiosquaramide Synthesis from the Vinylogous Butyl Thionoester

On the basis of the above findings, vinylogous butyl ester-amide **49** was made and treated with Lawesson's reagent (Scheme 14). Unlike it's corresponding methyl derivative **46**, the

vinylogous butyl ester was stable to dithionation conditions employing Lawesson's reagent, and after silica gel chromatography, could be isolated in 57% yield. What is interesting to note is that the methyl derivative **46** could (although in low yield) be dithionated with P_4S_{10}-pyridine complex, a thionating agent that was used in the only previously known synthesis of diaryl thiosquaramides in a reported 37 - 66% yield (Scheme 15).[8] The authors mentioned that Lawesson's reagent was ineffective for dithionation of the diaryl squaramides. For vinylogous butyl ester-amide **49**, P_4S_{10}-pyridine complex was found to be ineffective, while Lawesson's reagent on the other hand was effective.

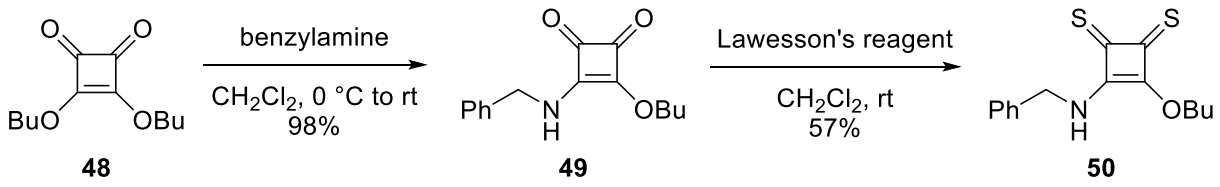

Scheme 14. Successful dithionation of vinylogous butyl ester-amide **49**.

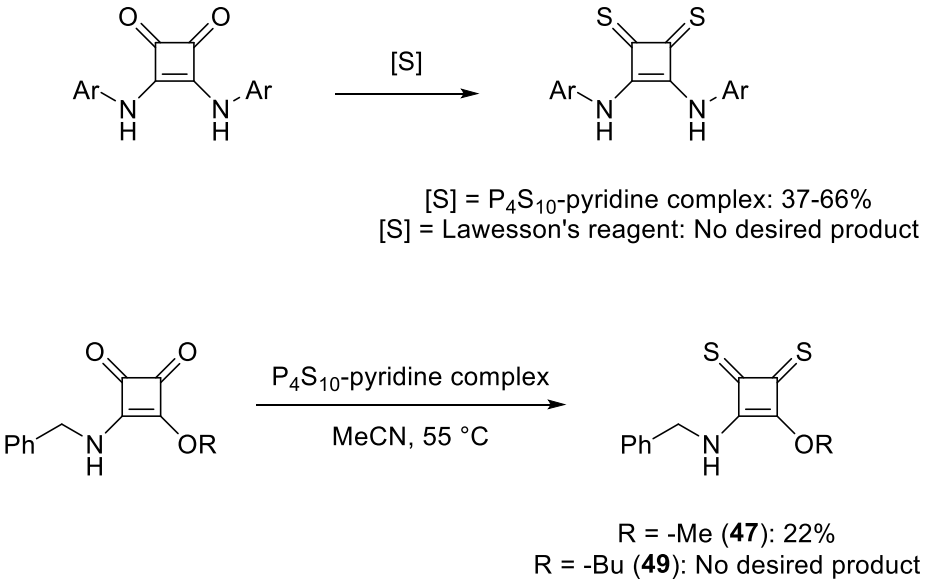

Scheme 15. Differences across thionating reagents and substrates.

[8] Busschaert, N.; Elmes, R. B. P.; Czech, D. D.; Wu, X.; Kirby, I. L.; Peck, E. M.; Hendzel, K. D.; Shaw, S. K.; Chan, B.; Smith, B. D.; Jolliffe, K. A.; Gale, P. A. *Chem. Sci*. **2014**, *5*, 3617.

Having identified substrate steric requirements for dithionation with Lawesson's reagent, a series of vinylogous butyl ester-amides was made and treated in the same way to produce the corresponding dithio-derivatives (Scheme 16). It should be noted that vinylogous butyl ester-amides derived from anilines were not suited for dithionation. This shortcoming to the methodology is fully addressed in a subsequent section.

The higher yields obtained with the *tert*-butyl and cumyl compounds **54** and **55** were consistent with the hypothesis that greater steric bulk around the squarate core imparts stability to the dithionated products. It was observed that subjecting compounds **49** and **53** to dithionation conditions for extended periods significantly worsened yields and purity. In contrast, compounds **51** and **52** were less sensitive to reaction time with respect to both yield and purity.

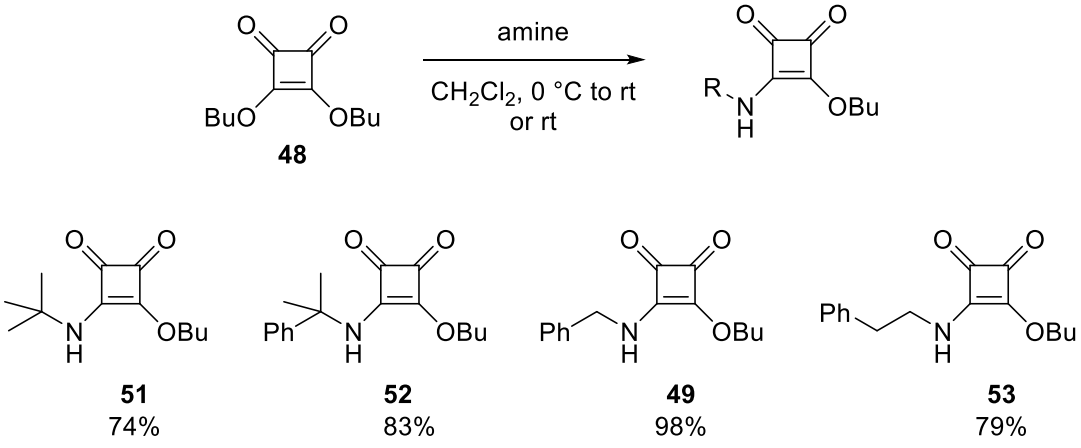

Scheme 16. Monoaddition of amines to dibutyl squarate.

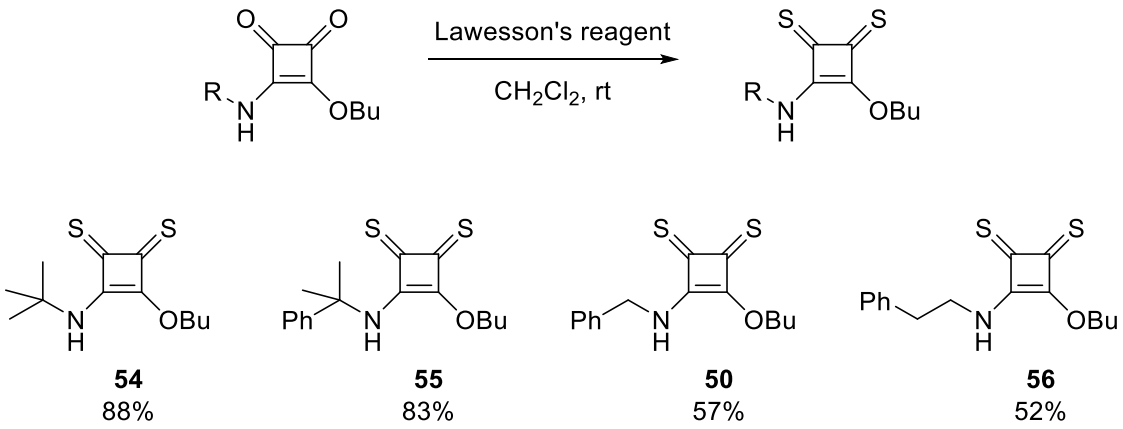

Scheme 17. Dithionation of the vinylogous butyl ester-amides.

The dithiosquarate intermediates all readily reacted with chiral diamines (Scheme 18), which after trituration produced pure bifunctional alkyl thiosquaramide catalysts. X-ray crystallography of **45** confirmed the structural assignment.

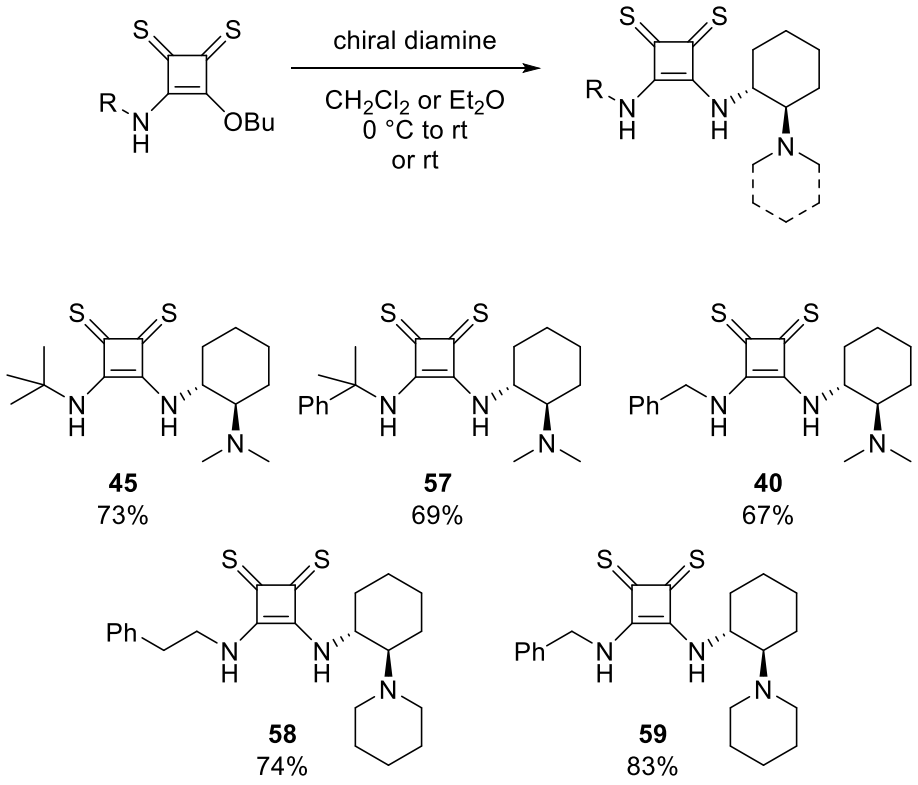

Scheme 18. Synthesis of bifunctional thiosquaramides from the vinylogous butyl thionoesters.

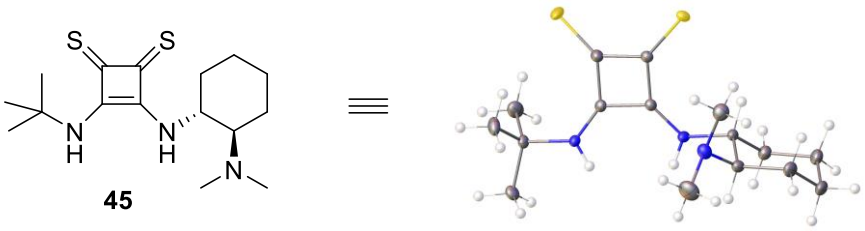

Figure 8. X-ray structure of thiosquaramide **45**.

This collection of results enabled the first general and reproducible synthesis of bifunctional alkyl thiosquaramides, and an outline of the overall synthesis from the commercially available dibutyl squarate is given in Scheme **19**. The catalysts prepared by this method were later applied to a highly enantioselective synthesis of chiral barbituric acids, which is described in detail in Chapter II.

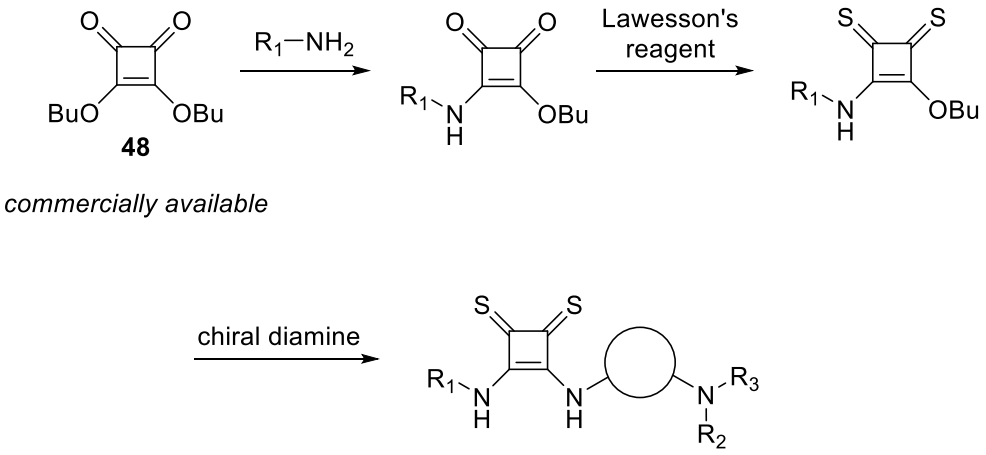

Scheme 19. Overall synthetic pathway to bifunctional alkyl thiosquaramides from dibutylsquarate.

II.4 Thiosquaramide Synthesis from the Dithiosquarate

Despite the progress made in bifunctional thiosquaramide synthesis with the above methodology, there remained substantial room for improvement. As already pointed out,

bifunctional aryl thiosquaramides remained inaccessible. Dithionated vinylogous butyl ester-amides are only moderately stable, and this has led to complications in their preparation. Moreover, the need to employ thionation conditions for each separate vinylogous butyl ester-amide creates a time-burden to the bench chemist. It was recognized that thioureas and squaramides have been widely-adopted not only for their excellent catalytic performance, but also due to the simple and routine nature of their preparation. An easy and standard synthetic sequence for the synthesis of thiosquaramides was therefore highly desireable.

Squaramides are most commonly made by two addition-elimination reactions of dimethyl squarate (Scheme 20). An analogous method of thiosquaramide preparation would therefore require identification of a stable alkyl dithiosquarate. Since it had already been found that steric bulk around the squarate core great impacts stability of the compound, it seemed reasonable that further increasing steric bulk around the core structure might impart the needed stability.

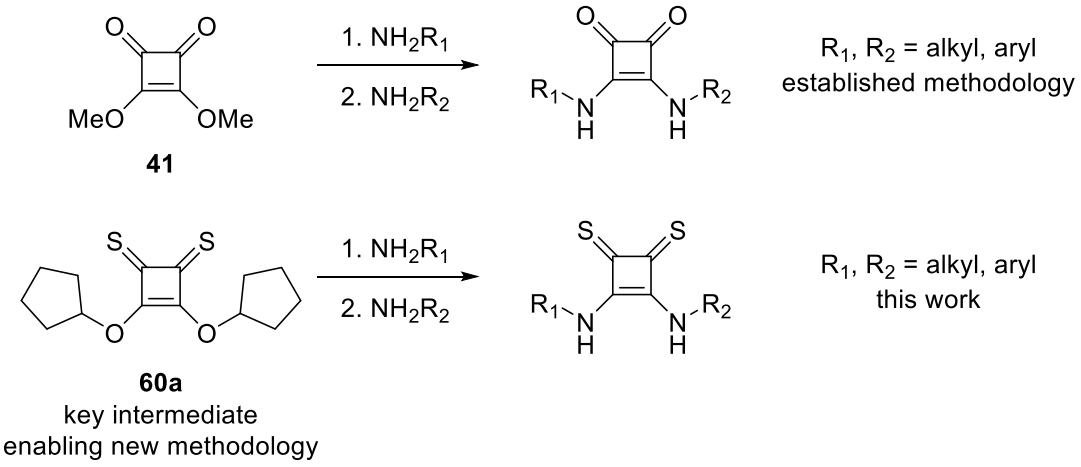

Scheme 20. General synthesis of squaramides and thiosquaramides.

Several alkyl squarates were thus prepared and treated with Lawesson's reagent (Table 2). Dithionation of dibutyl squarate gave an unstable gel. Due to decomposition of the product under reaction conditions, the reaction had to be stopped early in order to isolate the product pure. As a

result, yields were poor. As noted earlier, dithionated intermediates with a butyl substitution had only moderate stability (as well as having difficult handling characteristics, often unwilling to solidify) and this was one feature of the previous synthesis we wished to improve here.

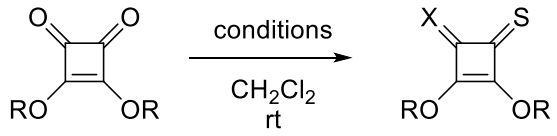

entry	R	Lawesson's reagent equivalents	time (h)	X	yield (%)
1	*n*-butyl (**48**)	1.0	7	S (**48a**)	14
2	3-pentyl (**61**)	1.0	14	S (**61a**), O (**61b**)	30, 39
3	3-pentyl (**61**)	1.0	46	S (**61a**)	80
4	cyclopentyl (**62**)	1.0	37	S (**60a**)	71
5	cyclopentyl (**62**)	0.5	25	O (**60b**)	68

Table 2. Dithionation of alkyl squarates with Lawesson's reagent.

Alkyl squarates derived from secondary alcohols gave better results. Dithionation of both 3-pentyl and cyclopentyl squarates gave good yield of the desired dithionation products after 80 hours and 71 hours, respectively. Due to superior handling characteristics and reactivity, dicyclopentyl dithiosquarate was the preferred intermediate for making thiosquaramides. Dicyclopentyl dithiosquarate is a solid and stable to ambient storage conditions for more than one week. On the other hand, di-3-pentyl dithiosquarate is a red oil that darkens upon standing. Monoaddition products of dicyclopentyl dithiosquarate are also solids and are stable to ambient storage conditions for months. Monoaddition products of di-3-pentyl dithiosquarate are only reluctant to solidify.

Dicyclopentyl dithiosquarate reacted well with a variety of electronically and sterically diverse amines to produce the diaddition products (Table 3). Reactions for less hindered amines such as benzylamine and cyclohexylamine are sufficiently exothermic so as to cause the solvent to boil if no cooling bath is employed. The main limitation appears to be the diaddition of very bulky amines. The diaddition of *tert*-butyl amine proceeds in only 30% yield. Prolonged reaction time, or using larger excess of amine, did not produce a substantial increase in yield.

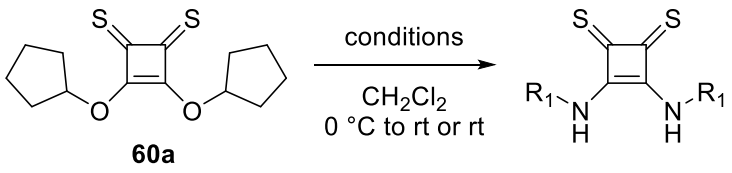

entry	product		amine equivalents	time (h)	yield (%)
1	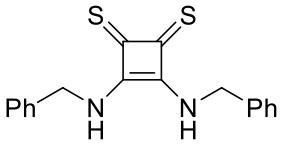	**63**	2.1	1.5	86
2	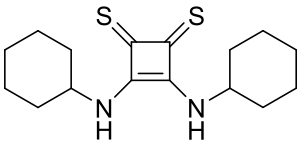	**64**	2.1	2	60
3	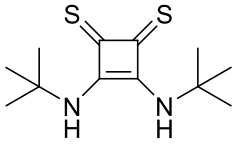	**65**	2.1	2	30
4	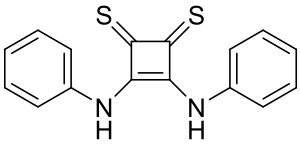	**66**	3.0	20	79
5	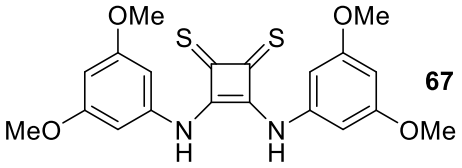	**67**	2.1	40	77
6	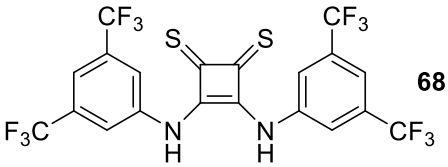	**68**	4.0	96	52

Table 3. Diaddition of amines to dicyclopentyl dithiosquarate.

Remarkably, the diaddition of 3,5-bis(trifluoromethyl)aniline to dicyclopentyl dithiosquarate occurs at room temperature and in the absence of catalyst (entry 6). For

comparison purposes, the diaddition of 3,5-bis(trifluoromethyl)aniline to diethyl squarate is usually carried out at 100 °C with $Zn(OTf)_2$ as catalyst (Scheme 21).[9]

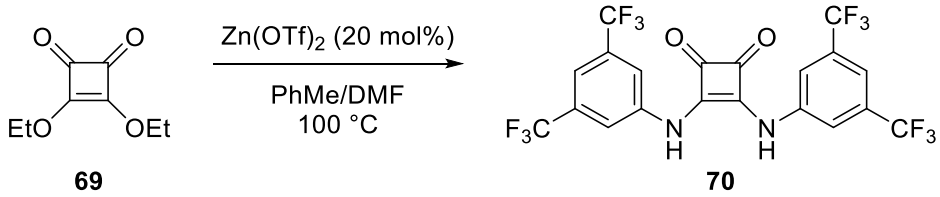

69 **70**

Scheme 21. Synthesis of an electron-deficient diaryl squaramide.

Synthesis of the simplest thiosquaramide **71** proved unsuccessful, likely due to the products presumed instability (Scheme 22).

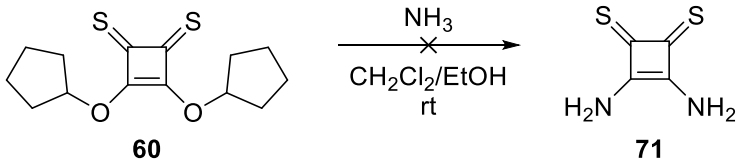

60 **71**

Scheme 22. Attempted synthesis of the simplest thiosquaramide.

Despite the high reactivity of dicyclopentyl dithiosquarate to addition-elimination reactions, monoaddition reactions of amines can still proceed in good yield (Table 4). The higher isolated yield of **75** compared to **74** is due to competitive diaddition of amine, indicating that the product **74** is similarly reactive to addition-elimination reactions as starting material **60a**.

[9] Rostami, A.; Colin, A.; Li, X. Y.; Chudzinski, M. G.; Lough, A. J.; Taylor, M. S. *J. Org. Chem.* **2010**, *75*, 3983.

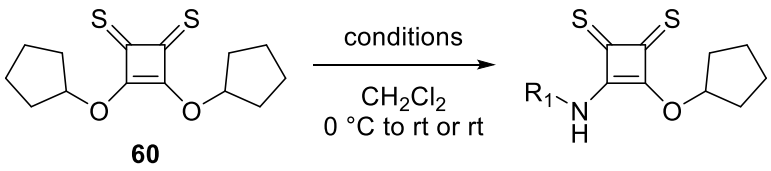

entry	product		amine equivalents	time (h)	yield (%)
7	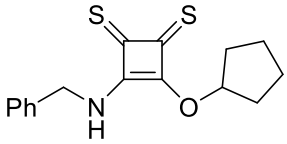	**72**	0.83	0.5	79
8	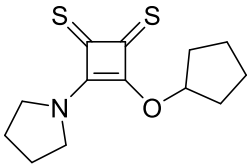	**73**	0.83	1	62
9	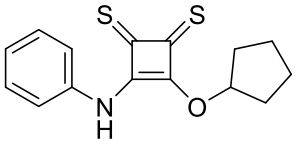	**74**	0.83	14	52
10	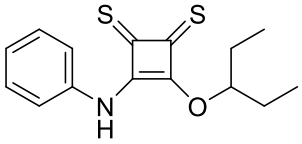	**75**	0.83	13	59
11	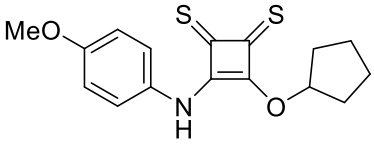	**76**	0.83	3	77
12	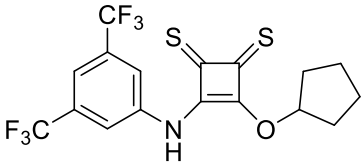	**77**	0.83	16	66

Table 4. Monoaddition of amines to dicyclopentyl dithiosquarate.

To gauge the reactivity of these intermediates to oxygen-centered nucleophiles, compound **73** was heated in *n*-butanol at 70 °C for 18 h. Transthionoesterification product **78**

was thus obtained in 38% yield. Intermediates **72** - **77** can be stored at ambient conditions for months without noticeable decomposition.

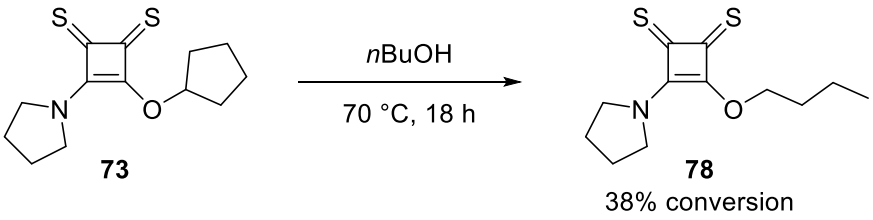

Scheme 23. Transthionoesterification of vinylogous thionoester **73**.

Reactivity of these intermediates with amines was of course much higher. Coupling of **72** - **77** with a chiral diamine at 0 °C leads to bifunctional thiosquaramides **59** and **79** - **84**. Notably, this includes the previously inaccessible bifunctional aryl thiosquaramides.

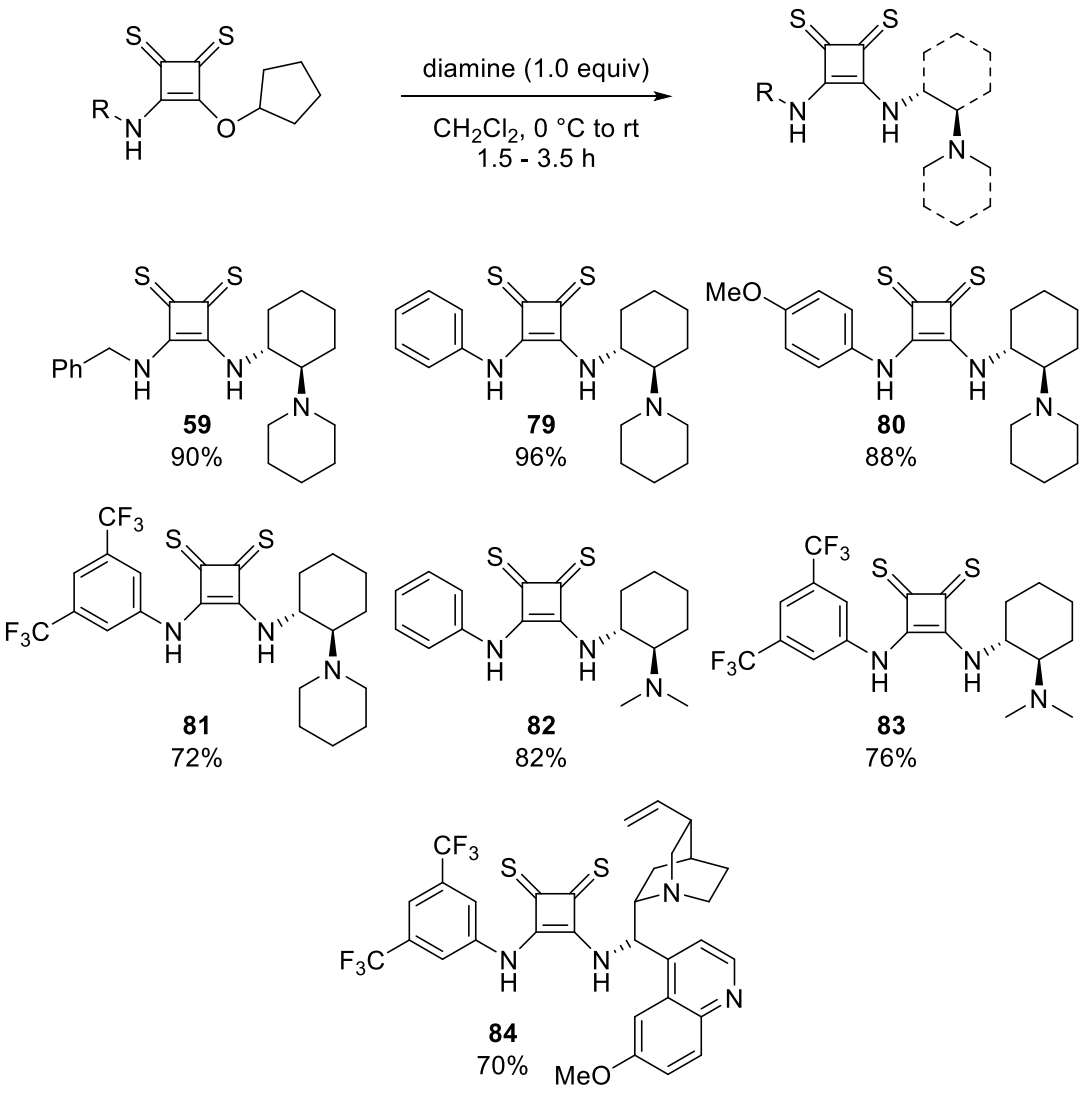

Scheme 24. Synthesis of bifunctional alkyl and aryl thiosquaramides.

An interesting divergence in reactivity between squarates **42** and **43** is shown in Scheme 25. When treated with ambident nucleophile **85**, the oxosquarate reacts with the primary amine as expected. Treatment of the thiosquarate with diamine **85** results in product **87**, which may arise either from addition-elimination of the secondary amine or rearrangement after a first addition-elimination of the primary amine. The reactivity of vinylogous butyl thionoesters or cyclopentyl thionoesters with ambident nucleophiles was not examined.

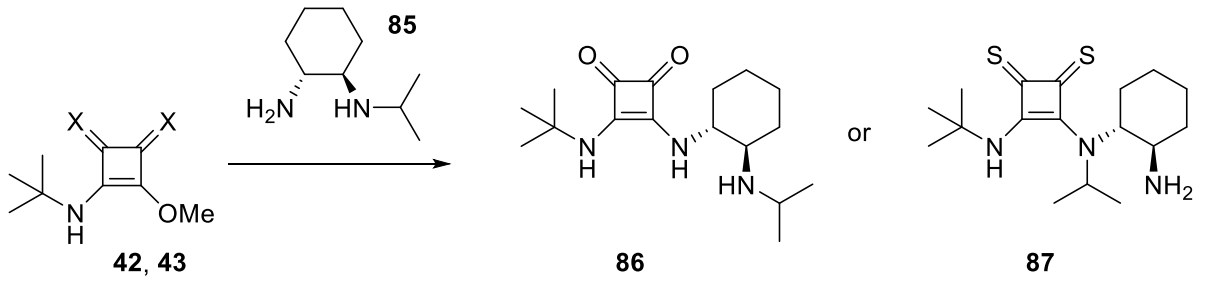

Scheme 25. Divergent reactivity of an oxo- and thiosquarate.

As can be seen in Table 2, using 0.5 equivalents of Lawesson's reagent for thionation gives access to monothionation product **60b** in good yield. This intermediate can undergo two addition-elimination reactions to produce a bifunctional monothiosquaramide catalyst with full regiocontrol (Scheme 26). The first amine addition-elimination occurs with the vinylogous thionoester. Predictably, the second amine addition-elimination reaction occurs much more sluggishly. Such bifunctional monothiosquaramide catalysts offer a new way to desymmetrize the hydrogen bond donor capabilities of the squaramide core. These new compounds remain untested for catalytic performance.

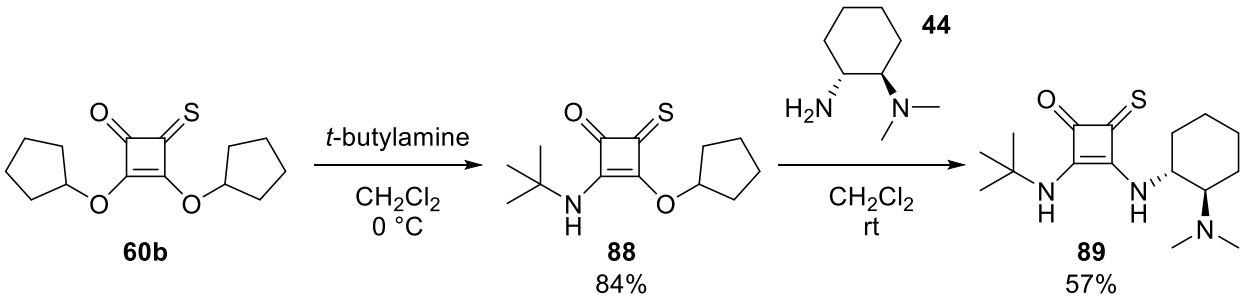

Scheme 26. Synthesis of a bifunctional monothiosquaramide.

II.5 Thiosquaramide Properties and Catalytic Performance

It was expected that thiosquaramides would be more acidic than their corresponding squaramides, and that this would in turn lead to better catalytic performance.[3] Acidities of bifunctional thiosquaramide **45** and its corresponding squaramide were measured by Dr. Chintan Sumaria using the Bordwell method.[10] The bifunctional thiosquaramide was found to be ~5 pK_a units more acidic than the corresponding squaramide in DMSO (Figure 9). Similar differences in acidity across other series of thiosquaramide and squaramides can be expected based on these results.

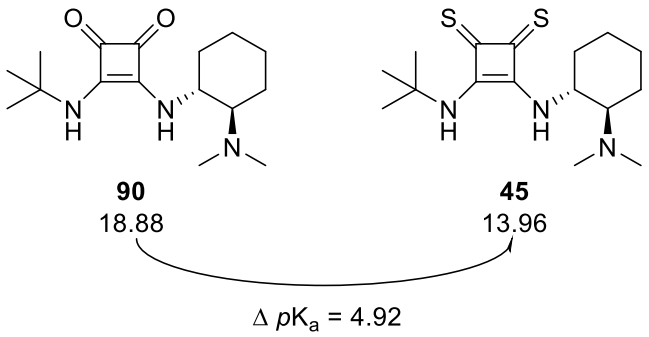

Figure 9. pK_a values of a bifunctional oxo- and thiosquaramide catalyst in DMSO.

Another difference we were expecting was in solubility. The solubility of thiosquaramide **59** was determined to be >3 mg/mL in toluene, compared with <0.1 mg/mL for the corresponding squaramide. Qualitatively, thiosquaramide **45** and monothiosquaramide **89** had similar solubilities in dichloromethane, and squaramide **90** was appreciably less soluble than either.

An examination of crystal structures provides some explanation for these differences in solubilities. Ureas and squaramides tend to crystallize by forming hydrogen bonded head-to-tail ladders in which adjacent molecules are coplanar with respect to the urea and squaramide core,

[10] Sumaria, C. S. Ph.D. Thesis, The University of Chicago, 2017.

while thioureas generally do not ladder in a coplanar fashion (Figure 10).[11] In the X-ray crystal structure of thiosquaramide **45**, it was found that the packing arrangement was similar to that seen in thioureas (Figure 11). A two-point H-bond is formed to a single thiocarbonyl unit in an adjacent molecule in a twisted geometry.

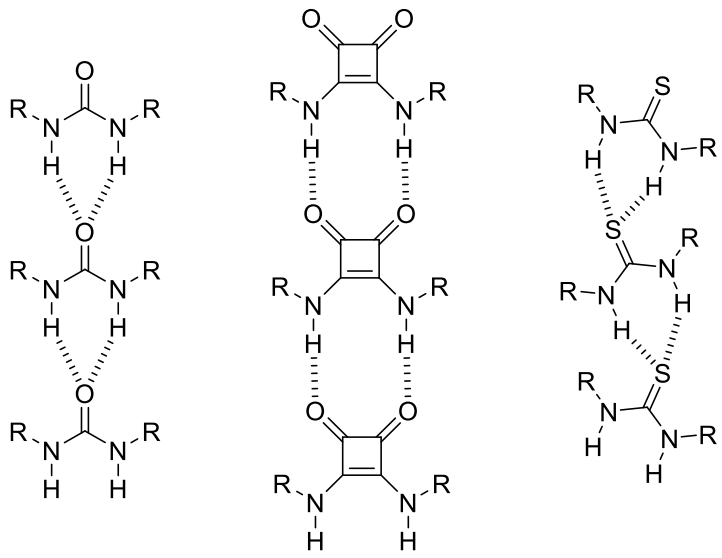

Figure 10. Common arrangement of ureas, squaramides, and thioureas in the solid state.

[11] Custelcean, R. *Chem. Commun.* **2008**, 295.

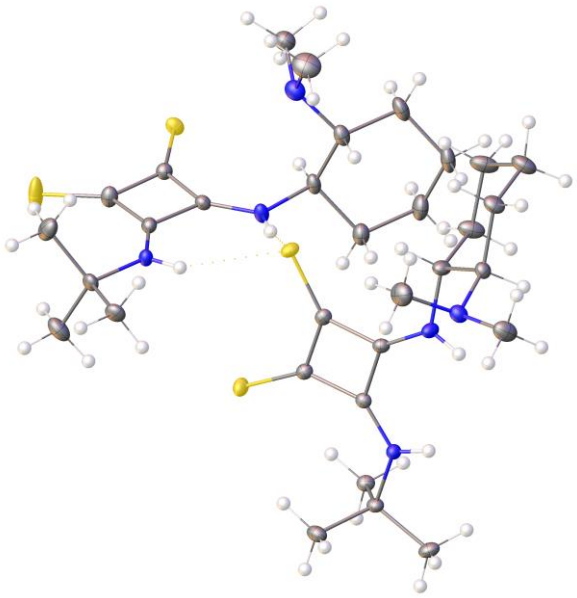

Figure 11. Packing arrangement of two adjacent thiosquaramide molecules in the solid state.

In the two rotameric forms of thiosquaramide **45** in the solid state, the two N−H hydrogen atoms in the thiosquaramide are 2.43 and 2.64 Å apart, compared to ~2.1 Å and ~2.7 Å for thioureas and squaramides, respectively. The smaller H−H distance is likely due to repulsive forces between the bulky *tert*-butyl group and adjacent thiocarbonyl unit rather than packing forces in the solid state, as Hartree-Fock calculations for the same structure at the 3-21G level of theory gives the H−H distance as 2.60 Å.

Due to restricted rotation about the vinylogous thioamide bond, asymmetric thiosquaramides can exist as up to four rotamers (Figure 12).[12] The bulkiness of the thiosquaramide substitution heavily influences its rotameric composition. Thiosquaramides with large substitutions tend to exist as one rotamer, and thiosquaramides with smaller substitutions tend to exist as multiple rotamers. Thiosquaramide **65** exists as a single rotamer in DMSO, while thiosquaramide **63** exists as three rotamers in a ratio of 26:9:2 (Figure 13).

[12] For a study on the conformational equilibria of squaramides, see: Rotger, M. C.; Piña, M. N.; Frontera, A.; Martorell, G.; Ballester, P.; Deyà, P. M.; Costa, A. *J. Org. Chem.* **2004**, *69*, 2302.

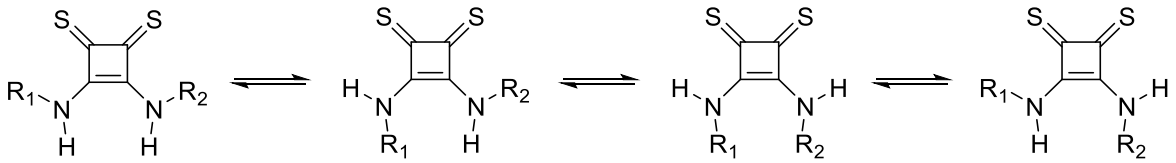

Figure 12. Multiple conformers of thiosquaramides observable by ^{1}H-NMR.

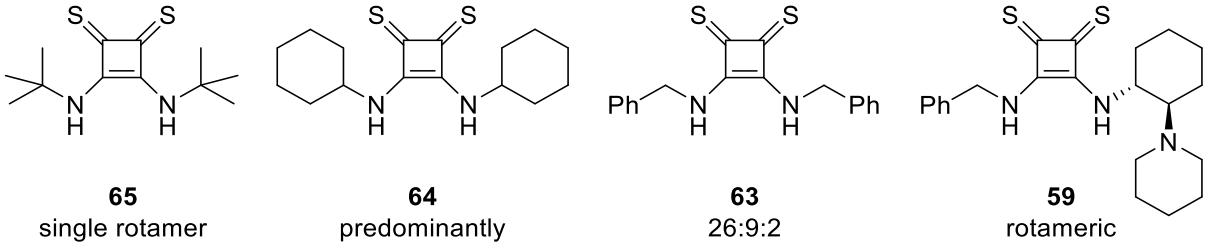

Figure 13. Rotameric composition of selected thiosquaramides in DMSO at rt.

The existence of thiosquaramide rotamers complicates NMR analysis of these compounds. Adding to complications is the presence of zwitterionic forms of bifunctional aryl thiosquaramide catalysts. NMR spectra of pure bifunctional (aryl) thiosquaramides can therefore appear very messy. It was found that forming the hydrochloride salt of bifunctional thiosquaramides (aryl or alkyl) eliminated both zwitterions and rotamers, thus greatly simplifying ^{1}H-NMR analysis and enabling routine structural assignment of bifunctional thiosquaramides (Scheme 27).

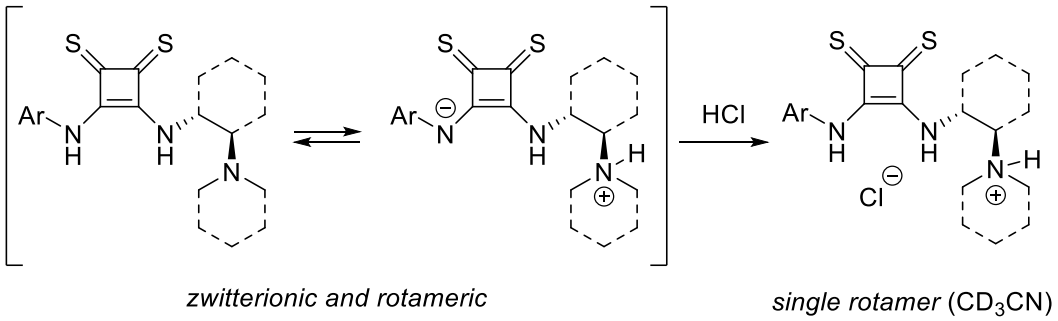

Scheme 27. Protonation of bifunctional thiosquaramides for ^{1}H-NMR characterization.

Unlike certain bifunctional alkyl thiosquaramides, several of the bifunctional aryl thiosquaramides were found to be stable to silica gel chromatography and were thus purified in this fashion. It appears as though these stability problems arise from the presence of the basic amine in the bifunctional thiosquaramides. Bifunctional thiosquaramide **45** was found to degrade after flushing through silica gel with dichloromethane and methanol. Thiosquaramide **65** lacking the basic amine portion underwent no detectable decomposition.

Benchmarking studies were carried out to evaluate the catalytic performance of bifunctional thiosquaramides against their squaramide counterparts in the known conjugate addition reaction of lawsone **91** to β,γ-unsaturated α-keto ester **92** (Scheme 28).[13] No substantial rate differences were observed between any catalysts in a pair. However, the thiosquaramide catalysts gave superior enantioselectivities for every pair of squaramide and thiosquaramide catalyst examined. This result was of great importance, as it provided proof of concept that thiosquaramides can provide better catalytic performance than squaramides.

[13] (a) Chen, X.; Zheng, C.; Zhao, S.; Chai, Z.; Yang, Y.; Zhao, G.; Cao, W. *Adv. Synth. Catal*. **2010**, *352*, 1648. (b) Wang, Y.; Zhang, W.; Luo, S.; Zhang, G.; Xia, A.; Xu, X.; Xu, D. *Eur. J. Org. Chem*. **2010**, *2010*, 4981. (c) Gao, Y.; Ren, Q.; Ang, S.; Wang, J. *Org. Biomol. Chem*. **2011**, *9*, 3691. (d) Lee, J. H.; Kim, D. Y. *Bull. Korean Chem. Soc.* **2013**, *34*, 1619

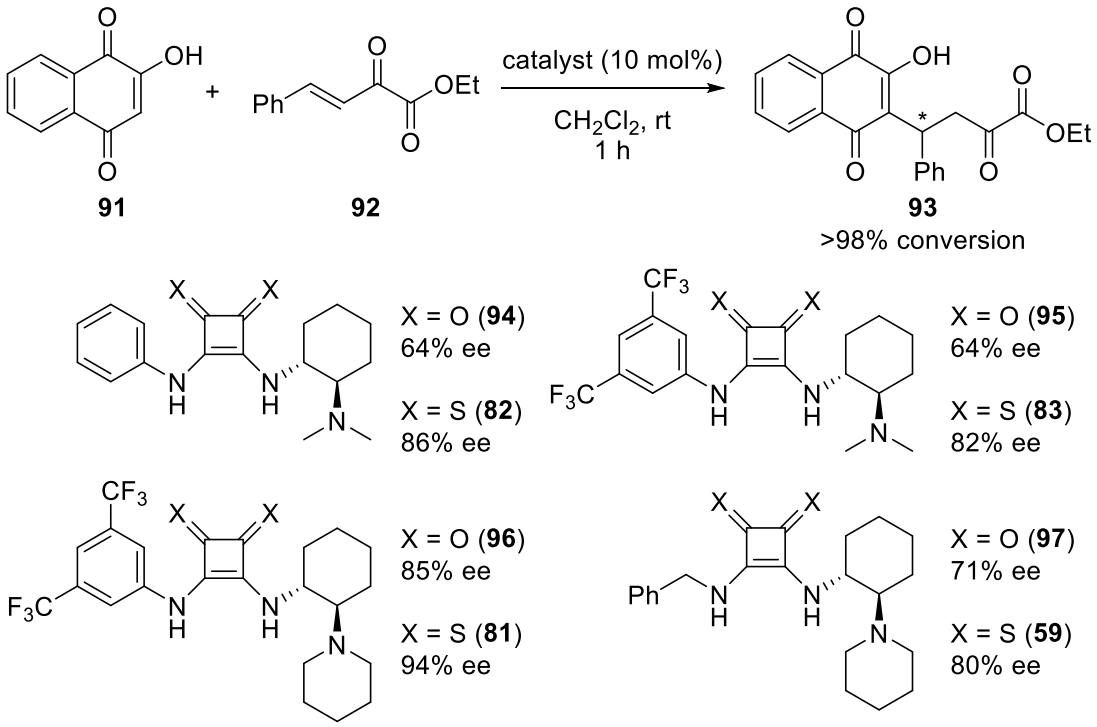

Scheme 28. Comparison of oxo- and thiosquaramide performance in a conjugate addition reaction of lawsone to a β,γ-unsaturated α-keto ester.

The lawsone reaction was originally chosen due to the acidity of lawsone (pK_a = 4.15 in H_2O).[14] Because bifunctional aryl thiosquaramides exist as zwitterions, they should be less basic than their corresponding squaramides, and as a result may not be effective for activating less acidic nucleophiles. The enantioselective Michael addition of acetylacetone (pK_a = 9 in H_2O)[15] to β-nitrostyrene is probably the most widely used reaction for benchmarking performance of bifunctional hydrogen bond donor catalysts. Thiosquaramide **83** and its corresponding squaramide were compared side-by-side in this reaction (Scheme 29). Although the thiosquaramide catalyzed reaction was slower, it did provide the product **33** in higher enantiopurity.

[14] Petrova, S. A.; Kolodyazhny, M. V.; Ksenzhek, O. S. *J. Electroanal. Chem.* **1990**, *277*, 189.
[15] Bordwell pK_a Table.

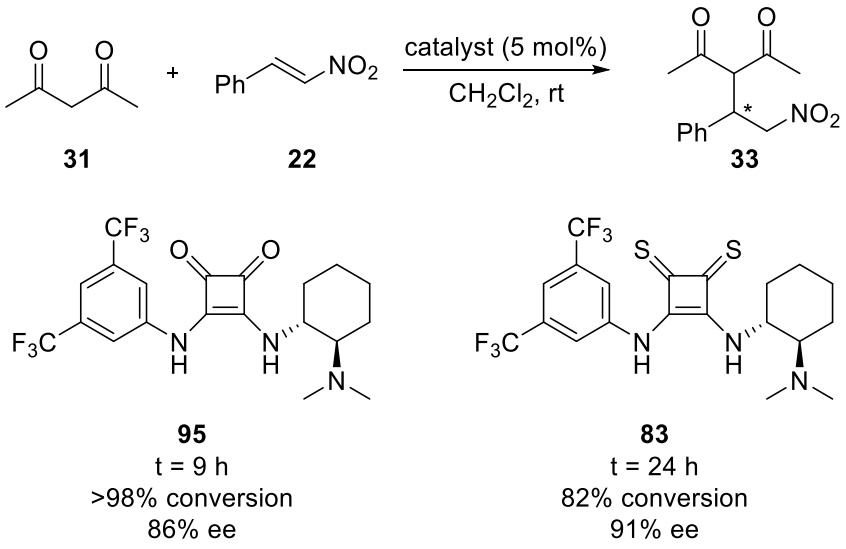

Scheme 29. Comparison of oxo- and thiosquaramide performance in a conjugate addition reaction of acetylacetone to β-nitrostyrene.

The acidity of the nucleophile does not appear to be a singular determinant of the efficacy of a bifunctional aryl thiosquaramide, however. The nitro-aldol reaction of nitromethane with isatin (Scheme 30) proceeds at similar rates with either a bifunctional aryl oxo- or thiosquaramide.

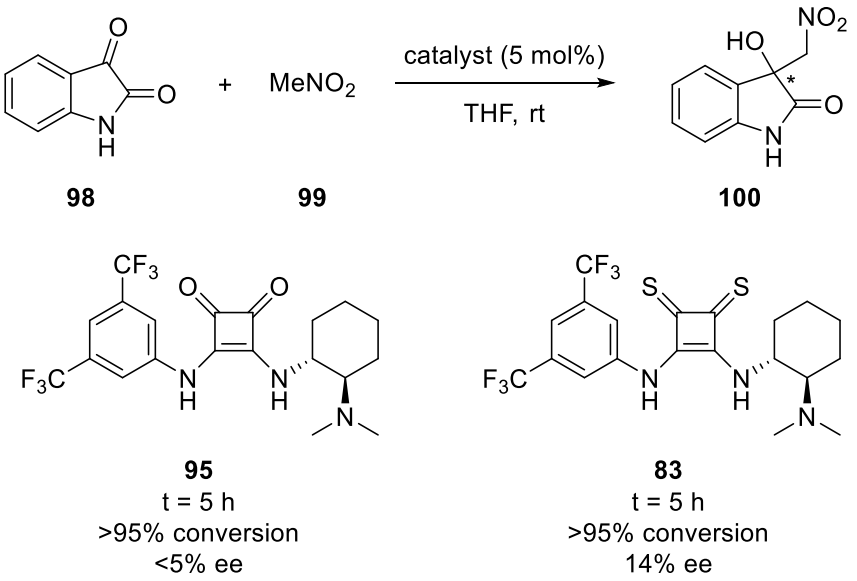

Scheme 30. Comparison of oxo- and thiosquaramide performance in a nitro-aldol reaction.

The increased acidity of the aryl thiosquaramides opens new doors for catalytic opportunities with the squaramide scaffold. It was hoped that the aryl thiosquaramides may be able to function as Brønsted acid catalysts. To test this, the aza-Diels-Alder reaction between 2-siloxydiene **101** and *N*-benzylideneaniline **102** was examined, which had been previously reported with bis(trifluoromethane)sulfonimide (Tf_2NH) as catalyst. [16] Excitingly, diarylthiosquaramide **68** was catalytically active, delivering the desired hetero-DA product **103** in 77% yield and 2.7:1 dr. The analogous squaramide gave no conversion, even in dichloromethane where its solubility is greater. Schreiner's catalyst was also entirely inactive.

[16] (a) Takasu, K.; Shindoh, N.; Tokuyama, H.; Ihara, M. *Tetrahedron* **2006**, *62*, 11900. For examples of Brønsted acid catalyzed enantioselective aza-Diels-Alder reactions, see: (b) Rueping, M.; Raja, S. *Beilstein J. Org. Chem.* **2012**, *8*, 1819. (c) Beceño, C.; Krappitz, T.; Raabe, G.; Enders, D. *Synthesis* **2015**, *47*, 3813. (d) Hatanaka, Y.; Nantaku, S.; Nishimura, Y.; Otsuka,T.; Sekikaw,T. *Chem. Commun*. **2017**, *53*, 8996.

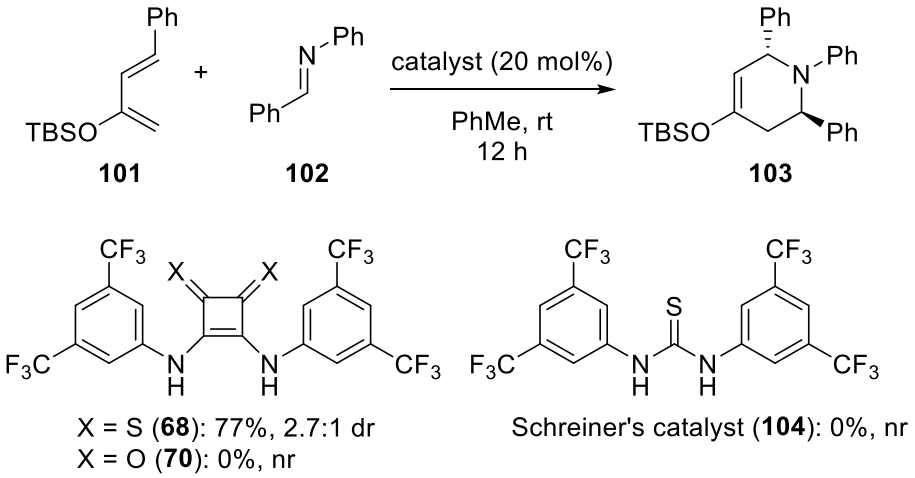

Scheme 31. Aza-Diels-Alder reaction using a thiosquaramide as a Brønsted acid catalyst.

II.6 Conclusion

In summary, the first synthesis of bifunctional thiosquaramides has been described.[17] Improvement of the synthesis resulted in the identification of dicyclopentyl dithiosquarate as a versatile intermediate for the construction of a wide variety of aryl and alkyl thiosquaramides.[18] Details of purification and characterization were uncovered which should assist in the routine preparation of these compounds in the future. Bifunctional thiosquaramides were found to be both more acidic and more soluble in nonpolar solvents their squaramide counterparts, and the superior performance of these catalysts was demonstrated in an enantioselective Michael addition. The higher acidity afforded by aryl thiosquaramides enabled them to function as Brønsted acids where squaramides could not. This result indicates high potential for thiosquaramides to expand the types of reactions amenable to catalysis by the (thio)squaramide scaffold in the future. The synthesis of bifunctional monothiosquaramides has also been

[17] Rombola, M.; Sumaria, C. S.; Montgomery, T. D.; Rawal, V. H. *J. Am. Chem. Soc*. **2017**, *139*, 5297.
[18] Rombola, M.; Rawal, V. H. *Org. Lett*. **2018**, *20*, 514.

described for the first time, and this new series of catalysts is expected to find unique applications in the future.

Chapter 3

Enantioselective Michael Additions of Barbituric Acids to Nitroalkenes Catalyzed by Bifunctional Thiosquaramides

III.1 Introduction

Barbituric acid was first synthesized in 1864 by the German chemist Adolf van Baeyer during his studies on uric acid and its derivatives.[1] As suggested by its name, barbituric acid is unusually acidic (pK_a = 4 in H_2O).[2] It was not until 1903 that the medicinal value of barbituric acid derivates (known as barbiturates) became appreciated, when Fischer and von Mering disclosed the synthesis of 5,5-diethyl barbituric acid (barbital) and reported on its therapeutic properties as a sedative,[3] and within a year the drug had been commercialized.

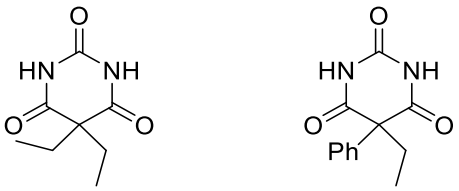

Figure 14. Barbital (left) and phenobarbital (right), two of the first medically applied barbiturates.

A brief history of barbiturates from the clinical perspective is given by López-Muñoz.[4] Shortly after the introduction of barbital by Fisher and von Mering, structural analogs based on the barbituric acid core were synthesized and tested. Phenobarbital was quickly discovered to

[1] Baeyer, A. *Annalen der Chemie* **1863**, *127*, 1.
[2] Krahl, M. E. *J. Phys. Chem.* **1940**, *44*, 449.
[3] Fischer, E.; Mering, J. *Therapie der Gegenwart* **1903**, *44*, 97.
[4] López-Muñoz, F.; Ucha-Udabe, R.; Alamo, C. *Neuropsychiatric Disease and Treatment* **2005**, *1*, 329.

offer certain pharmacological improvements over barbital, such as prolonged action, and thus replaced the original barbiturate in clinical settings. Notably, this drug remains in use to this day, chiefly for the treatment of seizures in small children, although it still finds occasional use as a general sedative.

The successful introduction of barbital into the clinical setting spurred research into chemical modifications of the barbituric acid core, and over 2,500 derivates ended up being synthesized. Of these, roughly 50 were to be used as medicines. Since the 1960s, the use of barbiturates has fallen greatly due to the availability of safer drugs, although several remain in current use. More recently, barbituric acids have been found possess a wide biological profile, including anti-tumor, immune system modulatory, and anti-depressive activity.[5] Shown below are merbarone, an anticancer thiobarbituric acid derivative that functions as a catalytic inhibitor of DNA topoisomerase II,[6] and **108**, a barbituric acid derivative and HIV-1 and HIV-2 protease inhibitor.[7]

[5] (a) Gulliya, K. S. Anti-Cancer Uses for Barbituric Acid Analogs. U.S. Patent 5674870A, Oct 7, 1997. (b) Gulliya, K. S. Uses for Barbituric Acid Analogs. U.S. Patent 5869494A, Feb 9, 1999. (c) Kaur, M.; Verma, P.; Singh, P. *Bioorg. Med. Chem. Lett*. **2009**, *19*, 3054. (d) Dhorajiya, B. D.; Ibrahim, A. S.; Badria, F. A.; Dholakiya, B. Z. *Med. Chem. Res*. **2014**, *23*, 839. (e) Penthala, N. R.; Ketkar, A.; Sekhar, K. R.; Freeman, M. L.; Eoff, R. L.; Balusu, R.; Crooks, P. A. *Bioorg. Med. Chem*. **2015**, *23*, 7226.

[6] Khélifa, T.; Beck, W. T. *Molecular Pharmacology* **1999**, *55*, 548.

[7] Guerin, D.J.; Mazeas, D.; Musale, M.S.; Naguib, F.N.M.; Safarjalani, O.N.A.; Kouni, M.H.; Panzica, R.P. *Bioorg. Med. Chem. Lett*. **1999**, *9*, 1477.

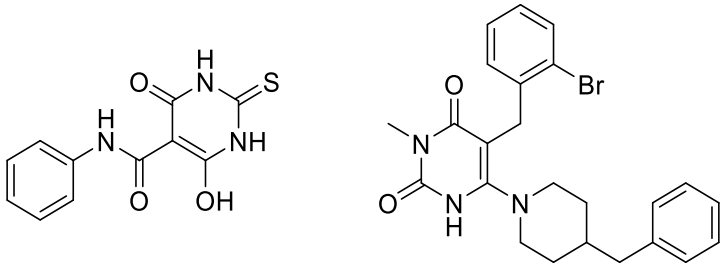

107 **108**

Figure 15. Merbarone (left) and an anti-HIV barbituric acid derivative (right).

III.2 Reaction Background: Asymmetric Catalysis with Barbituric Acid Nucleophiles and Racemic Michael Additions of Barbituric Acids

Despite the diffuse biological properties of barbiturates being well-documented, examples of the syntheses of chiral barbituric acids via asymmetric catalysis remain very few. Prior to our work, only three examples employing barbituric acids as nucleophiles in asymmetric catalyzed processes had been reported, all of which were palladium-catalyzed allylation reactions. The first two examples come from Brunner, who in 1998 employed a new chiral phosphane imine ligand **111** to allylate barbituric acid **109** in 77% yield and 34% ee (Scheme 32).[8] This methodology was later extended to the synthesis of enantioenriched Methohexital, a short-acting anesthetic.[9]

[8] Brunner, H.; Deml, I.; Dirnberger, W.; Nuber, B.; Reißer, W. *Eur. J. Inorg. Chem*. **1998**, *1998*, 43.
[9] Brunner, H.; Deml, I.; Dirnberger, W.; Ittner, K.-P.; Reißer, W.; Zimmermann, M. *Eur. J. Inorg. Chem*. **1999**, *1999*, 51.

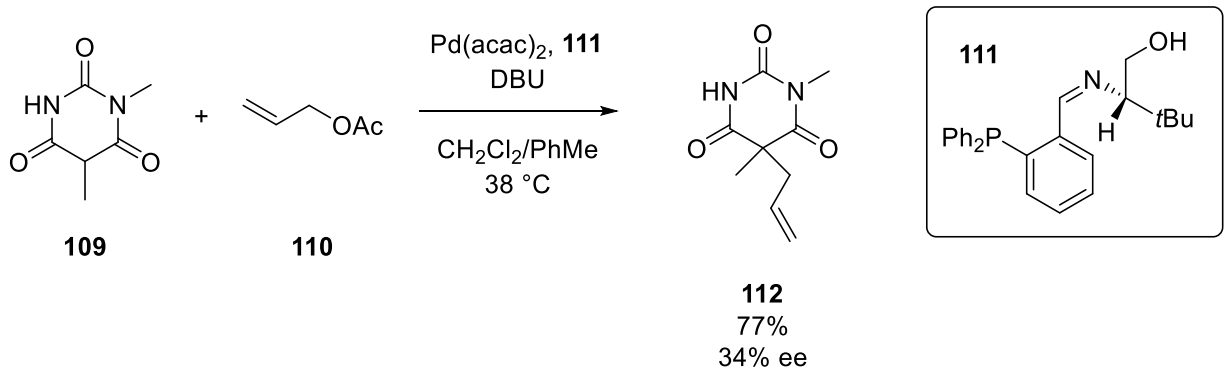

Scheme 32. Enantioselective allylation of a barbituric acid.

The third and final example is from Trost, who used chiral bisphosphine ligand **115** to synthesize two medically relevant barbiturates, cyclopentylbarbital and pentylbarbital, in enantioenriched form.[10]

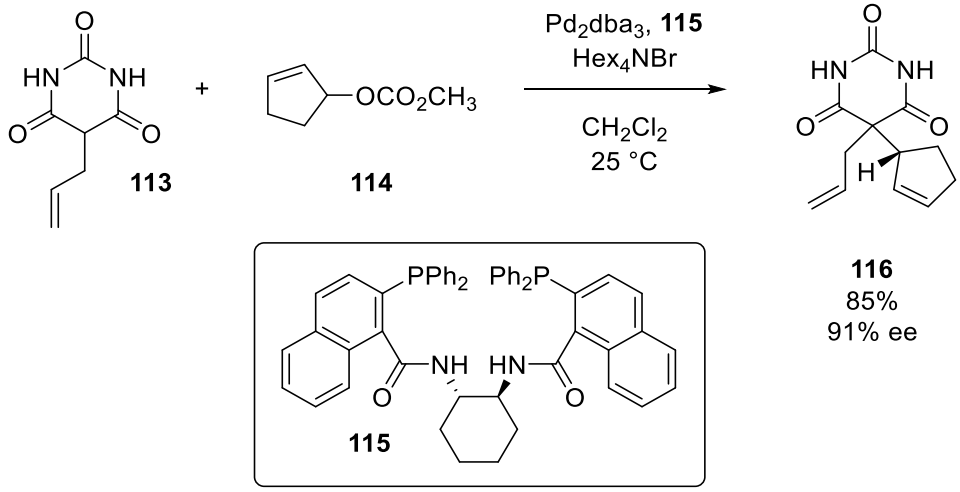

Scheme 33. Enantioselective synthesis of cyclopentylbarbital.

[10] Trost, B. M.; Schroeder, G. M. *J. Org. Chem.* **2000**, *65*, 1569.

Although no enantioselective Michael additions of barbituric acid nucleophiles have been reported prior to our work, many racemic reactions have been reported. Several recent examples are shown below.

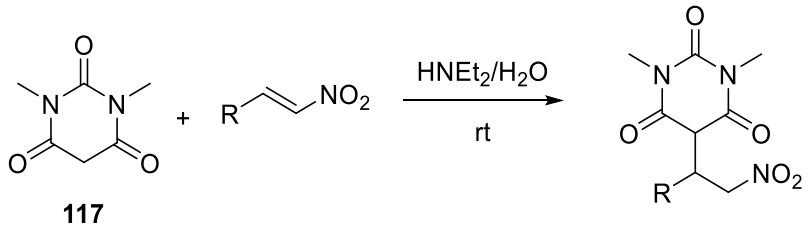

Scheme 34. MA of 1,3-dimethylbarbituric acid to nitroalkenes.[11]

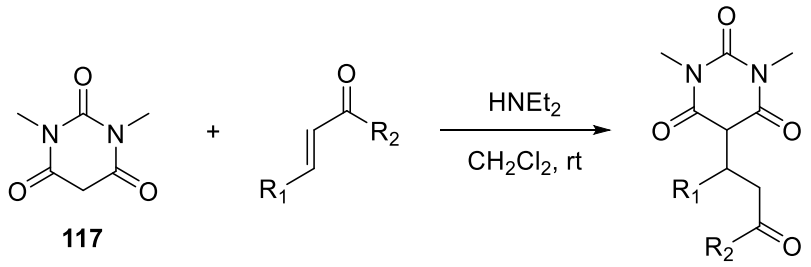

Scheme 35. MA of 1,3-dimethylbarbituric acid to chalcones.[12]

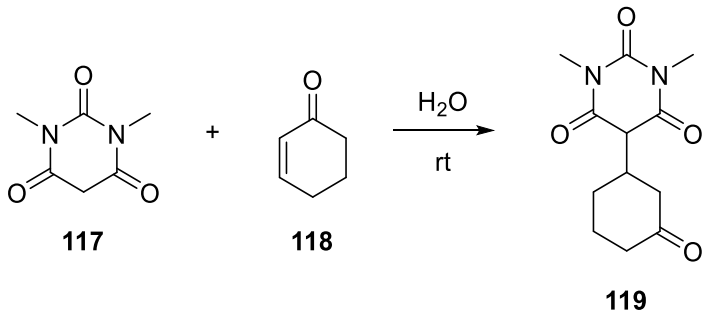

Scheme 36. MA of 1,3-dimethylbarbituric acid to cyclohexenone.[13]

[11] Al-Najjar, H. J.; Barakat, A.; Al-Majid, A. M.; Mabkhot, Y. N.; Weber, M.; Ghabbour. H. A.; Fun, H. *Molecules* **2014**, *19*, 1150.
[12] Barakat, A.; Islam, M. S.; Al-Majid, A. M.; Soliman, S. M.; Mabkhot, Y. N.; Al-Othman, Z. A.; Ghabbour, H. A.; Fun, H. *Tetrahedron Lett.* **2015**, *56*, 6984.

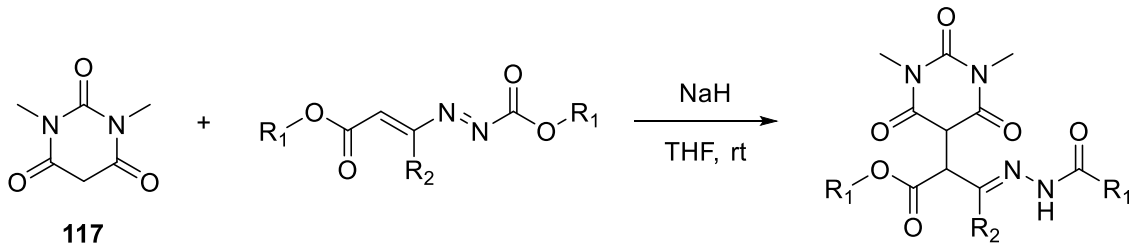

Scheme 37. MA of 1,3-dimethylbarbituric acid to diazadienes.[14]

III.3 Reaction Optimization of Enantioselective Michael Additions of Barbituric Acids to Nitroalkenes

Using methodology described in Chapter II.3, a series of bifunctional thiosquaramides was synthesized. Working with Dr. Chintan Sumaria, several commonly used bifunctional squaramide and thiourea catalysts (**95**, **122,** and **123**) were also prepared. Using the MA of *N*,*N'*-diphenylbarbituric acid to β-nitrostyrene as a model reaction, the catalysts were evaluated for enantioinduction. The addition products thus obtained are chiral barbiturate-containing oxidized phenethylamines; phenethylamines are themselves known for their bioactivity.[15] The results are given in Scheme 38.

[13] Callant, P.; Waumans, B. Infrared Dyes for Laser Marking. U.S. Patent 2015261080, Sep 17, 2015.
[14] Crescentini, L.; Attanasi, O. A.; Campisi, L. A.; Favi, G.; Lillini, S.; Ursini, F.; Mantellini, F. *Tetrahedron* **2015**, *71*, 7282.
[15] Shulgin, A.; Shulgin, A. *PiHKAL: A Chemical Love Story*, Transform Press, 1991.

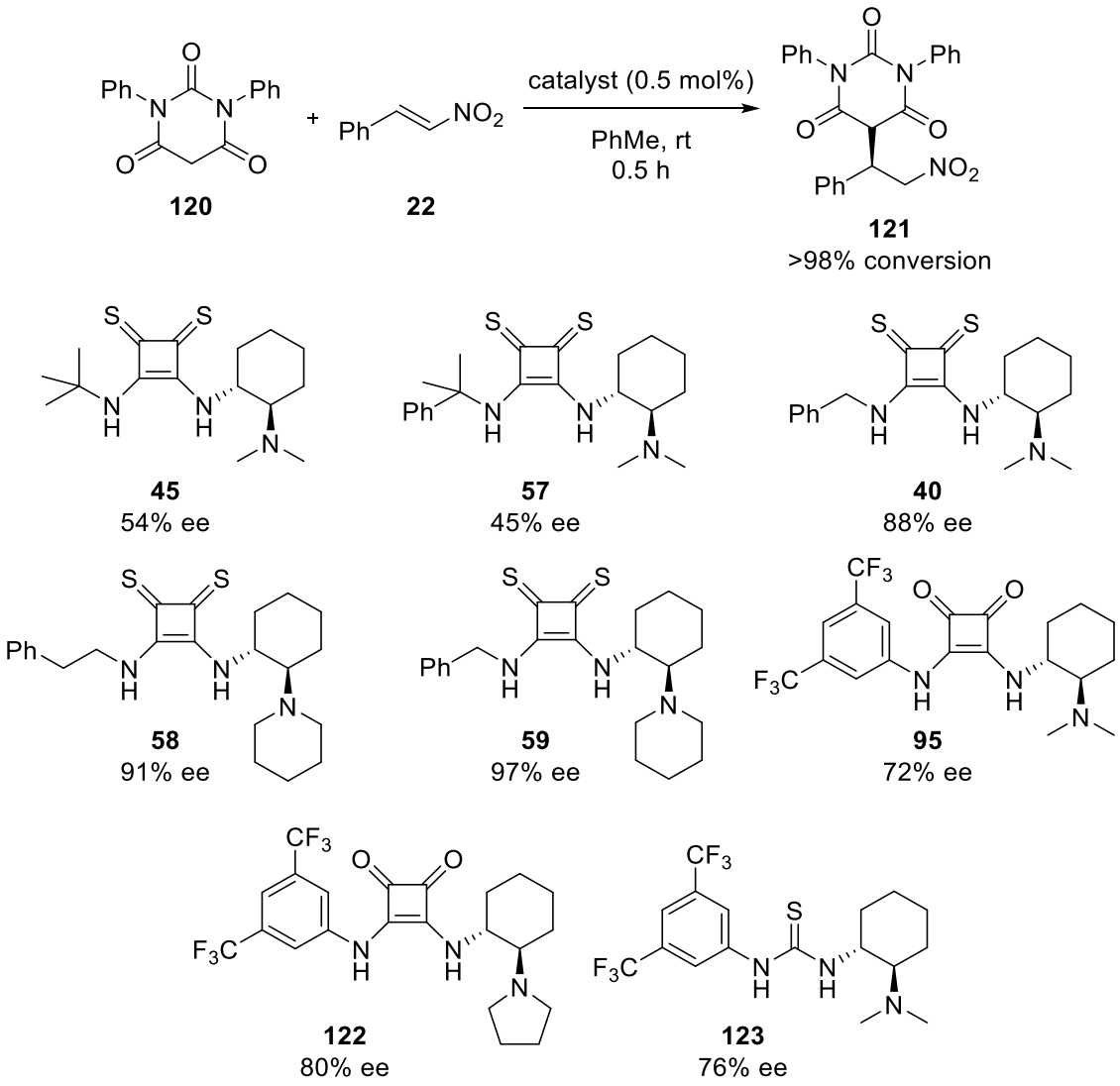

Scheme 38. Catalyst screen for the MA of *N,N*'-diphenylbarbituric acid to β-nitrostyrene.

At 0.5 mol% catalyst loading, all reactions were finished with essentially full conversion in half an hour. Reduction of steric bulk on the left half of the thiosquaramide catalyst produced drastically improved enantioselectivities. Replacement of the dimethylamino bifunctionality with a piperidine ring also afforded substantial improvement in enantioselectivity (**40** and **59**). Consequently, the best catalyst contained a benzylamine left half and a piperidine right half. These two "halves" had not been previously used in a squaramide or thiourea catalyst. The

analogous squaramide and thiourea catalysts were thus prepared in order to make a single variable comparison of the H-bond donor scaffolds.

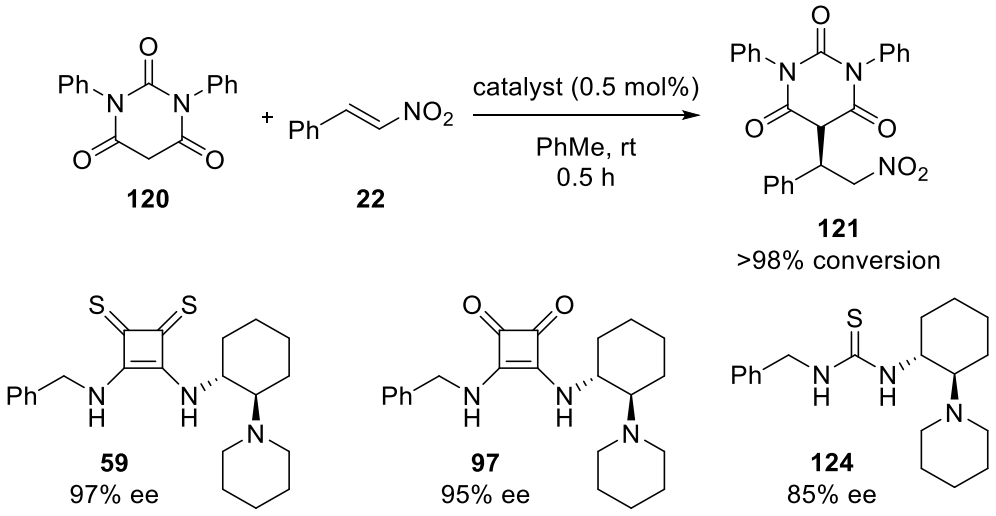

Scheme 39. Single variable comparison of H-bond donor scaffolds.

The thiosquaramide core was found to provide the greatest degree of enantioselectivity (Scheme 39). The seemingly small difference in enantioselectivities between thiosquaramide and squaramide (97% ee vs 95% ee) corresponds to selectivity ratios of 70:1 and 40:1, respectively. Both the thiosquaramide and squaramide catalysts provided substantial improvement in enantioselectivity over thiourea catalyst **124**.

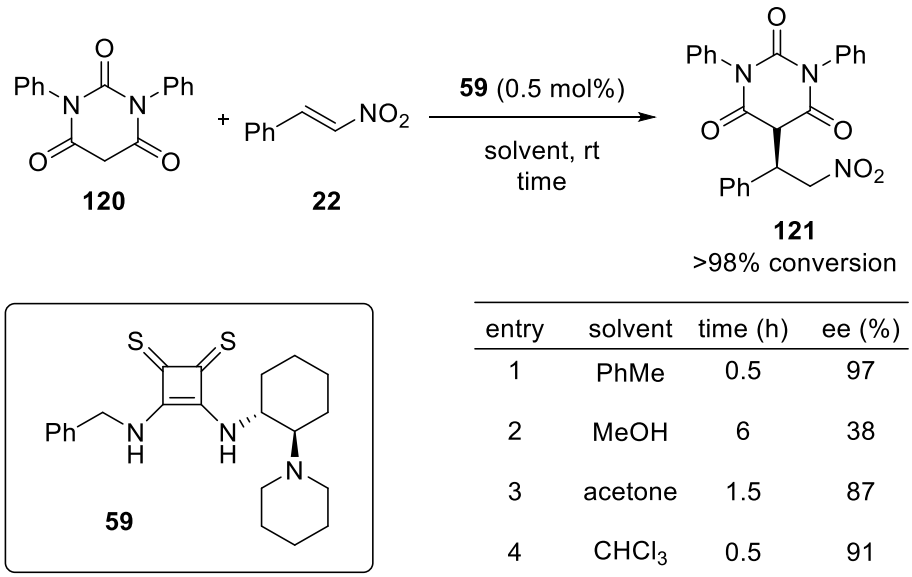

entry	solvent	time (h)	ee (%)
1	PhMe	0.5	97
2	MeOH	6	38
3	acetone	1.5	87
4	$CHCl_3$	0.5	91
5	EtOAc	0.5	92
6	CH_2Cl_2	0.5	94

Table 5. Solvent screen for the MA of *N*,*N*'-diphenylbarbituric acid to β-nitrostyrene.

Dr. Chintan Sumaria carried out an extensive solvent screen for the reaction, and an abridged but illustrative set of entries from his studies are shown above. Toluene was found to be the best solvent with respect to enantioselectivity. Enantioselectivies for H-bond promoted reactions tend to be worse in H-bond donor/acceptor solvents such as methanol or acetone, which is consistent with entries 2 and 3. Ethyl acetate was a surprisingly effective solvent considering its ability to form hydrogen bonds to the thiosquaramide catalyst and thus interrupt substrate-catalyst interactions. Nonpolar solvents were nonetheless generally better, and toluene was best among those.

III.4 Reaction Scope

The scope of the asymmetric MA was then examined to probe the generality of the reaction (Scheme 40).

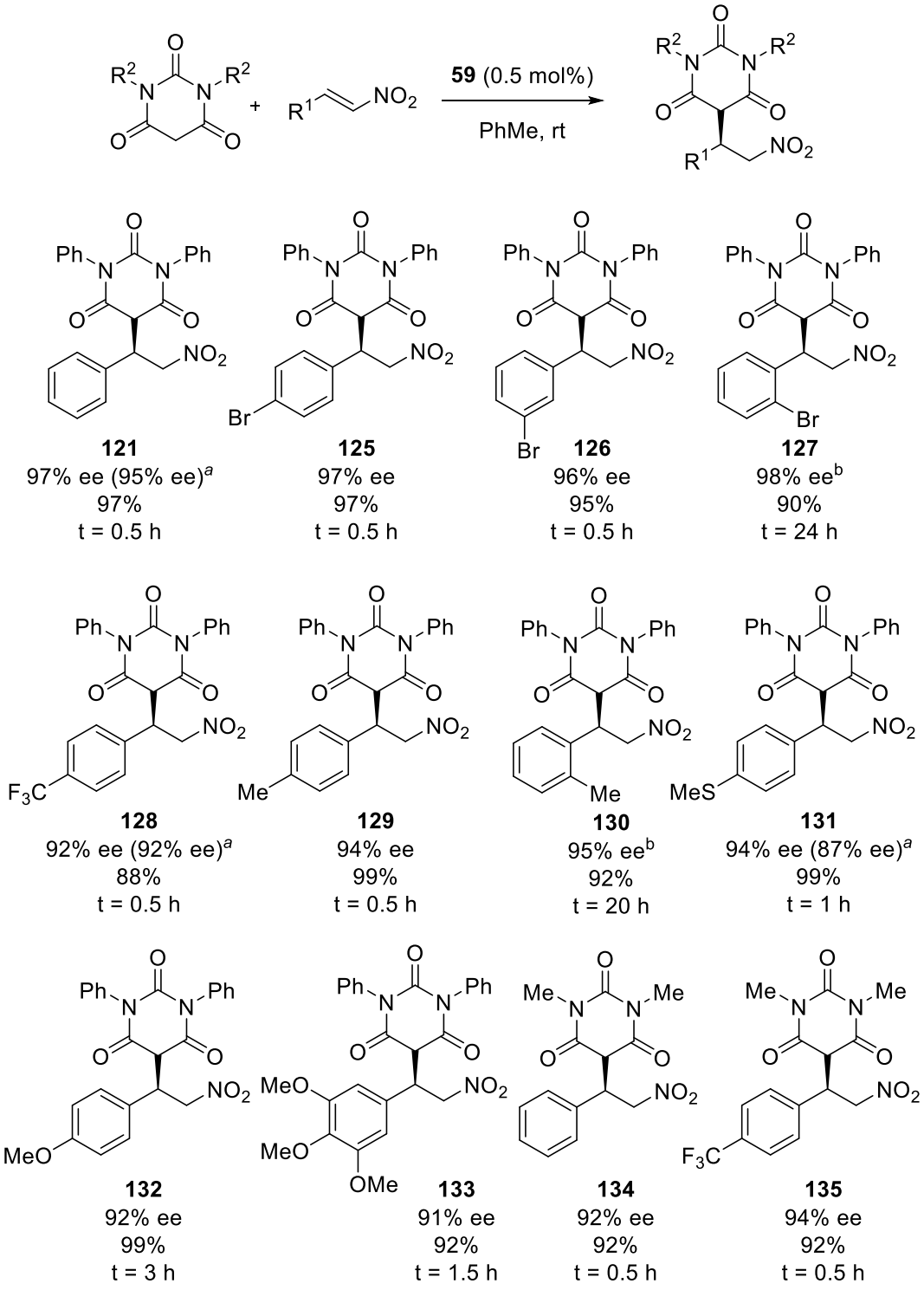

Scheme 40. Conjugate addition of barbituric acids to nitroolefins.

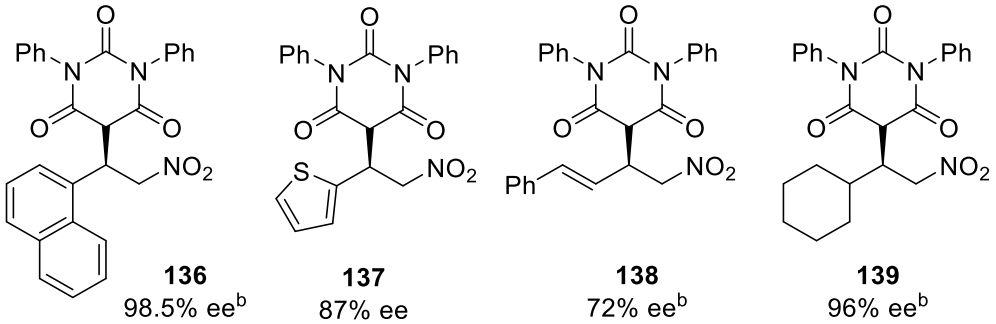

Scheme 40. (continued) Conjugate addition of barbituric acids to nitroolefins. [a] Catalyst **97** used instead of **59**. [b] 5 mol% catalyst **59** used.

The reaction proceeded well regarding both yield and enantioselectivity for a variety of nitrostyrenes. Unhindered electron-rich and electron-poor nitrostyrene substrates both gave high yield and enantioselectivities at 0.5 mol% catalyst loading. Ortho-substitutions slowed down the reaction significantly, which required higher (5 mol%) catalyst loadings and longer reaction times. The enantioselectivities for these substrates were nonetheless excellent.

The main determinant of enantioselectivity appeared to be steric bulk around the newly formed C-C bond. As such, thiophenyl and alkenyl substituted nitroalkenes gave the two lowest enantioselectivities, while the bulky cyclohexyl substituted nitroalkene gave very good enantioselectivity. *N*,*N'*-dimethylbarbituric acid was a suitable reaction partner, although enantioselectivity was marginally worse.

For comparison purposes, the corresponding squaramide of thiosquaramide **59** was used for two additional examples. Interestingly, thiosquaramide **59** performed better than the squaramide for an electron-rich nitrostyrene to give **131** but performed the same as the squaramide for an electron-poor nitrostyrene to give **128**.

The MA products streaked on chiral HPLC columns due to the presence of the highly acidic C-5 proton which made accurate measurements of enantioselectivities difficult. Addition

of acetic acid to the mobile phase was unsuccessful in preventing this streaking. The acidic C-5 position was thus blocked by bromination or chlorination prior to chiral HPLC (Scheme 41). One of these chlorination products ultimately crystallized, thereby establishing the absolute stereochemical configuration of the addition product via X-ray crystallography (Figure 16).

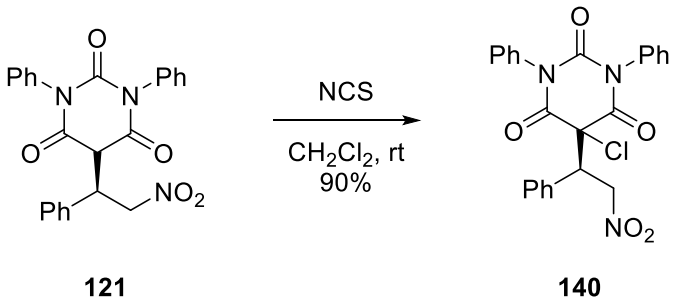

121 **140**

Scheme 41. Chlorination of MA adduct **121**.

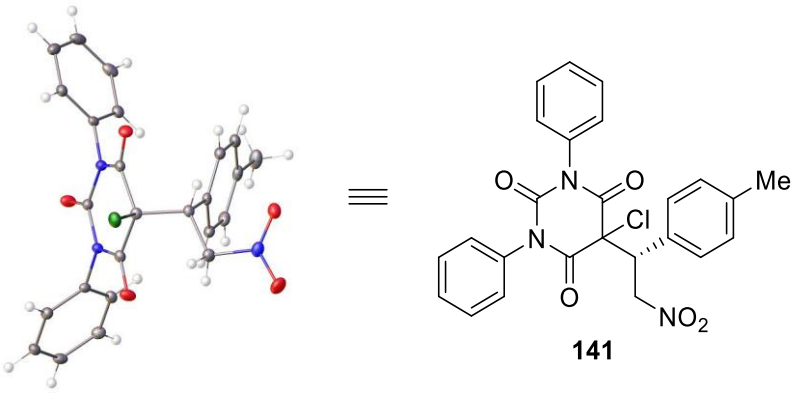

141

Figure 16. X-ray structure of a chlorinated barbiturate.

Dr. Chintan Sumaria carried out experiments to determine the lowest possible catalyst loading (Table 6). It was found that catalyst loadings could be reduced to a mere 0.05 mol% without appreciable loss in enantioselectivity or yield. At a catalyst loading of 0.02 mol%, loss in enantioselectivity was observed. It should be noted that these reactions were carried out with reagent grade solvents under an ambient atmosphere.

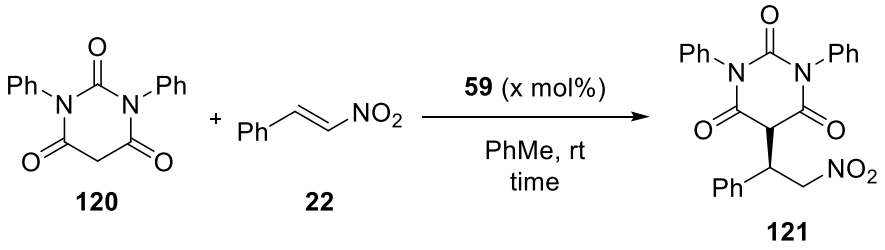

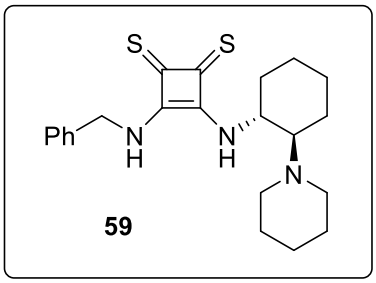

entry	mol%	time (h)	conv (%)	ee (%)
1	0.5	0.5	>98	97
2	0.1	2	>98	97
3	0.05	10	>98	96
4	0.02	10	83	72

Table 6. Catalyst loading experiments for the barbituric acid MA.

The reaction scaled up almost perfectly (Scheme 42). With just 8.0 mg of catalyst, 1.65 g of highly enantioenriched barbiturate could be produced in half an hour with no appreciable loss in yield or enantioselectivity compared with a small-scale reaction.

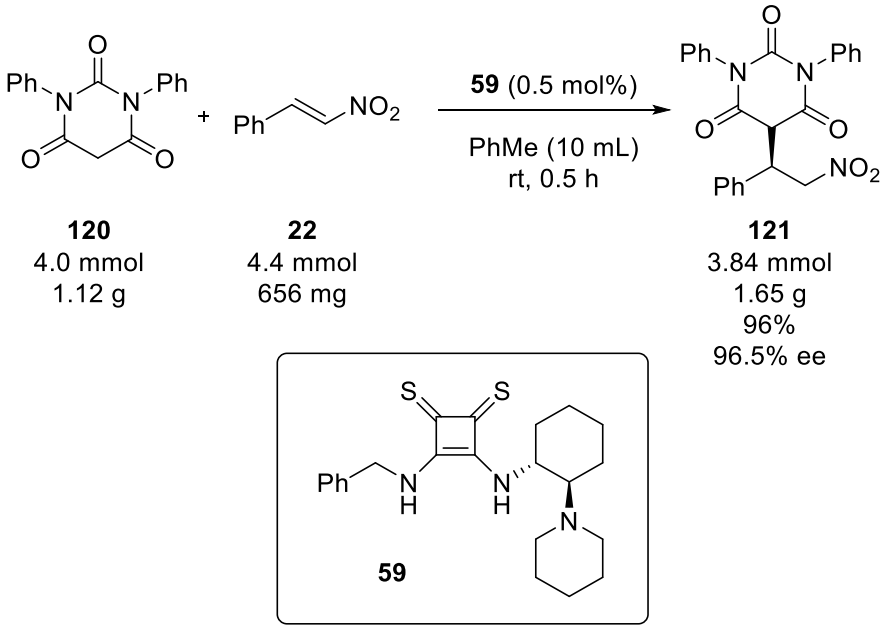

Scheme 42. Gram scale synthesis of a chiral barbiturate.

III.5 Recent Examples of Enantioselective Michael Additions with Barbituric Acids

Within several months of the disclosure of our thiosquaramide catalyzed reaction, two new organocatalytic methodologies for the synthesis of chiral barbiturates were published, both based on bifunctional squaramide catalysis. In a report by Wang, a variety of bifunctional hydrogen bond donor catalysts were screened for enantioselectivites in the Michael addition of *N,N*'-dialkyl barbituric acids with chalcone.[16] Bifunctional squaramide catalyst **144** derived from the Cinchona alkaloid quinine was found to give high yields and ee's (Scheme 43).

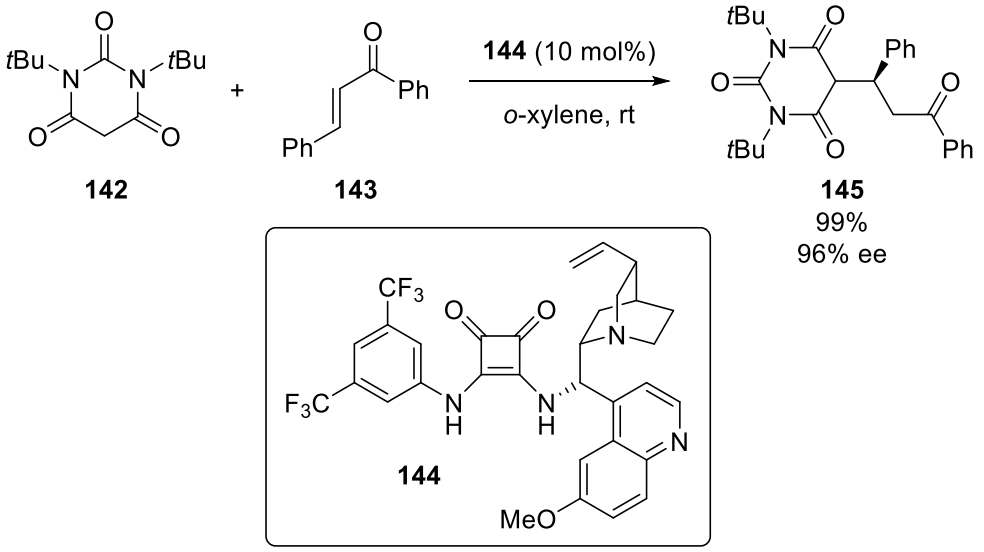

Scheme 43. Enantioselective barbituric acid addition to chalcone.

At the same time, Palomo reported the use of 2-alkylthio-4,6-dioxopyrimidines as barbituric acid equivalents.[17] Under bifunctional squaramide catalysis, these prochiral barbituric acid precursors add to β-unsubstituted enones or allylic bromides in highly enantioselective fashion, producing a chiral carbon at the barbituric acid C-5 position after deprotection.

[16] Liu, Y.; Zhang, Y.; Duan, H.; Wanyan, D.; Wang, Y. *Org. Biomol. Chem.* **2017**, *15*, 8669.
[17] Pozo, S.; Vera, S.; Oiarbide, M.; Palomo, C. *J. Am. Chem. Soc.* **2017**, *139*, 15308.

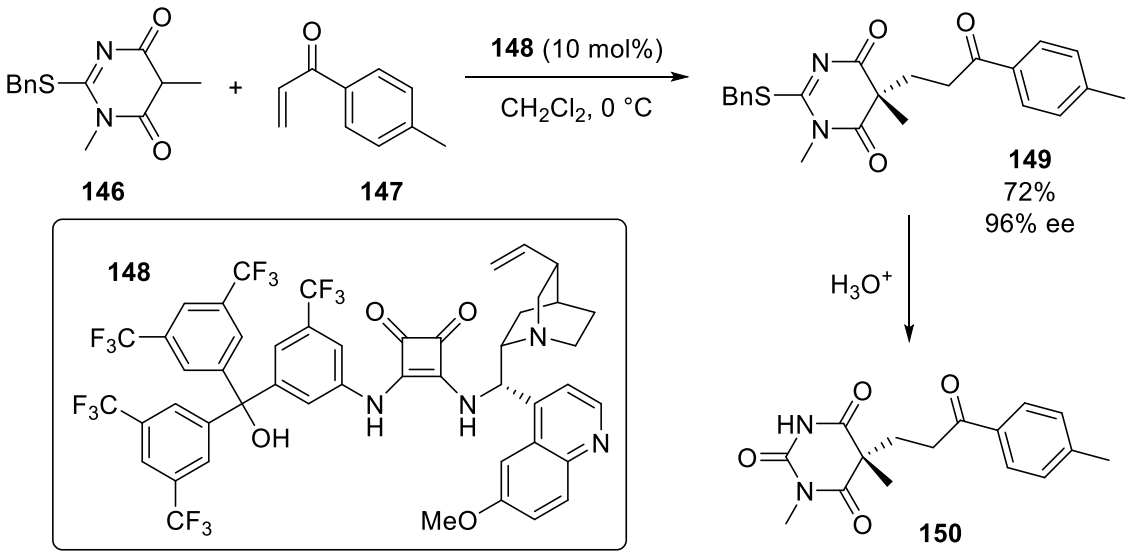

Scheme 44. Enantioselective addition of a prochiral barbituric acid equivalent to an enone.

III.6 Conclusion

In summary, the first enantioselective Michael addition of the barbituric acid pharmacophore to nitroalkenes has been described.[18] High yields and enantioselectivities were obtained using bifunctional thiosquaramides as catalysts, even at catalyst loadings as low as 0.05 mol%. The thiosquaramide scaffold was found to deliver superior enantioselectivities when compared with the corresponding squaramide or thiourea. This asymmetric conjugate addition reaction is also the first reported example of thiosquaramide catalysis.

[18] Rombola, M.; Sumaria, C. S.; Montgomery, T. D.; Rawal, V. H. *J. Am. Chem. Soc*. **2017**, *139*, 5297.

Chapter 4

Bispyridinium Catalyzed Nitro-Diels-Alder Reactions

IV.1 Introduction

In 1928, Otto Diels and Kurt Alder reported on the reaction of cyclopentadiene with quinone (Scheme 45).[1]

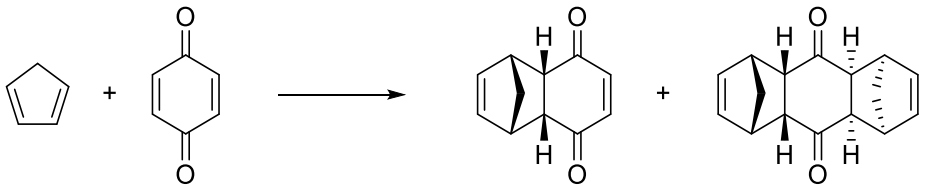

Scheme 45. First reported [4+2] cycloaddition reaction.

Belonging to a broader class of reactions now known as the [4+2] cycloaddition, this type of transformation would emerge as one of the most powerful and synthetically important reactions in all of organic synthesis.[2d]

Since the seminal report by Diels and Alder, the reaction which now bears their name has been studied intensively for decades up to the present time.[2] A general discussion of the Diels-Alder reaction is far beyond the scope of this introduction. However, the general form of the

[1] Diels, O.; Alder, K. *Justus Liebigs Ann. Chem*. **1928**, *460*, 98.
[2] For reviews on the Diels-Alder reaction, see: (a) Kagan, H. B.; Riant, O. *Chem. Rev.* **1992**, *92*, 1007. (b) Jørgensen, K. A. *Angew. Chem. Int. Ed*. **2000**, *39*, 3558. (c) Nicolaou, K. C.; Snyder, S. A.; Montagnon, T.; Vassilikogiannakis, G. *Angew. Chem. Int. Ed*. **2002**, *41*, 1668. (d) Corey, E. J. *Angew. Chem. Int. Ed*. **2002**, *41*, 1650. (e) Williams, R. M.; Stocking, E. M. *Angew. Chem. Int. Ed*. **2003**, *42*, 3078. (f) Yamamoto, Y.; Yamamoto, H. *Eur. J. Org. Chem.* **2006**, 2031. (g) Jiang, X.; Wang, R. *Chem. Rev.* **2013**, *113*, 5515. (h) Heravi, M. M.; Vavsari, V. F. *RSC Adv*. **2015**, *5*, 50890.

Diels-Alder reaction (shown in Scheme 46) serves as a useful starting point for introducing the content of this chapter.

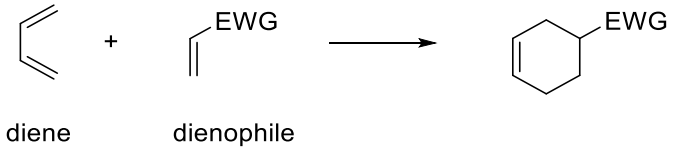

Scheme 46. General form of the Diels-Alder reaction.

In its most general form, the normal demand Diels-Alder reaction is a pericyclic cycloaddition reaction between a diene and dienophile. In practice, the dienophile is commonly equipped with an electron-withdrawing group (abbreviated EWG) which has the effect of accelerating the reaction via lowering of the LUMO (lowest unoccupied molecular orbital) energy.[3] When this EWG is a nitro group, its reaction with a diene may be referred to as a nitro-Diels-Alder reaction. Thermal Diels-Alder reactions of nitroalkenes have been known for almost as long as the original report by Diels and Alder. Two of the earliest examples comes from Alder[4] and researchers at Eastman Kodak Company[5] who reported on the reactivity of dienes with aliphatic nitroalkenes and β-nitrostyrene, respectively.

The most common mode of catalysis for Diels-Alder reactions utilizes a LUMO lowering strategy, whereby coordination of a Lewis acid or Brønsted acid to the dienophile EWG lowers the energy of the LUMO and thus accelerates the reaction.[3] Application of this strategy to activating nitroolefins has proven to be exceptionally difficult, and a primary reason for that is

[3] Carey, F. A.; Sundberg, R. J. *Advanced Organic Chemistry: Part A: Structure and Mechanisms*, 5th ed., Springer, New York, NY, 2007.
[4] Alder, K.; Rickert, H. F.; Windemuth, E. *Chem. Ber.* **1938**, *71*, 2451.
[5] Allen, C. F. H.; Bell, A. *J. Am. Chem. Soc.* **1939**, *61*, 521.

presented in Scheme 47.[6] Under thermal conditions, the diene and nitroalkene react as the 4π component and 2π component, respectively. But under Lewis acid conditions, a hetero-DA pathway is often preferred, with the nitroalkene acting as the 4π component and the diene as the 2π component in an inverse electron demand Diels-Alder reaction to yield a cyclic nitronic ester. This hetero-DA reactivity has been studied extensively by Denmark.[7]

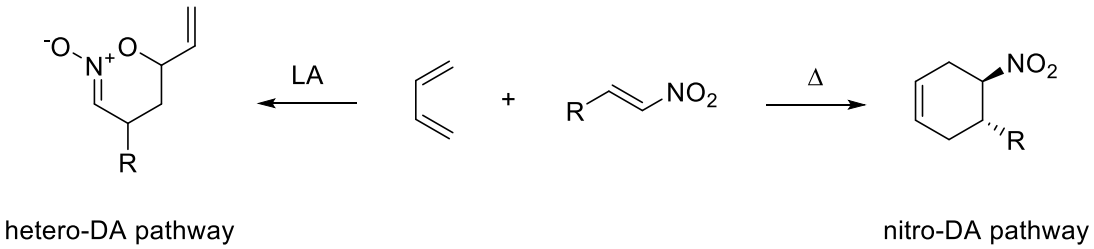

Scheme 47. Divergent reactivities of a diene and nitroalkene under Lewis acid or thermal conditions.

Consequently, a relatively large proportion of catalyzed nitro-DA reactions have been based on increasing the reactivity of the diene by raising the HOMO (highest occupied molecular orbital) energy. Successful strategies for the catalysis of nitro-Diels-Alder reactions are given below.

[6] Denmark, S. E.; Kesler, B. S.; Moon, Y. *J. Org. Chem.* **1992**, *57*, 4912.
[7] (a) Denmark, S. E.; Stolle, A.; Dixon, J. A.; Guagnano, V. *J. Am. Chem. Soc.* **1995**, *117*, 2100. (b) Denmark, S. E.; Schnule, M. E. *J. Org. Chem*. **1994**, *59*, 4576. (C) Denmark, S. E.; Baiazitov, R. Y.; Nguyen, S. T. *Tetrahedron* **2009**, *65*, 6535. (d) Denmark, S. E.; Nguyen, S. T.; Baiazitov, R. Y. *Heterocycles* **2008**, *76*, 143. (e) Denmark, S. E.; Baiazitov, R. Y. *Org. Lett.* **2005**, *7*, 5617. (f) Denmark, S. E.; Gomez, L. *J. Org. Chem.* **2003**, *68*, 8015. (g) Denmark, S. E.; Seierstad, M. *J. Org. Chem.* **1999**, *64*, 1610. (h) Denmark, S. E.; Parker, D. L.; Dixon, J. A. *J. Org. Chem.* **1997**, *62*, 435.

IV.2 Reaction Background: Catalysis of Nitro-Diels-Alder Reactions

IV.2.1 LUMO-Lowering Strategies

Despite being considered generally inert, silica gel is mildly acidic ($pK_a \approx 10$)[8] due to the permeation of silanol moieties on its surface. Consequently, the material has found to be catalytically active for a variety of transformations.[9] In 1991, Knochel used silica gel in hexanes to catalyze an intramolecular nitro-DA reaction after finding that the thermal cycloaddition was non-stereospecific.[10]

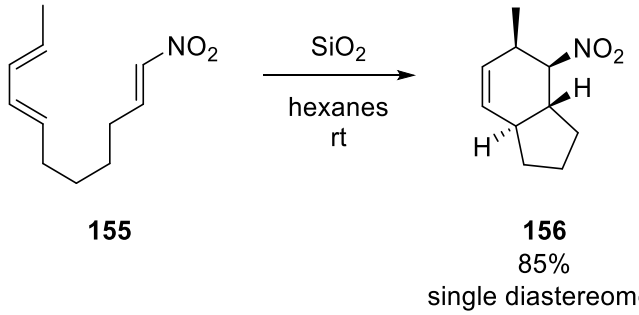

155 **156** 85% single diastereomer

Scheme 48. SiO_2 catalyzed intramolecular nitro-DA reaction.

At the same time, Rawal and coworkers found that concentrated solutions of lithium perchlorate[11] were potent catalysts for the nitro-DA reaction of isoprene and β-nitrostyrene.[12] They noted that use of these highly polar conditions resulted in a marked improvement in regioselectivity (3:1 to >25:1) and allowed for the reduction of reaction temperature by about 70 °C.

[8] Greenberg, S. A. *J. Am. Chem. Soc*. **1958**, *80*, 6508.
[9] For a review on silica gel catalysis, see: Basu, B.; Paul, S. *Journal of Catalysts* **2013**, *2013*, 1.
[10] Retherford, C.; Knochel, P. *Tetrahedron Lett.* **1991**, *32*, 441.
[11] Grieco, P. A.; Nunes, J. J.; Gaul, M. D. *J. Am. Chem. Soc*. **1990**, *112*, 4595.
[12] Rawal, V. H.; Michoud, C. *Tetrahedron Lett.* **1991**, *32*, 1695.

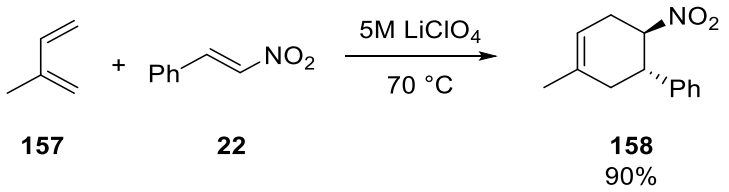

Scheme 49. $LiClO_4$ catalyzed nitro-DA reaction.

During studies towards the synthesis of norzoanthamine, Williams examined multiple Lewis acids to affect an intramolecular nitro-DA reaction (Scheme 50).[13] His results typify the difficulties encountered when using Lewis acids to promote the desired cycloaddition. Although diethylaluminum chloride improved the *endo* selectivity of the reaction, yield was poor (38% vs. 80% under thermal conditions). Several other Lewis acids were tried, all giving less than 10% yield due to substantial byproduct formation.

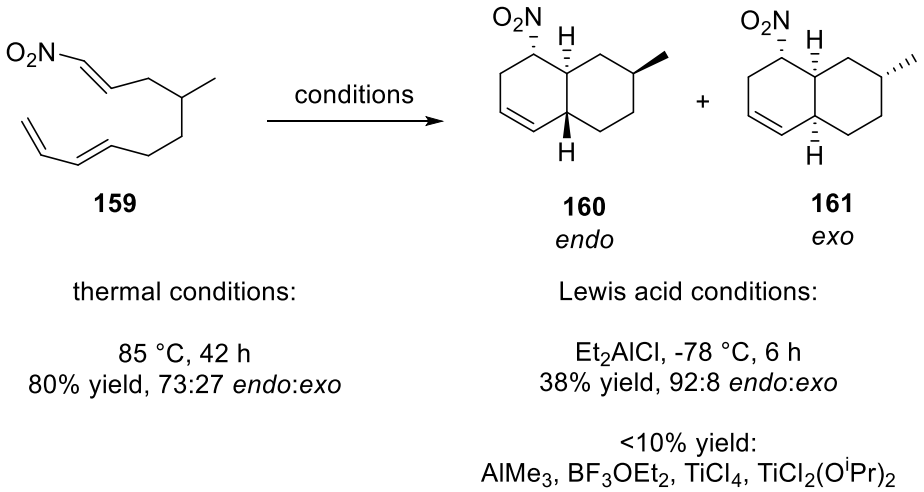

Scheme 50. Lewis acid screen for a nitro-DA reaction.

In 2007, Takenaka and coworkers reported on the use of 2-aminopyridiniums as hydrogen bond donor catalysts for the Diels-Alder reaction between cyclopentadiene and various

[13] Williams, D. R.; Brugel, T. A. *Org. Lett.* **2000**, *2*, 1023.

nitrostyrenes.[14] Five years later, they disclosed an asymmetric variation employing chiral helical amidinium **164** in the reaction of hexasubstituted cyclopentadienes with nitroethylene (Scheme 51).[15]

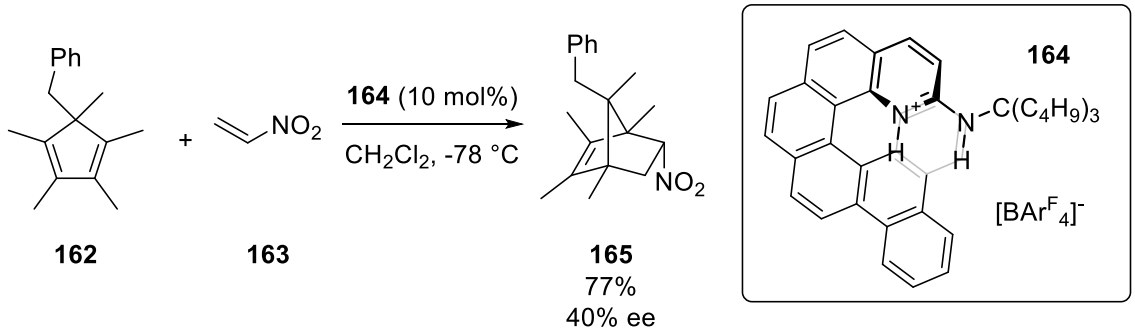

Scheme 51. Amidinium catalyzed nitro-DA reaction.

Several examples of a formal [4+2] cycloaddition between 2-vinyl indoles and nitroalkenes have been reported by Xiao. These reactions are in essence a tandem Friedel-Crafts/Michael addition and thus occupy a special subset of nitro-DA reactions. In his first report, Xiao found that chiral Brønsted acid **167** can catalyze the transformation with a variety of aromatic nitroalkenes (Scheme 52).[16]

[14] Takenaka, N.; Sarangthem, R. S.; Seerla, S. K. *Org. Lett.* **2007**, *9*, 2819.
[15] Narcis, M. J.; Sprague, D. J.; Captain, B.; Takenaka, N. *Org. Biomol. Chem.* **2012**, *10*, 9134.
[16] Wang, X.; Chen, J.; Cao, Y.; Cheng, H.; Xiao, W. *Org. Lett.* **2010**, *12*, 1140.

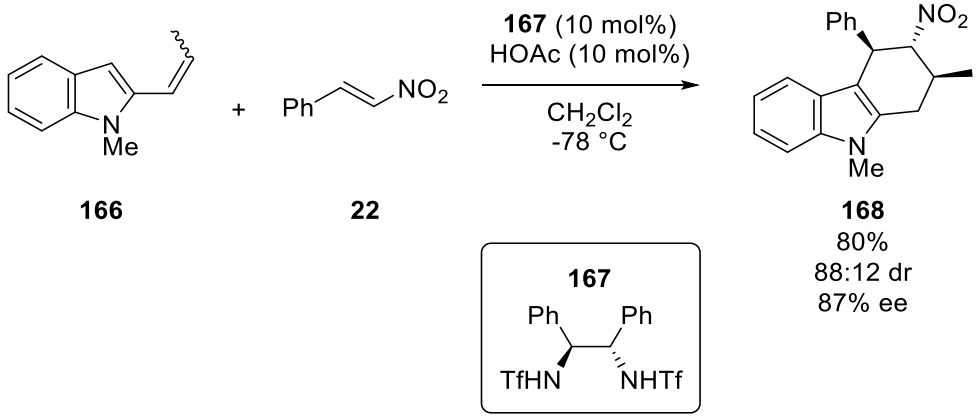

Scheme 52. Brønsted acid catalyzed nitro-DA reaction.

The same group later reported a similar reaction with 3-nitro-2*H*-chromenes catalyzed by a chiral zinc complex (Scheme 53).[17] This example is interesting because the Lewis acidic zinc complex is catalyzing the desired nitro-DA pathway rather than the often problematic hetero-DA pathway. It should be noted that all nitroalkene substrates contained the cyclic ether core, although no mention was made if this was necessary for reactivity.

[17] (a) Tan, F.; Li, F.; Zhang, X.; Wang, X.; Cheng, H.; Chen, J.; Xiao, W. *Tetrahedron* **2011**, *67*, 446. (b) Tan, F.; Xiao, C.; Cheng, H.; Wu, W.; Ding, K.; Xiao, W. *Chem. Asian J.* **2012**, *7*, 493.

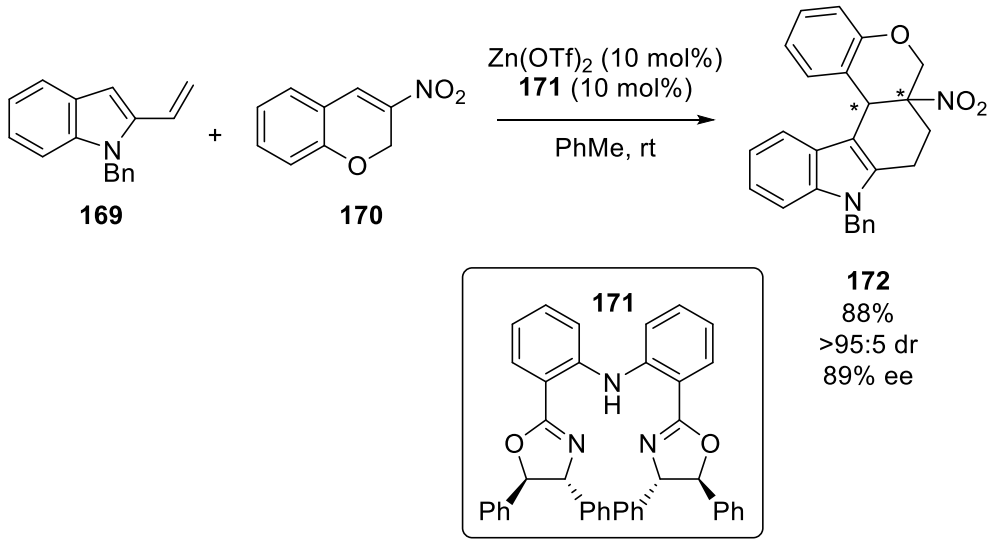

Scheme 53. Zinc catalyzed nitro-DA reaction.

In 2013, Oro used an iridinium complex of the type shown in Scheme 54 to react cyclopentadiene with a variety of nitrostyrenes.[18] As in the above example, this iridium catalyzed process is a rare example of metal catalysis providing the desired nitro-DA product over the hetero-DA product. Rate enhancements appear to be very modest, as the background reaction also occurs at room temperature (although only slowly).

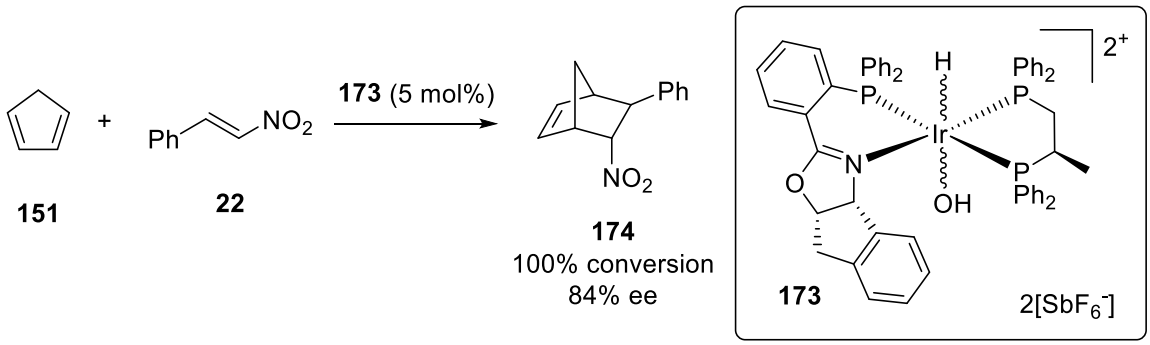

Scheme 54. Iridinium catalyzed nitro-DA reaction.

[18] Carmona, D.; Ferrer, J.; García, N.; Ramírez, P.; Lahoz, F. J.; García-Orduña, P.; Oro, L. A. *Organometallics* **2013**, *32*, 1609.

IV.2.2 HOMO-Raising Strategies

Application of enamine catalysis to the nitro-DA reaction was first reported by Barbas[19] and later improved upon by Melchiorre (Scheme 55).[20,21] In these bodies of work, a β-substituted vinyl ketone is reacted with a nitrostyrene in the presence of a chiral primary or secondary amine. While Melchiorre's catalytic systems enabled high enantioselectivities (almost all examples are over 90% ee) they require high catalyst loadings (20 - 30 mol%) and long reaction times (24 - 48 h).

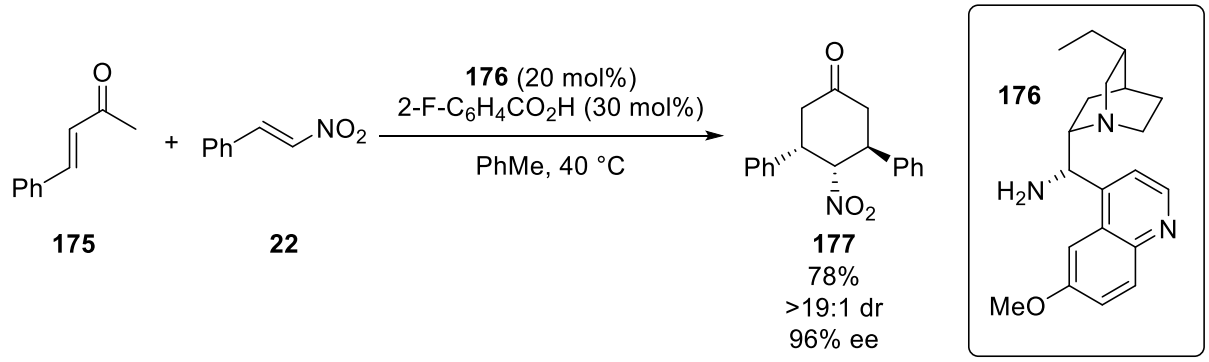

Scheme 55. Primary amine catalyzed nitro-DA reaction.

Trienamine catalysis has also been reported.[22] An example from Chen is shown below.

[19] Thayumanavan, R.; Dhevalapally, B.; Sakthivel, K.; Tanaka, F.; Barbas, C. F. *Tetrahedron Lett.* **2002**, *43*, 3817.
[20] Wu, L.; Bencivenni, G.; Mancinelli, M.; Mazzanti, A.; Bartoli, G.; Melchiorre, P. *Angew. Chem. Int. Ed.* **2009**, *48*, 7196.
[21] For other examples of enone activation for the nitro-DA reaction: (a) Yang, D.; Wang, L.; Han, F.; Zhao, D.; Zhang, B.; Wang, R. *Angew. Chem. Int. Ed.* **2013**, *52*, 6739. (b) Vamisetti, G. B.; Chowdhury, R.; Kumar, M.; Ghosh, S. K. *Org. Lett.* **2016**, *18*, 1964. (c) Möhlmann, L.; Chang, G.; Reddy, G. M.; Lee, C.; Lin, W. *Org. Lett.* **2016**, *18*, 688.
[22] (a) Jia, Z.; Zhou, Q.; Zhou, Q.; Chen, P.; Chen, Y. *Angew. Chem. Int. Ed.* **2011**, *50*, 8638. (b) Liu, Y.; Nappi, M.; Arceo, E.; Vera, S.; Melchiorre, P. *J. Am. Chem. Soc.* **2011**, *133*, 15212.

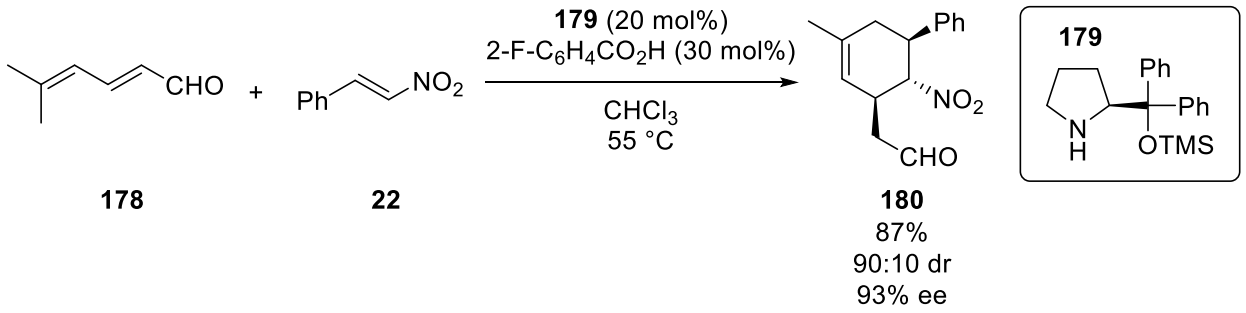

Scheme 56. Secondary amine catalyzed nitro-DA reaction.

In 2011, Deng and coworkers found that Cinchona alkaloid derivative **183** is capable of activating 3-hydroxy-2-pyrones for a highly enantioselective nitro-DA reaction with aliphatic nitroalkenes (Scheme 57).[23]

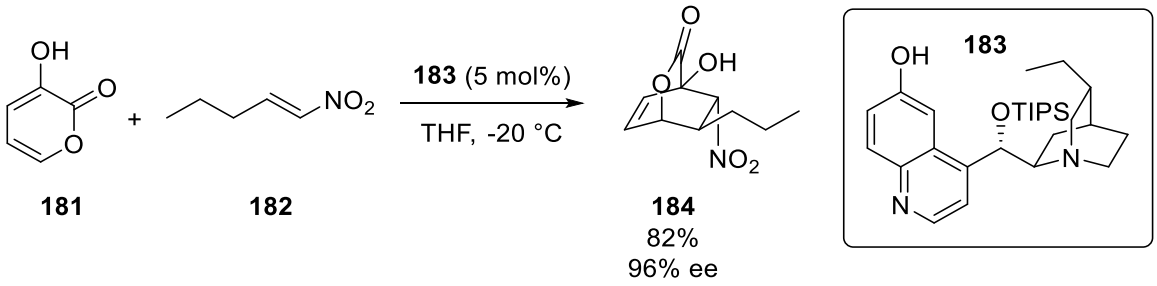

Scheme 57. Base catalyzed nitro-DA reaction.

The above examples represent the state-of-the-art in nitro-DA catalysis. The first couple of examples which utilize SiO_2 and $LiClO_4$ have no prospect for finding an asymmetric variation. The iridinium and aminopyridinium catalysts have only been demonstrated with highly reactive cyclopentadienes. The examples employing enamine catalysis are also highly limited in substrate scope, requiring aryl or alkenyl substitutions on both diene and dienophile. The final example is limited to 3-hydroxy-2-pyrones. These shortcomings motivated the exploration of bispyridiniums as possible solutions to the nitro-DA problem.

[23] Bartelson, K. J.; Singh, R. P.; Foxman, B. M.; Deng, L. *Chem. Sci.* **2011**, *2*, 1940.

IV.3 Background to Bispyridinium Catalysis

Conventional Brønsted acid catalysis utilizes a single proton to activate a substrate. Methods for increasing catalytic activity have often centered on lowering pK_a to bring about desired reactivity. This approach is limited in that simple proton transfer will be the operative mechanism beyond a certain pK_a threshold, at which point many compounds succumb to general acid catalyzed degradation. An alternative and milder approach is to use multiple acidic H-bond donors to active a substrate. Prior to my arrival in the Rawal group, this strategy had been realized: Dr. Yunus Türkmen had discovered bispyridinium salts to be powerful catalysts for the activation of carbonyl-containing substrates.[24] His benchmarking studies of the Diels-Alder reaction between cyclopentadiene and MVK are shown below.

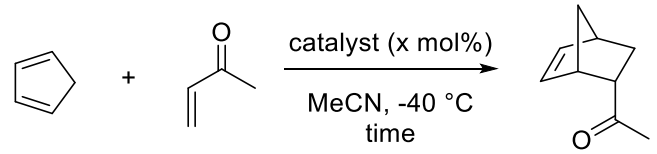

151 **185** **186**

entry	catalyst		mol%	time (h)	conv (%)
1	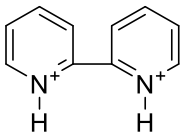	**187**	0.5	2	>99
2	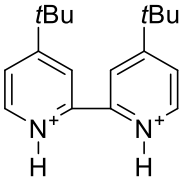	**188**	0.1	3	>99[a]

Table 7. Benchmarking studies of the catalytic activity of bispyridiniums and other H-bond donor catalysts.

[24] Türkmen, Y. E. Ph.D. Thesis, The University of Chicago, 2012.

entry	catalyst		mol%	time (h)	conv (%)
3	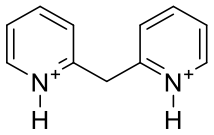	**189**	10	2	>99
4	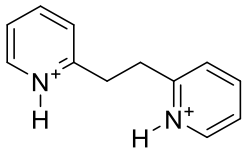	**190**	10	2	>99
5	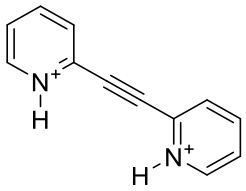	**191**	10	3	81
6	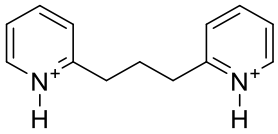	**192**	5	3	<5
7	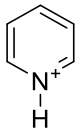	**193**	20	8.5	<5
8	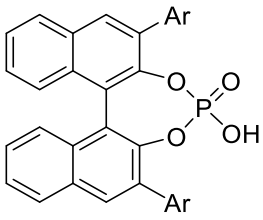 Ar: 2,4,6-*i*Pr$_3$(C$_6$H$_2$)	**194**	5	3.5	13[a]

Table 7. (continued) Benchmarking studies of the catalytic activity of bispyridiniums and other H-bond donor catalysts. [a] Reaction run in CH_2Cl_2.

During a search for other functional groups amenable to bispyridinium catalysis, activation of the nitro group was examined. The resistance of the nitro-DA reaction to catalysis made it an attractive target and so it was explored.

IV.4 Evaluation of Catalysts for the Nitro-Diels-Alder Reaction

Using the nitro-DA reaction of 2-siloxy diene **195** and β-nitrostyrene as a model system, several (bis)pyridinium and H-bond donor catalysts were evaluated with respect to conversion. The results are given in Table 8.

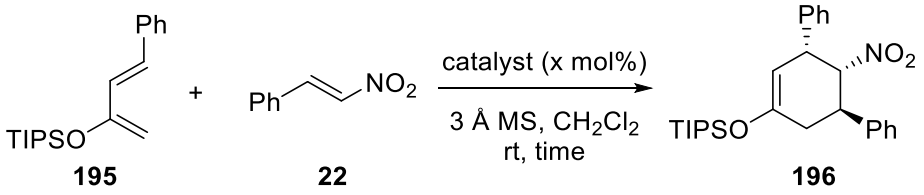

195 **22** **196**

entry	catalyst		mol%	time (h)	conv (%)
1	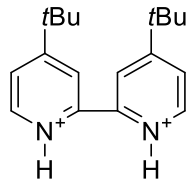	**188**	0.5	0.25	>98
2	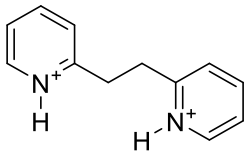	**190**	0.5	0.25	>98
3	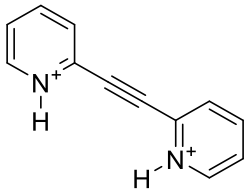	**191**	0.5	0.25	>98
4	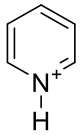	**193**	10	14	16
5	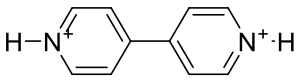	**197**	5	3	18

Table 8. Evaluation of the catalytic activity of several H-bond donor catalysts for a nitro-DA reaction.

entry	catalyst		mol%	time (h)	conv (%)
6	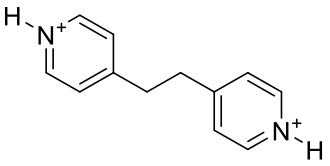	**198**	5	3	20
7	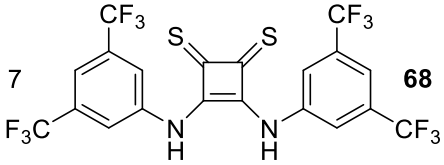	**68**	5	14	0
8	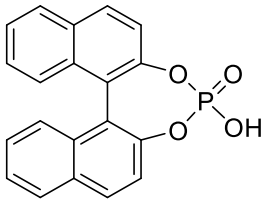	**199**	5	3	0

Table 8. (continued) Evaluation of the catalytic activity of several H-bond donor catalysts for a nitro-DA reaction.

Excitingly, bispyridinium catalysts capable of forming two-point H-bonds were found to be excellent catalysts (entries 1 - 3). At 0.5 mol% catalyst loading, these catalysts were able to achieve full conversion in just 15 minutes. Bispyridinium salts incapable of forming two-point H-bonds gave very low yield of product, even with an order of magnitude increase in both catalyst loading and reaction time (entries 5 and 6).

These results are consistent with our hypothesis that a two-point H-bond is critical to the catalytic activity of bispyridiniums. Bispyridiniums **188** and **197**, which have the same tether type, should have comparable acidities, yet bispyridinium **188**, being capable of forming a two-point H-bond, possesses catalytic activity orders of magnitude higher than **197**. The same holds true for bispyridiniums **190** and **198**. Bispyridiniums **188** and **197**, being electronically-coupled, are substantially more acidic than the others, and it has been found that the high acidity of these

catalysts can cause diene degradation. For bispyridinium **188**, which also catalyzes the nitro-DA reaction due to its two-point H-bonding ability, this is not a substantial problem. For bispyridinium **197** however, which cannot form a two-point H-bond to catalyze the nitro-DA as efficiently, the diene is entirely consumed with only limited nitro-DA product.

Since the bispyridinium catalysts were so effective with the originally chosen model reaction, a less reactive pair of substrates were examined for further investigation into catalyst performance. The results are given in Table 9.

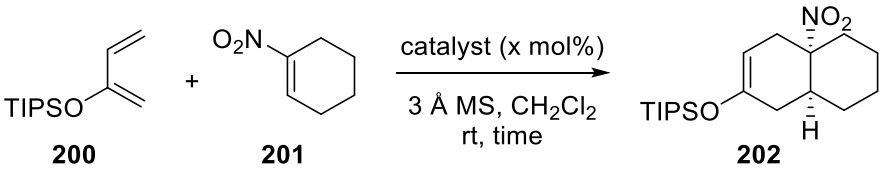

200 **201** **202**

entry	catalyst		mol%	time (h)	conv (%)
1	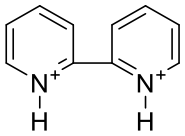	**187**	10	1	81
2	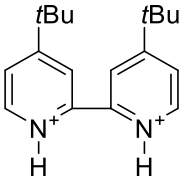	**188**	10	1	71
3	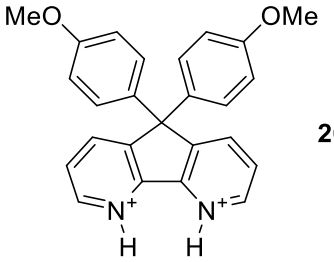	**203**	10	3	42

Table 9. Evaluation of the catalytic activity of several (bis)pyridiniums for a challenging nitro-DA reaction.

entry	catalyst		mol%	time (h)	conv (%)
4	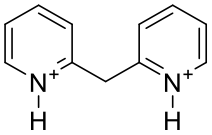	**189**	10	3	63
5	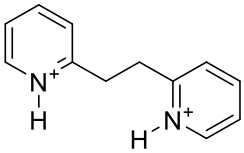	**190**	10	3	53
6	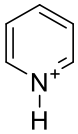	**193**	10	14	16
7	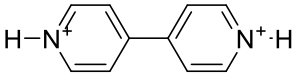	**197**	10	1	0
8	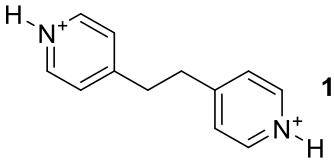	**198**	10	3	0

Table 9. (continued) Evaluation of the catalytic activity of several (bis)pyridiniums for a challenging nitro-DA reaction.

Bispyridinium salts capable of forming two-point H-bonds continued to perform exceptionally well, although higher catalyst loadings were required. Bispyridiniums incapable of forming two-point H-bonds were entirely ineffective for this more challenging reaction. Monopyridinium **193** was also entirely ineffective. Conformationally restrained bispyridinium **203** was surprisingly less effective than many other bispyridinium catalysts, including the other 2,2'-linked bispyridiniums. This suggests the most active conformer of the 2,2'-linked catalysts is not a coplanar pair of pyridiniums, a finding which may be useful in guiding design of chiral bispyridinium scaffolds in the future.

The reaction of 2-siloxybutadiene **200** with β-nitrostyrene also required a two-point H-bond donor bispyridinium catalyst to achieve conversion, as shown below in Scheme 58.

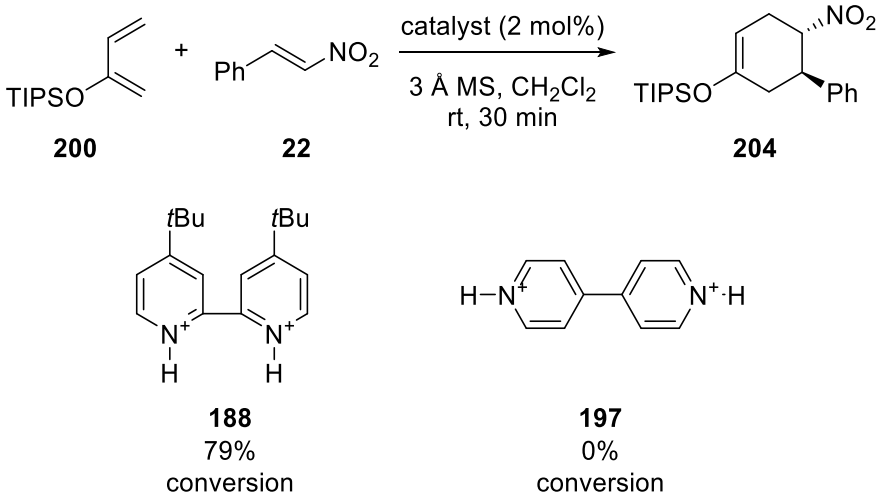

Scheme 58. Evaluation of the catalytic activity of two bispyridiniums for a more challenging nitro-DA reaction.

IV.5 Reaction Scope

Using bispyridinium catalyst **188**, the scope of the nitro-DA reaction was then examined to probe the generality of the reaction (Scheme 59). Bispyridinium **188** was chosen as catalyst due to its high catalytic activity, high solubility in chlorinated solvents, and commercial availability of the bispyridine. Dichloromethane was selected as solvent due to the extremely poor solubility of bispyridinium salts in hydrocarbon solvents and the severely diminished reactivity of the catalysts in H-bond accepting solvents such as acetonitrile or THF.

Molecular sieves were added since they were found to slow the rate of diene degradation. Increasing the concentration of the reaction was found to hasten diene degradation as well for some reactions. Although all reactions were finished with the given catalyst loading in under an

hour, it was observed that lowering the catalyst loading in some instances would result in incomplete conversion, even at prolonged reaction times.

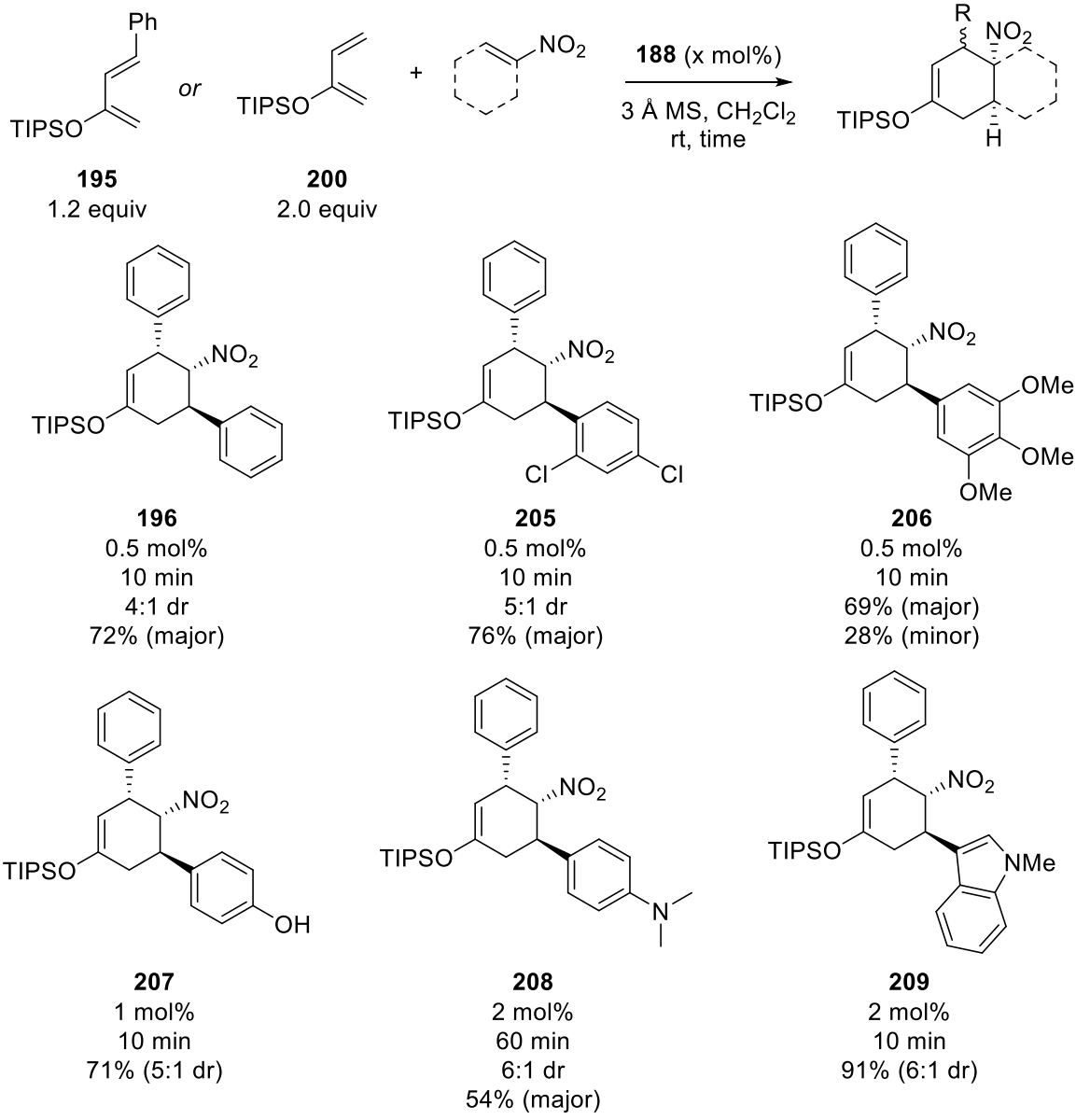

Scheme 59. Nitro-DA reaction of 2-siloxy dienes and nitroalkenes.

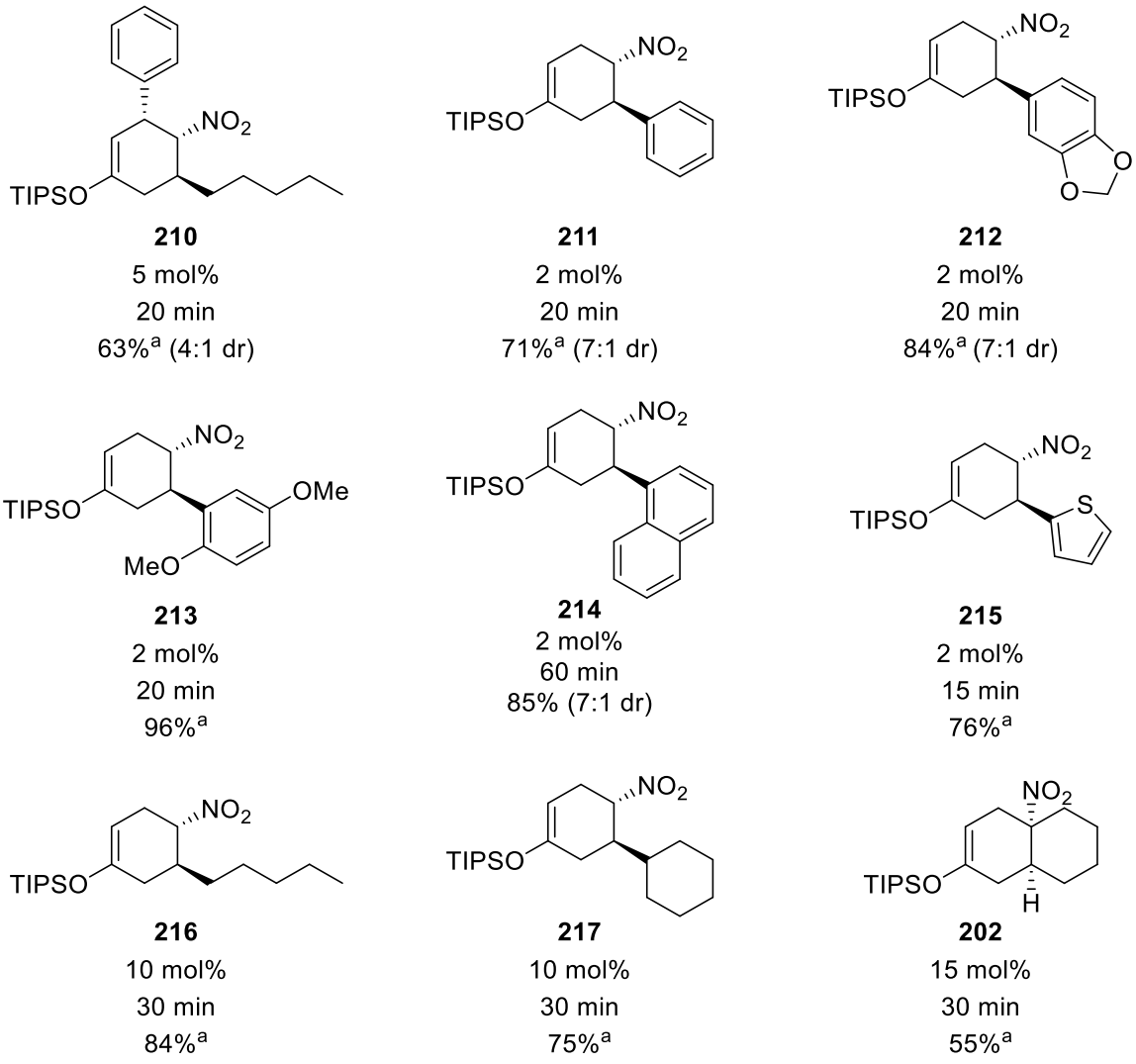

Scheme 59. (continued) Nitro-DA reaction of 2-siloxy dienes and nitroalkenes. [a] Isolated yield over two steps after TIPS deprotection.

As can be seen in the above substrate table, a wide variety of nitroalkenes can be used in this methodology. Electron-rich and electron-poor nitrostyrenes are both good reaction partners. Phenols and aniline nitrogens are tolerated under the reaction conditions. Aliphatic nitroalkenes react readily with both dienes **195** and **200**. Interestingly, electron-rich nitrostyrenes were found to be the best reaction partners for diene **200**. Heterocycle substituted nitroalkenes such as indole and thiophene also give good yields. Products obtained by the nitro-DA reaction of dienes with

3-nitrovinyl indole are essentially tryptamine-embedded carbocycles, a molecular framework commonly found in natural products.

Importantly, nitrocyclohexenes are also suitable reaction partners and lead to products such as **202**. Diels-Alder adducts of nitrocyclohexenes can be radically denitrated to afford trans-decalin systems, and therefore represent a method of achieving formal trans-DA products as discussed by Danishefsky (Scheme 60).[25] The nitro-DA reaction under bispyridinium catalysis compares favorably to the thermal conditions employed by Danishefsky, which requires large excess of diene, high temperature, and long reaction time.

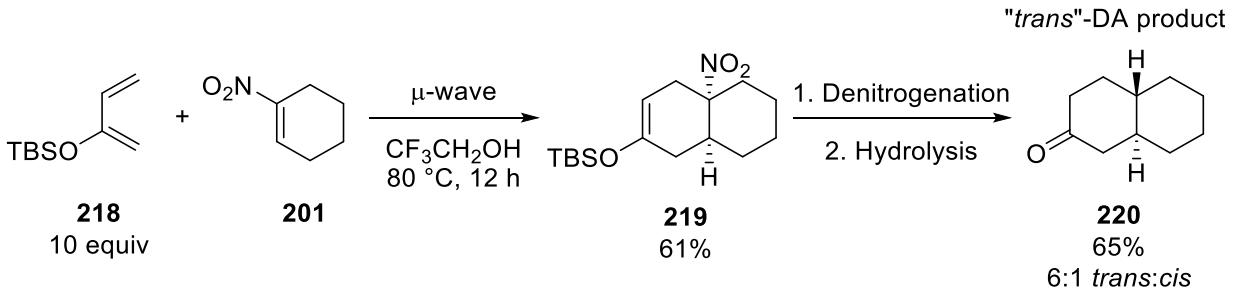

Scheme 60. Thermal nitro-DA reaction and denitration.

The presence of *cis*-isomers in some reactions of diene **200** point to a stepwise mechanism. This is consistent with the finding that dienes lacking the 2-siloxy substitution were unreactive. A list of some ineffective dienes is shown in Figure 17. Cyclopentadiene and 2-siloxy cyclohexadiene polymerized under the reaction conditions.

[25] Kim, W. H.; Lee, J. H.; Danishefsky, S. J. *J. Am. Chem. Soc*. **2009**, *131*, 12576.

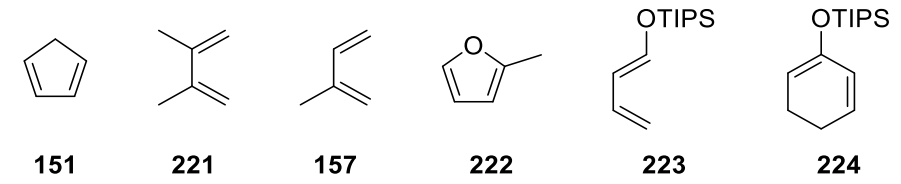

Figure 17. Dienes incompatible with the bispyridinium catalyzed nitro-DA reaction.

Using the most reactive substrates, catalyst loading experiments were set up to determine how low a catalyst loading is possible. At 0.01 mol% catalyst loading, substantial conversion occurred in only 14 h (Scheme 61).

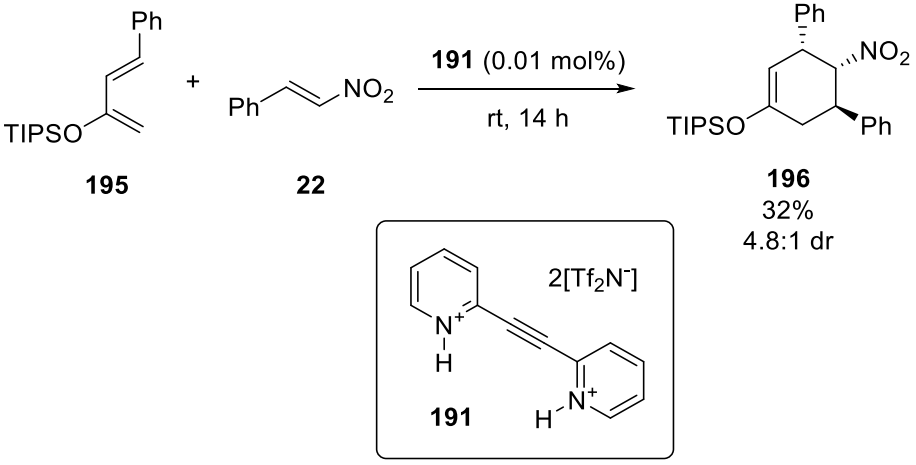

Scheme 61. Catalyst loading experiment for a nitro-DA reaction.

IV.6 Conclusion

In summary, bispyridinium salts have been found to be highly active catalysts for the nitro-Diels-Alder reaction of 2-siloxy dienes and nitroalkenes. A wide-range of nitroalkenes were susceptible to the catalytic method employed, and the main limitation on the diene is the

presence of a 2-siloxy substitution. The availability of chiral bispyridiniums opens the possibility of rendering the process asymmetric, and that is the subject of the following chapter.

Chapter 5

Asymmetric Bispyridinium Catalysis

V.1 Initial Studies

The successful demonstration of racemic bispyridinium catalysis demanded an investigation into chiral bispyridiniums to carry out the transformations asymmetrically. Prior to my arrival in the Rawal group, Dr. Julius Reyes had synthesized an assortment of chiral bispyridiniums, some of which are shown in Figure 18. The chiral catalysts were highly active for a number of different reactions, including Diels-Alder reactions and Nazarov cyclizations (Figure 19). Despite this, no enantioselectivities were observed.

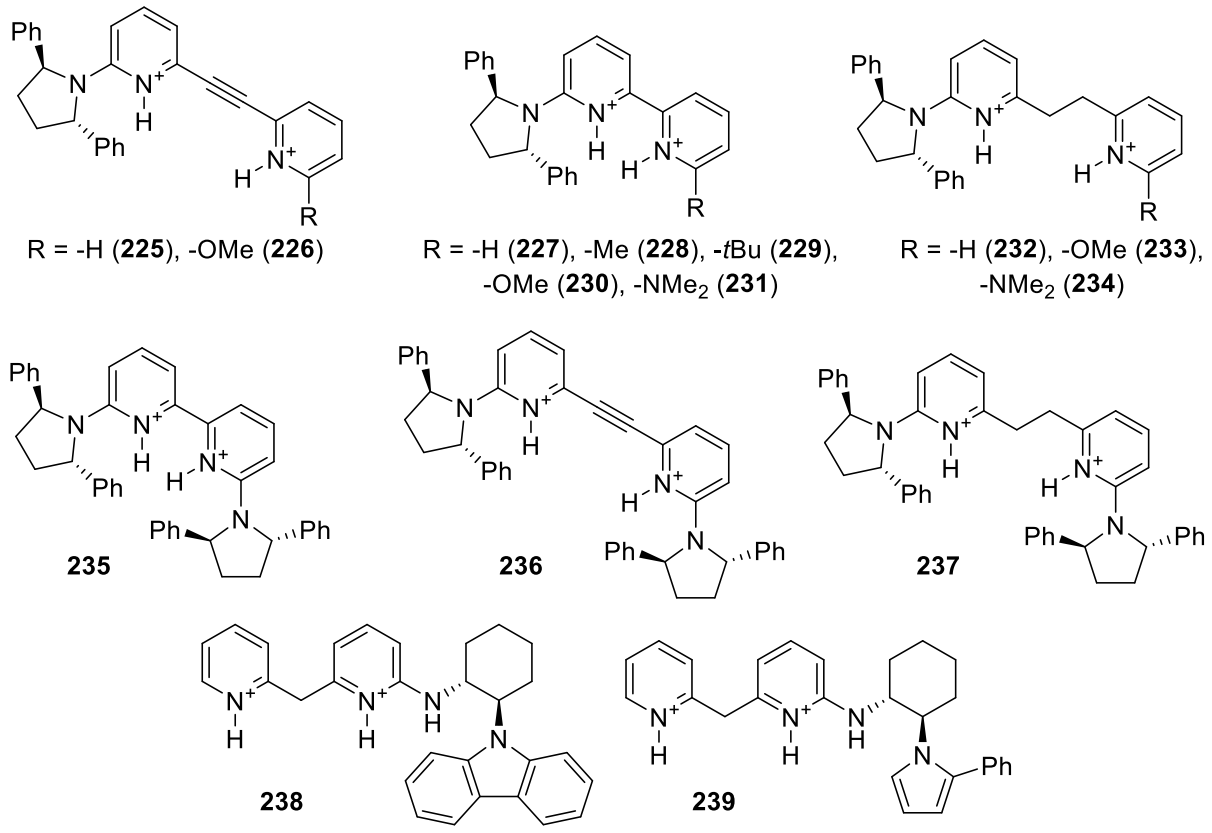

Figure 18. Previously synthesized chiral bispyridinium catalysts.

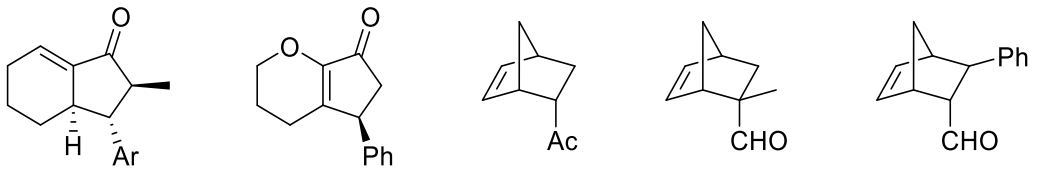

240 **241** **186** **242** **243**

Figure 19. Racemic products obtained with chiral bispyridinium catalysts.

The high catalytic activity coupled with racemic products raised the possibility that an added element of molecular recognition was needed to better differentiate the diastereotopic transition states. Substrates bearing multiple carbonyl units would possibly form additional hydrogen bonds to the catalyst and thus provide a greater chance of enantioinduction.

Using one of the previously synthesized chiral bispyridinium catalysts, a Friedel-Crafts reaction of 1-methyl indole and ethyl glyoxylate was carried out (Scheme 62). The desired product was obtained in 58% ee and 53% yield, thus providing proof-of-concept for chiral bispyridinium catalysis.

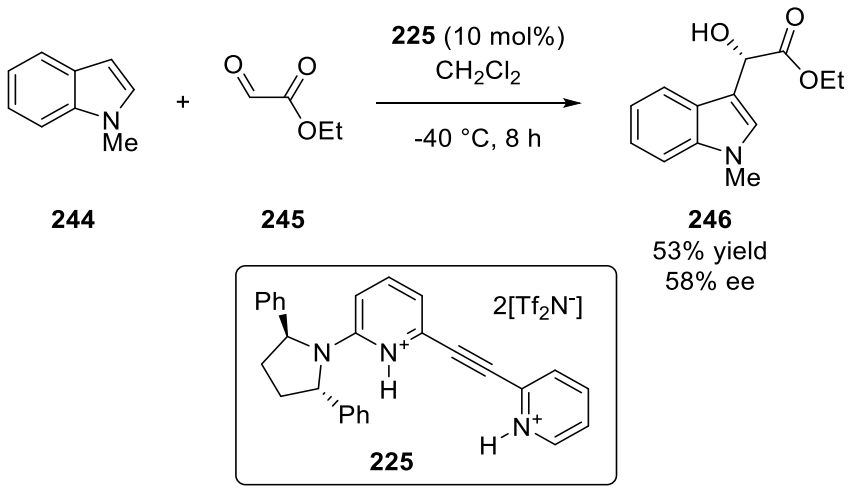

244 **245** **246**
53% yield
58% ee

225

Scheme 62. First asymmetric reaction catalyzed by a chiral bispyridinium.

Based on the absolute stereochemical configuration of the chiral alcohol product, a potential reaction pathway could be proposed (Figure 20). The bulkier ester half of the glyoxylate should extend away from the diphenyl pyrrolidine, and a secondary H-bonding interaction between the carbonyl ester and catalyst could provide both molecular recognition and moderate rate enhancements. The phenyl ring on the pyrrolidine would shield one face of the glyoxylate and thus force the indole into a *Re*-face attack.

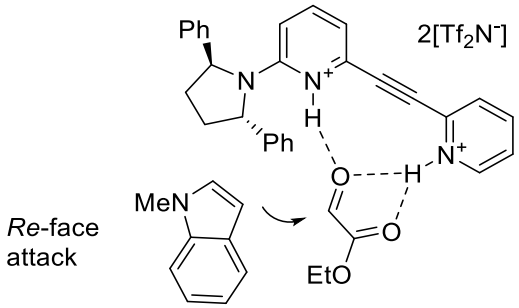

Figure 20. Possible mode of catalysis for the bipyridinium catalyzed Friedel-Crafts reaction.

The successful application of asymmetric bispyridinium catalysis motivated continued exploration of the chiral space.

V.2 Synthesis of New Chiral Bispyridiniums

V.2.1. From a (−)-β-Pinene-Derived Chloropyridine

One of the drawbacks of the previously made chiral bispyridiniums was that there was no easy way to systematically tweak the chiral handles. A new class of chiral bispyridiums that enabled easy modification of the chirality was therefore developed based on the previously

reported chloropyridine **247** (Figure 21).[1,2] It should be pointed out that bispyridinium activity is dependent on the anion being highly dissociated. Diprotonation of a bispyridine with one of the common chiral Brønsted acid has therefore not been a viable strategy for asymmetric catalysis, as the counter anions are not sufficiently dissociated for catalytic activity.

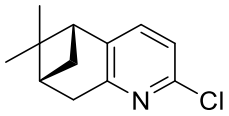

247

Figure 21. Previously synthesized chiral chloropyridine.

Synthesis of the chloropyridine begins with (−)-β-pinene, which is oxidized to pinocarvone by a modified literature procedure.[3] Kröhnke annulation to afford the pyridine was carried out according to the literature.[1]

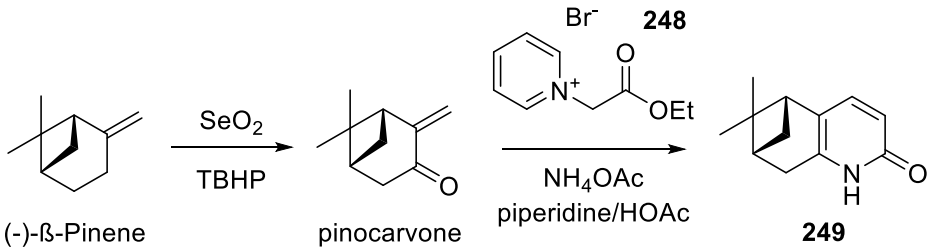

Scheme 63. Reported synthesis of chiral pyridone **249**.

Chlorination of the pyridone has been reported twice. The first report proceeds in two steps: triflation followed by nucleophilic aromatic substitution with a chloride source.[1] A second

[1] Chelucci, G.; Marchetti, M.; Malkov, A. V.; Friscourt, F.; Swarbrick, M. E.; Kocovský. *Tetrahedron* **2011**, *67*, 5421.
[2] For a review on chiral pyridine-containing ligands, see: Kwong, H.; Yeung, H.; Yeung, C.; Lee, W.; Lee, C.; Wong, W. *Coordination Chemistry Reviews* **2007**, *251*, 2188.
[3] Höld, K. M.; Sirisoma, N. S.; Sparks, S. E.; Casida, J. E. *Xenobiotica* **2008**, *32*, 251.

report uses phosphoryl chloride at 135 °C.[4] This second procedure was reported to proceed in high yield, although conversions above 15% were never obtained in our hands. A survey of the literature would indicate that chlorination of non-electronically activated pyridines requires addition of phosphorous pentachloride. Using a mixture of phosphoryl chloride and phosphorous pentachloride gave the desired chloropyridine in good yield (Scheme 64).

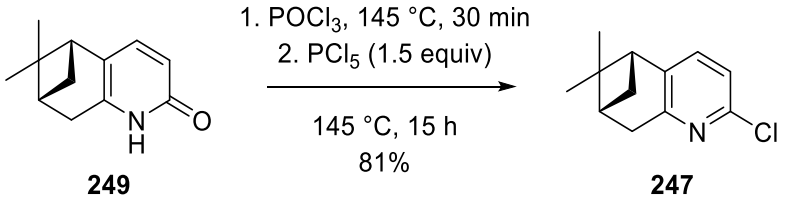

Scheme 64. Modification of the chloropyridine synthesis using PCl_5.

Chloropyridine **247** is readily elaborated into a variety of chiral bispyridiniums, and a representative synthesis is shown in Scheme 65. Lithiation of chloropyridine **247** followed by electrophilic trapping with fluorenone yields alcohol **250** as a single diastereomer. Ionic reduction of the alcohol leads to intermediate **251**. Heck-alkynylation of chloropyridine **251** is enabled by XPhos ligand as reported by Buchwald.[5] Ethynylpyridine was not used due to Buchwald's finding that aryl alkynes react poorly under these conditions. Deprotection with TBAF gives alkyne **253**, which is then Sonogoshira coupled to 2-bromopyridine to give bispyridine **254**.

[4] Boobalan, R.; Chinpiao, C. *Tetrahedron Letters* **2016**, *57*, 1930.
[5] Gelman, D.; Buchwald, S. L. *Angew. Chem. Int. Ed.* **2003**, *42*, 5993.

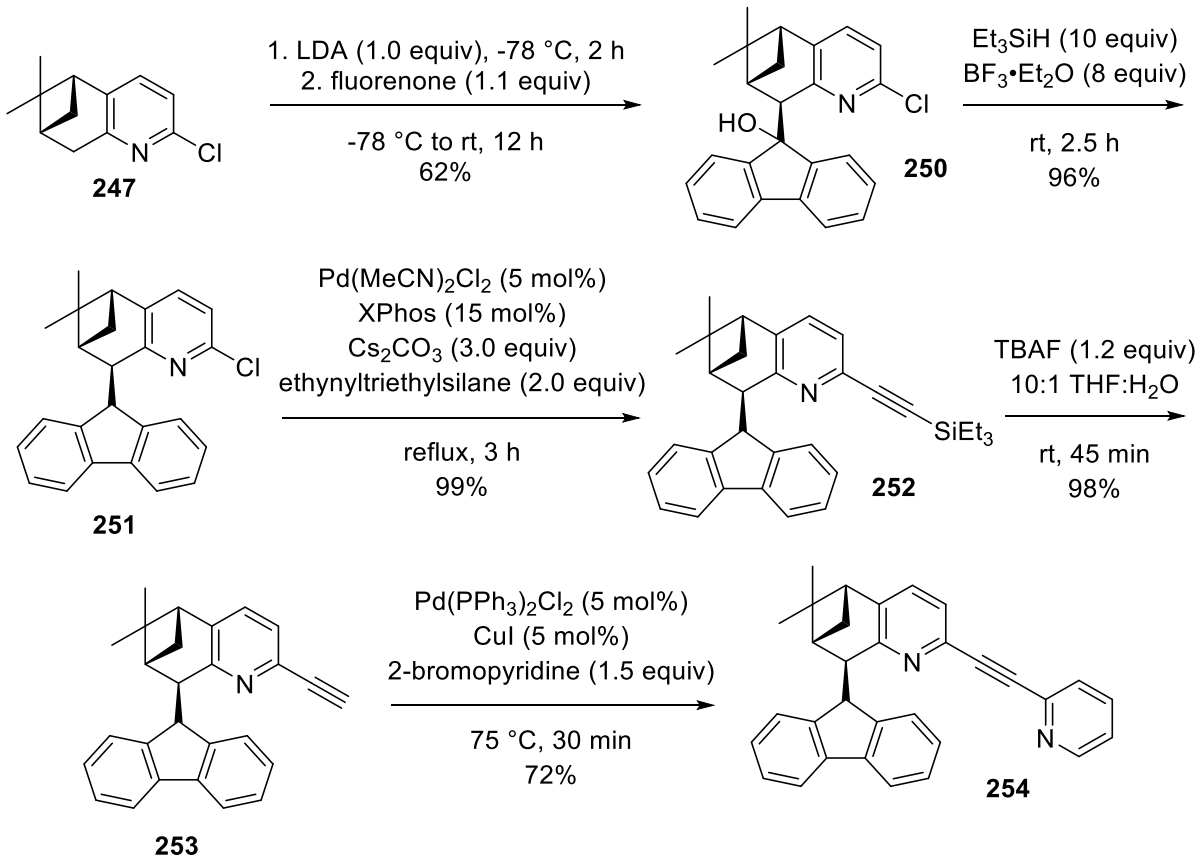

Scheme 65. Synthesis of a chiral bispyridine from chloropyridine **247**.

A variety of bispyridines were synthesized by this method and are shown below.

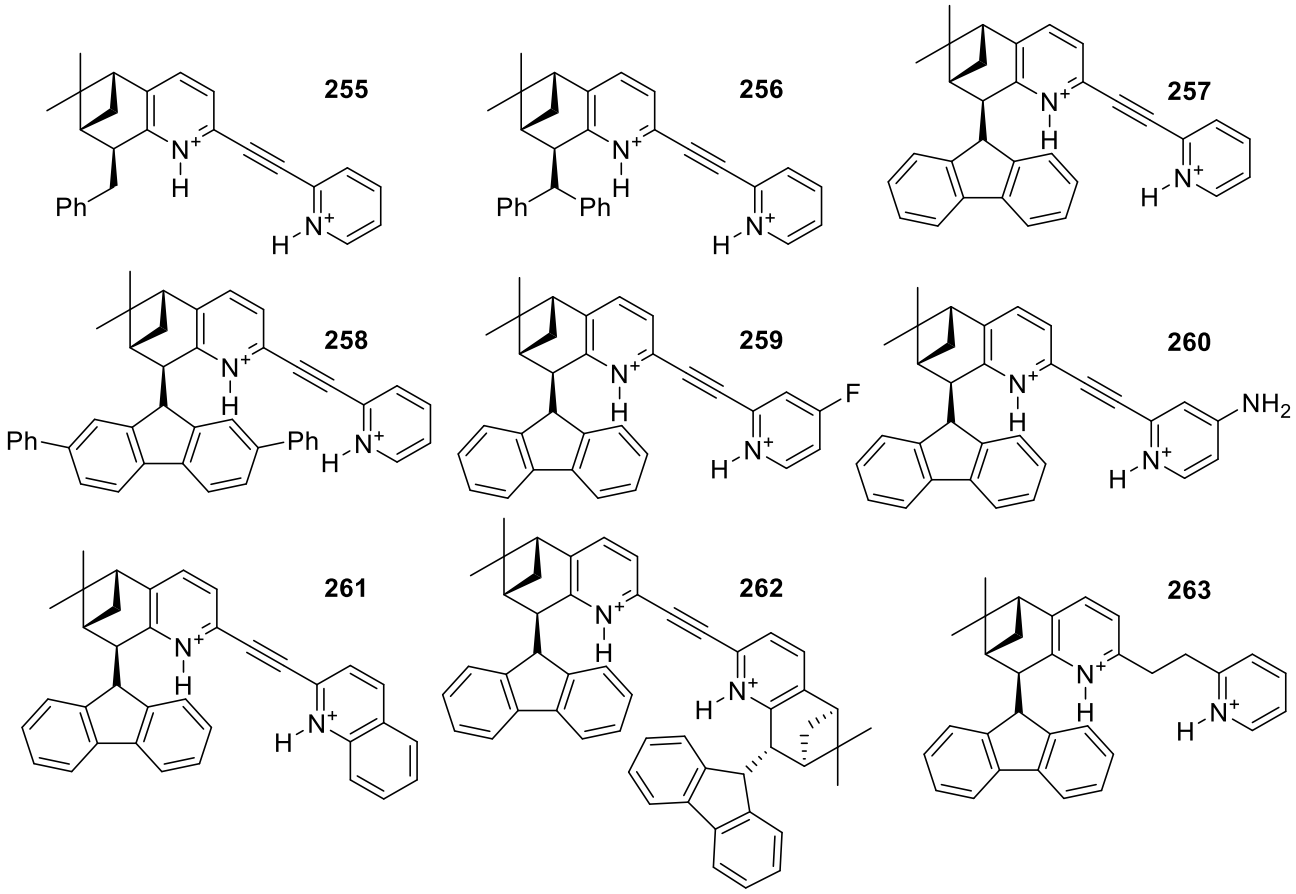

Figure 22. Synthesized chiral bispyridiniums.

It should be noted that alkylation of bispyridine **265** was unsuccessful (Scheme 66). Similarly, efforts to lithiate and alkylate triflated pyridine **264** led exclusively to thia-Fries rearrangement product **266**, a finding which had been reported several years earlier.[6]

[6] Xu, X.; Wang, X.; Lio, G.; Tokunaga, E.; Shibata, N. *Org. Lett.* **2012**, *14*, 2544.

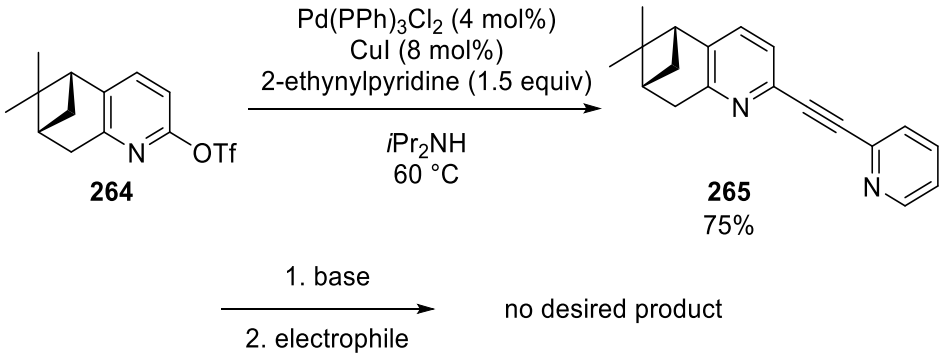

Scheme 66. Attempted alkylation of bispyridine **265**.

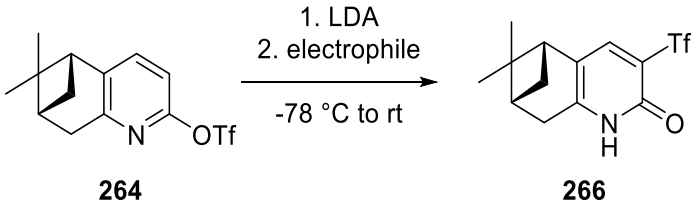

Scheme 67. Attempted alkylation of triflated pyridine **264**.

V.2.2 From a (−)-β-Pinene-Derived Bromoketopyridine

Since the route shown above requires multiple synthetic steps after introduction of the chiral handle, a shorter route was devised that would allow late stage diversification of chirality (Scheme 68).

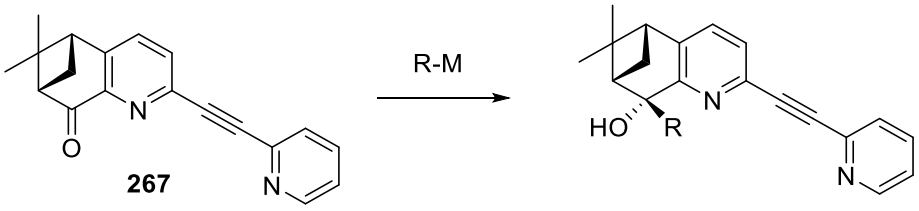

Scheme 68. Addition of an organometallic reagent to bispyridine **267**.

Late stage chiral diversification would be enabled by a ketone functionality on a chiral bispyridine so that an organometallic reagent could be added as the chiral handle just prior to bispyridine protonation. The corresponding bromoketopyridine was therefore synthesized as shown in the following schemes starting from chloropyridine **247**.

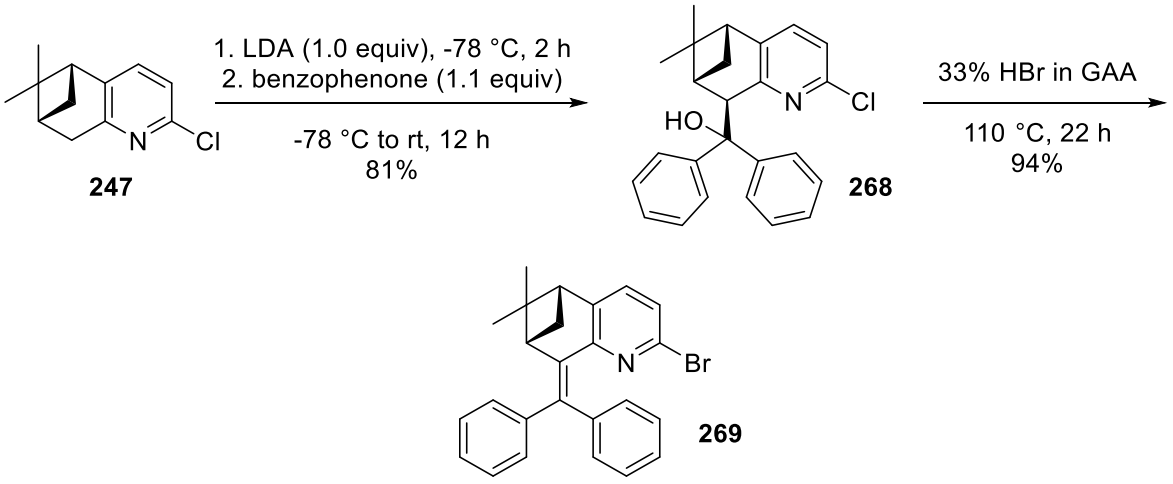

Scheme 69. Synthesis of bromopyridine **269**.

Lithiation of chloropyridine **247** followed by electrophilic trapping with benzophenone occurs according to the literature.[4] Simultaneous nucleophilic aromatic substitution and dehydration occurs in near-quantitative yield by refluxing with 33% HBr in GAA for 22 h. The exocyclic double bond that forms during dehydration of **268** is likely important for this relatively fast reaction; nucleophilic aromatic substitution of **251** requires 4 days to achieve good yield (Scheme 70). One possible explanation for this difference in reactivity is that the exocyclic double bond is protonated to form the dibenzylic cation, inductively activating the adjacent chloropyridine for nucleophilic aromatic substitution with the bromide.

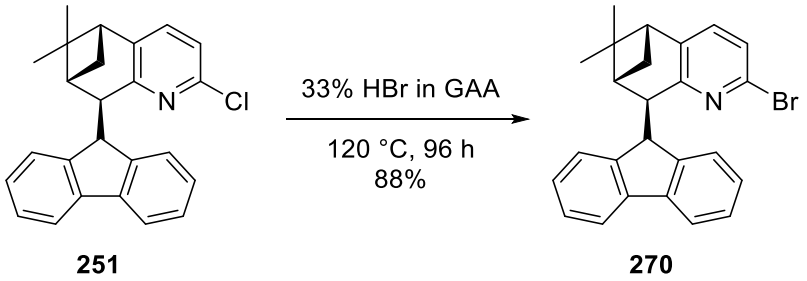

Scheme 70. Synthesis of bromopyridine **270** from chloropyridne **251**.

Ozonolysis of the double bond of bromopyridine **269** gave a nearly perfect 1:1 mixture of desired product **274** and the corresponding *N*-oxide **275** after workup (Scheme 71). This likely originates from a nonselective retro [3+2] cycloaddition of molozonide **271** to yield equally **272** and **273**. Rearrangement of carbonyl *O*-oxide **273** prior to the usual second [3+2] cycloaddition to form the trioxolane would then explain the outcome.

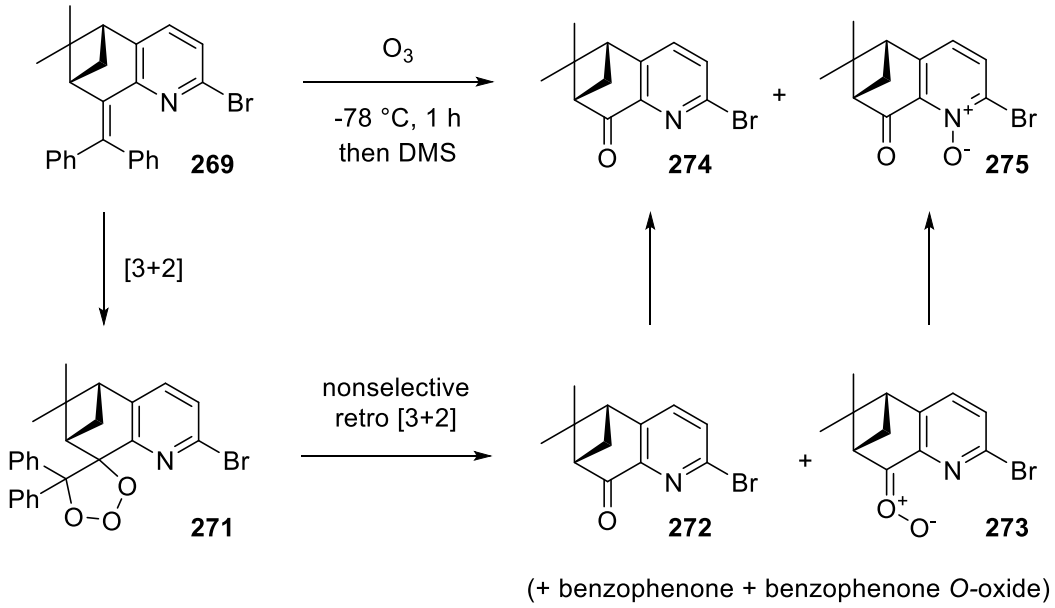

Scheme 71. Ozonolysis of bromopyridine **269**.

Pyridine has been reported as an organocatalyst for the reductive ozonolysis of alkenes, and the proposed mechanism is shown below in Scheme 72.[7] It was originally hoped that the substrate itself would catalyze this transformation. While this was not the case, it was found that the addition of 4 equivalents of pyridine to the reaction mixture entirely prevented formation of pyridine *N*-oxide **275** (Scheme 73), presumably through interception of the carbonyl *O*-oxide prior to rearranging into the *N*-oxide. This intermolecular reductive process is therefore apparently faster than the carbonyl *O*-oxide rearrangement even at -78 °C.

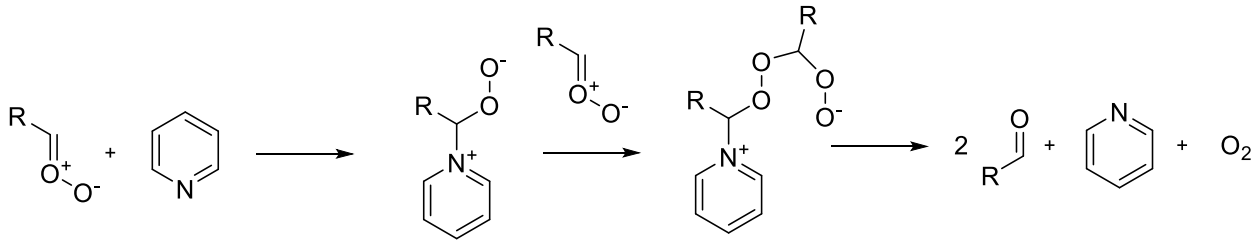

Scheme 72. Mechanism for the pyridine catalyzed reduction of carbonyl *O*-oxides.

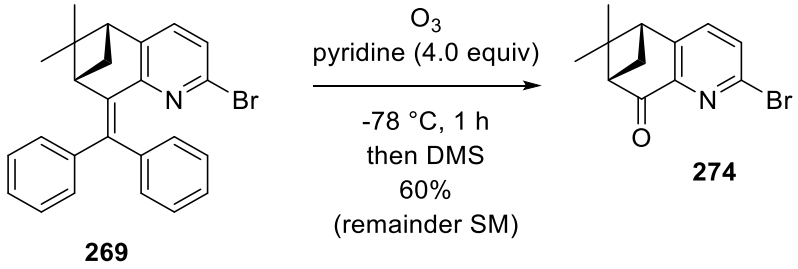

Scheme 73. Ozonolysis of bromopyridine **269** in the presence of exogeneous pyridine.

Sonogashira coupling of bromoketopyridine **274** with 2-ethynylpyridine yields bispyridine **267**, which can be reacted with various organometallic reagents as different chiral handles just prior to diprotonation (Scheme 74). The benzylic alcohol is stable to these acidic

[7] Willand-Charnley, R.; Fisher, T. J.; Johnson, B. M.; Dussault, P. H. *Org. Lett.* **2012**, *14*, 2242.

conditions presumably due to the adjacent pyridinium which would destabilize any benzylic cation formation.

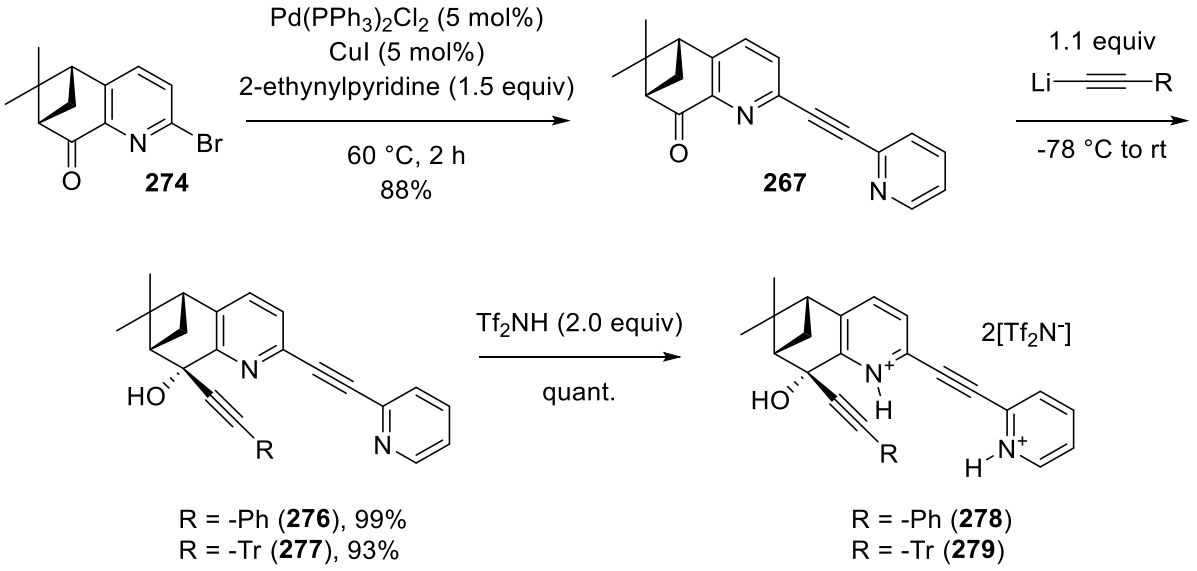

Scheme 74. Synthesis of dialkynyl bispyridiniums.

Reduction of the triple bond prior to addition of an organometallic reagent to the ketone affords bispyridines with an ethane linkage (Scheme 75).

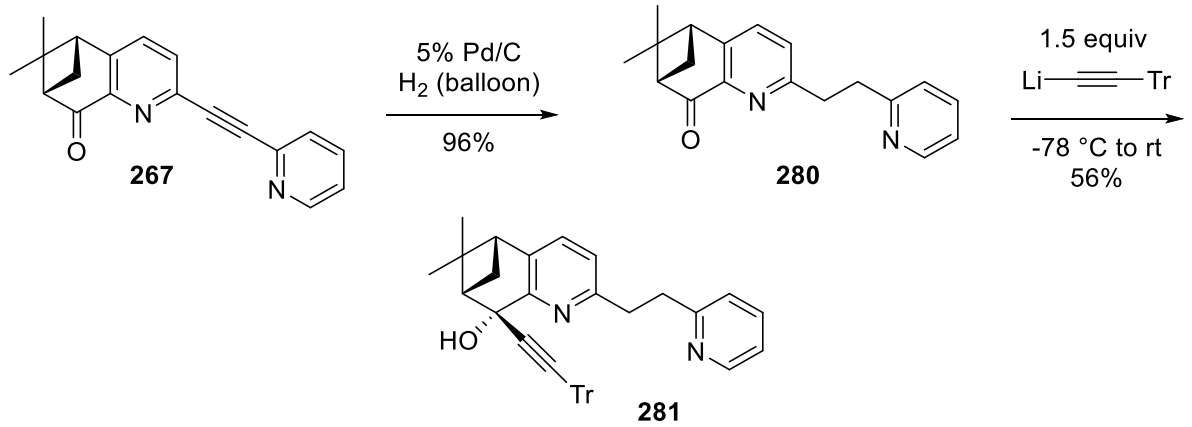

Scheme 75. Addition of an organometallic reagent to ethane-linked bispyridine **280**.

V.2.3 From Pinocarvone

Synthesis of a rigid chiral bispyridine from pinocarvone is also possible following a modified literature procedure (Scheme 76).[1] Presumably, bispyridine **285** can be further elaborated by functionalization of the benzylic position through lithiation and alkylation.

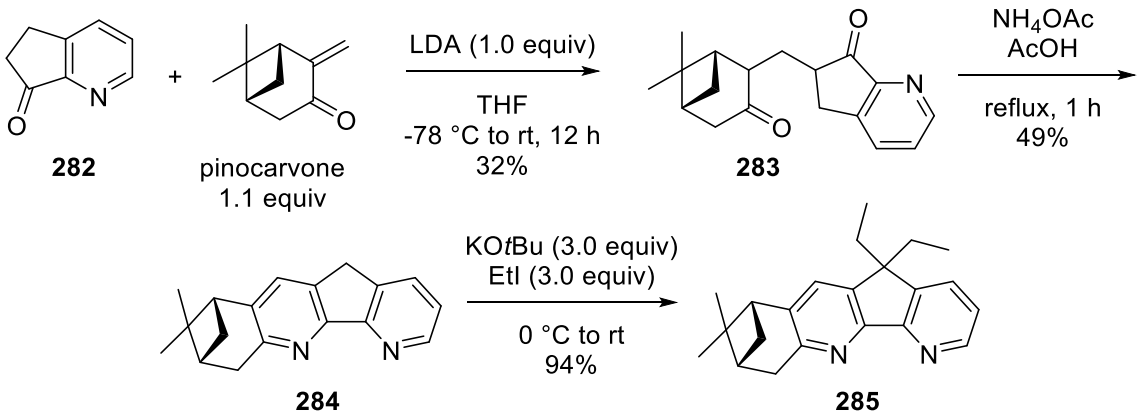

Scheme 76. Synthesis of a rigid chiral bispyridine.

V.3 Enantioselective Friedel-Crafts Reactions Catalyzed by Chiral Bispyridiniums

The chiral bispyridiniums synthesized were then evaluated for asymmetric induction in the Friedel-Crafts reaction between 1-methyl indole and ethyl glyoxylate (Table 10).

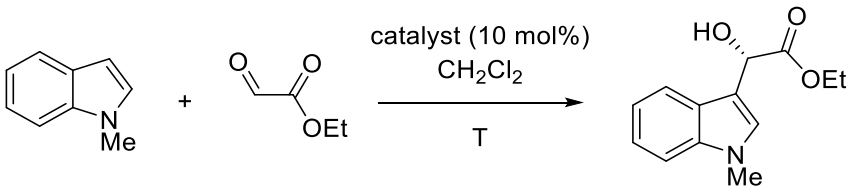

244 **245** **246**

entry	catalyst		T (°C)	ee (%)
1	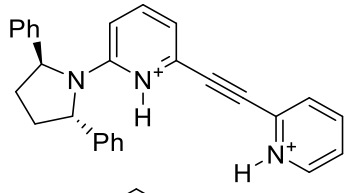	**225**	-40	58
2	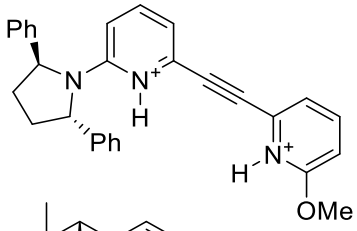	**226**	-40	-30
3	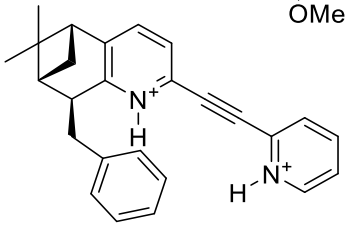	**255**	-40 to -30	0
4	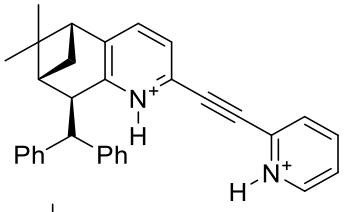	**256**	-40	11
5	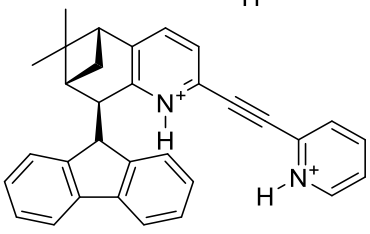	**257**	-50 to -40	37

Table 10. Evaluation of chiral catalysts for an asymmetric Friedel-Crafts reaction between 1-methyl indole and ethyl glyoxylate.

entry	catalyst		T (°C)	ee (%)
6	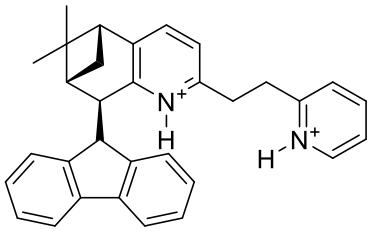	**263**	-30	12
7	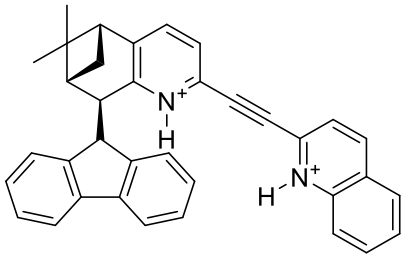	**261**	-60 to -40	-6
8	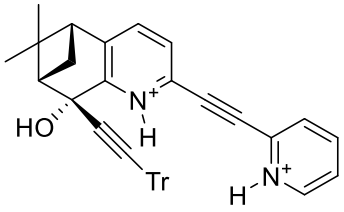	**279**	-40	26
9	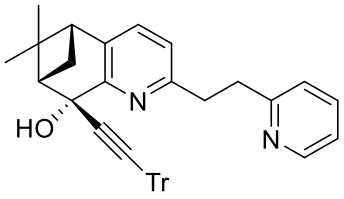	**286**	-40	18

Table 10. (continued) Evaluation of chiral catalysts for the asymmetric Friedel-Crafts reaction between 1-methyl indole and ethyl glyoxylate.

Increasing steric bulk on the achiral pyridine results in either substantially diminished enantioselectivity or even reversed enantioselectivity. Increasing steric bulk at the chiral pyridinium from benzyl to dibenzyl to fluorene results in improved enantioselectivity, while the triple bond linker was found to be better than the ethane linker.

Above some threshold temperature, bispyridiniums catalyze a bisindole formation from the desired Friedel-Crafts product and indole (Scheme 77).

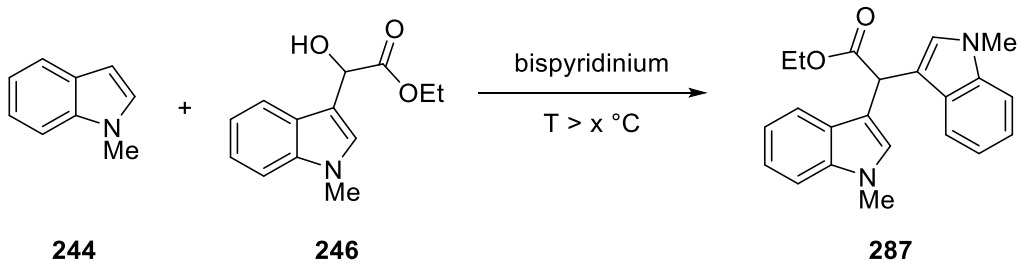

244 **246** **287**

Scheme 77. Bisindole formation above some threshold temperature under bispyridinium catalysis.

This temperature was found to be dependent on the catalyst and solvent. As a result of this competitive bisindole formation which required careful temperature control, ethyl 3,3,3-trifluoropyruvate was substituted for ethyl glyoxylate since this substrate avoids bisindole temperature even at higher temperatures.

Using this substrate and bispyridinium **257**, a solvent screen was carried out which identified THF and other ethereal solvents as being best for asymmetric induction (Table 11).

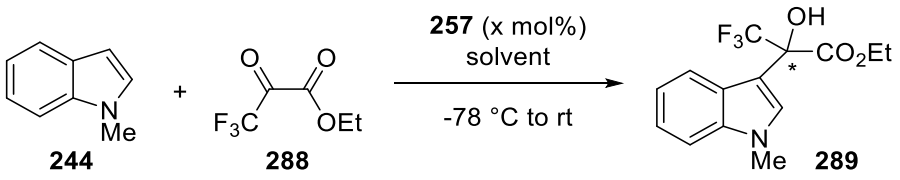

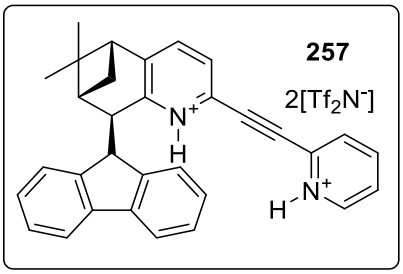

entry	solvent	mol%	ee (%)
1[a]	CH_2Cl_2	10	18
2	THF	10	47
3	THF	5	38
4	Et_2O	5	28
5	CPME	10	29
6	MeCN	10	<5

[a]Reaction performed at -50 °C.

Table 11. Solvent and catalyst loading experiments for the Friedel-Crafts reaction between 1-methyl indole and ethyl 3,3,3-trifluoropyruvate.

Several other catalysts were then tested in this Friedel-Crafts reaction using THF as solvent (Scheme 78).

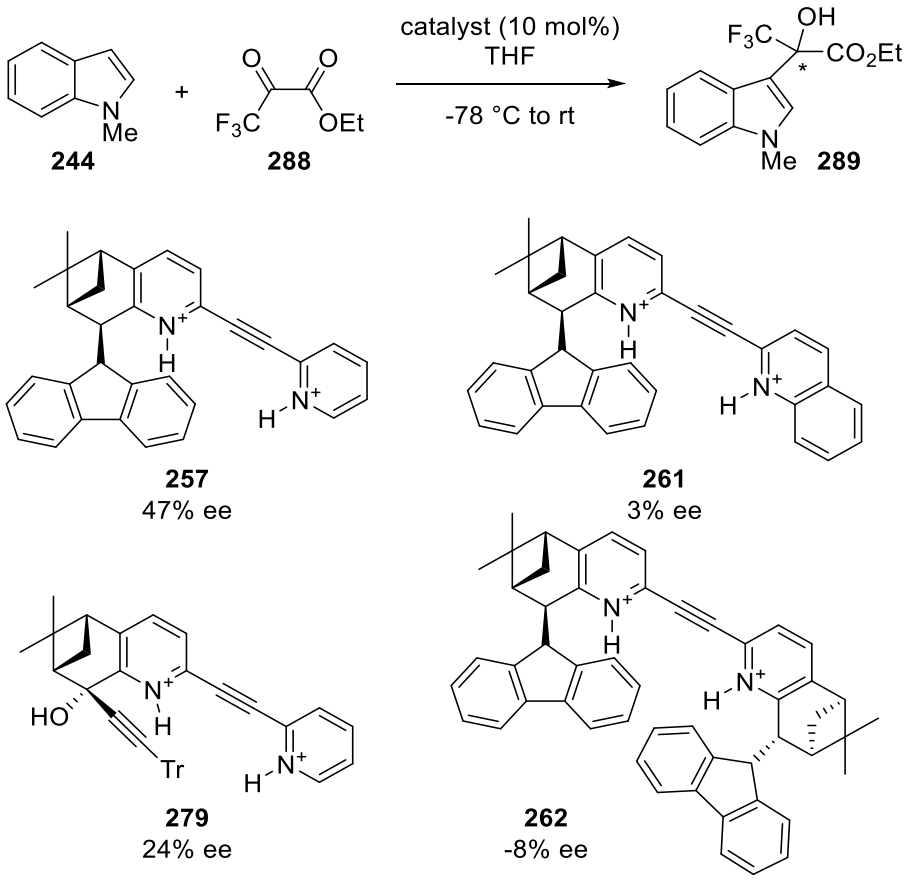

Scheme 78. Evaluation of chiral catalysts for the asymmetric Friedel-Crafts reaction between 1-methyl indole and ethyl 3,3,3-trifluoropyruvate.

With optimal catalyst and solvent identified, a substrate table was produced to probe the generality of the reaction (Scheme 79).

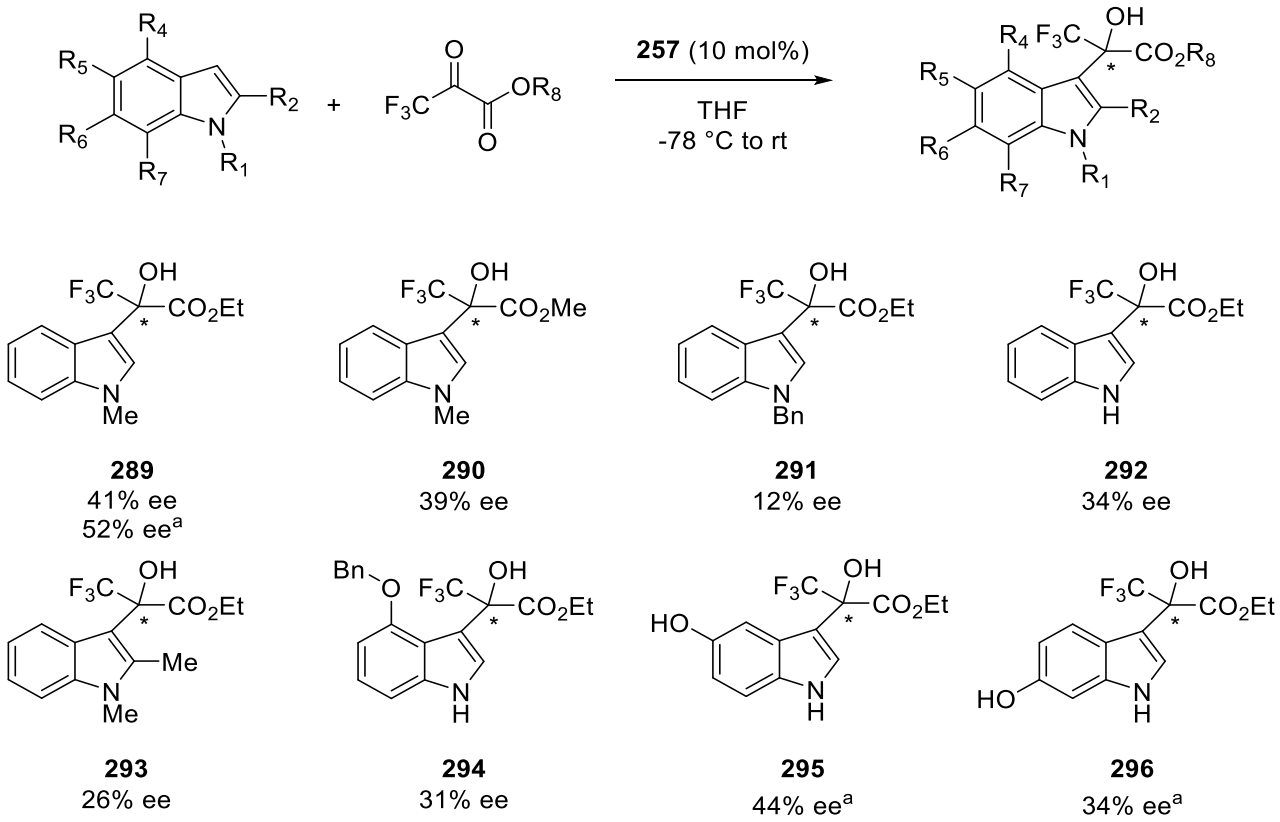

Scheme 79. Friedel-Crafts reactions of various indoles with pyruvates.

1-Methyl indoles gave better results than free indoles, which in turn were better than 1-benzyl indoles. Switching from ethyl pyruvate to methyl pyruvate had very little impact on ee. Substitutions including free hydroxy groups around the indole benzene ring were well-tolerated, although C-2 methyl substituted indoles gave somewhat lower ee's.

The necessity of a second carbonyl in the electrophilic substrate for enantioselectivity was demonstrated by the Friedel-Crafts reaction between 1-methyl indole and chloral as catalyzed by chiral bispyridinium **257** (Scheme 80).

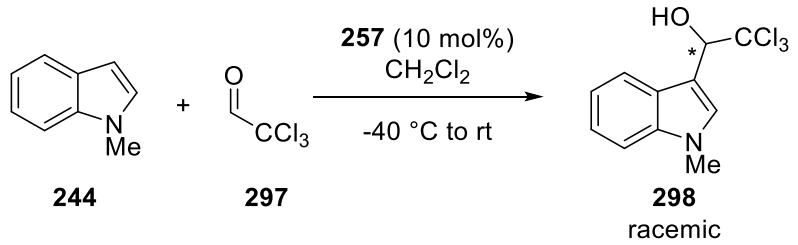

244 **297** **298** racemic

Scheme 80. Friedel-Crafts reaction of 1-methyl indole with chloral.

Despite the moderate enantioselectivities afforded by chiral bispyridiniums in this Friedel-Crafts reaction, the nitro-Diels-Alder reaction discussed in Chapter 4 remained resistant to asymmetric induction under chiral bispyridinium catalysis.

V.4 Conclusion

In summary, a family of new chiral bispyridinium catalysts has been synthesized. The synthetic route utilizes known chloropyridine **247** and allows for easy modification of the chiral unit, thereby enabling a more facile exploration of the chiral space. A fluorene-tethered chiral bispyridinium synthesized by this method was found to be an effective catalyst for the asymmetric Friedel-Crafts reaction between indoles and glyoxylates or trifluoropyruvates. The relatively easy modification of bispyridinium chirality by this method may enable the identification of effective chirality for reactions not yet explored.

Experimental Procedures and Characterization Data

V1.1 General Information

Thin-layer chromatography (TLC) was performed using Whatman silica gel 60 Å F254 plates (250 μm) with F-254 fluorescent indicator and visualized by UV fluorescence quenching, ceric ammonium molybdate, or potassium permanganate staining. SiliCycle SiliaFlash P60 silica gel (particle size 40 - 63 μm) was used for flash chromatography. NMR spectra were measured on Bruker DRX and DMX spectrometers at 500 MHz for ^{1}H spectra and 125 MHz for ^{13}C spectra, respectively, and calibrated to either TMS ($\delta = 0$ for ^{1}H), residual $CHCl_3$ ($\delta = 7.26$ for ^{1}H and $\delta = 77.23$ for ^{13}C), residual DMSO ($\delta = 2.50$ for ^{1}H and $\delta = 39.51$ for ^{13}C), or residual CD_3CN ($\delta = 1.94$ for ^{1}H and $\delta = 1.39$ for ^{13}C). Splitting patterns are reported as apparent. Mass spectral data was measured on Agilent technologies 6224 TOF LC/MS. Infrared spectra were recorded on a Nicolet iS5 FT-IR or Nicolet 6700 FT-IR spectrometer and are reported in frequency of absorption (cm^{-1}) using NaBr salt plates using a thin film. All reactions were run under a nitrogen atmosphere unless otherwise noted.

V1.2 Experimental Procedures and Characterization Data for Chapter 2

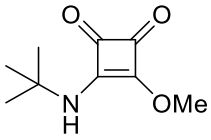

42

(**42**). To a solution of dimethyl squarate (1.15 g, 8.1 mmol, 1.00 equiv) in CH_2Cl_2 (10 mL) was added *tert*-butyl amine (0.90 mL, 8.5 mmol, 1.05 equiv) and the resulting solution was stirred for

1.5 h at rt. The reaction mixture was then concentrated and the residue chromatographed on silica gel (CH_2Cl_2 → 1% MeOH in CH_2Cl_2) to afford **42** (1.15 g, 78%) as a white solid. The product exists as two rotamers in DMSO at room temperature in a ratio of 1:1. ^{1}H NMR (500 MHz, DMSO-d_6): δ = 8.77 (s, 1H), 8.62 (s, 1H), 4.35 (s, 3H), 4.30 (s, 3H), 1.33 (s, 9H), 1.29 (s, 9H).

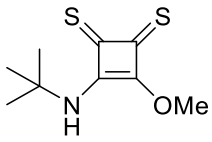

43

(**43**). To a solution of **42** (733 mg, 4.0 mmol, 1.0 equiv) in dry CH_2Cl_2 (20 mL) was added Lawesson's reagent (1.62 g, 4.0 mmol, 1.0 equiv) and the resulting solution was stirred for 13 h at rt. The reaction mixture was then concentrated and the residue chromatographed on silica gel (CH_2Cl_2) to afford **43** (424 mg, 49%) as a reddish-brown solid. The product exists as two rotamers in DMSO at room temperature in a ratio of 6:1. Major rotamer: ^{1}H NMR (500 MHz, DMSO-d_6): δ = 9.47 (s, 1H), 4.74 (s, 3H), 1.39 (s, 9H). Minor rotamer: ^{1}H NMR (500 MHz, DMSO-d_6): δ = 9.67 (s, 1H), 4.67 (s, 3H), 1.53 (s, 9H).

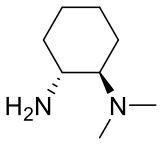

44

(**44**). Diamine **44** was prepared according to the literature.[8]

[8] Suez, G.; Bloch, V.; Nisnevich, G.; Gandelman, M. *Eur. J. Org. Chem*. **2012**, *2012*, 2118.

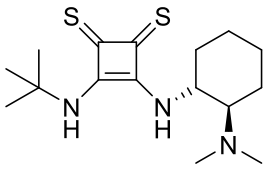

45

(**45**). To a solution of **43** (323 mg, 1.0 mmol, 1.50 equiv) in dry CH_2Cl_2 (5 mL) was added diamine **44** (214 mg, 1.5 mmol, 1.00 equiv) and the resulting solution was stirred for 1 h at rt. The reaction mixture was then concentrated and the reddish-brown solid thus obtained was washed with ice-cold CH_2Cl_2 to afford **45** (227 mg, 47%) as a yellow solid. Several milligrams of **45** were suspended in a 1:2 hexanes:CH_2Cl_2 solution, and a few drops of MeOH were added to achieve total dissolution. Slow evaporation yielded crystals suitable for X-ray analysis. ^{1}H NMR (500 MHz, DMSO-d_6): δ = 8.68 (d, J = 8.7 Hz, 1H), 8.63 (s, 1H), 4.90 (m, 1H), 2.45 (m, 1H), 2.20 (s, 6H), 2.06 (m, 1H), 1.86 (m, 1H), 1.74 (m, 1H), 1.64 (m, 1H), 1.60 (s, 9H), 1.33 (m, 1H), 1.20 (m, 3H). ^{13}C NMR (125 MHz, DMSO-d_6): δ = 204.6, 201.8, 171.2, 170.6, 65.6, 54.5, 53.9, 39.8, 35.3, 31.1, 24.1, 21.0. HRMS (ESI) calcd for $C_{16}H_{28}N_3S_2^+(M+H)^+$: 326.1719, Found: 326.1716. IR (film): 2929, 1695, 1559, 1480, 1281, 1226, 1144 cm^{-1}

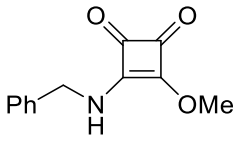

46

(**46**). To a solution of dimethylsquarate (2.01 g, 14.1 mmol, 1.00 equiv) in CH_2Cl_2 (10 mL) was added benzylamine (1.62 mL, 14.8 mmol, 1.05 equiv) and the resulting solution was stirred for 24 h at rt. The reaction mixture was then diluted with 100 mL CH_2Cl_2 and washed sequentially with 50 mL 1 M HCl and 50 mL water and then dried with $MgSO_4$. Removal of solvent afforded **46** (2.66 g, 87%) as a white solid. The product exists as two rotamers in DMSO at room

temperature in a ratio of nearly 1:1. ^{1}H NMR (500 MHz, DMSO-d_6): δ = 9.28 (s, 1H), 9.06 (s, 1H), 7.26-7.40 (m, 5H) x2, 4.68 (d, *J* = 6.2 Hz, 2H), 4.46 (d, *J* = 6.3 Hz, 2H), 4.30 (s, 3H), 4.28 (s, 3H).

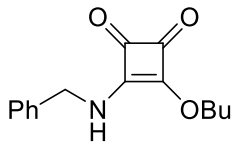

49

(**49**). To a solution of dibutylsquarate (1.19 g, 5.26 mmol, 1.00 equiv) in CH_2Cl_2 (15 mL) was added benzylamine (0.60 mL, 5.52 mmol, 1.05 equiv) dropwise at 0 °C. The mixture was stirred at 0 °C for 30 min then at room temperature for 6 h. The reaction mixture was then concentrated and the residue was chromatographed on silica gel (CH_2Cl_2 → 10% MeOH in CH_2Cl_2) to afford **49** (1.33 g, 98%) as a white solid. The product exists as two rotamers in DMSO at room temperature in a ratio of 1.3:1. Major rotamer: ^{1}H NMR (500 MHz, DMSO-d_6): δ = 9.31 (s, 1H), 7.33 (m, 5H), 4.62 (t, *J* = 6.4 Hz, 2H), 4.47 (d, *J* = 6.1 Hz, 2H), 1.69 (m, 2H), 1.34 (m, 2H), 0.89 (m, 3H). Minor rotamer: ^{1}H NMR (500 MHz, DMSO-d_6): δ = 9.07 (s, 1H), 7.33 (m, 5H), 4.67 (d, *J* = 6.1 Hz, 2H), 4.62 (t, *J* = 6.4 Hz, 2H), 1.69 (m, 2H), 1.34 (m, 2H), 0.89 (m, 3H). ^{13}C NMR (125 MHz, $CDCl_3$): δ = 189.4, 189.0, 182.4, 182.1, 177.4, 176.8, 172.6, 171.9, 138.4, 138.1, 128.5, 128.3, 127.5, 127.4, 127.2, 72.4, 47.2, 46.8, 31.4, 18.0, 13.4. HRMS (ESI) calcd for $C_{15}H_{18}NO_3^+(M+H)^+$: 260.1281, Found: 260.1279. IR (film): 3257, 2960, 1804, 1707, 1601, 1412, 1345, 1063, 700 cm^{-1}

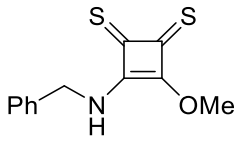

47

(**47**). To a solution of **46** (650 mg, 3.0 mmol, 1.0 equiv) in dry MeCN (32 mL) was added P_2S_5·pyridine complex (1.47 g, 3.9 mmol, 1.3 equiv) at rt and the resulting solution was then placed in a preheated oil bath and heated at 55 °C for 1 h. The reaction was then concentrated and the residue chromatographed on silica gel (CH_2Cl_2) to afford **47** (2.66 g, 87%) as an orange solid. The product exists as two rotamers in DMSO at room temperature in a ratio of 1.2:1. Major rotamer: ^{1}H NMR (500 MHz, DMSO-d_6): δ = 10.23 (t, *J* = 6.2 Hz, 1H), 7.35 (m, 5H), 4.69 (s, 3H), 4.57 (d, *J* = 6.5 Hz, 2H). Minor rotamer: ^{1}H NMR (500 MHz, DMSO-d_6): δ = 10.19 (t, *J* = 6.2 Hz, 1H), 7.35 (m, 5H), 5.21 (d, *J* = 6.5 Hz, 2H), 4.63 (s, 3H).

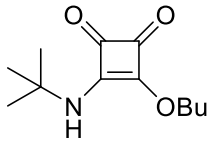

51

(**51**). To a solution of dibutylsquarate (1.19 g, 5.26 mmol, 1.00 equiv) in CH_2Cl_2 (5 mL) was added *tert*-butylamine (0.58 mL, 5.52 mmol, 1.05 equiv). The mixture was stirred at room temperature for 20 h. The reaction was then concentrated and the residue was chromatographed on silica gel (CH_2Cl_2) to afford **51** (871 mg, 74%) as a white solid. The product exists as two rotamers in DMSO at room temperature in a ratio of 1.2:1. Major rotamer: ^{1}H NMR (500 MHz, DMSO-d_6): δ = 8.77 (s, 1H), 4.72 (s, 2H), 1.72 (dt, *J* = 14.3, 6.5 Hz, 2H), 1.40 (td, *J* = 14.9, 7.5 Hz, 2H), 1.30 (s, 9H), 0.91 (t, *J* = 7.4 Hz, 3H). Minor rotamer: ^{1}H NMR (500 MHz, DMSO-d_6): δ = 8.60 (s, 1H), 4.63 (s, 2H), 1.72 (dt, *J* = 14.3, 6.5 Hz, 2H), 1.40 (td, *J* = 14.9, 7.5 Hz, 2H),

1.34 (s, 9H), 0.91 (t, *J* = 7.4 Hz, 3H). ^{13}C NMR (125 MHz, DMSO-*d*$_6$): δ = 189.9, 187.9, 182.7, 181.7, 178.3, 175.3, 173.0, 171.2, 72.4, 72.2, 52.9, 52.3, 31.5, 30.0, 29.6, 18.1, 13.4. HRMS (ESI) calcd for $C_{12}H_{20}NO_3^+$ $(M+H)^+$: 226.1438, Found: 226.1431. IR (film): 3255, 2966, 1799, 1705, 1598, 1435, 1368, 1215 cm^{-1}

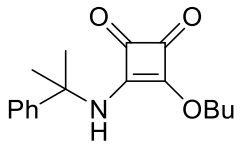

52

(**52**). To a solution of dibutylsquarate (1.58 g, 7.0 mmol, 1.0 equiv) in CH_2Cl_2:MeOH (9 mL:3 mL) was added cumylamine (1.1 mL, 7.7 mmol, 1.1 equiv). The mixture was stirred at room temperature for 24 h. The solvent was then concentrated and the residue was chromatographed on silica gel (CH_2Cl_2) to afford the desired product **52** (1.67 g, 83%) as a white solid. The product exists as two rotamers in DMSO at room temperature in a ratio of 2.6:1. Major rotamer: ^{1}H NMR (500 MHz, DMSO-*d*$_6$): δ = 9.30 (s, 1H), 7.31 (m, 4H), 7.22 (m, 1H), 4.30 (t, *J* = 5.5 Hz, 2H), 1.62 (s, 6H), 1.25 (m, 2H), 0.93 (m 2H), 0.73 (t, *J* = 7.0 Hz, 3H). Minor rotamer: ^{1}H NMR (500 MHz, DMSO-*d*$_6$): δ = 9.05 (s, 1H), 7.31 (m, 4H), 7.22 (m, 1H), 4.65 (s, 2H), 1.75 (m, 2H), 1.69 (s, 6H), 1.42 (m, 2H), 0.93 (m, 3H). ^{13}C NMR (125 MHz, DMSO-*d*$_6$): δ = 189.5, 183.3, 176.7, 171.9, 146.6, 128.2, 126.4, 124.7, 71.6, 57.5, 31.1, 30.5, 17.7, 13.3. HRMS (ESI) calcd for $C_{17}H_{22}NO_3^+$ $(M+H)^+$: 288.1594, Found: 288.1593. IR (film): 3264, 2962, 1803, 1706, 1598, 1414, 1352, 1179, 700 cm^{-1}

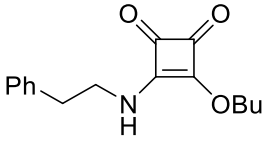

53

(**53**). To a solution of dibutylsquarate (634 mg, 2.80 mmol, 1.00 equiv) in CH_2Cl_2 (3 mL) was added phenethylamine (0.37 mL, 2.94 mmol, 1.05 equiv). The mixture was stirred at room temperature for 1.5 h. The reaction was filtered and the residue chromatographed on silica gel (5% MeOH in CH_2Cl_2) to afford the desired product **53** (604 mg, 79%) as a white solid. The product exists as two rotamers in DMSO at room temperature in a ratio of 1.6:1. Major rotamer: ^{1}H NMR (500 MHz, DMSO-d_6): δ = 8.88 (t, *J* = 5.8 Hz, 1H), 7.29 (t, *J* = 7.4 Hz, 2H), 7.20 (m, 3H), 4.57 (m, 2H), 3.50 (dd, *J* = 13.7, 6.8 Hz, 2H), 2.82 (m, 2H), 1.69 (m, 2H), 1.37 (m, 2H), 0.91 (t, *J* = 7.4 Hz, 3H). Minor rotamer: ^{1}H NMR (500 MHz, DMSO-d_6): δ = 8.67 (t, *J* = 5.7 Hz, 1H), 7.29 (t, *J* = 7.4 Hz, 2H), 7.20 (m, 3H), 4.57 (m, 2H), 3.71 (dd, *J* = 13.7, 6.8 Hz, 2H), 2.82 (m, 2H), 1.69 (m, 2H), 1.37 (m, 2H), 0.91 (t, *J* = 7.4 Hz, 3H). ^{13}C NMR (125 MHz, DMSO-d_6): δ = 189.2, 189.0, 182.1, 182.0, 177.0, 176.6, 172.5, 172.2, 138.2, 128.7, 128.3, 126.3, 72.2, 45.2, 44.7, 36.5, 36.2, 31.4, 18.1, 18.0, 13.4. HRMS (ESI) calcd for $C_{16}H_{20}NO_3^+$ $(M+H)^+$: 274.1438, Found: 274.1434. IR (film): 3157, 2958, 1800, 1710, 1587, 1416, 1378 cm^{-1}

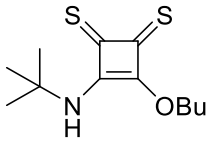

54

(**54**). To a solution of **51** (451 mg, 2.0 mmol, 1.0 equiv) in dry CH_2Cl_2 (10 mL) was added Lawesson's reagent (809 mg, 2.0 mmol, 1.0 equiv). The mixture was stirred at room temperature for 5 h. The reaction mixture was then concentrated and the residue chromatographed on silica gel (CH_2Cl_2) to afford the desired product **54** (452 mg, 88%) as an orange solid. Major rotamer: ^{1}H NMR (500 MHz, DMSO-d_6): δ = 9.48 (s, 1H), 5.26 (t, *J* = 6.3 Hz, 2H), 1.81 (m, 2H), 1.45 (m, 2H), 1.39 (s, 9H), 0.93 (t, *J* = 7.4 Hz, 3H). ^{13}C NMR (125 MHz, DMSO-d_6): δ = 218.5, 205.1, 181.1, 173.5, 73.5, 54.9, 54.1, 31.8, 31.7, 30.9, 29.6, 18.1, 17.9, 13.4. HRMS (ESI) calcd for

$C_{12}H_{20}NOS_2^+(M+H)^+$: 258.0981, Found: 258.0980. IR (film): 3223, 2959, 1671, 1514, 1433, 1327, 980 cm^{-1}

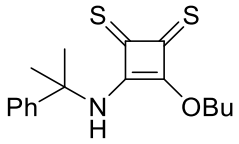

55

(**55**). To a solution of **52** (862 mg, 3.0 mmol, 1.0 equiv) in dry CH_2Cl_2 (15 mL) was added Lawesson's reagent (1.21 g, 3.0 mmol, 1.0 equiv). The mixture was stirred at room temperature for 5 h. The reaction mixture was then concentrated and the residue chromatographed on silica gel (CH_2Cl_2) to afford the desired product **55** (796 mg, 83%) as an orange solid. Major rotamer: ^{1}H NMR (500 MHz, DMSO-d_6): δ = 10.10 (s, 1H), 7.34 (m, 4H), 7.27 (m, 1H), 4.83 (t, *J* = 6.2 Hz, 2H), 1.72 (s, 6H), 1.30 (m, 2H), 0.97 (m, 2H), 0.75 (t, *J* = 7.4 Hz, 3H). ^{13}C NMR (125 MHz, DMSO-d_6): δ = 218.0, 206.2, 181.9, 174.6, 146.2, 128.4, 126.8, 124.7, 72.8, 59.0, 31.2, 30.5, 17.6, 13.3. HRMS (ESI) calcd for $C_{17}H_{22}NOS_2^+(M+H)^+$: 320.1137, Found: 320.1134. IR (film): 3239, 2959, 1676, 1508, 1422, 1315, 1187, 1025 cm^{-1}

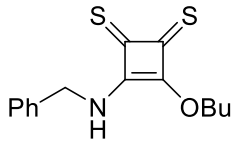

50

(**50**). To a solution of **49** (778 mg, 3.0 mmol, 1.0 equiv) in dry CH_2Cl_2 (14 mL) was added Lawesson's reagent (1.21 g, 3.0 mmol, 1.0 equiv). The mixture was stirred at room temperature for 3 h. The reaction mixture was then concentrated and the residue chromatographed on silica gel (CH_2Cl_2) to afford the desired product **50** (502 mg, 57%) as an orange solid. The product exists as two rotamers in DMSO at room temperature in a ratio of 1.4:1. Major rotamer: ^{1}H NMR

(500 MHz, DMSO-d_6): δ = 10.27 (t, J = 6.2 Hz, 1H), 7.35 (m, 5H), 5.16 (m, 2H), 4.58 (d, J = 6.5 Hz, 2H), 1.77 (m, 2H), 1.38 (m, 2H), 0.90 (m, 3H). Minor rotamer: ^{1}H NMR (500 MHz, DMSO-d_6): δ = 10.21 (t, J = 6.4 Hz, 1H), 7.35 (m, 5H), 5.16 (m, 4H), 1.77 (m, 2H), 1.38 (m, 2H), 0.90 (m, 3H). ^{13}C NMR (125 MHz, DMSO-d_6): δ = 217.7, 217.4, 205.4, 205.4, 183.5, 182.8, 174.6, 172.4, 137.2, 137.0, 128.6, 128.6, 127.8, 127.7, 127.6, 127.5, 73.5, 73.5, 48.0, 46.0, 31.7, 31.6, 17.9, 13.4, 13.4. HRMS (ESI) calcd for $C_{15}H_{18}NOS_2^+(M+H)^+$: 292.0824, Found: 292.0818. IR (film): 3231, 2958, 1694, 1521, 1290, 1107 cm^{-1}

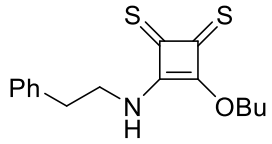

56

(**56**). To a solution of **53** (273 mg, 1.0 mmol, 1.0 equiv) in dry CH_2Cl_2 (3 mL) was added Lawesson's reagent (404 mg, 1.0 mmol, 1.0 equiv). The mixture was stirred at room temperature for 2 h. The reaction mixture was then concentrated and the residue chromatographed on silica gel (CH_2Cl_2) to afford the desired product **56** (158 mg, 52%) as an orange solid. The product exists as two rotamers in DMSO at room temperature in a ratio of 2.2:1. Major rotamer: ^{1}H NMR (500 MHz, DMSO-d_6): δ = 9.83 (s, 1H), 7.30 (m, 2H), 7.21 (m, 3H), 5.07 (t, J = 6.5 Hz, 2H), 3.62 (m, 2H), 2.91 (m, 2H), 1.76 (m, 2H), 1.40 (m, 2H), 0.92 (m, 3H). Minor rotamer: ^{1}H NMR (500 MHz, DMSO-d_6): δ = 9.83 (s, 1H), 7.30 (m, 2H), 7.21 (m, 3H), 5.11 (t, J = 6.6 Hz, 2H), 4.15 (m, 2H), 2.91 (m, 2H), 1.76 (m, 2H), 1.40 (m, 2H), 0.92 (m, 3H). ^{13}C NMR (125 MHz, DMSO-d_6): δ = 217.6, 204.6, 183.3, 182.6, 174.5, 137.8, 137.8, 128.7, 128.7, 128.3, 128.3, 126.5, 126.4, 73.3, 73.3, 46.1, 44.1, 36.5, 35.7, 31.7, 31.6, 17.9, 17.9, 13.4, 13.4. HRMS (ESI) calcd for $C_{16}H_{20}NOS_2^+(M+H)^+$: 306.0981, Found: 306.0977. IR (film): 3127, 2957, 1693, 1520, 1296, 990 cm^{-1}

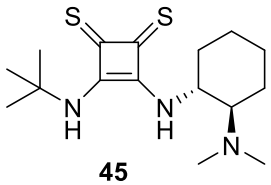

45

(**45**). To a solution of **54** (162 mg, 0.63 mmol, 1.05 equiv) in dry Et_2O (16 mL) at 0 °C was added diamine **44** (86 mg, 0.60 mmol, 1.00 equiv) in 4 mL dry Et_2O. The mixture was stirred at 0 °C for 5 min, then allowed to warm to room temperature and stirred an additional 1 h. The reaction mixture was then concentrated and the yellow solid thus obtained was washed with ice-cold CH_2Cl_2 to afford the desired product **45** (143 mg, 73%) as a yellow solid. Analytical data matched the above reported data.

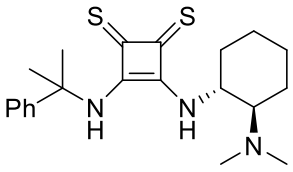

57

(**57**). To a solution of **55** (118 mg, 0.83 mmol, 1.0 equiv) in dry CH_2Cl_2 (5 mL) was added diamine **44** (265 mg, 0.83 mmol, 1.0 equiv). The mixture was stirred at room temperature for 0.5 h. The reaction mixture was then concentrated and the yellow solid thus obtained was washed with Et_2O to afford the desired product **57** (220 mg, 69%) as a yellow solid. ^1H NMR (500 MHz, DMSO-d_6): δ = 8.90 (s, 1H), 8.77 (d, *J* = 8.1 Hz, 1H), 7.48 (d, *J* = 7.4 Hz, 2H), 7.38 (t, *J* = 7.7 Hz, 2H), 7.29 (t, *J* = 7.3 Hz, 1H), 4.91 (br s, 1H), 2.44 (br s, 1H), 2.21 (s, 6H), 2.08 (m, 1H), 2.01 (s, 3H), 2.00 (s, 3H), 1.86 (m, 1H), 1.75 (m, 1H), 1.66 (m, 1H), 1.35 (m, 1H), 1.22 (m, 3H). ^{13}C NMR (125 MHz, $CDCl_3$): δ = 205.6, 201.9, 171.5, 170.6, 146.3, 128.3, 127.1, 125.4, 65.6, 59.2, 53.9, 35.3, 31.6, 31.3, 24.1, 21.1. HRMS (ESI) calcd for $C_{21}H_{30}N_3S_2^+(M+H)^+$: 388.1876, Found: 388.1875. IR (film): 3168, 2934, 1694, 1558, 1237 cm^{-1}

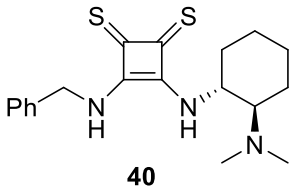

40

(**40**). To a solution of **50** (178 mg, 0.61 mmol, 1.05 equiv) in dry Et_2O (14 mL) at 0 °C was added diamine **44** (83 mg, 0.58 mmol, 1.00 equiv) in 3 mL dry Et_2O. The mixture was stirred at 0 °C for 0.5 h, then allowed to warm to room temperature and stirred an additional 0.5 h. The reaction mixture was then concentrated and the orange solid thus obtained was washed with Et_2O to afford the desired product **40** (141 mg, 67%) as an orange solid. The product is rotameric in DMSO at room temperature. ^{1}H NMR (500 MHz, DMSO-d_6, T = 60 °C): δ = 8.89 (br s, 1H), 8.49 (br s, 1H), 7.41 (m, 4H), 7.34 (m, 1H), 5.33 (m, 2H), 4.89 (s, 1H), 2.57 (m, 1H), 2.29 (s, 6H), 2.11 (m, 1H), 1.89 (br s, 1H), 1.77 (br s, 1H), 1.66 (br s, 1H), 1.36 (m, 1H), 1.24 (m, 3H). ^{13}C NMR (125 MHz, DMSO-d_6): δ = 203.8, 202.8, 170.1, 169.9, 137.4, 128.7, 128.1, 127.8, 65.7, 64.7, 53.4, 47.0, 45.9, 35.0, 30.1, 24.3, 24.0, 24.0, 23.6, 21.2. HRMS (ESI) calcd for $C_{19}H_{26}N_3S_2^+(M+H)^+$: 360.1563, Found:360.1561. IR (film): 3173, 2935, 1709, 1576, 1453, 1234 cm^{-1}

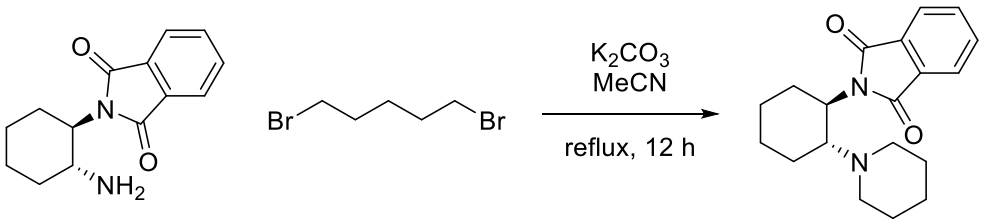

299 **300**

(**300**). To a solution of **299**[9] (1.51 g, 6.18 mmol, 1.0 equiv) and 1,5-dibromopentane (1.56 g, 6.80 mmol, 1.1 equiv) in dry MeCN (30 mL) was added K_2CO_3 (1.88 g, 13.59 mmol, 2.2 equiv) at room temperature. The reaction mixture was then brought to reflux. After 12 h at reflux, the reaction was allowed to cool and diluted with water. The reaction mixture was then extracted three times with CH_2Cl_2, dried with $MgSO_4$, and concentrated. The residue was chromatographed on silica gel ($CHCl_3$) to afford impure **300**, which was further purified by heating on the Kugelrohr to remove remaining starting material. The resulting residue was allowed to solidify, and was then ground up and washed with Et_2O to afford pure **300** (1.51 g, 78%) as a light yellow solid. ^{1}H NMR (500 MHz, $CDCl_3$): δ = 7.81 (dd, *J* = 5.4, 3.1 Hz, 2H), 7.69 (dd, *J* = 5.4, 3.0 Hz, 2H), 4.13 (td, *J* = 11.9, 4.0 Hz, 1H), 3.16 (td, *J* = 11.5, 3.4 Hz, 1H), 2.56 (m, 2H), 2.24 (m, 3H), 1.86 (m, 4H), 1.28 (m, 9H). ^{13}C NMR (125 MHz, $CDCl_3$): δ = 169.1, 133.7, 132.5, 123.0, 63.9, 52.5, 50.0, 30.3, 27.1, 26.0, 25.6, 25.1, 24.8. HRMS (ESI) calcd for $C_{19}H_{25}N_2O_2^+(M+H)^+$: 313.1911, Found: 313.1916. IR (film): 2930, 2854, 2799, 1766, 1707, 1391, 1371, 718 cm^{-1}

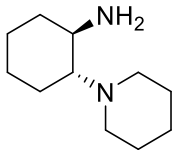

301

(**301**). To a solution of **300** (446 mg, 1.43 mmol, 1.0 equiv) in EtOH (4 mL) was added H_2NNH_2 (33 wt.% in H_2O, 0.54 mL, 5.72 mmol, 4.0 equiv). The reaction was placed in a preheated oil bath and refluxed for 1 h, after which time it was allowed to cool to room temperature. Et_2O (20 mL) was added, and the slurry was stirred at 0 °C for 15 min. The mixture was then filtered, and

[9] Kaik, M.; Gawroński, J. *Tetrahedron: Asymmetry* **2003**, *14*, 1559.

the filtrate concentrated to afford the desired product **301** (161 mg, 62%) as a pale yellow oil. Analytical data matched previously reported values.[10]

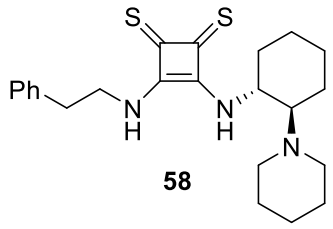

58

(**58**). To a solution of **56** (125 mg, 0.41 mmol, 1.05 equiv) in dry Et_2O (15 mL) was added diamine **301** (71 mg, 0.39 mmol, 1.00 equiv) in 5 mL dry Et_2O. The mixture was stirred at room temperature for 10 min. The reaction mixture was then concentrated and the orange solid thus obtained was washed with Et_2O to afford the desired product **58** (120 mg, 74%) as an orange solid. The product is rotameric in DMSO at room temperature. ^{1}H NMR (500 MHz, DMSO-d_6, T = 60 °C): δ = 8.49 (br s, 1H), 8.36 (br s, 1H), 7.31 (m, 4H), 7.23 (m, 1H), 4.89 (br s, 1H), 4.30 (m, 2H), 2.97 (t, *J* = 7.1 Hz, 2H), 2.70 (m, 2H), 2.35 (m, 3H), 2.08 (m, 1H), 1.88 (br s, 1H), 1.75 (br s, 1H), 1.66 (br s, 1H), 1.33 (m, 10H). ^{13}C NMR (125 MHz, DMSO-d_6): δ = 203.8, 202.9, 170.6, 170.2, 138.0, 128.7, 128.3, 126.4, 67.2, 53.2, 49.1, 43.8, 37.1, 34.7, 26.0, 24.4, 24.2, 24.1, 23.3. HRMS (ESI) calcd for $C_{23}H_{32}N_3S_2^+$ $(M+H)^+$: 414.2032, Found: 414.2033. IR (film): 3176, 2932, 1708, 1576, 1451, 1238 cm^{-1}

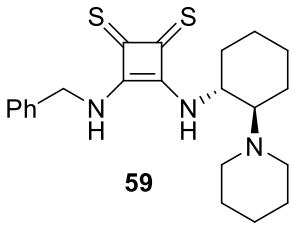

59

[10] Baran, R.; Veverkova, E.; Skvorcova, A.; Sebesta, R. *Org. Biomol. Chem*. **2013**, *11*, 7705.

(**59**). To a solution of **50** (306 mg, 1.05 mmol, 1.05 equiv) in dry Et_2O (26 mL) at 0 °C was added diamine **301** (182 mg, 1.00 mmol, 1.00 equiv) in 4 mL dry Et_2O. The mixture was stirred at 0 °C for 5 min, then allowed to warm to room temperature and stirred an additional 1 h. The reaction mixture was then concentrated and the orange solid thus obtained was washed with pentane to afford the desired product **59** (332 mg, 83%) as an orange solid. The product is rotameric in DMSO at room temperature. ^{1}H NMR (500 MHz, DMSO-*d*$_6$, T = 60 °C): δ = 8.74 (br s, 1H), 8.25 (br s, 1H), 7.38 (m, 5H), 5.34 (m, 2H), 4.87 (br s, 1H), 2.68 (m, 2H), 2.30 (m, 3H), 2.10 (m, 1H), 1.87 (br s, 1H), 1.75 (br s, 1H), 1.66 (br s, 1H), 1.27 (m, 10H). ^{13}C NMR (125 MHz, DMSO-*d*$_6$): δ = 204.4, 201.5, 170.3, 170.2, 137.6, 137.4, 128.7, 128.5, 128.4, 127.9, 127.8, 127.7, 127.3, 67.4, 66.9, 55.5, 53.4, 49.7, 49.1, 46.0, 45.9, 45.5, 34.5, 26.2, 24.8, 24.5, 24.3, 24.1, 23.8, 23.3. HRMS (ESI) calcd for $C_{22}H_{30}N_3S_2^+$(M+H)$^+$: 400.1876, Found: 400.1869. IR (film): 3173, 2931, 1707, 1575, 1451, 1233 cm^{-1}

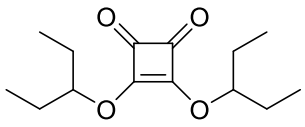

61

(**61**). To a suspension of squaric acid (3.42 g, 30 mmol, 1.0 equiv) in PhMe (21 mL) was added 3-pentanol (21 mL, 195 mmol, 6.5 equiv) and the resulting mixture was refluxed in a Dean-Stark apparatus. After 24 h, the reaction mixture was concentrated. Purification by flash column chromatography (CH_2Cl_2 → 3% MeOH in CH_2Cl_2) afforded **61** (5.92 g, 78%) as an oil. ^{1}H NMR (500 MHz, $CDCl_3$): δ = 5.03 (p, *J* = 6.1 Hz, 2H), 1.76 (m, 8H), 0.98 (t, *J* = 7.4 Hz, 12H). ^{13}C NMR (125 MHz, $CDCl_3$): δ = 189.7, 184.5, 88.8, 27.5, 9.5. HRMS (ESI) cald for $C_{14}H_{22}O_4$ (M+H)$^+$: 255.1591. Found: 255.1593. IR (film): 1812, 1733, 1596 cm^{-1}

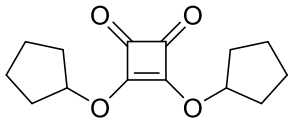

62

(**62**). To a suspension of squaric acid (4.56 g, 40 mmol, 1.0 equiv) in PhMe (30 mL) was added cyclopentanol (24 mL, 264 mmol, 6.5 equiv) and the resulting mixture was refluxed with Dean-Stark apparatus. After 7 h, the reaction mixture was concentrated. Purification by flash column chromatography (CH_2Cl_2 → 1% MeOH in CH_2Cl_2 → 2% MeOH in CH_2Cl_2) gave a brown solid, which was washed with ice-cold hexanes to afford **62** (7.31 g, 73%) as a white solid. ^{1}H NMR (500 MHz, $CDCl_3$): δ = 5.54 (tt, *J* = 5.3, 2.5 Hz, 2H), 1.96 (m, 8H), 1.81 (m, 4H), 1.68 (m, 4H). ^{13}C NMR (125 MHz, $CDCl_3$): δ = 189.8, 184.3, 88.1, 33.9, 23.8. HRMS (ESI) cald for $C_{14}H_{18}O_4$ $(M+H)^+$: 251.1278. Found: 251.1283. IR (film): 1721 cm^{-1}.

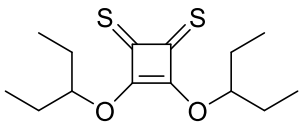

61a

(**61a**). To a solution of Lawesson's reagent (4.33 g, 10.7 mmol, 1.0 equiv) in dry CH_2Cl_2 (45 mL) was added **61** (2.71 g, 10.7 mmol, 1.0 equiv). The reaction was stirred for 46 h, during which time dry CH_2Cl_2 was added as needed to maintain constant volume. The reaction mixture was then gravity filtered, concentrated to roughly half the original volume, and immediately loaded onto column. Quickly eluting with 1:1 hexanes:CH_2Cl_2 afforded **61a** (2.46 g, 80%) as a red oil. ^{1}H NMR (500 MHz, $CDCl_3$): δ = 5.69 (m, 2H), 1.82 (m, 8H), 1.01 (t, *J* = 7.4 Hz, 12H). ^{13}C NMR (125 MHz, $CDCl_3$): δ = 218.6, 186.6, 89.2, 27.6, 9.4. HRMS (ESI) cald for $C_{14}H_{22}O_2S_2$ $(M+H)^+$: 287.1134. Found: 287.1119. IR (film): 1648 cm^{-1}

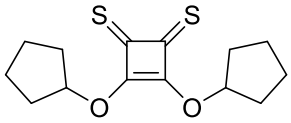

60a

(**60a**). To a solution of Lawesson's reagent (3.70 g, 9.15 mmol, 1.0 equiv) in dry CH_2Cl_2 (40 mL) was added **62** (2.29 g, 9.15 mmol, 1.0 equiv). The reaction was stirred for 37 h, during which time dry CH_2Cl_2 was added as needed to maintain constant volume. The reaction mixture was then gravity filtered, concentrated to roughly half the original volume, and immediately loaded onto column. Quickly eluting with 1:1 hexanes:CH_2Cl_2 afforded **60a** (1.83 g, 71%) as an amorphous orange solid. ^{1}H NMR (500 MHz, $CDCl_3$): δ = 6.06 (m, 2H), 2.02 (m, 8H), 1.86 (m, 4H), 1.70 (m, 4H). ^{13}C NMR (125 MHz, $CDCl_3$): δ = 218.8, 186.3, 88.9, 34.4, 23.9. HRMS (ESI) cald for $C_{14}H_{18}O_2S_2$ $(M+H)^+$: 283.0821. Found: 283.0733. IR (film): 1648 cm^{-1}

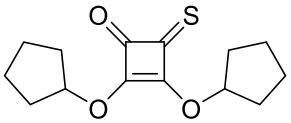

60b

(**60b**). To a solution of Lawesson's reagent (737 mg, 1.82 mmol, 0.5 equiv) in dry CH_2Cl_2 (8 mL) was added **62** (911 mg, 3.64 mmol, 1.0 equiv). After 25 h, the reaction mixture was concentrated to roughly half the original volume and immediately loaded onto column. Quickly eluting with 1:1 hexanes:CH_2Cl_2 → CH_2Cl_2 afforded **60b** (659 mg, 68%) as a pink solid. ^{1}H NMR (500 MHz, $CDCl_3$): δ = 5.88 (m, 1H), 5.58 (tt, *J* = 5.3, 2.6 Hz, 1H), 1.99 (m, 8H), 1.83 (m, 4H), 1.70 (m, 4H). ^{13}C NMR (125 MHz, $CDCl_3$): δ = 223.2, 187.7, 185.2, 185.0, 89.3, 88.0, 34.1, 33.9, 23.9, 23.7. HRMS (ESI) cald for $C_{14}H_{18}O_3S$ $(M+Na)^+$: 289.0869. Found: 289.0841. IR (film): 1780, 1612 cm^{-1}.

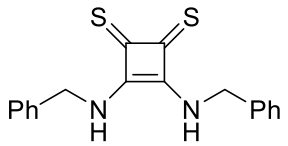

63

(**63**). To a solution of **60a** (141 mg, 0.50 mmol, 1.0 equiv) in dry CH_2Cl_2 (1 mL) was added benzylamine (115 µL, 1.05 mmol, 2.1 equiv) at 0 °C and the resulting solution was stirred for 5 min at that temperature, then 1.5 h at room temperature. 1 mL hexanes was then added and the suspension filtered to afford **63** (139 mg, 86%) as an amorphous yellow solid. The compound exists as three rotamers in DMSO at room temperature in a ratio of 26:9:2. Major rotamer: ^{1}H NMR (500 MHz, DMSO-d_6): δ = 8.81 (t, *J* = 6.2 Hz, 2H), 7.34 (m, 10H), 5.31 (d, *J* = 6.4 Hz, 4H). ^{13}C NMR (125 MHz, DMSO-d_6): δ = 204.1, 170.0, 137.4, 128.7, 128.0, 127.7, 46.0. HRMS (ESI) cald for $C_{18}H_{16}N_2S_2$ $(M+H)^+$: 325.0828. Found: 325.0826. IR (film): 1708, 1569 cm^{-1}

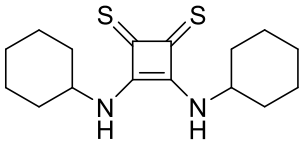

64

(**64**). To a solution of **60a** (141 mg, 0.50 mmol, 1.0 equiv) in dry CH_2Cl_2 (1 mL) was added cyclohexylamine (120 µL, 1.05 mmol, 2.1 equiv) at 0 °C and the resulting solution was stirred for 5 min at that temperature, then 2 h at room temperature. 1 mL hexanes was then added and the suspension filtered to afford **64** (92 mg, 60%) as an amorphous yellow solid. Major rotamer: ^{1}H NMR (500 MHz, DMSO-d_6): δ = 8.40 (d, *J* = 8.6 Hz, 2H), 4.70 (m, 2H), 1.05-2.10 (m, 20H). ^{13}C NMR (125 MHz, DMSO-d_6): δ = 203.5, 169.6, 51.6, 33.5, 24.5, 23.8. HRMS (ESI) cald for $C_{16}H_{24}N_2S_2$ $(M+H)^+$: 309.1454. Found: 309.1451. IR (film): 1705, 1567 cm^{-1}

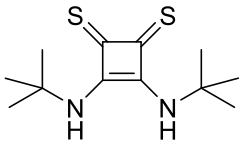

65

(**65**). To a solution of **60a** (141 mg, 0.50 mmol, 1.0 equiv) in dry CH_2Cl_2 (1 mL) was added *tert*-butyl amine (110 µL, 1.05 mmol, 2.1 equiv) at 0 °C and the resulting solution was stirred for 5 min at that temperature, then 2 h at room temperature. 1 mL hexanes was then added and the suspension filtered to afford **65** (39 mg, 30%) as an amorphous yellow solid. ^{1}H NMR (500 MHz, DMSO-d_6): δ = 8.70 (s, 2H), 1.60 (s, 18H). ^{13}C NMR (125 MHz, DMSO-d_6): δ = 203.9, 172.1, 54.6, 31.0. HRMS (ESI) cald for $C_{12}H_{20}N_2S_2$ $(M+H)^+$: 257.1141. Found: 257.1142. IR (film): 1682, 1546 cm^{-1}

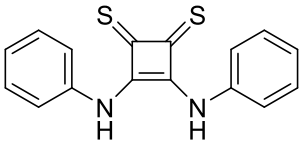

66

(**66**). To a solution of **60a** (94 mg, 0.33 mmol, 1.0 equiv) in dry CH_2Cl_2 (1 mL) was added aniline (90 µL, 0.99 mmol, 3.0 equiv) and the resulting solution stirred for 20 h, during which time a yellow precipitate appeared. 1 mL hexanes was then added and the suspension filtered to afford **66** (76 mg, 79%) as an amorphous yellow solid. Analytical data matched previously reported values:[11] ^{1}H NMR (500 MHz, DMSO-d_6): δ = 10.86 (s, 2H), 6.90-7.40 (m, 10H). ^{13}C NMR (125 MHz, DMSO-d_6): δ = 207.9, 169.4, 136.9, 128.5, 125.3, 122.1.

[11] Busschaert, N.; Elmes, R. B. P.; Czech, D. D.; Wu, X.; Kirby, I. L.; Peck, E. M.; Hendzel, K. D.; Shaw, S. K.; Chan, B.; Smith, B. D.; Jolliffe, K. A.; Gale, P. A. *Chem. Sci.* **2014**, *5*, 3617.

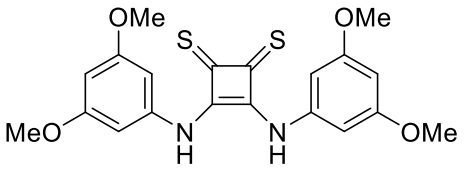

67

(**67**). To a solution of **60a** (85 mg, 0.30 mmol, 1.0 equiv) in dry CH_2Cl_2 (0.7 mL) was added 3,5-dimethoxyaniline (97 mg, 0.63 mmol, 2.1 equiv) and the resulting solution was stirred for 40 h, during which time a yellow precipitate formed. 1 mL hexanes was then added and the suspension filtered to afford **67** (95 mg, 77%) as an amorphous yellow solid. ^{1}H NMR (500 MHz, CD_3CN): δ = 8.72 (s, 2H), 6.31 (s, 4 H), 6.12 (s, 2H), 3.68 (s, 12H). ^{13}C NMR (125 MHz, DMSO-d_6): δ = 169.7, 160.2, 139.0, 100.5, 97.7, 55.1. HRMS (ESI) cald for $C_{20}H_{20}N_2O_4S_2$ $(M+H)^+$: 417.0937. Found: 417.0939. IR (film): 1694, 1597, 1540 cm^{-1}

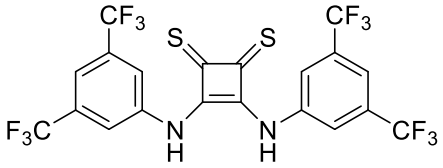

68

(**68**). To a solution of **60a** (141 mg, 0.5 mmol, 1.0 equiv) in dry CH_2Cl_2 (1.5 mL) was added 3,5-bis(trifluoromethyl)aniline (0.31 mL, 2.0 mmol, 4.0 equiv) and the resulting solution was stirred for 4 days, during which time the solution turned dark and a yellow precipitate formed. About 2 mL hexanes was then added and the suspension filtered to afford **68** (145 mg, 52%) as an amorphous yellow solid. Spectroscopic data for **68** was consistent with that of **66** and **67**, but differed from previously reported values.[11] ^{1}H NMR (500 MHz, CD_3CN): δ = 9.16 (s, 2H), 7.69 (s, 2H), 7.62 (s, 1H). ^{13}C NMR (125 MHz, CD_3CN): δ = 213.3, 170.2, 139.9, 133.0 (q, J = 33.8

Hz), 125.0, 123.2, 122.9, 120.0. HRMS (ESI) cald for $C_{20}H_8F_{12}N_2S_2$ $(M+H)^+$: 569.0010. Found: 568.9991. IR (film): 1683, 1625, 1558 cm^{-1}

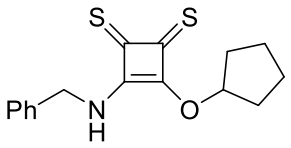

72

(**72**). To a solution of **60a** (237 mg, 0.84 mmol, 1.2 equiv) in dry CH_2Cl_2 (2 mL) was added benzylamine (76 µL, 0.70 mmol, 1.0 equiv) at 0 °C and the resulting solution was stirred for 15 min at that temperature, then 15 min at room temperature. The solution was then loaded directly onto column and quickly eluted with CH_2Cl_2 to afford **72** (166 mg, 79%) as an amorphous yellow solid. The compound exists as two rotamers in DMSO at room temperature in a ratio of 0.55:0.33. Major rotamer: ^{1}H NMR (500 MHz, DMSO-d_6): δ = 10.26 (t, *J* = 6.2 Hz, 1H), 7.35 (m, 5H), 6.37 (m, 1H), 4.56 (d, *J* = 6.5 Hz, 2H), 1.81-2.08 (m, 4H), 1.53-1.81 (m, 4H). Minor rotamer: ^{1}H NMR (500 MHz, DMSO-d_6): δ = 10.15 (t, *J* = 6.3 Hz, 1H), 7.35 (m, 5H), 6.32 (m, 1H), 5.19 (d, *J* = 6.5 Hz, 1H), 1.81-2.08 (m, 4H), 1.53-1.81 (m, 4H). ^{13}C NMR (125 MHz, DMSO-d_6): δ = 217.7, 217.4, 205.6, 182.8, 182.2, 175.2, 172.7, 137.2, 137.2, 128.6, 128.6, 127.9, 127.7, 127.6, 127.4, 87.3, 87.2, 47.9, 45.9, 33.7, 23.2, 23.0. HRMS (ESI) cald for $C_{16}H_{17}NOS_2$ $(M+H)^+$: 304.0824. Found: 304.0807. IR (film): 1691, 1513 cm^{-1}

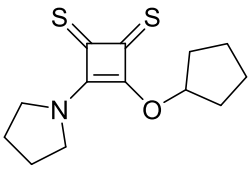

73

(**73**). To a solution of **60a** (169 mg, 0.60 mmol, 1.2 equiv) in dry CH_2Cl_2 (1.5 mL) was added pyrrolidine (42 µL, 0.50 mmol, 1.0 equiv) at 0 °C and the resulting solution was stirred for 20 min at that temperature, then 30 min at room temperature. The solution was then loaded directly onto column and quickly eluted with 1:1 hexanes:CH_2Cl_2 → CH_2Cl_2 to afford **73** (84 mg, 62%) as an amorphous yellow solid. ^{1}H NMR (500 MHz, $CDCl_3$): δ = 6.45 (m, 1H), 4.17 (m, 2H), 3.69 (m, 2H), 1.92-2.14 (m, 8H), 1.65-1.84 (m, 4H). ^{13}C NMR (125 MHz, $CDCl_3$): δ = 218.0, 205.5, 182.3, 171.3, 87.8, 50.1, 49.5, 34.5, 25.3, 24.7, 23.9. HRMS (ESI) cald for $C_{13}H_{17}NOS_2$ $(M+H)^+$: 268.0824. Found: 268.0825. IR (film): 1708, 1506 cm^{-1}

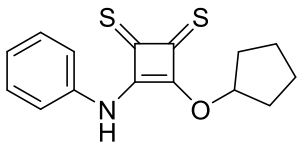

74

(**74**). To a solution of **60a** (339 mg, 1.2 mmol, 1.2 equiv) in dry CH_2Cl_2 (3 mL) was added aniline (91 µL, 1.0 mmol, 1.0 equiv) and the resulting solution was stirred for 14 h, during which time a yellow precipitate appeared (diaryl thiosquaramide byproduct). The suspension was then loaded directly onto column and quickly eluted with 1:1 hexanes:CH_2Cl_2 → CH_2Cl_2 to afford **74** (150 mg, 52%) as an orange solid. ^{1}H NMR (500 MHz, DMSO-d_6): δ = 11.59 (s, 1H), 7.40 (m, 4H), 7.26 (m, 1H), 6.47 (s, 1H), 1.94 (s, 4H), 1.66 (s, 4H). ^{13}C NMR (125 MHz, DMSO-d_6): δ = 217.5, 208.0, 181.6, 172.5, 136.3, 128.7, 126.0, 122.2, 87.8, 33.7, 23.0. HRMS (ESI) cald for $C_{15}H_{15}NOS_2$ $(M+H)^+$: 290.0668. Found: 290.0655. IR (film): 1674, 1598, 1520 cm^{-1}.

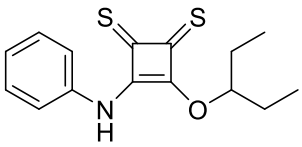

75

(**75**). To a solution of **61a** (1.00 g, 3.49 mmol, 1.2 equiv) in dry CH_2Cl_2 (2 mL) was added aniline (0.26 mL, 2.90 mmol, 1.0 equiv) and the resulting solution was stirred for 13 h. The solution was then loaded directly onto column and quickly eluted with 1:1 hexanes:CH_2Cl_2 → CH_2Cl_2 → 1% MeOH in CH_2Cl_2 to afford **75** (499 mg, 59%) as an amorphous orange solid. ^{1}H NMR (500 MHz, DMSO-d_6): δ = 11.63 (s, 1H), 7.40 (m, 4H), 7.28 (m, 1H), 6.15 (m, 1H), 1.75 (m, 4H), 0.91 (s, 6H). ^{13}C NMR (125 MHz, DMSO-d_6): δ = 217.4, 207.7, 182.1, 172.3, 136.3, 128.8, 126.1, 122.2, 87.0, 26.3, 8.7. HRMS (ESI) cald for $C_{15}H_{17}NOS_2$ $(M+H)^+$: 292.0824. Found: 292.0826. IR (film): 1674, 1598, 1520 cm^{-1}

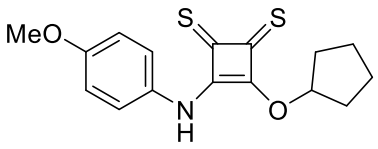

76

(**76**). To a solution of **60a** (220 mg, 0.79 mmol, 1.2 equiv) in dry CH_2Cl_2 (1.5 mL) was added *p*-anisidine (81 mg, 0.66 mmol, 1.0 equiv) and the resulting solution was stirred for 3 h. The solution was then loaded directly onto column and quickly eluted with 1:1 hexanes:CH_2Cl_2 → 1:2 hexanes:CH_2Cl_2 → CH_2Cl_2 to afford **76** (164 mg, 77%) as an orange solid. ^{1}H NMR (500 MHz, DMSO-d_6): δ = 11.49 (s, 1H), 7.33 (d, J = 8.8 Hz, 2H), 6.95 (d, J = 8.8 Hz, 2H), 6.46 (s, 1H), 3.76 (s, 3H), 1.93 (s, 4H), 1.65 (m, 4H). ^{13}C NMR (125 MHz, DMSO-d_6): δ = 217.7, 206.8, 181.6, 172.1, 157.6, 129.3, 123.7, 113.9, 87.6, 55.4, 33.7, 23.0. HRMS (ESI) cald for $C_{16}H_{17}NO_2S_2$ $(M+H)^+$: 320.0773. Found: 320.0745. IR (film): 1680, 1511 cm^{-1}.

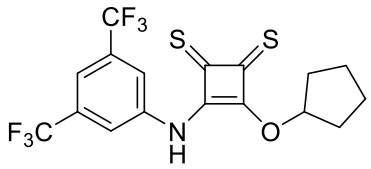

77

(**77**). To a solution of **60a** (261 mg, 0.92 mmol, 1.2 equiv) in dry CH_2Cl_2 (1 mL) was added 3,5-bis(trifluoromethyl)aniline (120 µL, 0.77 mmol, 1.0 equiv) and the resulting solution was stirred for 16 h. The solution was then loaded directly onto column and quickly eluted with 1:1 hexanes:CH_2Cl_2 → 1:2 hexanes:CH_2Cl_2 → CH_2Cl_2 to afford **77** (218 mg, 66%) as an orange solid. ^{1}H NMR (500 MHz, DMSO-d_6): δ = 11.85 (s, 1H), 8.14 (s, 2H), 7.97 (s, 1H), 6.46 (s, 1H), 1.98 (m, 4H), 1.62 (m, 4H). ^{13}C NMR (125 MHz, DMSO-d_6): δ = 216.5, 210.1, 181.9, 173.0, 138.6, 130.9 (q, J = 33.4 Hz), 126.2, 124.0, 122.2, 121.9, 119.7, 118.4, 88.4, 33.7, 23.2. HRMS (ESI) cald for $C_{17}H_{13}F_6NOS_2$ $(M+H)^+$: 426.0416. Found: 426.0389. IR (film): 1672, 1534 cm^{-1}

Synthesis of hydrochloride salts of bifunctional thiosquaramide catalysts. Due to zwitterionic and rotameric forms of bifunctional thiosquaramide catalysts, their HCl salts were used for NMR characterization. Representative example: To solid thiosquaramide catalyst was added 1.0 M hydrochloric acid in Et_2O (0.4 mL, 0.4 mmol, 4.0 equiv) and the resulting suspension stirred for 2 min at room temperature. 0.6 mL CH_2Cl_2 was then added, followed by 1.0 M hydrochloric acid in Et_2O (0.2 mL, 0.2 mmol, 2.0 equiv) and the suspension stirred for another 2 min at room temperature. About 1 mL hexanes was then added and the suspension filtered to afford the HCl salts of thiosquaramide catalysts which were used for NMR characterization.

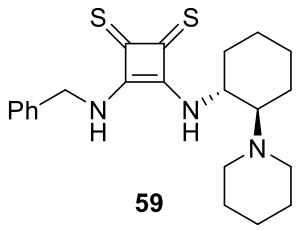

59

(**59**). To a solution of **72** (156 mg, 0.51 mmol, 1.0 equiv) in dry CH_2Cl_2 (1.5 mL) was added diamine **301** (93 mg, 0.51 mmol, 1.0 equiv) at 0 °C and the resulting solution was stirred for 1 h at that temperature, then 0.5 h at room temperature. Hexanes was then added and the resulting solution concentrated to give a solid, which was washed with pentane to afford **59** (185 mg, 90%) as an orange solid. Analytical data matched data reported above. NMR characterization for **59**.HCl: ^{1}H NMR (500 MHz, CD_3CN): δ = 10.04 (s, 1H), 9.20 (s, 1H), 8.53 (s, 1H), 7.45 (d, *J* = 7.3 Hz, 2H), 7.39 (t, *J* = 7.4 Hz, 2H), 7.32 (t, *J* = 7.2 Hz, 1H), 5.35 (m, 2H), 4.90 (m, 1H), 3.48 (d, *J* = 11.3 Hz, 1H), 3.39 (t, *J* = 10.6 Hz, 1H), 3.23 (m, 2H), 2.91 (m, 1H), 2.45 (d, *J* = 13.4 Hz, 1H), 1.89 (m, 4H), 1.32-1.82 (m, 9H). ^{13}C NMR (125 MHz, CD_3CN): δ = 207.9, 205.5, 173.0, 172.1, 138.8, 129.9, 129.0, 128.9, 68.8, 54.0, 53.6, 48.2, 47.9, 36.6, 24.9, 24.5, 24.3, 24.2, 24.0, 22.5.

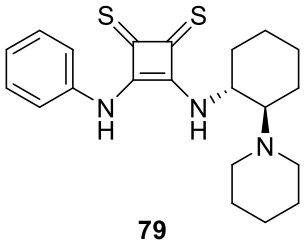

79

(**79**). To a solution of **74** (80 mg, 0.28 mmol, 1.0 equiv) in dry CH_2Cl_2 (1 mL) was added diamine **301** (51 mg, 0.28 mmol, 1.0 equiv) at 0 °C and the resulting solution was stirred for 1 h at that temperature, then 1 h at room temperature. The solution was then loaded directly onto column and quickly eluted with CH_2Cl_2 → 1% MeOH in CH_2Cl_2 → 3% MeOH in CH_2Cl_2 → 5%

MeOH in CH_2Cl_2 to afford **79** (104 mg, 96%) as an orange solid. NMR characterization for **79**.HCl: ^{1}H NMR (500 MHz, CD_3CN): δ = 11.05 (s, 1H), 9.99 (s, 1H), 8.48 (s, 1H), 7.77 (d, *J* = 7.6 Hz, 2H), 7.38 (t, *J* = 7.9 Hz, 2H), 7.21 (t, *J* = 7.4 Hz, 1H), 4.95 (s, 1H), 3.47 (m, 2H), 3.27 (m, 2H), 2.94 (m, 1H), 2.46 (d, *J* = 13.5 Hz, 1H), 1.88-2.21 (buried, 5H), 1.80 (m, 3H), 1.60 (m, 2H), 1.42 (m, 3H). ^{13}C NMR (125 MHz, CD_3CN): δ = 208.5, 207.0, 173.0, 171.2, 137.7, 129.9, 126.5, 123.1, 68.9, 54.1, 53.8, 48.2, 36.5, 24.8, 24.5, 24.3, 24.2, 24.0, 22.5. HRMS (ESI) cald for $C_{21}H_{27}N_3S_2$ $(M+H)^+$: 386.1719. Found: 386.1719. IR (film): 1691, 1598, 1559 cm^{-1}

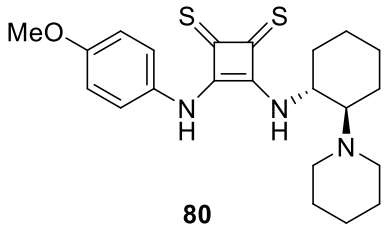

80

(**80**). To a solution of **76** (109 mg, 0.34 mmol, 1.0 equiv) in dry CH_2Cl_2 (1 mL) was added diamine **301** (62 mg, 0.34 mmol, 1.0 equiv) at 0 °C and the resulting solution was stirred for 0.5 h at that temperature, then 1.5 h at room temperature. The solution was then loaded directly onto column and quickly eluted with CH_2Cl_2 → 1% MeOH in CH_2Cl_2 → 3% MeOH in CH_2Cl_2 → 5% MeOH in CH_2Cl_2 to afford **80** (126 mg, 88%) as an orange solid. NMR characterization for **80**.HCl: ^{1}H NMR (500 MHz, CD_3CN): δ = 10.99 (s, 1H), 9.93 (s, 1H), 8.47 (s, 1H), 7.67 (d, *J* = 8.1 Hz, 2H), 6.93 (d, *J* = 8.9 Hz, 2H), 4.95 (m, 1H), 3.79 (s, 3H), 3.46 (m, 2H), 3.25 (m, 2H), 2.94 (q, *J* = 11.5 Hz, 1H), 2.46 (d, *J* = 12.7 Hz, 1H), 1.88-2.21 (buried, 5H), 1.80 (m, 3H), 1.60 (m, 2H), 1.42 (m, 3H). ^{13}C NMR (125 MHz, CD_3CN): δ = 207.1, 207.0, 170.7, 158.8, 130.7, 124.7, 115.0, 68.9, 56.3, 54.1, 53.7, 48.3, 36.4, 24.8, 24.4, 24.3, 24.2, 23.9, 22.5. HRMS (ESI) cald for $C_{22}H_{29}N_3OS_2$ $(M+H)^+$: 416.1825. Found: 416.1823. IR (film): 1694, 1606 cm^{-1}

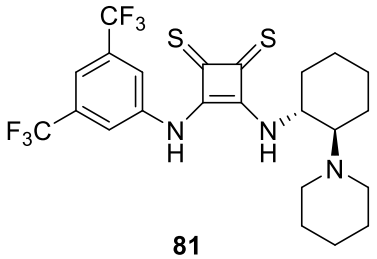

81

(**81**). To a solution of **77** (213 mg, 0.50 mmol, 1.0 equiv) in dry CH_2Cl_2 (1 mL) was added diamine **301** (91 mg, 0.50 mmol, 1.0 equiv) at 0 °C and the resulting solution was stirred for 1 h at that temperature, then 0.5 h at room temperature. About 5 mL hexanes was then added. The suspension was then filtered and washed with ice-cold 4:1 hexanes:CH_2Cl_2 to afford **81** (187 mg, 72%) as an orange-red solid. NMR characterization for **81**.HCl: ^{1}H NMR (500 MHz, CD_3CN): δ = 11.60 (s, 1H), 9.98 (s, 1H), 8.42 (s, 2H), 8.33 (s, 1H), 7.75 (s, 1H), 4.93 (s, 1H), 3.47 (m, 2H), 3.32 (m, 2H), 2.96 (m, 1H), 2.44 (m, 1H), 2.17 (m, 3H), 1.90 (m, 2H), 1.80 (m, 3H), 1.52-1.73 (m, 2H), 1.34-1.52 (m, 2H). ^{13}C NMR (125 MHz, CD_3CN): δ = 210.9, 206.9, 173.0, 171.3, 139.7, 132.6 (q, *J* = 33.3 Hz), 125.4, 123.3, 122.5, 68.9, 54.1, 54.0, 48.4, 36.4, 24.8, 24.4, 24.2, 24.2, 24.0, 22.4. HRMS (ESI) cald for $C_{23}H_{25}F_6N_3S_2$ $(M+H)^+$: 522.1467. Found: 522.1472. IR (film): 1688, 1568 cm^{-1}

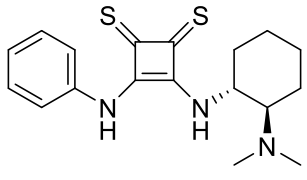

82

(**82**). To a solution of **74** (80 mg, 0.28 mmol, 1.0 equiv) in dry CH_2Cl_2 (1 mL) was added diamine **44** (44 μL, 0.28 mmol, 1.0 equiv) at 0 °C and the resulting solution was stirred for 1 h at that temperature, then 1 h at room temperature. The solution was then loaded directly onto column and quickly eluted with CH_2Cl_2 → 1% MeOH in CH_2Cl_2 → 3% MeOH in CH_2Cl_2 → 5%

MeOH in CH_2Cl_2 to afford **82** (80 mg, 82%) as a yellow solid. NMR characterization for **82**.HCl: ^{1}H NMR (500 MHz, CD_3CN): δ = 11.51 (s, 1H), 10.35 (s, 1H), 8.42 (s, 1H), 7.79 (d, *J* = 6.5 Hz, 2H), 7.38 (t, *J* = 7.9 Hz, 2H), 7.22 (t, *J* = 7.4 Hz, 1H), 5.21 (s, 1H), 3.39 (td, *J* = 11.9, 3.5 Hz, 1H), 2.87 (d, *J* = 3.9 Hz, 3H), 2.78 (d, *J* = 4.5 Hz, 3H), 2.32 (m, 1H), 2.10 (m, 1H), 1.89 (m, 1H), 1.79 (m, 1H), 1.48-1.69 (m, 2H), 1.33-1.46 (m, 2H). ^{13}C NMR (125 MHz, CD_3CN): δ = 208.3, 206.8, 173.4, 171.3, 137.6, 129.9, 126.6, 123.3, 68.9, 53.7, 43.6, 38.0, 35.4, 24.5, 24.4, 23.4. HRMS (ESI) cald for $C_{18}H_{23}N_3S_2$ $(M+H)^+$: 346.1406. Found: 346.1404. IR (film): 1691, 1598, 1559 cm^{-1}

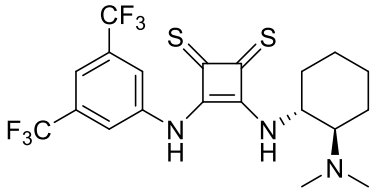

83

(**83**). To a solution of **77** (213 mg, 0.50 mmol, 1.0 equiv) in dry CH_2Cl_2 (1.5 mL) was added diamine **44** (78 µL, 0.50 mmol, 1.0 equiv) at 0 °C and the resulting solution was stirred for 1 h at that temperature, then 0.5 h at room temperature. About 2 mL hexanes was then added and the suspension filtered to afford **83** (182 mg, 76%) as a yellow solid. NMR characterization for **83**.HCl: ^{1}H NMR (500 MHz, CD_3CN): δ = 12.06 (s, 1H), 10.32 (s, 1H), 8.47 (s, 2H), 8.25 (s, 1H), 7.74 (s, 1H), 5.17 (m, 1H), 3.45 (td, *J* = 11.8, 3.7 Hz, 1H), 2.91 (s, 3H), 2.78 (s, 3H), 2.31 (m, 1H), 2.13 (m, 1H), 1.90 (m, 1H), 1.80 (m, 1H), 1.51-1.68 (m, 2H), 1.33-1.50 (m, 2H). ^{13}C NMR (125 MHz, CD_3CN): δ = 210.8, 206.7, 173.5, 171.4, 139.9, 132.7 (q, *J* = 33.3 Hz), 125.5, 123.3, 122.6, 69.1, 53.9, 43.6, 38.1, 35.5, 24.4, 24.4, 23.5. HRMS (ESI) cald for $C_{20}H_{21}F_6N_3S_2$ $(M+H)^+$: 482.1154. Found: 482.1157. IR (film): 1684, 1568 cm^{-1}

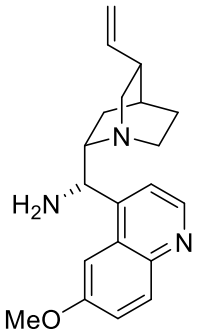

302

Quinine-derived diamine **302** was synthesized according to the literature.[12]

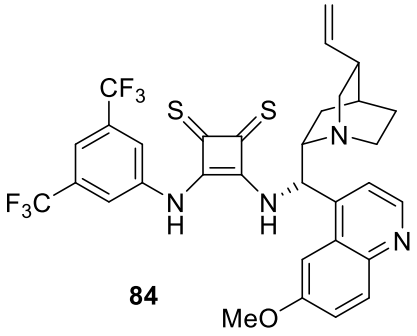

84

(**84**). To a solution of **77** (85 mg, 0.20 mmol, 1.0 equiv) in dry CH_2Cl_2 (1 mL) was added a solution of diamine **302** in dry CH_2Cl_2 (0.5 M, 0.4 mL, 1.0 equiv) at 0 °C and the resulting solution was stirred for 0.5 h at that temperature, then 3 h at room temperature. About 4 mL hexanes was then added. The suspension was filtered and washed with ice-cold 4:1 hexanes:CH_2Cl_2 to afford **84** (93 mg, 70%) as an amorphous yellow solid. NMR characterization for **84**.2HCl: ^{1}H NMR (500 MHz, CD_3CN): δ = 12.36 (s, 1H), 11.72 (s, 1H), 9.82 (s, 1H), 9.03 (s, 1H), 8.61 (s, 1H), 8.55 (d, *J* = 8.8 Hz, 1H), 8.37 (s, 2H), 8.06 (s, 1H), 7.71 (m, 2H), 7.53 (s, 1H), 5.85 (m, 1H), 5.18 (d, *J* = 16.5 Hz, 1H), 5.12 (d, *J* = 10.0 Hz, 1H), 4.38 (s, 1H), 4.15 (s, 3H), 4.15 (buried, 1H), 3.70 (m, 1H), 3.34 (s, 2H), 2.81 (s, 1H), 1.54-2.09 (m, 5H), 1.14 (s, 1H). ^{13}C

[12] Medina, S.; Harper, M. J.; Balmond, E. I.; Miranda, S.; Crisenza, G. E. M.; Coe, D. M.; McGarrigle, E. M.; Galan, M. C. *Org. Lett*. **2016**, *18*, 4222.

NMR (125 MHz, CD_3CN): δ = 209.6, 207.2, 171.6, 168.9, 162.0, 141.9, 139.4, 138.7, 138.5, 136.6, 132.7 (q, *J* = 33.8 Hz), 129.9, 128.8, 125.3, 125.3, 123.2, 122.9, 121.0, 119.3, 117.8, 103.9, 58.1, 55.0, 43.7, 37.4, 27.5, 24.6, 24.1. HRMS (ESI) cald for $C_{32}H_{28}F_6N_4OS_2$ $(M+H)^+$: 663.1681. Found: 663.1680. IR (film): 1681, 1622, 1566, 1510 cm^{-1}

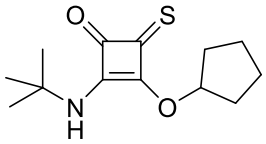

88

(**88**). To a solution of **60b** (278 mg, 1.04 mmol, 1.2 equiv) in dry CH_2Cl_2 (2 mL) was added *tert*-butyl amine (91 µL, 0.87 mmol, 1.0 equiv) at 0 °C and the resulting solution was stirred for 3 h at that temperature. The solution was then loaded directly onto column and quickly eluted with CH_2Cl_2 → 5% MeOH in CH_2Cl_2 to afford **88** (186 mg, 84%) as an amorphous yellow solid. The compound exists as two rotamers in DMSO at room temperature in a ratio of 0.54:0.40. Major rotamer: ^1H NMR (500 MHz, DMSO-d_6): δ = 9.43 (s, 1H), 6.32 (m, 1H), 1.82-2.06 (m, 4H), 1.55-1.82 (m, 4H), 1.38 (s, 9H); Minor rotamer: ^1H NMR (500 MHz, DMSO-d_6): δ = 9.74 (s, 1H), 6.50 (m, 1H), 1.82-2.06 (m, 4H), 1.55-1.82 (m, 4H), 1.34 (s, 9H). ^{13}C NMR (125 MHz, DMSO-d_6): δ = 205.5, 203.4, 184.6, 183.2, 181.0, 178.5, 176.8, 175.6, 85.7, 54.4, 53.8, 33.7, 33.7, 29.7, 29.5, 23.3, 23.1. HRMS (ESI) cald for $C_{13}H_{19}NO_2S$ $(M+H)^+$: 254.1209. Found: 254.1212. IR (film): 1765, 1633 cm^{-1}

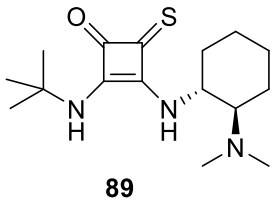

89

(**89**). To a solution of **88** (230 mg, 0.91 mmol, 1.0 equiv) in dry CH_2Cl_2 (0.5 mL) was added diamine **44** (142 µL, 0.91 mmol, 1.0 equiv) at room temperature. A precipitate formed within 30 min, at which point an additional 1 mL dry CH_2Cl_2 was added to facilitate stirring. After stirring an additional 24 h, about 2 mL hexanes was added and the suspension filtered to afford **89** (162 mg, 57%) as an amorphous yellow solid. ^{1}H NMR (500 MHz, DMSO-d_6): δ = 8.46 (s, 1H), 7.83 (d, J = 8.5 Hz, 1H), 4.82 (m, 1H), 2.35 (m, 1H), 2.20 (s, 6H), 2.08 (m, 1H), 1.84 (m, 1H), 1.73 (m, 1H), 1.62 (m, 1H), 1.42 (s, 9H), 1.11-1.30 (m, 4H). ^{13}C NMR (125 MHz, DMSO-d_6): δ = 200.1, 178.5, 171.8, 169.2, 65.8, 53.7, 53.0, 38.9-40.3 (buried x2), 35.9, 29.9, 24.3, 24.1, 21.1. HRMS (ESI) cald for $C_{16}H_{27}N_3OS$ $(M+H)^+$: 310.1948. Found: 310.1947. IR (film): 1756, 1594, 1538 cm^{-1}

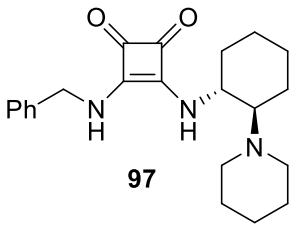

97

(**97**). To a solution of **46** (280 mg, 1.29 mmol, 1.1 equiv) in CH_2Cl_2 (8 mL) was added **301** (220 mg, 1.21 mmol, 1.0 equiv) in 2 mL CH_2Cl_2. The mixture was stirred at room temperature for 3 h and then concentrated. The resulting solid was then washed with ice-cold CH_2Cl_2 to afford the desired product **97** (288 mg, 65%) as a white solid. ^{1}H NMR (500 MHz, DMSO-d_6): δ = 7.73 (br s, 1H), 7.33 (m, 5H), 7.16 (br s, 1H), 4.73 (br s, 2H), 3.81 (s, 1H), 2.59 (m, 2H), 2.23 (m, 3H), 2.01 (br s, 1H), 1.79 (m, 1H), 1.71 (m, 1H), 1.63 (m, 1H), 1.24 (m, 10H). ^{13}C NMR (125 MHz, DMSO-d_6): δ = 182.5, 182.1, 168.4, 167.0, 139.1, 128.5, 127.4, 127.3, 68.3, 53.8, 49.3, 46.7, 34.1, 26.2, 24.8, 24.4, 23.5. HRMS (ESI) calcd for $C_{22}H_{30}N_3O_2^+$$(M+H)^+$: 368.2333, Found: 368.2331. IR (film): 3163, 2938, 1798, 1639, 1564, 1488, 1347, 1269 cm^{-1}

Squaramides **94**,[13] **95**, **96**[14] and **70**[15] are known.

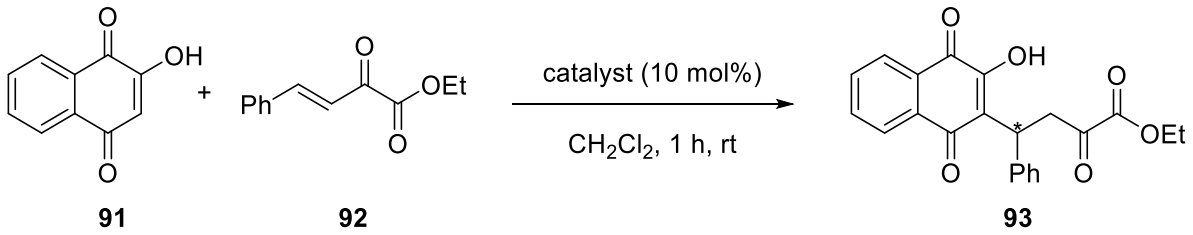

91 **92** **93**

Asymmetric Michael addition of lawsone (**91**) to β,γ-unsaturated α-oxo ester **92**[16] catalyzed by an oxo- or thiosquaramide catalyst. Representative example: To a solution of lawsone (17.4 mg, 0.10 mmol, 1.0 equiv) and catalyst (0.01 mmol, 10 mol%) in CH_2Cl_2 (0.5 mL) was added α-oxo ester **92** (22.5 mg, 0.11 mmol, 1.1 equiv) and the resulting solution was stirred for 1 h at room temperature. About half of the solution was then loaded directly onto a preparatory TLC plate and eluted with 1:2 EtOAc:hexanes to afford pure **93** for HPLC analysis. The remaining solution was concentrated and conversion measured by ^{1}H-NMR spectroscopy. NMR data matched previously reported values.[17] HPLC conditions: Daicel Chiralpak IC column, 80:20 hexanes:iPrOH, 1.0 mL/min, λ = 250 nm, t_{minor} = 15.3 min, t_{major} = 19.7 min.

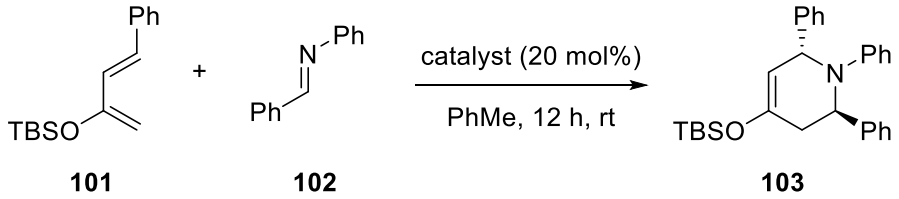

101 **102** **103**

[13] Yang, C.; Wang, J.; Liu, Y.; Ni, X.; Li, X.; Cheng, J. *Chem. Eur. J*. **2017**, *23*, 5488.
[14] Konishi, H.; Lam, T. Y.; Malerich, J. P.; Rawal, V. H. *Org. Lett.* **2010**, *12*, 2028.
[15] Rostami, A.; Colin, A.; Li, X. Y.; Chudzinski, M. G.; Lough, A. J.; Taylor, M. S. *J. Org. Chem.* **2010**, *75*, 3983.
[16] Chen, S.; Li, X.; Zhao, H.; Li, B. *J. Org. Chem.* **2014**, *79*, 4137.
[17] Gao, Y.; Ren, Q.; Ang, S.; Wang, J. *Org. Biomol. Chem.* **2011**, *9*, 3691.

Aza-Diels-Alder reaction of 2-siloxydiene **101**[18] with *N*-benzylideneaniline **102** catalyzed by thiosquaramide **68**, oxosquaramide **70**, or Schreiner's thiourea catalyst **104**. Representative example: To a solution of *N*-benzylideneaniline **102** (36 mg, 0.20 mmol, 1.0 equiv) and catalyst (0.04 mmol, 20 mol%) in dry PhMe (1 mL) or dry CH_2Cl_2 (1 mL) was added 2-siloxydiene **101** (63 mg, 0.24 mmol, 1.2 equiv) and the resulting reaction mixture was stirred for 12 h at room temperature. 1,3,5-Trimethoxybenzene was then added, the reaction mixture was concentrated, and the resulting residue taken up in $CDCl_3$ for determination of yield of **103** by ^{1}H-NMR spectroscopy. NMR data matched previously reported values.[19]

The below thiourea synthesis and procedure is by Dr. Chintan Sumaria.

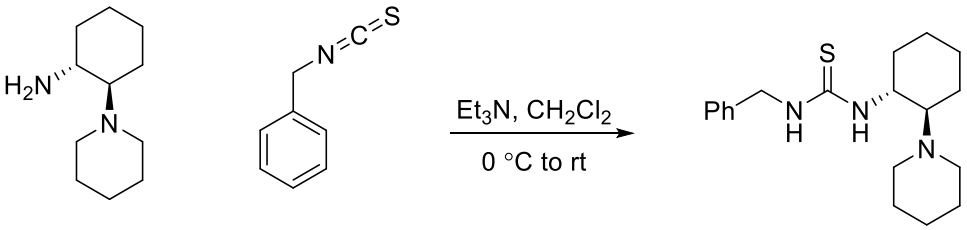

301 **303** **124**

(**124**). A solution of **301** (266 mg, 1.46 mmol, 1.1 equiv) in CH_2Cl_2 (4 mL) was cooled to 0 °C followed by the addition of triethylamine (0.37 mL, 2.66 mmol, 2.0 equiv). Benzyl isothiocyanate **303** (199 mg, 1.33 mmol, 1.0 equiv) was added and the reaction mixture was stirred at room temperature for 12 hours (monitored by TLC). The reaction mixture was washed with water, brine, and the organic layers were dried with $MgSO_4$ and concentrated. The crude product was purified by silica gel chromatography using MeOH:$CHCl_3$:NH_4OH (5:94:1) as the eluent to give catalyst **124** (312 mg, 71%) as a white solid. ^{1}H NMR (500 MHz, $CDCl_3$): δ = 7.35-7.31 (m, 4H), 7.30-7.26 (m, 1H), 6.45 (br s, 1H), 4.8-4.5 (m, 2H), 3.59 (br s, 1H), 2.7-2.5

[18] Aono, T.; Sasagawa, H.; Fuchibe, K.; Ichikawa, J. *Org. Lett.* **2015**, *17*, 5736.
[19] Takasu, K.; Shindoh, N.; Tokuyama, H.; Ihara, M. *Tetrahedron* **2006**, *62*, 11900.

(m, 3H), 2.38-2.24 (m, 3H), 1.87 (d, *J* = 12.0 Hz, 1H), 1.82-1.76 (m, 1H), 1.71-1.64 (m, 1H), 1.46-1.02 (m, 11H). ^{13}C NMR (125 MHz, $CDCl_3$): δ = 128.7, 127.6, 127.5, 68.7, 55.7, 49.5 (br), 48.3, 33.1, 26.2, 25.3, 24.4, 23.4. HRMS (ESI) calcd for $C_{19}H_{30}N_3S^+(M+H)^+$: 332.2155, Found: 332.216. IR (film): 3853, 3258, 2930, 2853, 2361, 2337, 1540 cm^{-1}

V1.3 Experimental Procedures and Characterization Data for Chapter 3

Asymmetric Michael addition of barbituric acids to nitroalkenes catalyzed by an oxo- or thiosquaramide. Representative example: To a mixture of nitroalkene (0.22 mmol, 1.1 equiv) and *N,N'*-disubstitutedbarbituric acid (0.20 mmol, 1.0 equiv) was added **59** (0.001 mmol, 0.005 equiv, 0.5 mol%)[20] in PhMe (0.5 mL) at rt. The reaction was stirred at room temperature, and the conversion monitored by TLC. Upon complete conversion, the reaction mixture was loaded directly onto column and eluted with a gradient of 0:1 to 1:1 EtOAc:CH_2Cl_2.

Note: Enantiomeric excesses are measured after C-5 chlorination of the addition product (see below).

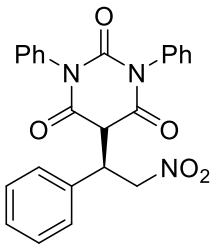

121

(**121**). Flash column chromatography afforded **121** (83.5 mg, 97%) as an off-white solid. ^{1}H NMR (500 MHz, $CDCl_3$): δ = 7.46 (m, 9H), 7.28 (m, 2H), 7.05 (br s, 2H), 6.91 (br s, 2H), 5.32

[20]For some reactions (see Scheme 40), 4.0 mg (0.01 mmol, 0.05 equiv, 5.0 mol%) of **59** is used.

(dd, *J* = 14.3, 8.0 Hz, 1H), 5.04 (dd, *J* = 14.3, 7.7 Hz, 1H), 4.67 (td, 7.8, 3.5 Hz, 1H), 4.20 (d, *J* = 3.5 Hz, 1H). ^{13}C NMR (125 MHz, $CDCl_3$) δ = 166.9, 166.7, 150.1, 134.3, 133.8, 133.7, 129.9, 129.8, 129.6, 129.6, 129.6, 129.5, 128.5, 128.3, 76.0, 52.0, 45.9. HRMS (ESI) calcd for $C_{24}H_{20}N_3O_5^+$ $(M+H)^+$: 430.1397, Found: 430.1398. IR (film): 1697, 1554, 1492, 1372, 1220 cm^{-1}. HPLC (after chlorination: AS-H, 88:12 hexanes:iPrOH, 1.0mL/min, 210 nm): t_{major} = 19.5 min, t_{minor} = 14.0 min, 97% ee.

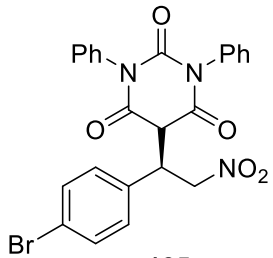

125

(**125**). Flash column chromatography afforded **125** (98.3 mg, 97%) as a light pink solid. ^{1}H NMR (500 MHz, $CDCl_3$): δ = 7.59 (m, 2H), 7.45 (m, 6H), 7.17 (m, 2H), 7.05 (d, *J* = 6.2 Hz, 2H), 6.95 (brs, 2H), 5.28 (dd, *J* = 14.3, 8.0 Hz, 1H), 5.00 (dd, *J* = 14.3, 7.7 Hz, 1H), 4.67 (td, *J* = 7.8, 3.4 Hz, 1H), 4.19 (d, *J* = 3.4 Hz, 1H). ^{13}C NMR (125 MHz, $CDCl_3$): δ = 166.8, 166.5, 150.1, 133.8, 133.7, 133.7, 133.0, 130.3, 130.0, 130.0, 129.8, 129.8, 129.7, 128.3, 124.0, 76.0, 51.8, 44.8. HRMS (ESI) calcd for $C_{24}H_{19}BrN_3O_5^+$$(M+H)^+$: 508.0503, Found: 508.0504. IR (film): 1698, 1554, 1491, 1372, 1219 cm^{-1}. HPLC (after chlorination: AS-H, 88:12 hexanes:iPrOH, 1.0 mL/min, 210 nm): t_{major} = 23.9 min, t_{minor} = 13.1 min, 97% ee.

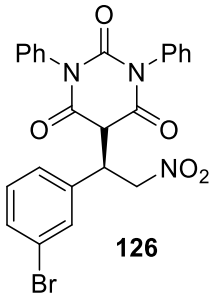

126

(**126**). Flash column chromatography afforded **126** (96.9 mg, 95%) as an off-white solid. ^{1}H NMR (500 MHz, $CDCl_3$): δ = 7.62 (d, *J* = 8.1 Hz, 1H), 7.46 (m, 7H), 7.36 (t, *J* = 7.9 Hz, 1H), 7.23 (d, *J* = 7.8 Hz, 1H), 7.08 (d, *J* = 6.6 Hz, 2H), 6.96 (br s, 2H), 5.29 (dd, *J* = 14.4, 7.9 Hz, 1H), 5.03 (dd, *J* = 14.4, 7.8 Hz, 1H), 4.66 (td, *J* = 7.8, 3.4 Hz, 1H), 4.18 (d, *J* = 3.4 Hz, 1H). ^{13}C NMR (125 MHz, $CDCl_3$): δ = 166.7, 166.5, 150.0, 136.7, 133.7, 133.5, 133.1, 131.3, 131.3, 129.7, 129.7, 129.7, 128.3, 128.3, 127.2, 124.0, 75.7, 51.7, 45.2. HRMS (ESI) calcd for $C_{24}H_{19}BrN_3O_5^+$ $(M+H)^+$: 508.0503, Found: 508.0488. IR (film): 1697, 1554, 1490, 1372, 1218 cm^{-1}. HPLC (after chlorination: AD-H, 80:20 hexanes:iPrOH, 0.8 mL/min, 210 nm): t_{major} = 10.9 min, t_{minor} = 12.3 min, 95% ee.

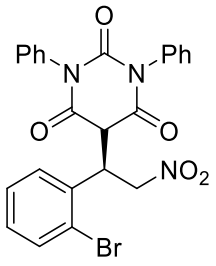

127

(**127**). Flash column chromatography afforded **127** (91.9 mg, 90%) as a pink solid. ^{1}H NMR (500 MHz, $CDCl_3$): δ = 7.68 (dd, *J* = 8.0, 1.1 Hz, 1H), 7.46 (m, 7H), 7.36 (m, 1H), 7.24 (m, 3H), 7.13 (d, *J* = 7.2 Hz, 2H), 5.38 (ddd, *J* = 9.8, 5.8, 2.6 Hz, 1H), 5.25 (dd, *J* = 13.4, 10.1 Hz, 1H), 4.83 (dd, *J* = 13.4, 5.9 Hz, 1H), 4.30 (d, *J* = 2.6 Hz, 1H). ^{13}C NMR (125 MHz, $CDCl_3$): δ = 166.5,

150.5, 135.8, 134.2, 134.1, 134.0, 130.5, 129.7, 129.6, 129.6, 129.5, 129.5, 128.5, 128.5, 128.4, 125.3, 74.9, 51.5, 42.1. HRMS (ESI) calcd for $C_{24}H_{19}BrN_3O_5^+$ $(M+H)^+$: 508.0503, Found: 508.0483. IR (film): 1698, 1553, 1491, 1371, 1216 cm^{-1}. HPLC (after chlorination: AS-H, 88:12 hexanes:iPrOH, 1.0 mL/min, 210 nm): t_{major} = 28.3 min, t_{minor} = 20.8 min, 98% ee.

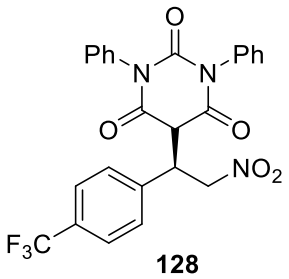

128

(**128**). Flash column chromatography afforded **128** (87.3 mg, 88%) as an off-white solid. ^1H NMR (500 MHz, $CDCl_3$): δ = 7.71 (d, *J* = 8.2 Hz, 2H), 7.46 (m, 8H), 7.05 (d, *J* = 5.4 Hz, 2H), 6.94 (br s, 2H), 5.34 (dd, *J* = 14.3, 8.3 Hz, 1H), 5.04 (dd, *J* = 14.3, 7.5 Hz, 1H), 4.80 (td, *J* = 7.9, 3.2 Hz, 1H), 4.25 (d, *J* = 3.3 Hz, 1H). ^{13}C NMR (125 MHz, $CDCl_3$): δ = 166.6, 166.3, 149.9, 139.2, 133.7, 133.6, 132.1, 131.8, 129.8, 129.7, 129.7, 129.2, 128.2, 128.2, 126.6, 126.6, 124.9, 122.7, 75.7, 51.8, 44.5. HRMS (ESI) calcd for $C_{25}H_{19}F_3N_3O_5^+(M+H)^+$: 498.1271, Found: 498.1275. IR (film): 1699, 1555, 1491, 1372, 1327, 1120 cm^{-1}. HPLC (after chlorination: AS-H, 88:12 hexanes:iPrOH, 1.0 mL/min, 210 nm): t_{major} = 17.0 min, t_{minor} = 9.5 min, 92% ee.

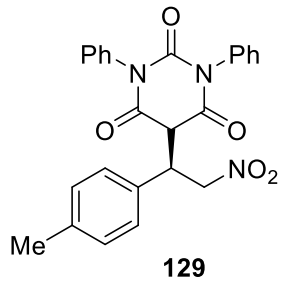

129

(**129**). Flash column chromatography afforded **129** (88.1 mg, 99%) as an off-white solid. Chlorination of **129** (for purposes of ee determination, see below) gave a white solid which, after slow evaporation from an 80:20 Hexanes:iPrOH mixture, yielded crystals suitable for X-ray analysis. ^{1}H NMR (500 MHz, $CDCl_3$): δ = 7.44 (m, 6H), 7.27 (d, *J* = 7.9 Hz, 2H), 7.14 (d, *J* = 8.1 Hz, 2H), 7.05 (d, *J* = 5.9 Hz, 2H), 6.91 (br s, 2H), 5.26 (dd, *J* = 14.3, 7.9 Hz, 1H), 5.00 (dd, *J* = 14.2, 7.9 Hz, 1H), 4.61 (td, *J* = 7.8, 3.6 Hz, 1H), 4.15 (d, *J* = 3.6 Hz, 1H), 2.41 (s, 3H). ^{13}C NMR (125 MHz, $CDCl_3$): δ = 166.9, 166.8, 150.2, 139.9, 133.8, 133.7, 131.0, 131.0, 131.0, 130.4, 129.6, 129.6, 129.5, 128.3, 76.2, 51.9, 45.7, 21.4. HRMS (ESI) calcd for $C_{25}H_{22}N_3O_5^+$(M+H)$^+$: 444.1554, Found: 444.1554. IR (film): 1698, 1553, 1491, 1372, 1220 cm^{-1}. HPLC (after chlorination: AS-H, 88:12 hexanes:iPrOH, 1.0 mL/min, 210 nm): t_{major} = 16.8 min, t_{minor} = 11.6 min, 94% ee.

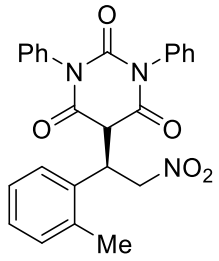

130

(**130**). Flash column chromatography afforded **130** (81.8mg, 92%) as an off-white solid. ^{1}H NMR (500 MHz, $CDCl_3$): δ = 7.40 (m, 10H), 7.22 (m, 2H), 6.78 (brs, 2H), 5.19 (dd, *J* = 14.0, 7.6 Hz, 1H), 5.01 (td, *J* = 7.6, 3.9 Hz, 1H), 4.88 (dd, *J* = 14.1, 7.8 Hz, 1H), 4.15 (d, *J* = 3.4 Hz, 1H), 2.36 (s, 3H). ^{13}C NMR (125 MHz, $CDCl_3$): δ = 167.2, 166.7, 150.2, 137.9, 133.9, 133.4, 133.4, 132.1, 129.6, 129.6, 129.6, 129.4, 129.4, 128.3, 128.2, 127.2, 126.6, 76.6, 51.5, 40.4, 19.7. HRMS (ESI) calcd for $C_{25}H_{22}N_3O_5^+$ (M+H)$^+$: 444.1554, Found: 444.1549. IR (film): 1696, 1553,

1491, 1372, 1214 cm^{-1}. HPLC (after chlorination: AS-H, 88:12 hexanes:iPrOH, 1.0 mL/min, 210 nm): t_{major} = 16.1 min, t_{minor} = 13.0 min, 95% ee.

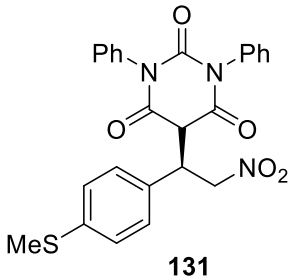

131

(**131**). Flash column chromatography afforded **131** (94.8 mg, 99%) as a light yellow solid. ^{1}H NMR (500 MHz, $CDCl_3$): δ = 7.44 (m, 6H), 7.29 (d, *J* = 8.3 Hz, 2H), 7.17 (d, *J* = 8.3 Hz, 2H), 7.04 (d, *J* = 5.7 Hz, 2H), 6.92 (brs, 2H), 5.24 (dd, *J* = 14.2, 7.8 Hz, 1H), 4.99 (dd, *J* = 14.2, 7.9 Hz, 1H), 4.61 (td, *J* = 7.8, 3.5 Hz, 1H), 4.15 (d, *J* = 3.5 Hz, 1H), 2.50 (s, 3H). ^{13}C NMR (125 MHz, $CDCl_3$): δ = 166.6, 166.4, 150.2, 135.8, 133.9, 133.7, 129.6, 129.6, 129.6, 128.6, 128.4, 128.4, 128.1, 127.8, 126.8, 76.8, 52.1, 41.0. HRMS (ESI) calcd for $C_{25}H_{22}N_3O_5S^+(M+H)^+$: 476.1275, Found: 476.1274. IR (film): 1697, 1553, 1492, 1372, 1265, 1221 cm^{-1}. HPLC (after chlorination: AS-H, 80:20 hexanes:iPrOH, 0.8 mL/min, 210 nm): t_{major} = 30.7 min, t_{minor} = 19.3 min, 94% ee.

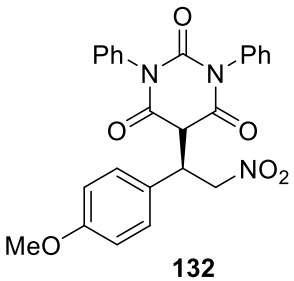

132

(**132**). Flash column chromatography afforded **132** (90.6 mg, 99%) as a light yellow solid. ^{1}H NMR (500 MHz, $CDCl_3$): δ = 7.43 (m, 6H), 7.17 (m, 2H), 7.06 (d, *J* = 6.4 Hz, 2H), 6.96 (m, 2H),

6.93 (br s, 2H), 5.24 (dd, *J* = 14.2, 7.8 Hz, 1H), 4.99 (dd, *J* = 14.2, 8.0 Hz, 1H), 4.60 (td, *J* = 7.9, 3.6 Hz, 1H), 4.13 (d, *J* = 3.6 Hz, 1H), 3.84 (s, 3H). ^{13}C NMR (125 MHz, $CDCl_3$): δ = 167.0, 166.9, 160.6, 150.1, 133.8, 133.7, 129.6, 129.6, 129.5, 128.3, 125.8, 115.0, 76.3, 55.6, 52.1, 45.3. HRMS (ESI) calcd for $C_{25}H_{22}N_3O_6^+(M+H)^+$: 460.1503, Found: 460.1505. IR (film): 1697, 1553, 1515, 1491, 1373, 1256, 1222 cm^{-1}. HPLC (after chlorination: AS-H, 80:20 hexanes:iPrOH, 0.8 mL/min, 210 nm): t_{major} = 24.2 min, t_{minor} = 16.4 min, 92% ee.

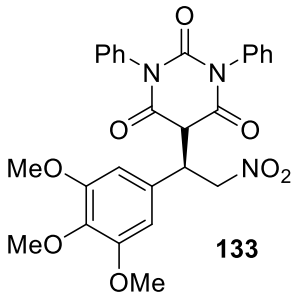

133

(**133**). Flash column chromatography afforded **133** (95.8 mg, 92%) as a light pink solid. ^{1}H NMR (500 MHz, $CDCl_3$): δ = 7.45 (m, 6H), 7.03 (d, *J* = 5.5 Hz, 2H), 6.97 (brs, 2H), 6.42 (s, 2H), 5.28 (dd, *J* = 14.3, 7.9 Hz, 1H), 5.07 (dd, *J* = 14.2, 7.9 Hz, 1H), 4.61 (td, *J* = 7.9, 3.3 Hz, 1H), 4.14 (d, *J* = 3.3 Hz, 1H), 3.88 (s, 3H), 3.77 (s, 6H). ^{13}C NMR (125 MHz, $CDCl_3$): δ = 167.0, 166.8, 154.1, 150.0, 139.1, 133.9, 133.7, 129.7, 129.6, 129.6, 128.5, 128.3, 128.3, 105.5, 76.1, 61.1, 56.6, 52.2, 45.9. HRMS (ESI) calcd for $C_{27}H_{26}N_3O_8^+(M+H)^+$: 520.1714, Found: 520.1721. IR (film): 1698, 1591, 1555, 1506, 1463, 1373, 1247, 1220 cm^{-1}. HPLC (after chlorination: AS-H, 94:6 hexanes:iPrOH, 1.0 mL/min, 210 nm): t_{major} = 52.3 min, t_{minor} = 25.1 min, 91% ee.

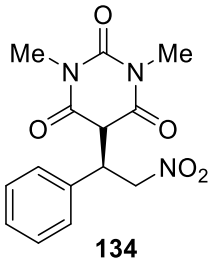

134

(**134**). Flash column chromatography afforded **134** (56.3 mg, 92%) as a pink solid. ^{1}H NMR (500 MHz, $CDCl_3$): δ = 7.30 (m, 3H), 7.05 (m, 2H), 5.29 (dd, *J* = 14.2, 7.9 Hz, 1H), 5.01 (dd, *J* = 14.2, 7.7 Hz, 1H), 4.51 (td, *J* = 7.8, 3.6 Hz, 1H), 3.86 (d, *J* = 3.6 Hz, 1H), 3.15 (s, 3H), 3.09 (s, 3H). ^{13}C NMR (125 MHz, $CDCl_3$): δ = 167.0, 150.7, 133.9, 129.6, 129.4, 128.4, 127.7, 76.1, 51.7, 45.7, 28.6, 28.5. HRMS (ESI) calcd for $C_{14}H_{16}N_3O_5^+(M+H)^+$: 306.1084, Found: 306.1079. IR (film): 1678, 1555, 1425, 1380, 1292 cm^{-1}. HPLC (after chlorination: AS-H, 80:20 hexanes:iPrOH, 0.8 mL/min, 210 nm): t_{major} = 16.0 min, t_{minor} = 13.7 min, 92% ee.

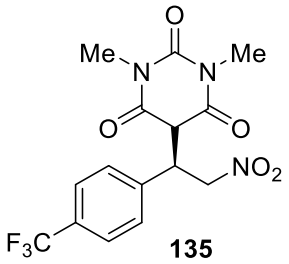

135

(**135**). Flash column chromatography afforded **135** (68.8 mg, 92%) as a light pink solid. ^{1}H NMR (500 MHz, $CDCl_3$): δ = 7.58 (d, *J* = 8.2 Hz, 2H), 7.30 (d, *J* = 8.2 Hz, 2H), 5.34 (dd, *J* = 14.3, 7.8 Hz, 1H), 5.08 (dd, *J* = 14.3, 7.8 Hz, 1H), 4.69 (td, *J* = 7.8, 3.4 Hz, 1H), 3.93 (d, *J* = 3.4 Hz, 1H), 3.20 (s, 3H), 3.16 (s, 3H). ^{13}C NMR (125 MHz, $CDCl_3$): δ = 166.6, 166.3, 150.5, 138.7, 131.7, 131.5, 128.7, 127.0, 126.4, 126.3, 124.8, 122.7, 120.5, 76.1, 51.3, 44.1, 28.9, 28.7. HRMS (ESI) calcd for $C_{15}H_{15}F_3N_3O_5^+(M+H)^+$: 374.0958, Found:374.0951. IR (film): 1684, 1559, 1425, 1384, 1327, 1123 cm^{-1}. HPLC (after chlorination: AS-H, 88:12 hexanes:iPrOH, 1.0 mL/min, 210 nm): t_{major} = 10.1 min, t_{minor} = 7.9 min, 94% ee.

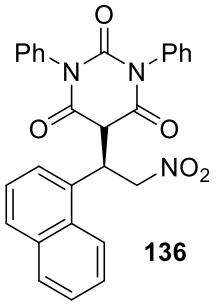

136

(**136**). Flash column chromatography afforded **136** (84.7 mg, 88%) as a light orange solid. ^{1}H NMR (500 MHz, $CDCl_3$): δ = 8.20 (d, *J* = 8.3 Hz, 1H), 7.95 (m, 2H), 7.51 (m, 9H), 7.29 (m, 1H), 7.22 (m, 2H), 7.12 (d, *J* = 7.4 Hz, 2H), 5.66 (m, 1H), 5.47 (dd, *J* = 13.8, 8.8 Hz, 1H), 5.09 (dd, *J* = 13.8, 6.8 Hz, 1H), 4.28 (d, *J* = 2.9 Hz, 1H). ^{13}C NMR (125 MHz, $CDCl_3$): δ = 167.1, 166.7, 150.1, 134.4, 133.9, 133.6, 131.3, 130.3, 129.6, 129.6, 129.4, 129.3, 129.3, 128.4, 128.2, 128.1, 128.0, 126.8, 125.3, 125.2, 123.1, 76.4, 52.0, 38.9. HRMS (ESI) calcd for $C_{28}H_{22}N_3O_5^+(M+H)^+$: 480.1554, Found: 480.1558. IR (film): 1697, 1554, 1491, 1372, 1216 cm^{-1}. HPLC (after chlorination: AS-H, 88:12 hexanes:iPrOH, 1.0 mL/min, 210 nm): t_{major} = 25.8 min, t_{minor} = 19.9 min, 98.5% ee.

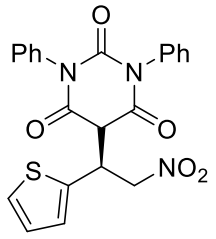

137

(**137**). Flash column chromatography afforded **137** (84.6 mg, 97%) as an off-white solid. ^{1}H NMR (500 MHz, $CDCl_3$): δ = 7.43 (m, 7H), 7.07 (m, 6H), 5.28 (m, 1H), 5.01 (m, 2H), 4.20 (d, *J* = 3.1 Hz, 1H). ^{13}C NMR (125 MHz, $CDCl_3$): δ = 166.6, 166.4, 150.2, 135.8, 133.9, 133.7, 129.6, 129.6, 129.6, 128.6, 128.4, 128.4, 128.1, 127.8, 126.8, 76.8, 52.1, 41.0. HRMS (ESI) calcd for

$C_{22}H_{18}N_3O_5S^+(M+H)^+$: 436.0962, Found: 436.0960. IR (film): 1697, 1555, 1491, 1373, 1218 cm^{-1}. HPLC (after chlorination: AD-H, 88:12 hexanes:iPrOH, 1.0 mL/min, 210 nm): t_{major} = 12.9 min, t_{minor} = 14.2 min, 87% ee.

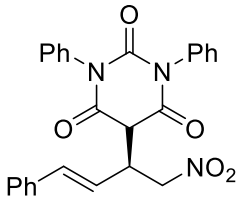

138

(**138**). Flash column chromatography afforded **138** (86.8 mg, 95%) as an orange solid. ^{1}H NMR (500 MHz, $CDCl_3$): δ = 7.44 (m, 6H), 7.33 (m, 5H), 7.19 (m, 2H), 7.11 (m, 2H), 6.72 (d, *J* = 15.8 Hz, 1H), 6.18 (dd, *J* = 15.8, 9.6 Hz, 1H), 4.95 (dd, *J* = 13.2, 8.0 Hz, 1H), 4.72 (dd, *J* = 13.1, 7.4 Hz, 1H), 4.25 (td, *J* = 9.9, 2.6 Hz, 1H), 4.06 (d, *J* = 2.7 Hz, 1H). ^{13}C NMR (125 MHz, $CDCl_3$): δ = 166.5, 150.5, 137.4, 135.4, 134.0, 133.9, 129.7, 129.6, 129.6, 129.5, 129.1, 128.4, 126.8, 121.5, 76.3, 51.5, 43.3. HRMS (ESI) calcd for $C_{26}H_{22}N_3O_5^+(M+H)^+$: 456.1554, Found: 456.1556. IR (film): 1699, 1552, 1491, 1372, 1217 cm^{-1}. HPLC (after chlorination: AS-H, 88:12 hexanes:iPrOH, 1.0 mL/min, 210 nm): t_{major} = 23.7 min, t_{minor} = 14.5 min, 72% ee.

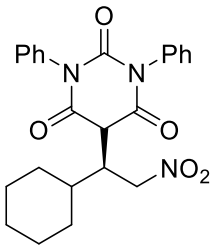

139

(**139**). Flash column chromatography afforded **139** (84.8 mg, 97%) as a pink solid. ^{1}H NMR (500 MHz, $CDCl_3$): δ = 7.45 (m, 6H), 7.25 (m, 4H), 4.91 (dd, *J* = 12.9, 11.4 Hz, 1H), 4.63 (dd, *J* =

12.9, 3.9 Hz, 1H), 4.11 (d, *J* = 1.9 Hz, 1H), 3.33 (m, 1H), 1.76 (m, 6H), 1.18 (m, 5H). ^{13}C NMR (125 MHz, $CDCl_3$): δ = 167.5, 167.0, 150.8, 134.4, 134.3, 129.6, 129.6, 129.4, 129.4, 128.5, 75.2, 48.4, 43.7, 39.1, 31.3, 31.3, 26.4, 26.2, 26.1. HRMS (ESI) calcd for $C_{24}H_{26}N_3O_5^+(M+H)^+$: 436.1867, Found: 436.1866. IR (film): 1700, 1549, 1491, 1366, 1211 cm^{-1}. HPLC (after chlorination: AS-H, 92:8 hexanes:iPrOH, 1.0 mL/min, 210 nm): t_{major} = 12.4 min, t_{minor} = 10.3 min, 96% ee.

Procedure for the determination of enantioselectivity: Due to poor solubility, high retention times, and a tendency to streak, barbituric acids adducts were chlorinated prior to ee measurement. A representative example is shown below for **121**.

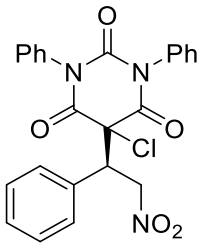

140

(**140**). To a solution of **121** (43 mg, 0.1 mmol, 1.0 equiv) in CH_2Cl_2 (1.0 mL) was added N-chlorosuccinimmide (13 mg, 0.1 mmol, 1.0 equiv). The mixture was stirred at room temperature for 20 min, and then filtered through a plug of silica gel (eluting with CH_2Cl_2) to afford the desired product **140** (41.9 mg, 90%) as a white solid. ^{1}H NMR (500 MHz, $CDCl_3$): δ = 7.49 (m, 6H), 7.42 (m, 3H), 7.33 (m, 2H), 7.13 (d, *J* = 6.4 Hz, 2H), 6.84 (br s, 2H), 5.49 (dd, *J* = 14.5, 3.4 Hz, 1H), 5.39 (dd, *J* = 14.4, 10.9 Hz, 1H), 4.86 (dd, *J* = 10.9, 3.4 Hz, 1H). ^{13}C NMR (125 MHz, $CDCl_3$): δ = 165.4, 164.6, 148.5, 133.4, 133.4, 131.9, 130.4, 130.0, 130.0, 129.9, 129.9, 129.8,

129.7, 128.1, 128.1, 75.8, 62.9, 50.8. HRMS (ESI) calcd for $C_{24}H_{19}ClN_3O_5^+$ $(M+H)^+$: 464.1008, Found: 464.1007. IR (film): 1708, 1557, 1491, 1370, 1224 cm^{-1}

V1.4 Experimental Procedures and Characterization Data for Chapter 4

Bispyridiniums **187** - **192** are known.[21]

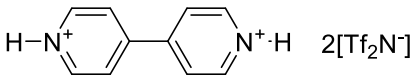

197

(**197**). To a solution of 4,4'-dipyridyl (31.2 mg, 0.20 mmol, 1.00 equiv) in CH_2Cl_2 (2 mL) was added a solution of bis(trifluoromethane)sulfonimide (0.2075 M, 1.88 mL, 0.39 mmol, 1.95 equiv) and the resulting mixture was stirred at rt for 45 min. 1 mL hexanes was then added. Filtration and washing with CH_2Cl_2 afforded **197** (121 mg, 86%) as a white solid. ^{1}H NMR (500 MHz, DMSO-d_6): δ = 8.92 (dd, J = 4.8, 1.6 Hz, 4H), 8.18 (dd, J = 4.9, 1.5 Hz, 4H). ^{13}C NMR (125 MHz, DMSO-d_6): δ = 148.0, 146.2, 123.8, 119.5 (q, J = 320 Hz).

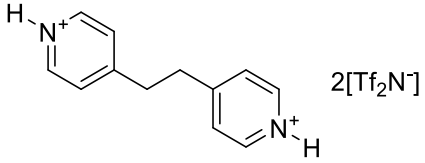

198

(**198**). To a solution of 1,2-bis(4-pyridyl)ethane (69 mg, 0.377 mmol, 1.00 equiv) in CH_2Cl_2 (2 mL) was added a solution of bis(trifluoromethane)sulfonimide (0.334 M, 2.2 mL, 0.735 mmol, 1.95 equiv) and the resulting mixture was stirred at rt for 45 min. 1 mL hexanes was then added.

[21] Türkmen, Y. E. Ph.D. Thesis, The University of Chicago, 2012.

Filtration and washing with CH_2Cl_2 afforded **198** (243 mg, 88%) as a white solid. ^{1}H NMR (500 MHz, DMSO-d_6): δ = 8.82 (dd, *J* = 5.2, 1.3 Hz, 4H), 7.93 (d, *J* = 6.5 Hz, 4H), 3.29 (s, 4H). ^{13}C NMR (125 MHz, DMSO-d_6): δ = 160.6, 142.0, 126.9, 119.5 (q, *J* = 320 Hz), 34.3.

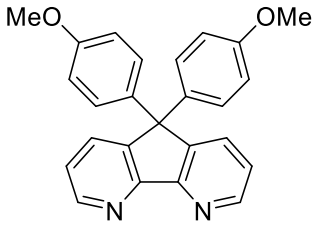

304

(**304**). Bispyridine **304** was prepared according to the literature.[22]

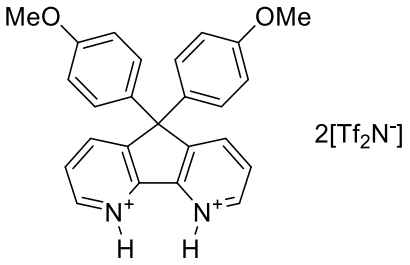

203

(**203**). Bispyridinium **203** was prepared in analogous fashion to bispyridinium **198**. ^{1}H NMR (500 MHz, DMSO-d_6): δ = 8.77 (m, 2H), 8.16 (d, *J* = 7.8 Hz, 2H), 7.60 (dd, *J* = 7.8, 5.0 Hz, 2H), 7.07 (d, *J* = 8.8 Hz, 4H), 6.85 (d, *J* = 8.8 Hz, 4H), 3.70 (s, 6H).

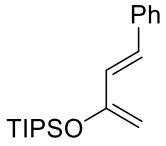

195

[22] Katsuhiko, O.; Tomoki, Y.; Masakazu, O.; Katsuhiro, S.; Matsushita, Y.; Shigeki, N.; Hiroyuki, O.; Hiroyoshi, O. *Chemistry Letters* **2004**, *33*, 276.

(**195**). Diene **195** was prepared according to the literature.[23]

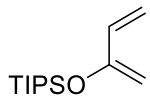

200

(**200**). Diene **200** was prepared according to the literature.[24]

Nitro-Diels-Alder reaction between 2-siloxy dienes and nitroalkenes catalyzed by a bispyridinium. Representative example: To a solution of bispyridinium **188** (2.1 mg - 62 mg, 0.0025 mmol - 0.075 mmol, 0.5 - 15 mol%) and nitroalkene (0.50 mmol, 1.0 equiv) in dry CH_2Cl_2 (2 - 4 mL) with activated 3 Å molecules sieves was added either diene **195** (182 mg, 0.60 mmol, 1.2 equiv) or diene **200** (226 mg, 1.0 mmol, 2.0 equiv) dropwise over 20 seconds. The reaction was stirred at room temperature for the given time. Reactions were worked up in one of three ways:

A: Quenched with 4 drops Et_3N, concentrated (crude ^{1}H-NMR taken for dr determination) and then purified by silica gel chromatography, or

B: Quenched with 4 drops Et_3N, concentrated, purified by silica gel chromatography and then deprotected/purified according to **C**, or

C: Concentrated and deprotected by stirring in 1,4-dioxane (4 mL) that had been acidified with 5 drops 12 N HCl. Upon completion of deprotection, the reaction mixture was diluted with H_2O (5 mL) and extracted with CH_2Cl_2 (10 mL x 5), dried with $MgSO_4$, concentrated and purified by silica gel chromatography to afford the desired product.

---

[23] Racine, S.; de Nanteuil, F.; Serrano, E.; Waser, J. *Angew. Chem. Int. Ed.* **2014**, *53*, 8484.
[24] Snyder, S. A.; Corey, E. J. *J. Am. Chem. Soc.* **2006**, *128*, 740.

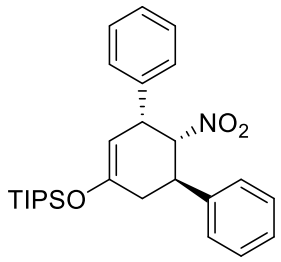

196

(**196**). Conditions: 0.5 mol% **188**, 2 mL CH_2Cl_2, 10 min. Purification by general procedure **A** (1:20 EtOAc:hexanes) afforded **196** (163 mg, 72%) as a single diastereomer and an off-white solid. ^{1}H NMR (500 MHz, $CDCl_3$): δ = 7.27-7.36 (m, 10H), 5.31 (dd, *J* = 12.0, 6.2 Hz, 1H), 4.99 (dd, *J* = 5.5, 1.3 Hz, 1H), 4.24 (t, *J* = 5.7 Hz, 1H), 3.58 (td, *J* = 11.3, 6.5 Hz, 1H), 2.69 (dd, *J* = 18.0, 6.6 Hz, 1H), 1.20 (m, 3H), 1.10 (dd, *J* = 7.2, 3.9 Hz, 18H). ^{13}C NMR (125 MHz, $CDCl_3$): δ = 151.0, 140.9, 138.2, 129.2, 129.0, 128.6, 128.3, 127.5, 127.4, 102.1, 90.1, 44.7, 38.7, 38.3, 18.2, 12.7.

Determination of relative stereochemistry: The above adduct **196** was deprotected according to general procedure **C** to give the corresponding ketone. Analytical data matched previously reported values.[25] Relative stereochemistry of other nitro-DA adducts are assigned by analogy.

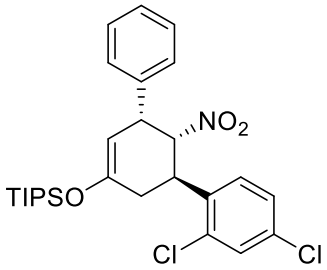

205

[25] Wu, L.; Bencivenni, G.; Mancinelli, M.; Mazzanti, A.; Bartoli, G.; Melchiorre, P. *Angew. Chem. Int. Ed.* **2009**, *48*, 7196.

(**205**). Conditions: 0.5 mol% **188**, 2 mL CH_2Cl_2, 10 min. Purification by general procedure **A** (4% EtOAc in hexanes) afforded **205** (198 mg, 76%) as a single diastereomer and a yellow solid. ^{1}H NMR (500 MHz, $CDCl_3$): δ = 7.33 (m, 4H), 7.19 (m, 3H), 7.13 (d, *J* = 8.4 Hz, 1H), 5.36 (br s, 1H), 5.00 (d, *J* = 5.3 Hz, 1H), 4.26 (t, *J* = 5.7 Hz, 1H), 4.20 (br s, 1H), 2.73 (dd, *J* = 17.5, 5.9 Hz, 1H), 2.25 (br s, 1H), 1.21 (m, 3H), 1.11 (dd, *J* = 7.2, 4.1 Hz, 18H). ^{13}C NMR (125 MHz, $CDCl_3$): δ = 150.7, 137.8, 133.7, 130.3, 129.3, 129.0, 129.0, 128.9, 128.6, 128.2, 128.1, 128.0, 102.4, 44.8, 18.3, 18.3, 12.9.

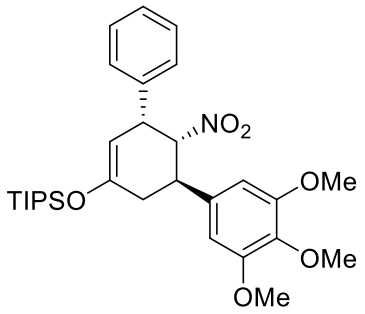

206

(**206**). Conditions: 0.5 mol% **188**, 2 mL CH_2Cl_2, 10 min. Purification by general procedure **A** (1:5 EtOAc:hexanes) afforded **206** (86.8 mg, 95%) as a single diastereomer and a light yellow solid. ^{1}H NMR (500 MHz, $CDCl_3$): δ = 7.34 (m, 3H), 7.23 (dd, *J* = 7.6, 1.8 Hz, 2H), 6.39 (s, 2H), 5.29 (dd, *J* = 11.9, 6.2 Hz, 1H), 4.98 (m, 1H), 4.23 (t, *J* = 5.7 Hz, 1H), 3.82 (s, 6H), 3.79 (s, 3H), 3.51 (td, *J* = 11.1, 6.6 Hz, 1H), 2.70 (dd, *J* = 18.0, 6.6 Hz, 1H), 2.44 (dd, *J* = 18.0, 10.8 Hz, 1H), 1.21 (m, 3H), 1.11 (dd, *J* = 7.2, 4.0 Hz, 18H). ^{13}C NMR (125 MHz, $CDCl_3$): δ = 153.7, 151.0, 138.3, 136.7, 129.3, 129.0, 128.8, 128.4, 128.0, 104.6, 102.0, 90.2, 61.1, 56.5, 44.8, 39.1, 38.3, 18.3, 12.9.

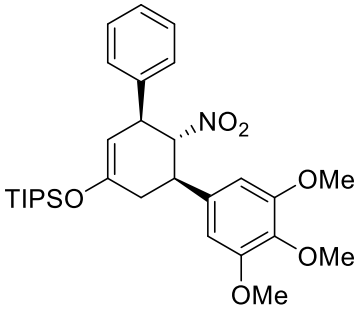

305

(**305**). Purification of the above reaction mixture also yielded minor diastereomer **305** (76 mg, 28%) as a light yellow solid. ^{1}H NMR (500 MHz, $CDCl_3$): δ = 7.28 (m, 5H), 6.43 (s, 2H), 5.07 (dd, *J* = 5.7, 3.1 Hz, 1H), 4.96 (s, 1H), 4.27 (s, 1H), 3.83 (s, 6H), 3.82 (s, 3H), 3.48 (ddd, *J* = 12.0, 6.0, 3.1 Hz, 1H), 3.14 (m, 1H), 2.43 (dd, *J* = 17.0, 6.0 Hz, 1H), 1.26 (m, 3H), 1.16 (dd, *J* = 11.8, 7.3 Hz, 18H). ^{13}C NMR (125 MHz, $CDCl_3$): δ = 153.8, 152.2, 139.5, 134.9, 129.1, 128.2, 128.1, 104.5, 100.8, 91.3, 61.1, 56.4, 46.1, 44.2, 31.6, 18.4, 18.3, 13.0.

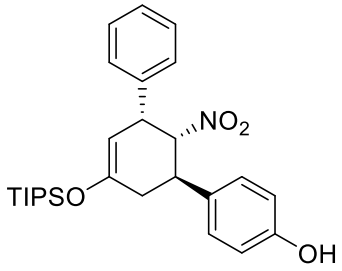

207

(**207**). Conditions: 1 mol% **188**, 4 mL CH_2Cl_2, 10 min. Purification by general procedure **A** (2:5 EtOAc:hexanes) afforded **207** (166 mg, 71%) as an orange-brown solid. Major diastereomer: ^{1}H NMR (500 MHz, $CDCl_3$): δ = 7.32 (m, 4H), 7.21 (m, 3H), 7.07 (d, *J* = 8.6 Hz, 2H), 6.72 (d, *J* = 8.6 Hz, 2H), 5.23 (dd, *J* = 12.0, 6.2 Hz, 1H), 4.97 (dd, *J* = 5.5, 1.2 Hz, 1H), 4.66 (s, 1H), 4.21 (t, *J* = 5.7 Hz, 1H), 3.51 (m, 1H), 2.66 (dd, *J* = 18.0, 6.5 Hz, 1H), 2.42 (m, 1H), 1.16 (m, 3H), 1.10 (dd, *J* = 7.2, 3.7 Hz, 18H). ^{13}C NMR (125 MHz, $CDCl_3$): δ = 155.3, 151.1, 138.3, 132.5, 129.3,

129.1, 128.7, 128.4, 128.0, 127.5, 116.0, 102.2, 90.7, 44.9, 38.3, 38.0, 18.3, 18.1, 18.0, 17.1, 12.9, 12.9, 12.8, 12.5.

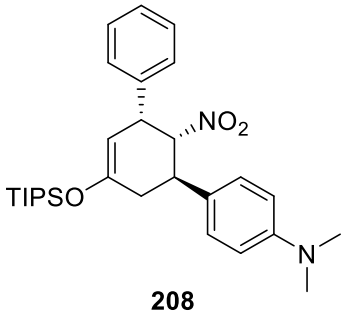

208

(**208**). Conditions: 2 mol% **188**, 2 mL CH_2Cl_2, 60 min. Purification by general procedure **A** (1:20 aetone:hexanes → 1:10 acetone:hexanes) afforded **208** (133 mg, 54%) as an orange solid. ^{1}H NMR (500 MHz, $CDCl_3$): δ = 7.31 (m, 3H), 7.21 (m, 2H), 7.06 (d, *J* = 8.8 Hz, 2H), 6.62 (d, *J* = 8.8 Hz, 2H), 5.23 (dd, *J* = 11.8, 6.2 Hz, 1H), 4.97 (dd, *J* = 5.4, 1.1 Hz, 1H), 4.19 (t, *J* = 5.7 Hz, 1H), 3.48 (td, *J* = 11.1, 6.6 Hz, 1H), 2.87 (s, 1H), 2.66 (dd, *J* = 18.0, 6.6 Hz, 1H), 2.44 (ddt, *J* = 18.0, 10.7, 1.7 Hz, 1H), 1.19 (m, 3H), 1.10 (dd, *J* = 7.2, 3.9 Hz, 18H). ^{13}C NMR (125 MHz, $CDCl_3$): δ = 151.3, 150.0, 138.6, 129.3, 128.7, 128.4, 128.2, 113.0, 102.3, 90.7, 44.8, 40.8, 38.3, 37.9, 30.9, 18.3, 12.8.

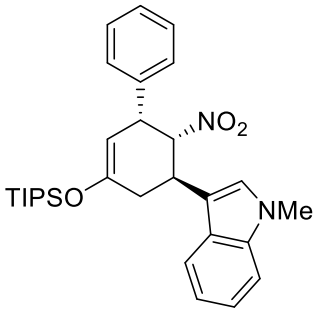

209

(**209**). Conditions: 2 mol% **188**, 2 mL CH_2Cl_2, 10 min. Purification by general procedure **A** (1:10 EtOAc:hexanes) afforded **209** (230 mg, 91%) in a 6:1 dr and as a yellow solid. ^{1}H NMR (500

MHz, $CDCl_3$): δ = 7.60 (d, *J* = 8.0 Hz, 1H), 7.32 (m, 3H), 7.22 (m, 3H), 7.10 (ddd, *J* = 8.0, 7.0, 1.0 Hz, 1H), 6.89 (s, 1H), 5.43 (dd, *J* = 11.1, 6.1 Hz, 1H), 5.02 (d, *J* = 5.1 Hz, 1H), 4.19 (t, *J* = 5.6 Hz, 1H), 3.92 (td, *J* = 9.9, 6.9 Hz, 1H), 3.69 (s, 3H), 2.82 (dd, *J* = 18.1, 6.9 Hz, 1H), 2.70 (ddt, *J* = 18.2, 9.8, 1.7 Hz, 1H), 1.19 (m, 3H), 1.12 (dd, *J* = 7.2, 4.0 Hz, 18H). ^{13}C NMR (125 MHz, $CDCl_3$): δ = 151.2, 138.8, 137.3, 129.3, 129.0, 128.7, 128.2, 128.2, 126.7, 126.6, 122.0, 119.4, 119.1, 113.7, 109.9, 102.3, 90.2, 44.6, 36.7, 32.8, 31.1, 18.4, 18.3, 18.3, 18.3, 18.0, 13.0, 12.9, 12.6.

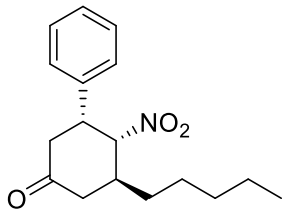

210a

(**210a**). Conditions: 5 mol% **188**, 2 mL CH_2Cl_2, 20 min. Purification by general procedure **C** (1:5 EtOAc:hexanes) afforded **210a** (91 mg, 63%) in a 4:1 dr and as a thick brown gel. ^1H NMR (500 MHz, $CDCl_3$): δ = 7.34 (m, 3H), 7.17 (m, 2H), 4.93 (t, *J* = 4.7 Hz, 1H), 3.64 (m, 1H), 3.42 (m, 1H), 2.94 (dd, *J* = 15.2, 12.0 Hz, 1H), 2.94 (dd, *J* = 15.3, 5.7 Hz, 1H), 2.67 (m, 2H), 2.36 (ddd, *J* = 15.4, 5.9, 1.0 Hz, 1H), 1.42 (m, 8H), 0.90 (t, *J* = 7.0 Hz, 1H). ^{13}C NMR (125 MHz, $CDCl_3$): δ = 208.4, 137.3, 129.5, 129.3, 128.7, 128.5, 127.6, 127.1, 91.0, 90.3, 45.7, 42.2, 42.1, 41.8, 41.5, 40.9, 40.6, 38.8, 33.7, 32.8, 31.8, 31.7, 26.6, 26.5, 22.7, 22.7, 14.2.

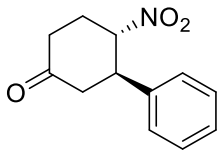

211a

(**211a**). Conditions: 2 mol% **188**, 2 mL CH_2Cl_2, 20 min. Purification by general procedure **C** (4% EtOAc in hexanes, then hexanes → 2:5 EtOAc:hexanes) afforded **211a** (78 mg, 71%) in a 7:1 dr and as an off-white solid. ^{1}H NMR (500 MHz, $CDCl_3$): δ = 7.33 (m, 3H), 7.23 (m, 2H), 5.06 (td, *J* = 10.4, 3.7 Hz, 1H), 3.71 (m, 1H), 2.64 (m, 6H). ^{13}C NMR (125 MHz, $CDCl_3$): δ = 206.0, 138.4, 129.5, 129.3, 128.6, 128.5, 127.6, 127.2, 88.3, 85.5, 47.2, 45.8, 45.3, 42.0, 38.2, 36.6, 29.8, 27.4.

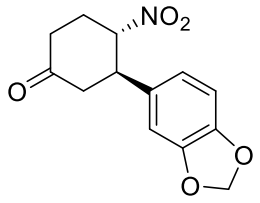

212a

(**212a**). Conditions: 2 mol% **188**, 3 mL CH_2Cl_2, 20 min. Purification by general procedure **B** (1:8 EtOAc:hexanes, then hexanes → 2:5 EtOAc:hexanes → 3:5 EtOAc:hexanes) afforded **212a** (111 mg, 84%) as an off-white solid. ^{1}H NMR (500 MHz, $CDCl_3$): δ = 6.76 (d, *J* = 8.0 Hz, 1H), 6.68 (m, 2H), 5.96 (m, 2H), 4.98 (td, *J* = 10.5, 3.8 Hz, 1H), 3.60 (ddd, *J* = 12.6, 10.5, 5.0 Hz, 1H), 2.60 (m, 6H). ^{13}C NMR (125 MHz, $CDCl_3$): δ = 205.8, 148.6, 147.9, 132.2, 121.1, 120.9, 109.2, 109.0, 108.0, 107.4, 101.7, 88.7, 85.7, 47.1, 46.1, 45.3, 42.5, 38.3, 36.7, 29.8, 27.5.

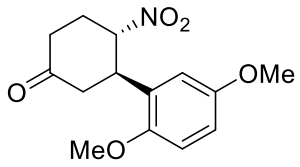

213a

(**213a**). Conditions: 2 mol% **188**, 2 mL CH_2Cl_2, 20 min. Purification by general procedure **B** (1:10 EtOAc:hexanes, then 3:5 EtOAc:hexanes) afforded **213a** (134 mg, 96%) as a single diastereomer and an off-white solid. ^{1}H NMR (500 MHz, $CDCl_3$): δ = 6.82 (d, *J* = 8.9 Hz, 1H),

6.78 (dd, *J* = 8.9, 3.0 Hz, 1H), 6.67 (d, *J* = 2.9 Hz, 1H), 5.41 (td, *J* = 10.0, 3.9 Hz, 1H), 3.87 (m, 1H), 3.83 (s, 3H), 3.74 (s, 3H), 2.94 (dd, *J* = 15.5, 11.6 Hz, 1H), 2.58 (m, 5H). ^{13}C NMR (125 MHz, $CDCl_3$): δ = 206.9, 154.0, 151.5, 127.3, 115.9, 113.5, 112.5, 85.5, 56.1, 55.9, 44.1, 43.6, 38.1, 29.5.

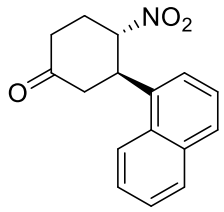

214a

(**214a**). Conditions: 2 mol% **188**, 2 mL CH_2Cl_2, 60 min. Purification by general procedure **C** (2:5 EtOAc:hexanes) afforded **214a** (114 mg, 85%) in a 5:1 dr and as an off-white solid. ^{1}H NMR (500 MHz, $CDCl_3$)

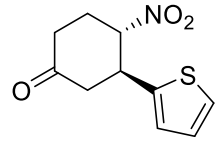

215a

(**215a**). Conditions: 2 mol% **188**, 2 mL CH_2Cl_2, 15 min. Purification by general procedure **C** (2:5 EtOAc:hexanes) afforded **215a** (86 mg, 76%) in a dr and as a thick brown gel. ^{1}H NMR (500 MHz, $CDCl_3$): δ = 7.25 (dd, *J* = 5.1, 1.2 Hz, 1H), 6.94 (dd, *J* = 5.1, 3.5 Hz, 1H), 6.90 (m, 1H), 4.97 (m, 1H), 4.09 (ddd, *J* = 11.5, 9.6, 5.1 Hz, 1H), 2.88 (ddd, *J* = 15.3, 5.1, 2.0 Hz, 1H), 2.74 (ddd, *J* = 15.3, 11.6, 0.8 Hz, 1H), 2.65 (m, 1H), 2.53 (m, 3H). ^{13}C NMR (125 MHz, $CDCl_3$): δ = 205.1, 141.5, 127.6, 126.1, 125.5, 89.1, 46.1, 42.3, 38.0, 29.2.

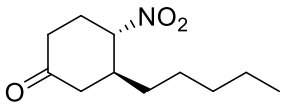

216a

(**216a**). Conditions: 10 mol% **188**, 4 mL CH_2Cl_2, 30 min. Purification by general procedure **C** (1:5 EtOAc:hexanes) afforded **216a** (90 mg, 84%) in >15:1 dr and as an off-white solid. ^{1}H NMR (500 MHz, $CDCl_3$): δ = 4.62 (m, 1H), 2.61 (m, 3H), 2.44 (m, 3H), 2.16 (m, 1H), 1.30 (m, 9H), 0.88 (t, *J* = 7.0 Hz, 3H). ^{13}C NMR (125 MHz, $CDCl_3$): δ = 207.1, 87.5, 43.2, 40.7, 38.0, 32.9, 31.7, 29.0, 25.6, 22.7, 18.6, 14.2, 13.6.

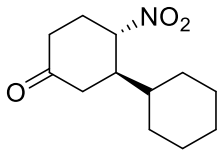

217a

(**217a**). Conditions: 10 mol% **188**, 4 mL CH_2Cl_2, 30 min. Purification by general procedure **C** (1:5 EtOAc:hexanes) afforded **217a** (85 mg, 75%) as an off-white solid. ^{1}H NMR (500 MHz, $CDCl_3$): δ = 4.84 (m, 1H), 2.58 (m, 1H), 2.44 (m, 5H), 2.26 (m, 1H), 1.77 (m, 3H), 1.68 (d, *J* = 12.9 Hz, 1H), 1.51 (d, *J* = 12.5 Hz, 1H), 1.15 (m, 6H). ^{13}C NMR (125 MHz, $CDCl_3$): δ = 207.8, 85.31, 45.9, 39.5, 38.9, 37.9, 30.8, 29.4, 27.3, 26.7, 26.5, 26.4.

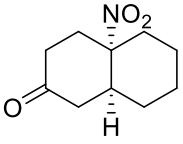

202

(**202**). Conditions: 15 mol% **188**, 4 mL CH_2Cl_2, 30 min. Purification by general procedure **B** (4% EtOAc in hexanes, then 1:5 EtOAc:hexanes) afforded **202** (54 mg, 55%) as an off-white solid. Analytical data matched previously reported values.[26]

V1.5 Experimental Procedures and Characterization Data for Chapter 5

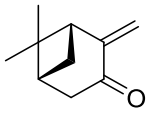

pinocarvone

(Pinocarvone). Prepared according to a modified literature procedure.[27] To a vigorously stirred mixture of SeO_2 (1.1 g, 10 mmol, 0.5 equiv) and *tert*-butyl hydroperoxide (70% in H_2O, 5.5 mL, 40 mmol, 2.0 equiv) in CH_2Cl_2 (15 mL) was added (−)-β-pinene (3.1 mL, 20 mmol, 1.0 equiv) dropwise at 0 °C over 30 minutes (CAUTION: Strongly exothermic. Ensure vigorous stirring and slow addition). After stirring at rt for 48 h, the reaction mixture was diluted with hexanes and washed with H_2O then brine. The organic layer was dried over $MgSO_4$ and concentrated under reduced pressure. Purification by flash column chromatography (3% EtOAc in hexanes → 10% EtOAc in hexanes) afforded pinocarvone (1.62 g, 54%) as a colorless oil. Analytical data matched previously reported values.[28]

[26] Kim, W. H.; Lee, J. H.; Danishefsky, S. J. *J. Am. Chem. Soc.* **2009**, *131*, 12576.
[27] Höld, K. M.; Sirisoma, N. S.; Sparks, S. E.; Casida, J. E. *Xenobiotica* **2008**, *32*, 251.
[28] Malkov, A. V.; Pernazza, D.; Bell, M.; Bella, M.; Massa, A.; Teplý, F.; Meghani, P.; Kočovský, P. *J. Org. Chem.* **2003**, *68*, 4727.

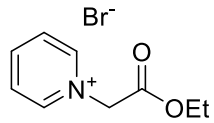

248

(**248**). Pyridinium salt **248** was prepared according to a literature procedure.[28]

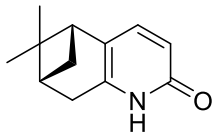

249

(**249**). Pyridone **249** was prepared according to a literature procedure.[29]

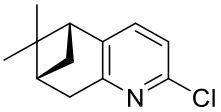

247

(**247**). A solution of pyridone **249** (2.84 g, 15 mmol, 1.0 equiv) in $POCl_3$ (10 mL) was heated in a bomb at 145 °C for 30 min. The reaction vessel was then cooled to rt, and PCl_5 (4.69 g, 22.5 mmol, 1.5 equiv) was added in one portion. The bomb was resealed and placed into a 145 °C oil bath for 15 h. The reaction was then cooled to rt and slowly added to H_2O (50 mL) at 0 °C over 45 min with vigorous stirring (CAUTION: Strongly exothermic. Ensure vigorous stirring and slow addition). The mixture is then made strongly basic (pH>12) by the slow addition of solid KOH pellets at 0 °C over 45 min with vigorous stirring (CAUTION: Strongly exothermic. Ensure vigorous stirring and slow addition). The aqueous phase is then extracted with CH_2Cl_2, dried over $MgSO_4$, filtered through Celite, and concentrated under reduced pressure. Purification

[29] Schmitz, C.; Leitner, W.; Franciò, G. *Eur. J. Org. Chem.* **2015**, 2889.

by flash column chromatography (10% EtOAc in hexanes) afforded **247** (2.52 g, 81%) as a pale yellow oil. Analytical data matched previously reported values.[30]

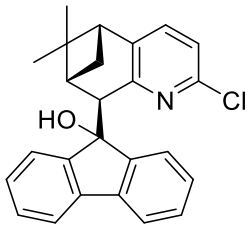

250

(**250**). To a solution of diisopropylamine (0.36 mL, 2.57 mmol, 1.1 equiv) in dry THF (5 mL) was added *n*-BuLi (1.5 M, 1.6 mL, 2.34 mmol, 1.0 equiv) dropwise at 0 °C and the resulting solution was stirred for 30 min at that temperature. The solution was then cooled to -78 °C and a solution of chloropyridine **247** (486 mg, 2.34 mmol, 1.0 equiv) in dry THF (5 mL) was added dropwise over 30 min. After stirring at -78 °C for 2 h, a solution of fluorenone (463 mg, 2.57 mmol, 1.1 equiv) in THF (5 mL) was added dropwise over 30 min. The resulting solution was allowed to gradually warm to rt overnight. The reaction mixture was then quenched with aqueous $NaHCO_3$, diluted with H_2O, and extracted three times with CH_2Cl_2. The combined organic layers were dried over $MgSO_4$ and concentrated under reduced pressure. The resulting solid is then suspended in CH_2Cl_2:hexanes (1 mL: 12 mL) and stored at -20 °C for 2 h before being filtered and washed with ice-cold hexanes to afford **250** (560 mg, 62%) as a white solid. ^{1}H NMR (500 MHz, $CDCl_3$): δ = 7.63 (s, 1H), 7.59 (m, 2H), 7.54 (d, *J* = 7.5 Hz, 1H), 7.36 (m, 2H), 7.22 (m, 3H), 6.95 (td, *J* = 7.5, 1.1 Hz, 1H), 6.49 (d, *J* = 7.6 Hz, 1H), 3.93 (d, *J* = 1.7 Hz, 1H), 2.52 (t, *J* = 5.6 Hz, 1H), 1.84 (dt, *J* = 10.4, 5.7 Hz, 1H), 1.36 (td, *J* = 6.0, 2.0 Hz, 1H), 1.12 (s, 3H), 0.64 (s, 3H), 0.20 (d, *J* = 10.2 Hz, 1H).

[30] Chelucci, G.; Marchetti, M.; Malkov, A. V.; Friscourt, F.; Swarbrick, M. E.; Kocovský. *Tetrahedron* **2011**, *67*, 5421.

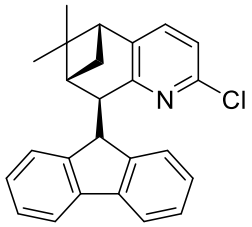

251

(**251**). To a solution of **250** (98 mg, 0.25 mmol, 1.0 equiv) and Et_3SiH (0.40 mL, 2.5 mmol, 10 equiv) in CH_2Cl_2 (2.5 mL) was added BF_3•Et_2O (0.25 mL, 2.0 mmol, 8.0 equiv) and the resulting solution was stirred for 2.5 h. The reaction mixture was then quenched with aqueous $NaHCO_3$, extracted twice with CH_2Cl_2, and the combined organic layers dried over $MgSO_4$ and concentrated under reduced pressure. Purification by flash column chromatography (1:1 CH_2Cl_2:hexanes) afforded **251** (90 mg, 96%) as a white solid. ^{1}H NMR (500 MHz, $CDCl_3$): δ = 7.75 (d, *J* = 7.4 Hz, 1H), 7.70 (d, *J* = 7.6 Hz, 1H), 7.55 (m, 1H), 7.37 (m, 2H), 7.21 (m, 2H), 6.95 (td, *J* = 7.5, 1.1 Hz, 1H), 6.46 (dd, *J* = 7.6, 0.8 Hz, 1H), 5.34 (d, *J* = 4.8 Hz, 1H), 4.03 (dd, *J* = 4.9, 1.7 Hz, 1H), 2.55 (t, *J* = 5.7 Hz, 1H), 1.88 (m, 1H), 1.47 (td, *J* = 6.1, 2.1 Hz, 1H), 1.12 (s, 3H), 0.65 (s, 3H), 0.63 (d, *J* = 10.1 Hz, 1H).

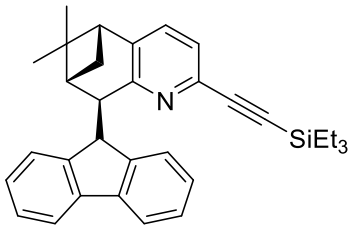

252

(**252**). To a flask containing $Pd(MeCN)_2Cl_2$ (19 mg, 0.074 mmol, 5 mol%), XPhos (106 mg, 0.222 mmol, 15 mol%), and Cs_2CO_3 (1.45 g, 4.44 mmol, 3.0 equiv) was added dry, degassed MeCN (12 mL). The resulting suspension was stirred at rt for 45 min. The reaction was then treated sequentially with chloropyridine **251** (550 mg, 1.48 mmol, 1.0 equiv) and

ethynyltriethylsilane (0.53 mL, 2.96 mmol, 2.0 equiv) and heated at reflux for 3 h. After cooling to rt, the reaction was filtered through Celite, eluting with CH_2Cl_2. Concentration of the reaction under reduced pressure followed by purification by flash column chromatography (1:2 CH_2Cl_2:hexanes) afforded **252** (696 mg, 99%) as a light yellow solid. ^{1}H NMR (500 MHz, $CDCl_3$): δ = 7.75 (d, *J* = 7.2 Hz, 1H), 7.69 (d, *J* = 7.6 Hz, 1H), 7.56 (d, *J* = 7.4 Hz, 1H), 7.35 (m, 3H), 7.23 (m, 2H), 6.94 (td, *J* = 7.5, 1.1 Hz, 1H), 6.44 (dd, *J* = 7.6, 0.7 Hz, 1H), 5.44 (d, *J* = 4.9 Hz, 1H), 4.08 (dd, *J* = 4.8, 1.8 Hz, 1H), 2.55 (t, *J* = 5.7 Hz, 1H), 1.88 (m, 1H), 1.48 (td, *J* = 6.0, 2.1 Hz, 1H), 1.12 (s, 3H), 1.09 (t, *J* = 7.9 Hz, 9H), 0.73 (q, *J* = 8.0 Hz, 6H), 0.65 (buried, 1H), 0.64 (s, 3H).

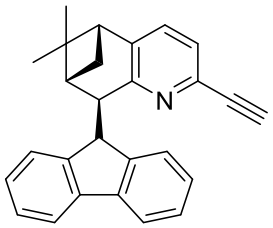

253

(**253**). To a solution of **252** (382 mg, 0.80 mmol, 1.0 equiv) in THF:H_2O (4 mL: 0.5 mL) was added TBAF (1.0 M in THF, 0.96 mL, 0.96 mmol, 1.2 equiv) and the resulting solution was stirred for 45 min. The reaction mixture was then quenched with aqueous $NaHCO_3$, extracted three times with CH_2Cl_2, and the combined organic layers dried over $MgSO_4$ and concentrated under reduced pressure. Purification by flash column chromatography (3:2 CH_2Cl_2:hexanes → 2:1 CH_2Cl_2:hexanes) afforded **253** (282 mg, 98%) as a white solid. ^{1}H NMR (500 MHz, $CDCl_3$): δ = 7.75 (d, *J* = 7.4 Hz, 1H), 7.69 (d, *J* = 7.5 Hz, 1H), 7.55 (d, *J* = 7.5 Hz, 1H), 7.35 (m, 3H), 7.23 (m, 2H), 6.93 (td, *J* = 7.5, 1.1 Hz, 1H), 6.42 (dd, *J* = 7.6, 0.8 Hz, 1H), 5.42 (d, *J* = 4.8 Hz,

1H), 4.06 (m, 1H), 3.19 (s, 1H), 2.57 (m, 1H), 1.89 (m, 1H), 1.49 (td, *J* = 6.0, 2.1 Hz, 1H), 1.13 (s, 3H), 0.66 (buried, 1H), 0.65 (s, 3H).

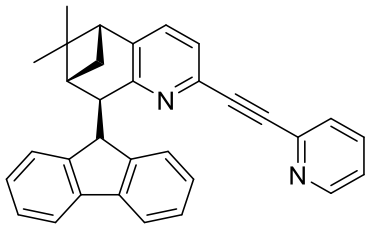

254

(**254**). To a solution of 2-bromopyridine (82 μL, 0.86 mmol, 1.5 equiv), $Pd(PPh_3)_2Cl_2$ (20 mg, 0.029 mmol, 5 mol%), and CuI (6 mg, 0.029 mmol, 5 mol%) in degassed 1,4-dioxane:Et_3N (1.5 mL: 1.5 mL) was added alkyne **253** (205 mg, 0.57 mmol, 1.0 equiv) and the resulting solution was then placed in a preheated oil bath and heated at 75 °C for 30 min. The reaction mixture was then cooled to rt, diluted with H_2O, extracted three times with CH_2Cl_2, and the combined organic layers dried over $MgSO_4$ and concentrated under reduced pressure. Purification by flash column chromatography (1% MeOH in CH_2Cl_2) afforded **254** (179 mg, 72%) as a light yellow solid. ^1H NMR (500 MHz, $CDCl_3$): δ = 8.65 (d, *J* = 4.6 Hz, 1H), 7.76 (d, *J* = 7.3 Hz, 1H), 7.69 (m, 3H), 7.57 (d, *J* = 7.4 Hz, 1H), 7.54 (d, *J* = 7.7 Hz, 1H), 7.36 (m, 4H), 7.23 (m, 1H), 6.94 (td, *J* = 7.5, 1.0 Hz, 1H), 6.45 (dd, *J* = 7.6, 0.6 Hz, 1H), 5.46 (d, *J* = 4.9 Hz, 1H), 4.11 (dd, *J* = 4.8, 1.7 Hz, 1H), 2.59 (t, *J* = 5.7 Hz, 1H), 1.90 (m, 1H), 1.51 (td, *J* = 6.0, 2.0 Hz, 1H), 1.14 (s, 3H), 0.67 (s, 3H), 0.66 (buried, 1H).

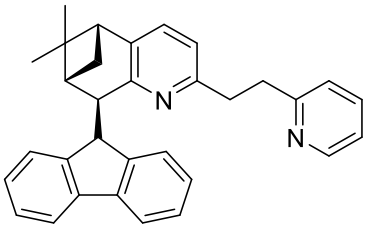

306

(**306**). To a flask containing 5% Pd/C (44 mg) and **254** (44 mg, 0.10 mmol) was added EtOH (1 mL). The reaction flask was equipped with an H_2 balloon and stirred for 96 h. The reaction mixture was then filtered through Celite and concentrated under reduced pressure. Purification by flash column chromatography (1% MeOH in CH_2Cl_2) afforded **306** (24.6 mg, 56%) as a pale brown gel. ^{1}H NMR (500 MHz, $CDCl_3$): δ = 8.56 (dd, *J* = 4.9, 0.9 Hz, 1H), 7.76 (d, *J* = 6.9 Hz, 1H), 7.69 (d, *J* = 7.6 Hz, 1H), 7.61 (d, *J* = 7.4 Hz, 1H), 7.52 (m, 1H), 7.36 (m, 2H), 7.21 (m, 2H), 7.12 (d, *J* = 7.6 Hz, 1H), 7.08 (ddd, *J* = 7.5, 4.9, 1.1 Hz, 1H), 6.99 (d, *J* = 7.6 Hz, 1H), 6.86 (td, *J* = 7.5, 1.1 Hz, 1H), 6.24 (m, 1H), 5.44 (d, *J* = 4.9 Hz, 1H), 4.06 (m, 1H), 3.37 (m, 4H), 2.50 (t, *J* = 5.7 Hz, 1H), 1.84 (m, 1H), 1.49 (td, *J* = 6.0, 2.1 Hz, 1H), 1.12 (s, 3H), 0.66 (s, 3H), 0.60 (d, *J* = 9.9 Hz, 1H).

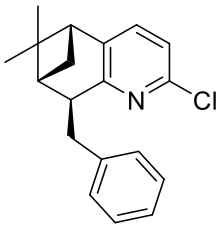

307

(**307**). To a solution of diisopropylamine (0.35 mL, 2.5 mmol, 1.1 equiv) in dry THF (4 mL) was added *n*-BuLi (1.5 M, 1.5 mL, 2.3 mmol, 1.0 equiv) dropwise at 0 °C and the resulting solution was stirred for 30 min at that temperature. The solution was then cooled to -78 °C and a solution of chloropyridine **247** (478 mg, 2.3 mmol, 1.0 equiv) in dry THF (4 mL) was added dropwise

over 30 min. After stirring at -78 °C for 2 h, a solution of benzyl bromide (0.3 mL, 2.5 mmol, 1.1 equiv) in THF (4 mL) was added dropwise over 30 min. The resulting solution was allowed to gradually warm to rt overnight. The reaction mixture was then quenched with aqueous $NaHCO_3$, diluted with H_2O, and extracted three times with CH_2Cl_2. The combined organic layers were dried over $MgSO_4$ and concentrated under reduced pressure. Purification by flash column chromatography afforded **307** (432 mg, 63%) as a thick brown gel. ^{1}H NMR (500 MHz, $CDCl_3$): δ = 7.30 (m, 2H), 7.22 (m, 4H), 7.05 (dd, *J* = 7.8, 0.6 Hz, 1H), 3.69 (dd, *J* = 13.6, 3.7 Hz, 1H), 3.27 (dt, *J* = 11.6, 3.1 Hz, 1H), 2.75 (t, *J* = 5.7 Hz, 1H), 2.62 (dd, *J* = 13.6, 11.6 Hz, 1H), 2.54 (dt, *J* = 10.0, 5.7 Hz, 1H), 2.03 (td, *J* = 6.1, 2.5 Hz, 1H), 1.39 (d, *J* = 9.9 Hz, 1H), 1.32 (s, 3H), 0.57 (s, 3H).

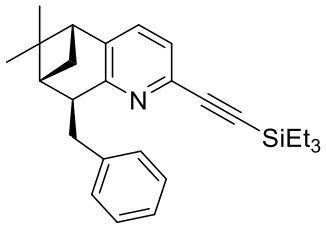

308

(**308**). To a flask containing $Pd(MeCN)_2Cl_2$ (19 mg, 0.073 mmol, 5 mol%), XPhos (104 mg, 0.218 mmol, 15 mol%), and Cs_2CO_3 (1.42 g, 4.35 mmol, 3.0 equiv) was added dry, degassed MeCN (16 mL). The resulting suspension was stirred at rt for 45 min. The reaction was then treated sequentially with chloropyridine **307** (432 mg, 1.45 mmol, 1.0 equiv) and ethynyltriethylsilane (0.52 mL, 2.90 mmol, 2.0 equiv) and heated at reflux for 3 h. After cooling to rt, the reaction was filtered through Celite, eluting with CH_2Cl_2. Concentration of the reaction under reduced pressure followed by purification by flash column chromatography afforded **308** (460 mg, 79%) as a light yellow solid. ^{1}H NMR (500 MHz, $CDCl_3$): δ = 7.30 (m, 2H), 7.23 (m,

4H), 7.16 (d, *J* = 7.7 Hz, 1H), 3.78 (dd, *J* = 13.7, 3.8 Hz, 1H), 3.33 (dt, *J* = 11.7, 3.2 Hz, 1H), 2.74 (t, *J* = 5.7 Hz, 1H), 2.61 (dd, *J* = 13.6, 11.7 Hz, 1H), 2.61 (dd, *J* = 13.6, 11.7 Hz, 1H), 2.52 (dt, *J* = 10.0, 5.7 Hz, 1H), 2.02 (td, *J* = 6.0, 2.5 Hz, 1H), 1.39 (d, *J* = 9.8 Hz, 1H), 1.31 (s, 3H), 1.07 (t, *J* = 7.9 Hz, 9H), 0.72 (q, *J* = 7.9 Hz, 6H), 0.56 (s, 3H).

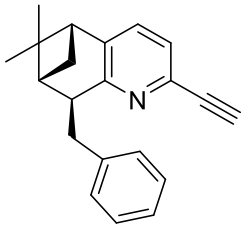

309

(**309**). To a solution of **308** (460 mg, 1.15 mmol, 1.0 equiv) in THF:H_2O (4 mL: 0.5 mL) was added TBAF (1.0 M in THF, 2.3 mL, 2.3 mmol, 2.0 equiv) and the resulting solution was stirred for 45 min. The reaction mixture was then quenched with aqueous $NaHCO_3$, extracted three times with CH_2Cl_2, and the combined organic layers dried over $MgSO_4$ and concentrated under reduced pressure. Purification by flash column chromatography afforded **309** (330 mg, quant.) as a light yellow solid. ^{1}H NMR (500 MHz, $CDCl_3$): δ = 7.30 (m, 2H), 7.22 (m, 5H), 3.77 (dd, *J* = 13.6, 3.7 Hz, 1H), 3.31 (m, 1H), 3.14 (s, 1H), 2.76 (t, *J* = 5.7 Hz, 1H), 2.62 (dd, *J* = 13.6, 11.7 Hz, 1H), 2.54 (dt, *J* = 10.1, 5.7 Hz, 1H), 2.03 (td, *J* = 6.1, 2.5 Hz, 1H), 1.41 (d, *J* = 9.9 Hz, 1H), 1.32 (s, 3H), 0.57 (s, 3H).

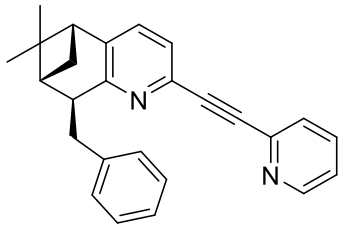

310

(**310**). To a solution of 2-bromopyridine (132 μL, 1.38 mmol, 1.2 equiv), $Pd(PPh_3)_2Cl_2$ (41 mg, 0.058 mmol, 5 mol%), and CuI (11 mg, 0.058 mmol, 5 mol%) in degassed 1,4-dioxane:Et_3N (4 mL: 4 mL) was added alkyne **309** (330 mg, 1.15 mmol, 1.0 equiv) and the resulting solution was then placed in a preheated oil bath and heated at 85 °C for 60 min. The reaction mixture was then cooled to rt, diluted with H_2O, extracted three times with CH_2Cl_2, and the combined organic layers dried over $MgSO_4$ and concentrated under reduced pressure. Purification by flash column chromatography (3:10 acetone:hexanes) afforded **310** (246 mg, 58%) as a brown solid. ^{1}H NMR (500 MHz, $CDCl_3$): δ = 8.65 (m, 1H), 7.68 (m, 2H), 7.39 (d, *J* = 7.6 Hz, 1H), 7.27 (m, 7H), 3.79 (dd, *J* = 13.7, 3.7 Hz, 1H), 3.35 (dt, *J* = 11.6, 3.1 Hz, 1H), 2.78 (t, *J* = 5.6 Hz, 1H), 2.66 (dd, *J* = 13.6, 11.7 Hz, 1H), 2.55 (m, 1H), 2.05 (td, *J* = 6.0, 2.5 Hz, 1H), 1.43 (d, *J* = 9.9 Hz, 1H), 1.33 (s, 3H), 0.59 (s, 3H).

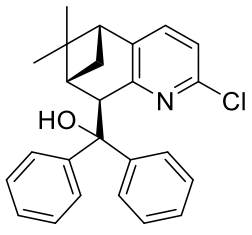

268

(**268**). Chloropyridine **268** was prepared according to a literature procedure.[31]

[31] Boobalan, R.; Chinpiao, C. *Tetrahedron Lett.* **2016**, *57*, 1930.

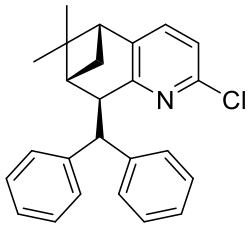

311

(**311**). To a solution of **268** (195 mg, 0.5 mmol, 1.0 equiv) and Et_3SiH (0.80 mL, 5.0 mmol, 10 equiv) in CH_2Cl_2 (2.5 mL) was added BF_3•Et_2O (0.5 mL, 4.0 mmol, 8.0 equiv) and the resulting solution was stirred for 2 h. The reaction mixture was then quenched with aqueous $NaHCO_3$, extracted three times with CH_2Cl_2, and the combined organic layers dried over $MgSO_4$ and concentrated under reduced pressure. Purification by flash column chromatography (1:2 CH_2Cl_2:hexanes) afforded **311** (262 mg, 70%) as a white solid. ^{1}H NMR (500 MHz, $CDCl_3$): δ = 7.30 (m, 4H), 7.20 (m, 1H), 7.12 (m, 4H), 7.00 (m, 3H), 5.23 (d, *J* = 4.5 Hz, 1H), 4.01 (d, *J* = 3.0 Hz, 1H), 2.54 (m, 2H), 2.12 (dt, *J* = 10.4, 5.7 Hz, 1H), 1.37 (s, 3H), 0.73 (s, 3H), 0.26 (d, *J* = 10.2 Hz, 1H).

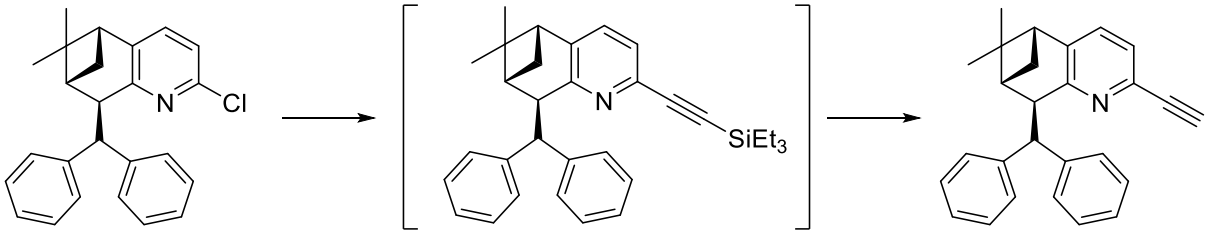

311 **312**

(**312**). To a flask containing $Pd(MeCN)_2Cl_2$ (6.0 mg, 0.023 mmol, 5 mol%), XPhos (32 mg, 0.068 mmol, 15 mol%), and Cs_2CO_3 (440 mg, 1.35 mmol, 3.0 equiv) was added dry, degassed MeCN (8 mL). The resulting suspension was stirred at rt for 45 min. The reaction was then treated sequentially with chloropyridine **311** (166 mg, 0.45 mmol, 1.0 equiv) and ethynyltriethylsilane (0.16 mL, 0.90 mmol, 2.0 equiv) and heated at reflux for 3 h. After cooling

to rt, the reaction was diluted with H_2O, extracted three times with CH_2Cl_2, and concentrated under reduced pressure. The residue was then dissolved in THF (4 mL) and treated with TBAF (1.0 M in THF, 4.0 mL, 4.0 mmol, 8.9 equiv). After 10 min, reaction mixture was quenched with aqueous $NaHCO_3$, extracted three times with CH_2Cl_2, and the combined organic layers dried over $MgSO_4$ and concentrated under reduced pressure. Purification by flash column chromatography (1:1 CH_2Cl_2:hexanes) afforded **312** (117 mg, 71%) as a white solid. ^{1}H NMR (500 MHz, $CDCl_3$): δ = 7.30 (m, 4H), 7.20 (m, 2H), 7.09 (m, 4H), 6.93 (m, 2H), 5.48 (d, *J* = 3.5 Hz, 1H), 4.04 (s, 1H), 3.10 (s, 1H), 2.58 (m, 2H), 2.08 (m, 1H), 1.38 (s, 3H), 0.75 (s, 3H), 0.08 (d, *J* = 10.2 Hz, 1H).

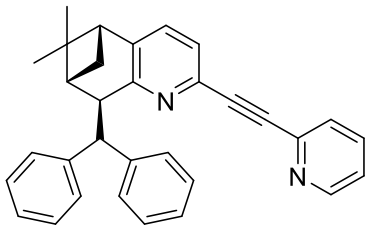

313

(**313**). To a solution of 2-bromopyridine (11 μL, 0.12 mmol, 1.2 equiv), $Pd(PPh_3)_2Cl_2$ (3.5 mg, 0.005 mmol, 5 mol%), and CuI (1.0 mg, 0.005 mmol, 5 mol%) in degassed 1,4-dioxane:Et_3N (1 mL: 1 mL) was added alkyne **312** (36 mg, 0.1 mmol, 1.0 equiv) and the resulting solution was then placed in a preheated oil bath and heated at 95 °C for 45 min. The reaction mixture was then cooled to rt, diluted with H_2O, extracted three times with CH_2Cl_2, and the combined organic layers dried over $MgSO_4$ and concentrated under reduced pressure. Purification by flash column chromatography (2:1 CH_2Cl_2:hexanes) afforded **313** (30.8 mg, 70%) as a brown solid. ^{1}H NMR (500 MHz, $CDCl_3$): δ = 8.65 (m, 1H), 7.70 (td, *J* = 7.7, 1.8 Hz, 1H), 7.62 (td, *J* = 7.8, 1.1 Hz, 1H), 7.28 (m, 7H), 7.10 (m, 4H), 6.97 (dd, *J* = 7.7, 1.7 Hz, 2H), 5.47 (d, *J* = 3.7 Hz, 1H), 4.07 (d,

J = 2.4 Hz, 1H), 2.60 (m, 2H), 2.11 (dd, *J* = 10.4, 5.6 Hz, 1H), 1.39 (s, 3H), 0.76 (s, 3H), 0.15 (d, *J* = 10.2 Hz, 1H).

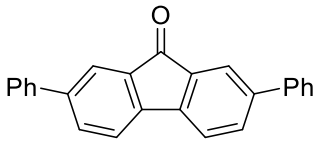

314

(**314**). Diphenylfluorenone **314** was prepared according to the literature.[32]

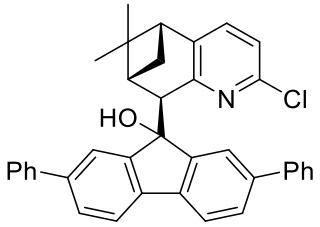

315

(**315**). To a solution of diisopropylamine (0.15 mL, 1.1 mmol, 1.1 equiv) in dry THF (5 mL) was added *n*-BuLi (1.2 M, 0.83 mL, 1.0 mmol, 1.0 equiv) dropwise at 0 °C and the resulting solution was stirred for 30 min at that temperature. The solution was then cooled to -78 °C and a solution of chloropyridine **247** (208 mg, 1.0 mmol, 1.0 equiv) in dry THF (5 mL) was added dropwise over 30 min. After stirring at -78 °C for 2 h, **314** (366 mg, 1.1 mmol, 1.1 equiv) was added as a solid, followed by THF (6 mL) dropwise over 30 min. The resulting solution was allowed to gradually warm to rt overnight. The reaction mixture was then quenched with aqueous $NaHCO_3$, diluted with H_2O, and extracted three times with CH_2Cl_2. The combined organic layers were dried over $MgSO_4$ and concentrated under reduced pressure. Purification by flash column chromatography (2:1 CH_2Cl_2:hexanes) afforded **315** (303 mg, 56%) as a yellow solid (~22%

[32] Kobin, B.; Bianchi, F.; Halm, S.; Leistner, J.; Blumstengel, S. *Advanced Functional Materials* **2014**, *24*, 7717.

impurity present). ^{1}H NMR (500 MHz, $CDCl_3$): δ = 7.86 (d, *J* = 1.0 Hz, 1H), 7.20-7.75 (m, 17H), 6.76 (d, *J*= 1.2 Hz, 1H), 4.01 (d, *J* = 1.7 Hz, 1H), 2.52 (m, 1H), 1.88 (m, 1H), 1.48 (td, *J* = 6.0, 2.0 Hz, 1H), 1.13 (s, 3H), 0.65 (s, 3H), 0.29 (d, *J* = 10.3 Hz, 1H).

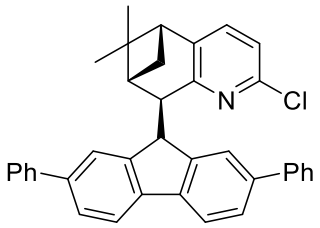

316

(**316**). To a solution of **315** (216 mg, 0.40 mmol, 1.0 equiv) and Et_3SiH (0.64 mL, 4.0 mmol, 10 equiv) in CH_2Cl_2 (4 mL) was added BF_3•Et_2O (0.4 mL, 3.2 mmol, 8.0 equiv) and the resulting solution was stirred for 5.5 h. The reaction mixture was then quenched with aqueous $NaHCO_3$, extracted three times with CH_2Cl_2, and the combined organic layers dried over $MgSO_4$ and concentrated under reduced pressure. Purification by flash column chromatography (2:1 CH_2Cl_2:hexanes) afforded **316** (145 mg, 70%) as a yellow solid (~24% impurity present). ^{1}H NMR (500 MHz, $CDCl_3$): δ = 7.22-7.84 (m, 18H), 6.70 (d, *J* = 0.8 Hz, 1H), 5.46 (d, *J* = 4.9 Hz, 1H), 4.12 (s, 1H), 2.57 (t, *J* = 5.7 Hz, 1H), 1.93 (m, 1H), 1.59 (m, 1H), 1.13 (s, 3H), 0.74 (d, *J* = 10.1 Hz, 1H), 0.67 (s, 1H).

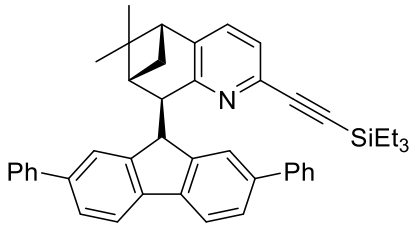

317

(**317**). To a flask containing $Pd(MeCN)_2Cl_2$ (21 mg, 0.08 mmol, 5 mol%), XPhos (114 mg, 0.24 mmol, 15 mol%), and Cs_2CO_3 (1.56 g, 4.8 mmol, 3.0 equiv) was added dry, degassed MeCN (20 mL). The resulting suspension was stirred at rt for 45 min. The reaction was then treated sequentially with chloropyridine **316** (839 mg, 1.6 mmol, 1.0 equiv) and ethynyltriethylsilane (0.57 mL, 3.2 mmol, 2.0 equiv) and heated at reflux for 2 h. After cooling to rt, the reaction was filtered through Celite, eluting with CH_2Cl_2. Concentration of the reaction under reduced pressure followed by flash column chromatography (1:2 CH_2Cl_2:hexanes) afforded **317** (834 mg, 83%) as a light yellow solid (~25% impurity). ^{1}H NMR (500 MHz, $CDCl_3$): δ = 7.19-7.84 (m, 18H), 6.69 (s, 1H), 5.57 (d, *J* = 5.0 Hz, 1H), 4.18 (d, *J* = 3.2 Hz, 1H), 2.56 (t, *J* = 5.6 Hz, 1H), 1.92 (dd, *J* = 10.1, 5.5 Hz, 1H), 1.61 (m, 1H), 1.13 (s, 3H), 1.07 (t, *J* = 7.9 Hz, 9H), 0.73 (m, 6H), 0.66 (s, 3H).

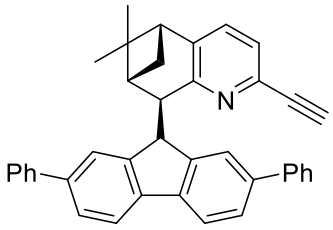

318

(**318**). To a solution of **317** (829 mg, 1.32 mmol, 1.0 equiv) in THF:H_2O (15 mL: 2 mL) was added TBAF (1.0 M in THF, 1.6 mL, 1.6 mmol, 1.2 equiv) and the resulting solution was stirred for 3.5 h. The reaction mixture was then quenched with aqueous $NaHCO_3$, extracted three times

with CH_2Cl_2, and the combined organic layers dried over $MgSO_4$ and concentrated under reduced pressure. Purification by flash column chromatography (1:1 CH_2Cl_2:hexanes) afforded **318** (550 mg, 81%) as a yellow solid. ^{1}H NMR (500 MHz, $CDCl_3$): δ = 7.19-7.86 (m, 18H), 6.66 (s, 1H), 5.55 (d, *J* = 4.6 Hz, 1H), 4.16 (s, 1H), 3.19 (s, 1H), 2.58 (m, 1H), 1.94 (m, 1H), 1.14 (s, 3H), 0.75 (d, *J* = 10.1 Hz, 1H), 0.66 (s, 3H).

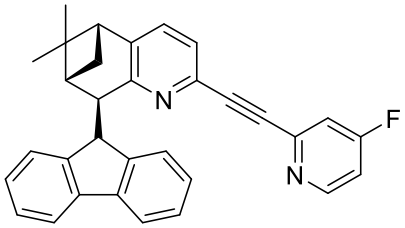

319

(**319**). To a flask containing pyridine **253** (64 mg, 0.18 mmol, 1.0 equiv), 2-bromo-4-fluoropyridine (28 µl, 0.27 mmol, 1.5 equiv), $Pd(PPh_3)_2Cl_2$ (7.0 mg, 0.01 mmol, 5 mol%), and CuI (1.9 mg, 0.01 mmol, 5 mol%) was added dry, degassed 1,4-dioxane:Et_3N (1 mL: 1 mL). The resulting suspension was then placed in a preheated oil bath and heated at 75 °C. After 1.5 h, the reaction was allowed to cool and diluted with water. The reaction mixture was then extracted three times with CH_2Cl_2, dried with $MgSO_4$, and concentrated under reduced pressure. Purification by flash column chromatography (2:1 EtOAc:hexanes → EtOAc) afforded **319** (51 mg, 61%) as a yellow solid. ^{1}H NMR (500 MHz, $CDCl_3$): δ = 8.61 (dd, *J* = 8.5, 5.7 Hz, 1H), 7.76 (d, *J* = 7.3 Hz, 1H), 7.70 (d, *J* = 7.6 Hz, 1H), 7.55 (m, 2H), 7.35 (m, 6H), 7.04 (m, 1H), 6.93 (m, 1H), 6.44 (d, *J* = 7.6 Hz, 1H), 5.45 (d, *J* = 4.8 Hz, 1H), 4.10 (d, *J* = 3.3 Hz, 1H), 2.60 (t, *J* = 5.6 Hz, 1H), 1.91 (m, 1H), 1.51 (m, 1H), 1.14 (s, 3H), 0.67 (s, 3H), 0.65 (buried, 1H).

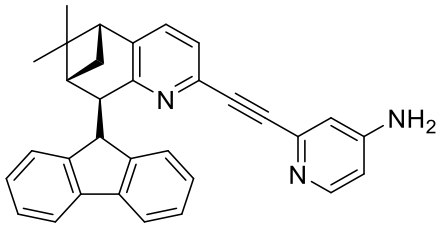

320

(**320**). To a flask containing pyridine **253** (72 mg, 0.20 mmol, 1.0 equiv), 4-amino-2-bromopyridine (52 mg, 0.30 mmol, 1.5 equiv), $Pd(PPh_3)_2Cl_2$ (7.0 mg, 0.01 mmol, 5 mol%), and CuI (1.9 mg, 0.01 mmol, 5 mol%) was added dry, degassed 1,4-dioxane:Et_3N (0.5 mL: 0.5 mL). The resulting suspension was then placed in a preheated oil bath and heated at 75 °C. After 1.5 h, the reaction was allowed to cool and diluted with water. The reaction mixture was then extracted three times with CH_2Cl_2, dried with $MgSO_4$, and concentrated under reduced pressure. Purification by flash column chromatography (2:1 EtOAc:hexanes → EtOAc) afforded **320** (30 mg, 33%) as a yellow solid. ^1H NMR (500 MHz, $CDCl_3$): δ = 8.24 (s, 1H), 7.20-7.78 (m, 10H), 6.93 (m, 2H), 6.48 (dd, *J* = 22.8, 5.7 Hz, 2H), 5.45 (d, *J* = 4.8 Hz, 1H), 4.21 (s, 2H), 2.57 (t, *J* = 5.6 Hz, 1H), 1.89 (m, 1H), 1.50 (m, 1H), 1.13 (s, 3H), 0.67 (s, 3H), 0.65 (d, *J* = 10.2 Hz, 1H).

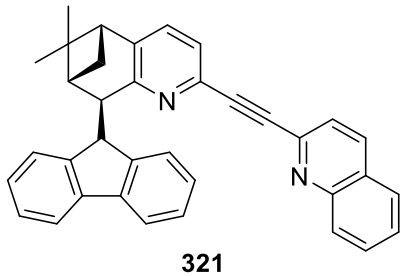

321

(**321**). To a flask containing pyridine **253** (145 mg, 0.40 mmol, 1.0 equiv), 2-bromoquinoline (125 mg, 0.60 mmol, 1.5 equiv), $Pd(PPh_3)_2Cl_2$ (14 mg, 0.02 mmol, 5 mol%), and CuI (3.8 mg, 0.01 mmol, 5 mol%) was added dry, degassed 1,4-dioxane:Et_3N (1 mL: 1 mL). The resulting suspension was then placed in a preheated oil bath and heated at 75 °C. After 1 h, the reaction

was allowed to cool and diluted with water. The reaction mixture was then extracted three times with CH_2Cl_2, dried with $MgSO_4$, and concentrated under reduced pressure. Purification by flash column chromatography (2:1 EtOAc:hexanes → EtOAc) afforded **321** (178 mg, 90%) as an orange solid. ^{1}H NMR (500 MHz, $CDCl_3$): δ = 8.17 (m, 2H), 7.82 (d, *J* = 7.5 Hz, 1H), 7.73 (m, 4H), 7.58 (m, 3H), 7.35 (m, 3H), 7.24 (m, 1H), 6.95 (m, 1H), 6.47 (d, *J* = 7.6 Hz, 1H), 5.48 (d, *J* = 4.9 Hz, 1H), 4.13 (d, *J* = 3.3 Hz, 1H), 2.60 (t, *J* = 5.7 Hz, 1H), 1.91 (m, 1H), 1.52 (td, *J* = 6.0, 1.9 Hz, 1H), 1.15 (s, 3H), 0.69 (s, 3H), 0.66 (buried, 1H).

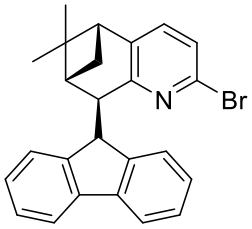

270

(**270**). A solution of chloropyridine **251** (268 mg, 0.72 mmol) in 33% HBr in acetic acid (3 mL) was heated at reflux for 96 h, with 33% HBr in acetic acid (2 mL) being added every 12 h. The reaction mixture was then cooled to rt, quenched with aqueous $NaHCO_3$, extracted three times with CH_2Cl_2, and the combined organic layers dried over $MgSO_4$ and concentrated under reduced pressure. Purification by flash column chromatography (1:1 CH_2Cl_2:hexanes) afforded **270** (262 mg, 88%) as a light yellow solid. ^{1}H NMR (500 MHz, $CDCl_3$): δ = 7.75 (d, *J* = 7.4 Hz, 1H), 7.70 (d, *J* = 7.6 Hz, 1H), 7.55 (d, *J* = 7.3 Hz, 1H), 7.17-7.41 (m, 4H), 7.16 (dd, *J* = 7.9, 1.1 Hz, 1H), 6.96 (t, *J* = 7.5 Hz, 1H), 6.46 (d, *J* = 7.6 Hz, 1H), 5.34 (d, *J* = 4.7 Hz, 1H), 4.05 (d, *J* = 4.6 Hz, 1H), 2.54 (t, *J* = 5.6 Hz, 1H), 1.88 (dt, *J* = 11.1, 5.6 Hz, 1H), 1.47 (t, *J* = 5.9 Hz, 1H), 1.12 (s, 3H), 0.65 (s, 3H), 0.62 (d, *J* = 10.1 Hz, 1H).

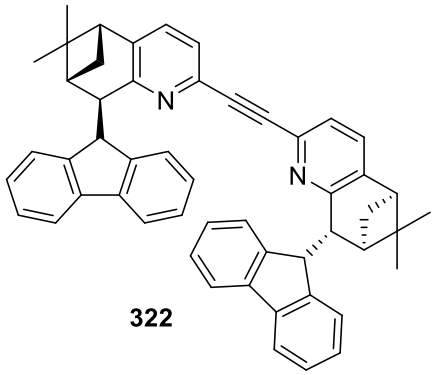

322

(**322**). To a solution of bromopyridine **270** (195 mg, 0.468 mmol, 1.2 equiv), $Pd(PPh_3)_2Cl_2$ (14 mg, 0.02 mmol, 5 mol%), and CuI (3.8 mg, 0.02 mmol, 5 mol%) in degassed 1,4-dioxane:Et_3N (2.5 mL: 2.5 mL) was added a solution of alkyne **253** (141 mg, 0.390 mmol, 1.0 equiv) in degassed 1,4-dioxane:Et_3N (0.75 mL: 0.75 mL) and the resulting solution was then placed in a preheated oil bath and heated at 70 °C for 40 min. The reaction mixture was then cooled to rt, diluted with H_2O, extracted three times with CH_2Cl_2, and the combined organic layers dried over $MgSO_4$ and concentrated under reduced pressure. Purification by flash column chromatography (1:10 EtOAc:hexanes) afforded **322** (165 mg, 61%) as a light brown solid. ^1H NMR (500 MHz, $CDCl_3$): δ = 7.75 (d, *J* = 7.2 Hz, 1H), 7.68 (d, *J* = 7.6 Hz, 1H), 7.56 (m, 2H), 7.35 (m, 4H), 7.22 (t, *J* = 7.2 Hz, 1H), 6.92 (t, *J* = 7.5 Hz, 1H), 6.47 (d, *J* = 7.6 Hz, 1H), 5.47 (d, *J* = 4.8 Hz, 1H), 4.12 (d, *J* = 3.0 Hz, 1H), 2.58 (t, *J* = 5.6 Hz, 1H), 1.89 (m, 1H), 1.51 (m, 1H), 1.14 (m, 3H), 0.68 (s, 3H), 0.66 (d, *J* = 10.2 Hz, 1H).

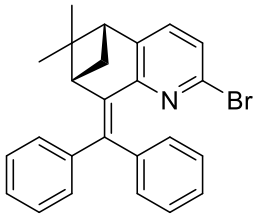

269

(**269**). A solution of chloropyridine **268** (268 mg, 0.72 mmol) in 33% HBr in acetic acid (12 mL) was heated at reflux for 22 h. The reaction mixture was then cooled to rt, quenched with aqueous $NaHCO_3$, extracted three times with CH_2Cl_2, and the combined organic layers dried over $MgSO_4$ and concentrated under reduced pressure to afford **269** (262 mg, 88%) as a yellow solid. ^{1}H NMR (500 MHz, $CDCl_3$): δ = 7.01-7.34 (m, 12H), 3.21 (t, *J* = 6.1 Hz, 1H), 2.83 (t, *J* = 5.8 Hz, 1H), 2.71 (m, 1H), 1.59 (d, *J* = 9.5 Hz, 1H), 1.55 (s, 3H), 0.87 (s, 3H).

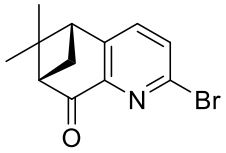

274

(**274**). A solution of bromopyridine **269** (1.67 g, 4.0 mmol, 1.0 equiv) and pyridine (1.3 mL, 16.0 mmol, 4.0 equiv) in dry CH_2Cl_2 (20 mL) at -78 °C was bubbled with ozone for 2 h. The reaction mixture was then quenched with DMS (1.47 mL, 20.0 mmol, 5.0 equiv) and allowed to gradually warm to rt. The reaction mixture was then concentrated and purified by flash column chromatography (CH_2Cl_2 → 1% MeOH in CH_2Cl_2) to afford **274** (659 mg, 62%) as a light brown solid. ^{1}H NMR (500 MHz, $CDCl_3$): δ = 7.49 (m, 2H), 3.09 (m, 3H), 2.15 (d, *J* = 8.3 Hz, 1H), 1.60 (s, 3H), 0.81 (s, 3H).

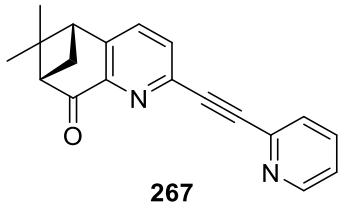

267

(**267**). To a solution of bromopyridine **274** (608 mg, 2.28 mmol, 1.0 equiv), $Pd(PPh_3)_2Cl_2$ (77 mg, 0.11 mmol, 5 mol%), and CuI (21 mg, 0.11 mmol, 5 mol%) in degassed 1,4-dioxane:Et_3N (2 mL: 2 mL) was added 2-ethynylpyridine (0.35 mL, 3.42 mmol, 1.5 equiv) and the resulting solution was then placed in a preheated oil bath and heated at 75 °C for 30 min. The reaction mixture was then cooled to rt, diluted with H_2O, extracted three times with CH_2Cl_2, and the combined organic layers dried over $MgSO_4$ and concentrated under reduced pressure. Purification by flash column chromatography (CH_2Cl_2 → 6% MeOH in CH_2Cl_2, then 1:1 EtOAc:hexanes → 4:1 EtOAc:hexanes → EtOAc) afforded **267** (650 mg, 99%) as a light brown solid. ^{1}H NMR (500 MHz, $CDCl_3$): δ = 8.64 (m, 1H), 7.68 (m, 4H), 7.29 (m, 1H), 3.12 (m, 3H), 2.17 (m, 1H), 1.62 (s, 3H), 0.82 (s, 3H).

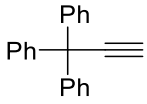

323

(**323**). Alkyne **323** was prepared according to a literature procedure.[33]

[33] Dominguez, Z.; Dang, H.; Strouse, M. J.; Garcia-Garibay, M. A. *J. Am. Chem. Soc.* **2002**, *124*, 2398.

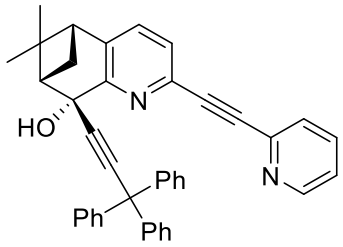

324

(**324**). To a solution of alkyne **323** (193 mg, 0.72 mmol, 1.2 equiv) in dry THF (8 mL) was added *n*-BuLi (1.55 M in hexanes, 0.43 mL, 0.66 mmol, 1.1 equiv) at -78 °C and the resulting solution was stirred for 5 min at that temperature then 5 min at rt. The reaction mixture was then cooled to -78 °C, and bispyridine **267** (173 mg, 0.60 mmol, 1.0 equiv) in dry THF (6 mL) was added dropwise. The resulting solution was stirred for 15 min at -78 °C, then 3 h at rt. The reaction mixture was then quenched with aqueous $NaHCO_3$, diluted with H_2O, extracted three times with CH_2Cl_2, and the combined organic layers dried over $MgSO_4$ and concentrated under reduced pressure. Purification by flash column chromatography (1:2 EtOAc:hexanes → 1:1 EtOAc:hexanes) afforded **324** (311 mg, 93%) as a light brown solid. ^{1}H NMR (500 MHz, $CDCl_3$): δ = 8.67 (d, *J* = 4.8 Hz, 1H), 7.72 (td, *J* = 7.7, 1.4 Hz, 1H), 7.65 (d, *J* = 7.8 Hz, 1H), 7.45 (d, *J* = 7.7 Hz, 1H), 7.24 (m, 17H), 3.62 (s, 1H), 2.84 (m, 1H), 2.79 (t, *J* = 5.6 Hz, 1H), 2.73 (t, *J* = 6.1 Hz, 1H), 1.87 (d, *J* = 10.4 Hz, 1H), 1.48 (s, 3H), 0.77 (s, 3H).

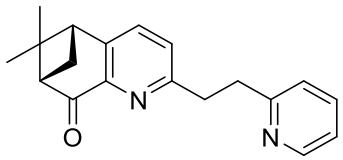

280

(**280**). To a flask containing 5% Pd/C (144 mg) and bispyridine **267** (144 mg, 0.5 mmol) was added EtOH (2 mL). The reaction flask was equipped with an H_2 balloon and stirred for 96 h.

The reaction mixture was then filtered through Celite and concentrated under reduced pressure to afford **280** (140 mg, 96%) as a pale brown gel. ^{1}H NMR (500 MHz, $CDCl_3$): δ = 8.54 (m, 1H), 7.56 (td, *J* = 7.7, 1.8 Hz, 1H), 7.45 (d, *J* = 7.8 Hz, 1H), 7.13 (m, 3H), 3.31 (m, 4H), 3.06 (m, 3H), 2.14 (dd, *J* = 6.6, 3.0 Hz, 1H), 1.59 (s, 3H), 0.78 (s, 3H).

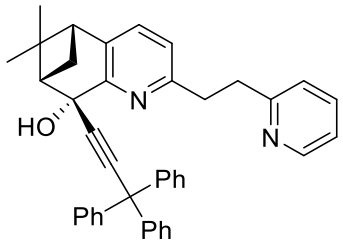

325

(**325**). To a solution of alkyne **323** (193 mg, 0.72 mmol, 1.5 equiv) in dry THF (2 mL) was added *n*-BuLi (1.55 M in hexanes, 0.43 mL, 0.67 mmol, 1.4 equiv) at -78 °C and the resulting solution was stirred for 5 min at that temperature then 5 min at rt. The reaction mixture was then cooled to -78 °C, and bispyridine **280** (140 mg, 0.48 mmol, 1.0 equiv) in dry THF (2 mL) was added dropwise. The resulting solution was stirred for 5 min at -78 °C, then 2 h at rt. The reaction mixture was then quenched with aqueous $NaHCO_3$, diluted with H_2O, extracted three times with CH_2Cl_2, and the combined organic layers dried over $MgSO_4$ and concentrated under reduced pressure. Purification by flash column chromatography (1:2 EtOAc:hexanes → 1:1 EtOAc:hexanes → EtOAc) afforded **325** (154 mg, 56%) as a light brown solid. ^{1}H NMR (500 MHz, $CDCl_3$): δ = 8.54 (d, *J* = 4.8 Hz, 1H), 7.44 (t, *J* = 7.6 Hz, 1H), 7.22 (m, 15H), 7.13 (d, *J* = 7.6 Hz, 1H), 7.07 (m, 1H), 6.99 (d, *J* = 7.8 Hz, 1H), 6.88 (d, *J* = 7.6 Hz, 1H), 3.58 (s, 1H), 3.26 (m, 4H), 2.81 (m, 1H), 2.71 (m, 2H), 1.86 (d, *J* = 10.3 Hz, 1H), 1.46 (s, 3H), 0.70 (s, 3H).

Diprotonation of bispyridines. Representative example: To a solution of bispyridine (1.00 equiv) in dry CH_2Cl_2 is added a solution of bis(trifluoromethane)sulfonimide (1.95 equiv) in dry CH_2Cl_2.

After 45 minutes, the solution is transferred to a 20 mL scintillation vial containing dry hexanes and concentrated under reduced pressure to afford the bispyridinium salt.

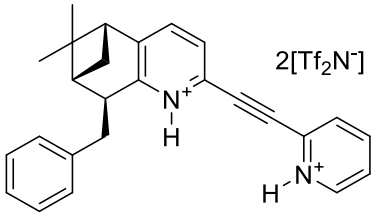

255

(**255**). ^{1}H NMR (500 MHz, DMSO-d_6): δ = 9.19 (br s, 2H), 8.69 (m, 1H), 7.99 (td, *J* = 7.8, 1.8 Hz, 1H), 7.80 (dt, *J* = 7.9, 1.0 Hz, 1H), 7.53 (m, 3H), 7.26 (m, 5H), 3.58 (dd, *J* = 13.5, 3.5 Hz, 1H), 3.23 (dd, *J* = 8.4, 2.7 Hz, 1H), 2.88 (t, *J* = 5.6 Hz, 1H), 2.67 (m, 1H), 2.57 (m, 1H), 1.94 (td, *J* = 6.0, 2.4 Hz, 1H), 1.39 (d, *J* = 10.0 Hz, 1H), 1.31 (s, 3H), 0.53 (s, 3H).

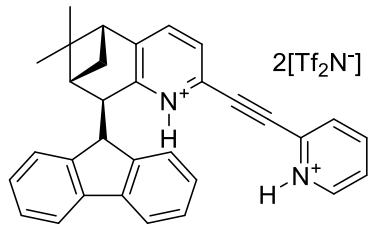

257

(**257**). ^{1}H NMR (500 MHz, DMSO-d_6): δ = 8.67 (d, *J* = 4.8 Hz, 1H), 7.95 (td, *J* = 7.8, 1.8 Hz, 1H), 7.88 (m, 1H), 7.84 (d, *J* = 7.6 Hz, 1H), 7.79 (d, *J* = 7.8 Hz, 1H), 7.74 (d, *J* = 6.5 Hz, 1H), 7.63 (d, *J* = 7.7 Hz, 1H), 7.55 (d, *J* = 7.8 Hz, 1H), 7.51 (ddd, *J* = 7.7, 4.9, 1.2 Hz, 1H), 7.39 (m, 2H), 7.27 (t, *J* = 7.5 Hz, 1H), 6.99 (m, 1H), 6.33 (d, *J* = 7.6 Hz, 1H), 5.28 (d, *J* = 4.9 Hz, 1H), 4.12 (d, *J* = 3.5 Hz, 1H), 2.68 (t, *J* = 5.7 Hz, 1H), 1.89 (m, 1H), 1.37 (m, 1H), 1.11 (s, 3H), 0.63 (s, 3H), 0.52 (d, *J* = 9.8 Hz, 1H).

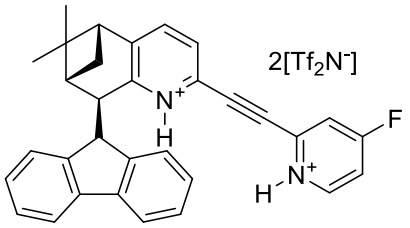

259

(**259**). ^{1}H NMR (500 MHz, DMSO-d_6): δ = 8.68 (dd, *J* = 8.8, 8.5 Hz, 1H), 7.88 (d, *J* = 6.6 Hz, 1H), 7.83 (d, *J* = 7.6 Hz, 1H), 7.76 (m, 2H), 7.64 (d, *J* = 7.7 Hz, 1H), 7.56 (d, *J* = 7.7 Hz, 1H), 7.43 (m, 3H), 7.27 (t, *J* = 7.5 Hz, 1H), 6.99 (t, *J* = 7.5 Hz, 1H), 6.33 (d, *J* = 7.6 Hz, 1H), 5.27 (d, *J* = 4.8 Hz, 1H), 4.12 (d, *J* = 3.6 Hz, 1H), 2.68 (t, *J* = 5.6 Hz, 1H), 1.90 (m, 1H), 1.37 (t, *J* = 5.2 Hz, 1H), 1.11 (s, 3H), 0.62 (s, 3H), 0.52 (d, *J* = 9.9 Hz, 1H).

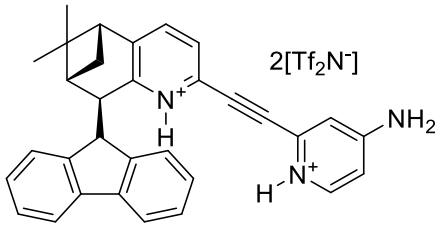

260

(**260**). ^{1}H NMR (500 MHz, DMSO-d_6): δ = 13.96 (s, 1H), 8.24 (s, 1H), 8.20 (s, 1H), 8.14 (d, *J* = 6.9 Hz, 1H), 7.88 (d, *J* = 6.6 Hz, 1H), 7.84 (d, *J* = 7.6 Hz, 1H), 7.73 (t, *J* = 7.2 Hz, 2H), 7.59 (m, 2H), 7.40 (m, 2H), 7.28 (t, *J* = 7.5 Hz, 1H), 7.08 (d, *J* = 2.3 Hz, 1H), 6.99 (t, *J* = 7.4 Hz, 1H), 6.82 (dd, *J* = 7.0, 2.4 Hz, 1H), 6.30 (d, *J* = 7.6 Hz, 1H), 5.23 (d, *J* = 4.7 Hz, 1H), 4.11 (d, *J* = 4.2 Hz, 1H), 2.72 (t, *J* = 5.7 Hz, 1H), 1.91 (m, 1H), 1.37 (t, *J* = 5.1 Hz, 1H), 1.11 (s, 3H), 0.62 (s, 3H), 0.51 (d, *J* = 9.9 Hz, 1H).

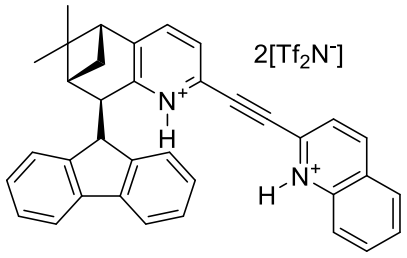

261

(**261**). ^{1}H NMR (500 MHz, DMSO-d_6): δ = 8.51 (d, *J* = 8.5 Hz, 1H), 8.05 (m, 2H), 7.87 (m, 4H), 7.71 (m, 3H), 7.58 (d, *J* = 7.8 Hz, 1H), 7.40 (m, 2H), 7.27 (t, *J* = 7.5 Hz, 1H), 7.00 (t, *J* = 7.5 Hz, 1H), 6.36 (d, *J* = 7.7 Hz, 1H), 5.31 (d, *J* = 4.8 Hz, 1H), 4.14 (d, *J* = 3.6 Hz, 1H), 2.70 (t, *J* = 5.6 Hz, 1H), 1.91 (m, 1H), 1.38 (t, *J* = 5.3 Hz, 1H), 1.12 (s, 3H), 0.64 (s, 3H), 0.53 (d, *J* = 9.9 Hz, 1H).

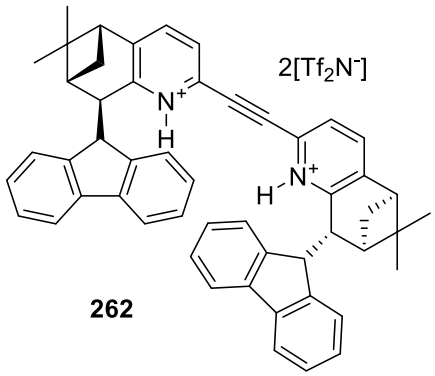

262

(**262**). ^{1}H NMR (500 MHz, DMSO-d_6): δ = 7.87 (m, 1H), 7.83 (d, *J* = 7.6 Hz, 1H), 7.72 (d, *J* = 7.0 Hz, 1H), 7.64 (d, *J* = 7.7 Hz, 1H), 7.54 (d, *J* = 7.8 Hz, 1H), 7.38 (m, 2H), 7.26 (t, *J* = 7.4 Hz, 1H), 6.98 (m, 1H), 6.35 (d, *J* = 7.7 Hz, 1H), 5.29 (d, *J* = 4.8 Hz, 1H), 4.11 (d, *J* = 4.8 Hz, 1H), 2.67 (t, *J* = 5.7 Hz, 1H), 1.89 (m, 1H), 1.37 (m, 1H), 1.11 (s, 3H), 0.63 (s, 3H), 0.52 (d, *J* = 9.8 Hz, 1H).

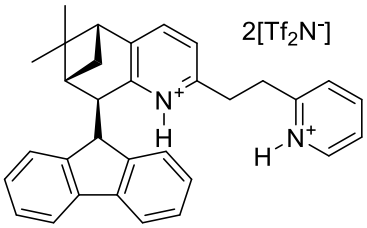

263

(**263**). ^{1}H NMR (500 MHz, DMSO-d_6): δ = 8.70 (d, *J* = 5.7 Hz, 1H), 8.38 (t, *J* = 7.8 Hz, 1H), 8.02 (d, *J* = 8.1 Hz, 1H), 7.87 (m, 1H), 7.81 (d, *J* = 7.6 Hz, 1H), 7.76 (t, *J* = 6.6 Hz, 1H), 7.68 (d, *J* = 6.2 Hz, 1H), 7.40 (m, 3H), 7.25 (m, 2H), 6.85 (td, *J* = 7.5, 0.9 Hz, 1H), 5.95 (d, *J* = 7.6 Hz, 1H), 5.11 (d, *J* = 4.8 Hz, 1H), 3.94 (d, *J* = 3.7 Hz, 1H), 3.58 (t, *J* = 7.3 Hz, 2H), 3.45 (m, 2H), 2.57 (t, *J* = 5.7 Hz, 1H), 1.82 (m, 1H), 1.32 (m, 1H), 1.08 (s, 3H), 0.57 (s, 3H), 0.44 (d, *J* = 9.7 Hz, 1H).

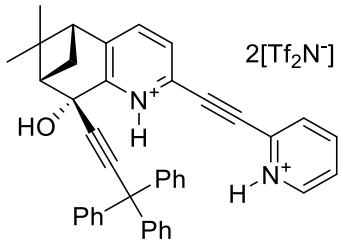

279

(**279**). ^{1}H NMR (500 MHz, DMSO-d_6): δ = 8.70 (d, *J* = 4.8 Hz, 1H), 7.99 (t, *J* = 7.7 Hz, 1H), 7.75 (d, *J* = 7.7 Hz, 1H), 7.54 (m, 3H), 7.23 (m, 15H), 2.83 (m, 2H), 2.54 (t, *J* = 6.2 Hz, 1H), 1.59 (d, *J* = 10.1 Hz, 1H), 1.43 (s, 3H), 0.72 (s, 1H).

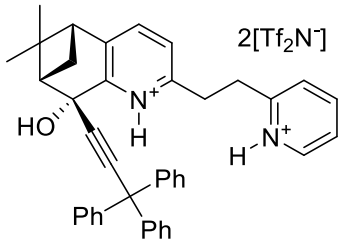

326

(**326**). ^{1}H NMR (500 MHz, DMSO-d_6): δ = 8.71 (d, *J* = 5.3 Hz, 1H), 8.31 (t, *J* = 7.8 Hz, 1H), 7.83 (d, *J* = 7.9 Hz, 1H), 7.75 (t, *J* = 6.6 Hz, 1H), 7.63 (d, *J* = 7.5 Hz, 1H), 7.25 (m, 10H), 7.07 (d, *J* = 7.1 Hz, 6H), 3.40 (m, 4H), 2.87 (m, 2H), 2.64 (t, *J* = 6.0 Hz, 1H), 1.66 (m, 1H), 1.45 (s, 3H), 0.67 (s, 3H).

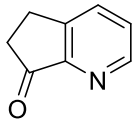

282

(**282**). Pyridine **282** was prepared according to a literature procedure.[34]

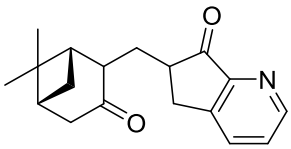

283

(**283**). To a solution of diisopropylamine (0.76 mL, 5.4 mmol, 1.0 equiv) in dry THF (12 mL) was added *n*-BuLi (1.6 M, 3.4 mL, 5.4 mmol, 1.0 equiv) dropwise at 0 °C and the resulting solution was stirred for 30 min at that temperature. The solution was then cooled to -78 °C and a solution of ketopyridine **282** (720 mg, 5.4 mmol, 1.0 equiv) in dry THF (22 mL) was added

[34] Andreotti, D.; Miserazzi, E.; Nalin, A.; Pozzan, A.; Profeta, R.; Spada, S. *Tetrahedron Lett.* **2010**, *51*, 6526.

dropwise over 30 min. After warming to -45 °C, pinocarvone (811 mg, 5.4 mmol, 1.1 equiv) was added dropwise. The resulting solution was allowed to gradually warm to rt overnight. The reaction mixture was then quenched with HOAc (0.3 mL), diluted with H_2O, and extracted three times with CH_2Cl_2. The combined organic layers were dried over $MgSO_4$ and concentrated under reduced pressure. Purification by flash column chromatography (3:1 EtOAc:hexanes) afforded **283** (491 mg, 32%) as a mixture of diastereomers and as a thick gel. ^{1}H NMR (500 MHz, $CDCl_3$): δ = 8.78 (t, *J* = 4.1 Hz, 1H), 7.86 (d, *J* = 7.7 Hz, 1H), 7.45 (m, 1H), 3.30-3.57 (m, 1H), 2.37-3.11 (m, 6H), 1.85-2.24 (m, 4H), 1.30 (m, 4H), 0.91 (m, 3H).

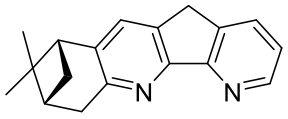

284

(**284**). To a solution of **283** (491 mg, 1.73 mmol, 1.0 equiv) in AcOH (10 mL) was added NH_4OAc (667 mg, 8.65 mmol, 5.0 equiv) and the resulting solution was reflux under an open-air atmosphere for 1 h. The reaction mixture was then quenched with aqueous K_2CO_3, diluted with H_2O, extracted three times with CH_2Cl_2, and washed with brine. The combined organic layers were dried over $MgSO_4$ and concentrated under reduced pressure. Purification by flash column chromatography (EtOAc) afforded **284** (220 mg, 49%) as a brown solid. ^{1}H NMR (500 MHz, $CDCl_3$): δ = 8.68 (d, *J* = 3.9 Hz, 1H), 7.82 (d, *J* = 7.0 Hz, 1H), 7.41 (s, 1H), 7.22 (dd, *J* = 7.6, 4.9 Hz, 1H), 3.78 (s, 2H), 3.31 (d, *J* = 2.7 Hz, 2H), 2.84 (t, *J*= 5.7 Hz, 1H), 2.72 (dt, *J* = 9.7, 5.7 Hz, 1H), 2.41 (m, 1H), 1.43 (s, 3H), 1.33 (d, *J* = 9.6 Hz, 1H), 0.68 (s, 3H).

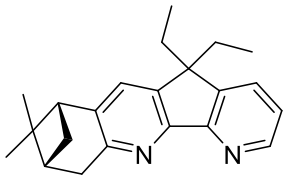

285

(**285**). To a solution of **284** (220 mg, 0.84 mmol, 1.0 equiv) and KO*t*Bu (283 mg, 2.52 mmol, 3.0 equiv) in dry THF (8 mL) was added ethyl iodide (0.20 mL, 2.52 mmol, 3.0 equiv) at 0 °C and the resulting solution was allowed to warm to rt and stirred at that temperature for 2 h. The reaction mixture was then quenched with H_2O, diluted with CH_2Cl2, extracted three times with CH_2Cl_2, and washed with brine. The combined organic layers were dried over $MgSO_4$ and concentrated under reduced pressure to afford **285** (252 mg, 94%) as a brown solid. ^{1}H NMR (500 MHz, $CDCl_3$): δ = 8.63 (dd, *J* = 4.9, 1.4 Hz, 1H), 7.65 (dd, *J* = 7.6, 1.4 Hz, 1H), 7.21 (m, 2H), 3.29 (d, *J* = 2.8 Hz, 2H), 2.83 (t, *J* = 5.7 Hz, 1H), 2.72 (dt, *J* = 9.7, 5.7 Hz, 1H), 2.40 (m, 1H), 2.03 (m, 4H), 1.43 (s, 3H), 1.36 (d, *J* = 9.6 Hz, 1H), 0.67 (s, 3H), 0.42 (t, *J* = 7.4 Hz, 3H), 0.35 (t, *J* = 7.3 Hz, 3H).

Asymmetric Friedel-Crafts reaction of indoles with pyruvates or glyoxylates catalyzed by a bispyridinium. Representative example: To a solution of indole (0.10 mmol, 1.0 equiv) and catalyst (0.01 mmol, 10 mol%) in dry solvent (1.5 mL) was added pyruvate or glyoxylate (0.20 mmol, 2.0 equiv) dropwise at the indicated temperature. The reaction was stirred for the given time before being quenched with 1 drop of triethylamine. About half of the solution was then loaded directly onto a preparatory TLC plate and eluted to afford pure Friedel-Crafts adduct for HPLC analysis.

Selected ^{1}H and ^{13}C NMR Spectra

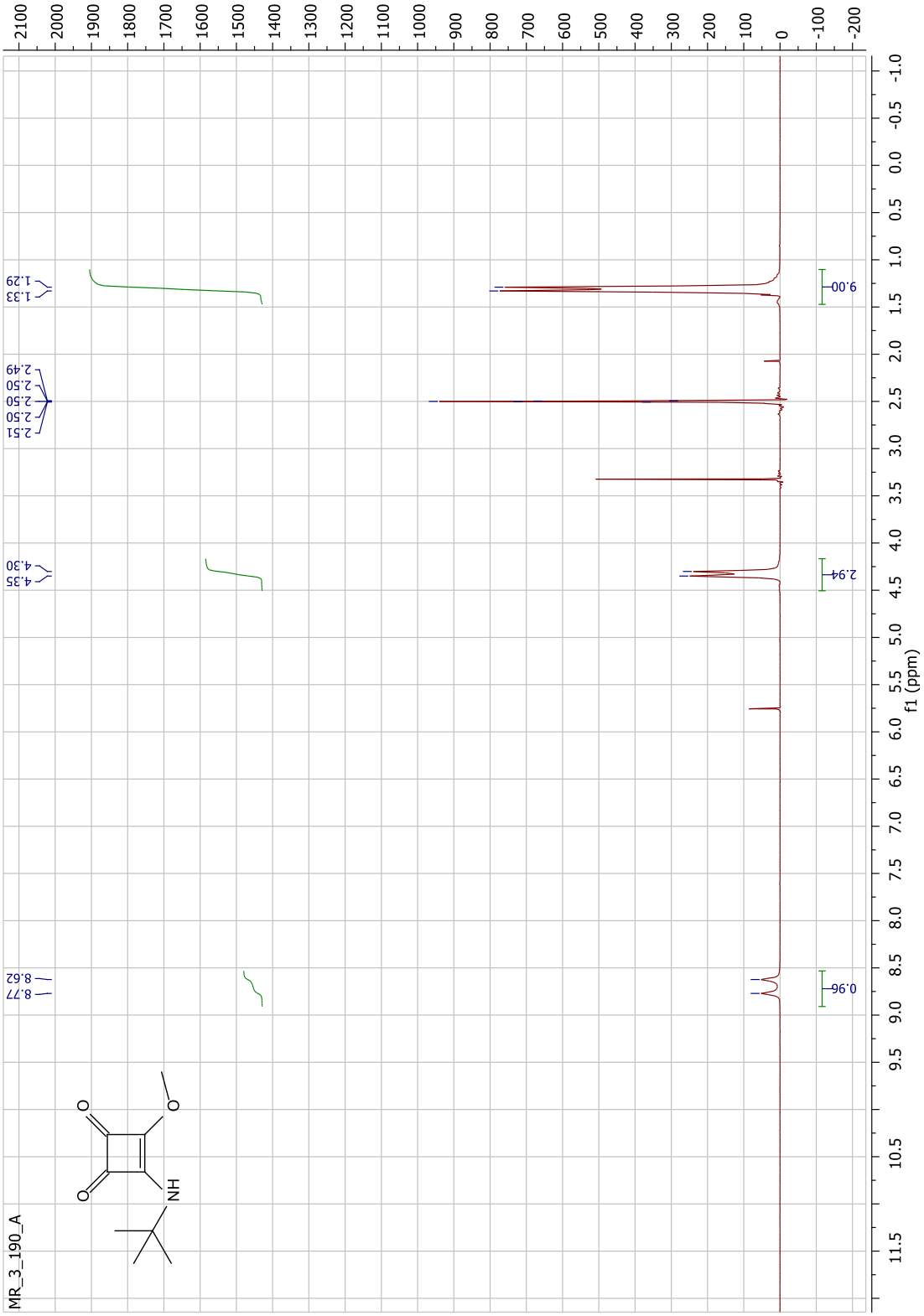

Figure 23. ^{1}H NMR spectrum of **42** (500 MHz, DMSO-d_6).

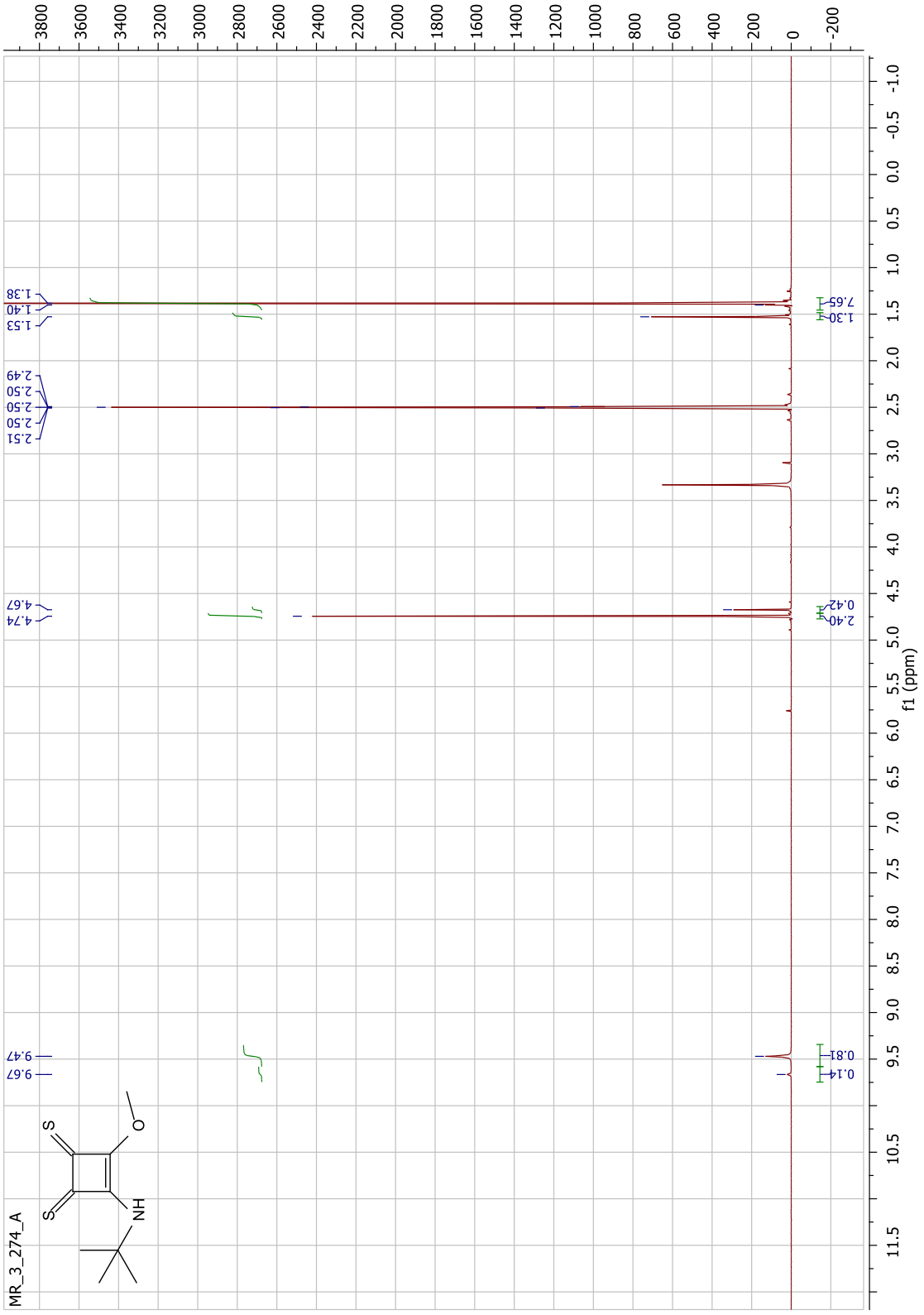

Figure 24. ^{1}H NMR spectrum of **43** (500 MHz, DMSO-d_6).

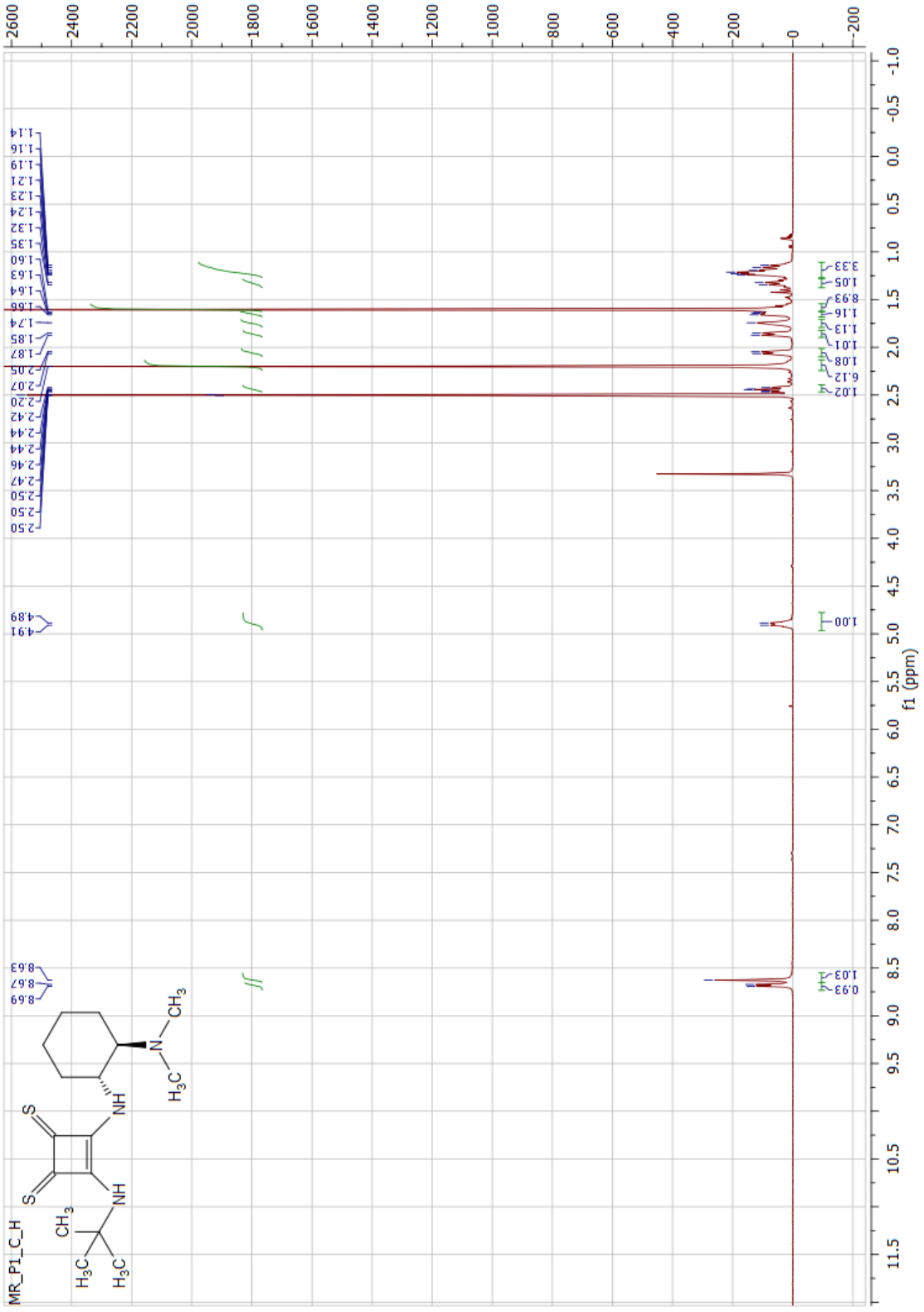

Figure 25. ^{1}H NMR spectrum of **45** (500 MHz, DMSO-d_6).

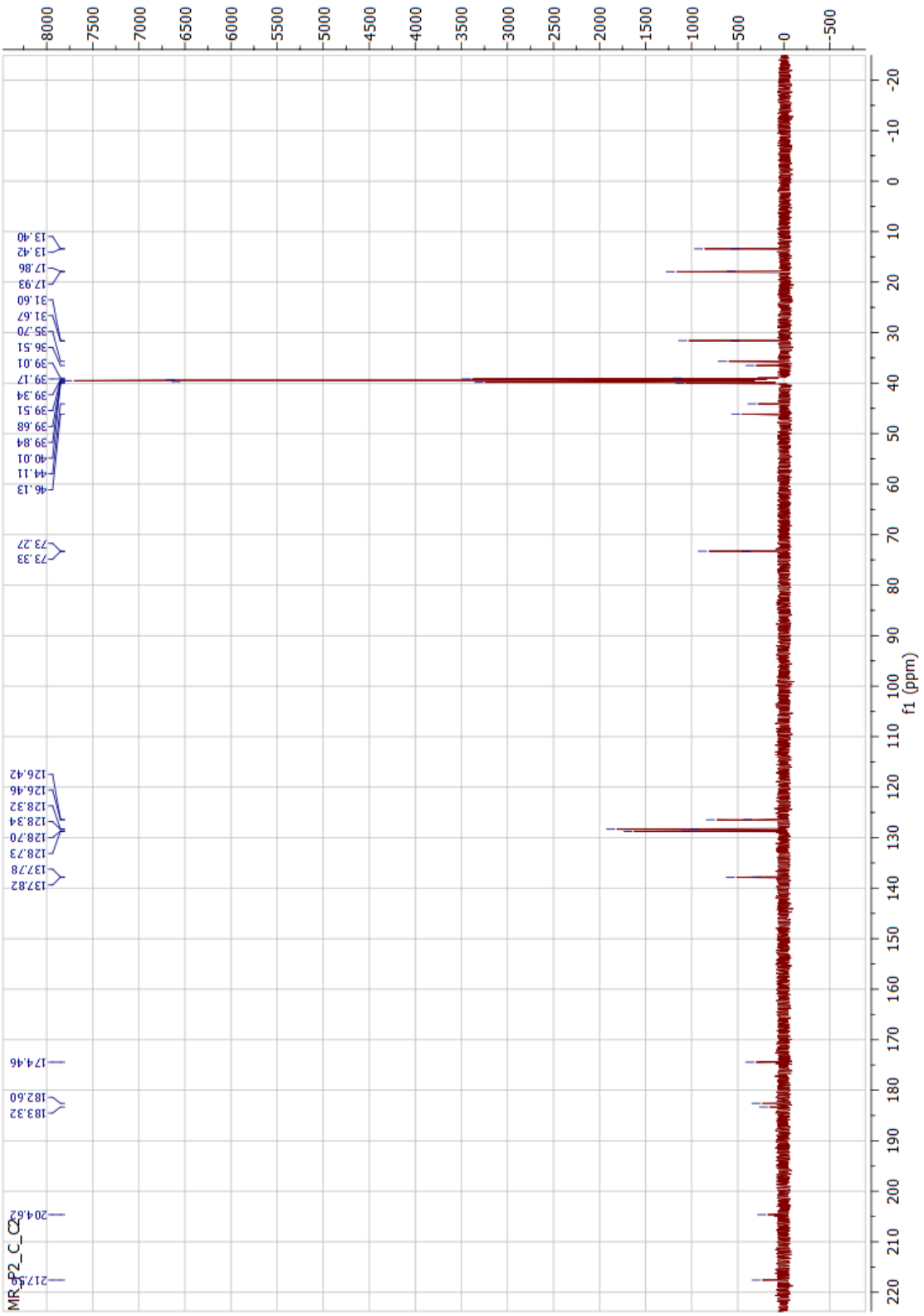

Figure 26. ^{13}C NMR spectrum of **45** (125 MHz, DMSO-d_6).

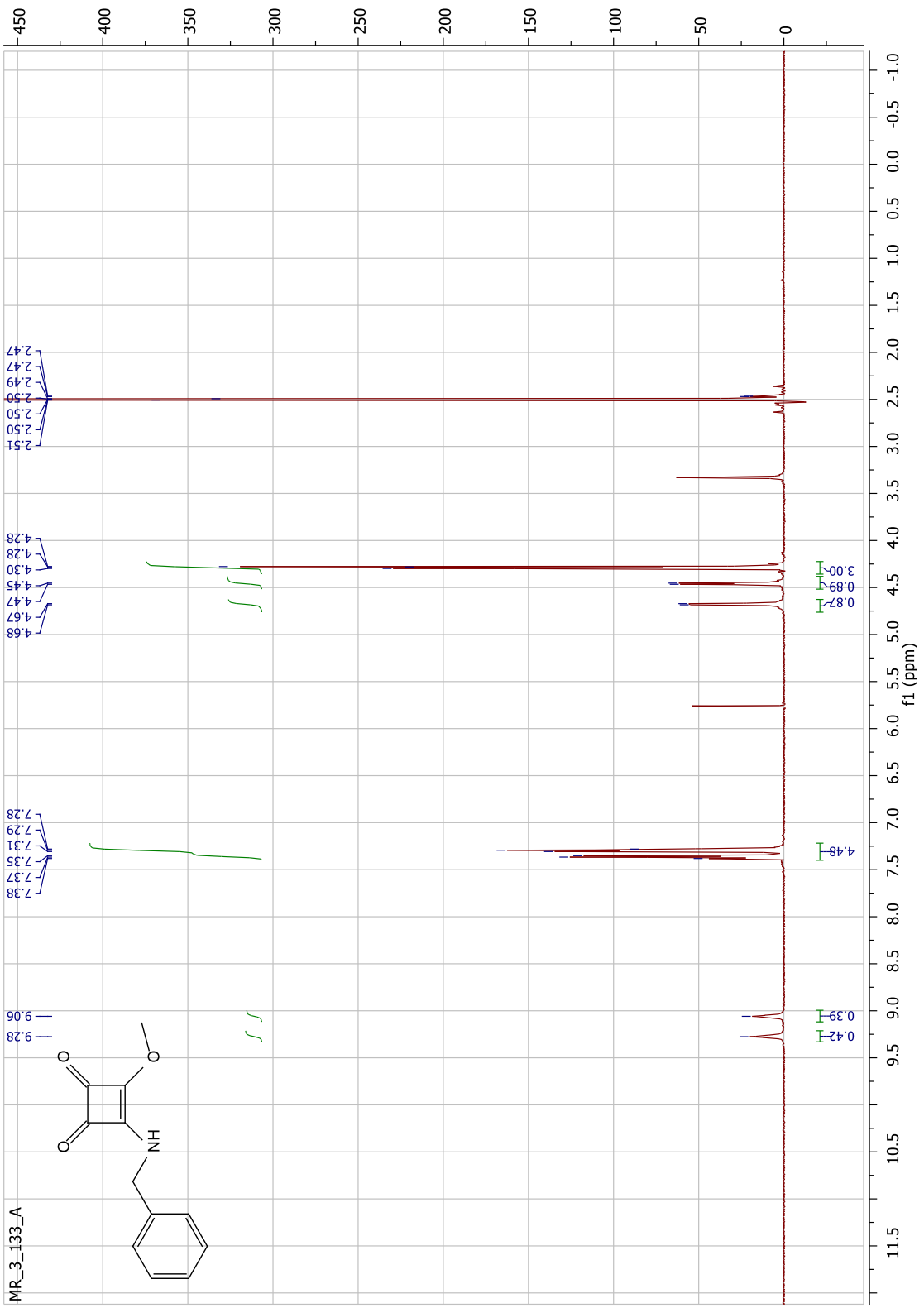

Figure 27. ^{1}H NMR spectrum of **46** (500 MHz, DMSO-d_6).

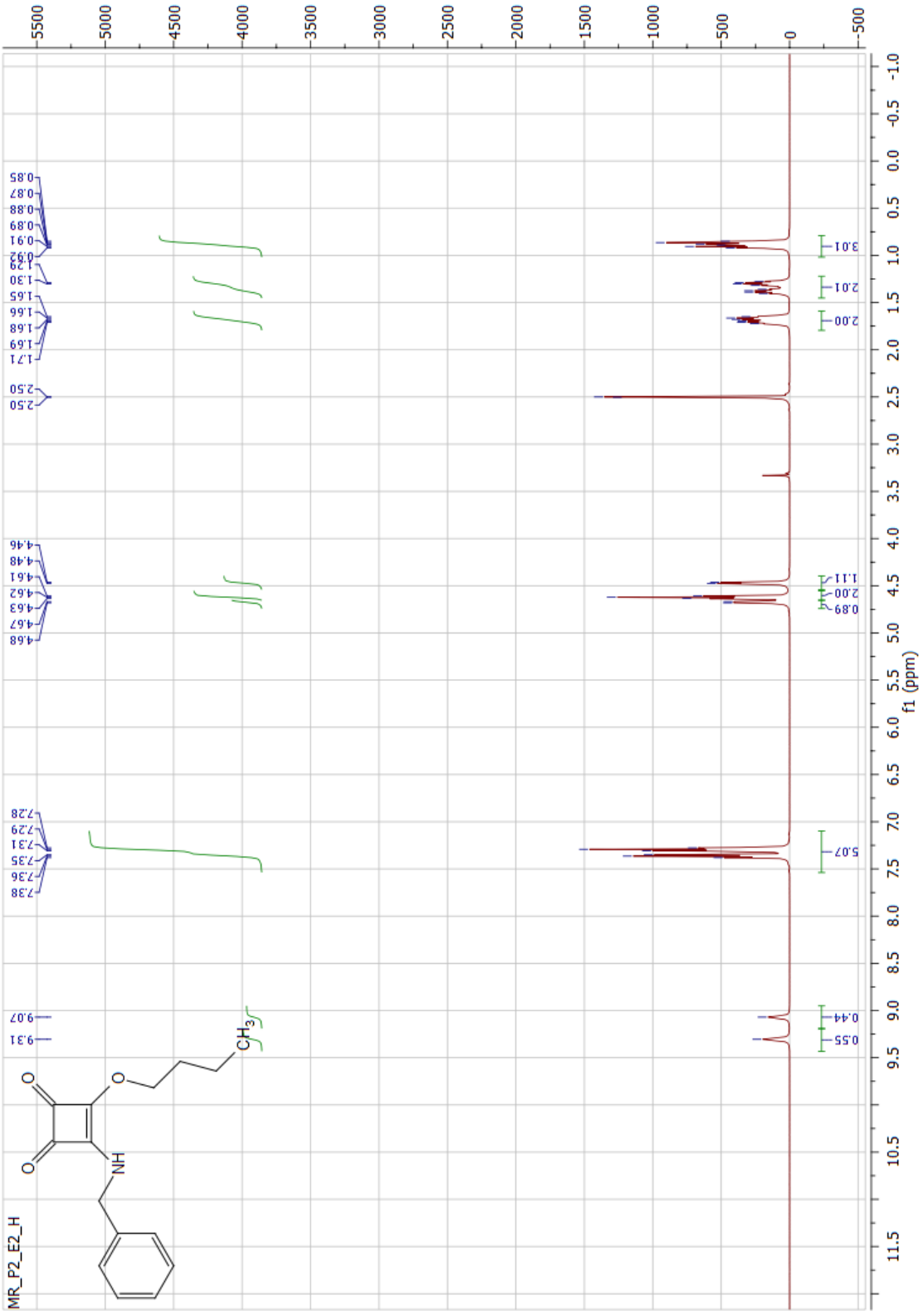

Figure 28. ^{1}H NMR spectrum of **49** (500 MHz, DMSO-d_6).

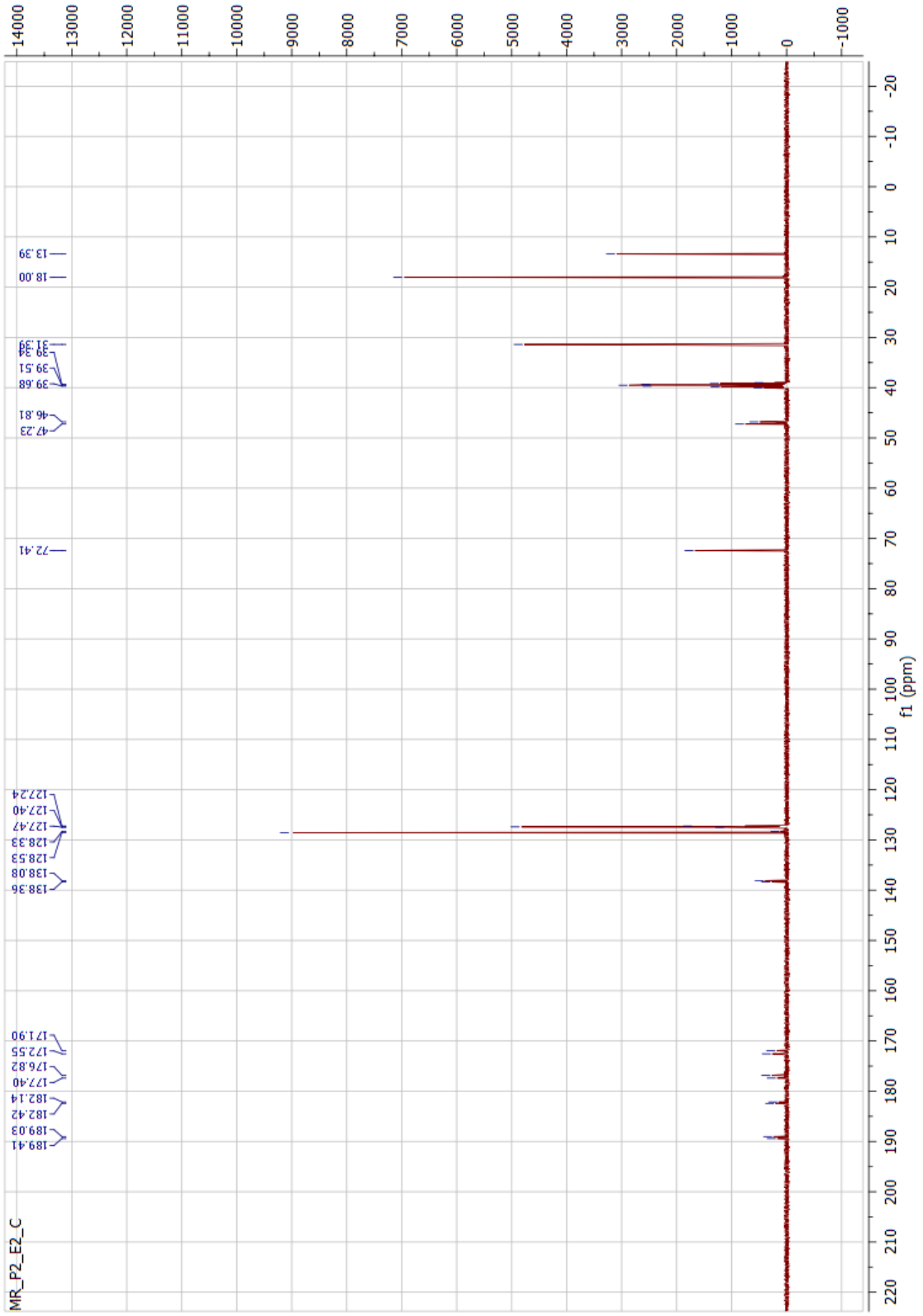

Figure 29. ^{13}C NMR spectrum of **49** (125 MHz, DMSO-d_6).

Figure 30. ^{1}H NMR spectrum of **47** (500 MHz, DMSO-d_6).

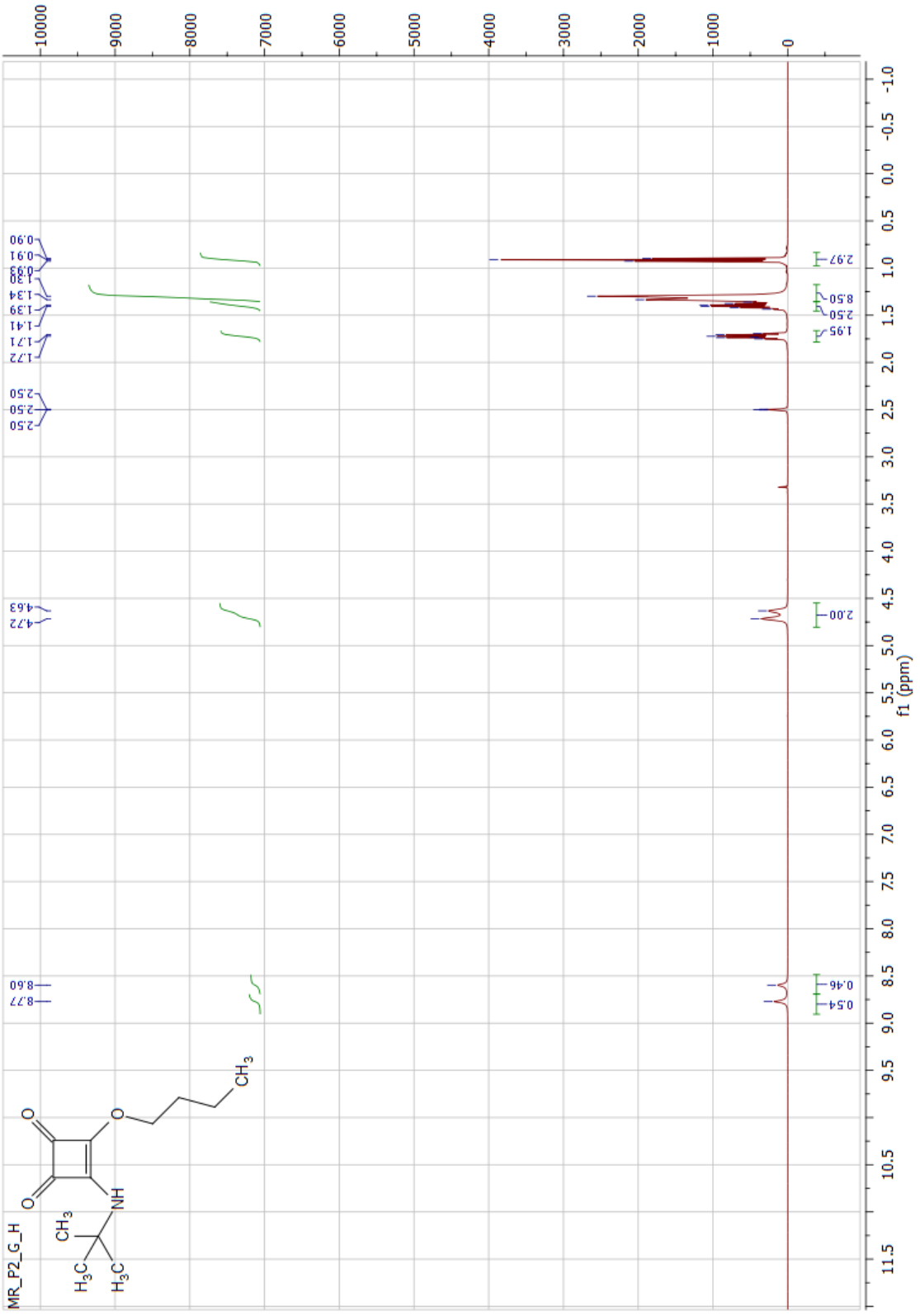

Figure 31. ^{1}H NMR spectrum of **51** (500 MHz, DMSO-d_6).

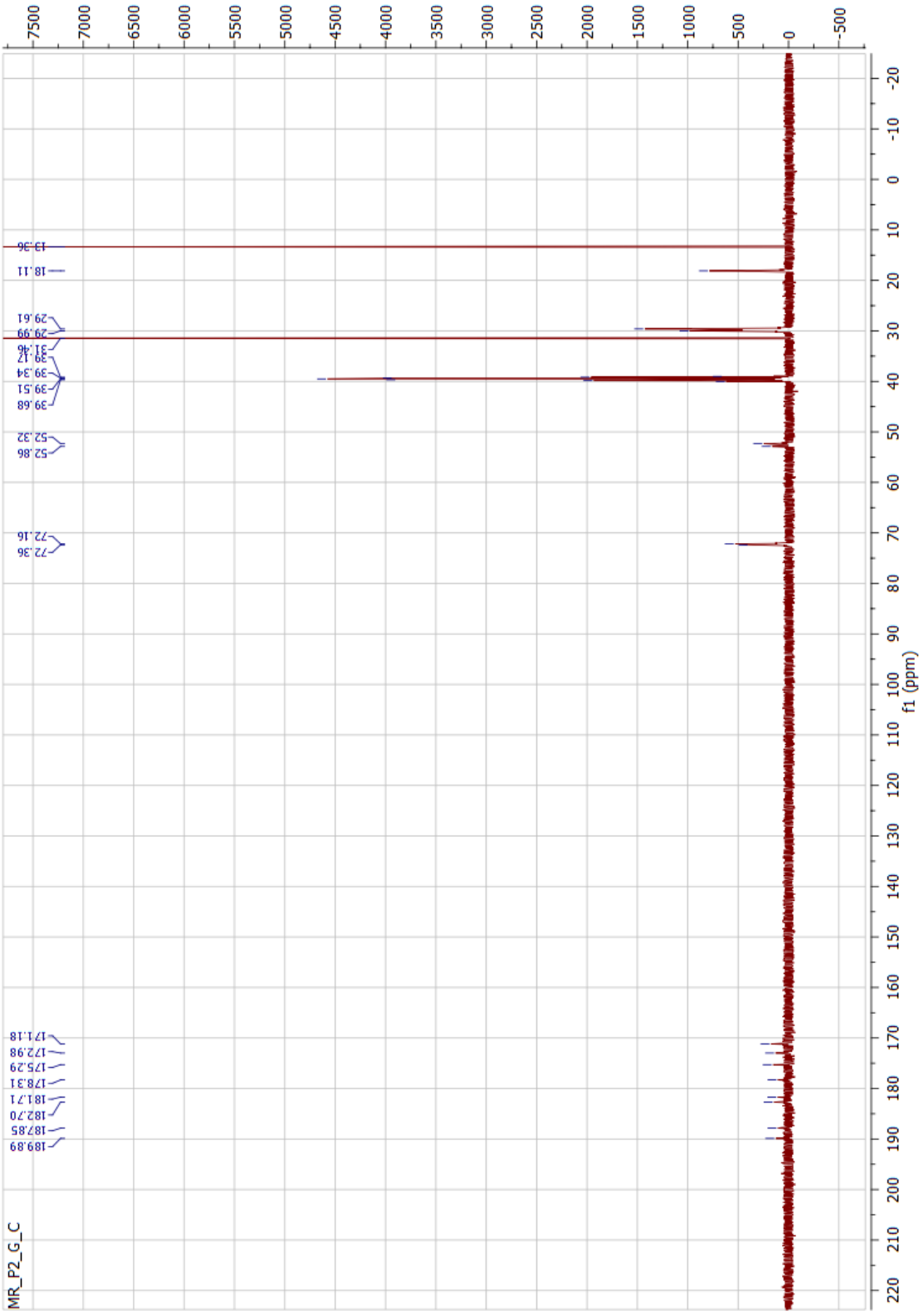

Figure 32. ^{13}C NMR spectrum of **51** (125 MHz, DMSO-d_6).

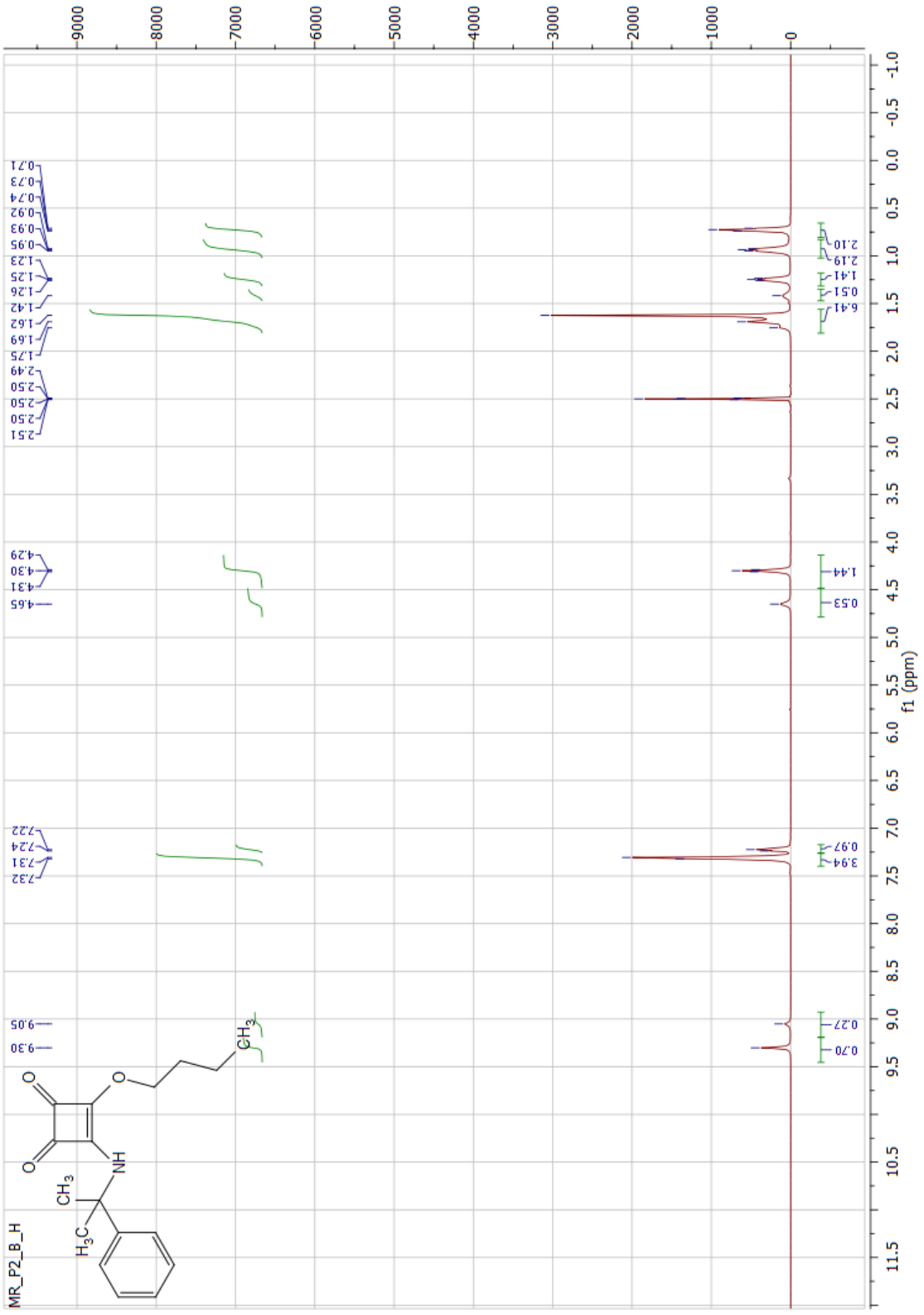

Figure 33. ^{1}H NMR spectrum of **52** (500 MHz, DMSO-d_6).

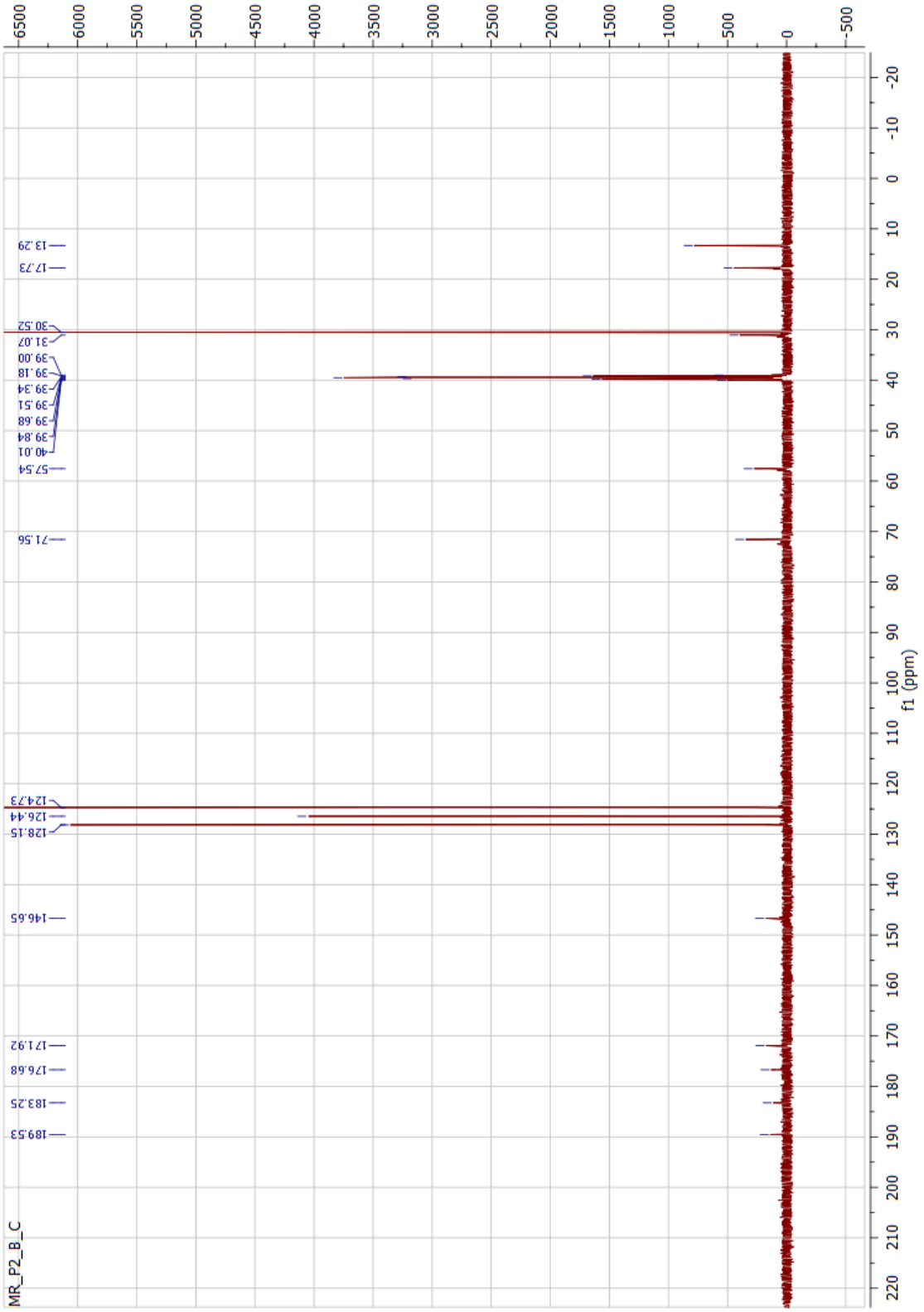

Figure 34. ^{13}C NMR spectrum of **52** (125 MHz, DMSO-d_6).

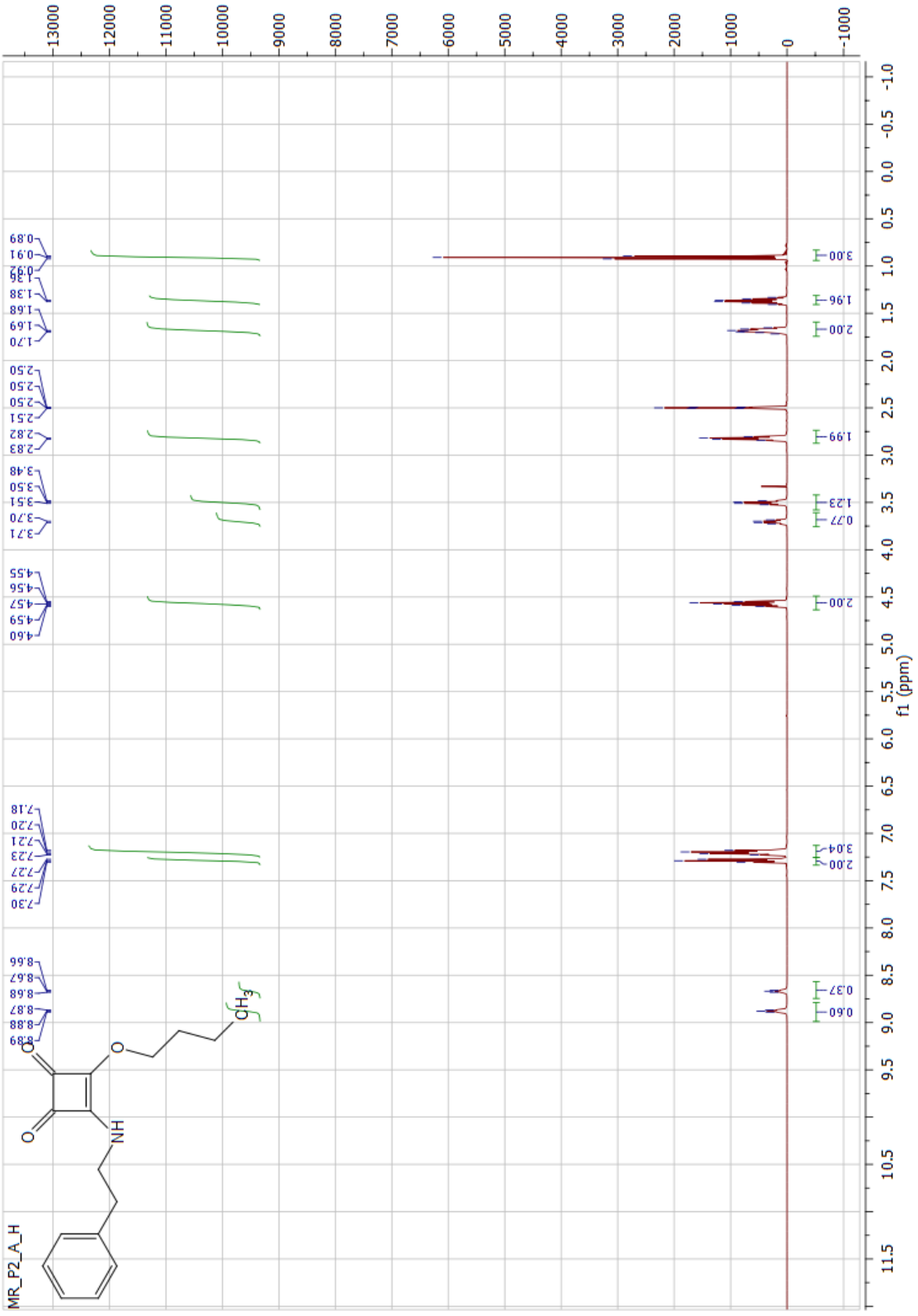

Figure 35. ^{1}H NMR spectrum of **53** (500 MHz, DMSO-d_6).

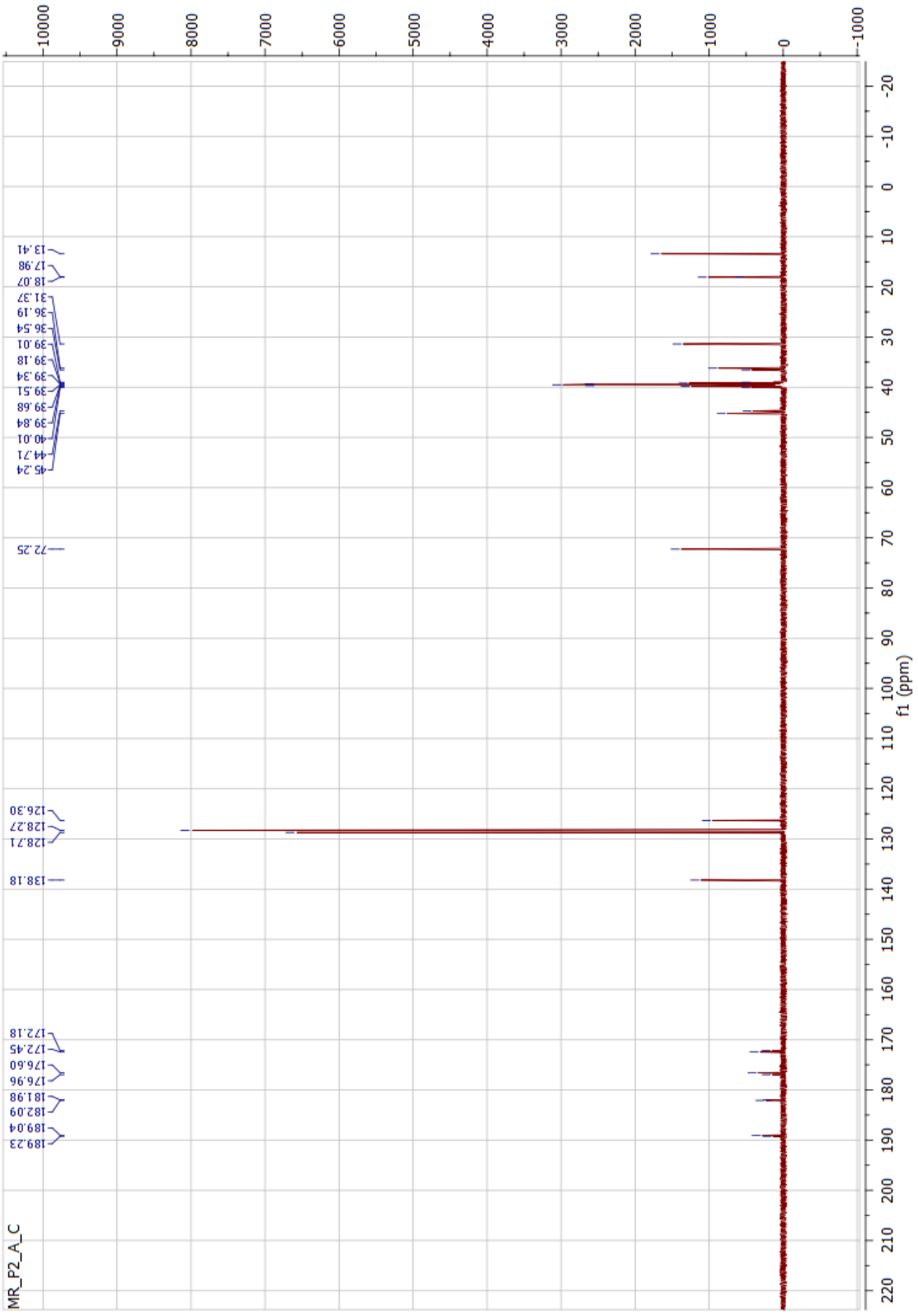

Figure 36. ^{13}C NMR spectrum of **53** (125 MHz, DMSO-d_6).

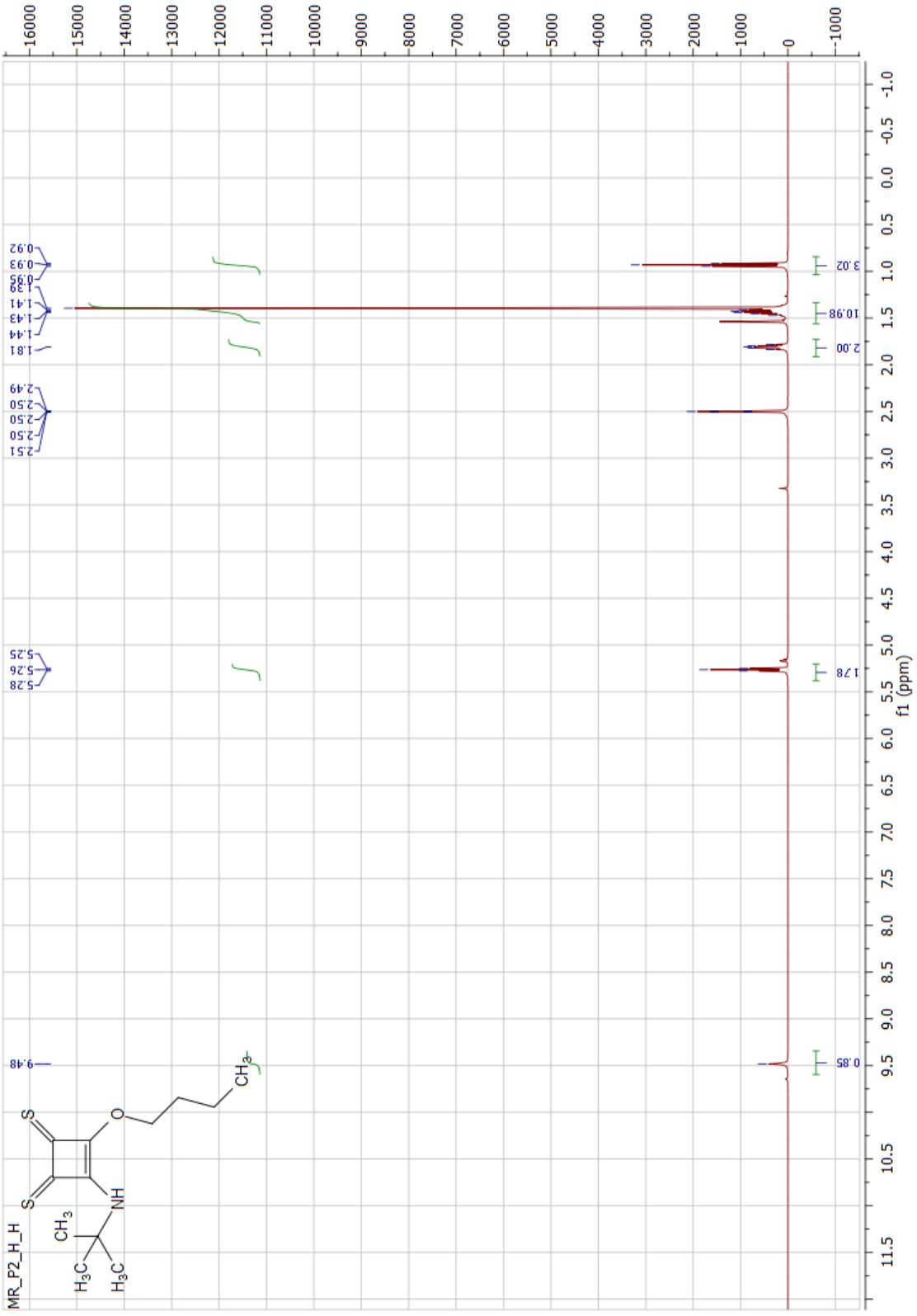

Figure 37. ^{1}H NMR spectrum of **54** (500 MHz, DMSO-d_6).

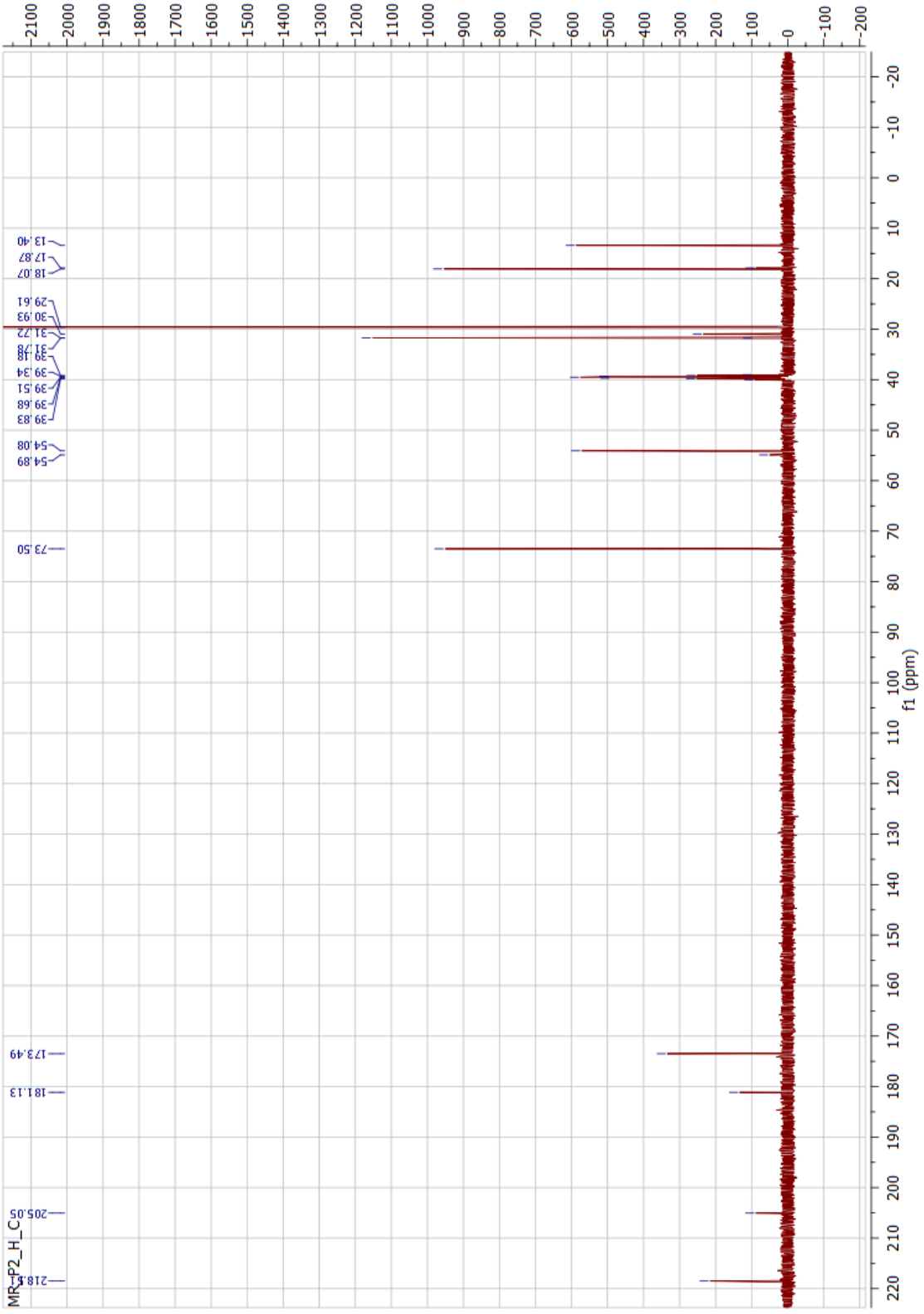

Figure 38. ^{13}C NMR spectrum of **54** (125 MHz, DMSO-d_6).

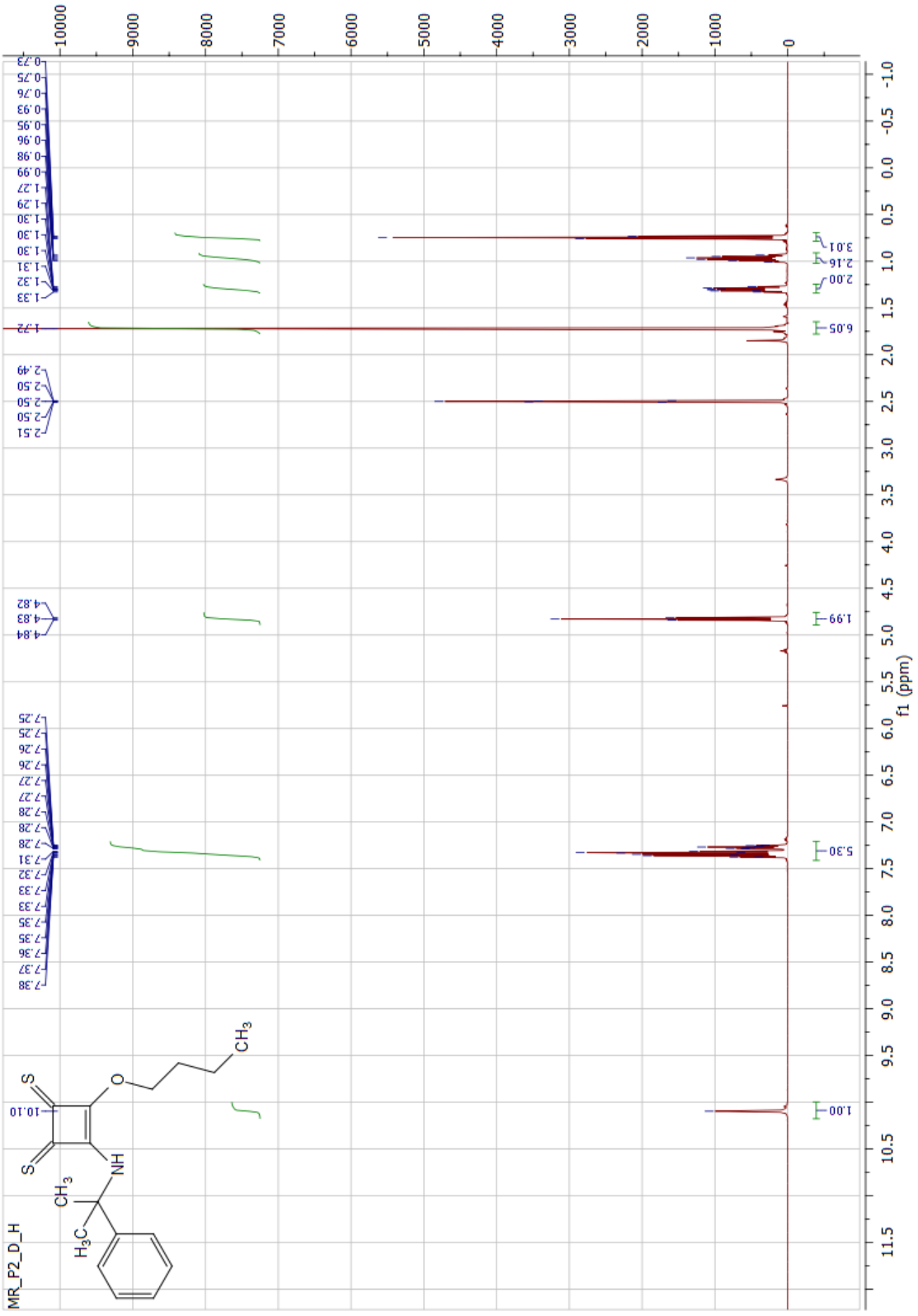

Figure 39. ^{1}H NMR spectrum of **55** (500 MHz, DMSO-d_6).

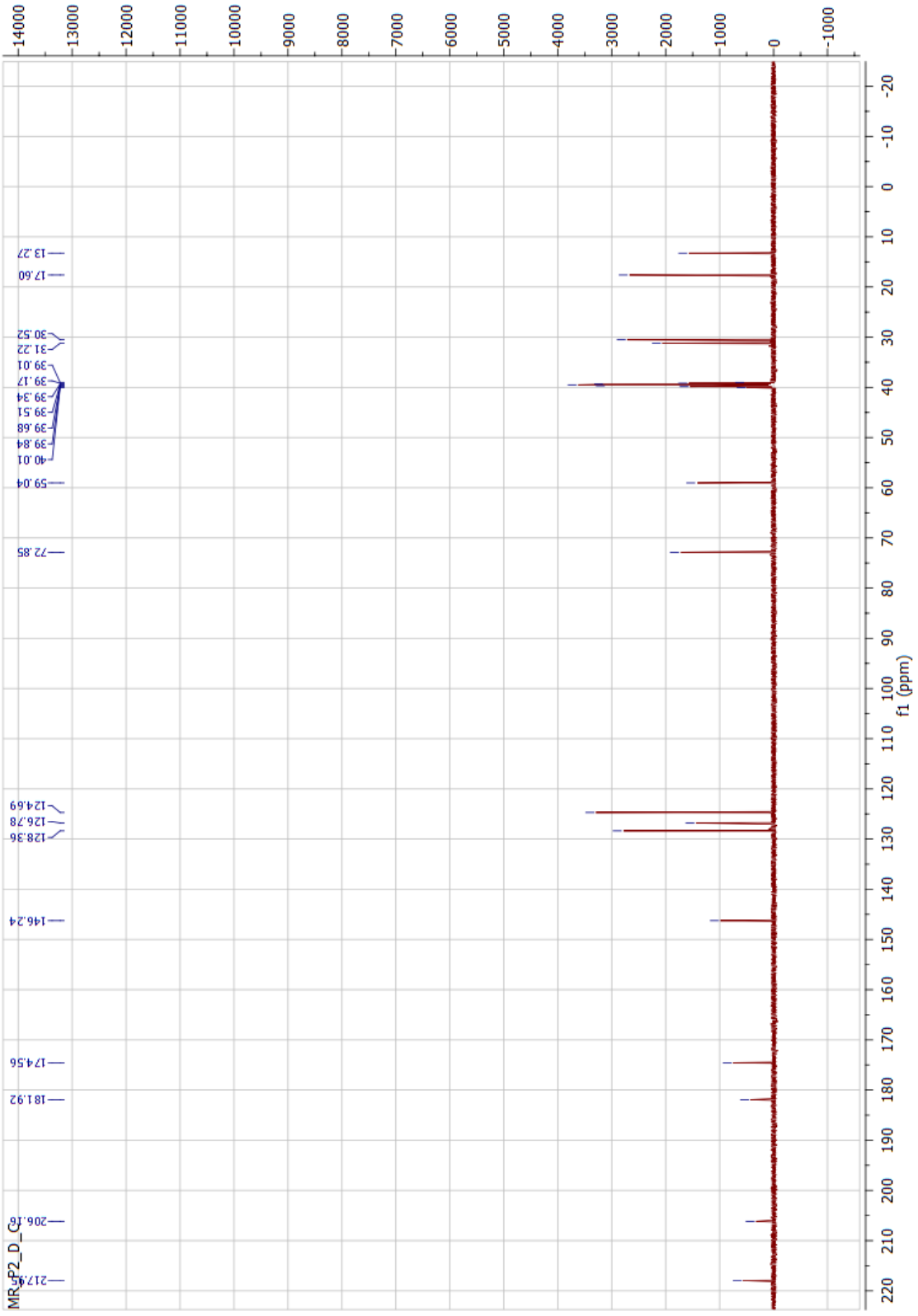

Figure 40. ^{13}C NMR spectrum of **55** (125 MHz, DMSO-d_6).

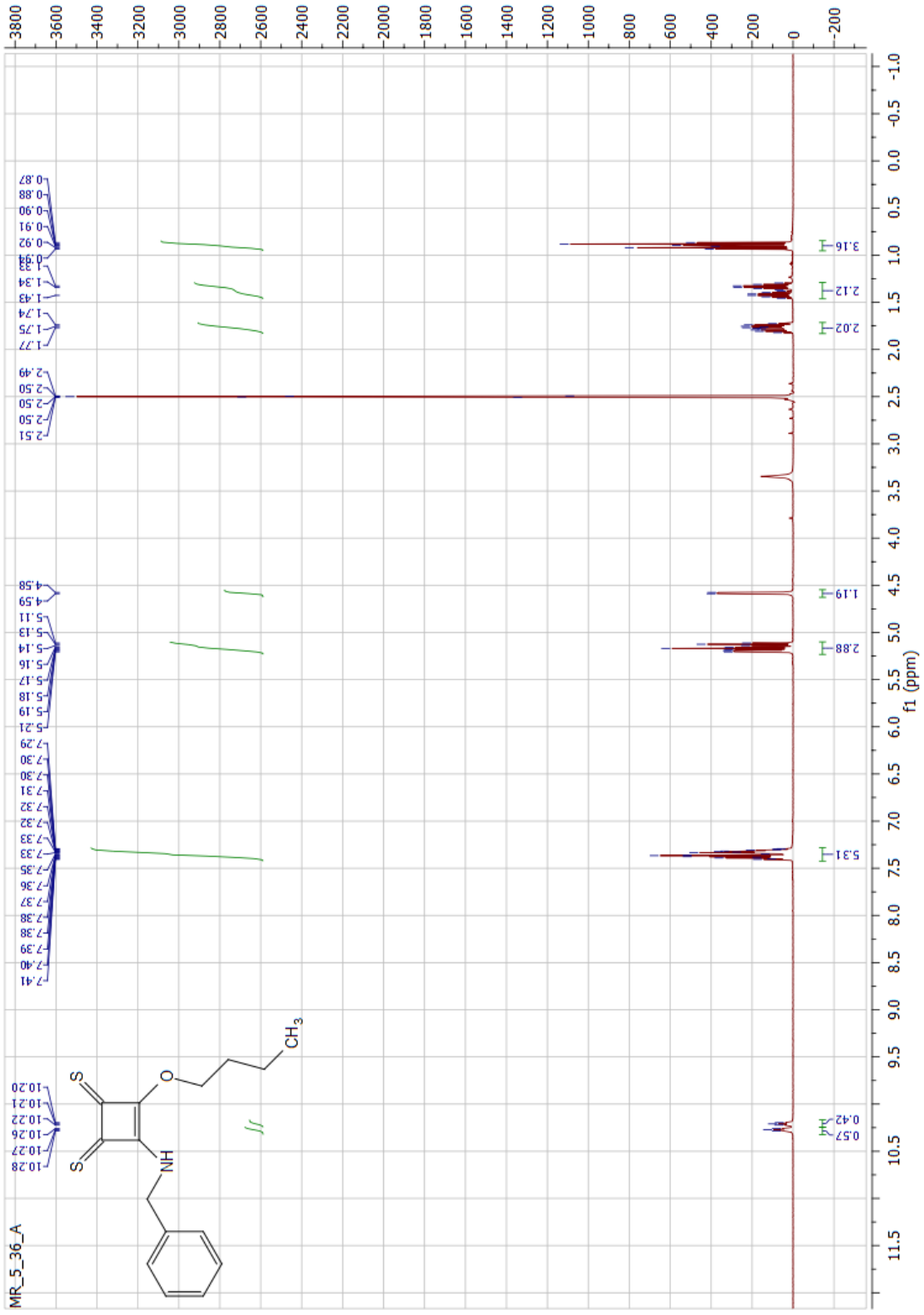

Figure 41. ^{1}H NMR spectrum of **50** (500 MHz, DMSO-d_6).

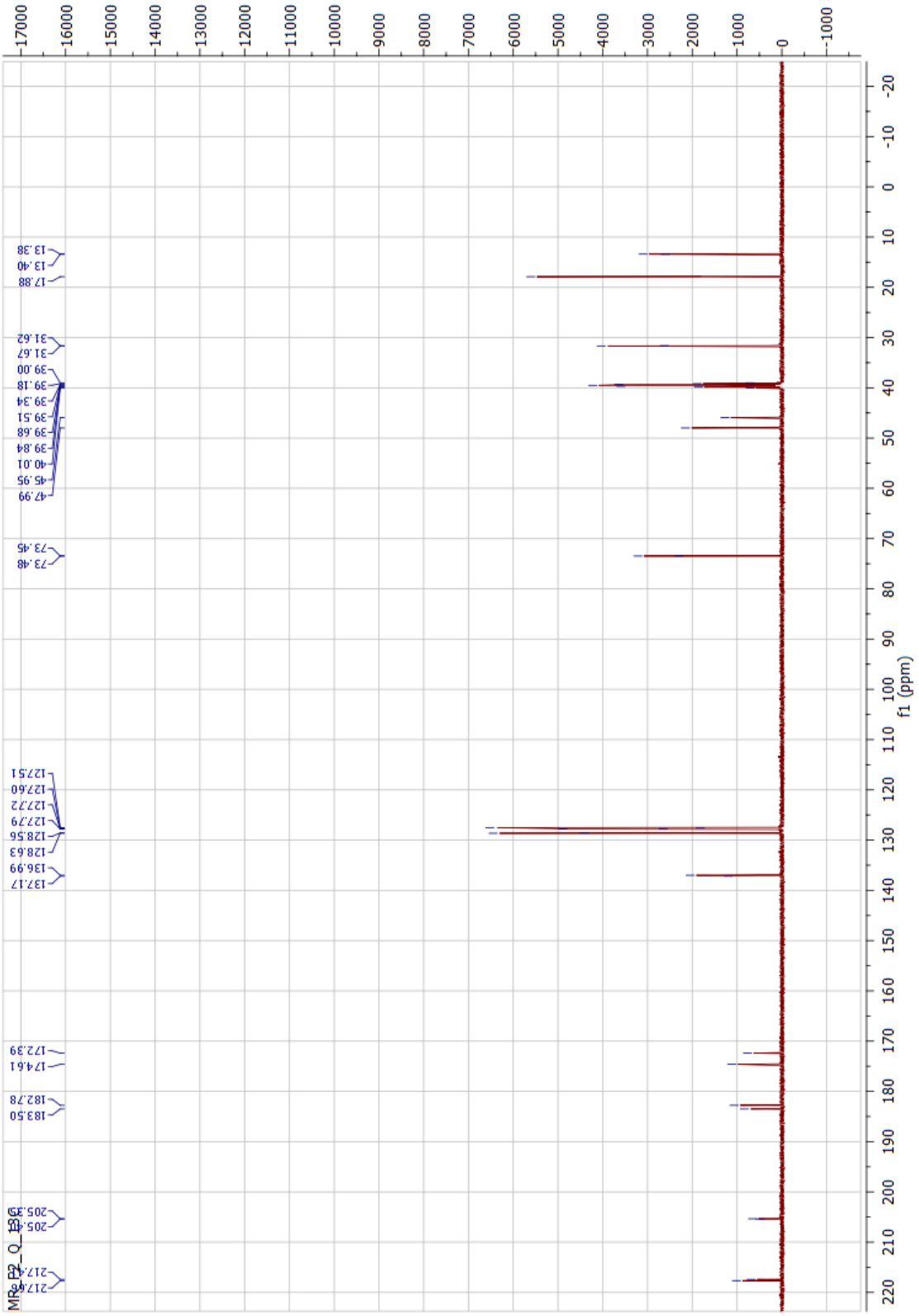

Figure 42. ^{13}C NMR spectrum of **50** (125 MHz, DMSO-d_6).

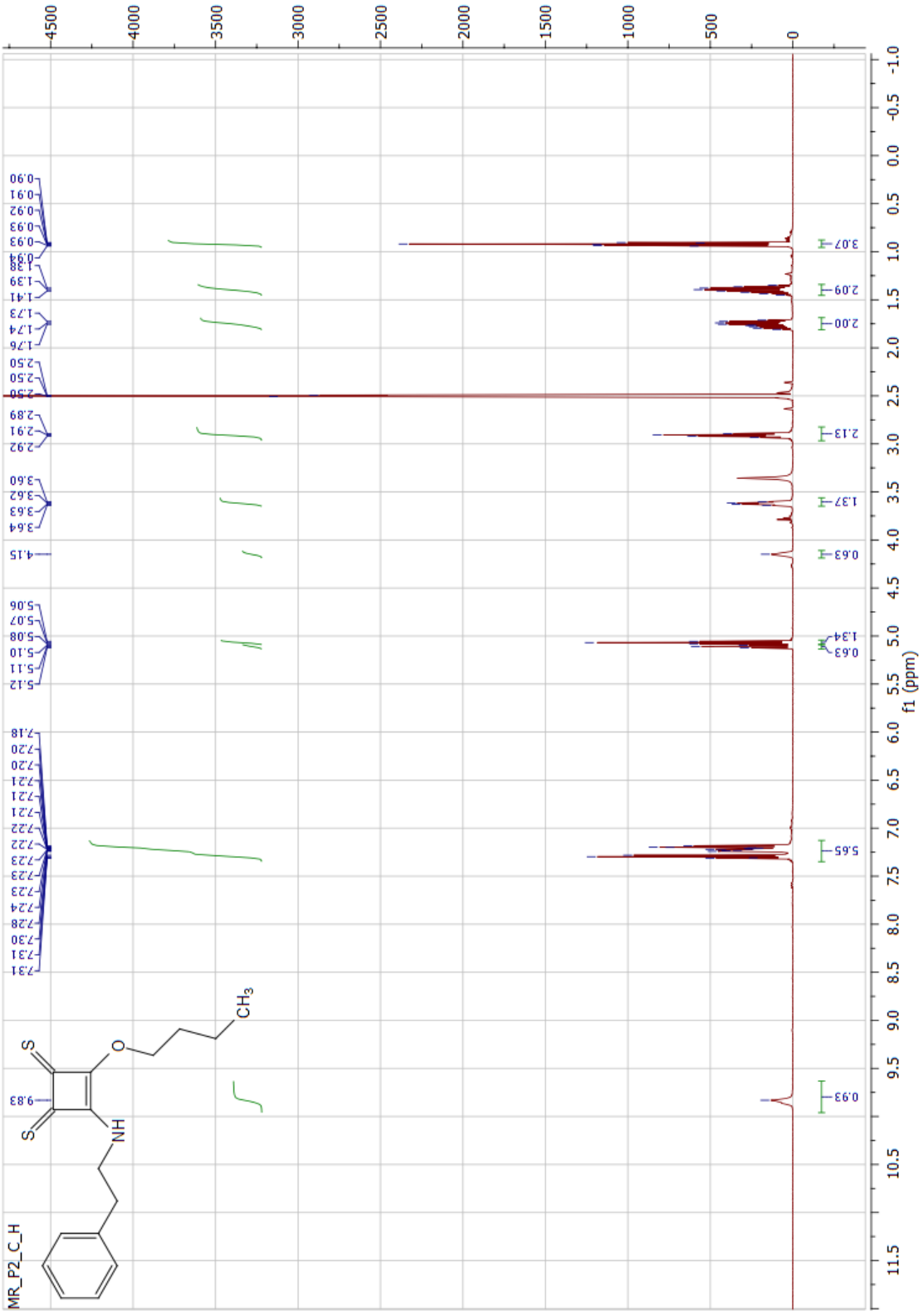

Figure 43. ^{1}H NMR spectrum of **56** (500 MHz, DMSO-d_6).

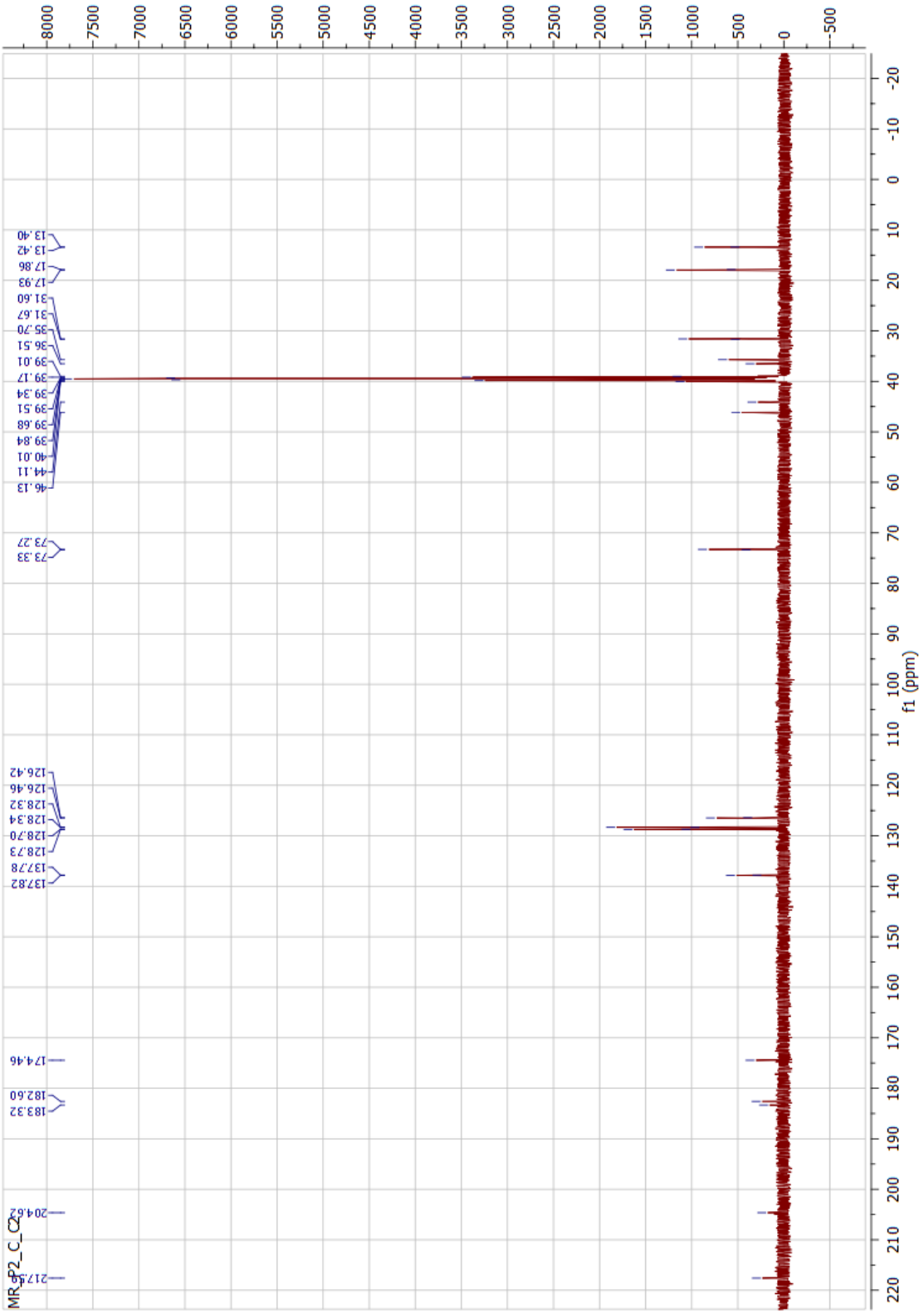

Figure 44. ^{13}C NMR spectrum of **56** (125 MHz, DMSO-d_6).

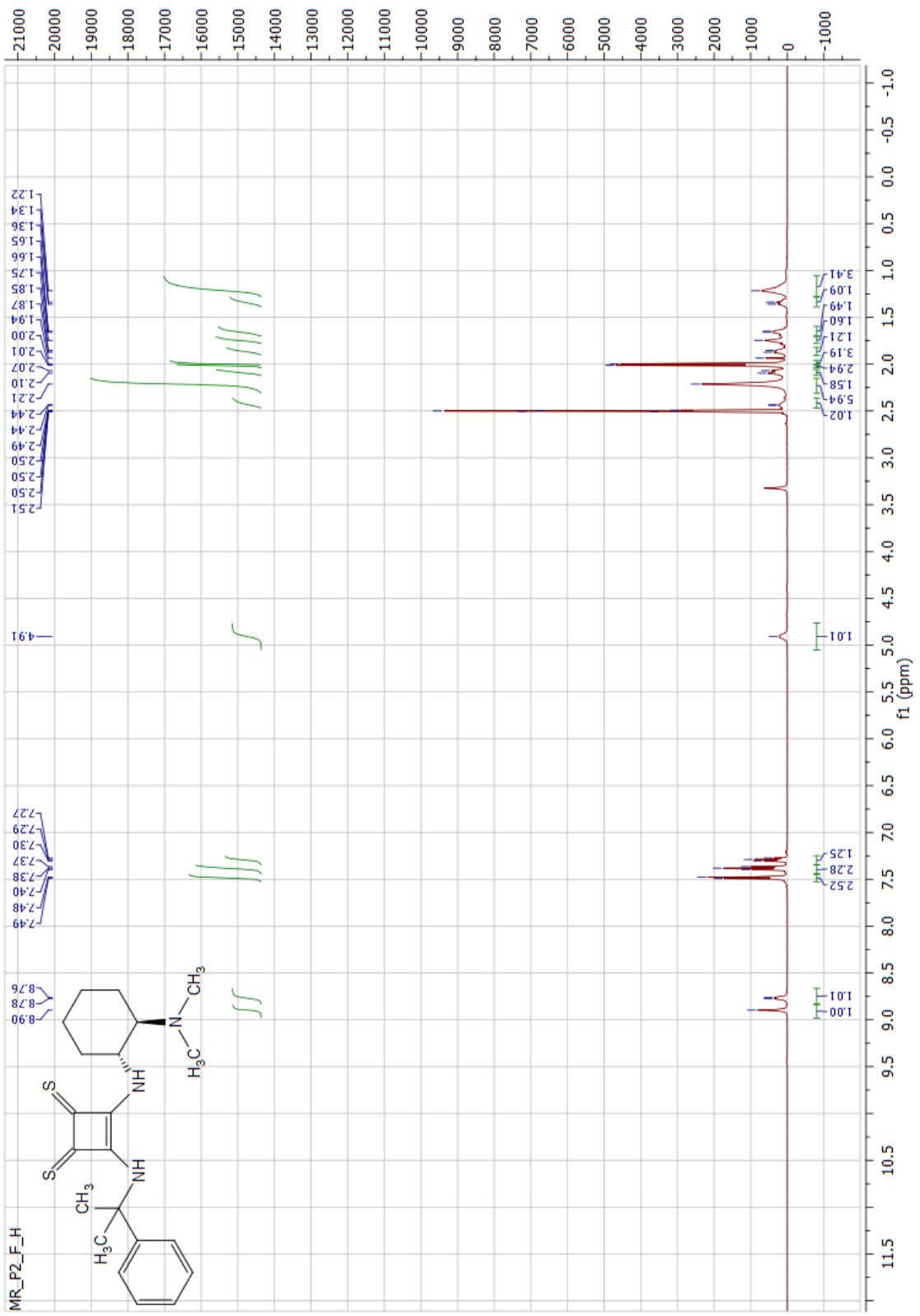

Figure 45. ^{1}H NMR spectrum of **57** (500 MHz, DMSO-d_6).

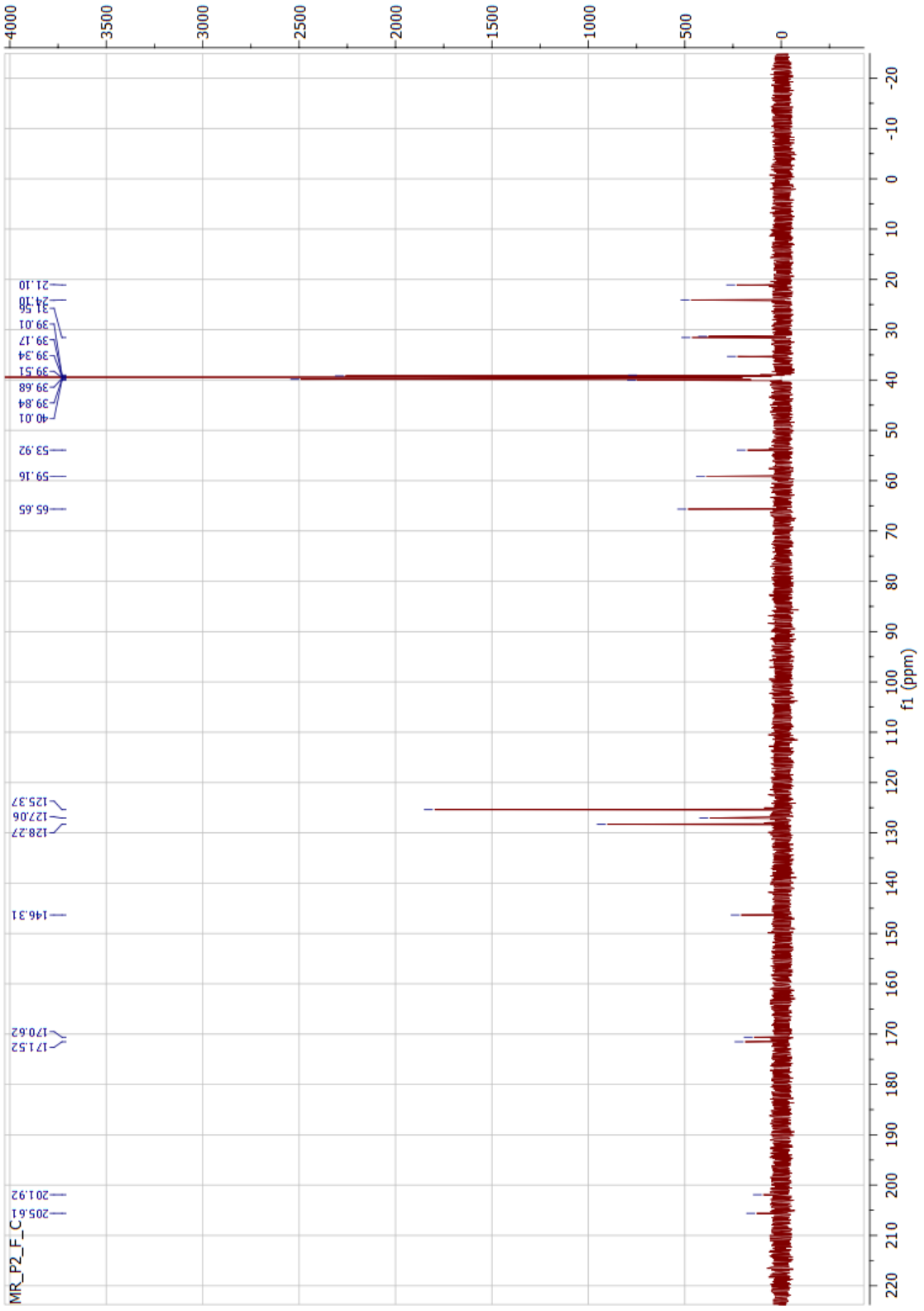

Figure 46. ^{13}C NMR spectrum of **57** (125 MHz, DMSO-d_6).

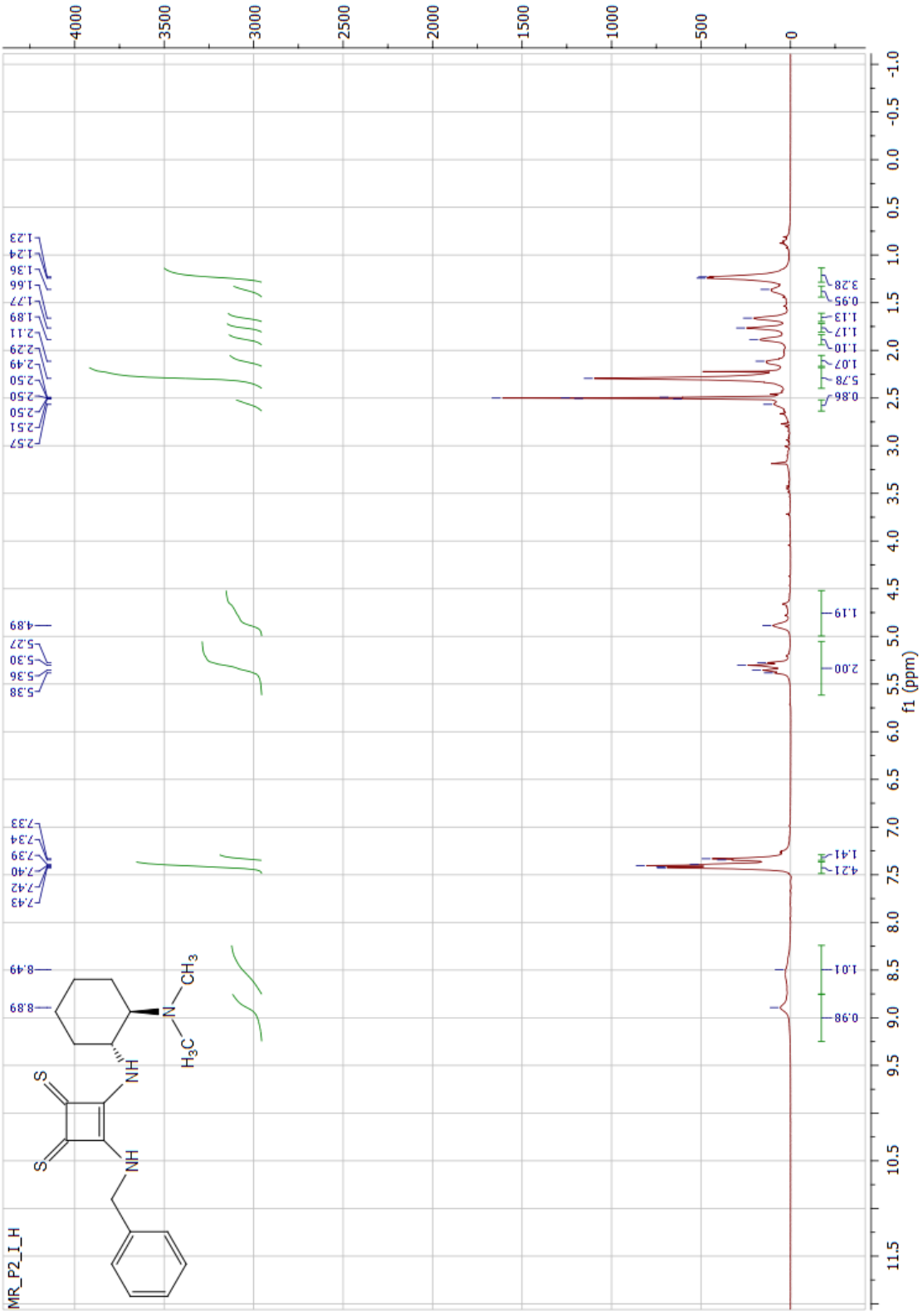

Figure 47. ^{1}H NMR spectrum of **40** (500 MHz, DMSO-d_6).

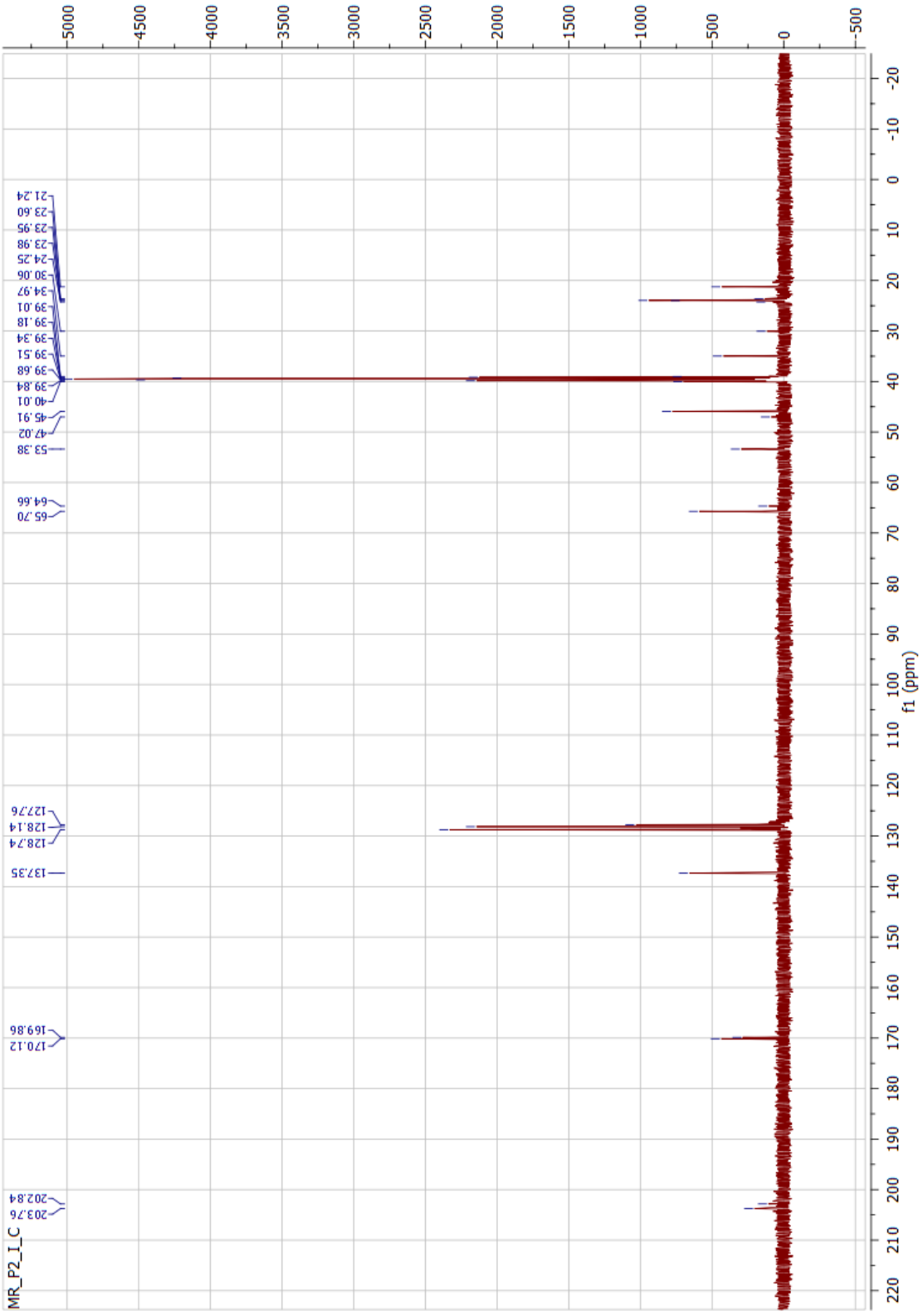

Figure 48. ^{13}C NMR spectrum of **40** (125 MHz, DMSO-d_6).

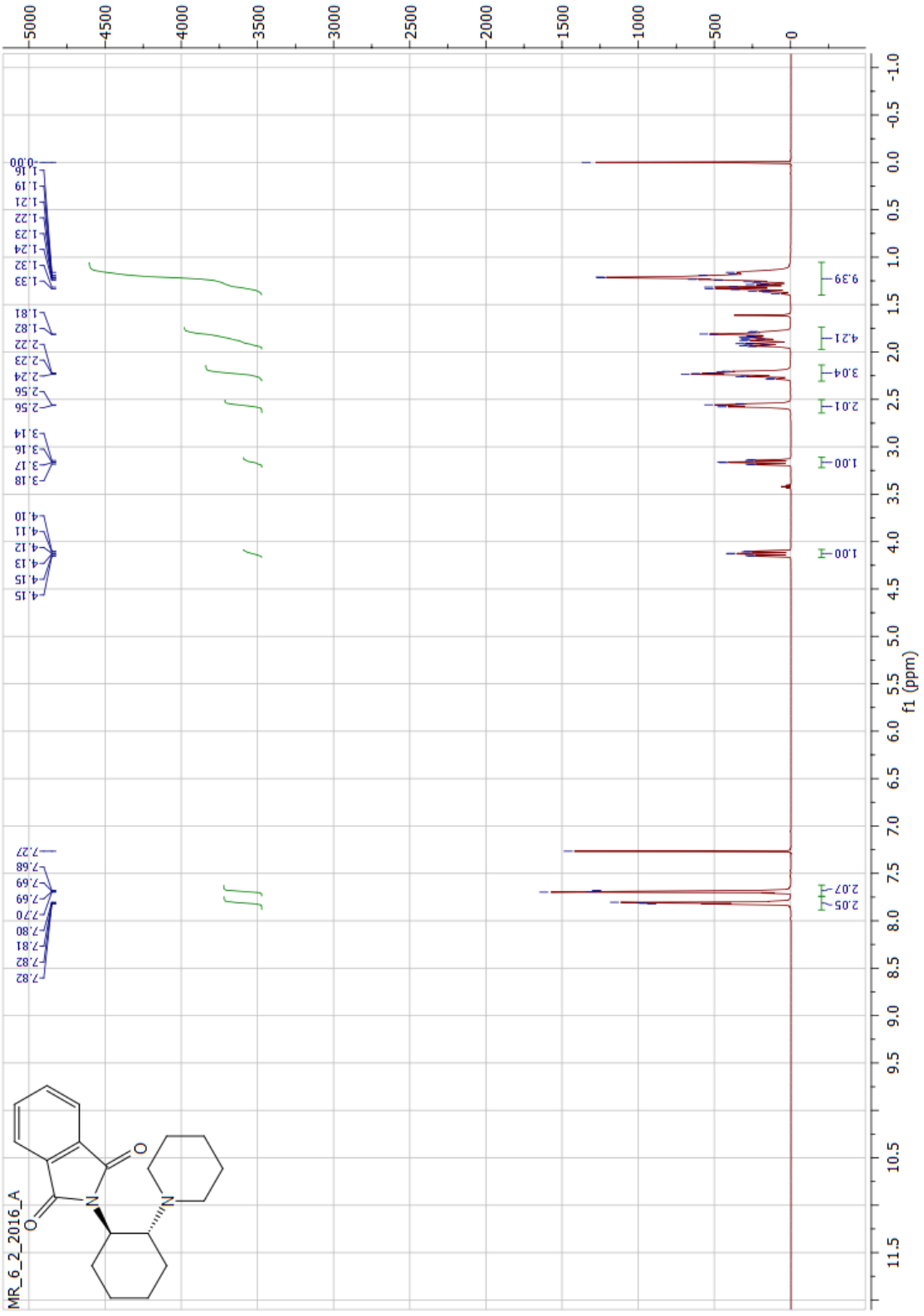

Figure 49. ^{1}H NMR spectrum of **300** (500 MHz, $CDCl_3$).

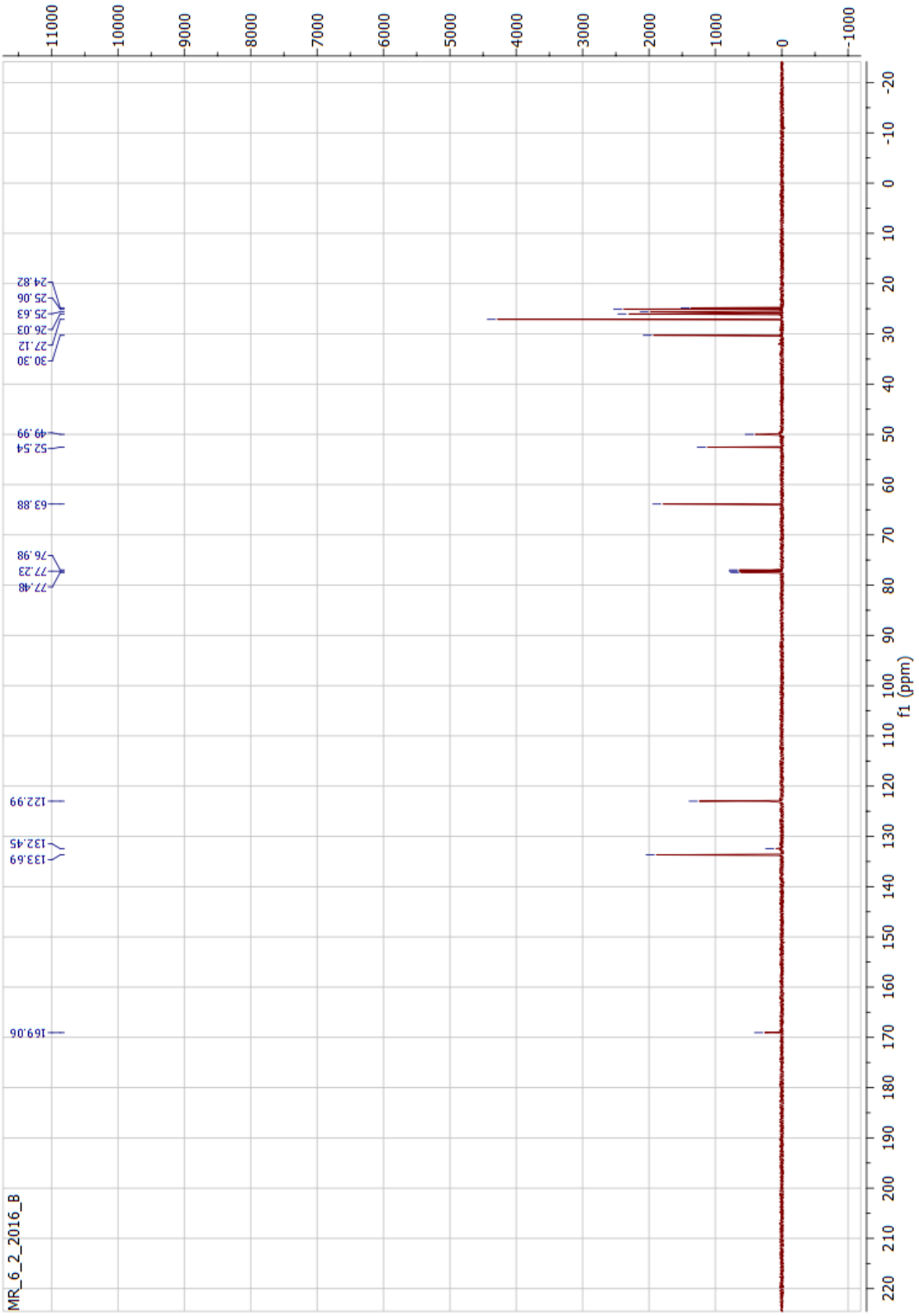

Figure 50. ^{13}C NMR spectrum of **300** (125 MHz, $CDCl_3$).

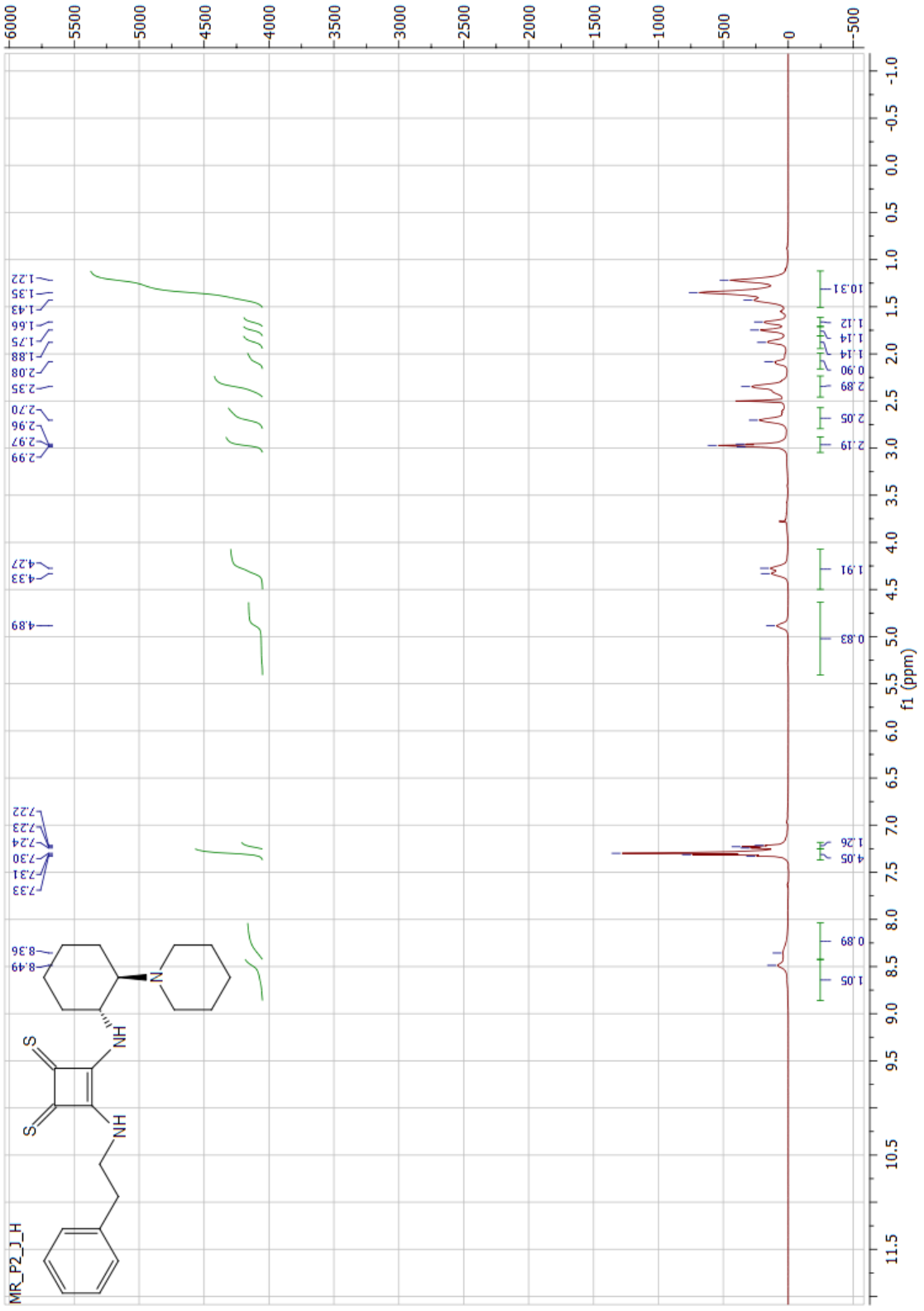

Figure 51. ^{1}H NMR spectrum of **58** (500 MHz, DMSO-d_6).

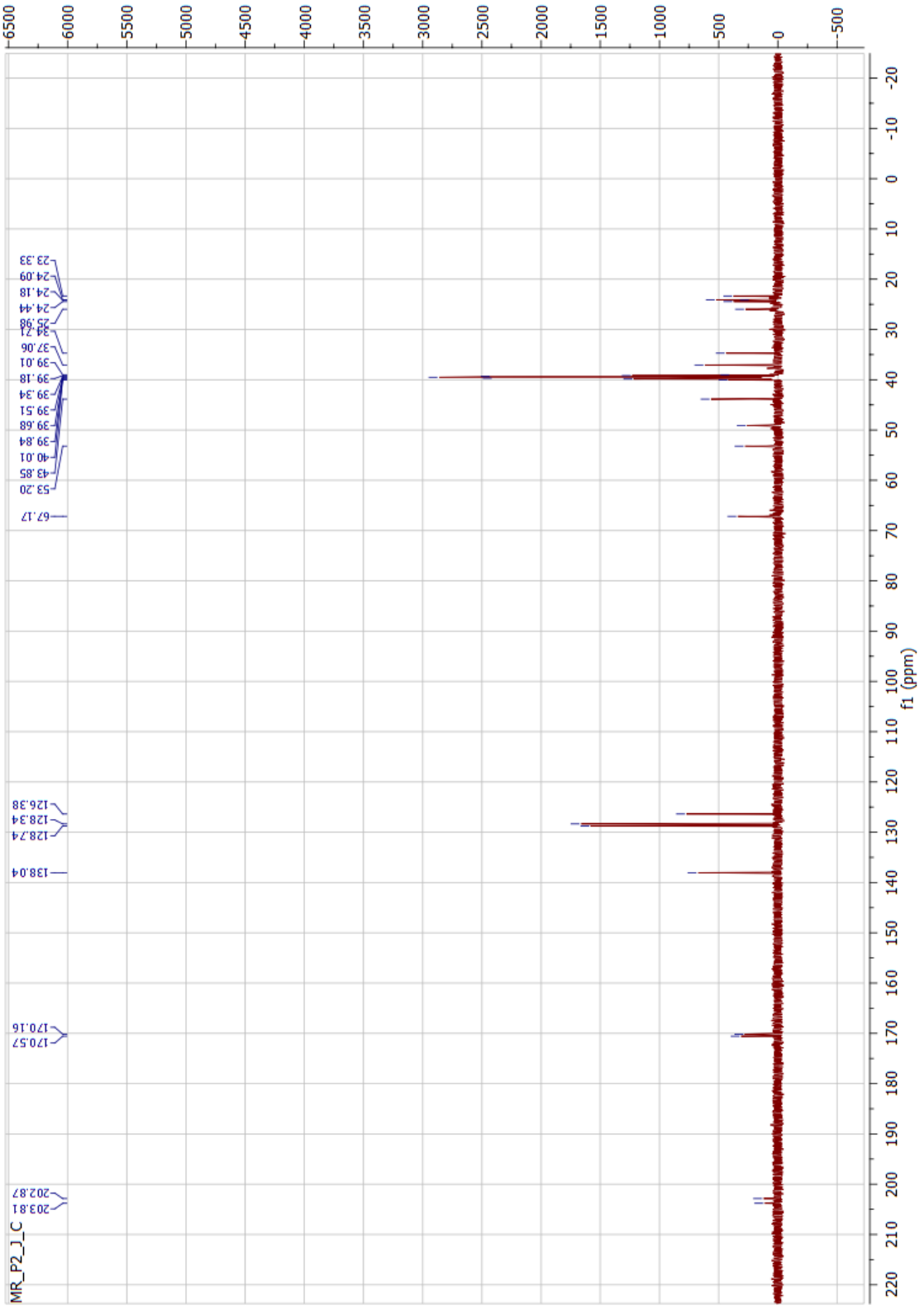

Figure 52. ^{13}C NMR spectrum of **58** (125 MHz, DMSO-d_6).

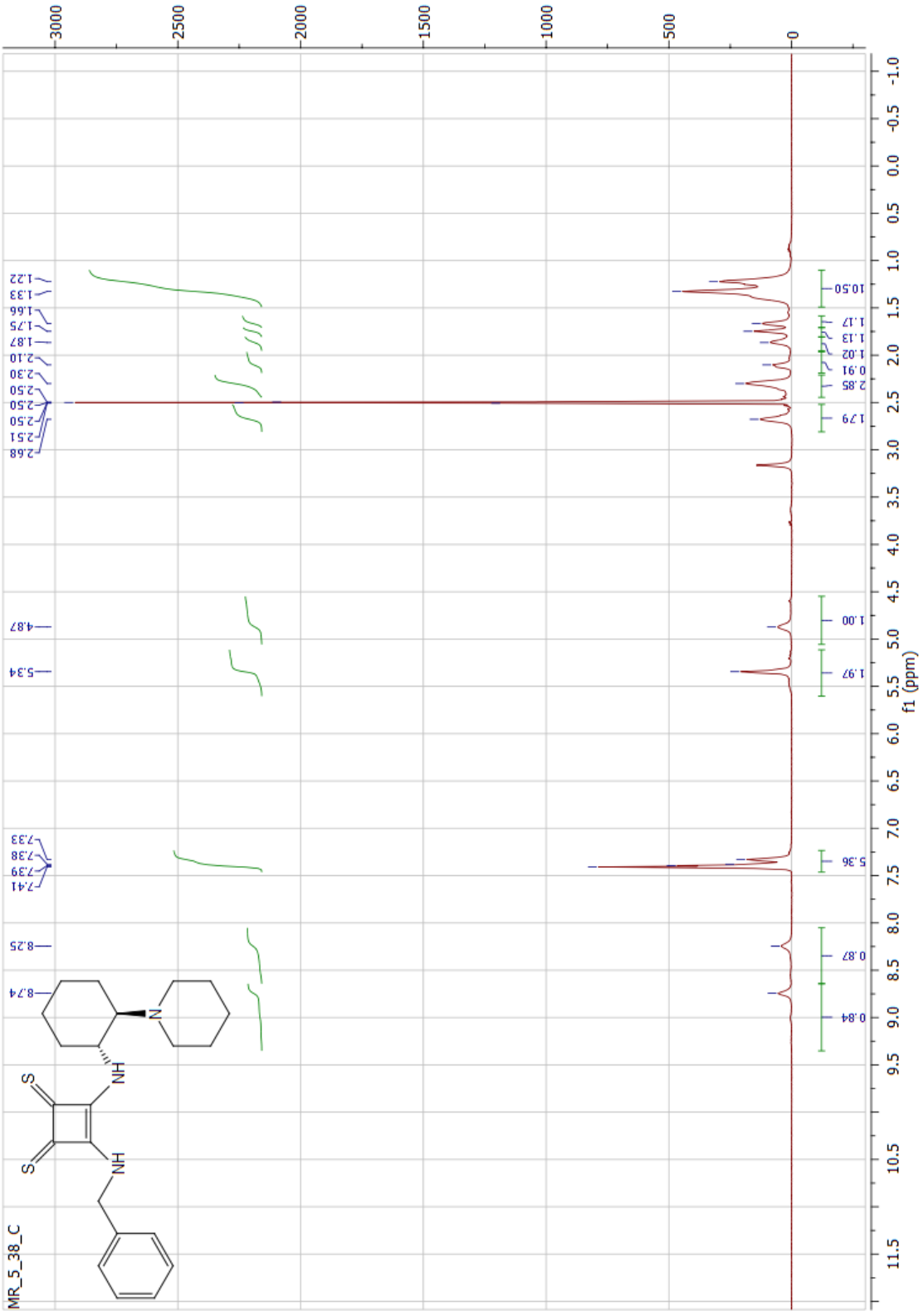

Figure 53. ^{1}H NMR spectrum of **59** (500 MHz, DMSO-d_6).

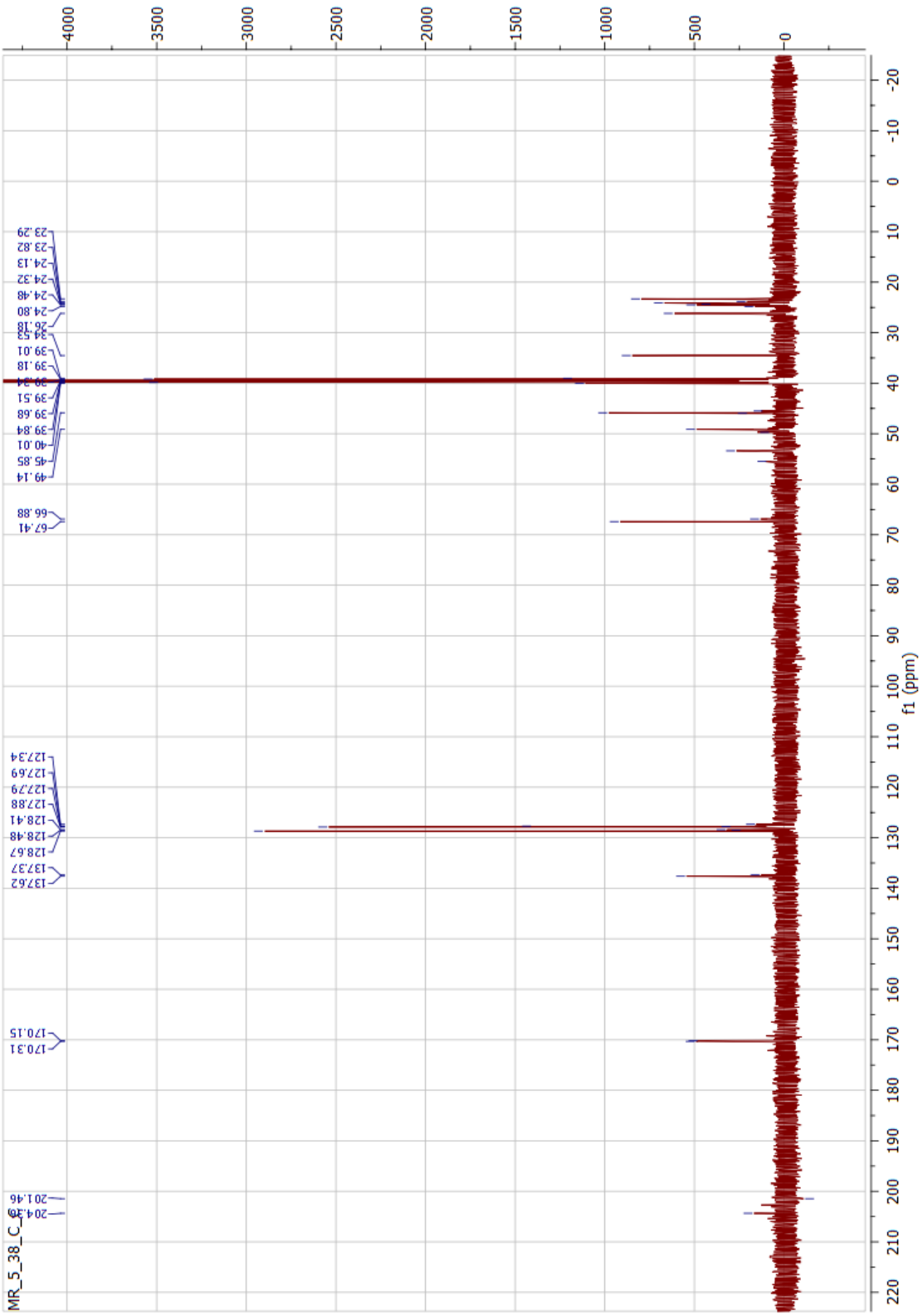

Figure 54. ^{13}C NMR spectrum of **59** (125 MHz, DMSO-d_6).

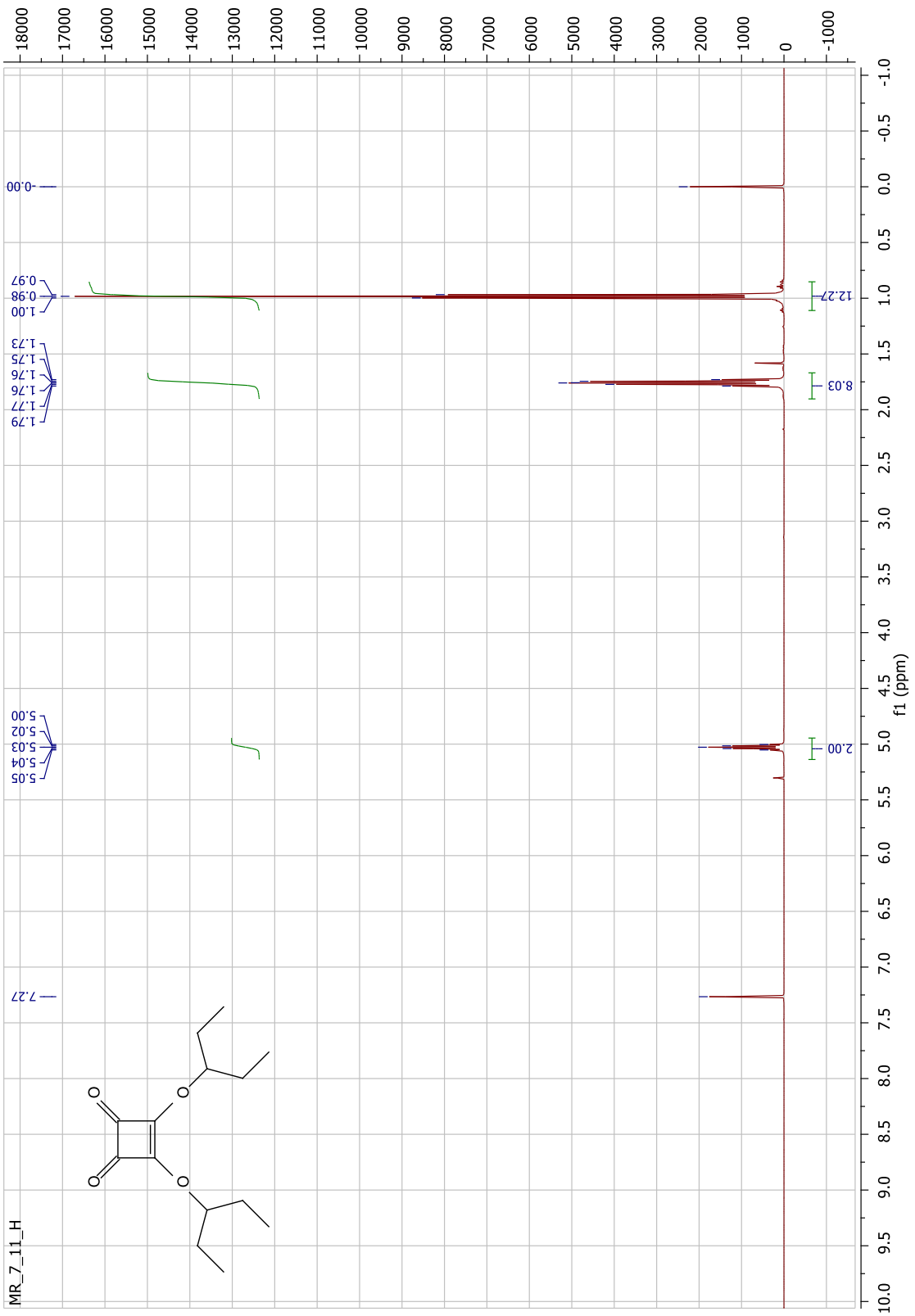

Figure 55. ^{1}H NMR spectrum of **61** (500 MHz, $CDCl_3$).

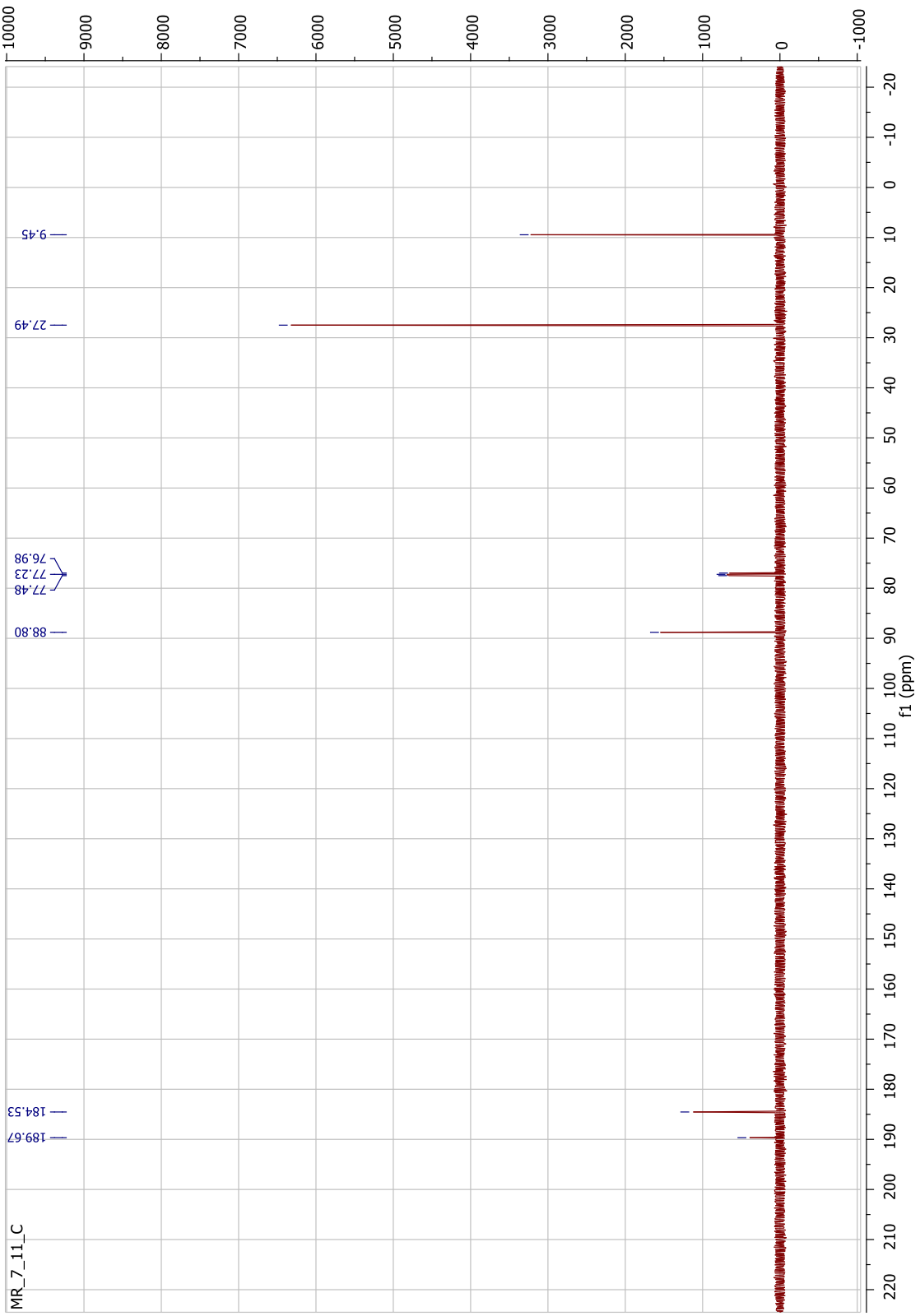

Figure 56. ^{13}C NMR spectrum of **61** (125 MHz, $CDCl_3$).

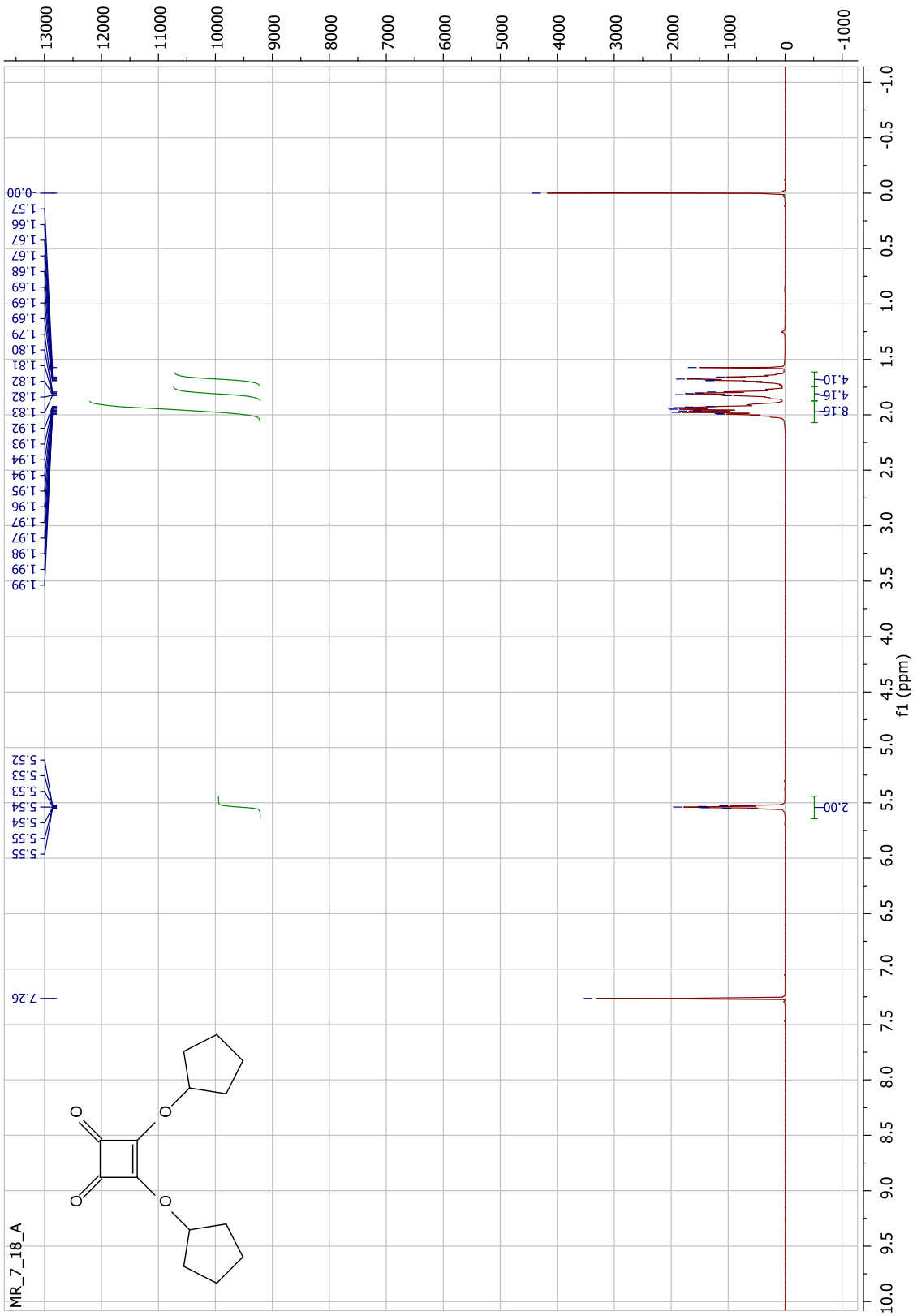

Figure 57. ^{1}H NMR spectrum of **62** (500 MHz, $CDCl_3$).

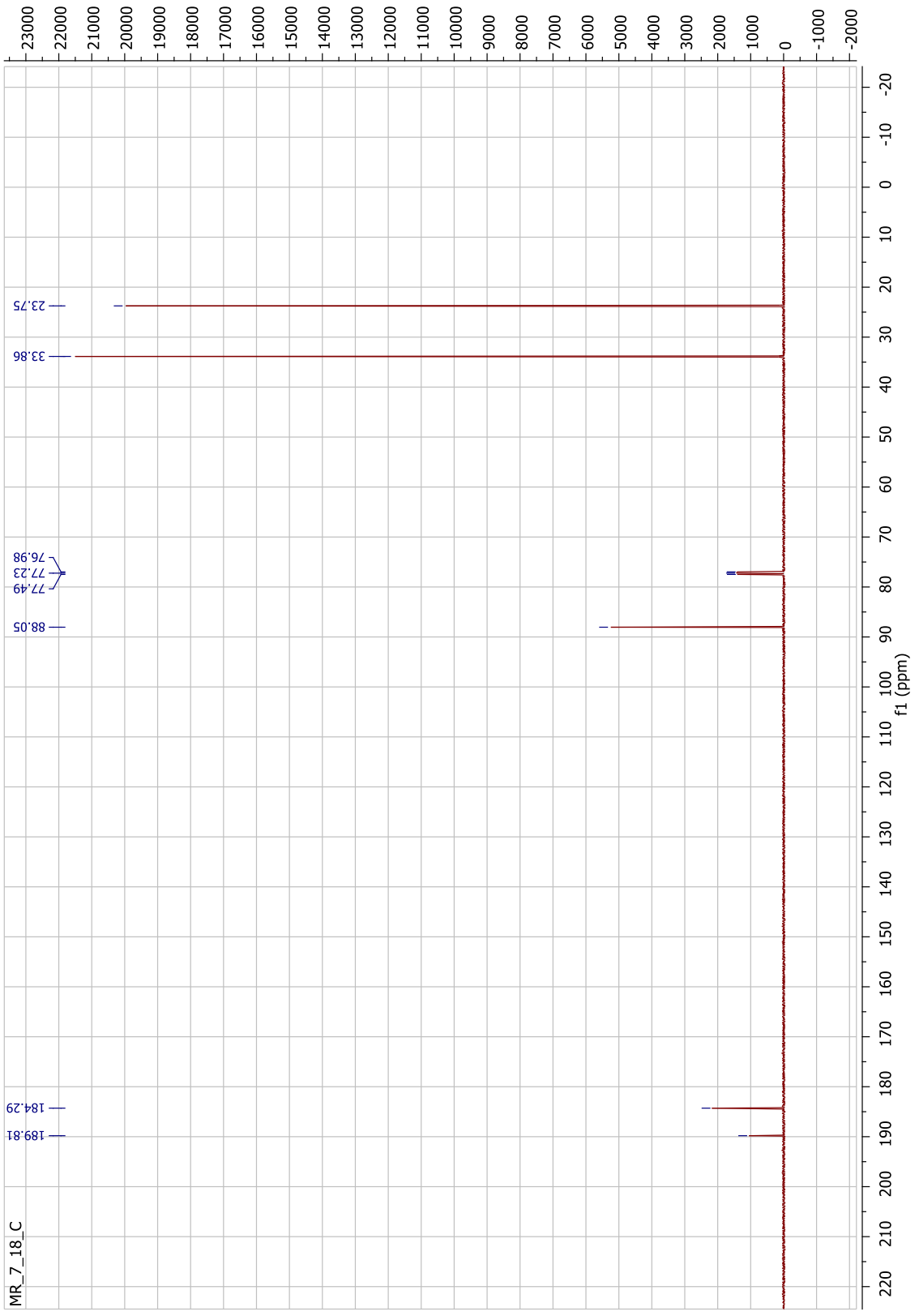

Figure 58. ^{13}C NMR spectrum of **62** (125 MHz, $CDCl_3$).

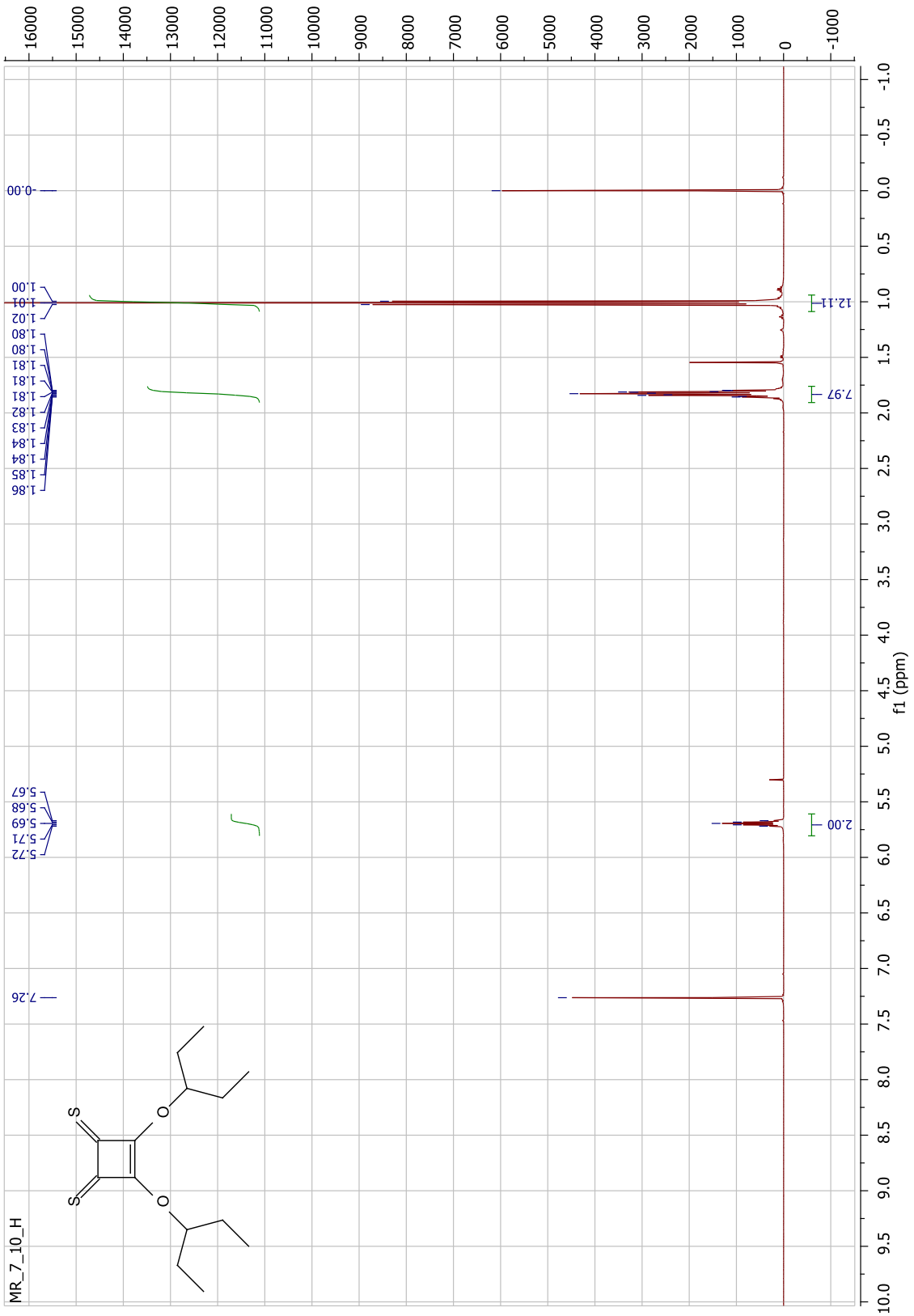

Figure 59. ^{1}H NMR spectrum of **61a** (500 MHz, $CDCl_3$).

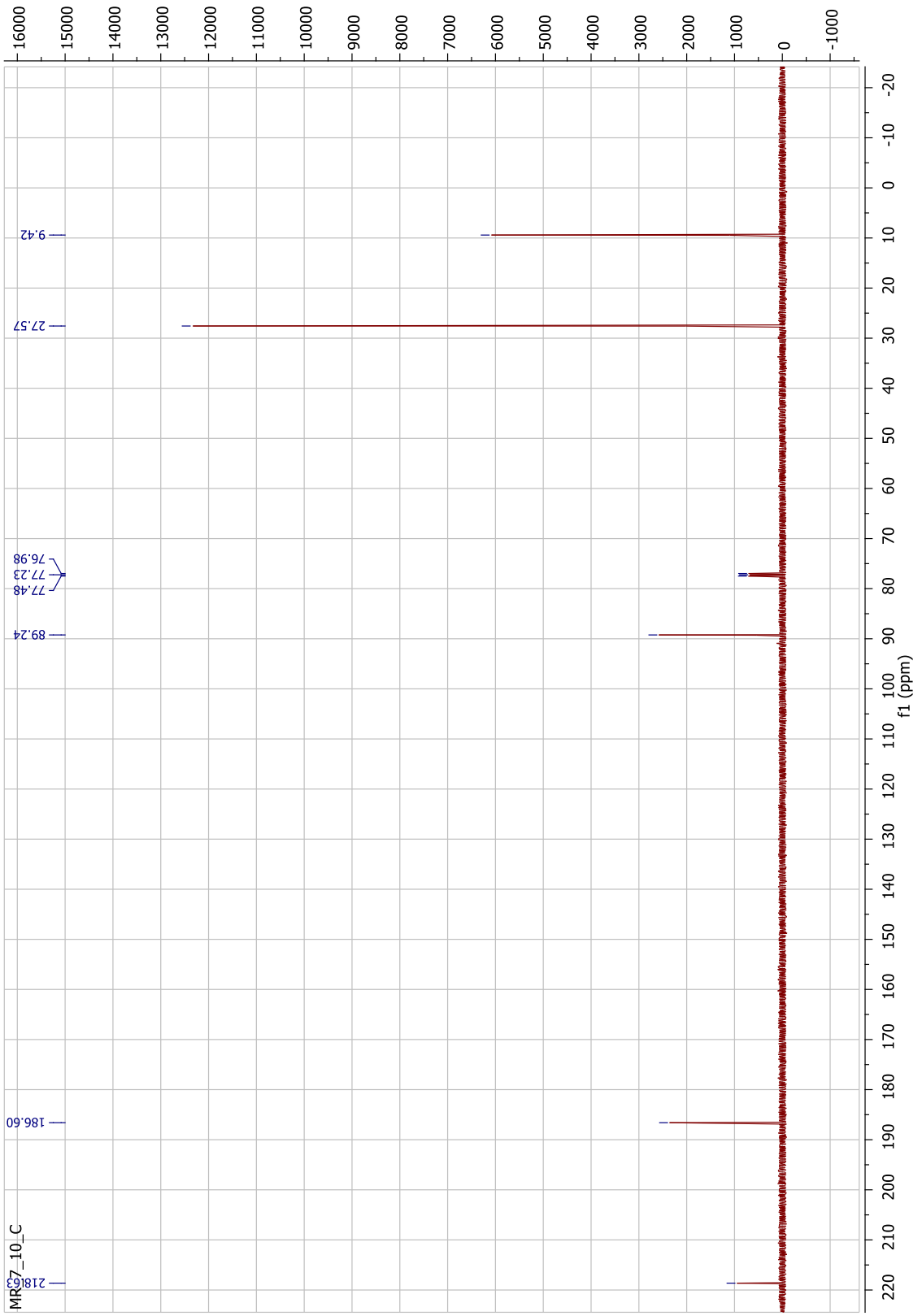

Figure 60. ^{13}C NMR spectrum of **61a** (125 MHz, $CDCl_3$).

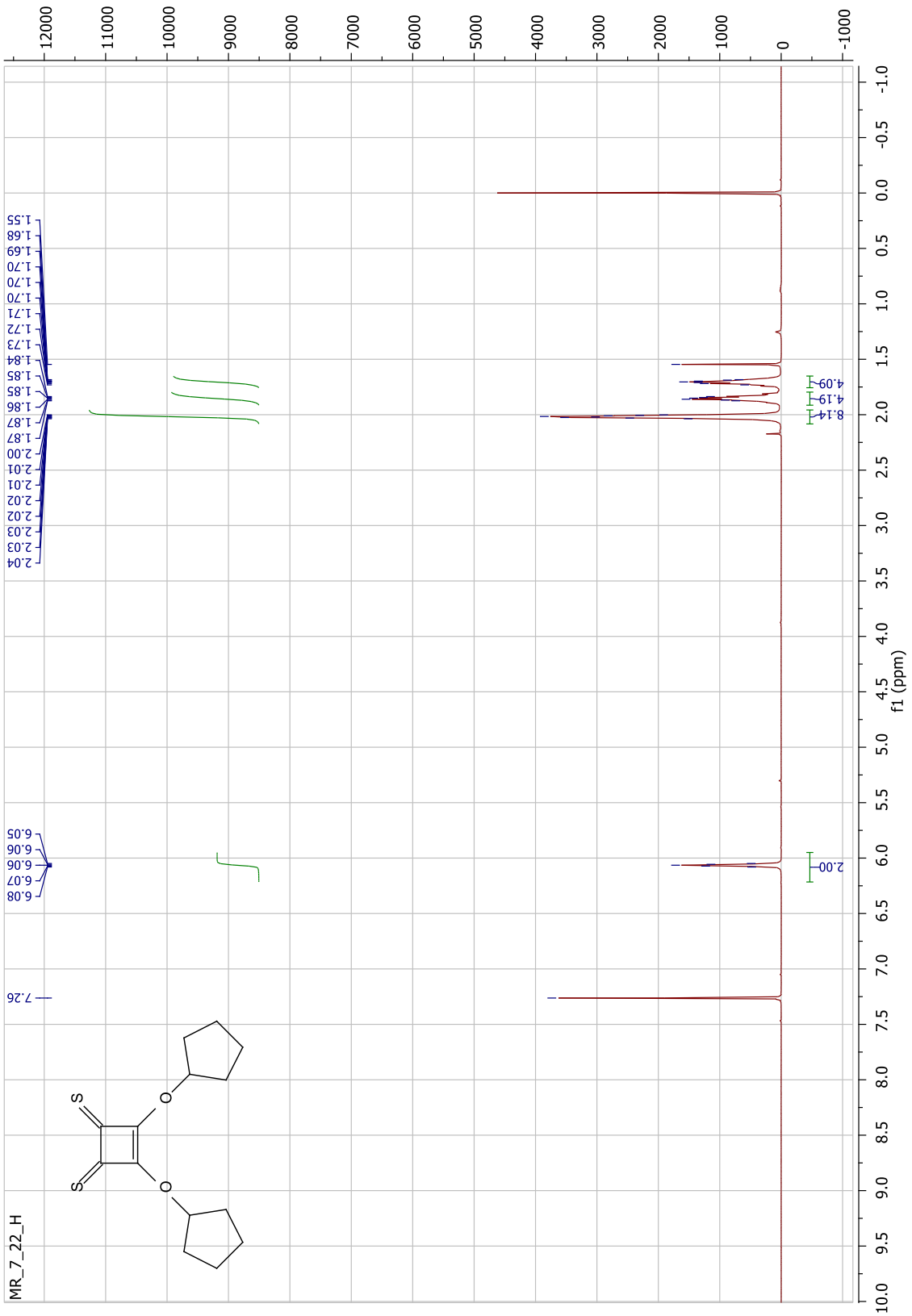

Figure 61. ^{1}H NMR spectrum of **60a** (500 MHz, $CDCl_3$).

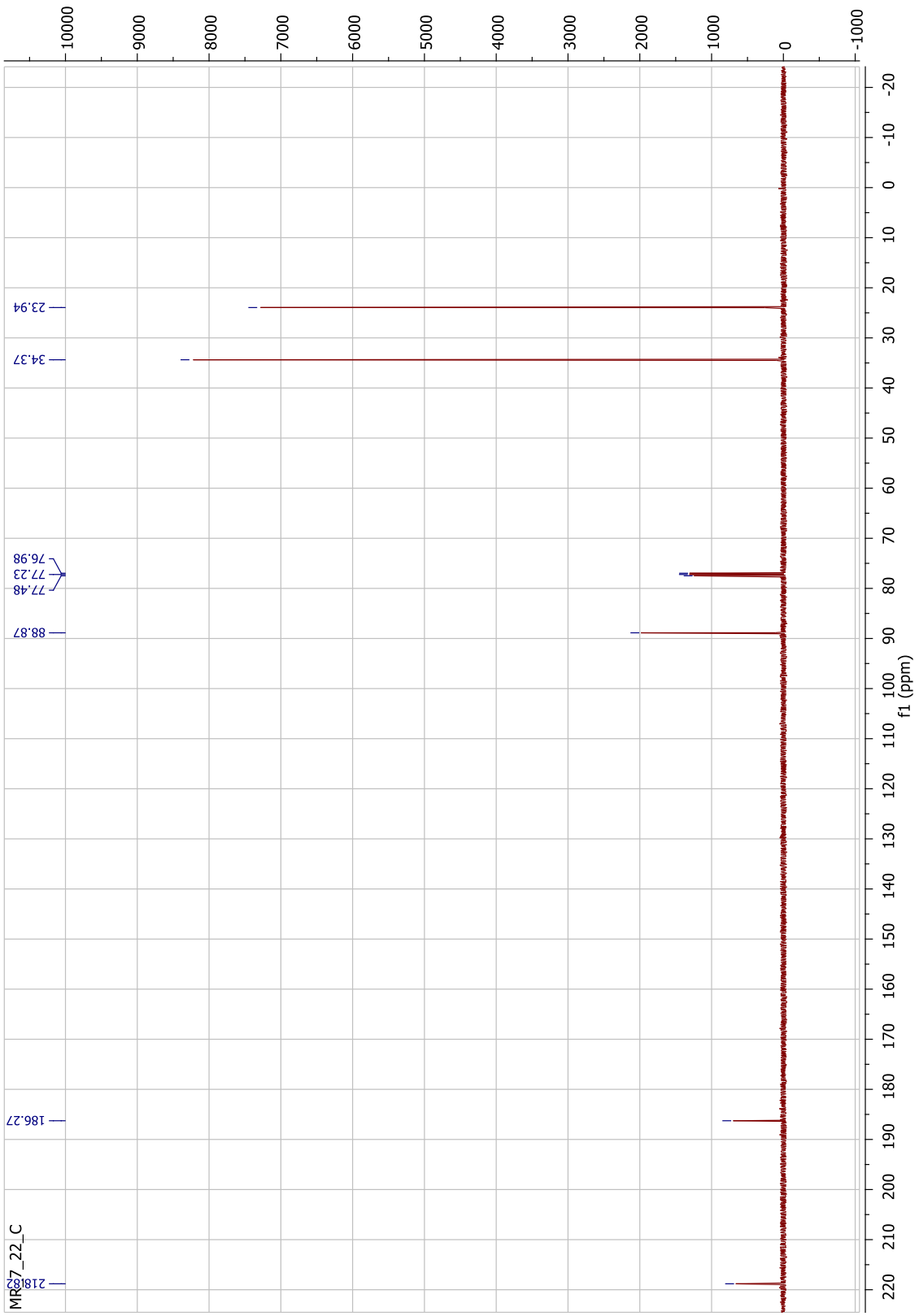

Figure 62. ^{13}C NMR spectrum of **60a** (125 MHz, $CDCl_3$).

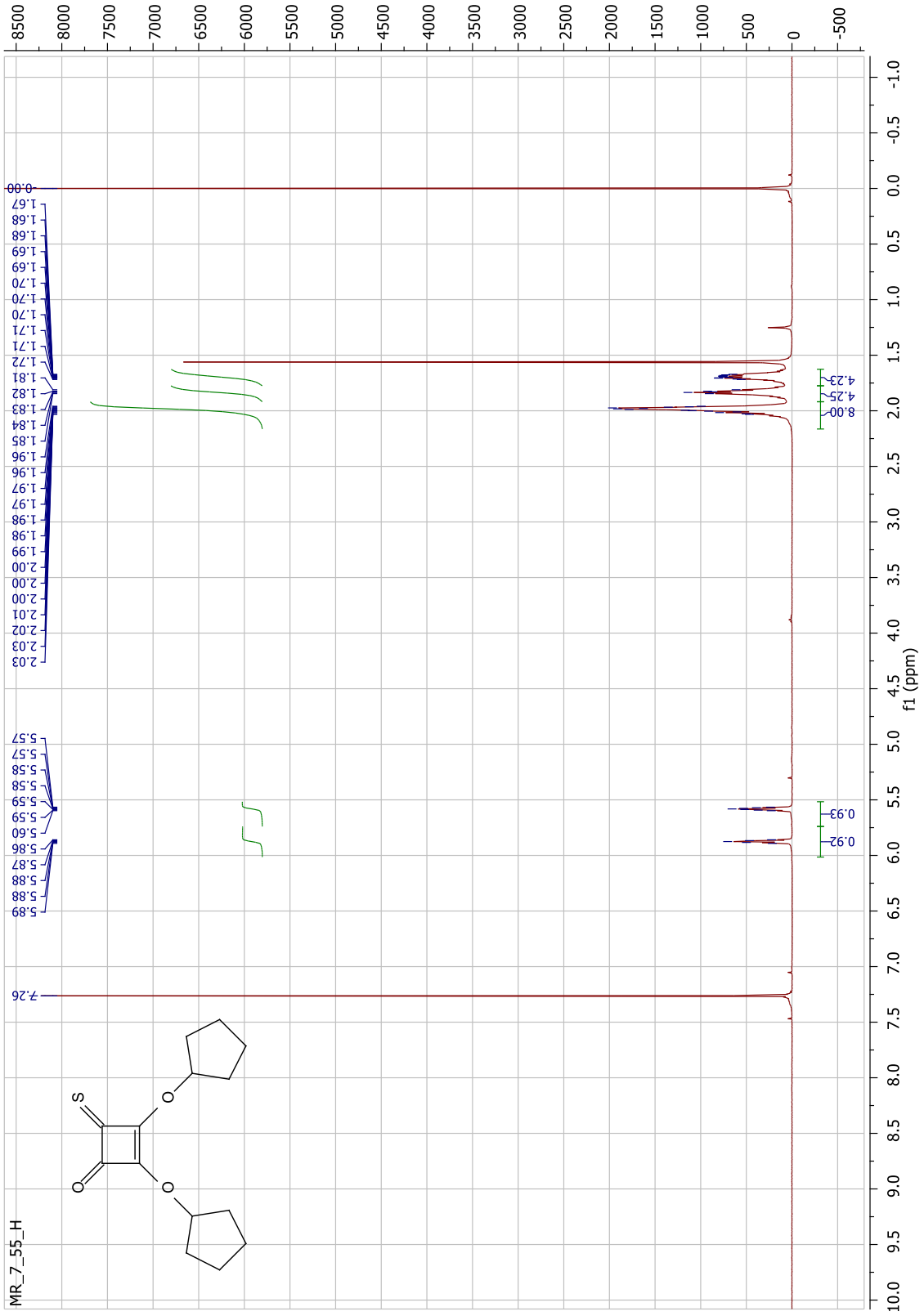

Figure 63. ^{1}H NMR spectrum of **60b** (500 MHz, $CDCl_3$).

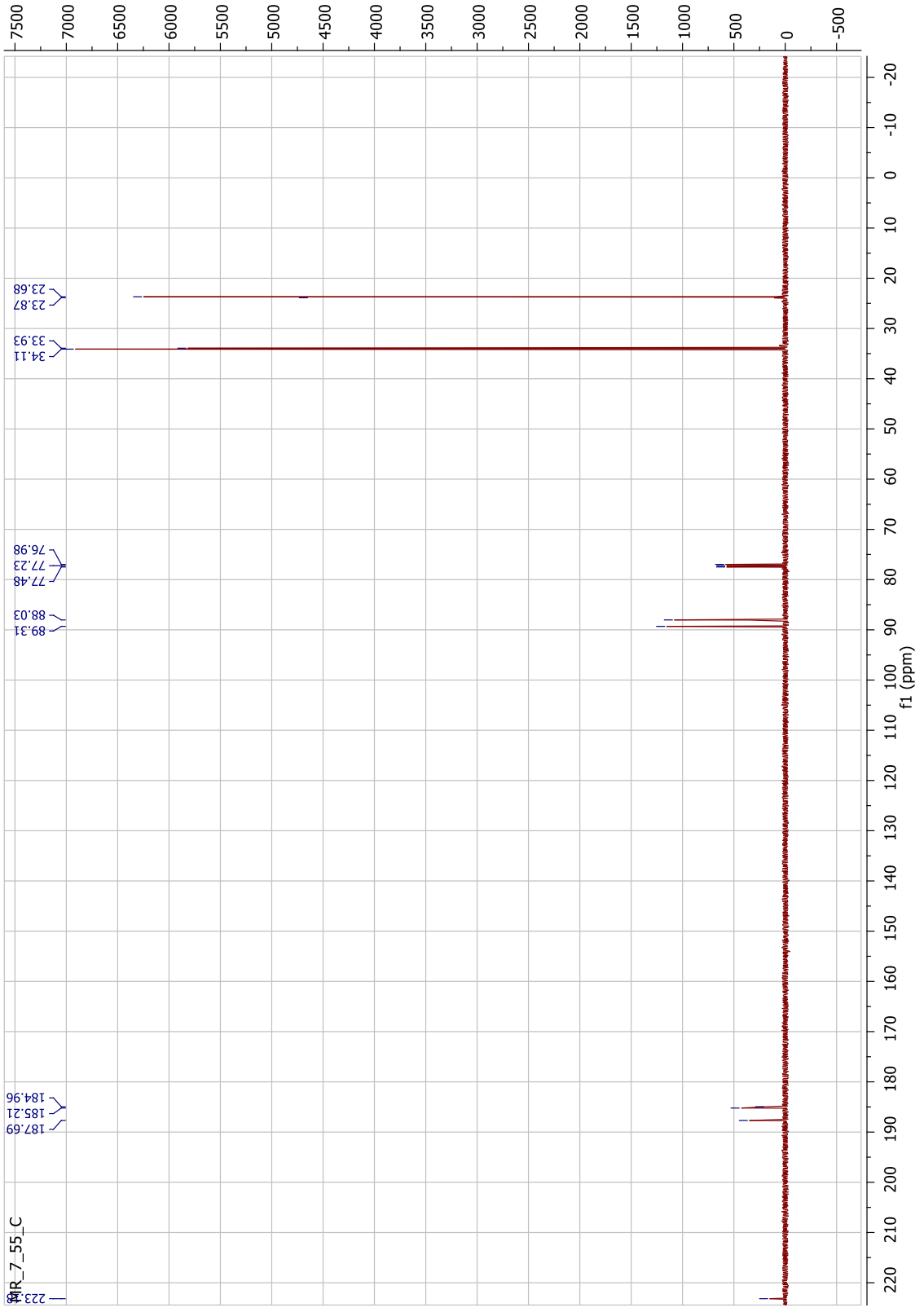

Figure 64. ^{13}C NMR spectrum of **60b** (125 MHz, $CDCl_3$).

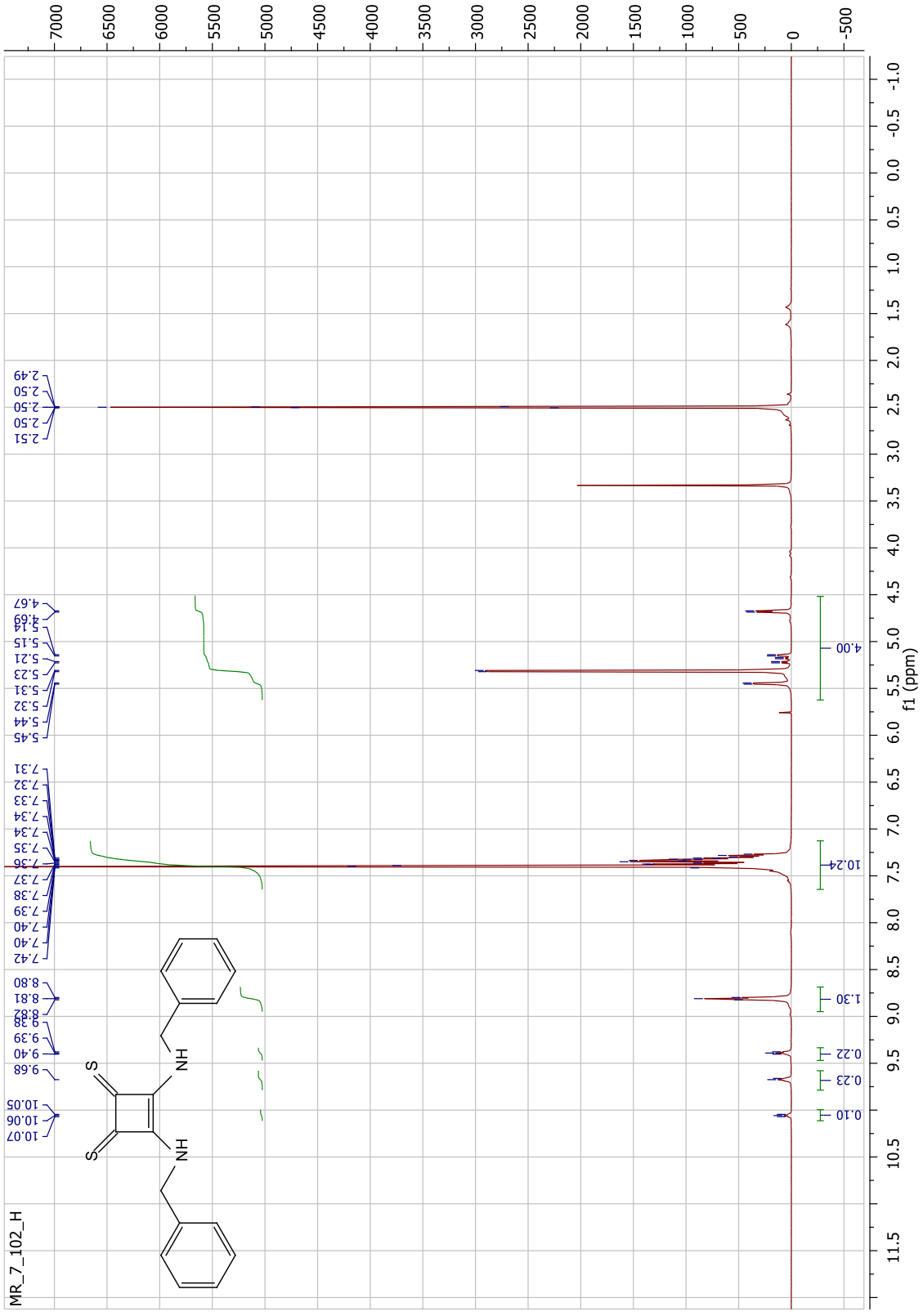

Figure 65. ^{1}H NMR spectrum of **63** (500 MHz, DMSO-d_6).

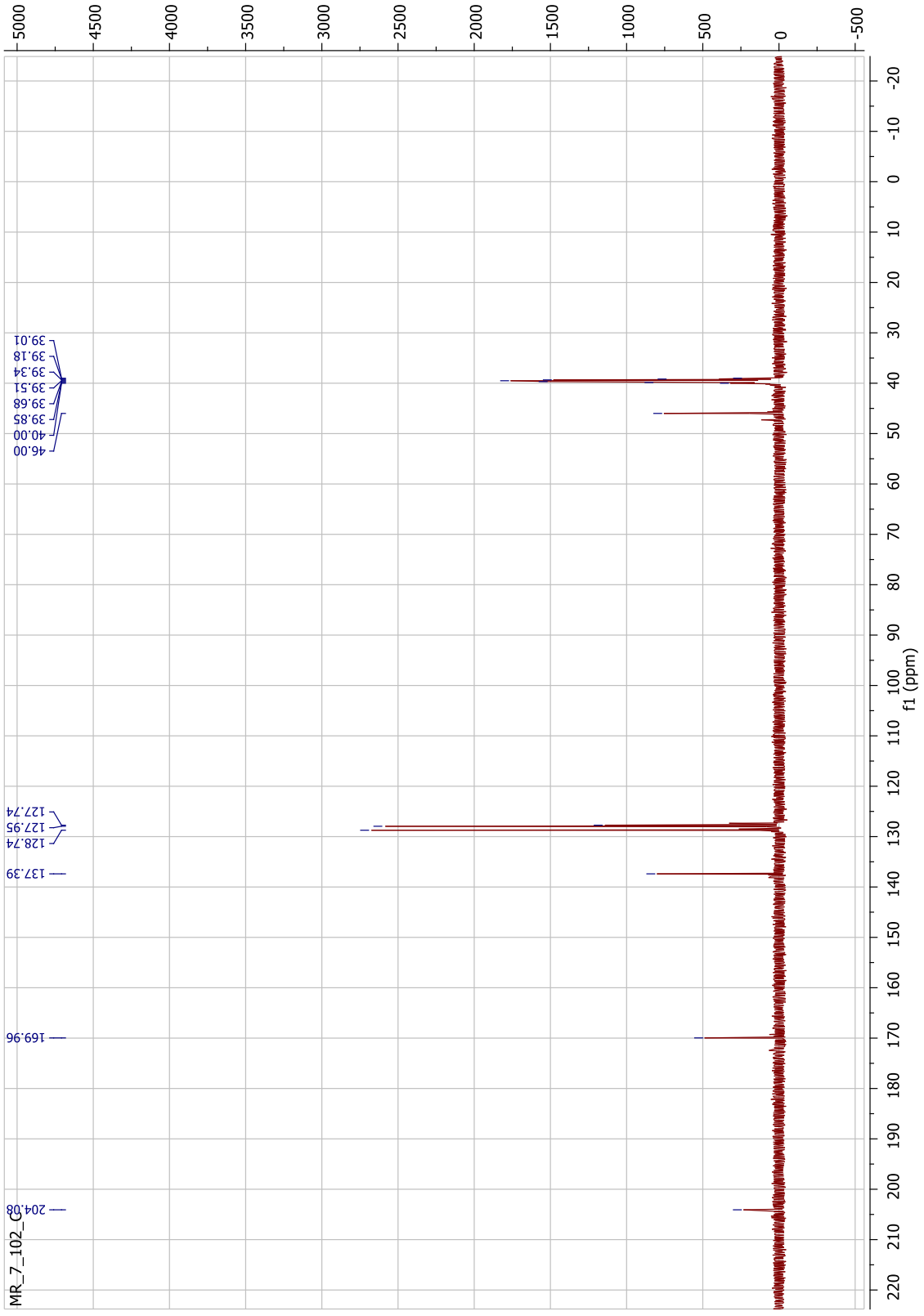

Figure 66. ^{13}C NMR spectrum of **63** (125 MHz, DMSO-d_6).

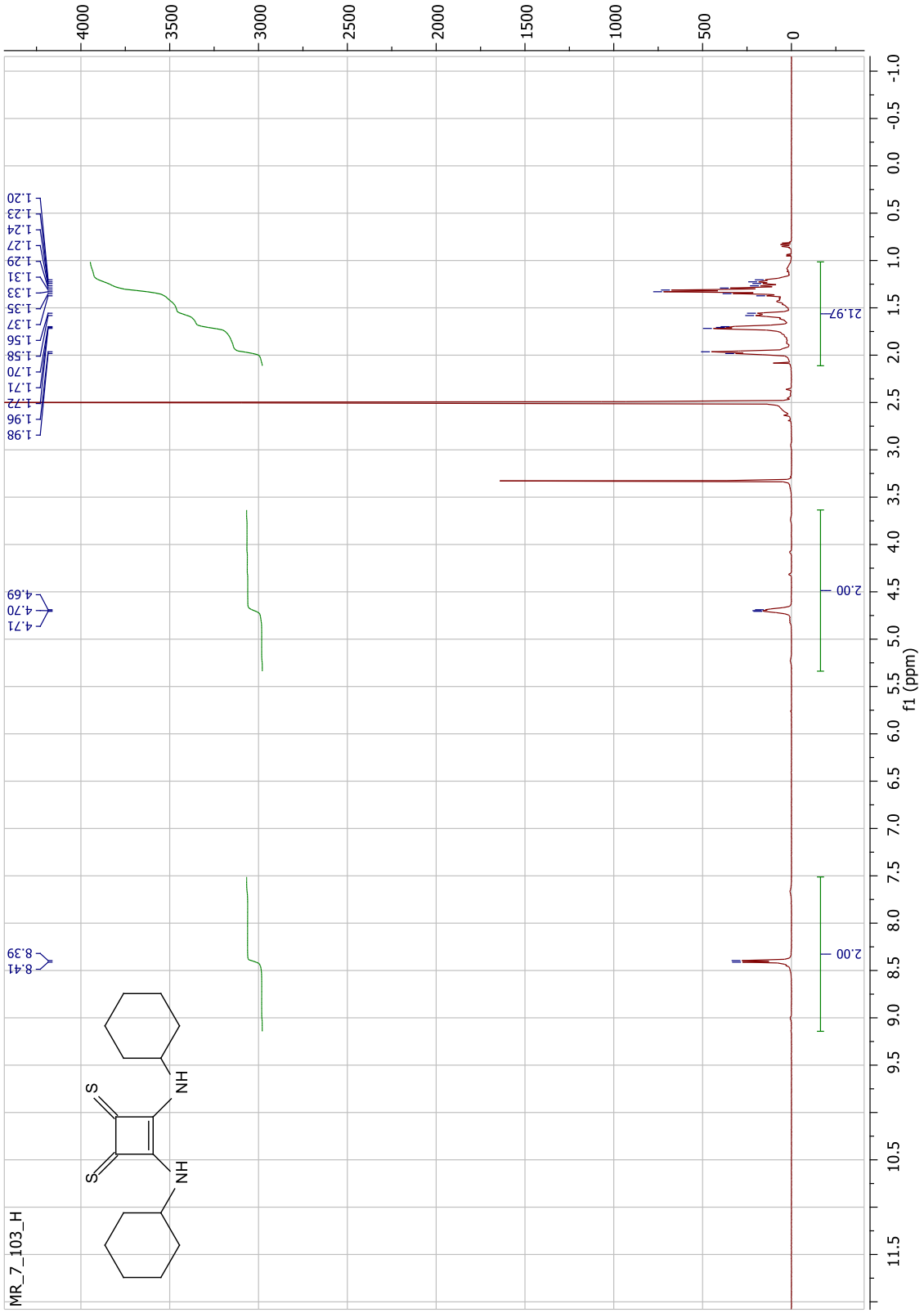

Figure 67. ^{1}H NMR spectrum of **64** (500 MHz, DMSO-d_6).

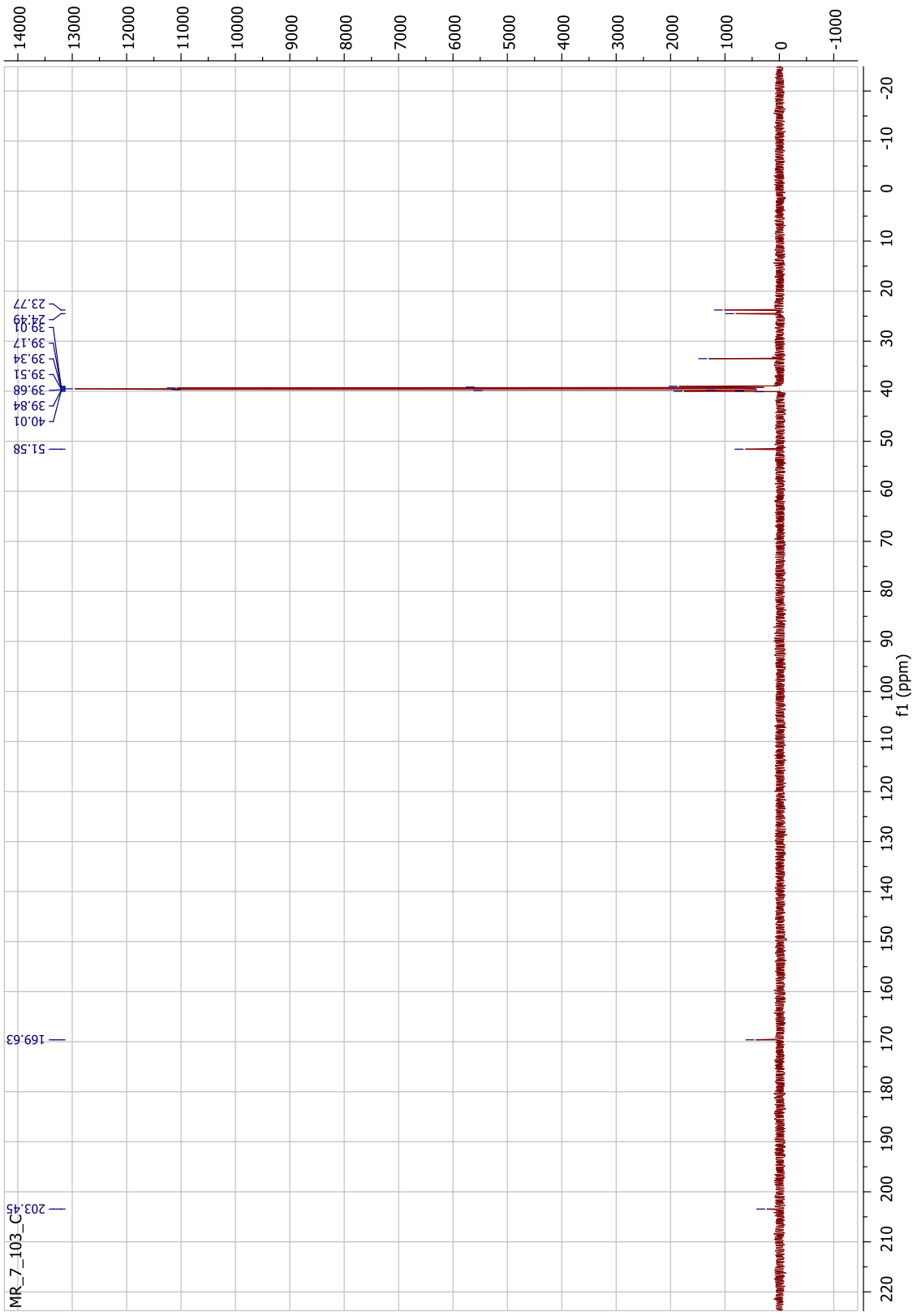

Figure 68. ^{13}C NMR spectrum of **64** (125 MHz, DMSO-d_6).

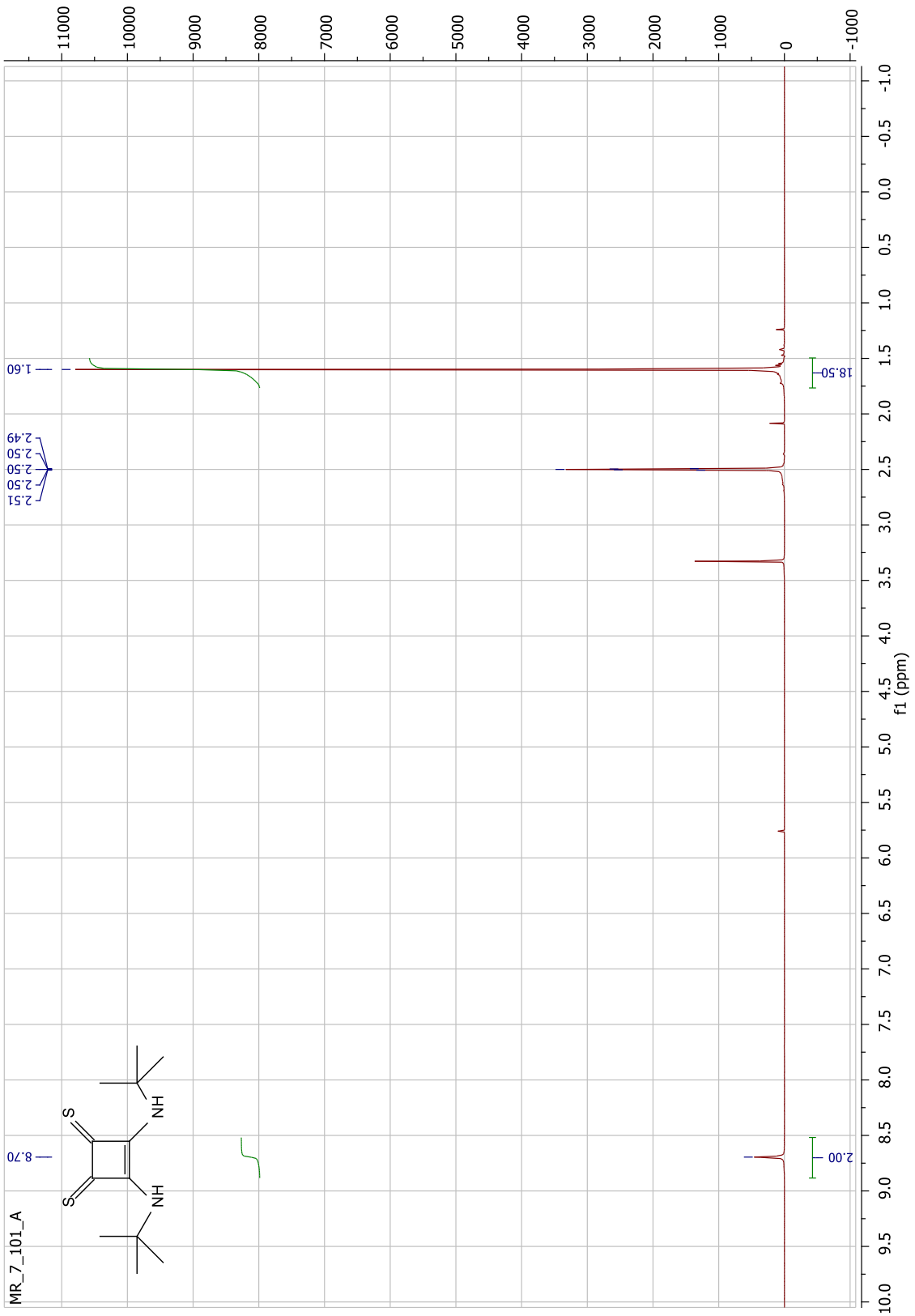

Figure 69. ^{1}H NMR spectrum of **65** (500 MHz, DMSO-d_6).

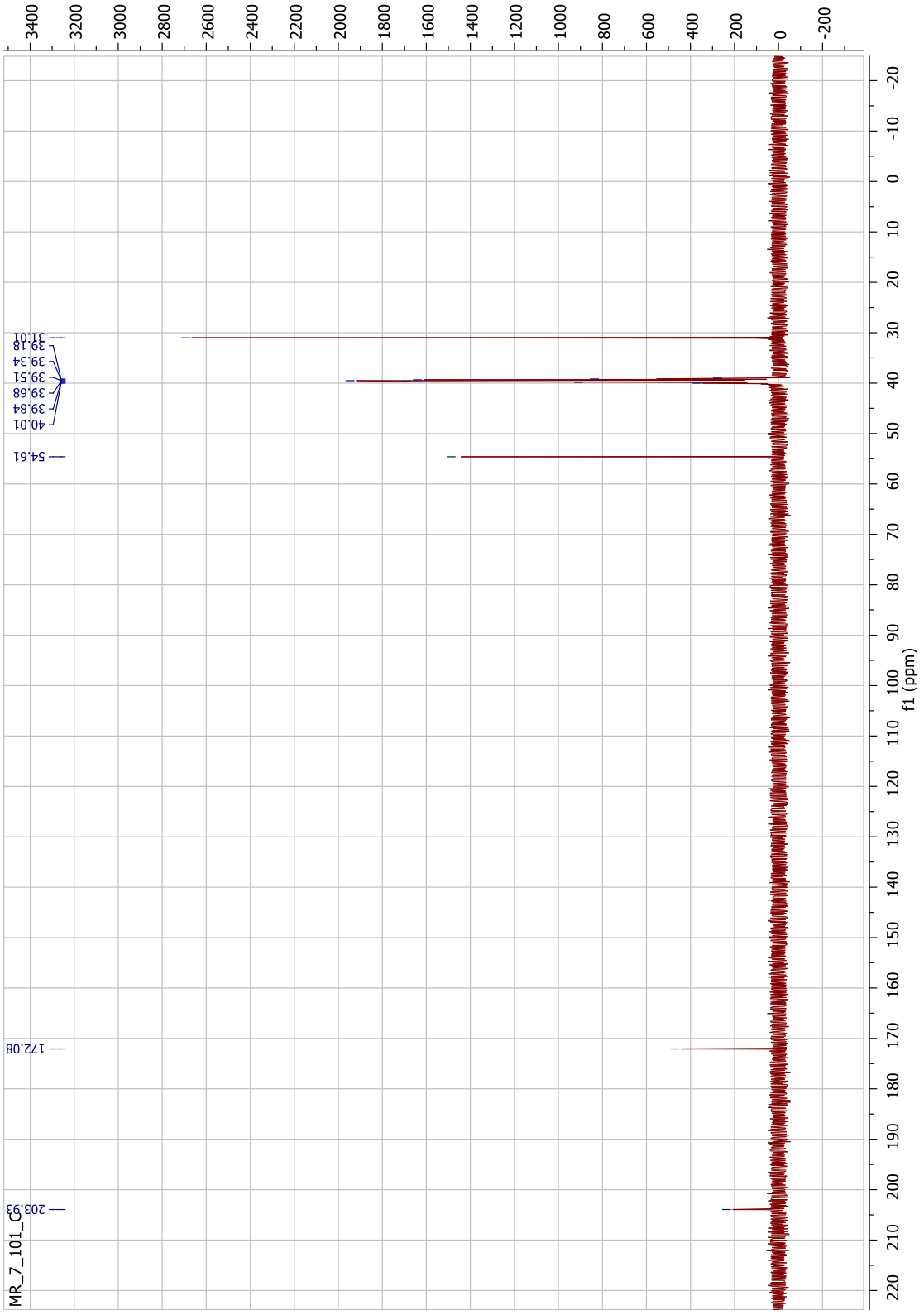

Figure 70. ^{13}C NMR spectrum of **65** (125 MHz, DMSO-d_6).

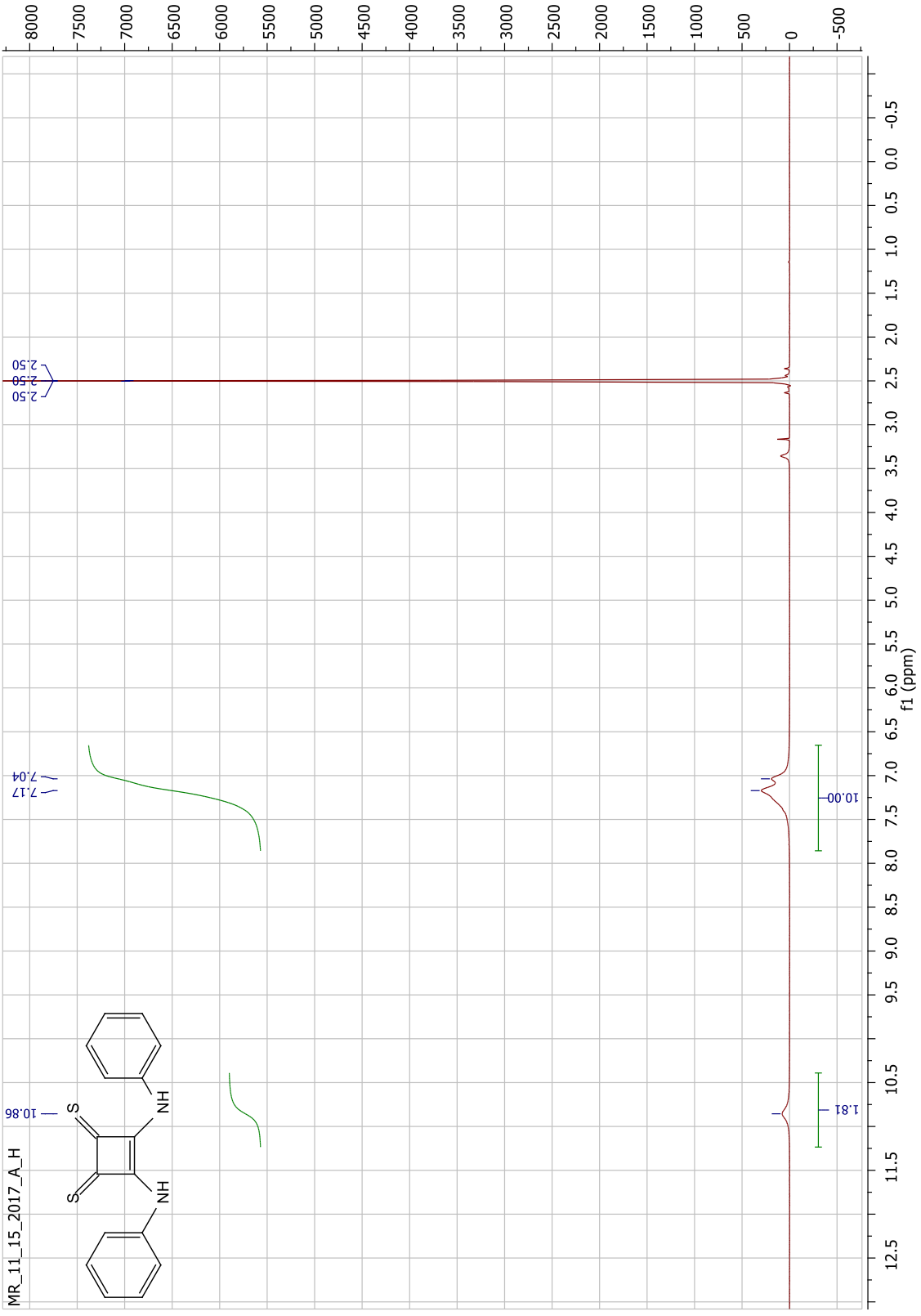

Figure 71. ^{1}H NMR spectrum of **66** (500 MHz, DMSO-d_6).

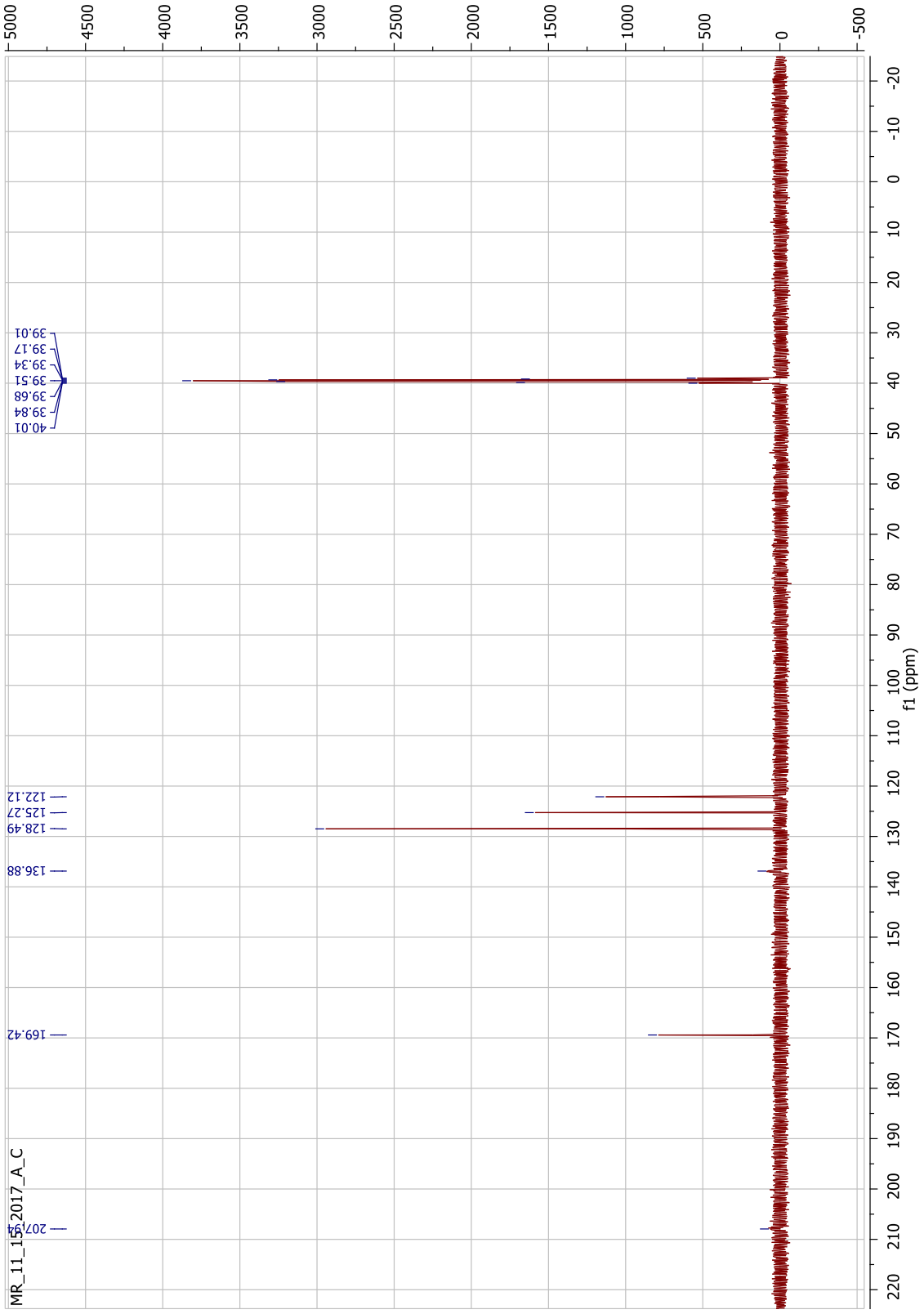

Figure 72. ^{13}C NMR spectrum of **66** (125 MHz, DMSO-d_6).

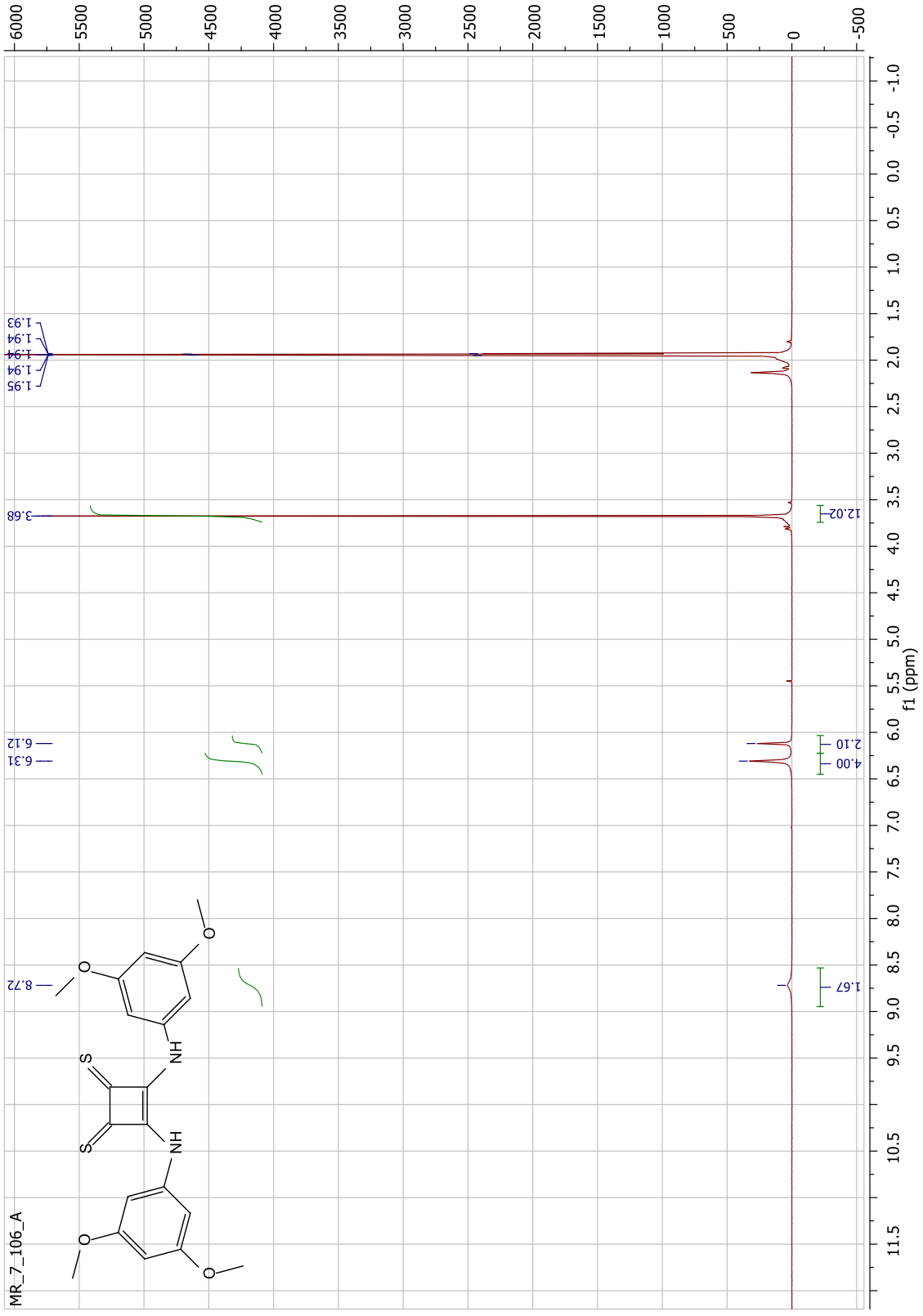

Figure 73. ^{1}H NMR spectrum of **67** (500 MHz, CD_3CN).

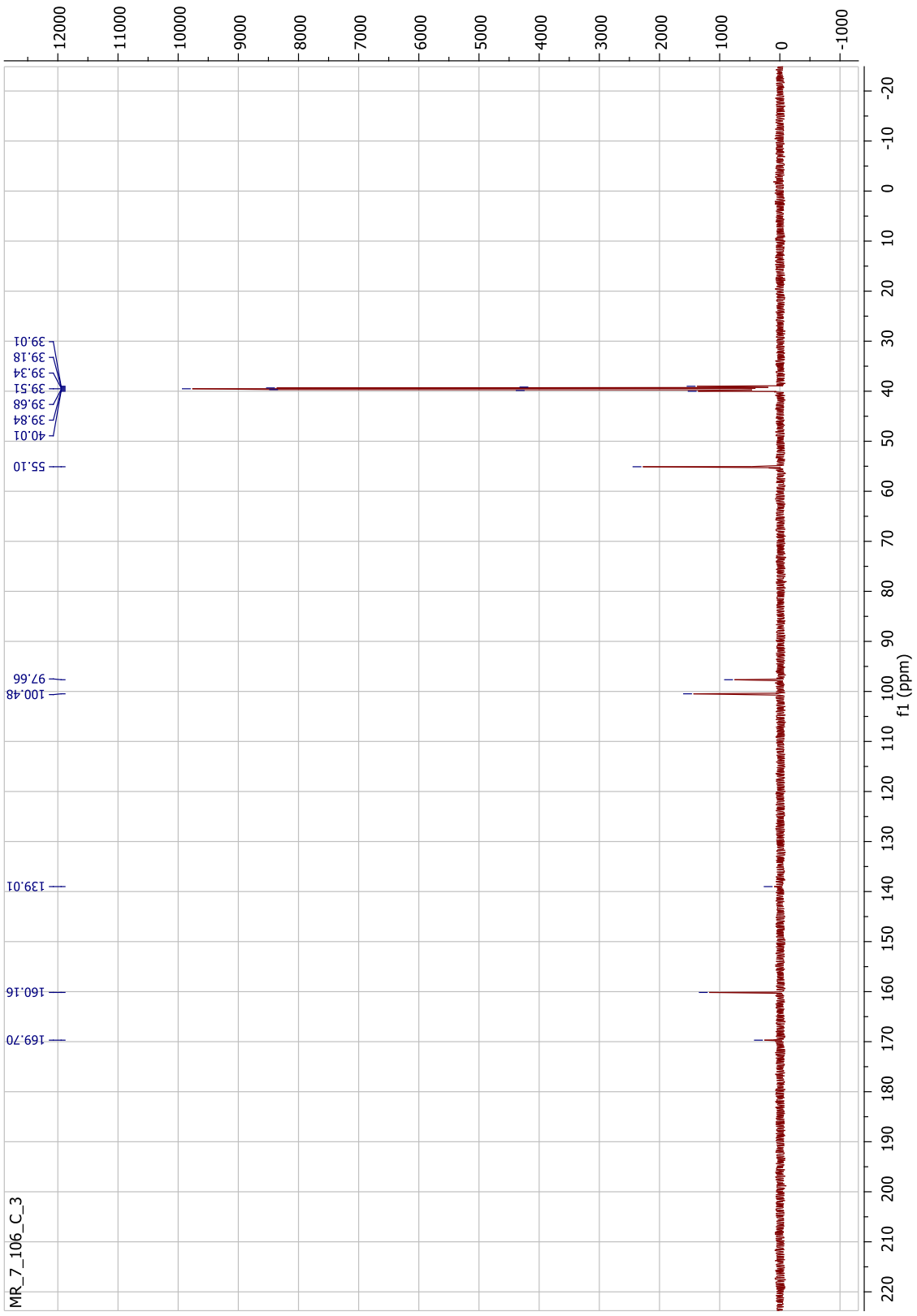

Figure 74. ^{13}C NMR spectrum of **67** (125 MHz, CD_3CN).

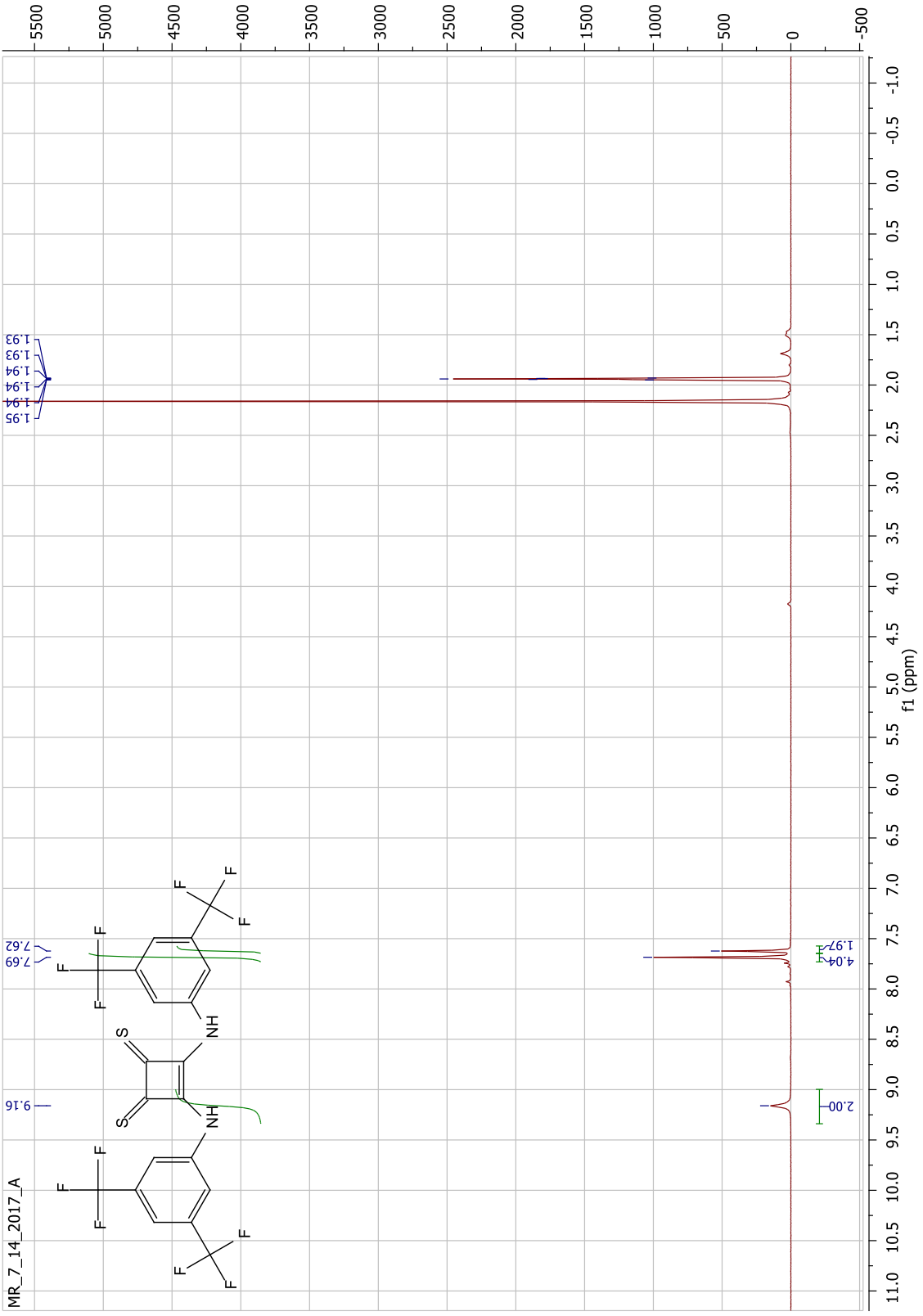

Figure 75. ^{1}H NMR spectrum of **68** (500 MHz, CD_3CN).

Figure 76. ^{13}C NMR spectrum of **68** (125 MHz, CD_3CN).

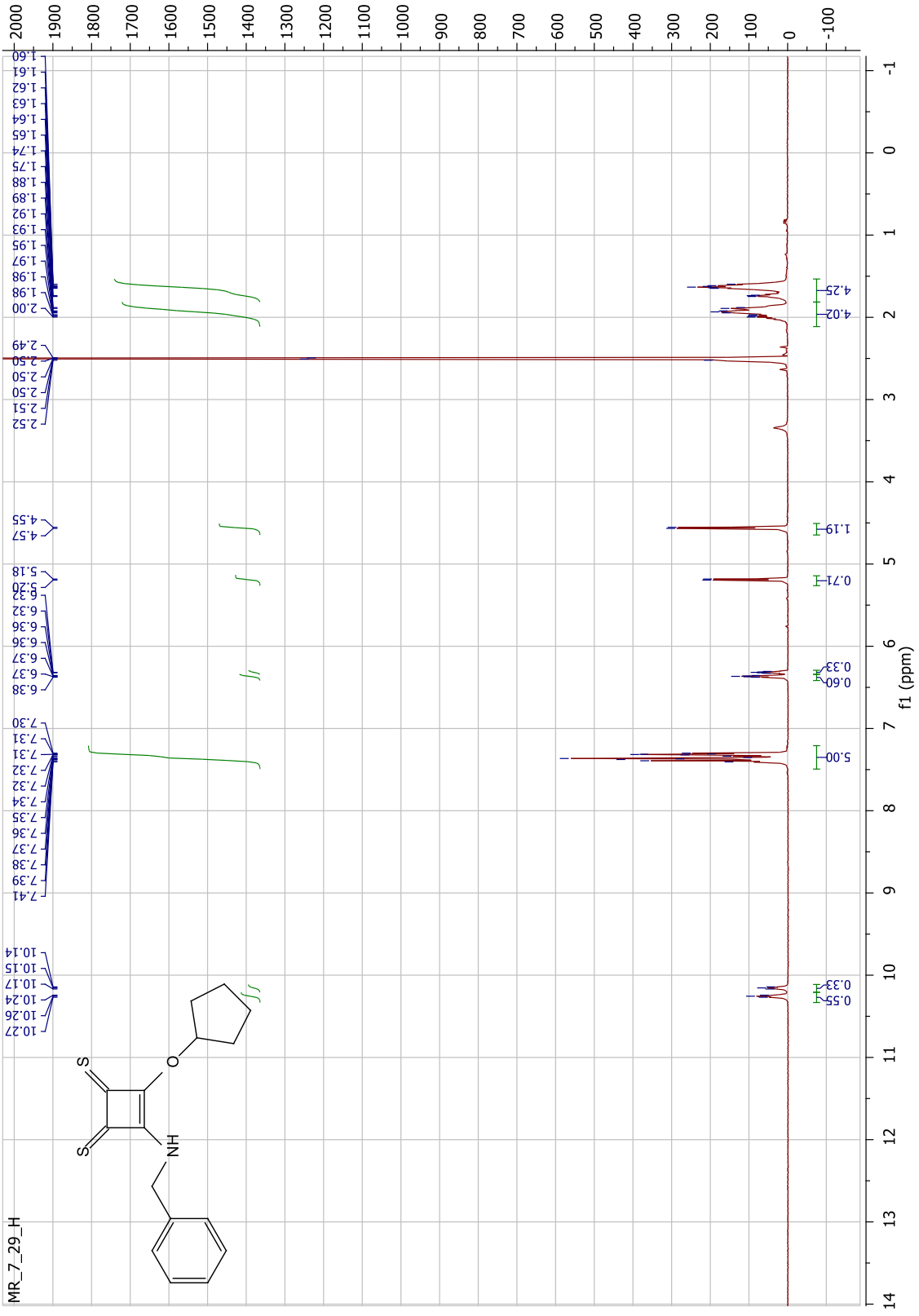

Figure 77. ^{1}H NMR spectrum of **72** (500 MHz, DMSO-d_6).

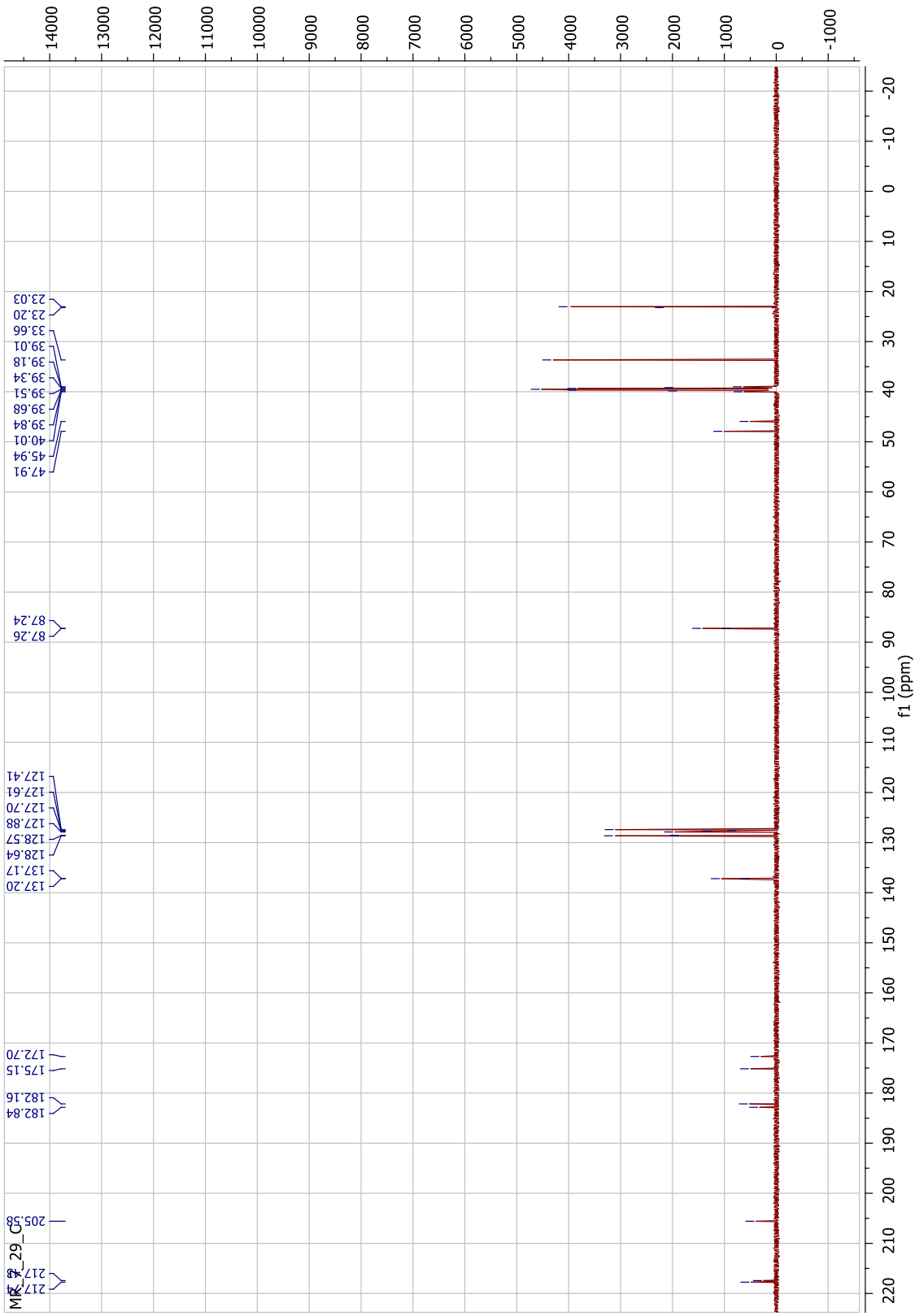

Figure 78. ^{13}C NMR spectrum of **72** (125 MHz, DMSO-d_6).

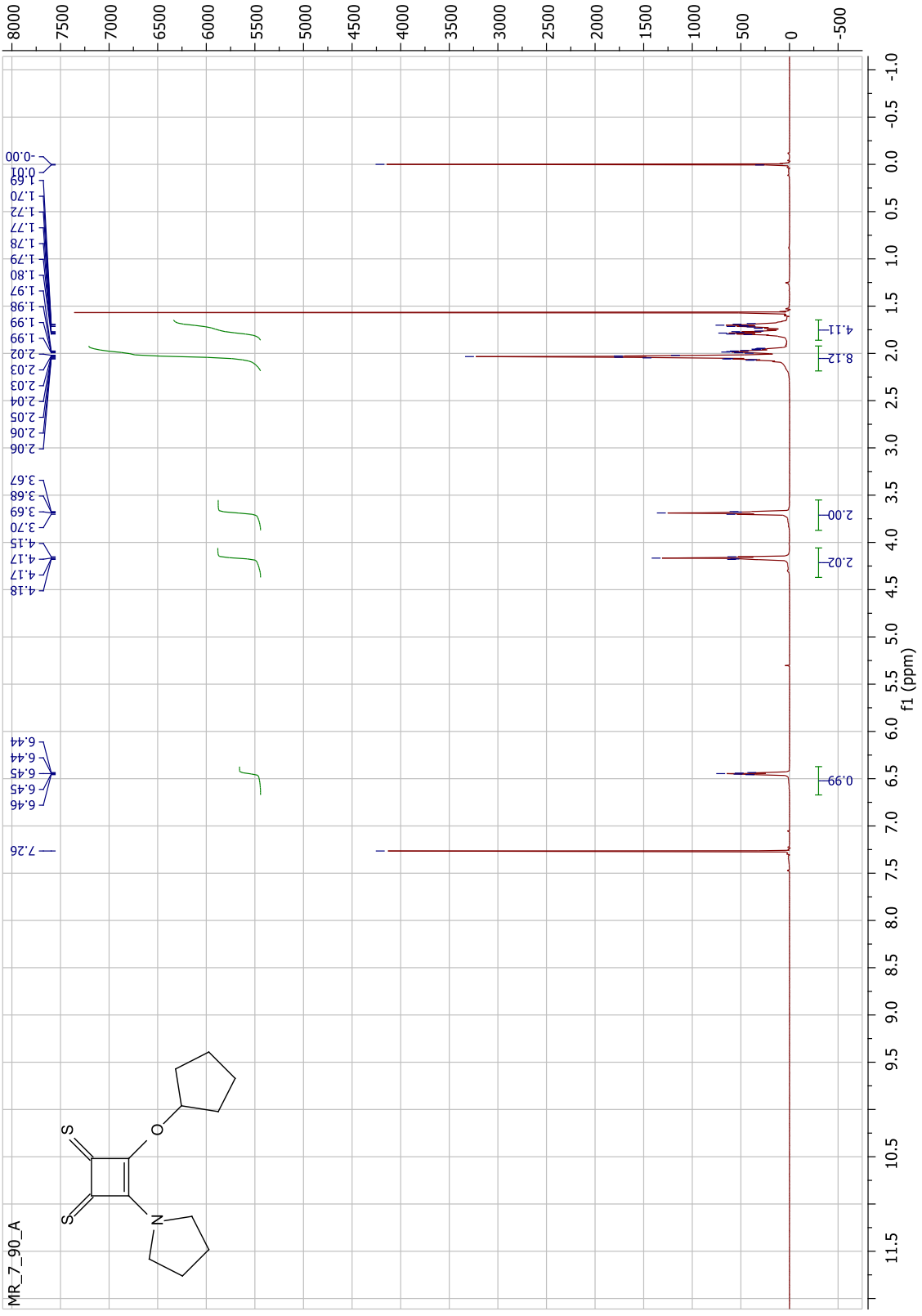

Figure 79. ^{1}H NMR spectrum of **73** (500 MHz, $CDCl_3$).

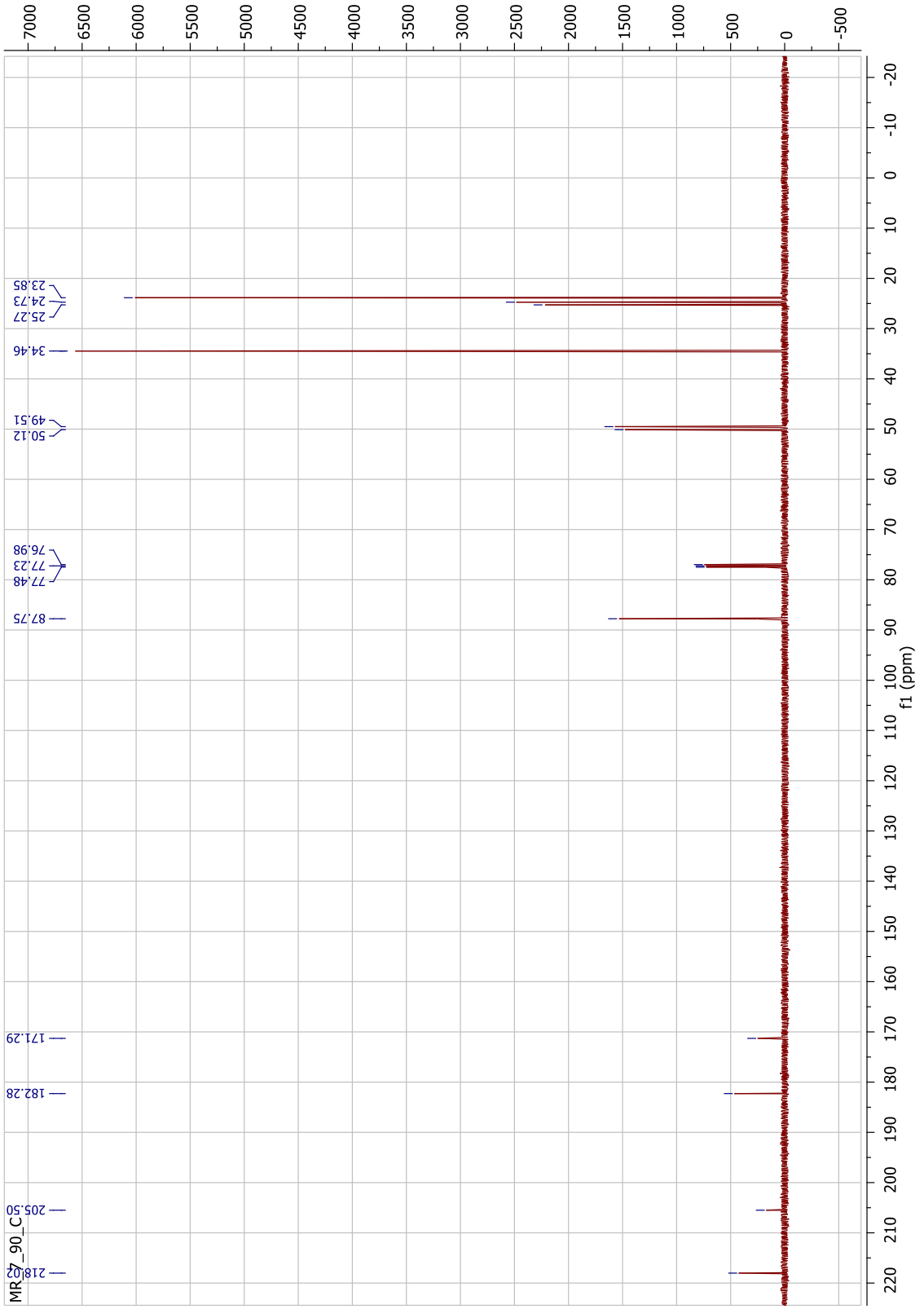

Figure 80. ^{13}C NMR spectrum of **73** (125 MHz, $CDCl_3$).

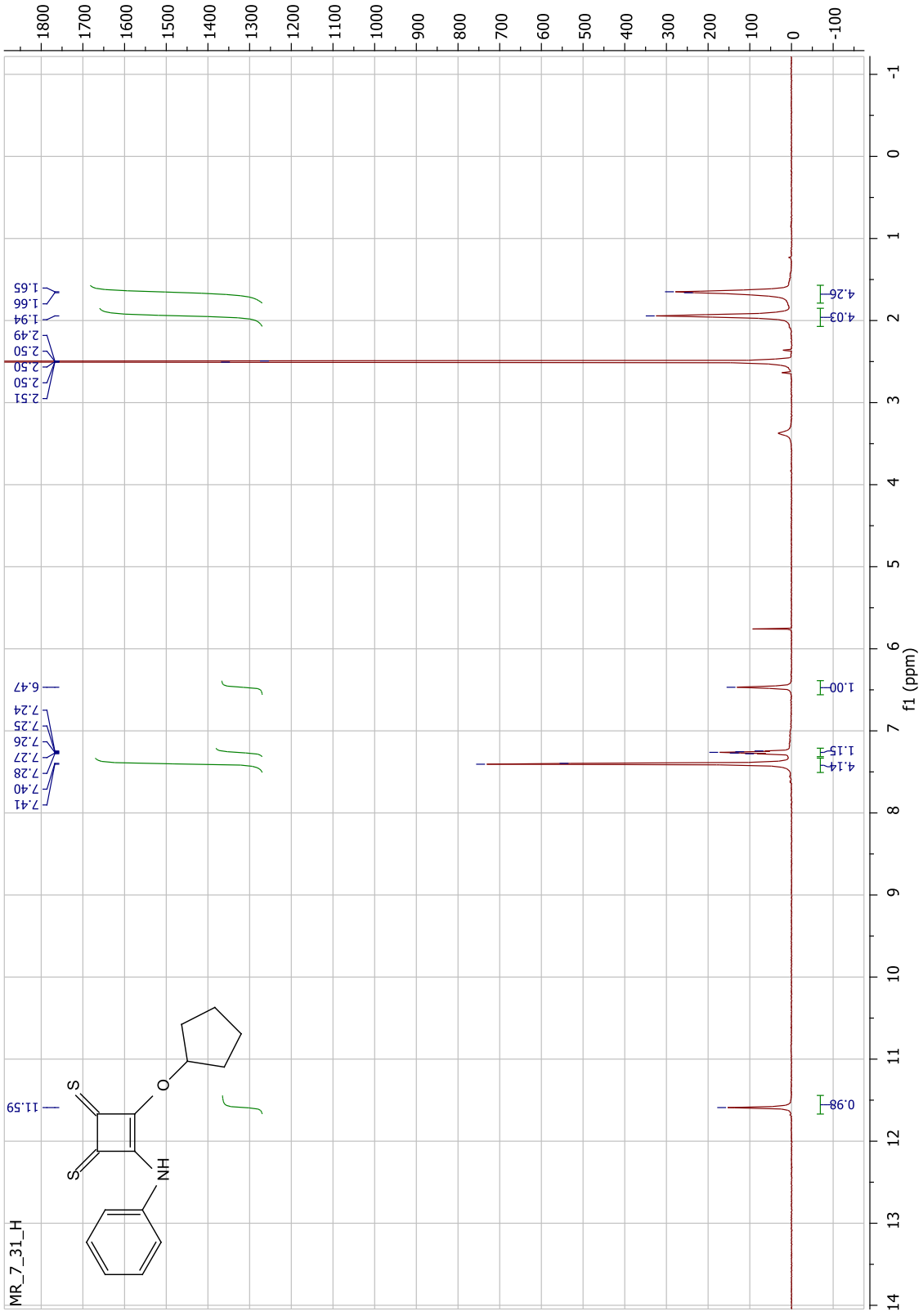

Figure 81. ^{1}H NMR spectrum of **74** (500 MHz, DMSO-d_6).

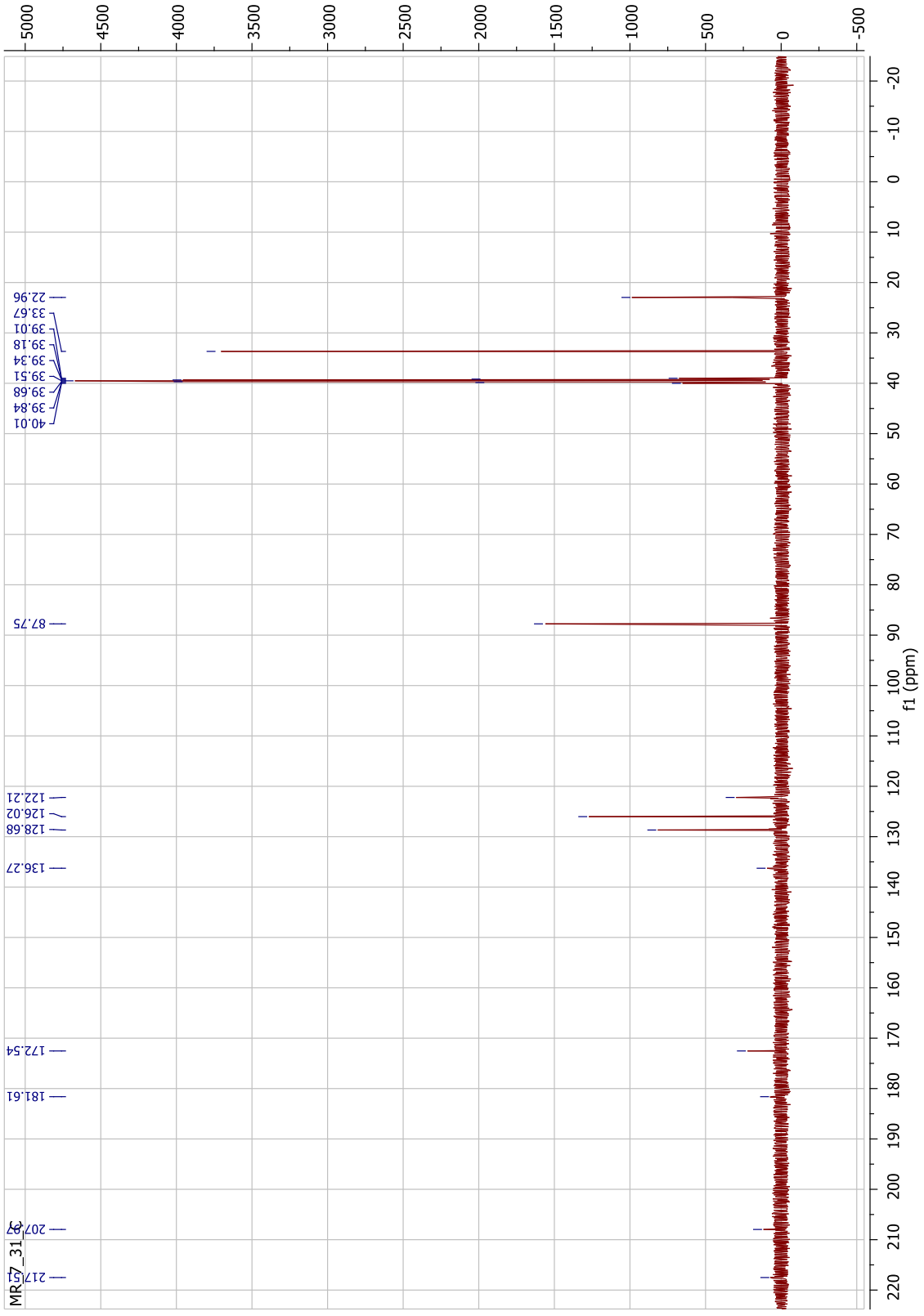

Figure 82. ^{13}C NMR spectrum of **74** (125 MHz, DMSO-d_6).

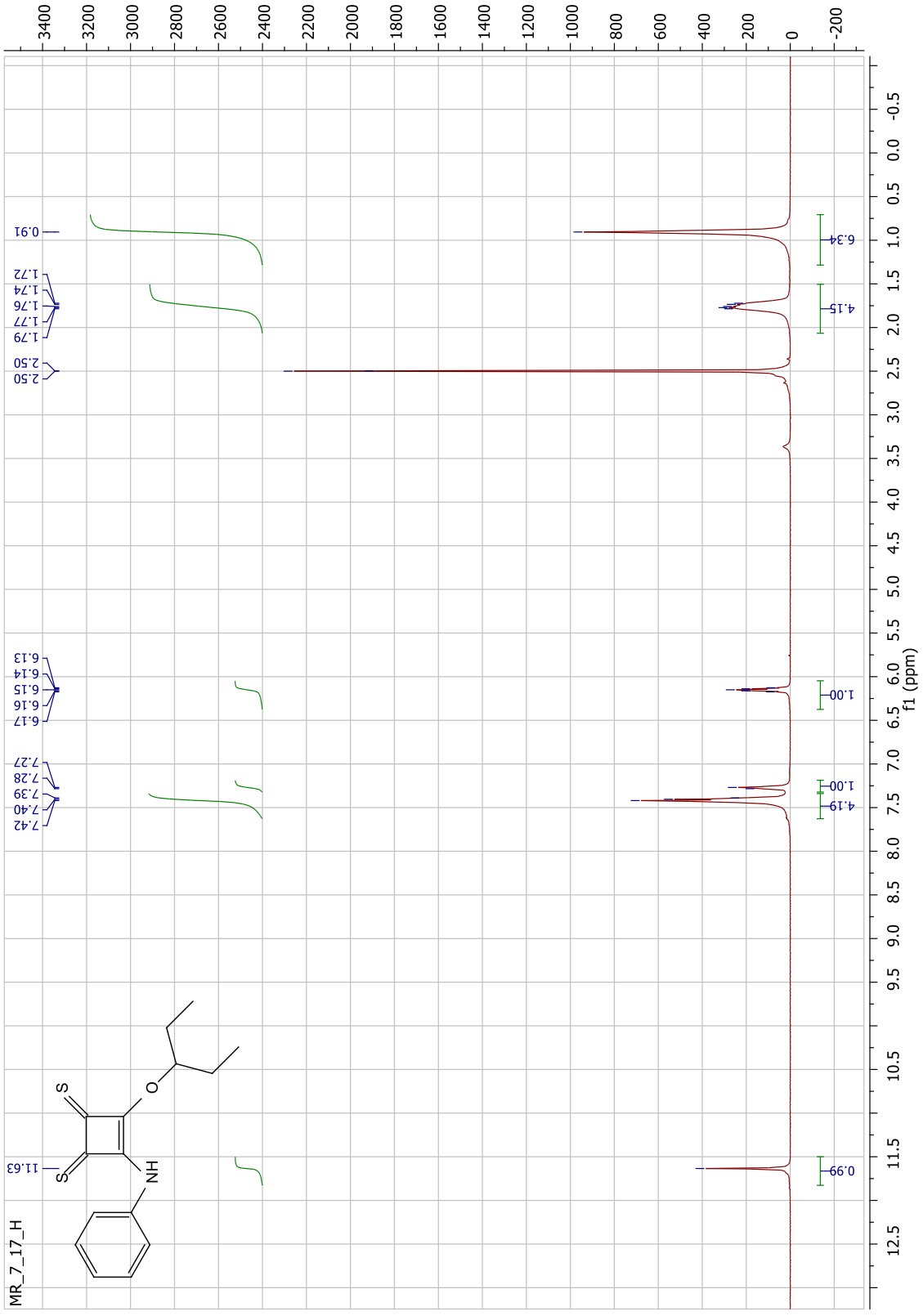

Figure 83. ^{1}H NMR spectrum of **75** (500 MHz, DMSO-d_6).

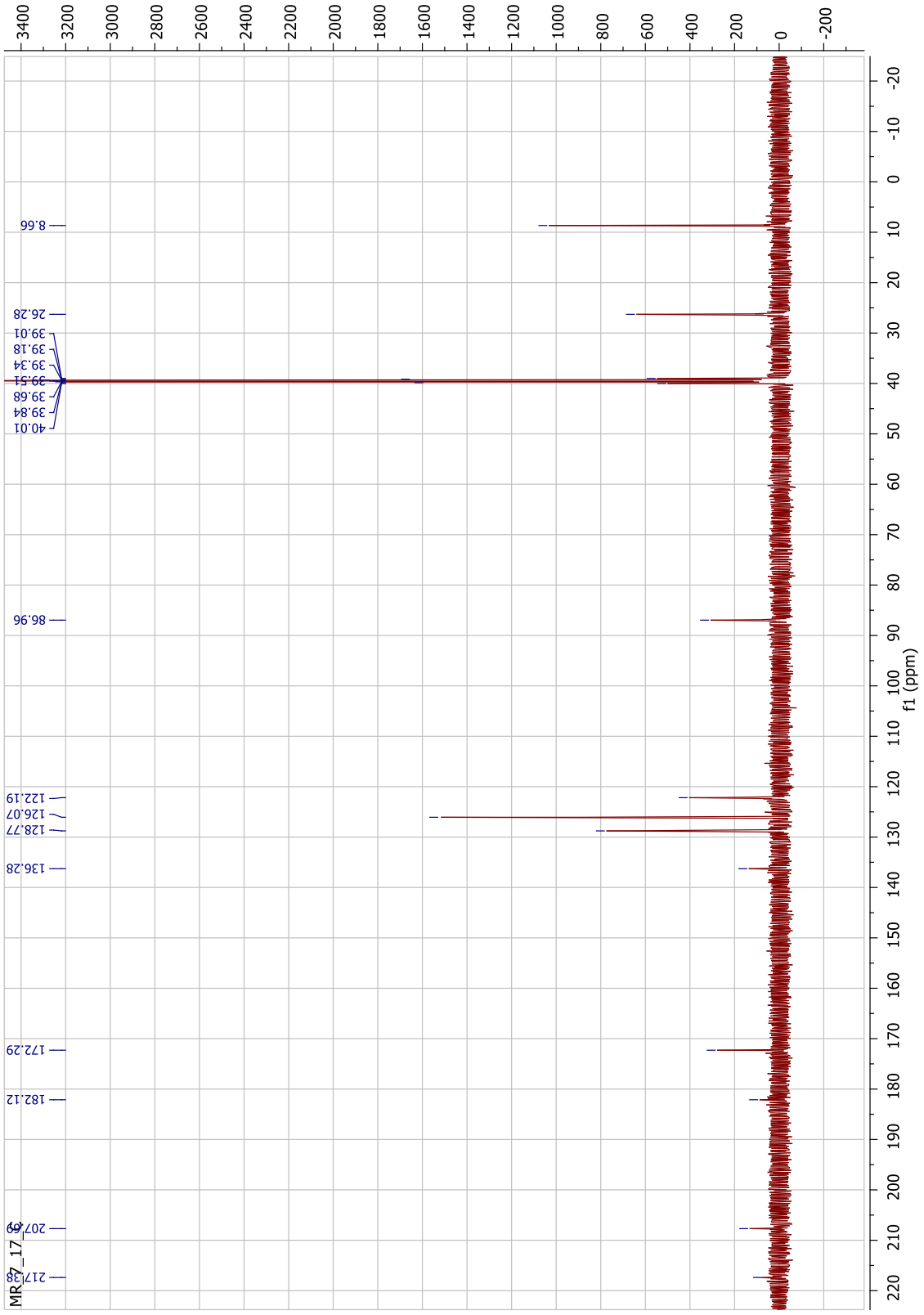

Figure 84. ^{13}C NMR spectrum of **75** (125 MHz, DMSO-d_6).

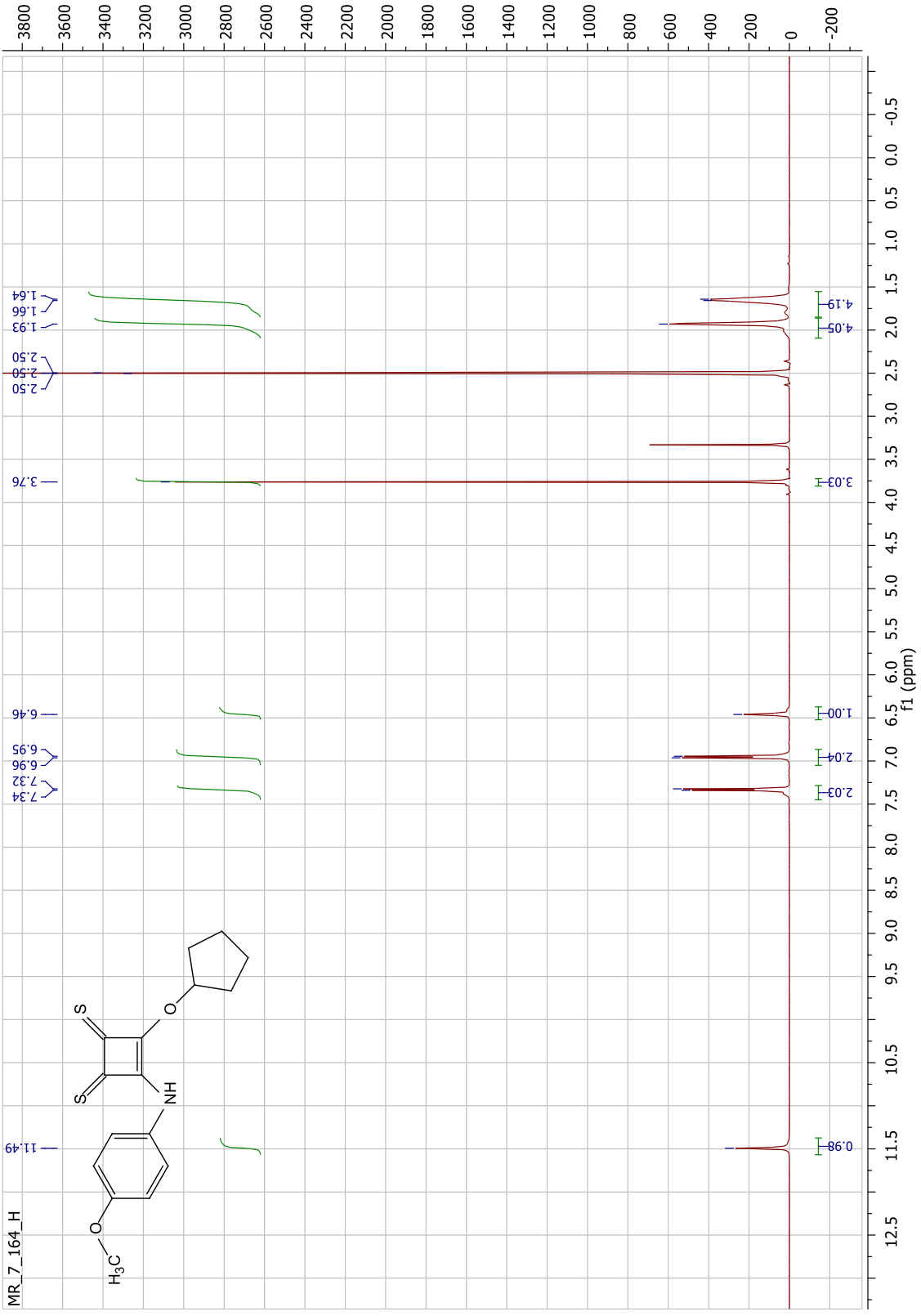

Figure 85. ^{1}H NMR spectrum of **76** (500 MHz, DMSO-d_6).

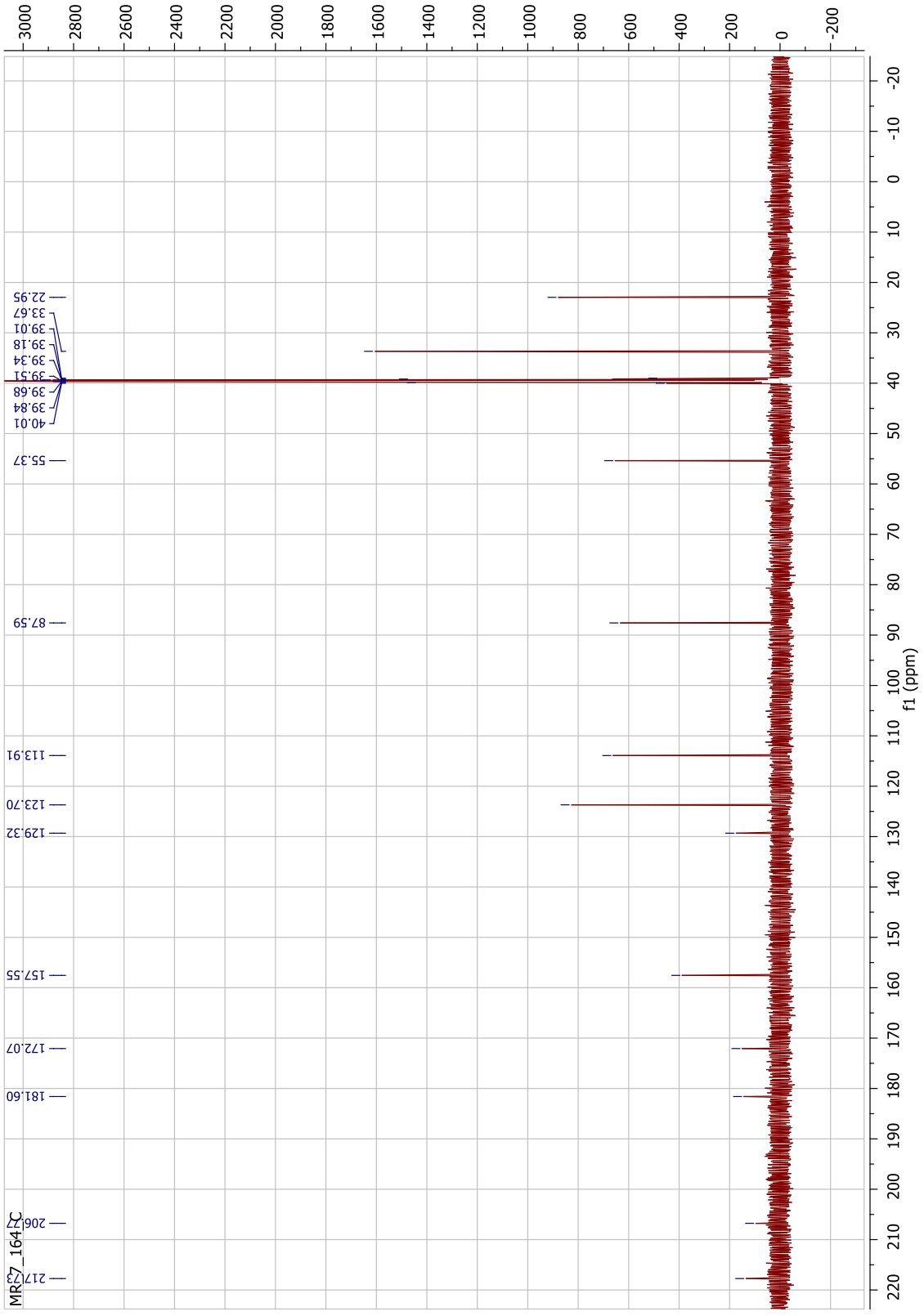

Figure 86. ^{13}C NMR spectrum of **76** (125 MHz, DMSO-d_6).

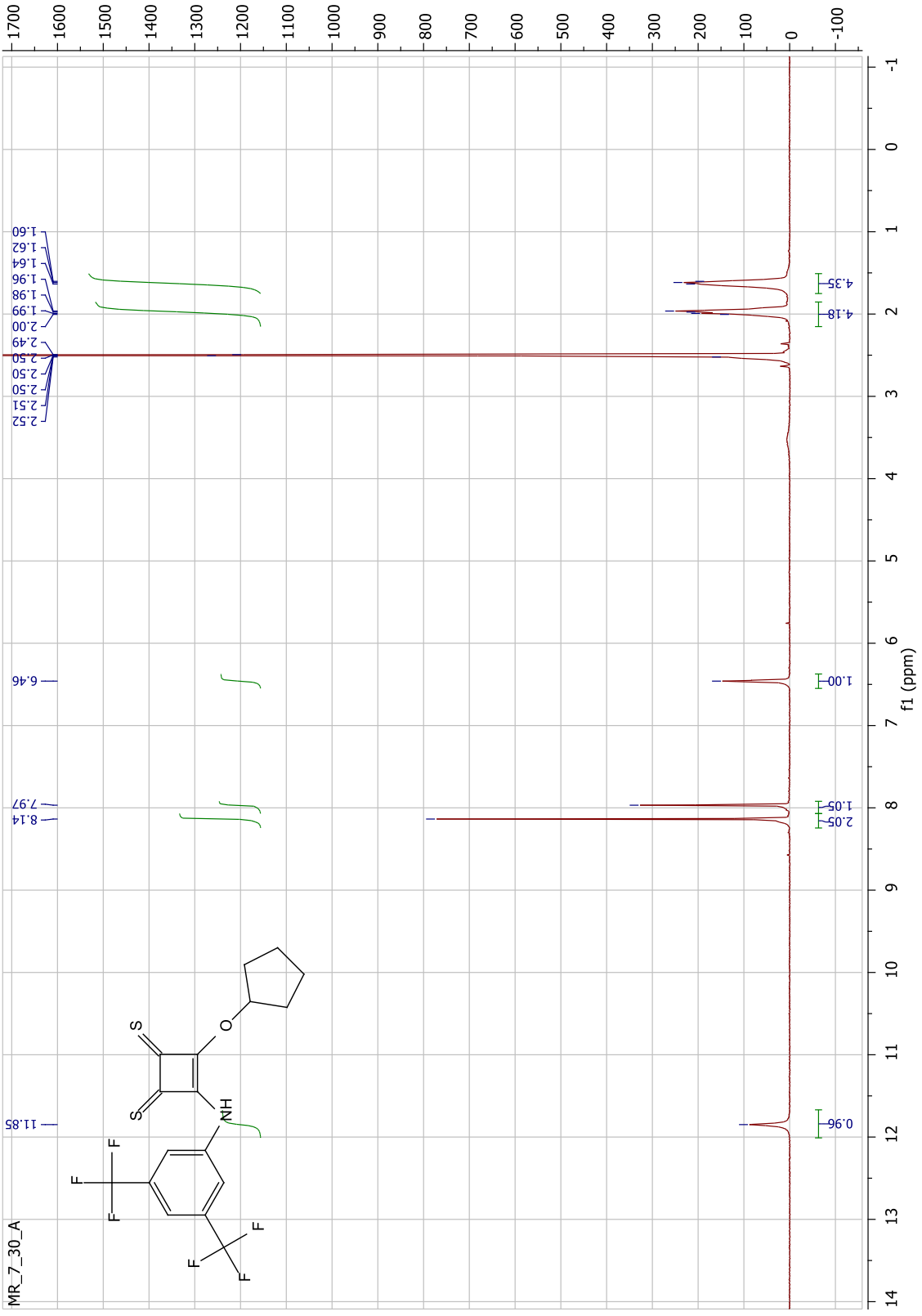

Figure 87. ^{1}H NMR spectrum of **77** (500 MHz, DMSO-d_6).

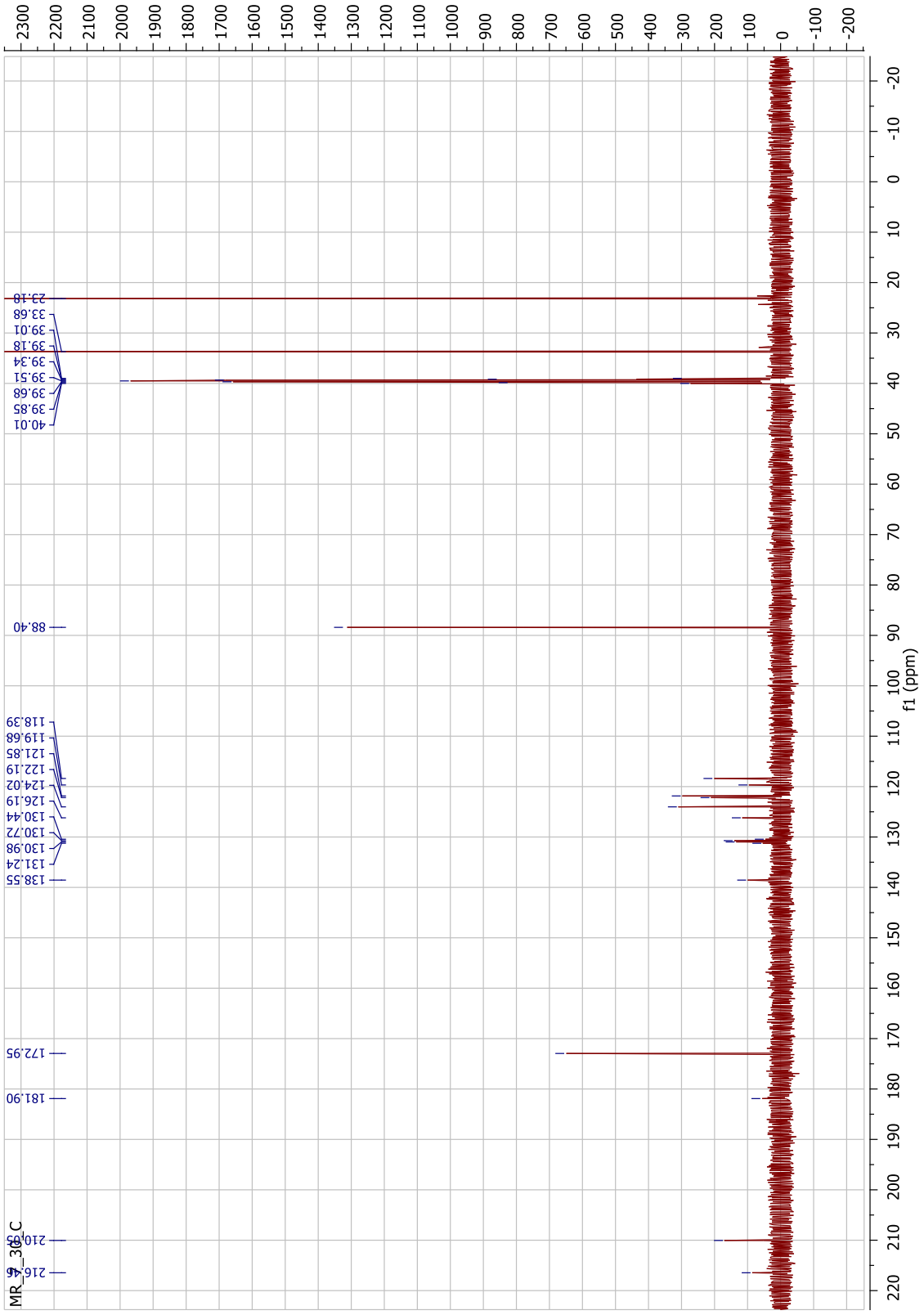

Figure 88. ^{13}C NMR spectrum of **77** (125 MHz, DMSO-d_6).

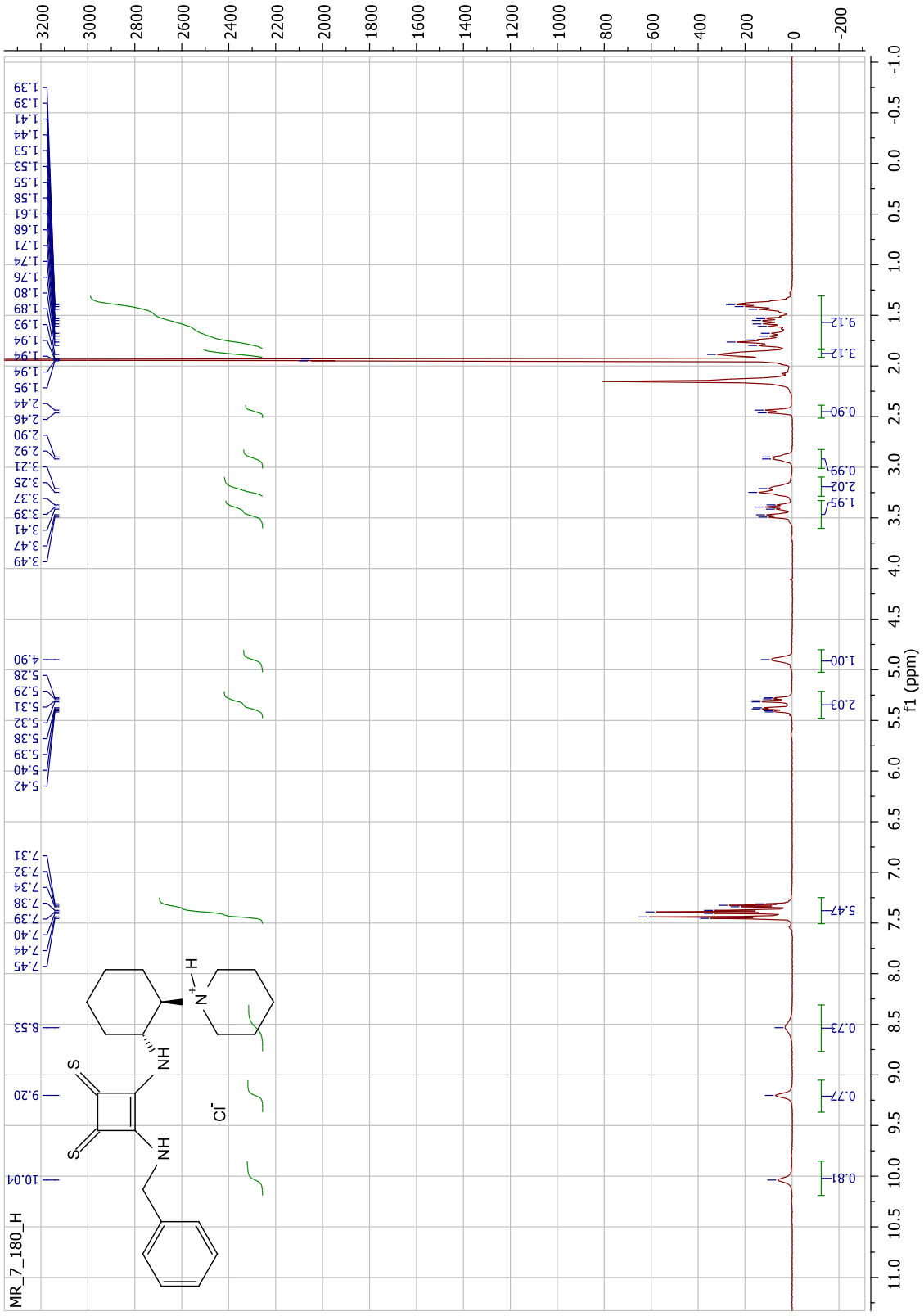

Figure 89. ^{1}H NMR spectrum of **59**.HCl (500 MHz, CD_3CN).

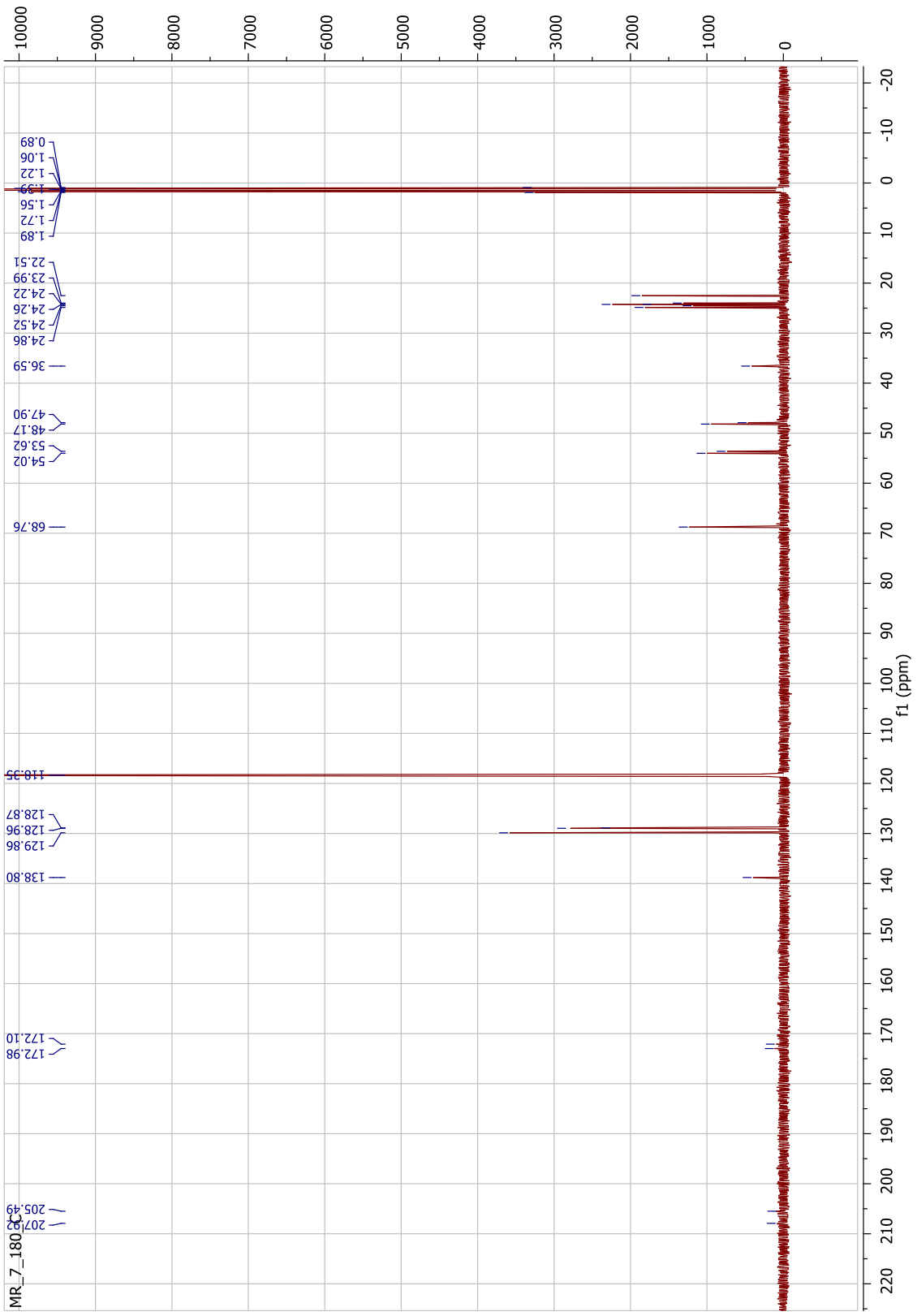

Figure 90. ^{13}C NMR spectrum of **59**.HCl (125 MHz, CD_3CN).

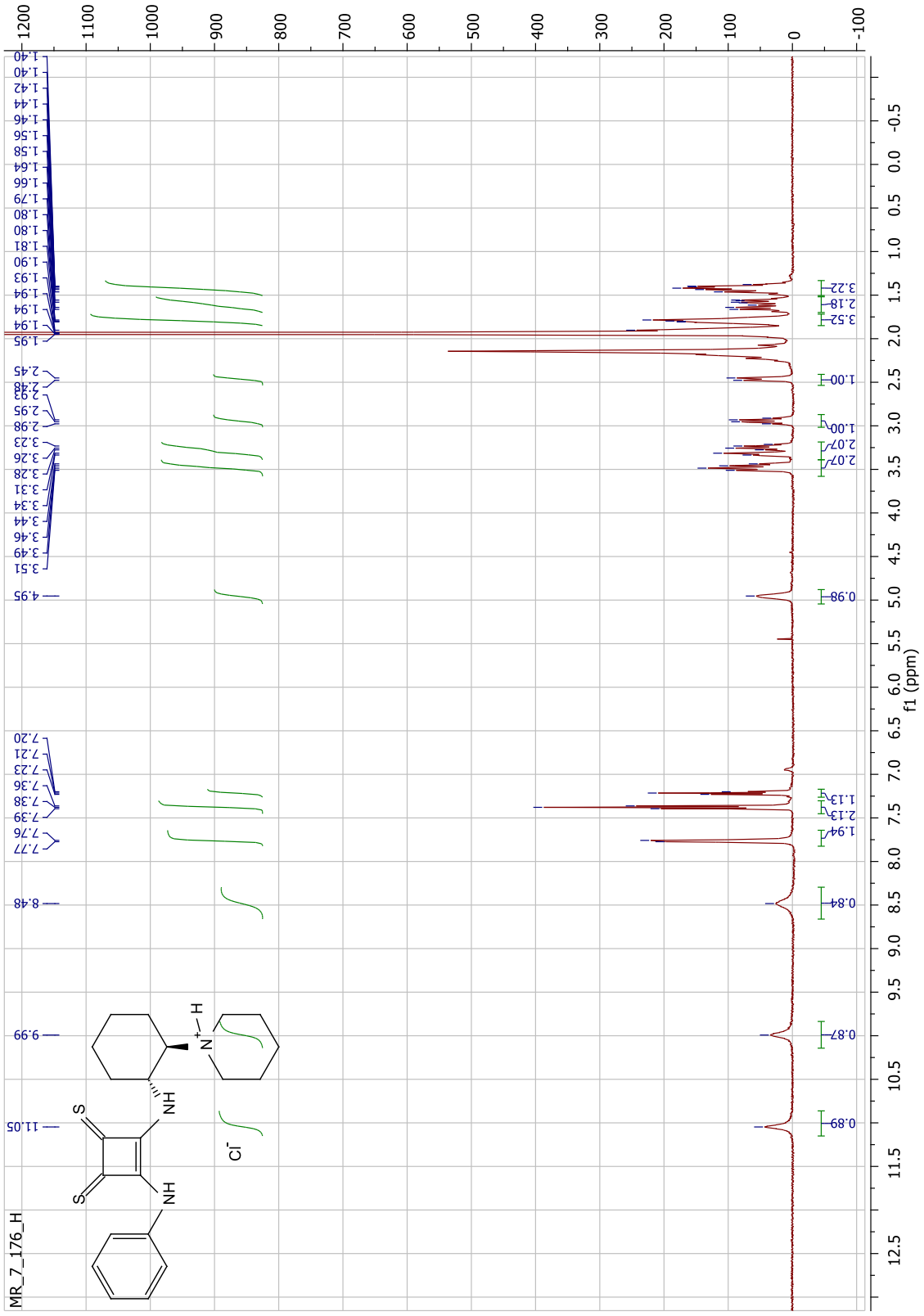

Figure 91. ^{1}H NMR spectrum of **79**.HCl (500 MHz, CD_3CN).

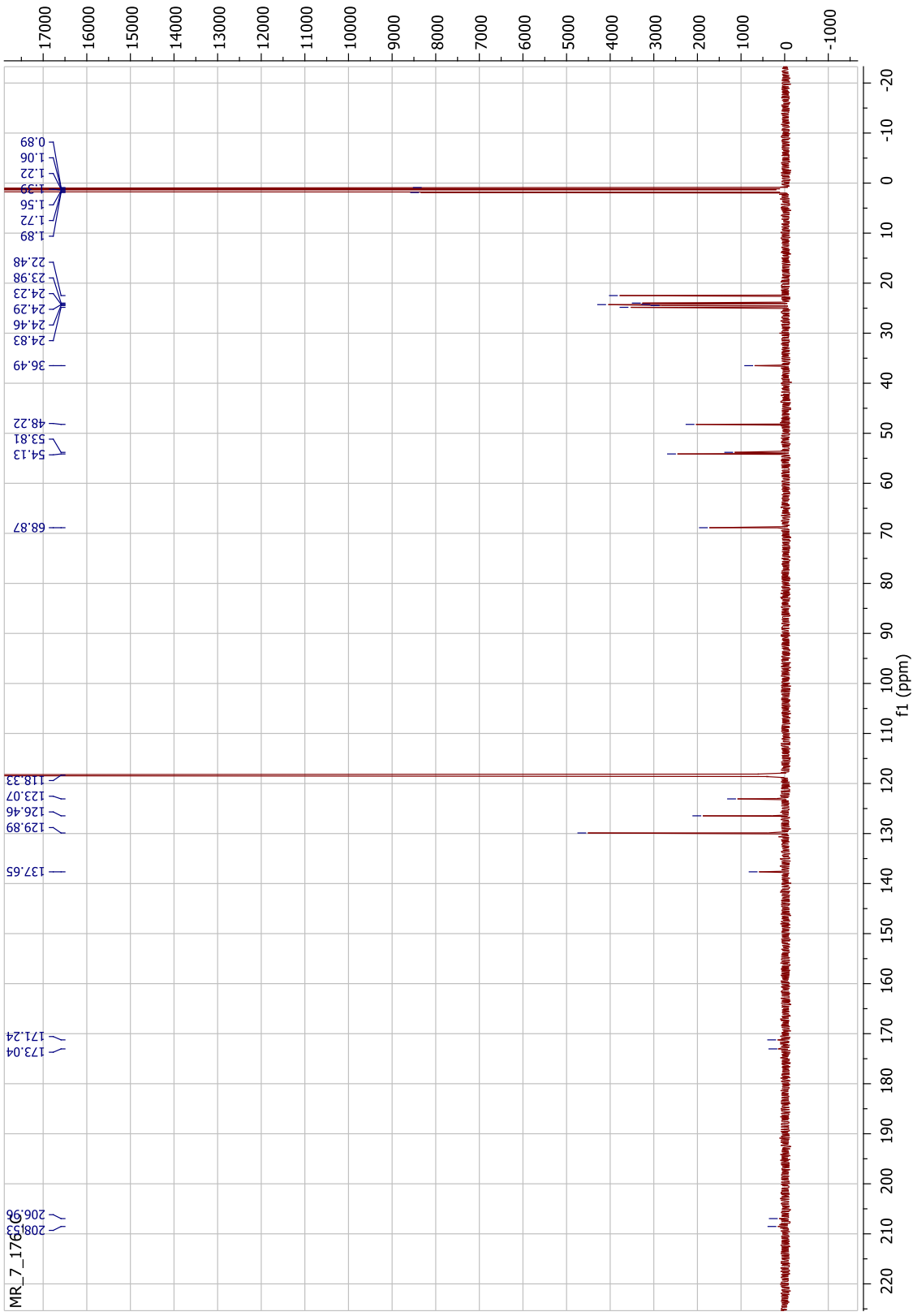

Figure 92. ^{13}C NMR spectrum of **79**.HCl (125 MHz, CD_3CN).

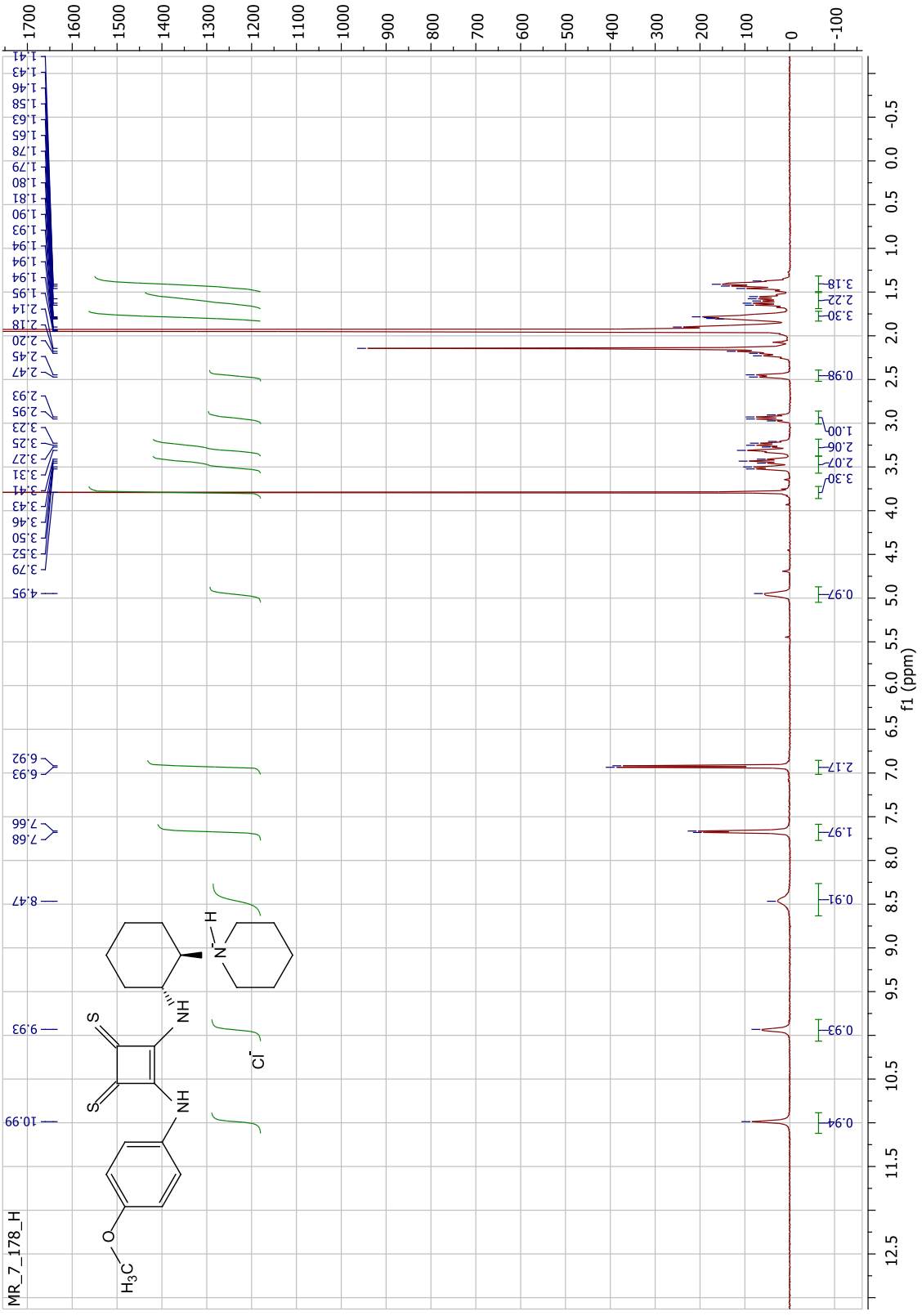

Figure 93. ^{1}H NMR spectrum of **80**.HCl (500 MHz, CD_3CN).

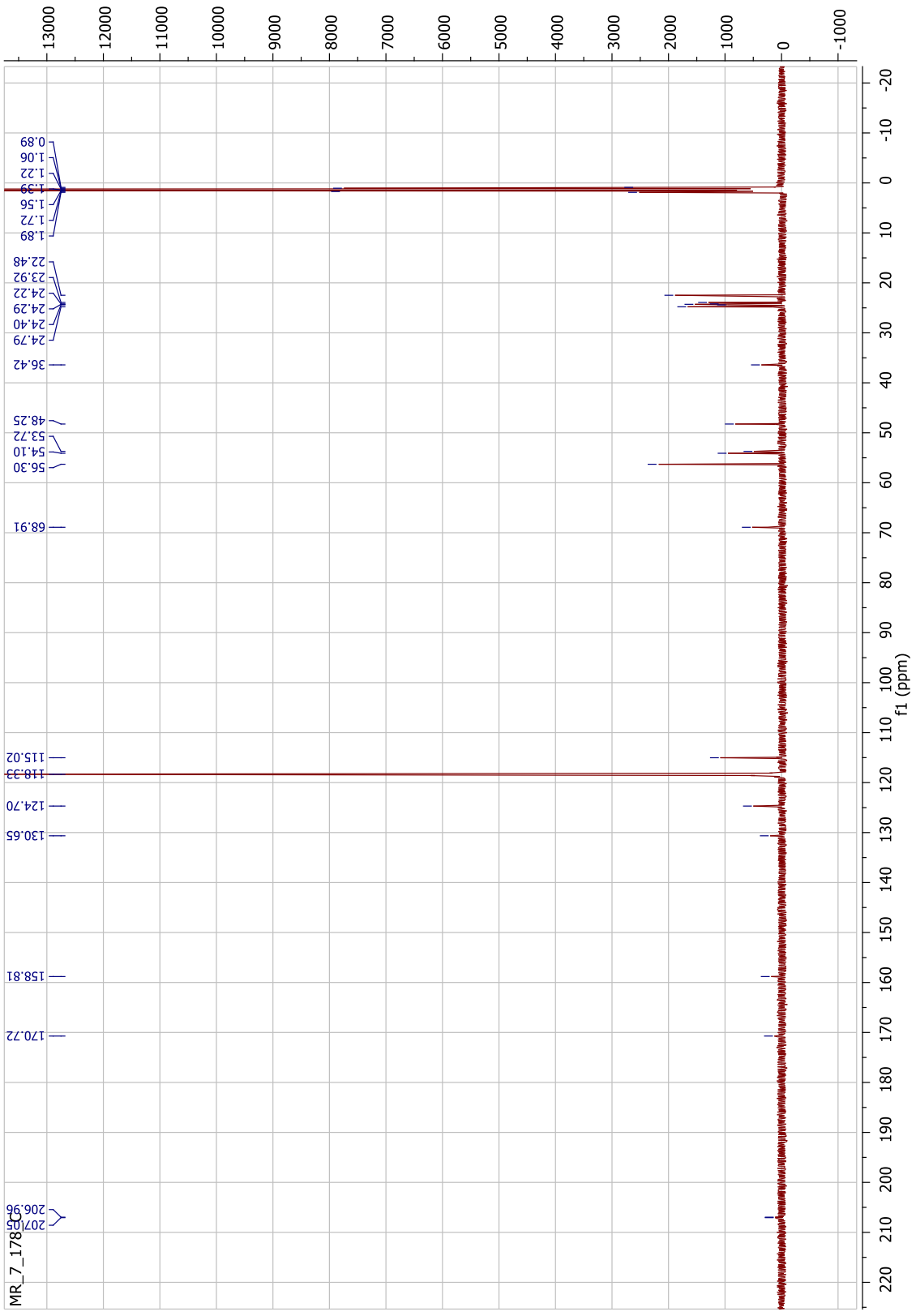

Figure 94. ^{13}C NMR spectrum of **80**.HCl (125 MHz, CD_3CN).

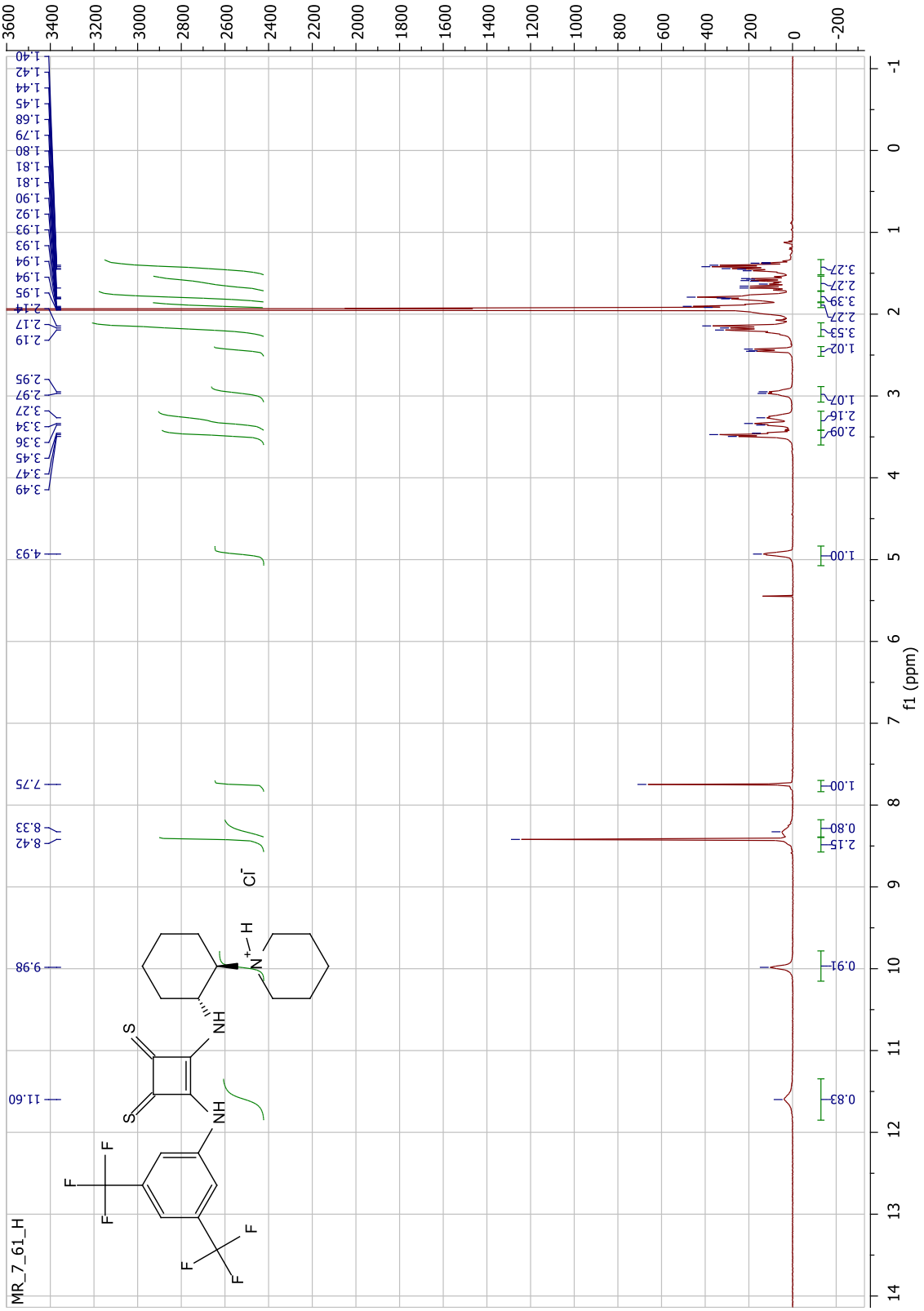

Figure 95. ^{1}H NMR spectrum of **81**.HCl (500 MHz, CD_3CN).

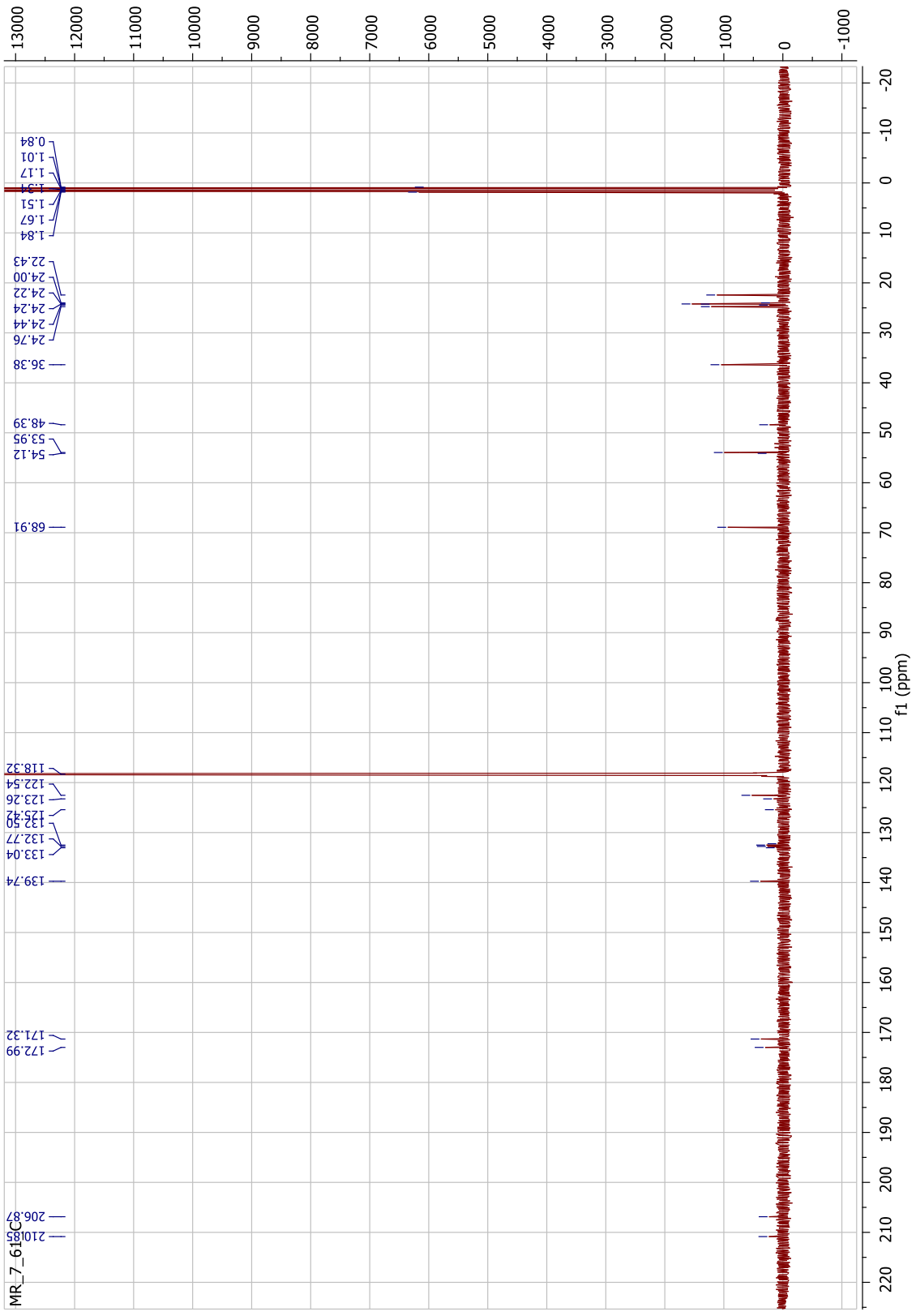

Figure 96. ^{13}C NMR spectrum of **81**.HCl (125 MHz, CD_3CN).

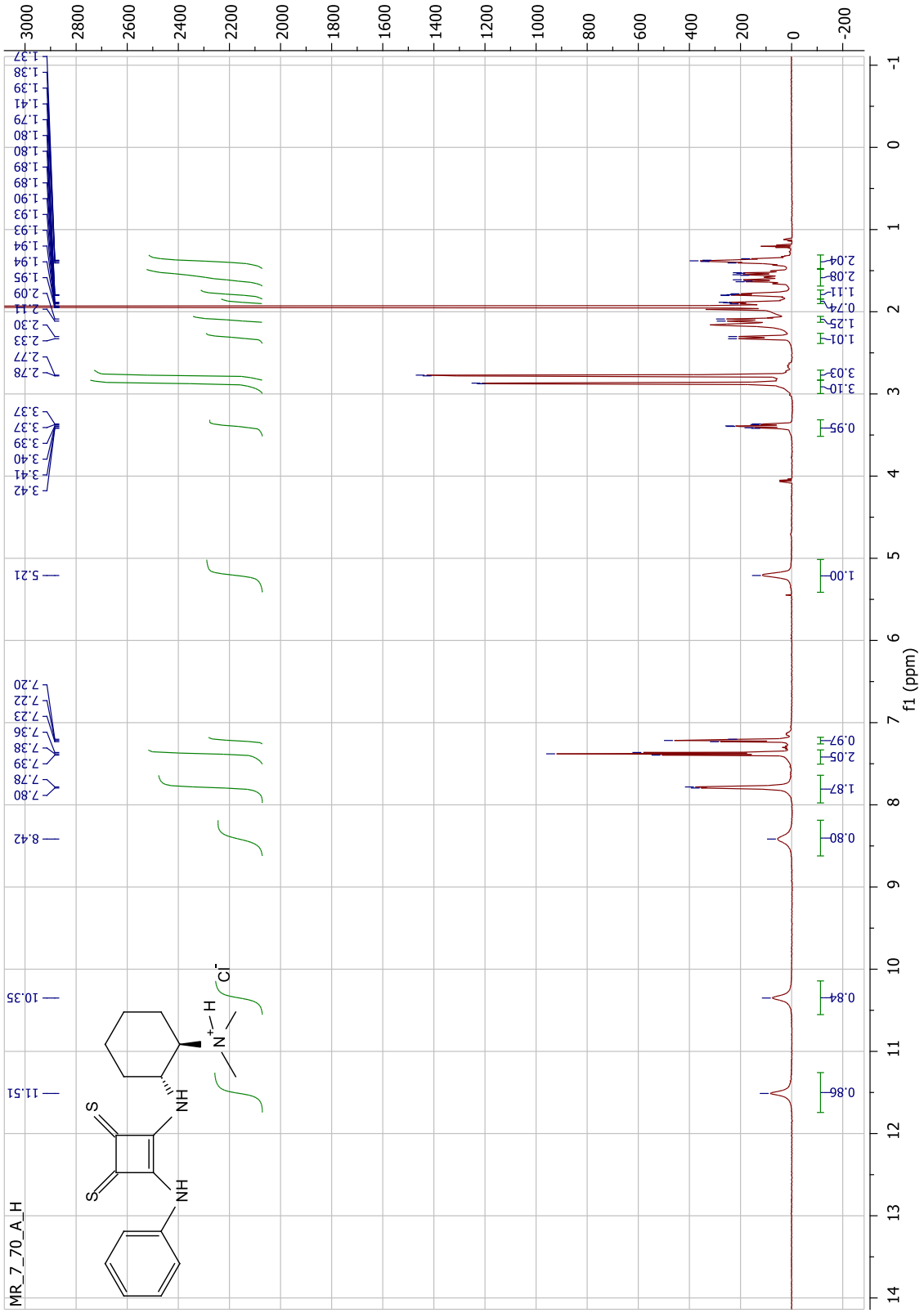

Figure 97. ^{1}H NMR spectrum of **82**.HCl (500 MHz, CD_3CN).

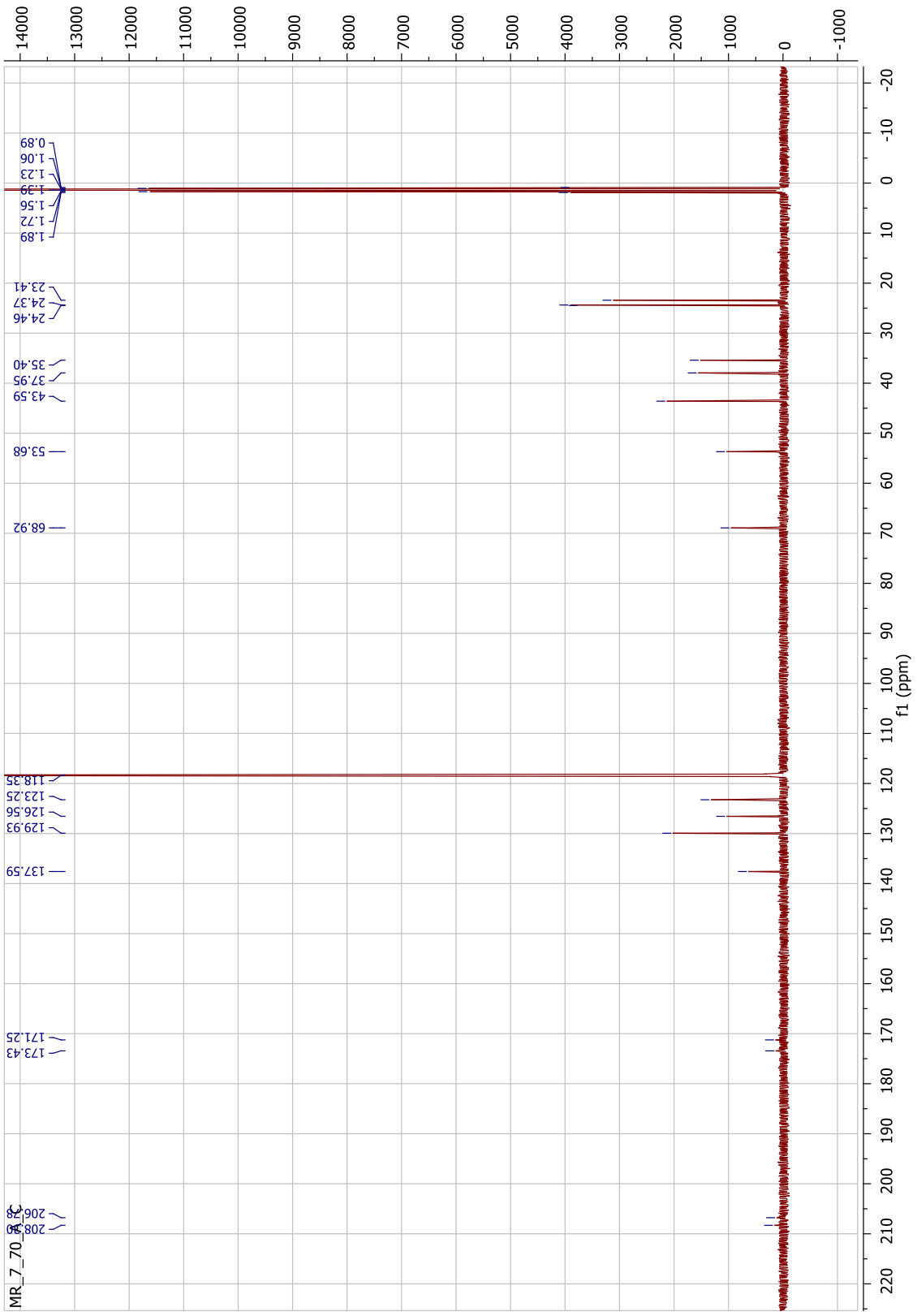

Figure 98. ^{13}C NMR spectrum of **82**.HCl (125 MHz, CD_3CN).

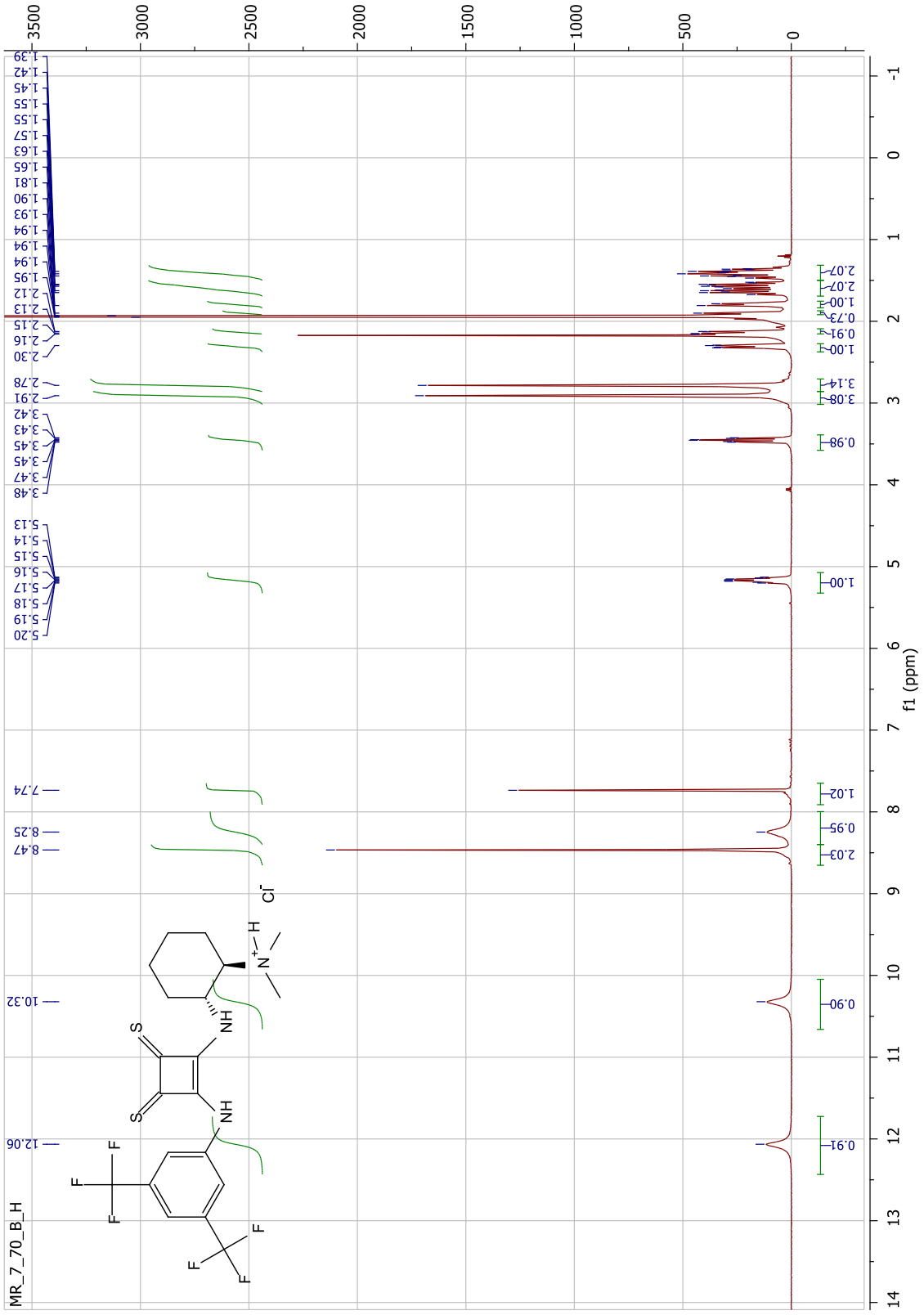

Figure 99. ^{1}H NMR spectrum of **83**.HCl (500 MHz, CD_3CN).

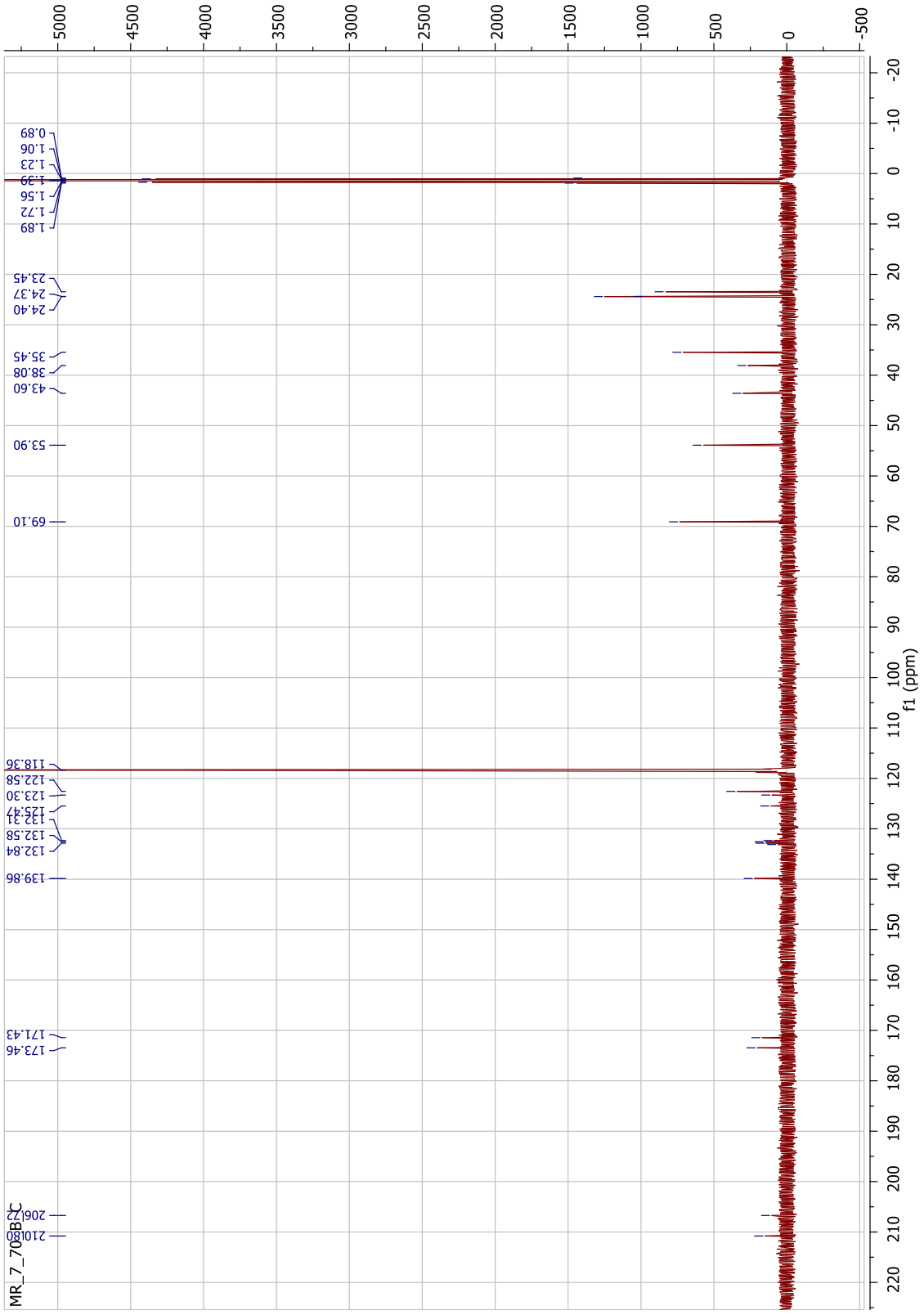

Figure 100. ^{13}C NMR spectrum of **83**.HCl (125 MHz, CD_3CN).

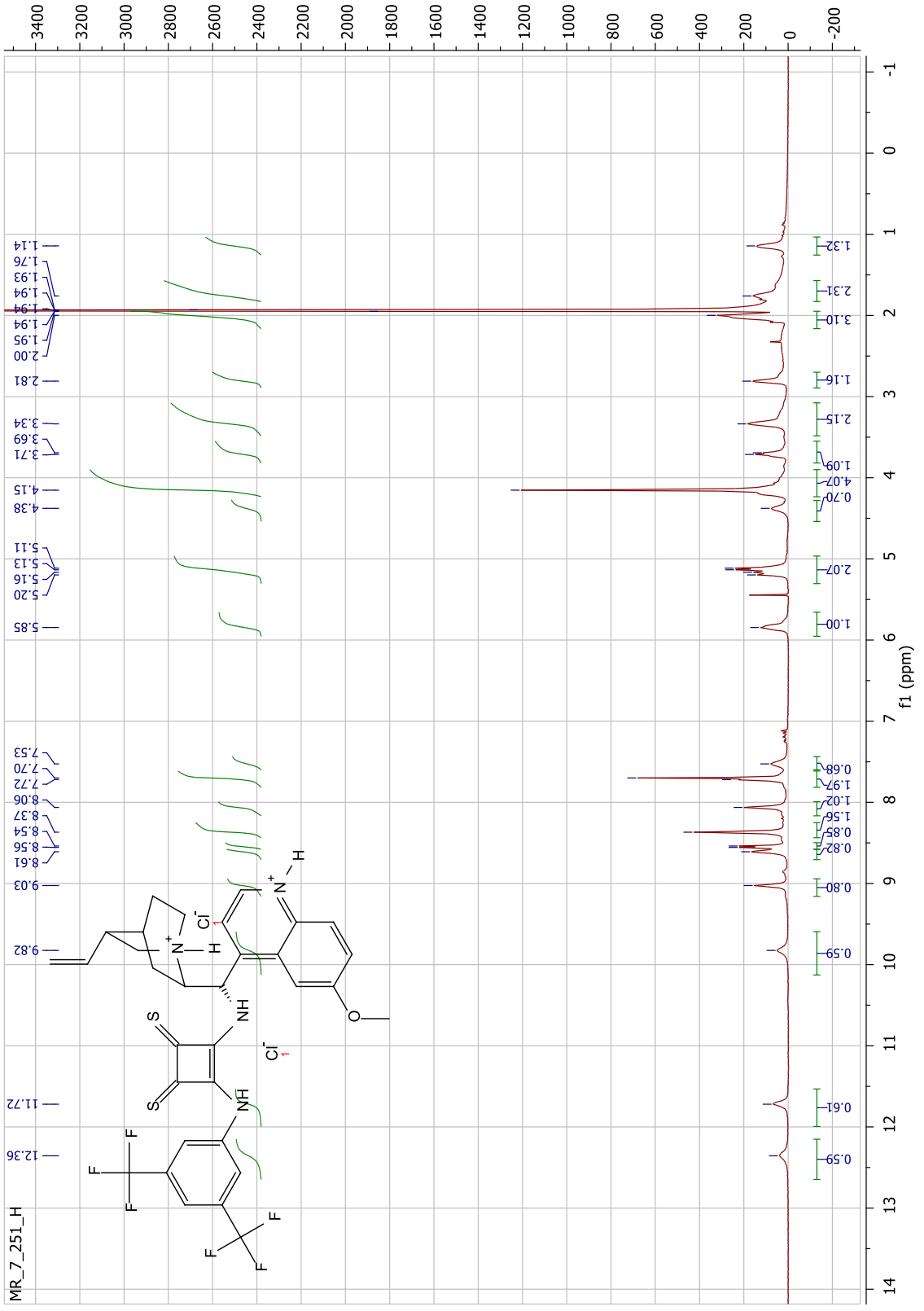

Figure 101. ^{1}H NMR spectrum of **84**.HCl (500 MHz, CD_3CN).

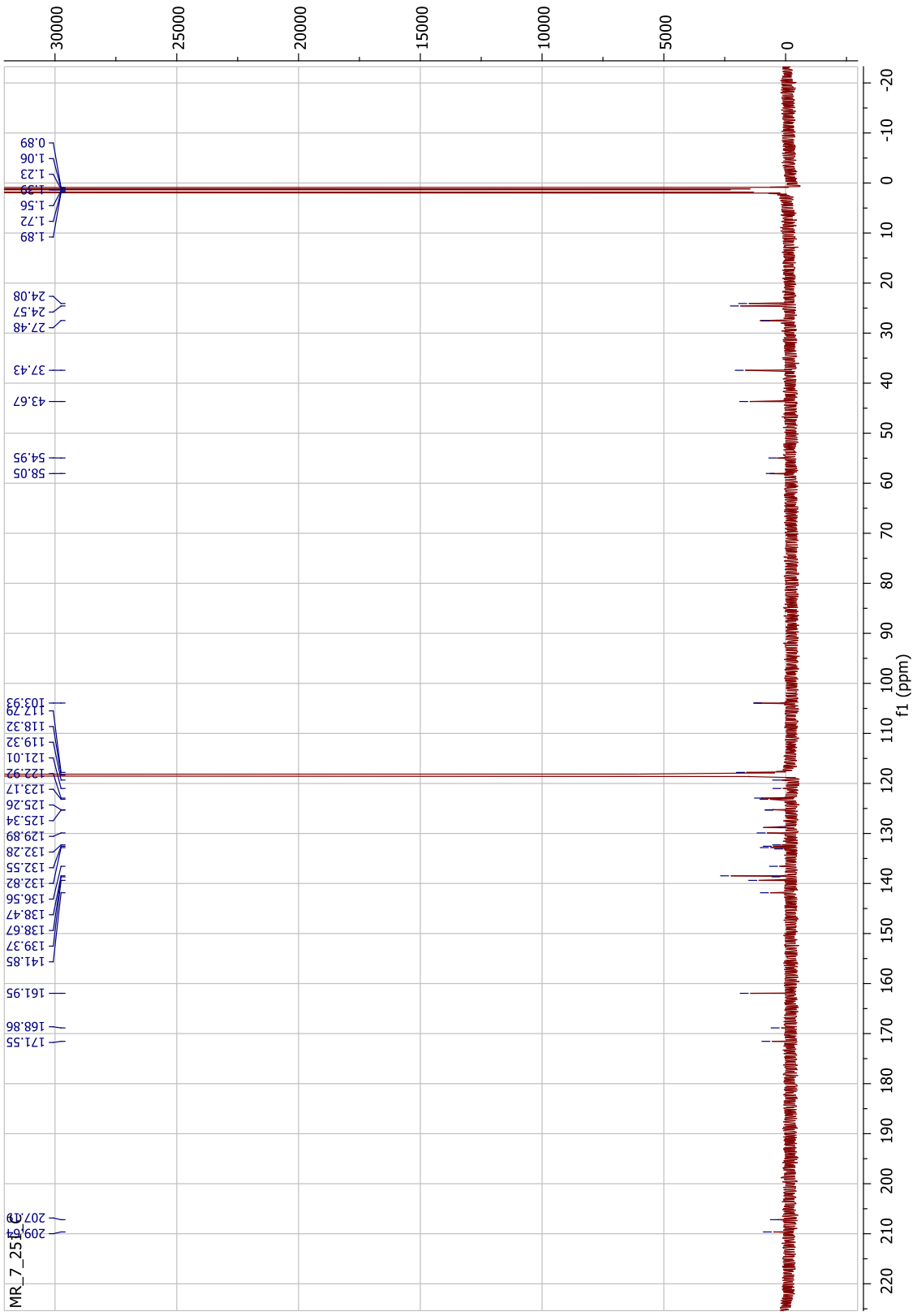

Figure 102. ^{13}C NMR spectrum of **84**.HCl (125 MHz, CD_3CN).

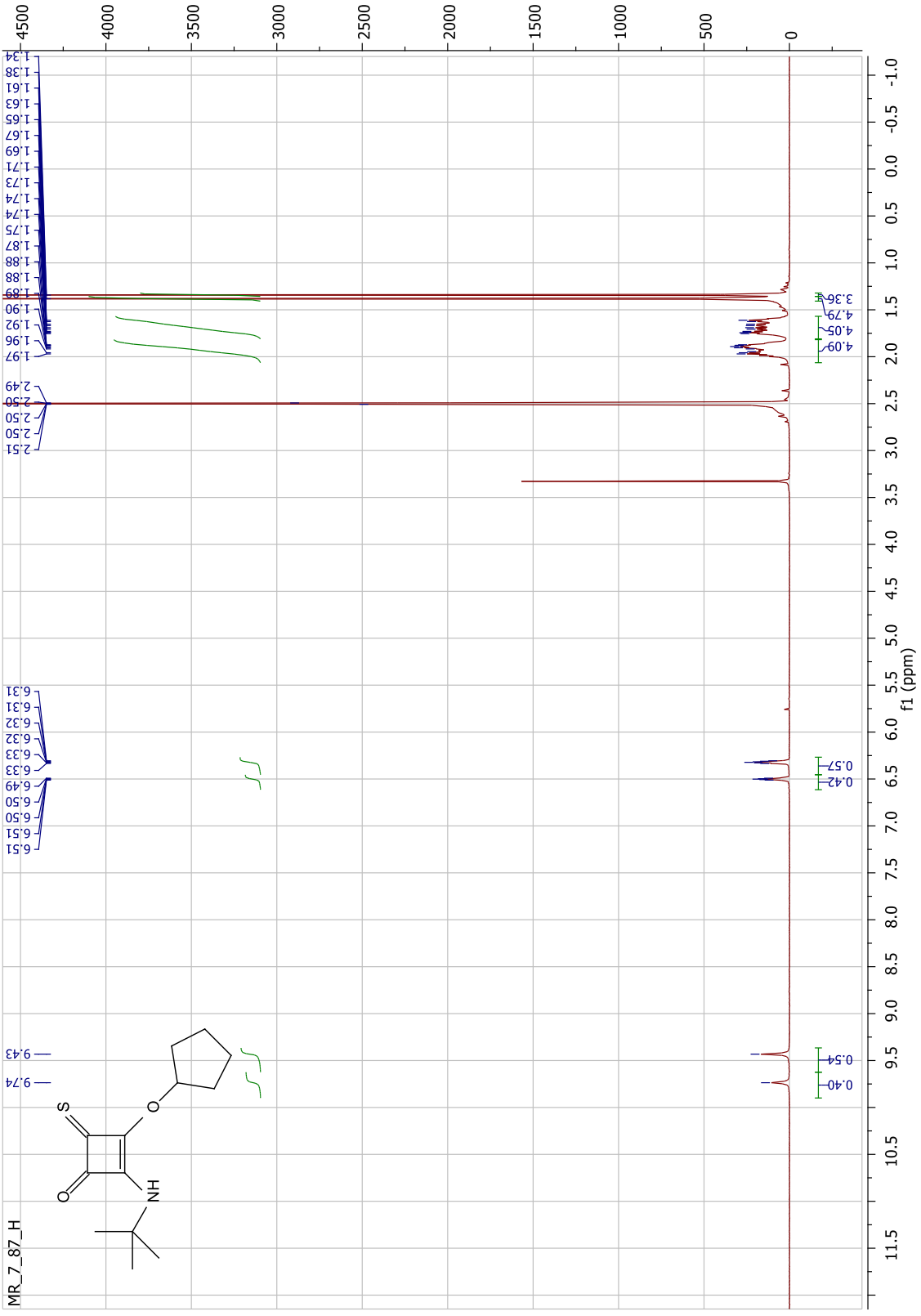

Figure 103. ^{1}H NMR spectrum of **88** (500 MHz, DMSO-d_6).

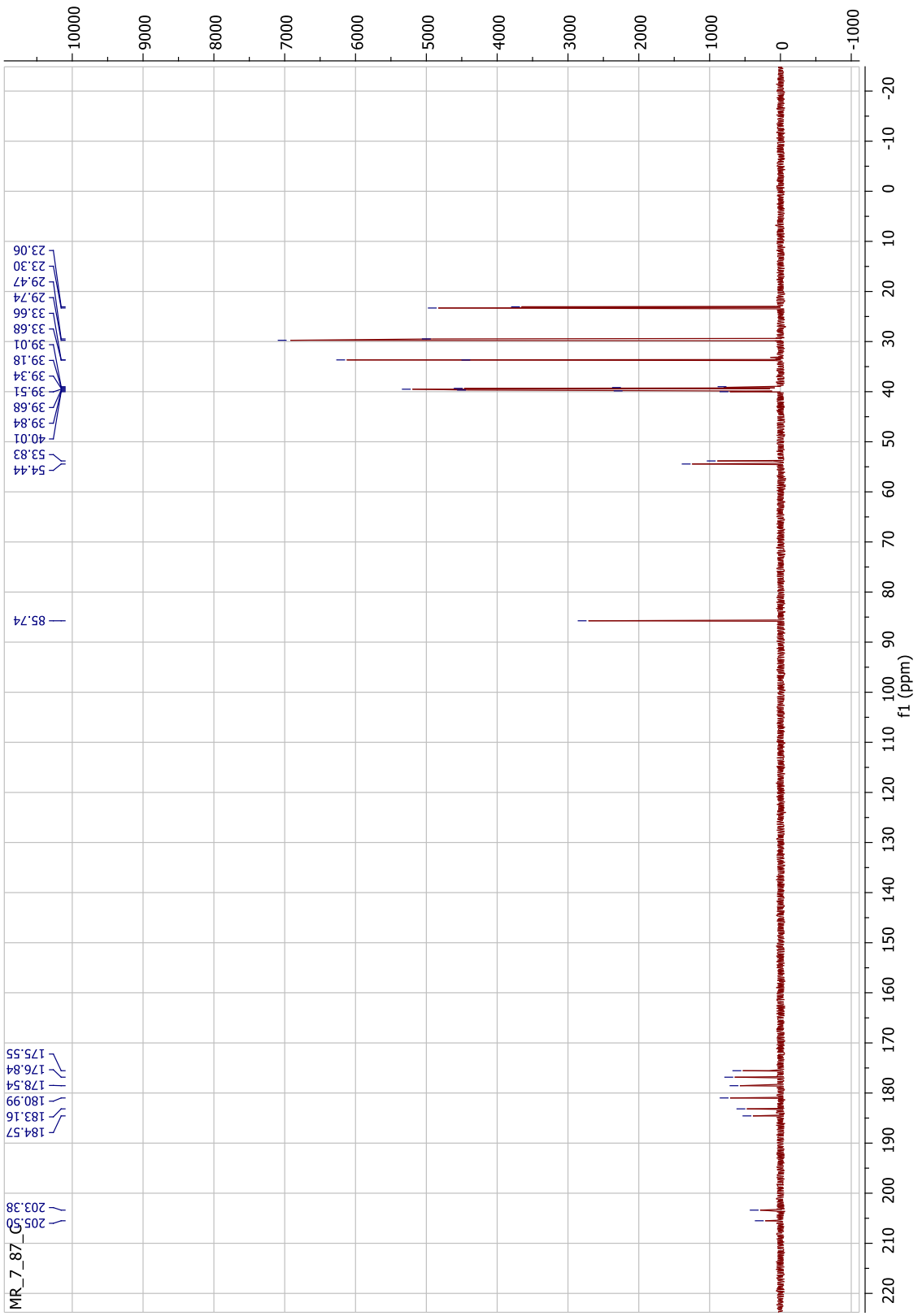

Figure 104. ^{13}C NMR spectrum of **88** (125 MHz, DMSO-d_6).

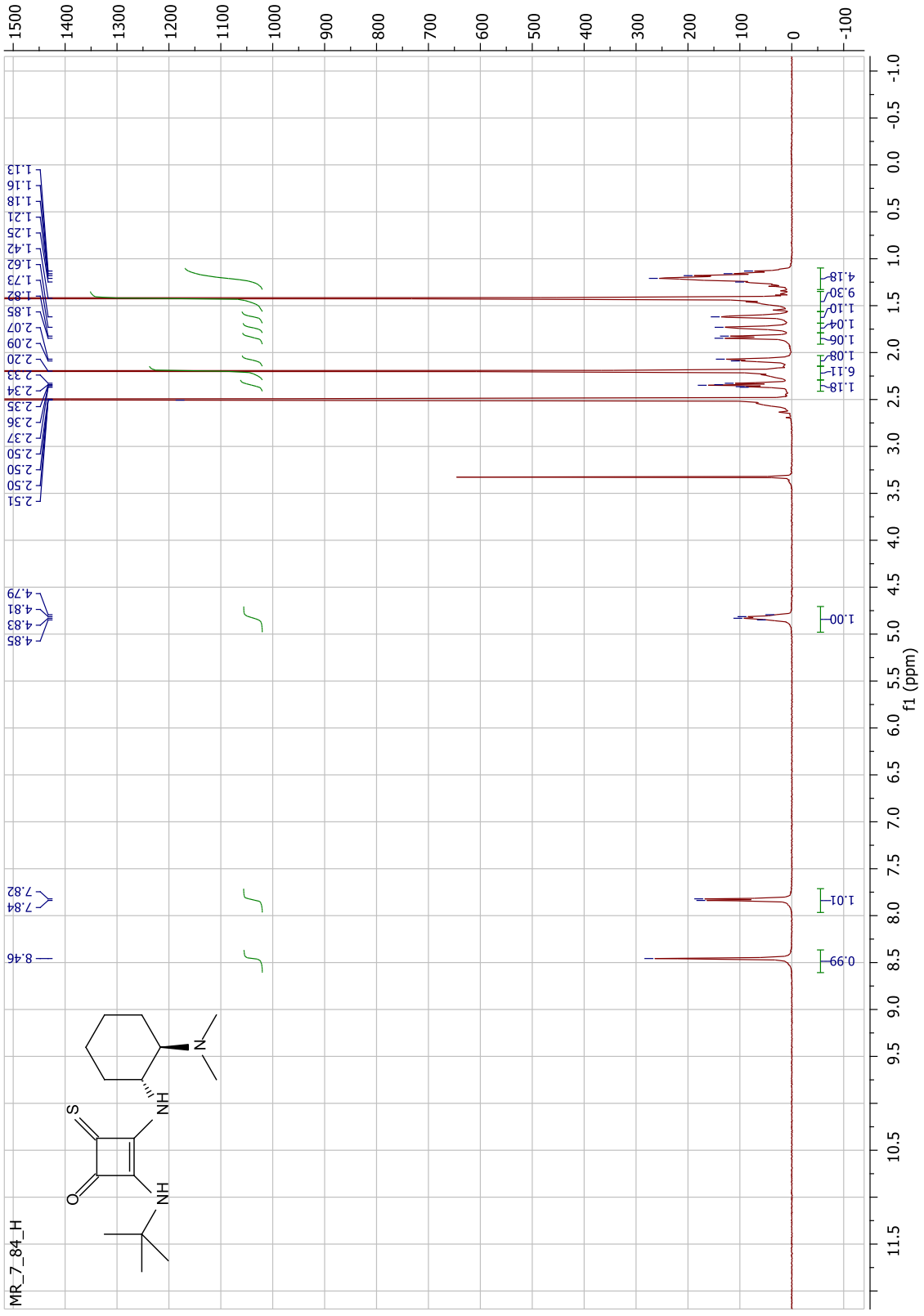

Figure 105. ^{1}H NMR spectrum of **89** (500 MHz, DMSO-d_6).

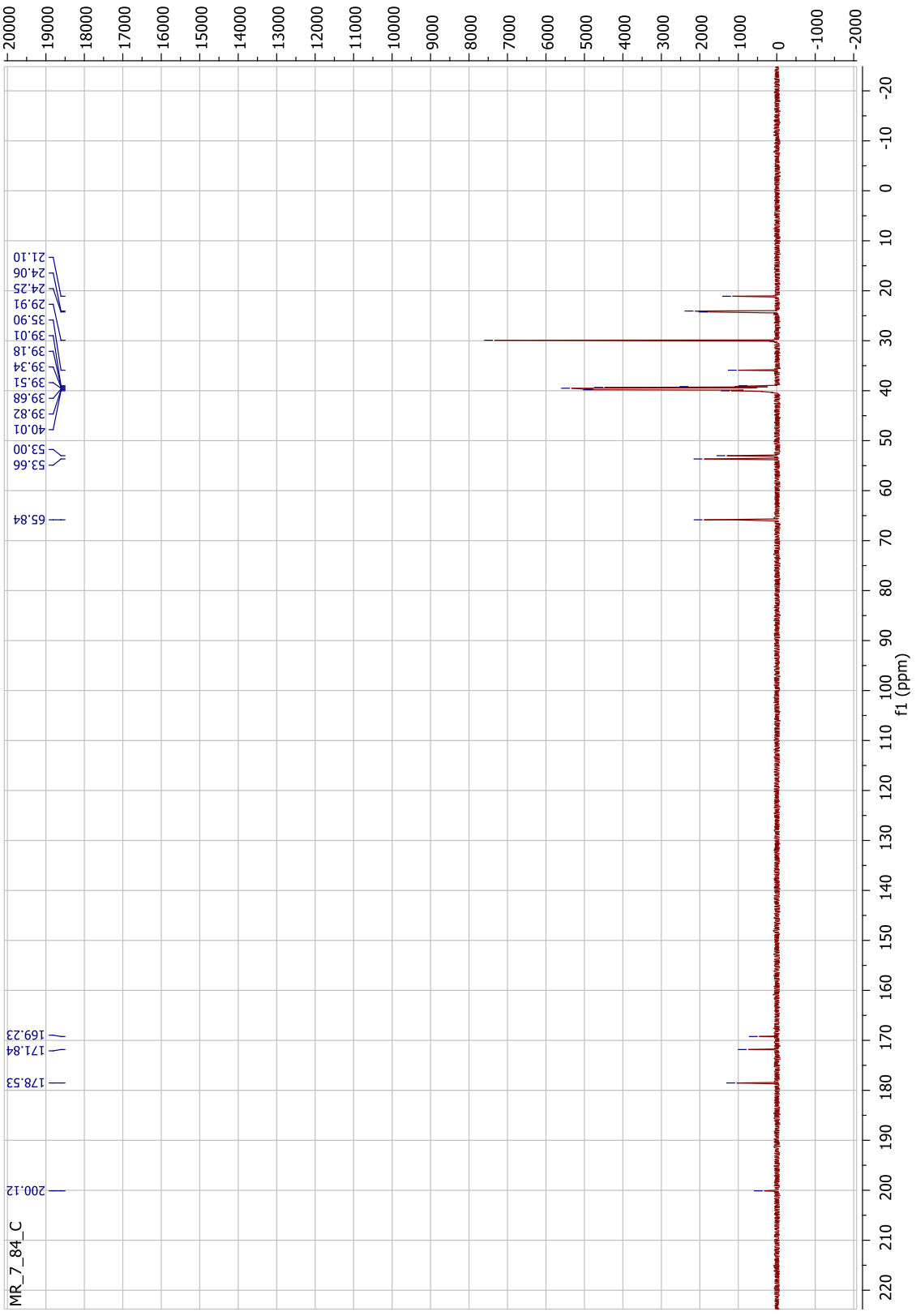

Figure 106. ^{13}C NMR spectrum of **89** (125 MHz, DMSO-d_6).

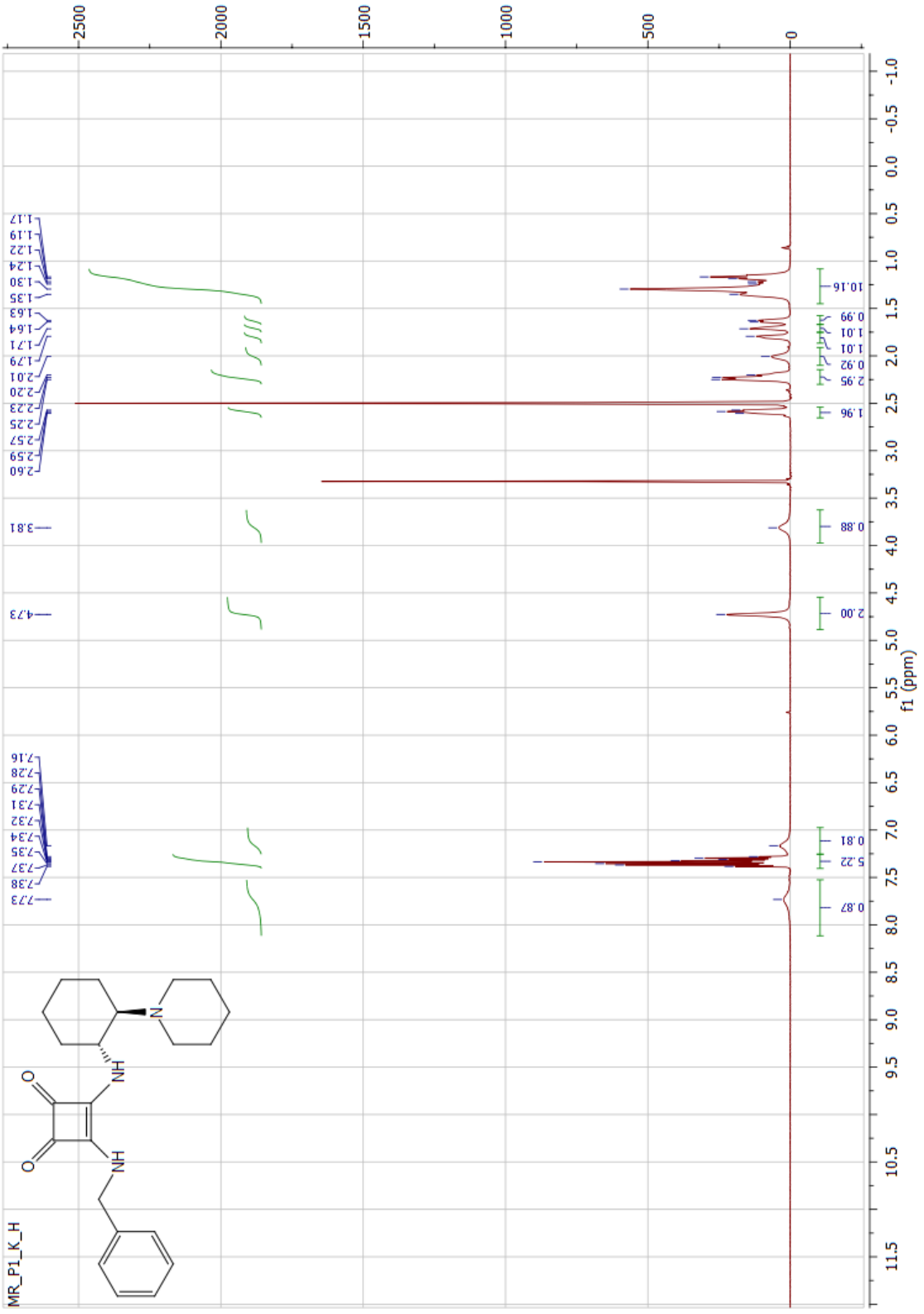

Figure 107. ^{1}H NMR spectrum of **97** (500 MHz, DMSO-d_6).

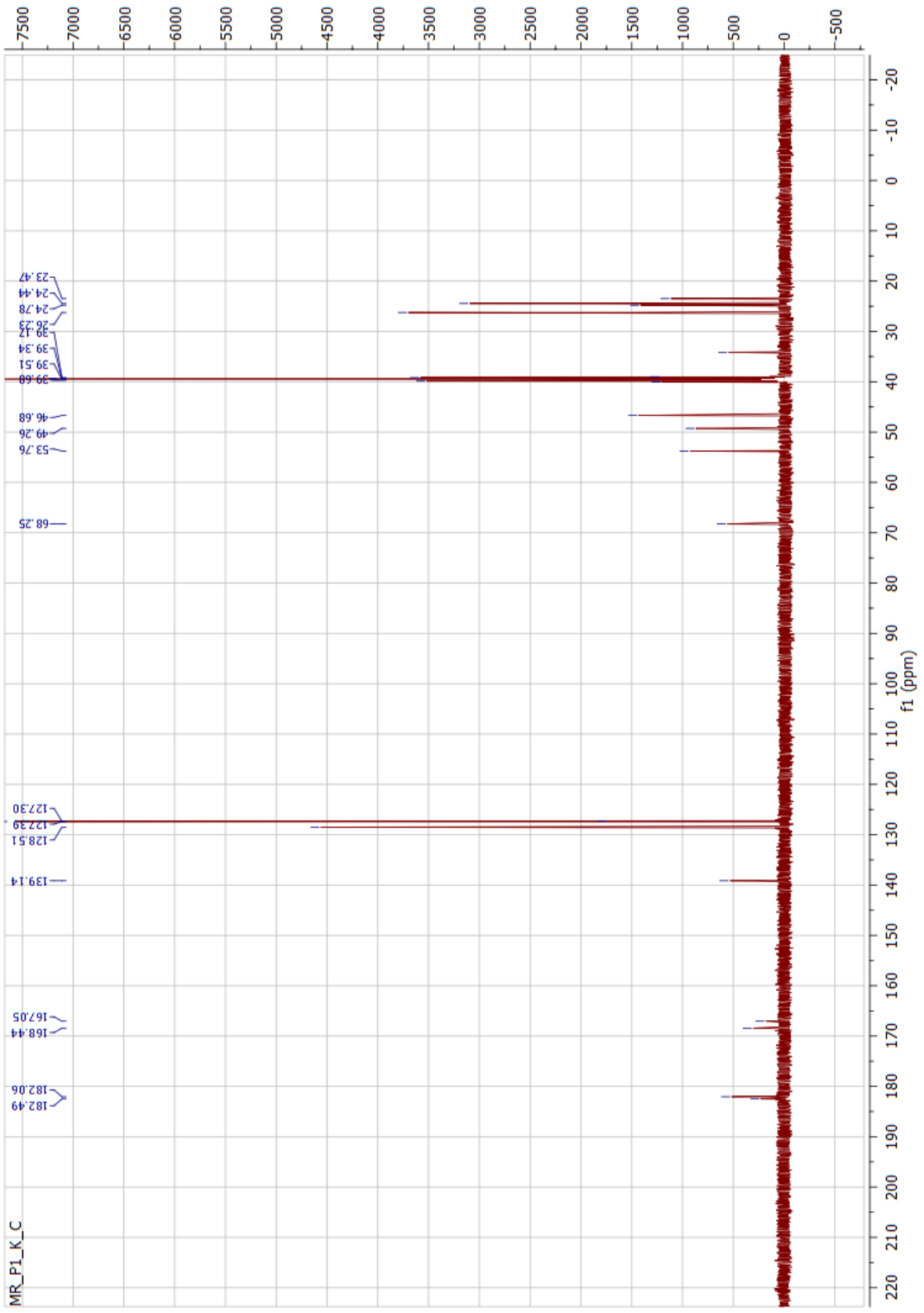

Figure 108. ^{13}C NMR spectrum of **97** (125 MHz, DMSO-d_6).

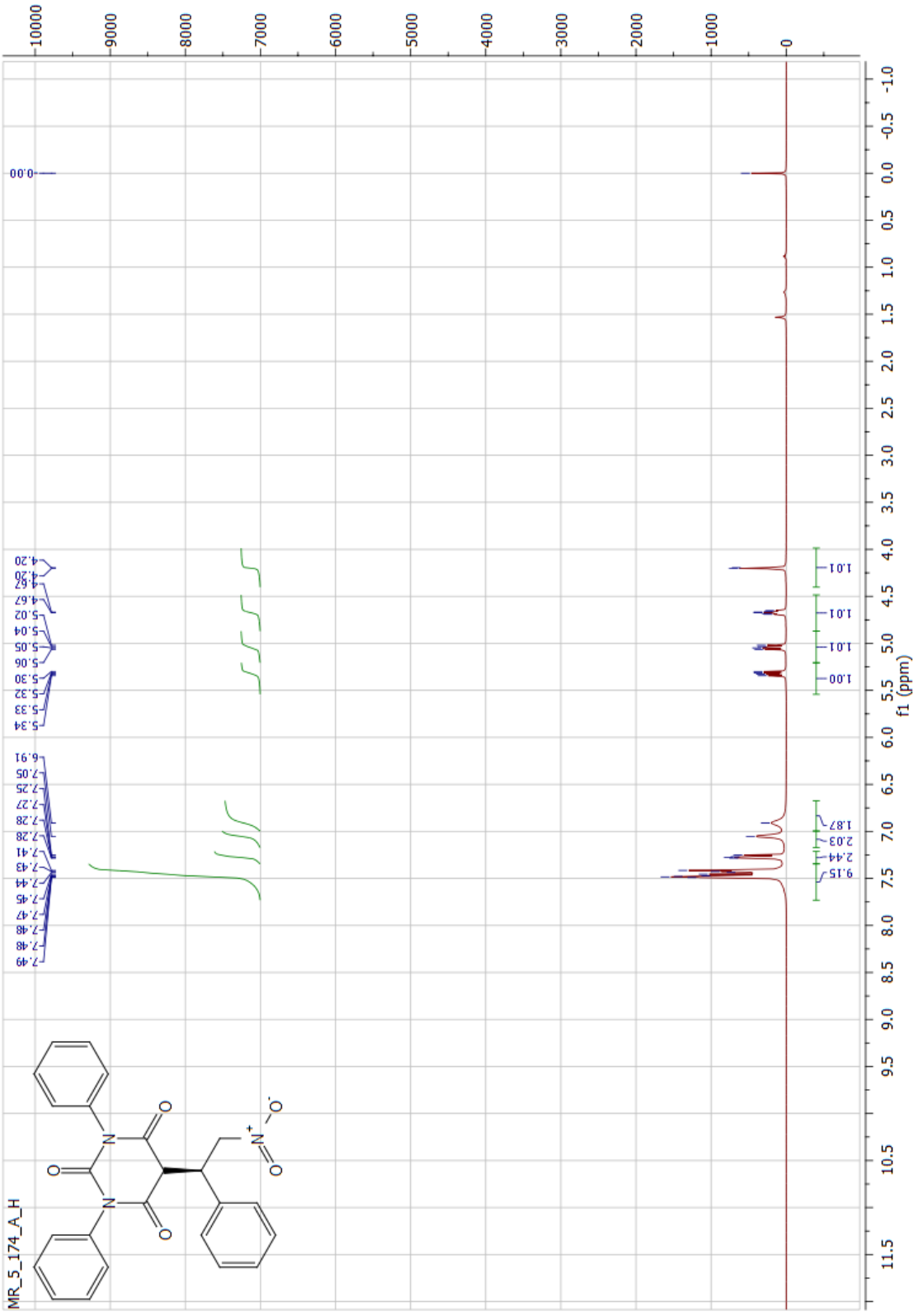

Figure 109. ^{1}H NMR spectrum of **121** (500 MHz, $CDCl_3$).

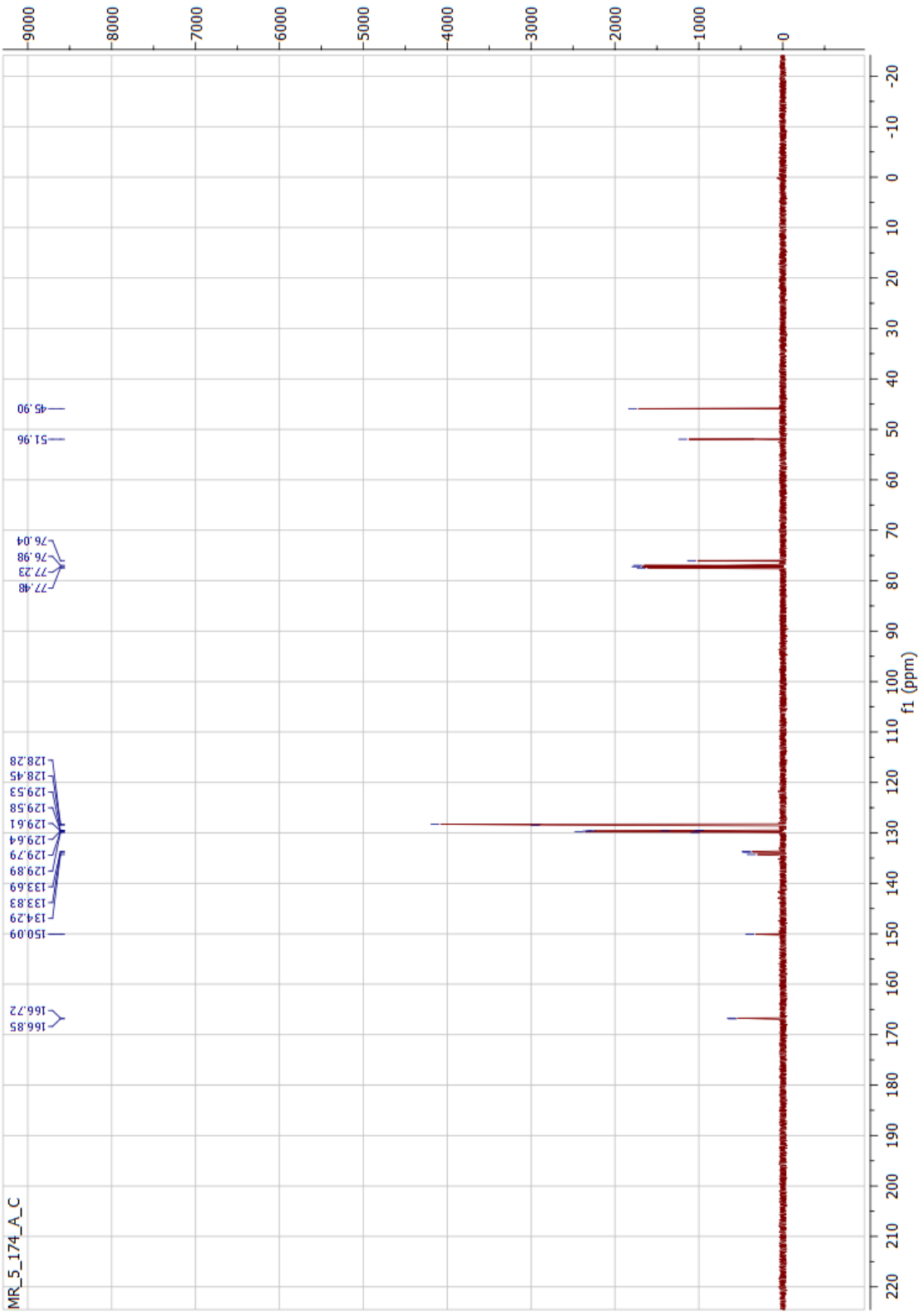

Figure 110. ^{13}C NMR spectrum of **121** (125 MHz, $CDCl_3$).

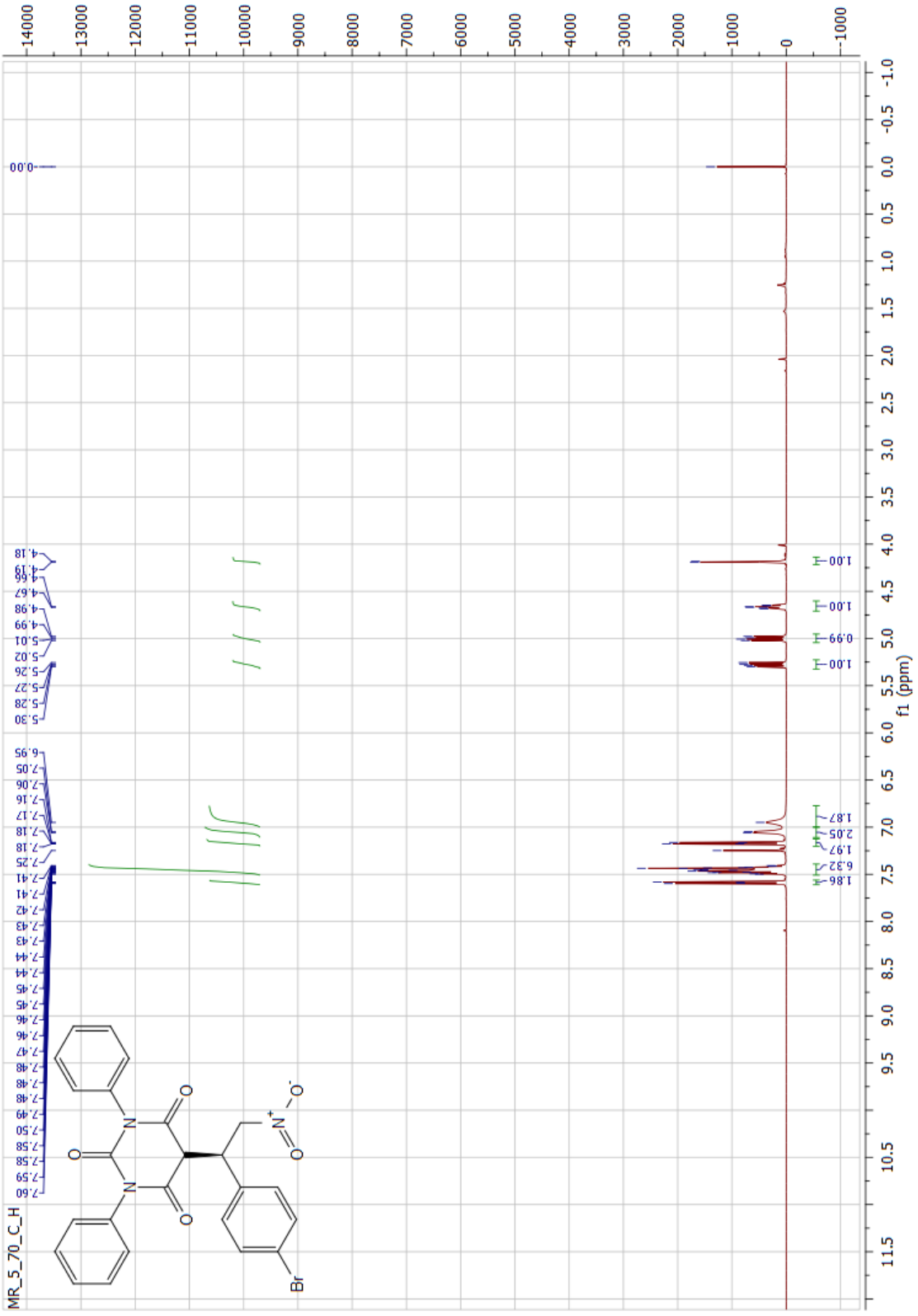

Figure 111. ^{1}H NMR spectrum of **125** (500 MHz, $CDCl_3$).

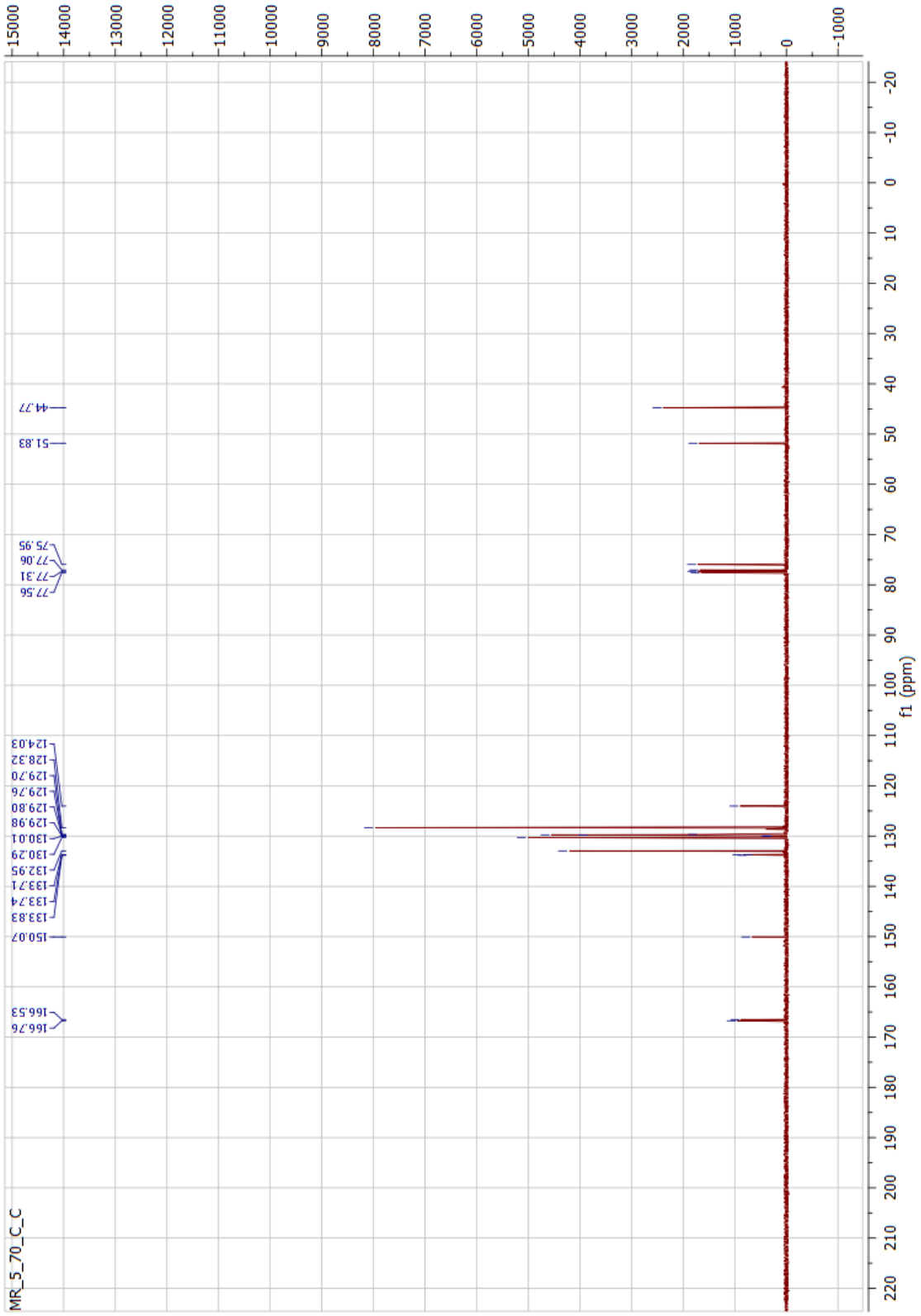

Figure 112. ^{13}C NMR spectrum of **125** (125 MHz, $CDCl_3$).

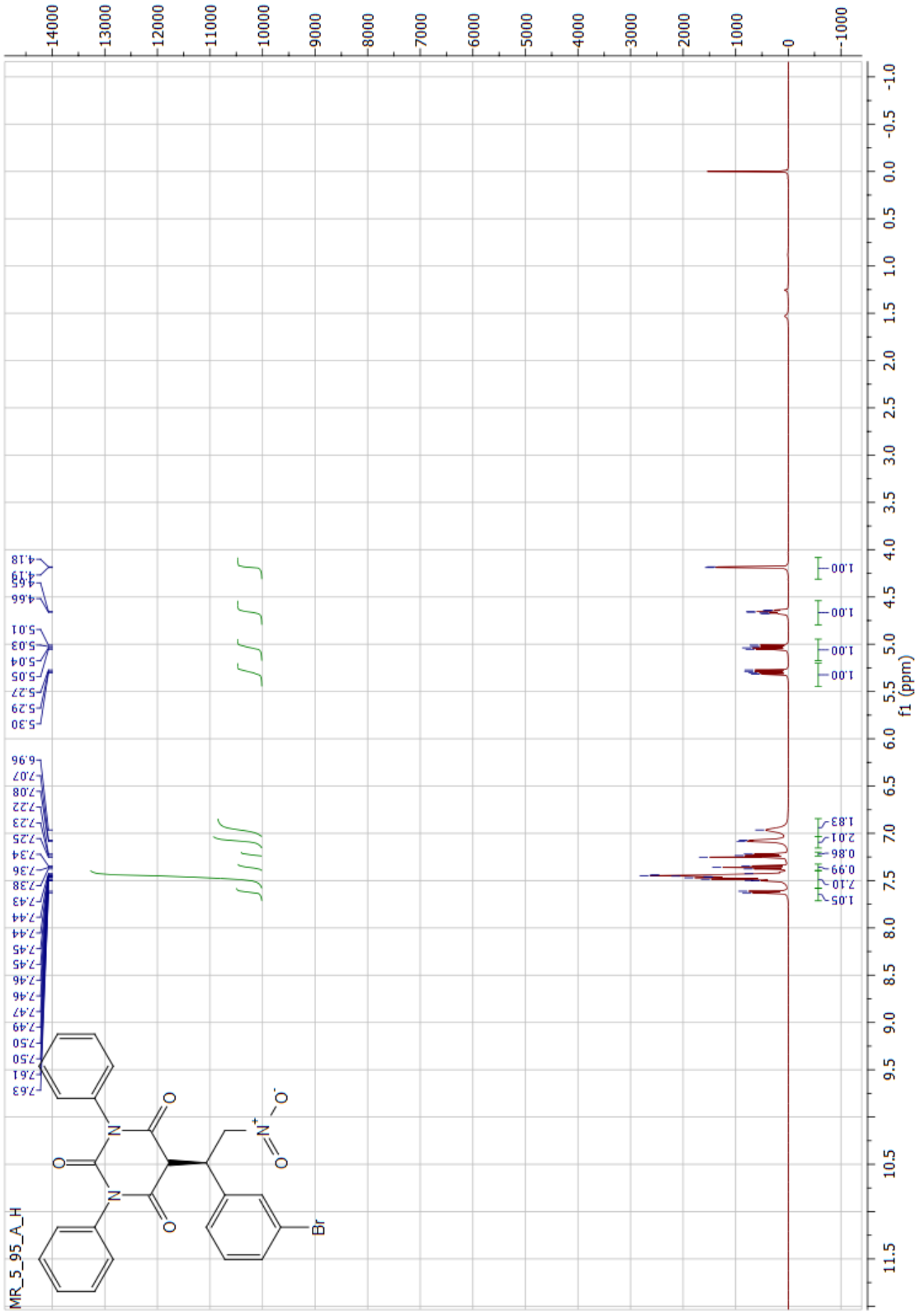

Figure 113. ^{1}H NMR spectrum of **126** (500 MHz, $CDCl_3$).

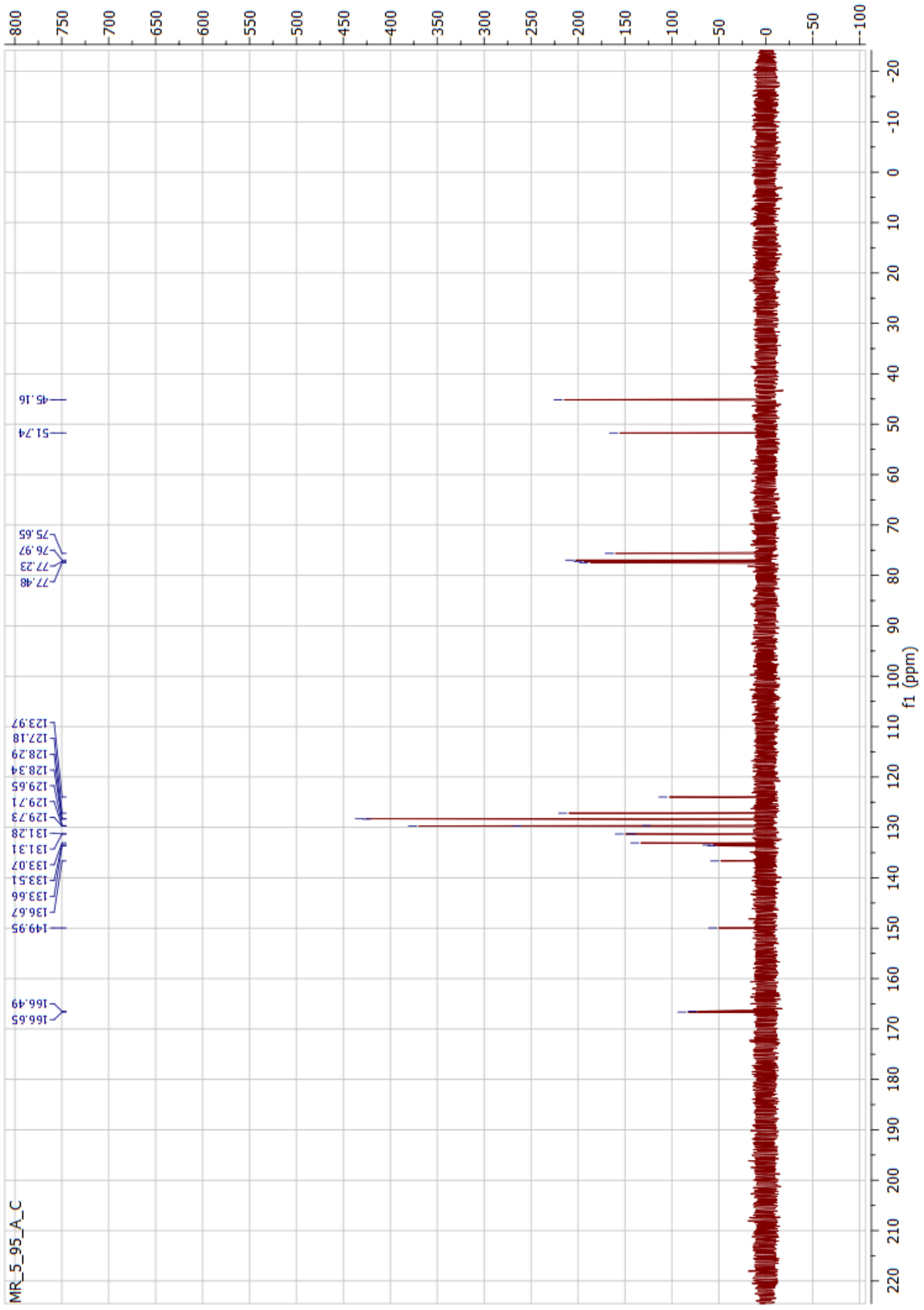

Figure 114. ^{13}C NMR spectrum of **126** (125 MHz, $CDCl_3$).

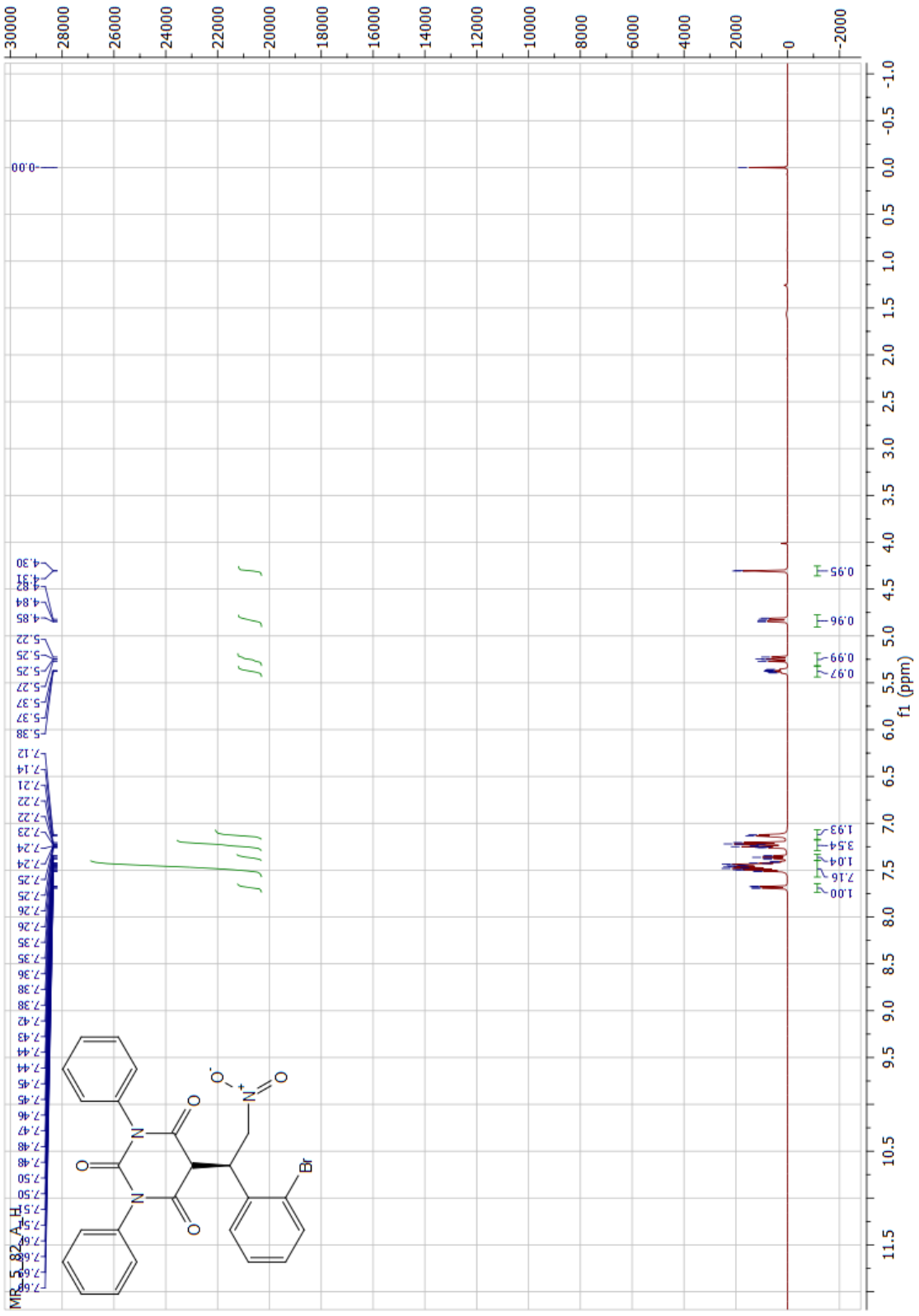

Figure 115. ^{1}H NMR spectrum of **127** (500 MHz, $CDCl_3$).

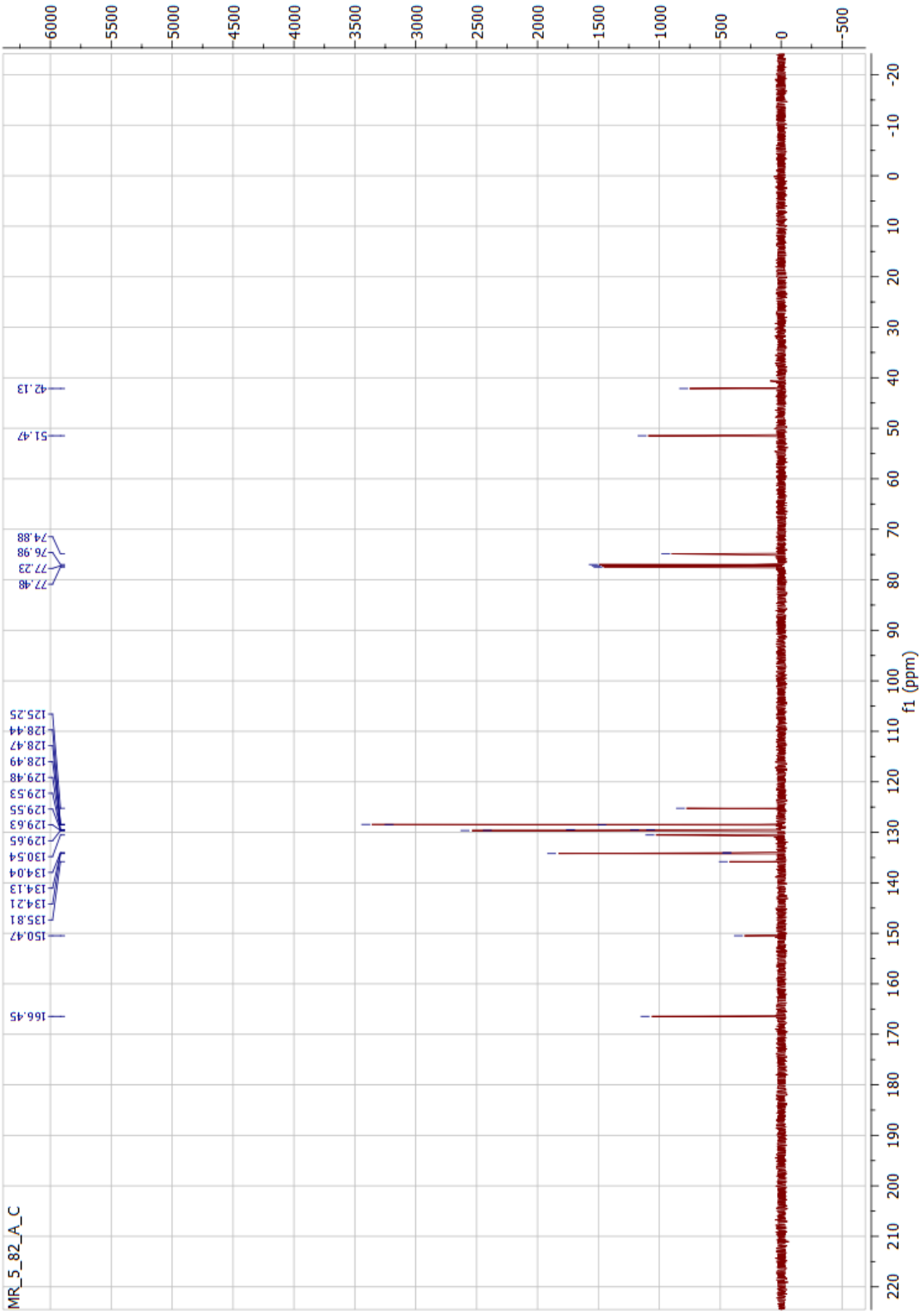

Figure 116. ^{13}C NMR spectrum of **127** (125 MHz, $CDCl_3$).

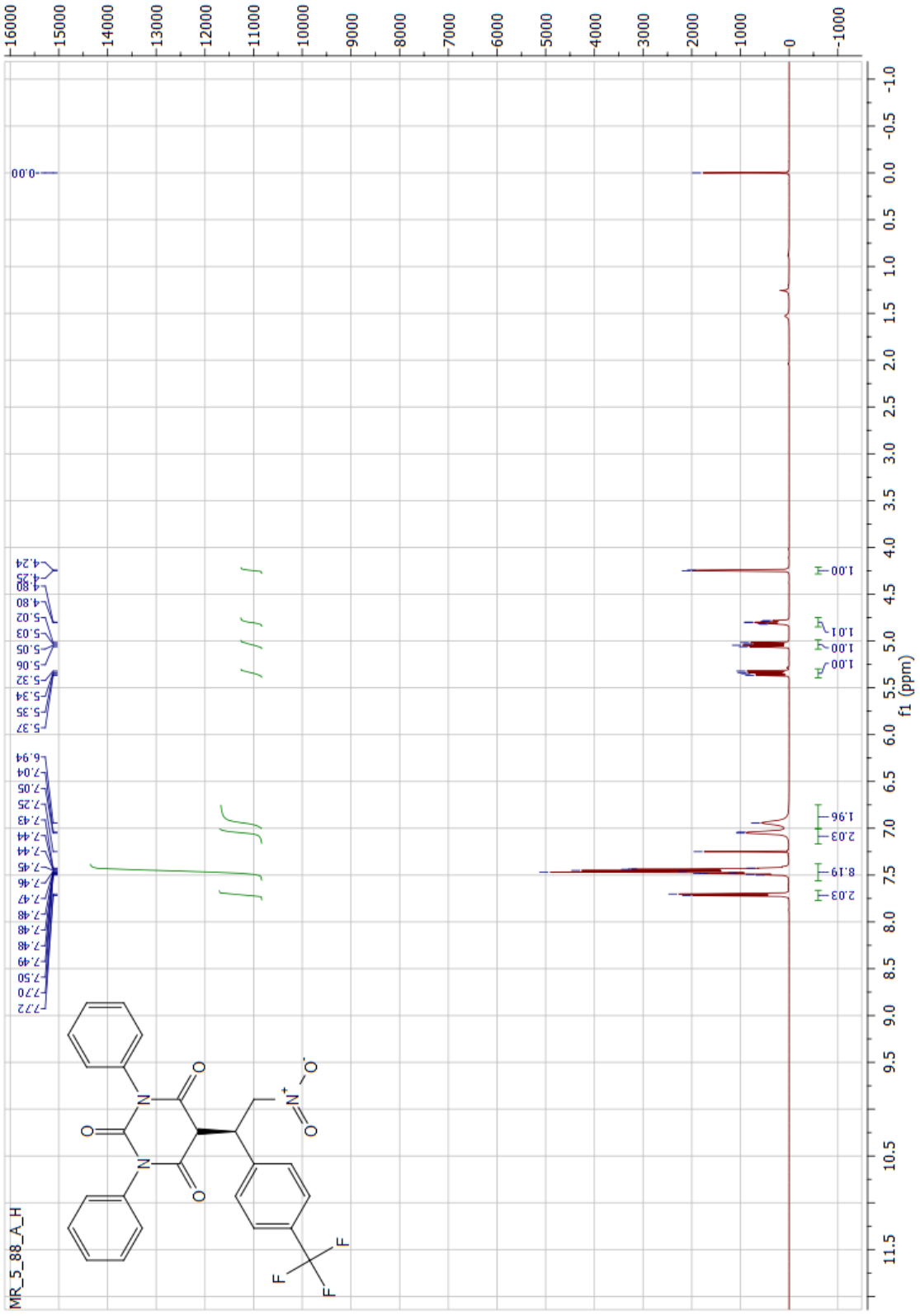

Figure 117. ^{1}H NMR spectrum of **128** (500 MHz, $CDCl_3$).

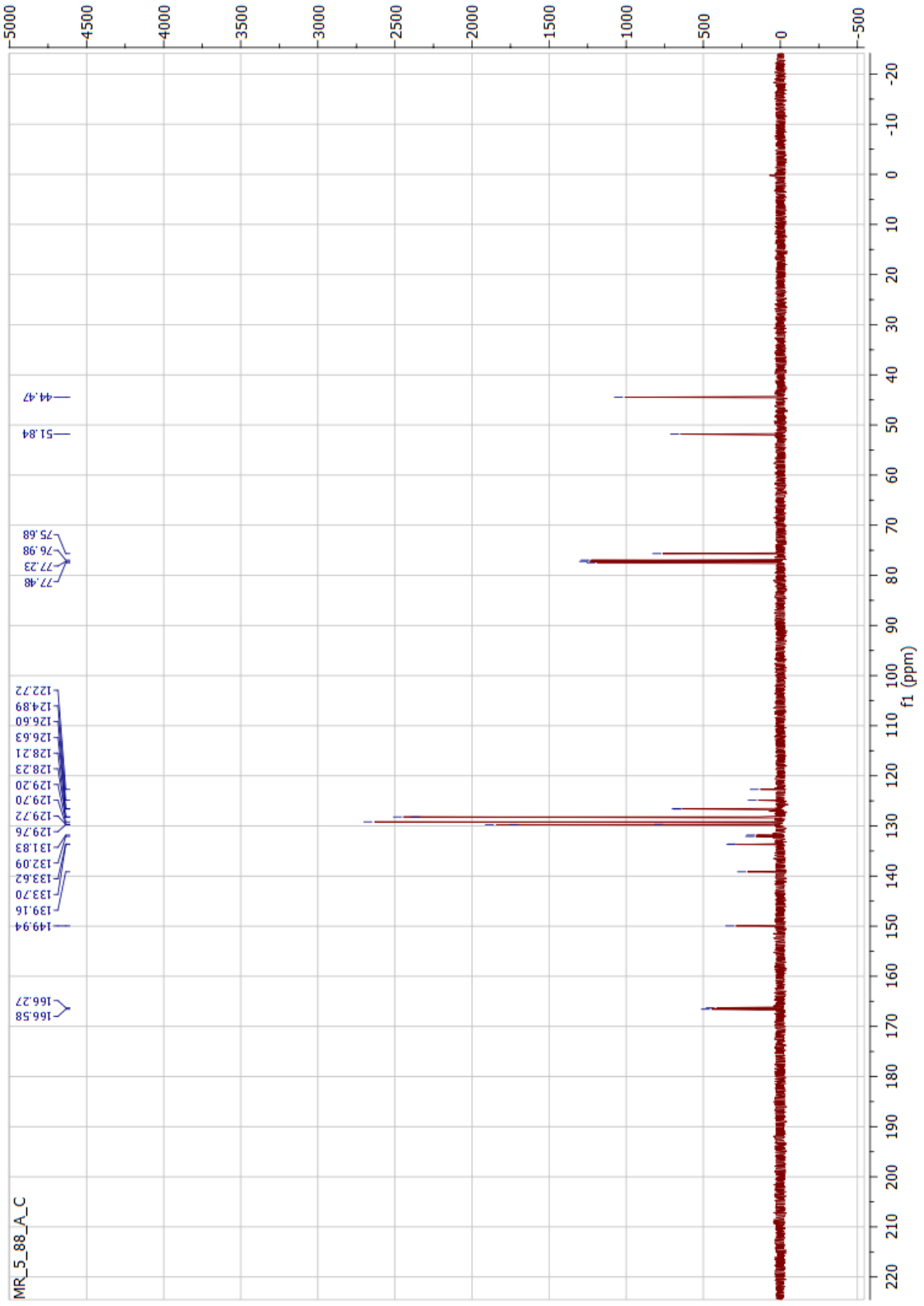

Figure 118. ^{13}C NMR spectrum of **128** (125 MHz, $CDCl_3$).

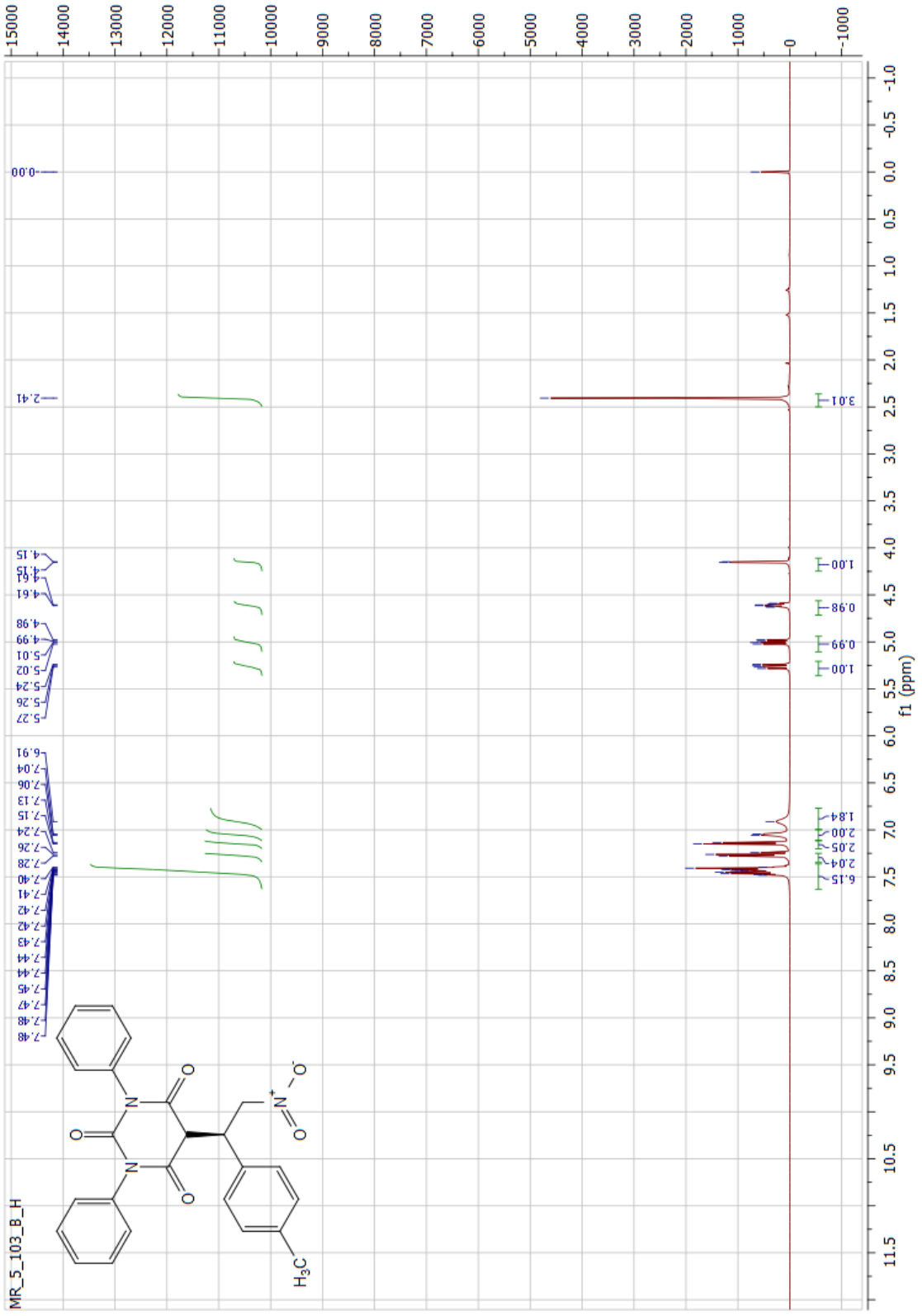

Figure 119. ^{1}H NMR spectrum of **129** (500 MHz, $CDCl_3$).

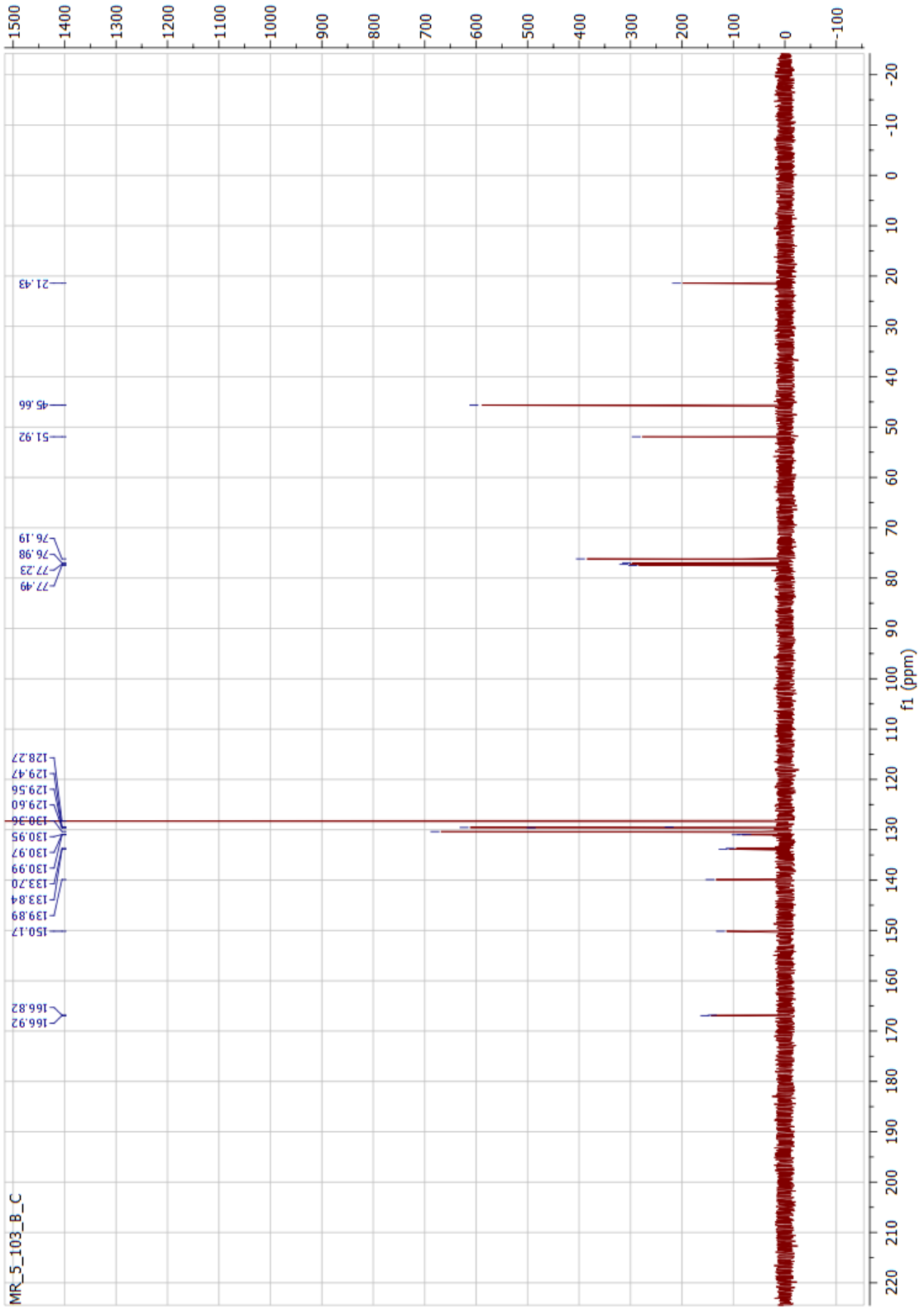

Figure 120. ^{13}C NMR spectrum of **129** (125 MHz, $CDCl_3$).

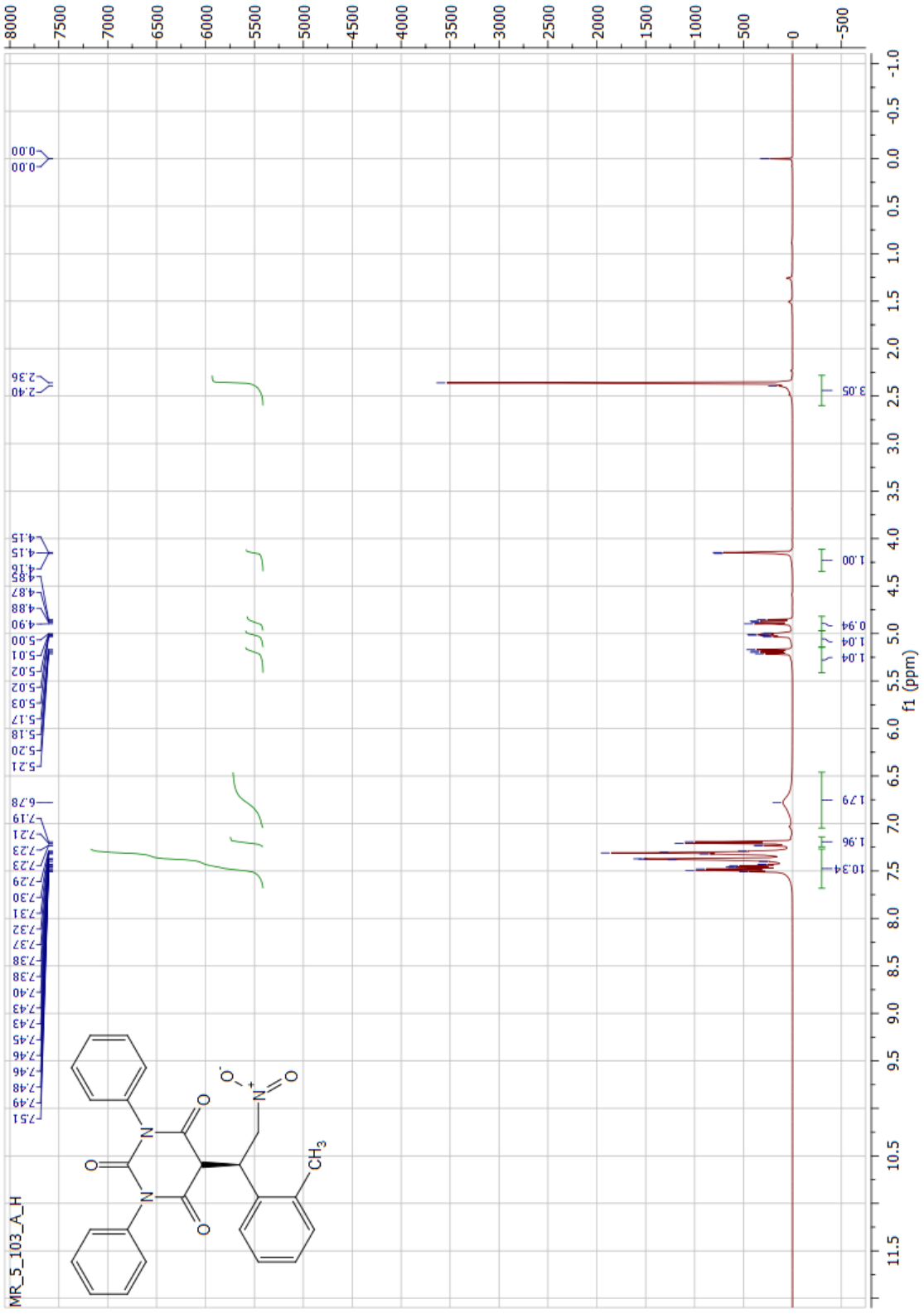

Figure 121. ^{1}H NMR spectrum of **130** (500 MHz, $CDCl_3$).

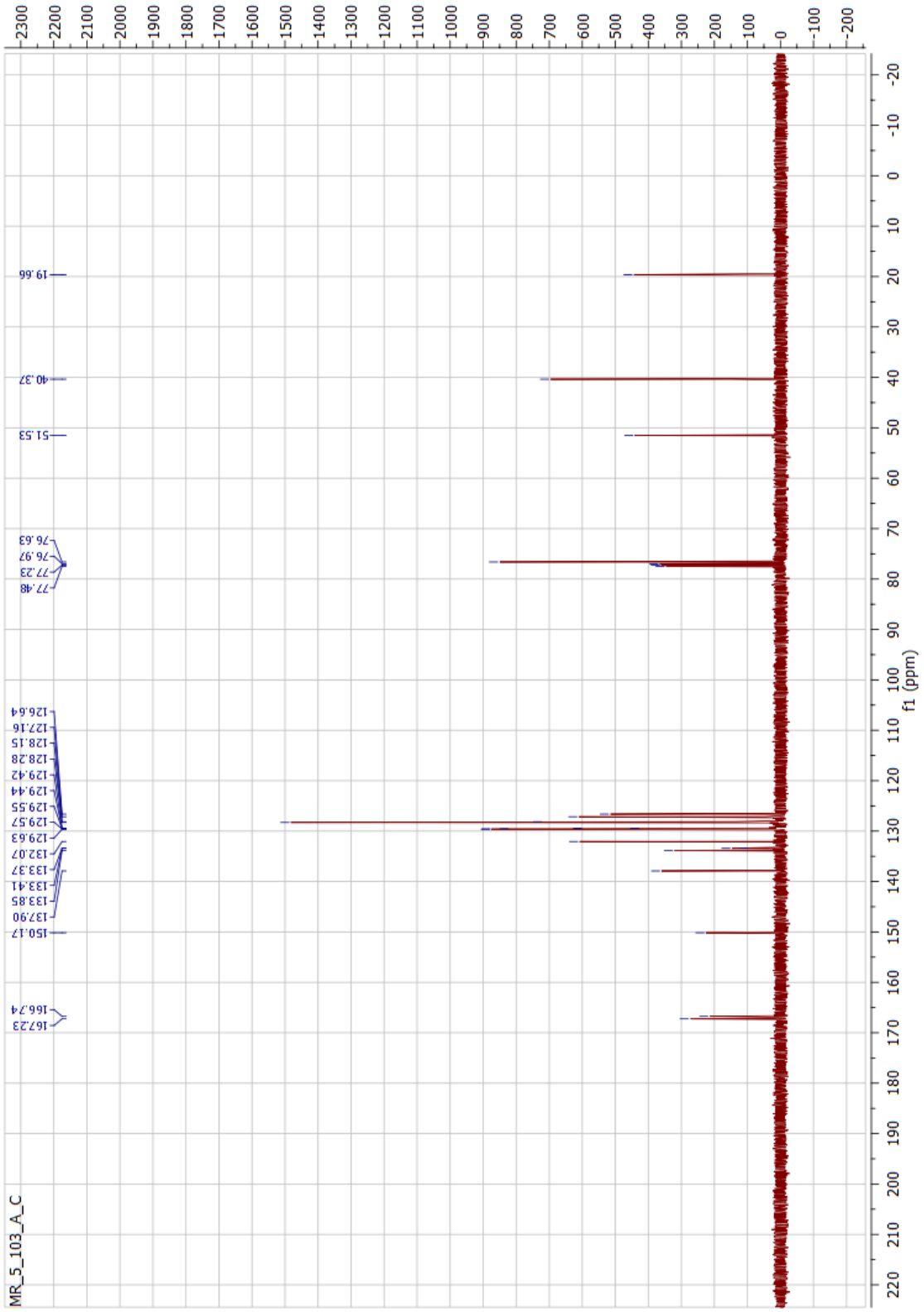

Figure 122. ^{13}C NMR spectrum of **130** (125 MHz, $CDCl_3$).

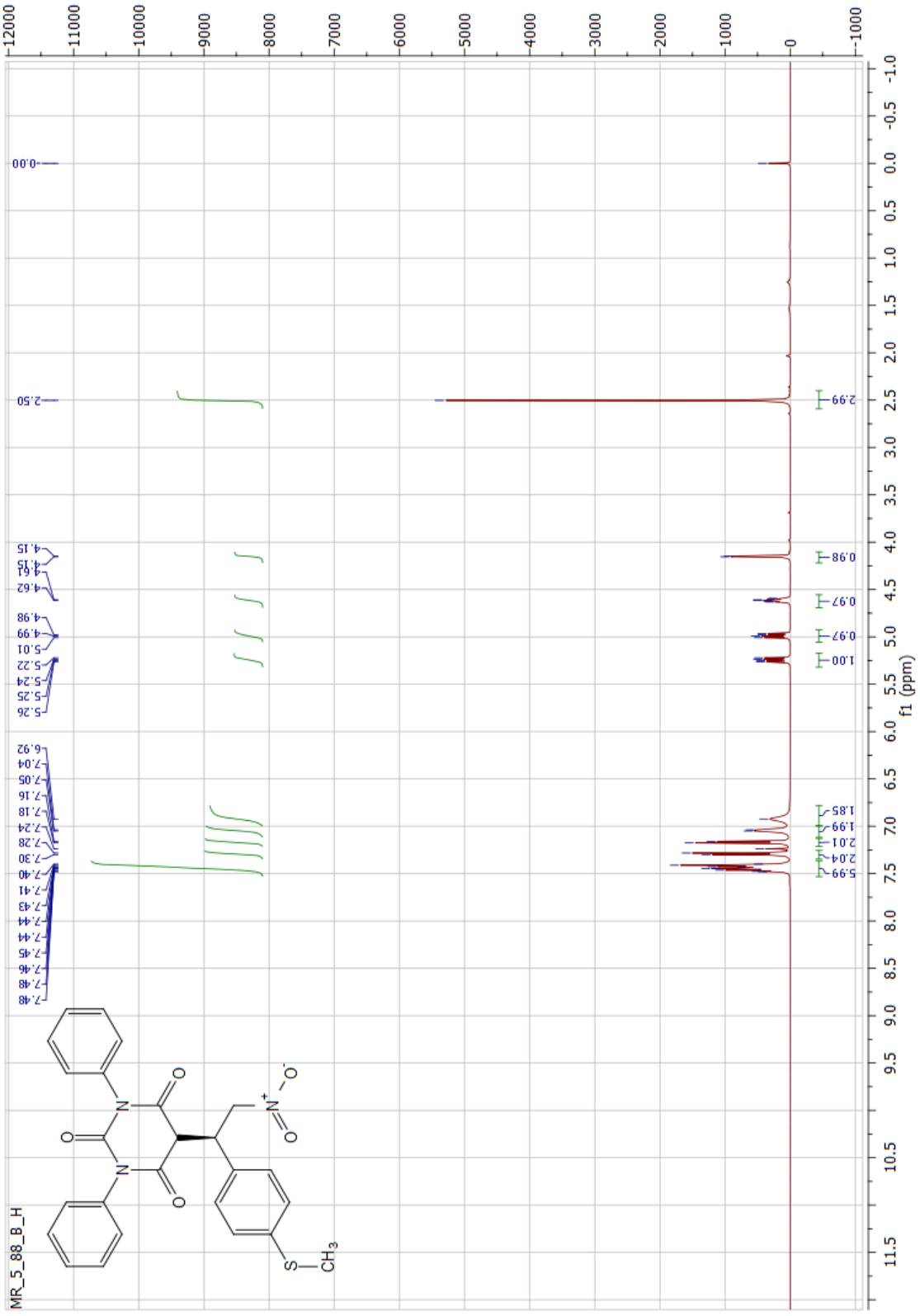

Figure 123. ^{1}H NMR spectrum of **131** (500 MHz, $CDCl_3$).

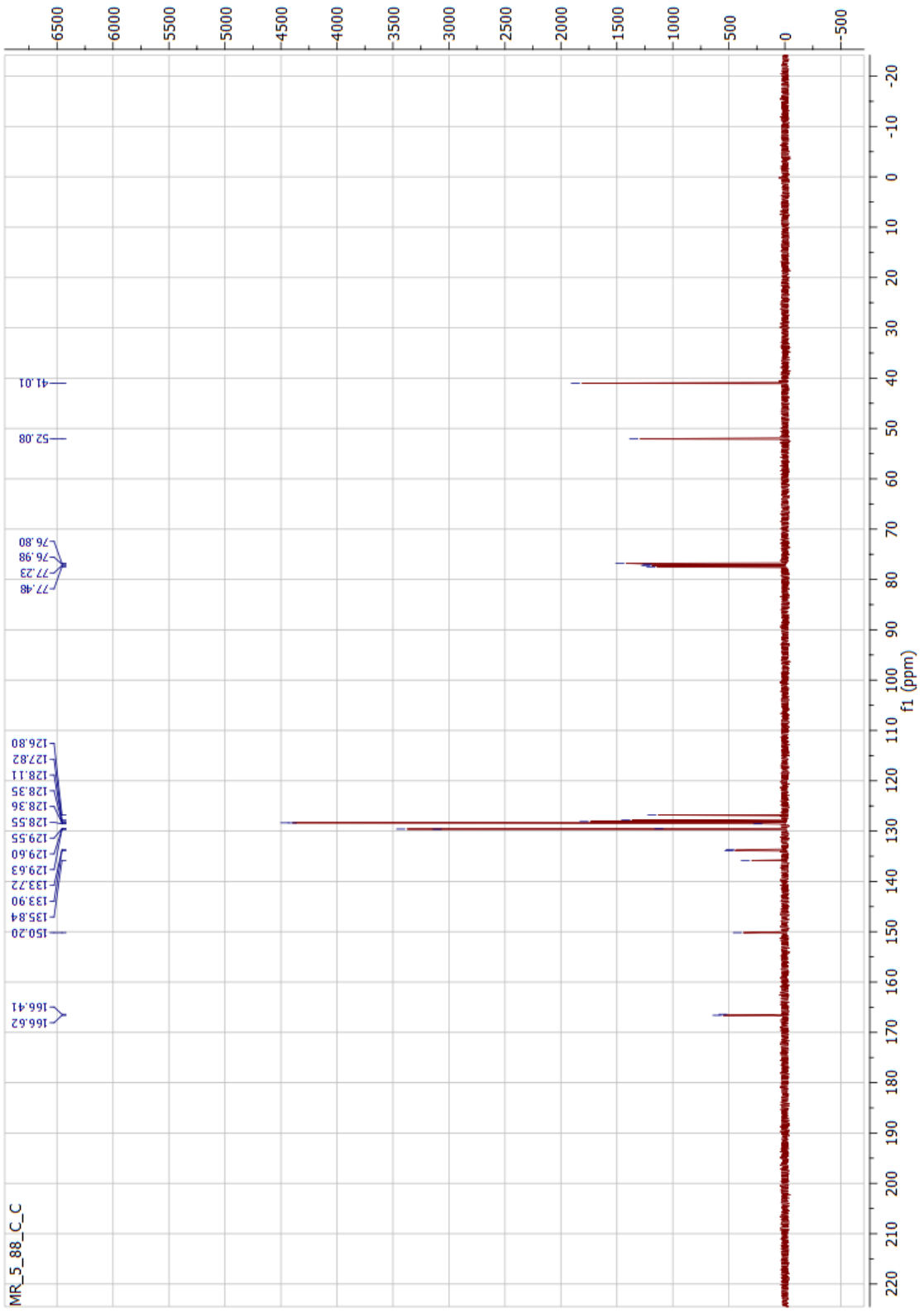

Figure 124. ^{13}C NMR spectrum of **131** (125 MHz, $CDCl_3$).

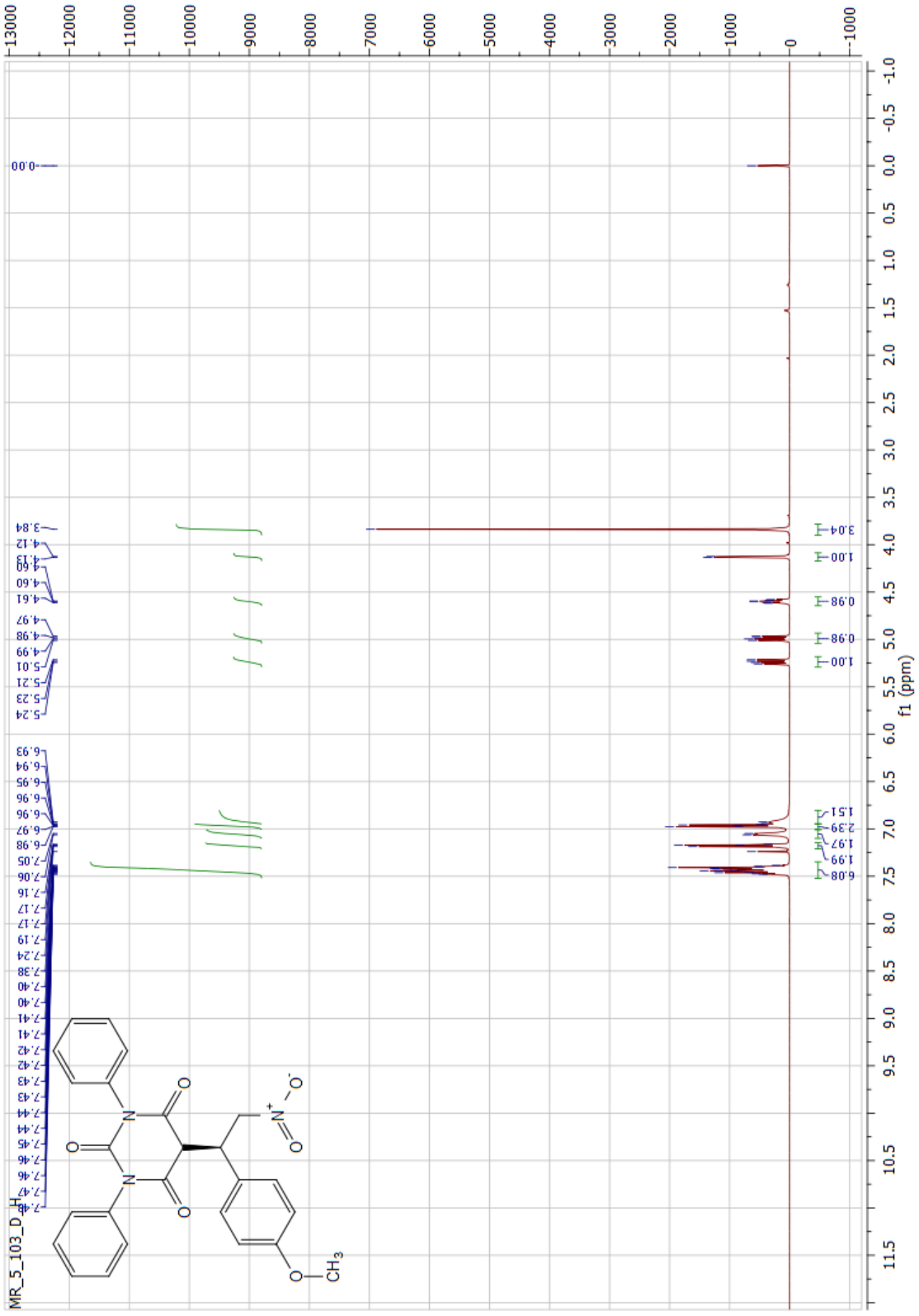

Figure 125. ^{1}H NMR spectrum of **132** (500 MHz, $CDCl_3$).

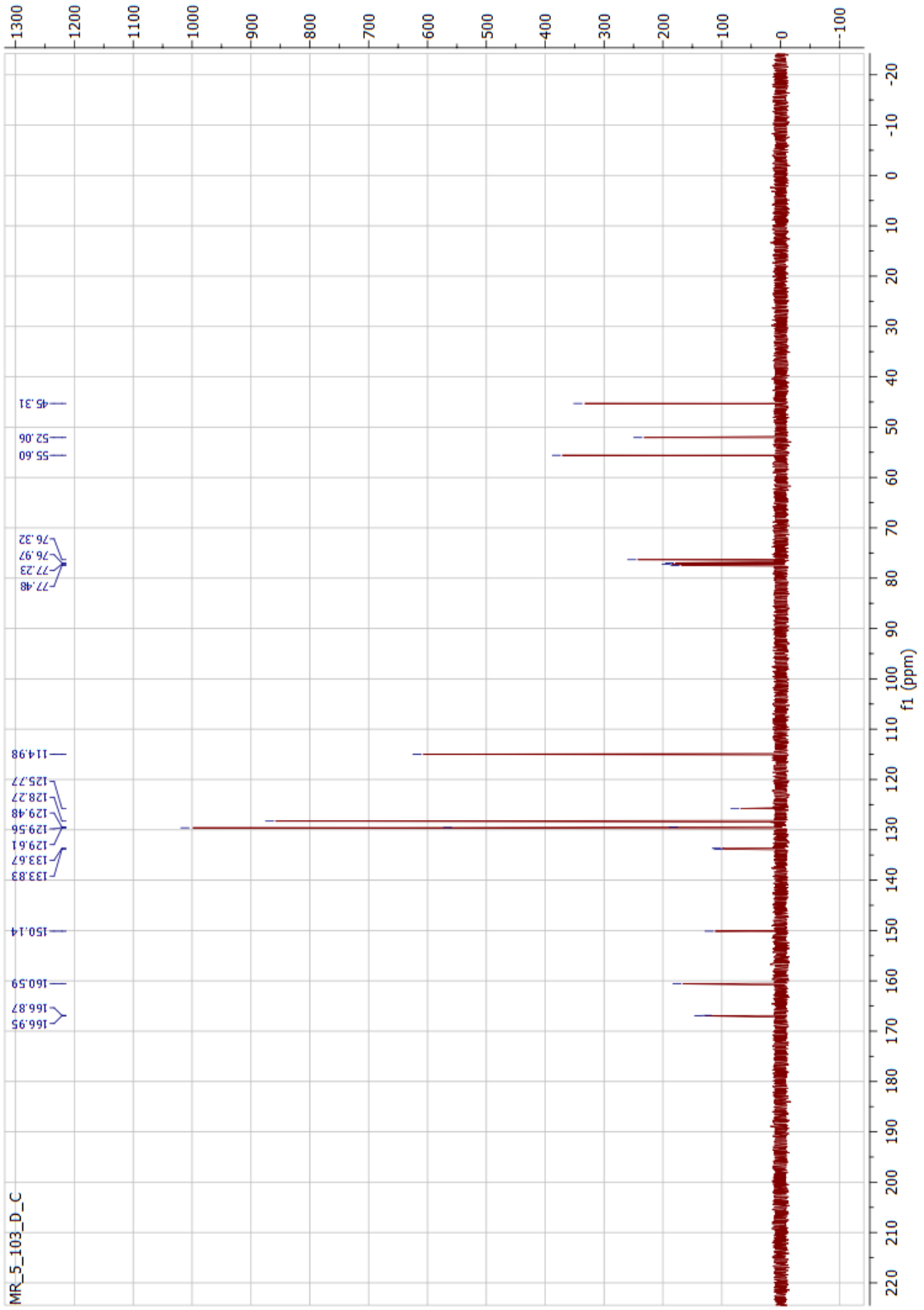

Figure 126. ^{13}C NMR spectrum of **132** (125 MHz, $CDCl_3$).

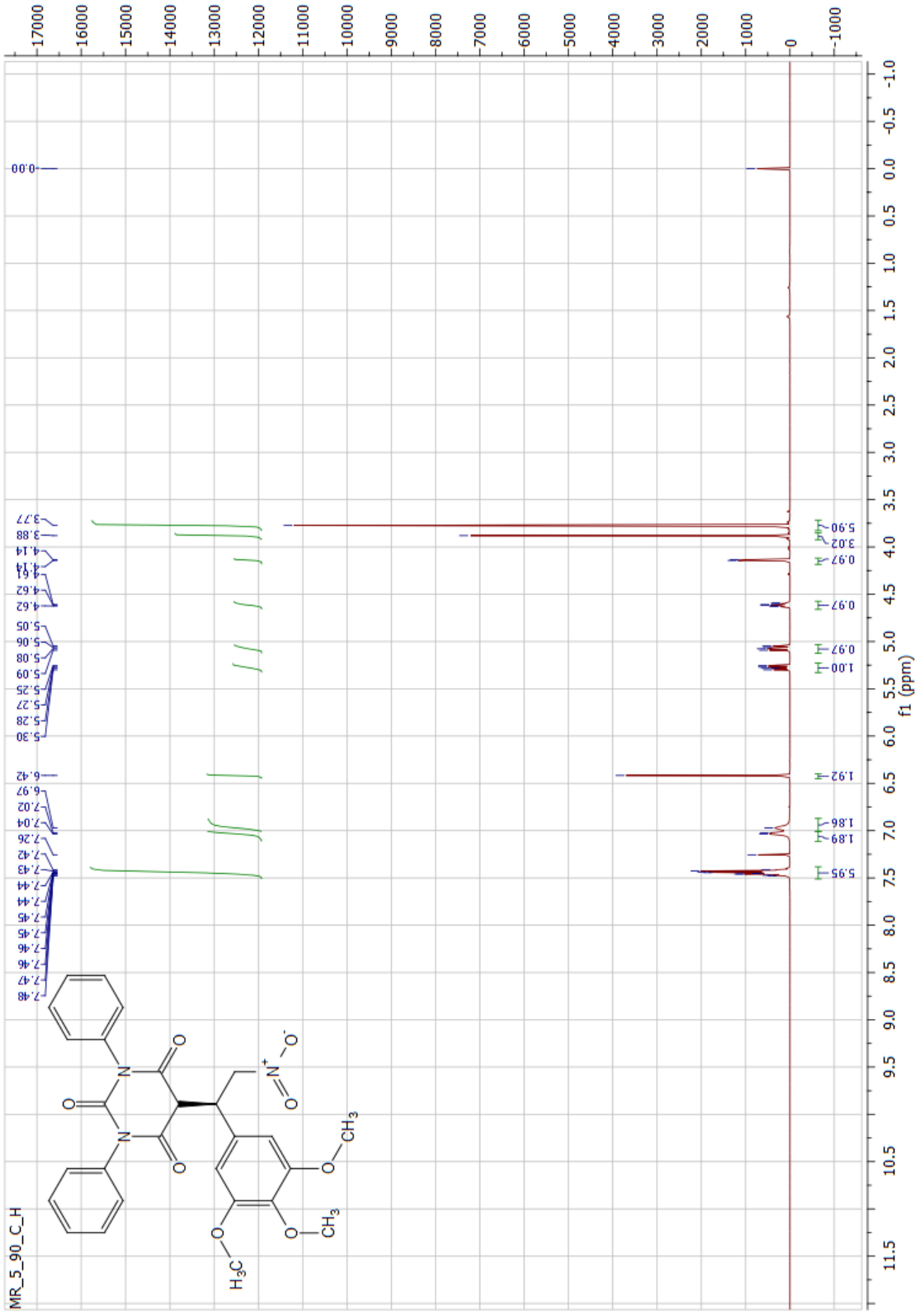

Figure 127. ^{1}H NMR spectrum of **133** (500 MHz, $CDCl_3$).

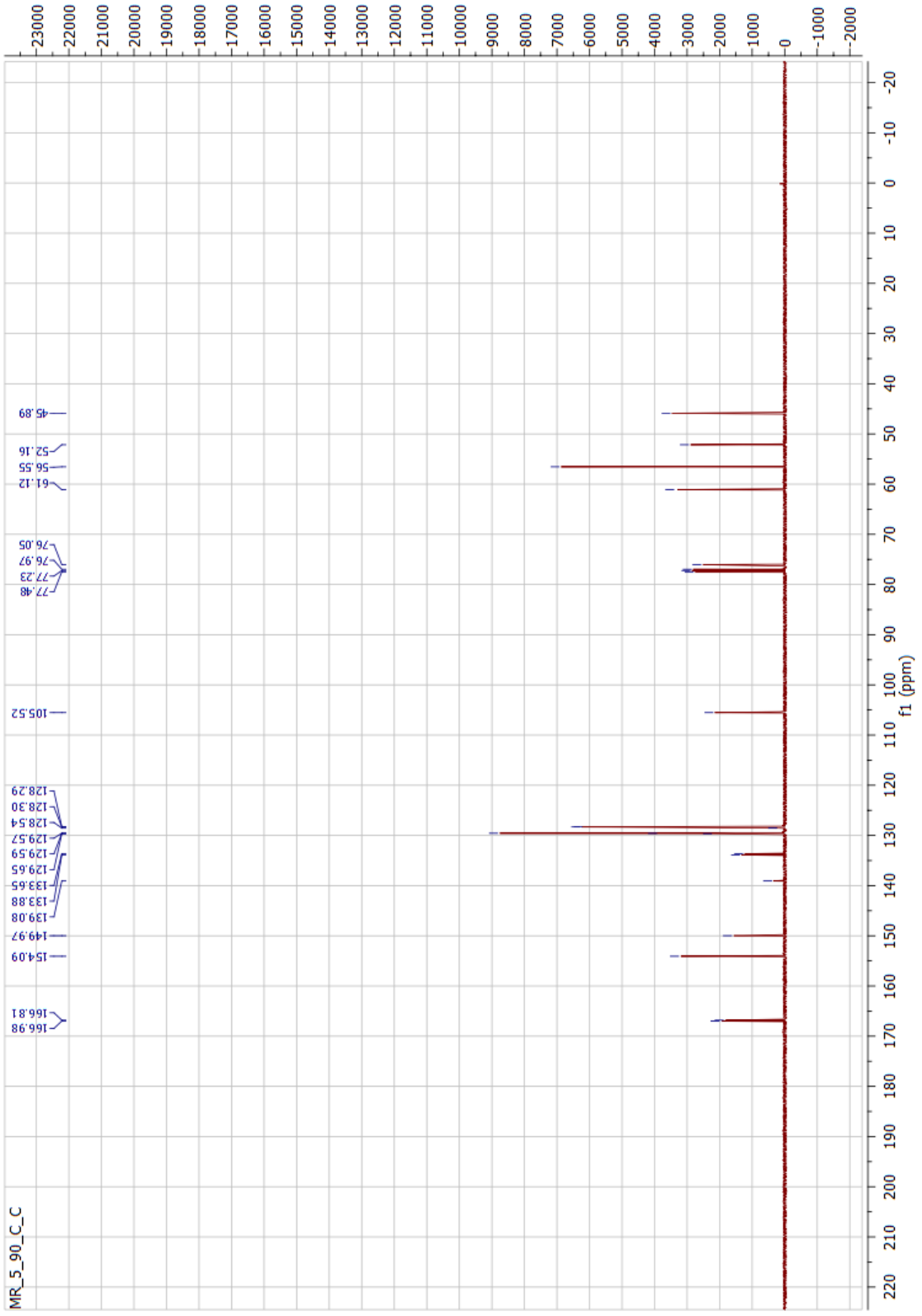

Figure 128. ^{13}C NMR spectrum of **133** (125 MHz, $CDCl_3$).

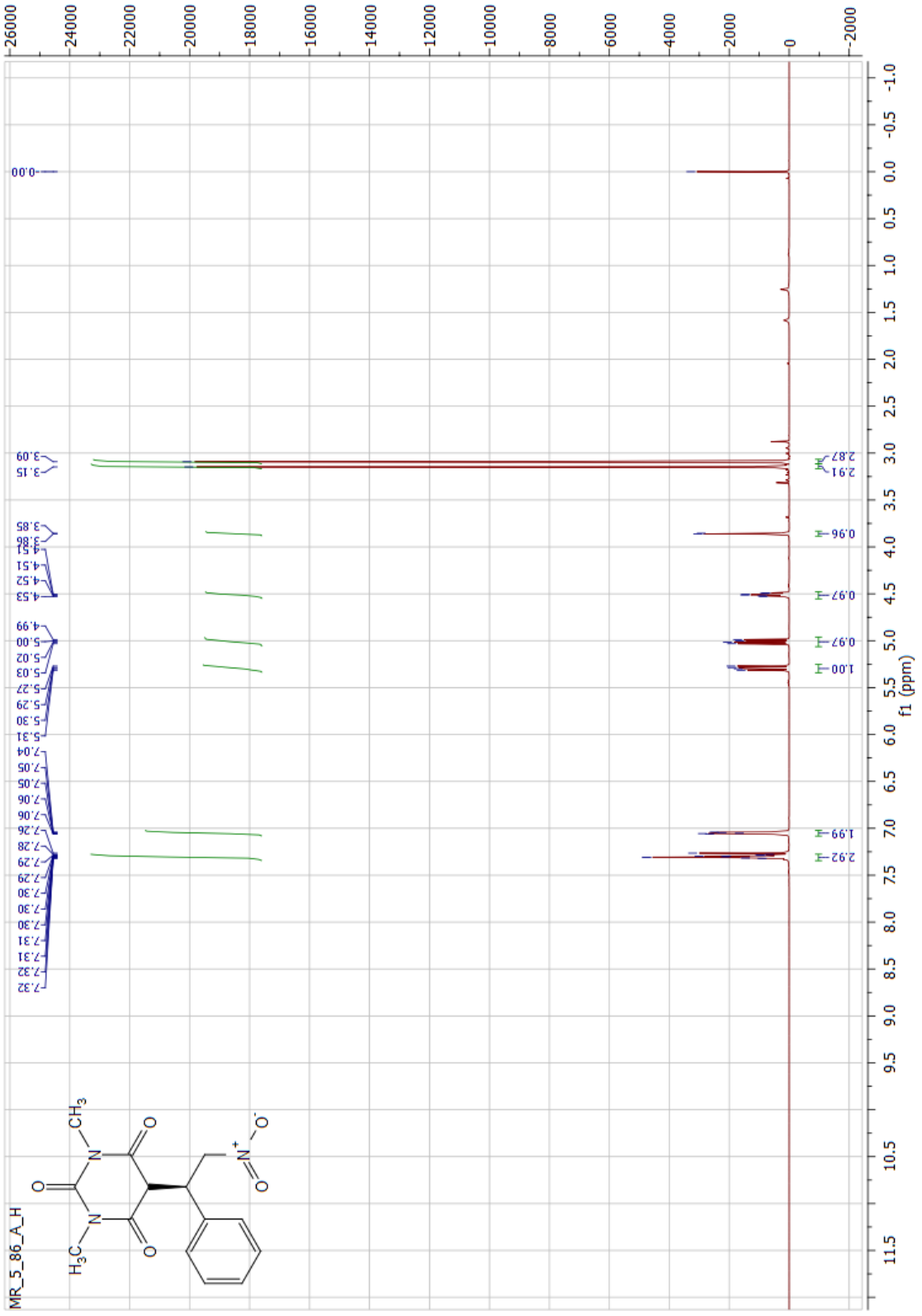

Figure 129. ^{1}H NMR spectrum of **134** (500 MHz, $CDCl_3$).

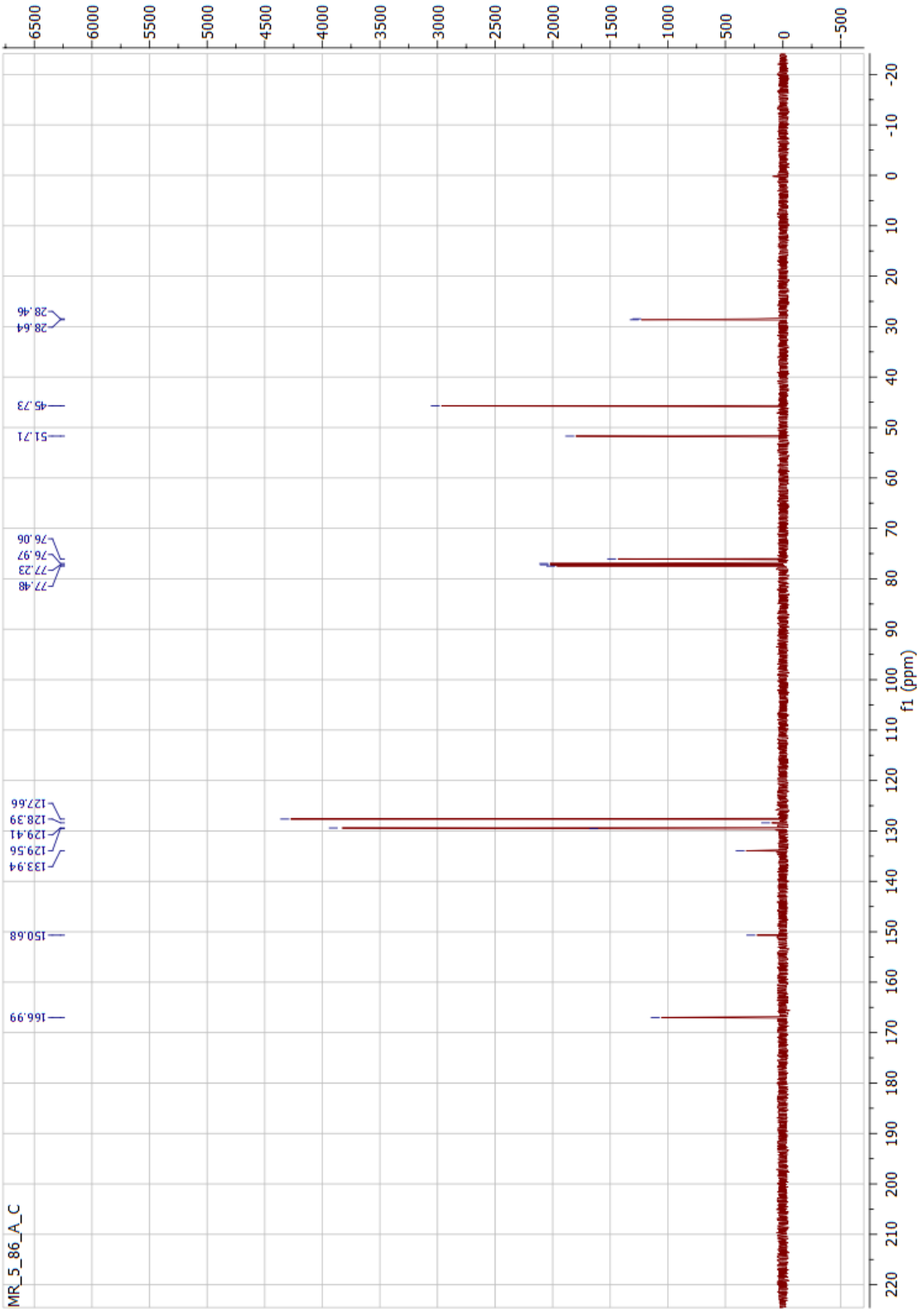

Figure 130. ^{13}C NMR spectrum of **134** (125 MHz, $CDCl_3$).

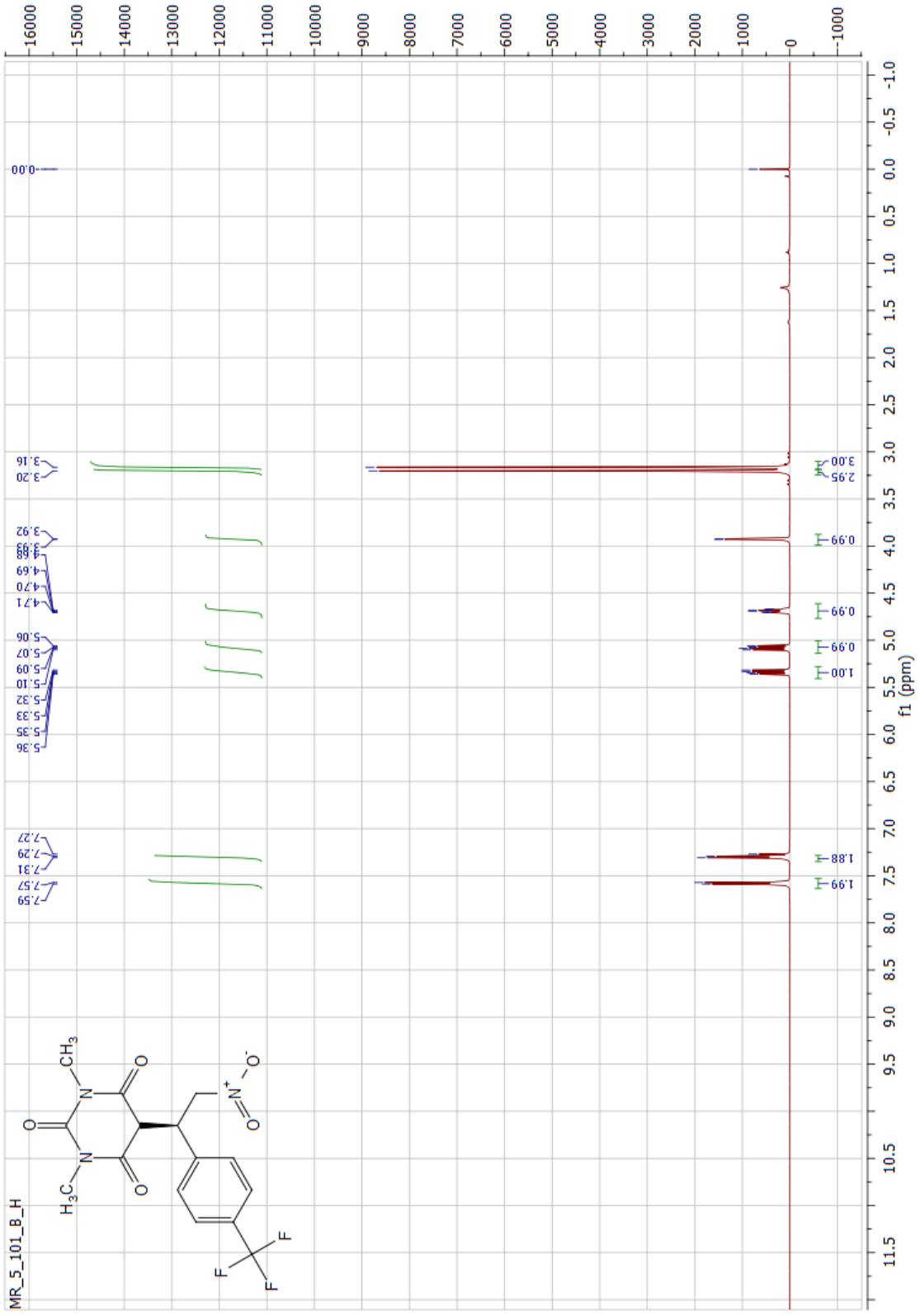

Figure 131. ^{1}H NMR spectrum of **135** (500 MHz, $CDCl_3$).

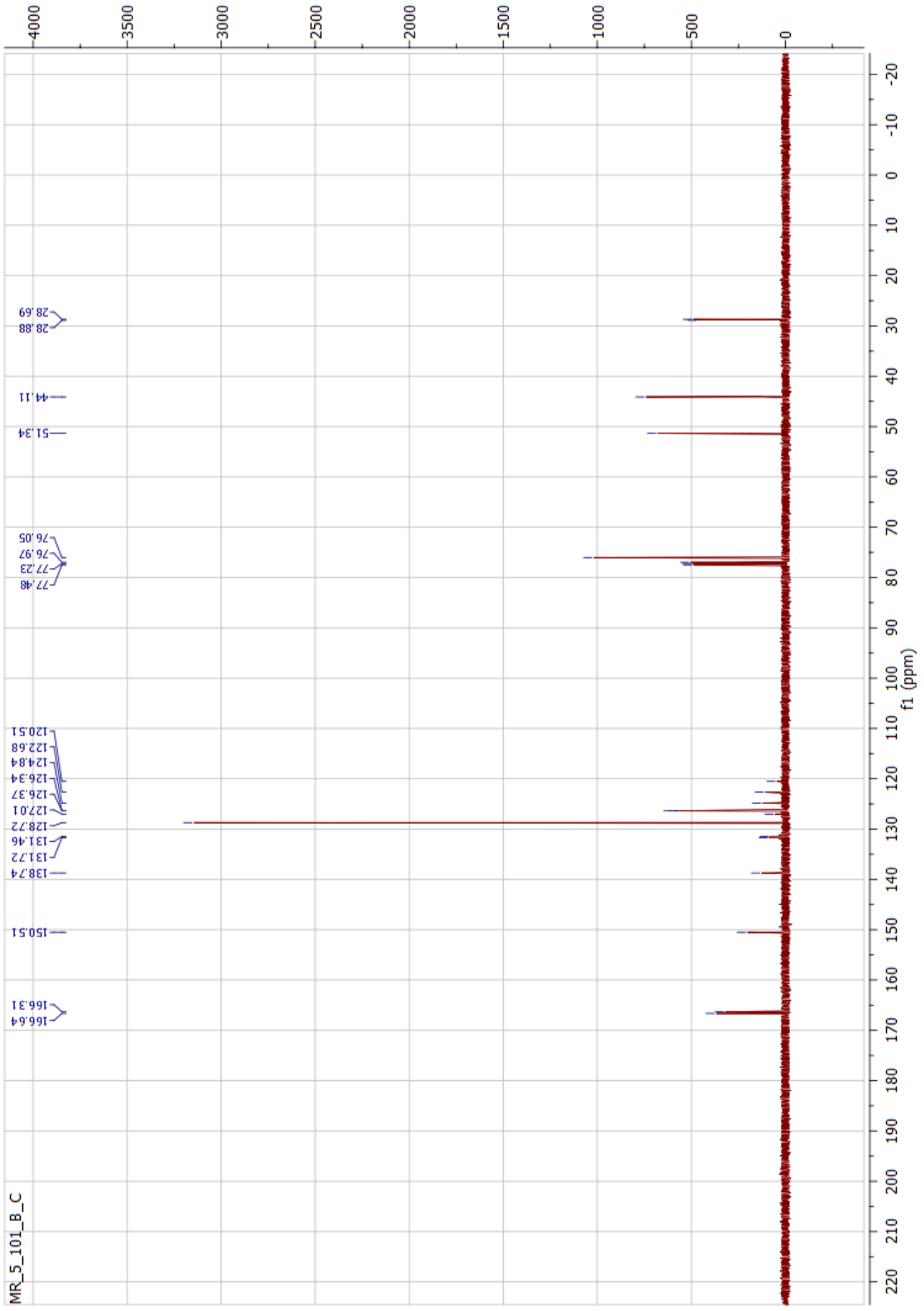

Figure 132. ^{13}C NMR spectrum of **135** (125 MHz, $CDCl_3$).

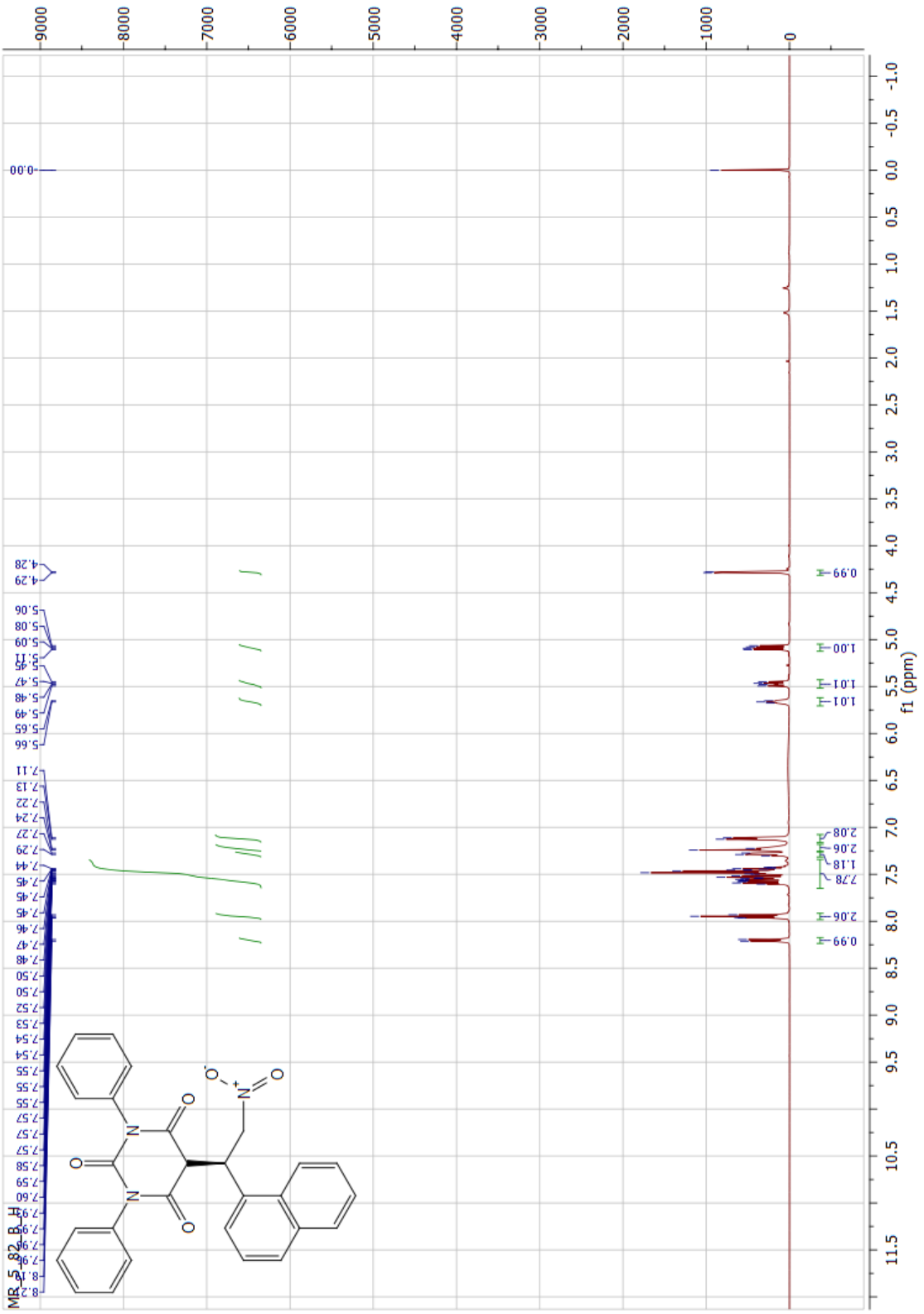

Figure 133. ^{1}H NMR spectrum of **136** (500 MHz, $CDCl_3$).

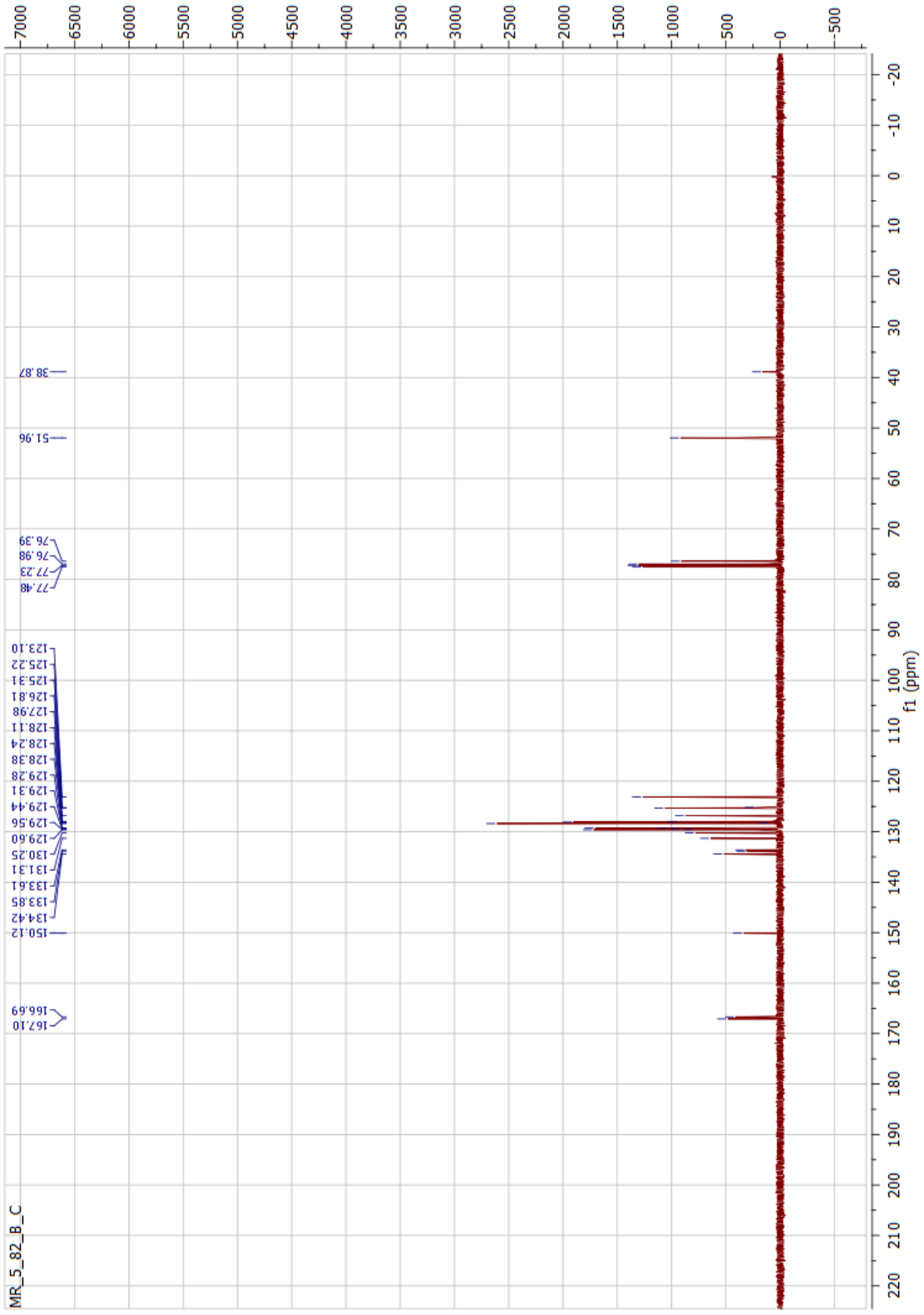

Figure 134. ^{13}C NMR spectrum of **136** (125 MHz, $CDCl_3$).

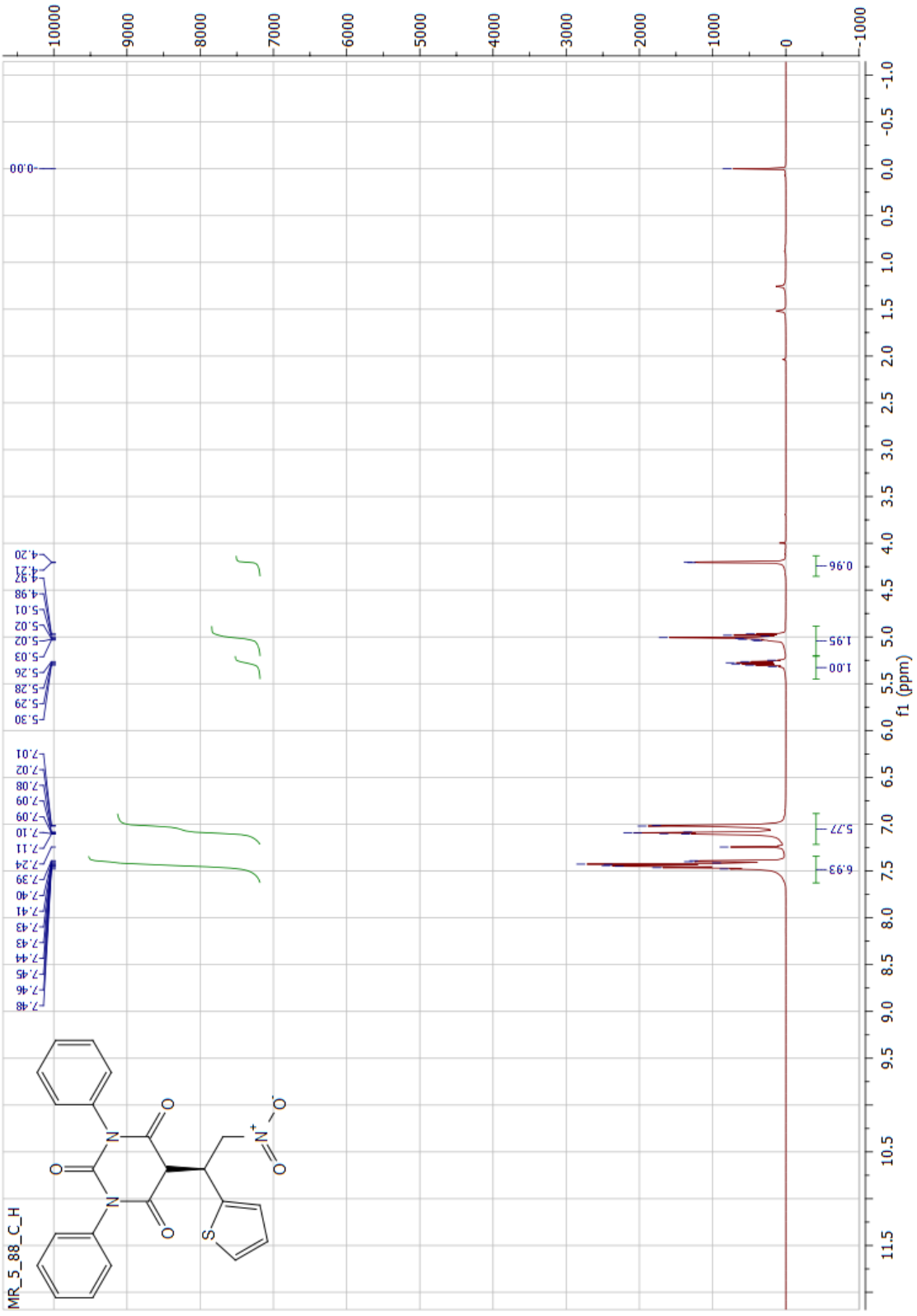

Figure 135. ^{1}H NMR spectrum of **137** (500 MHz, $CDCl_3$).

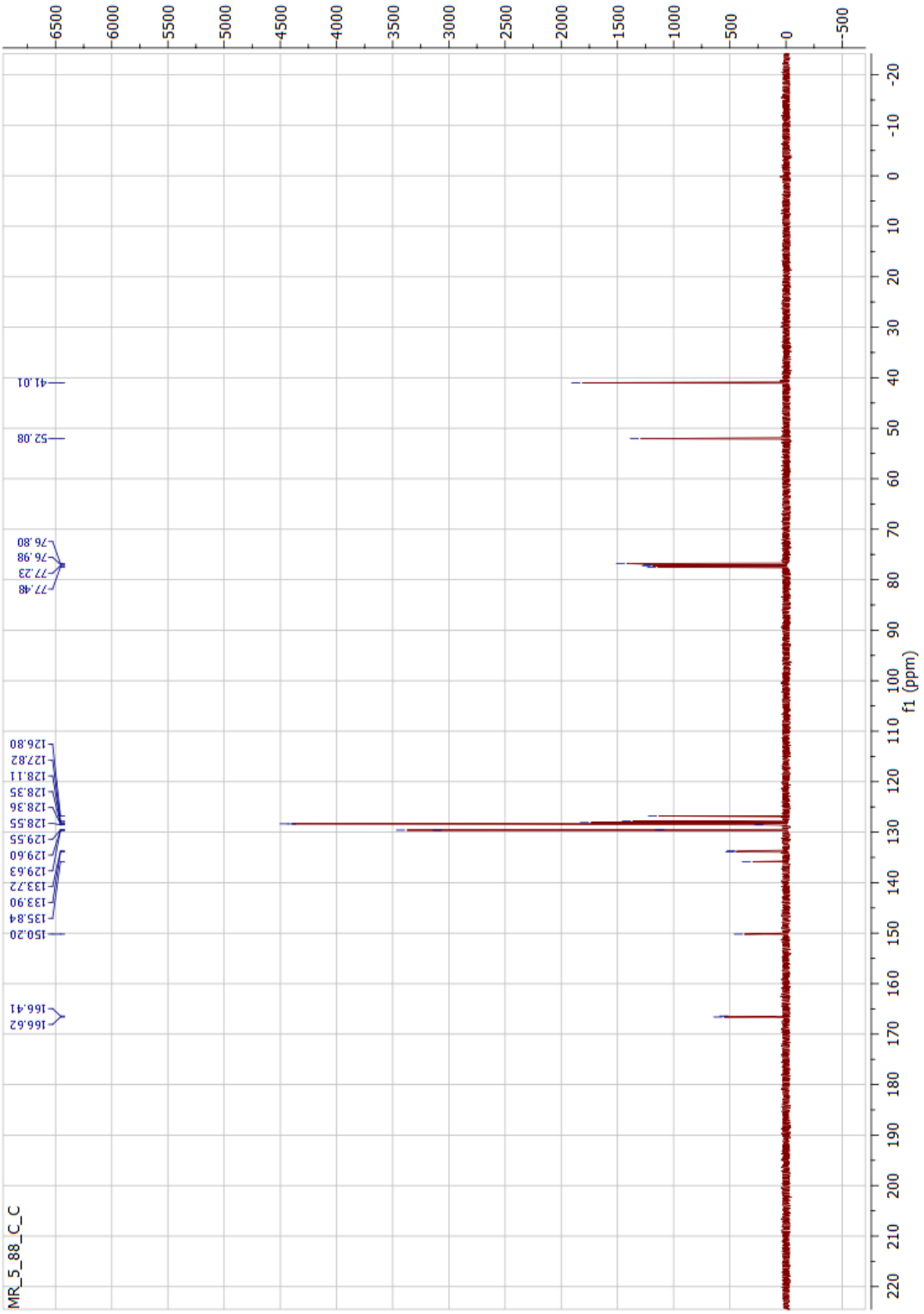

Figure 136. ^{13}C NMR spectrum of **137** (125 MHz, $CDCl_3$).

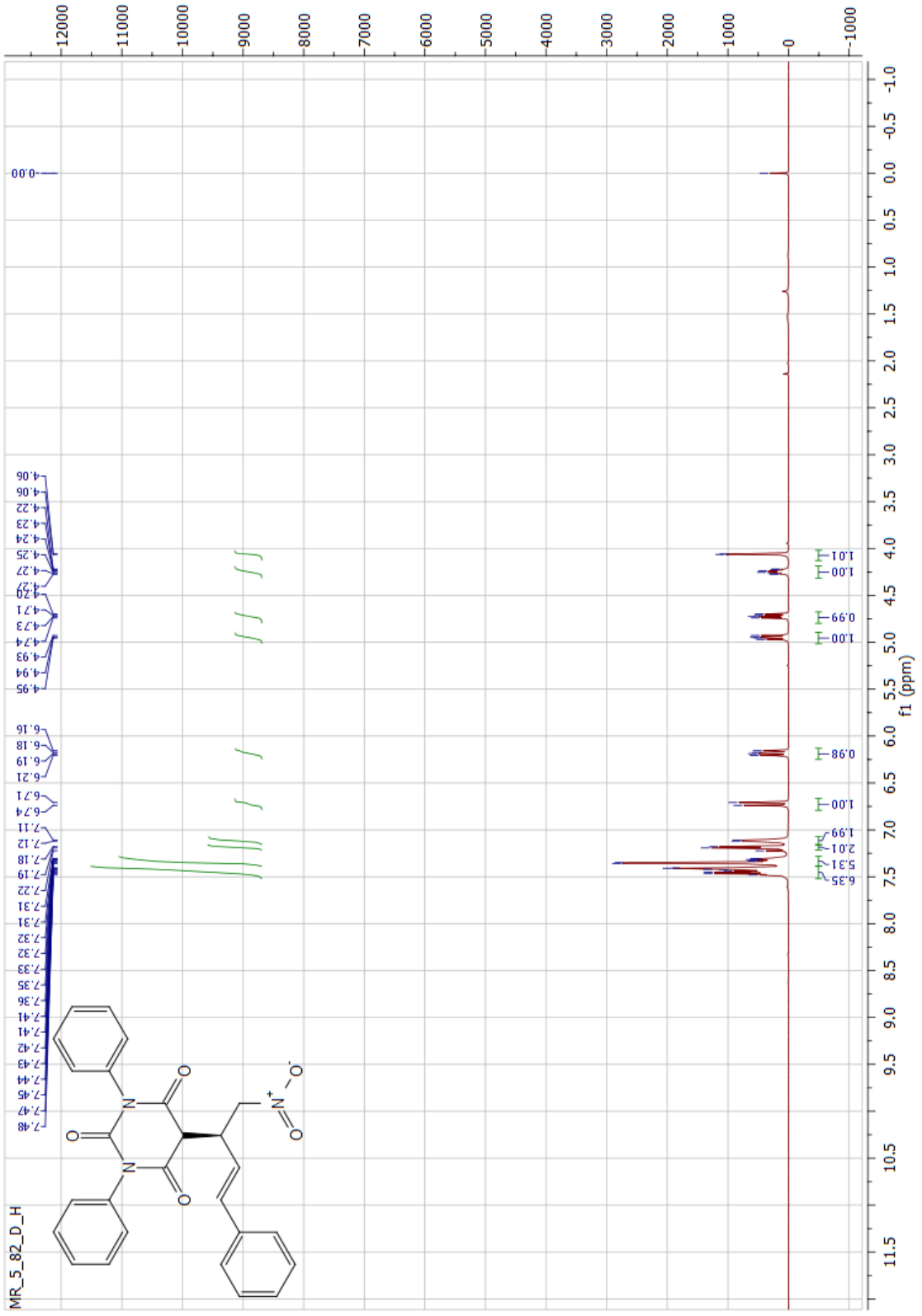

Figure 137. ^{1}H NMR spectrum of **138** (500 MHz, $CDCl_3$).

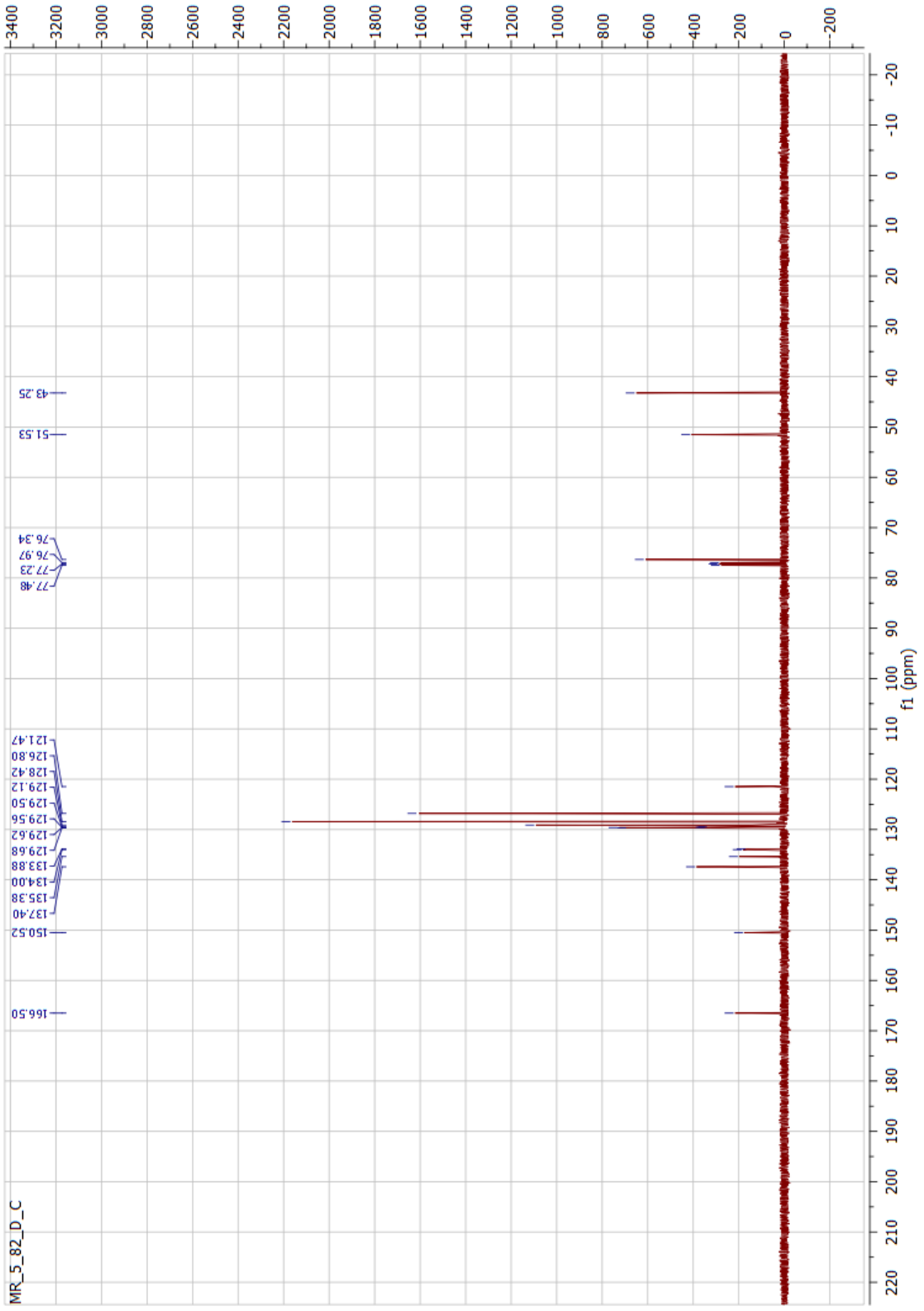

Figure 138. ^{13}C NMR spectrum of **138** (125 MHz, $CDCl_3$).

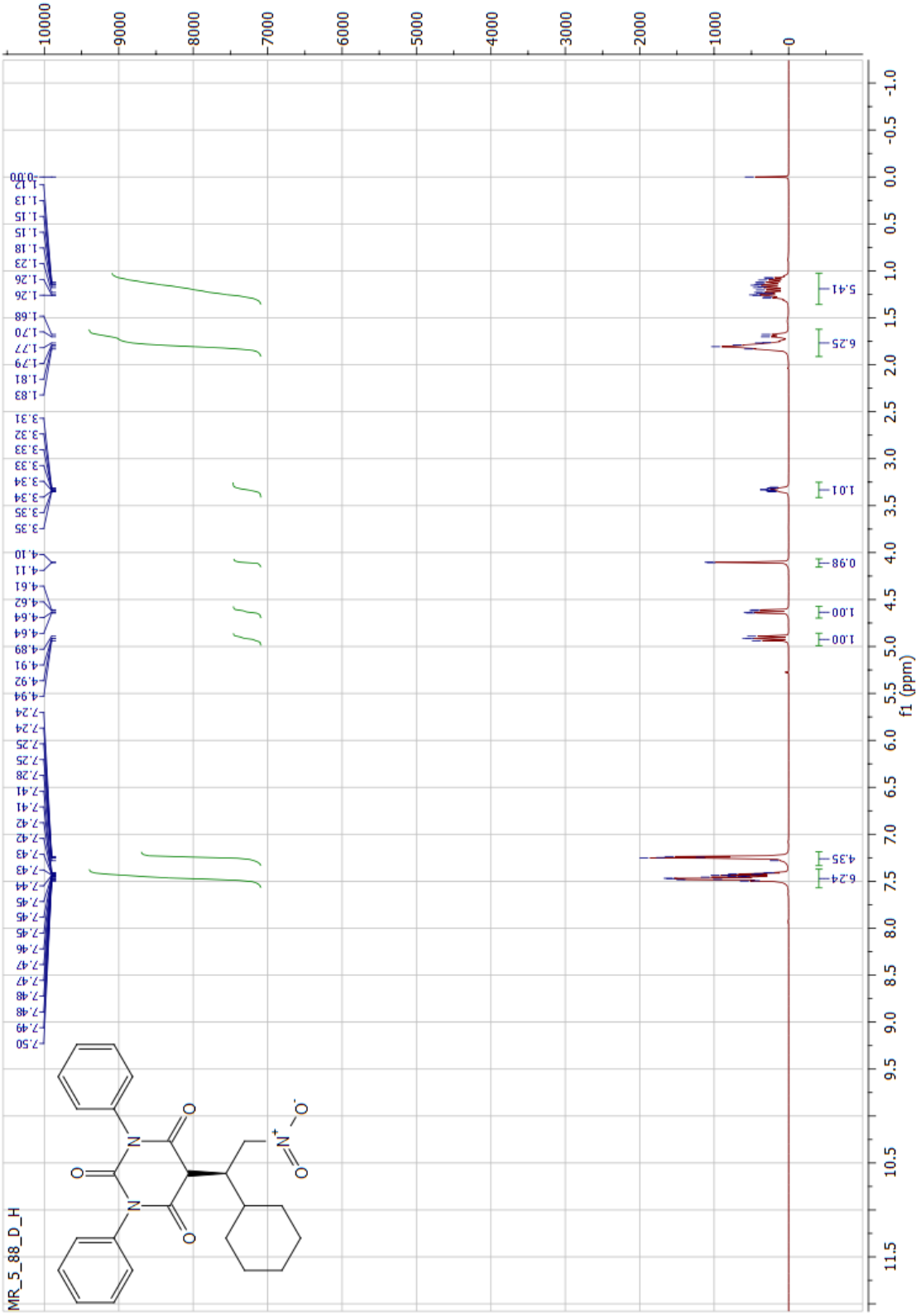

Figure 139. ^{1}H NMR spectrum of **139** (500 MHz, $CDCl_3$).

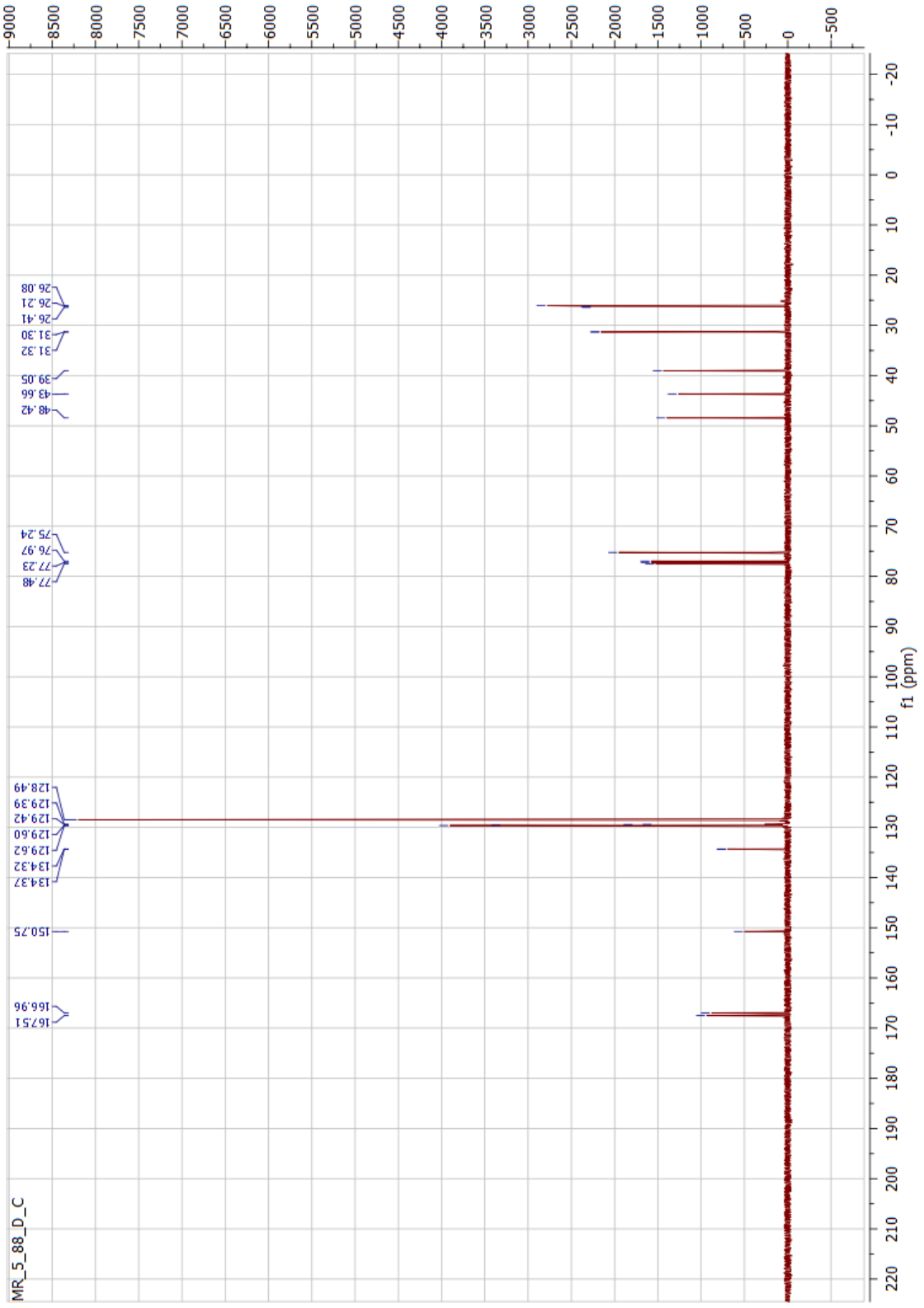

Figure 140. ^{13}C NMR spectrum of **139** (125 MHz, $CDCl_3$).

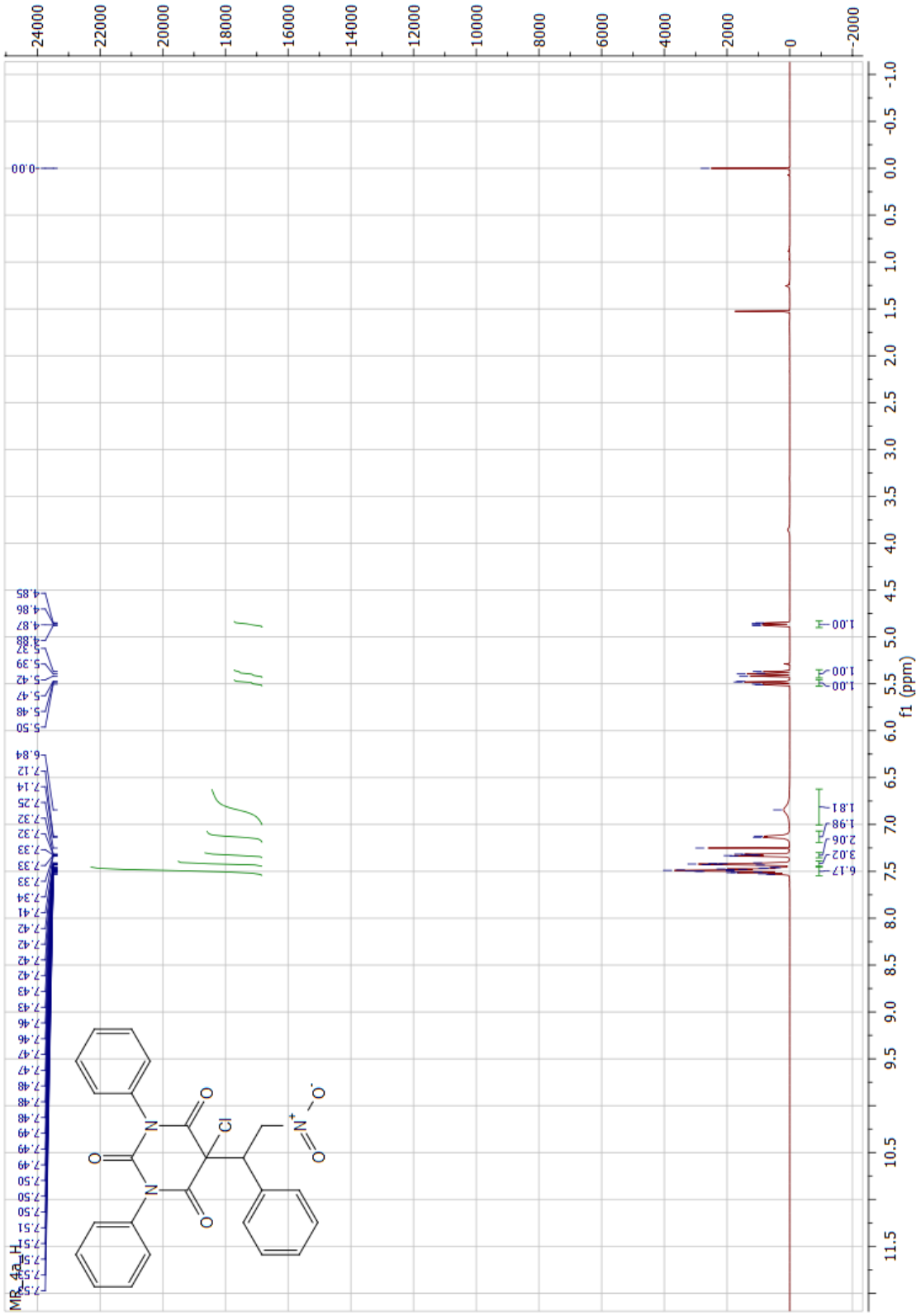

Figure 141. ^{1}H NMR spectrum of **140** (500 MHz, $CDCl_3$).

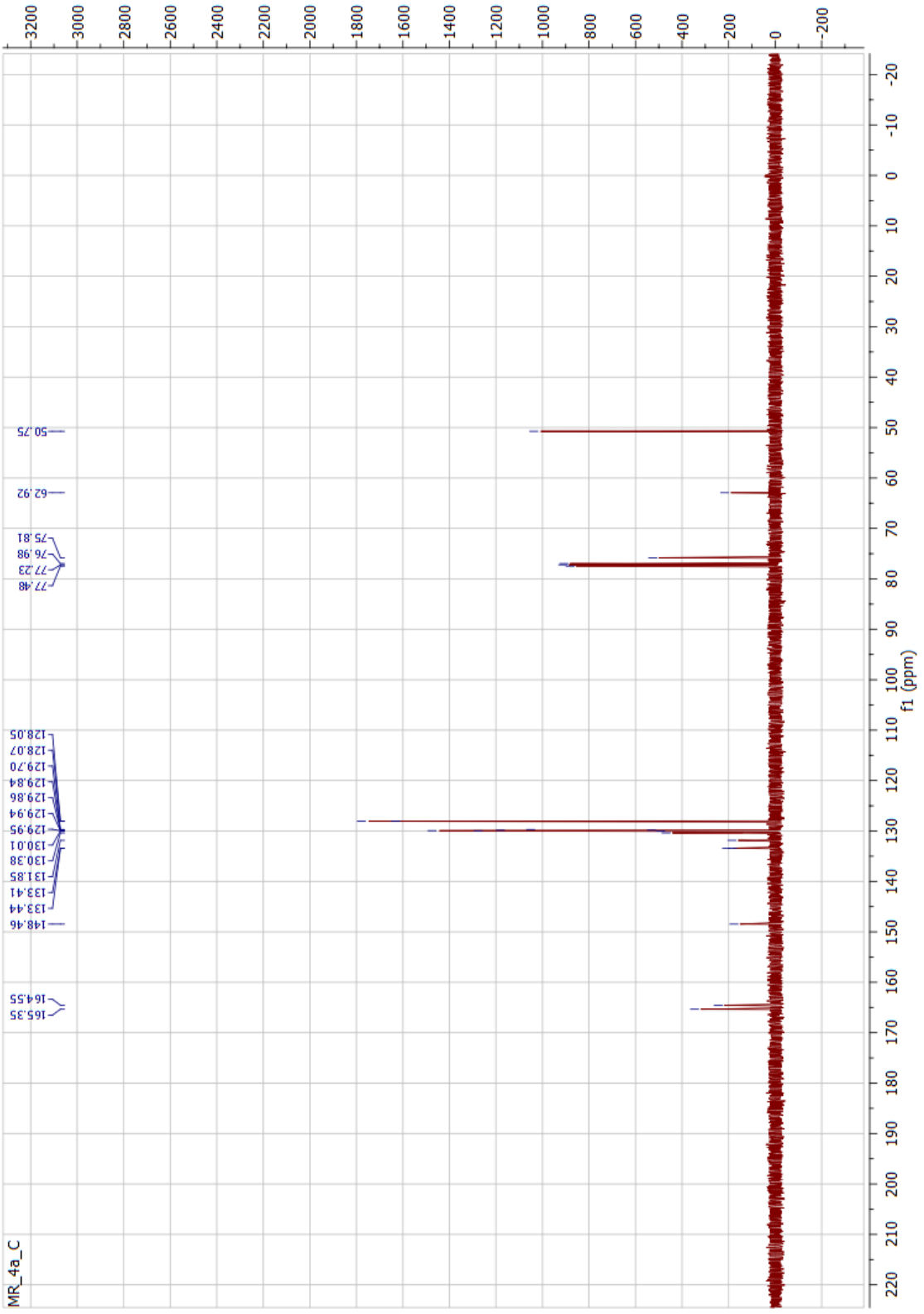

Figure 142. ^{13}C NMR spectrum of **140** (125 MHz, $CDCl_3$).

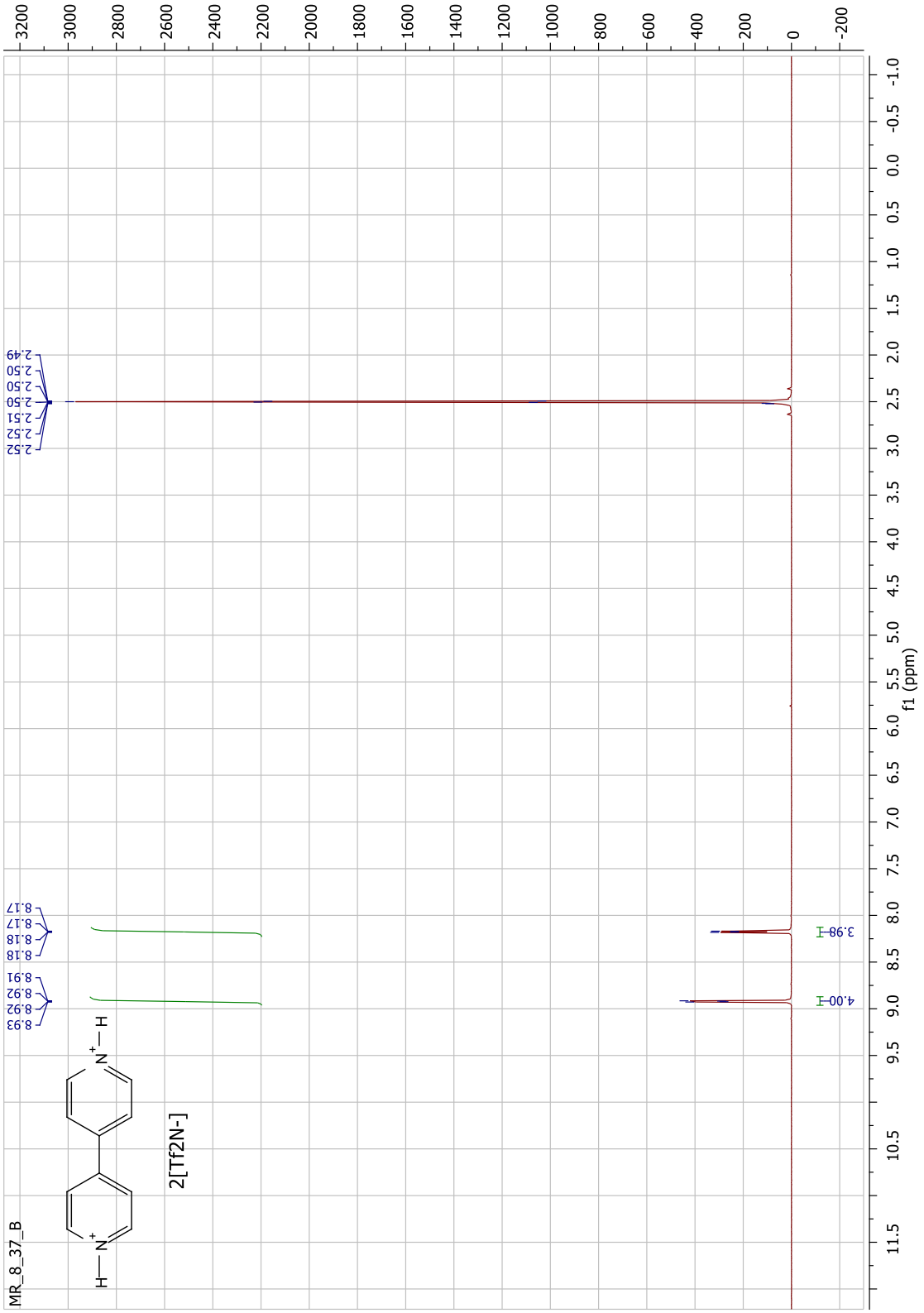

Figure 143. ^{1}H NMR spectrum of **197** (500 MHz, DMSO-d_6).

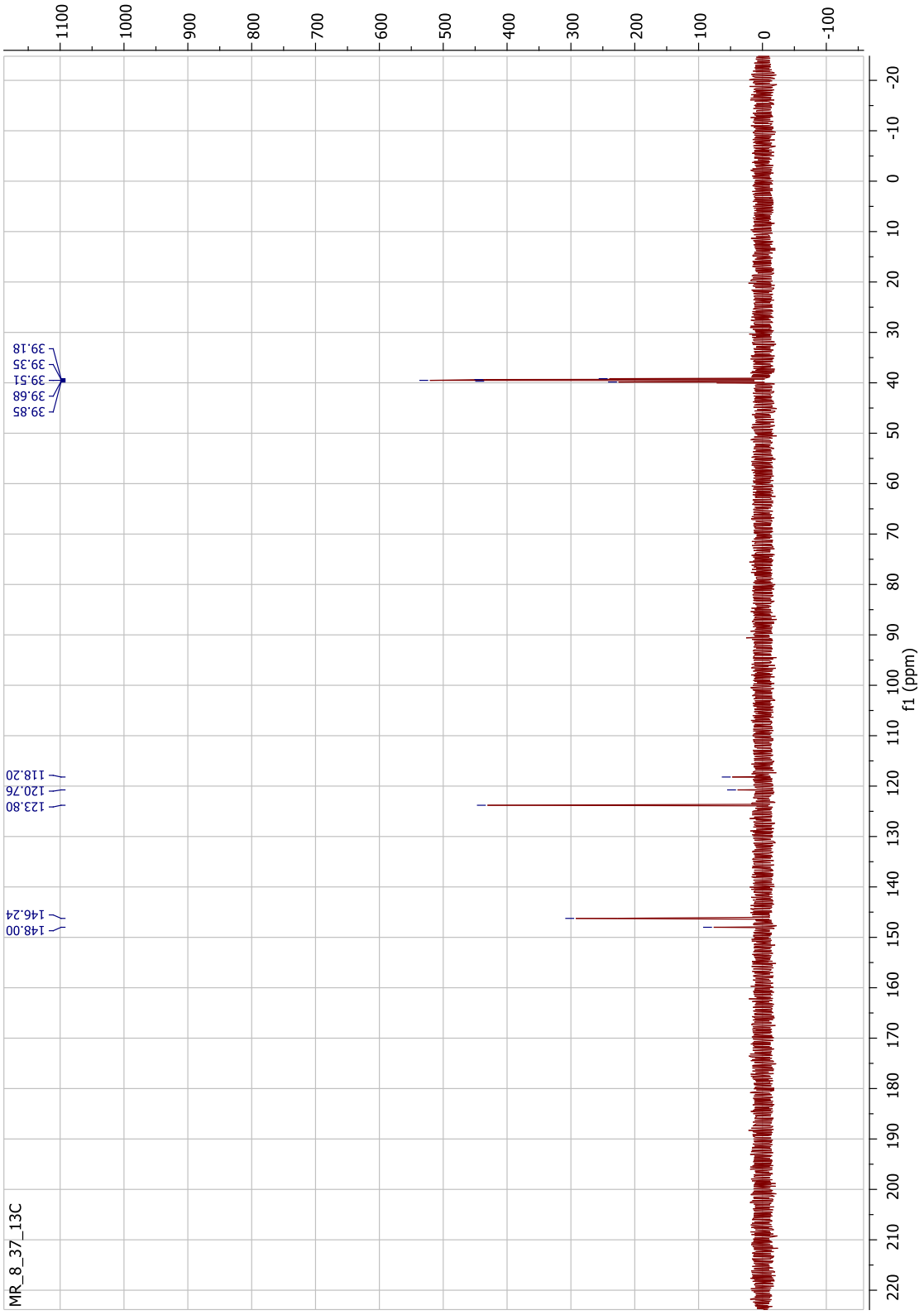

Figure 144. ^{13}C NMR spectrum of **197** (125 MHz, DMSO-d_6).

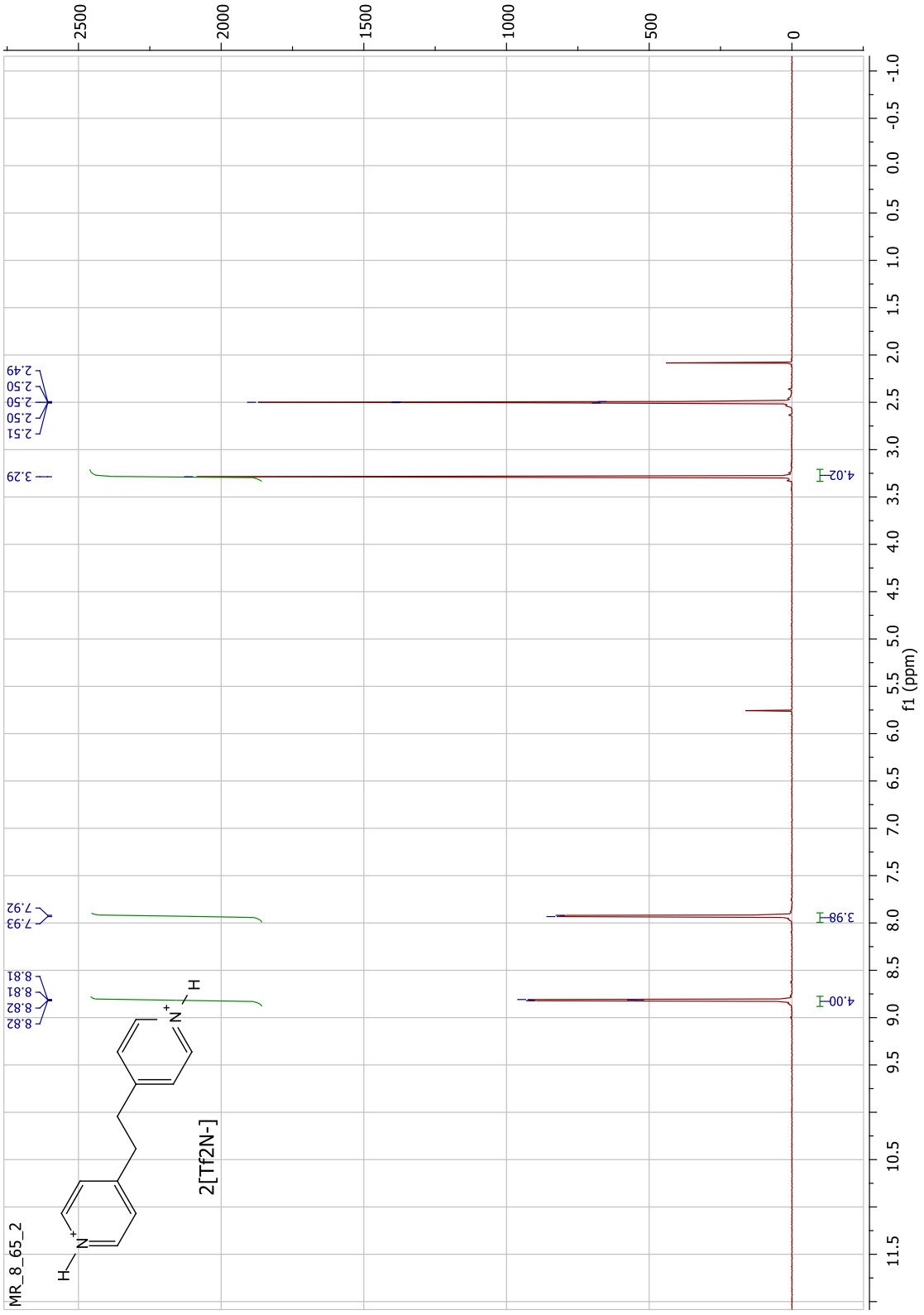

Figure 145. ^{1}H NMR spectrum of **198** (500 MHz, DMSO-d_6).

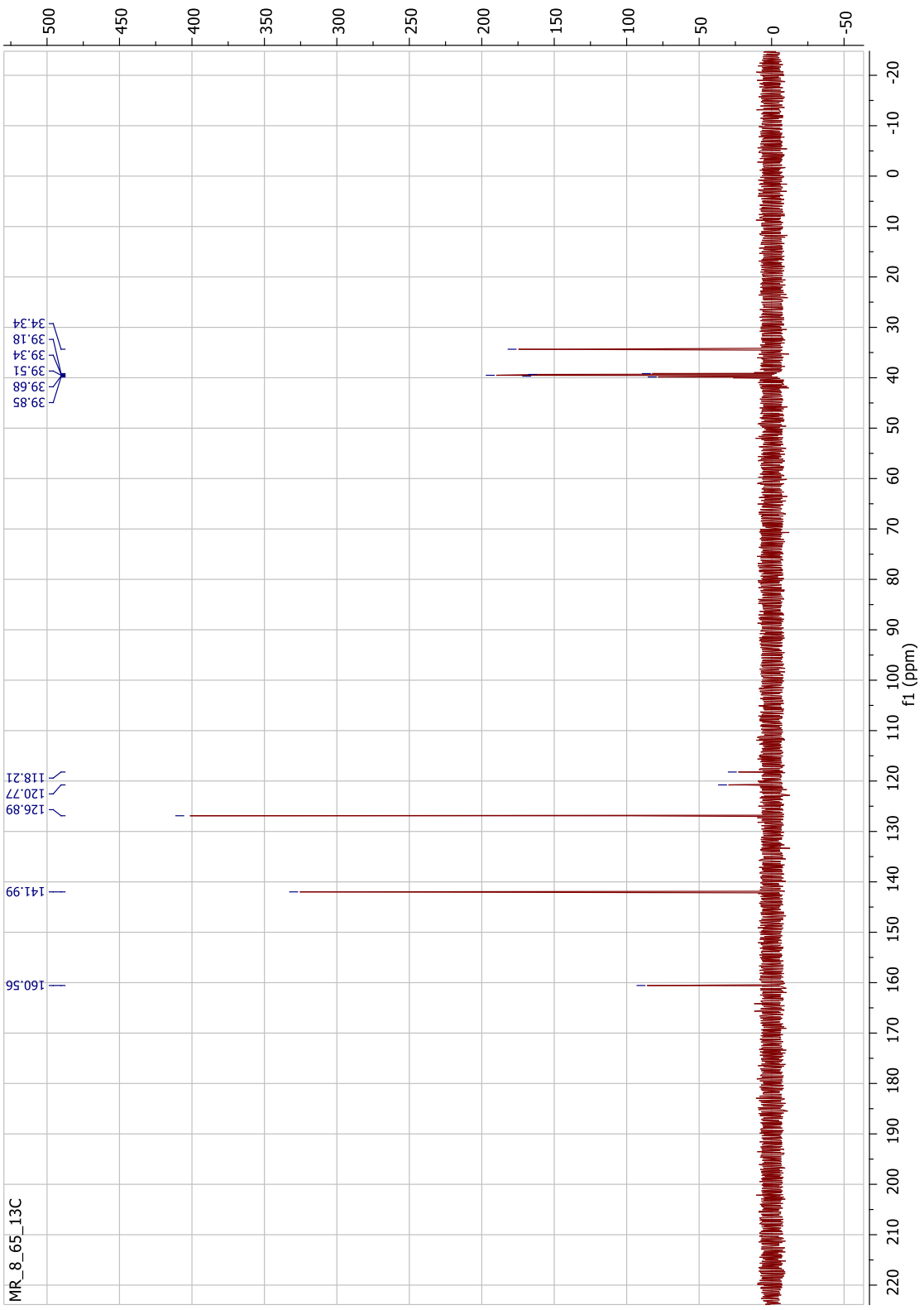

Figure 146. ^{13}C NMR spectrum of **198** (125 MHz, DMSO-d_6).

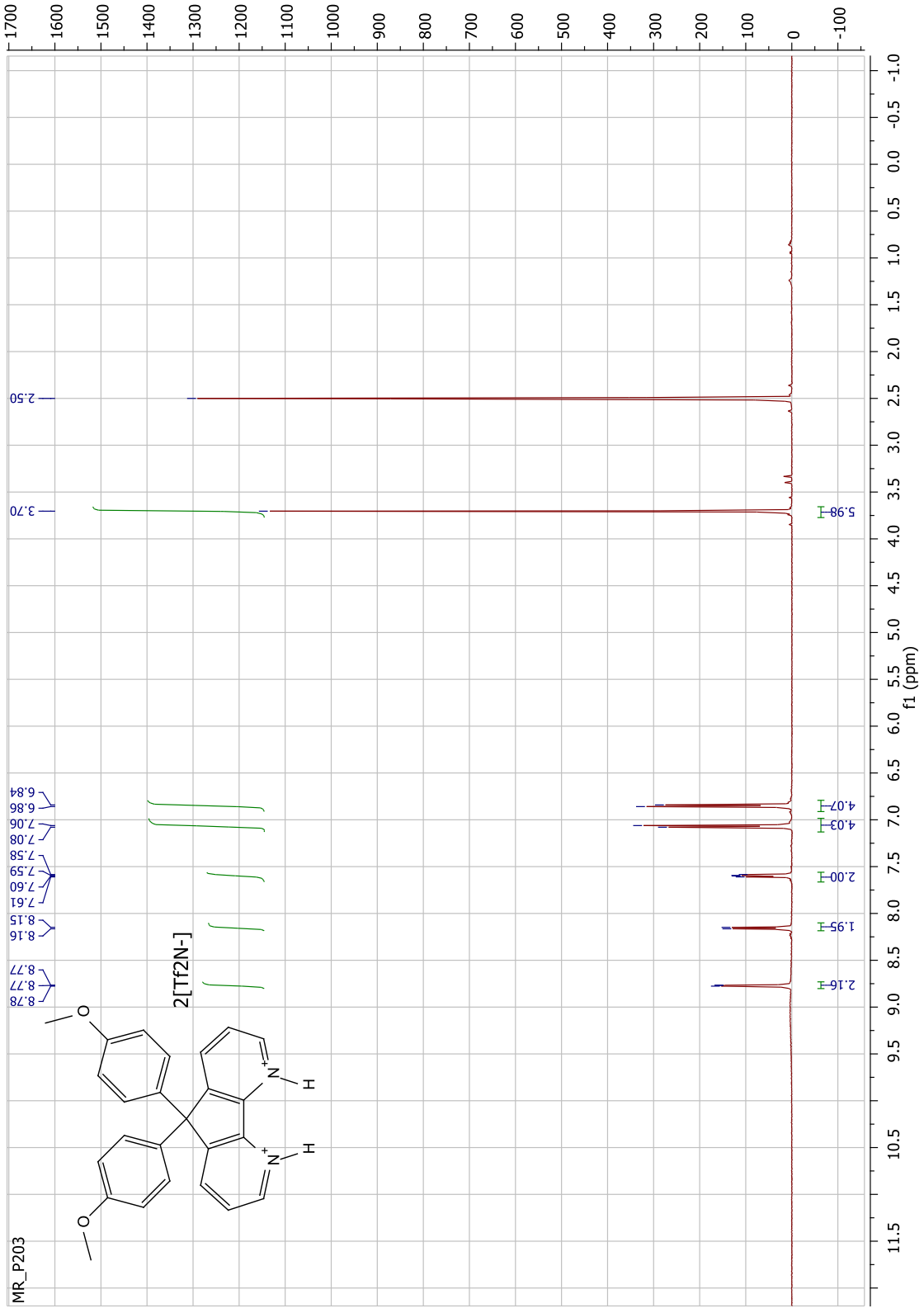

Figure 147. ^{1}H NMR spectrum of **203** (500 MHz, DMSO-d_6).

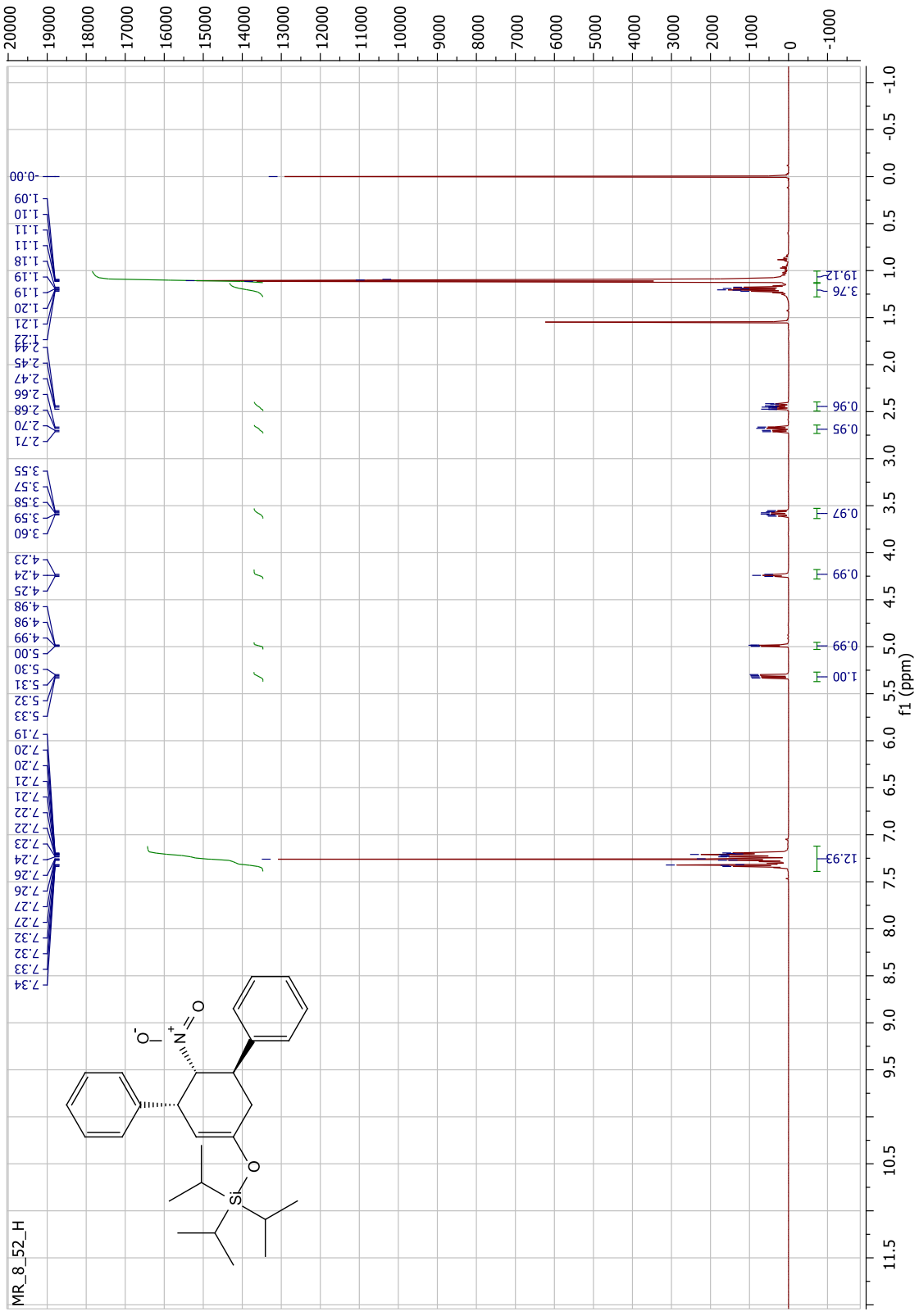

Figure 148. ^{1}H NMR spectrum of **196** (500 MHz, $CDCl_3$).

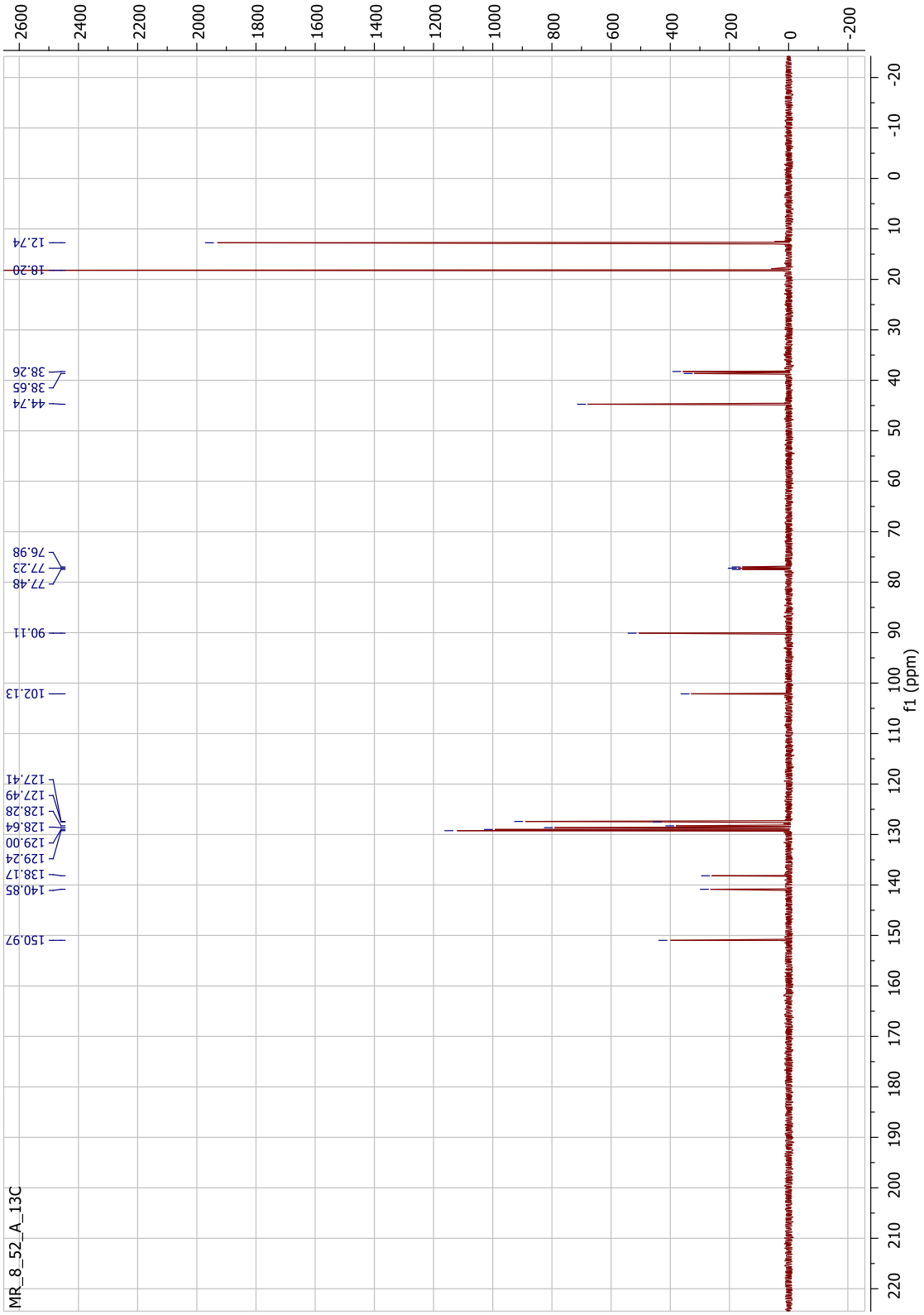

Figure 149. ^{13}C NMR spectrum of **196** (125 MHz, $CDCl_3$).

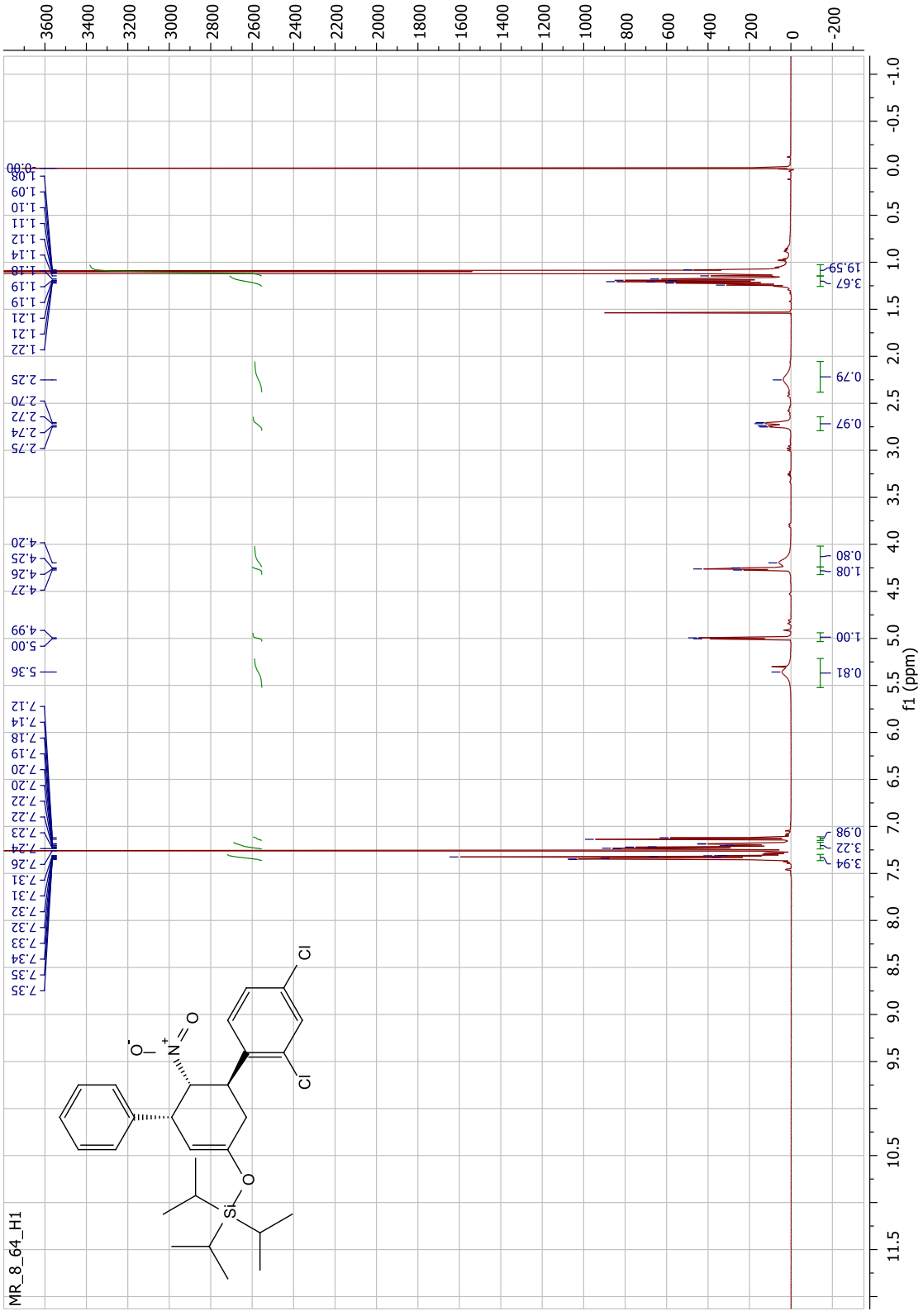

Figure 150. ^{1}H NMR spectrum of **205** (500 MHz, $CDCl_3$).

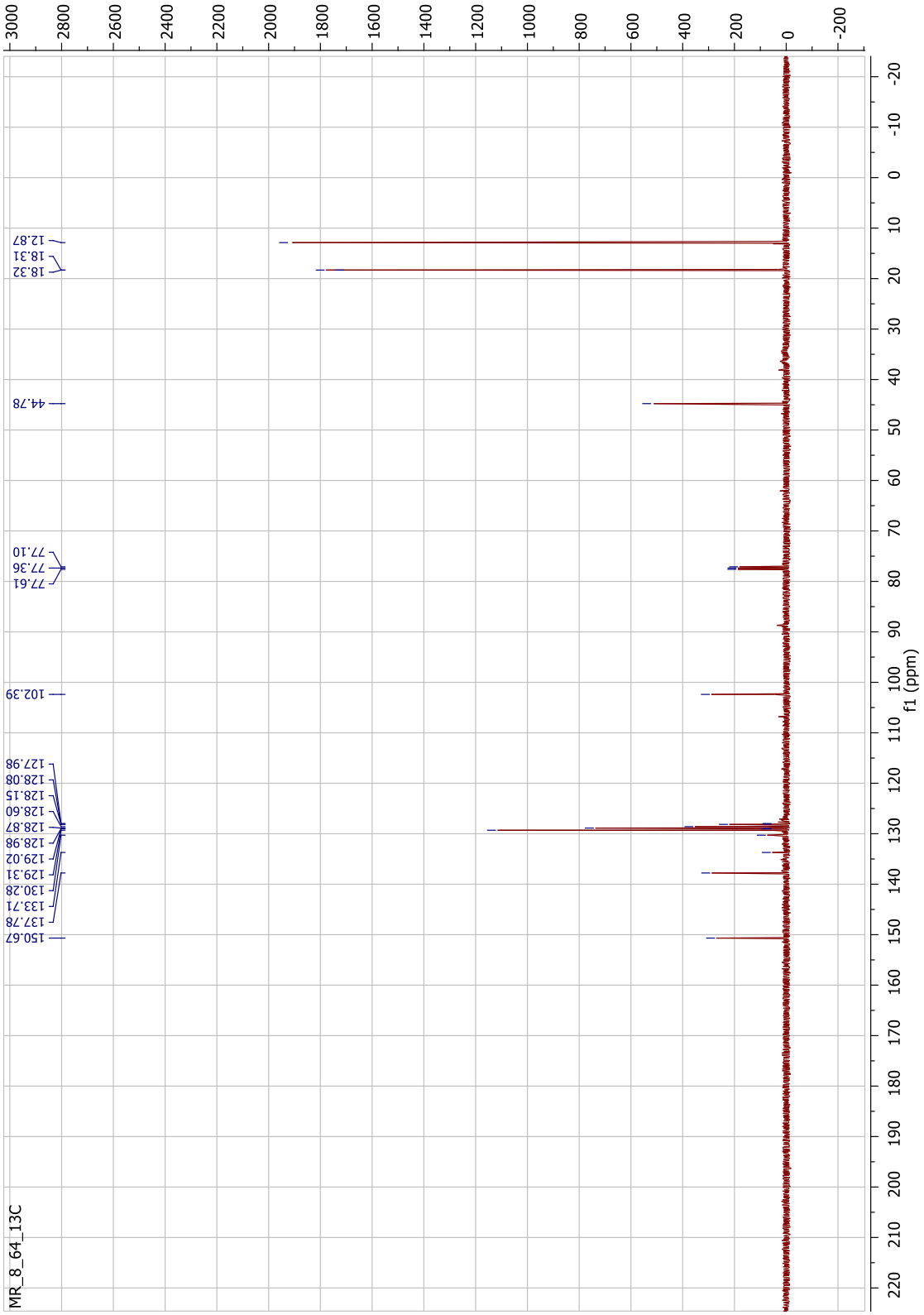

Figure 151. ^{13}C NMR spectrum of **205** (125 MHz, $CDCl_3$).

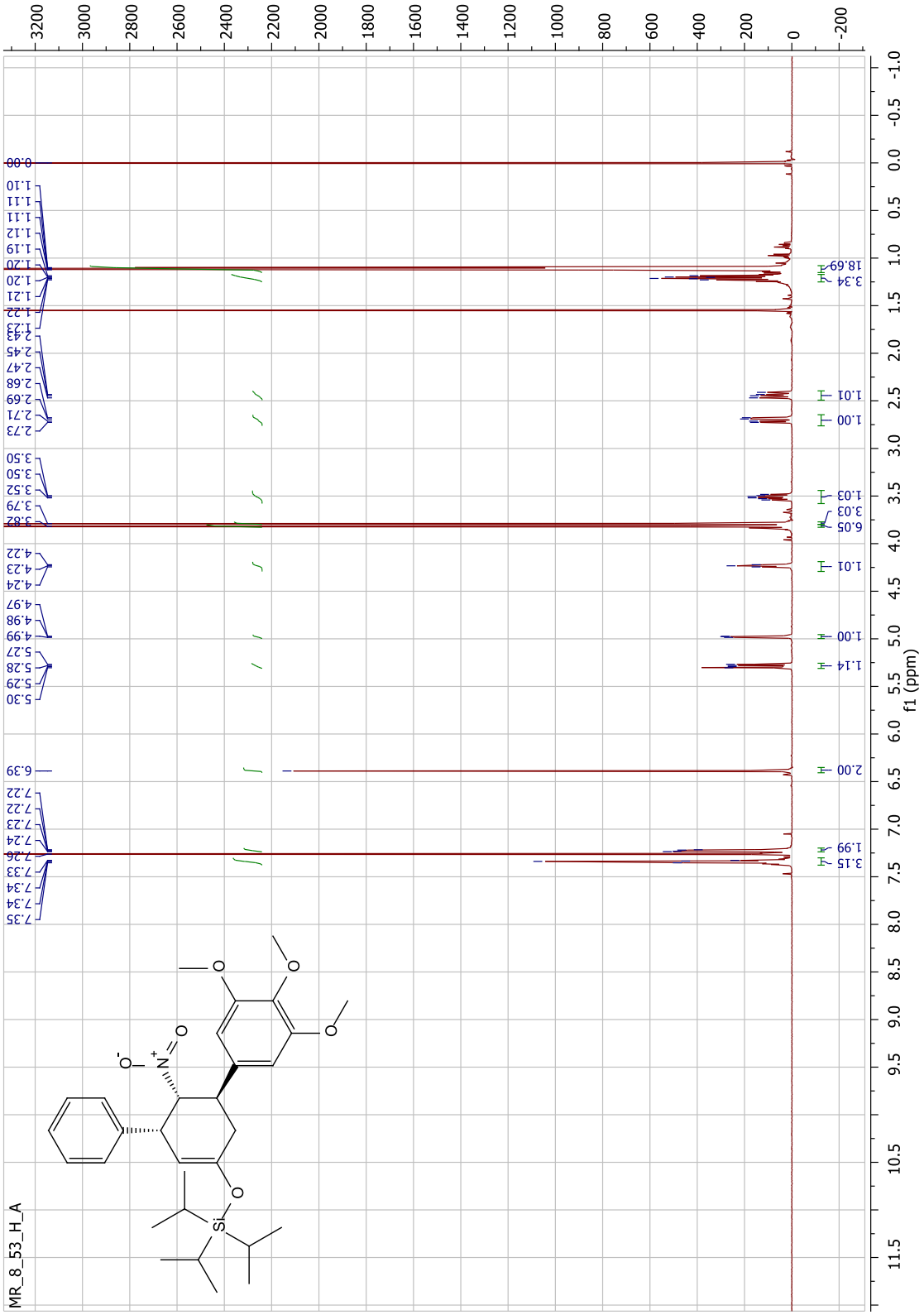

Figure 152. ^{1}H NMR spectrum of **206** (500 MHz, $CDCl_3$).

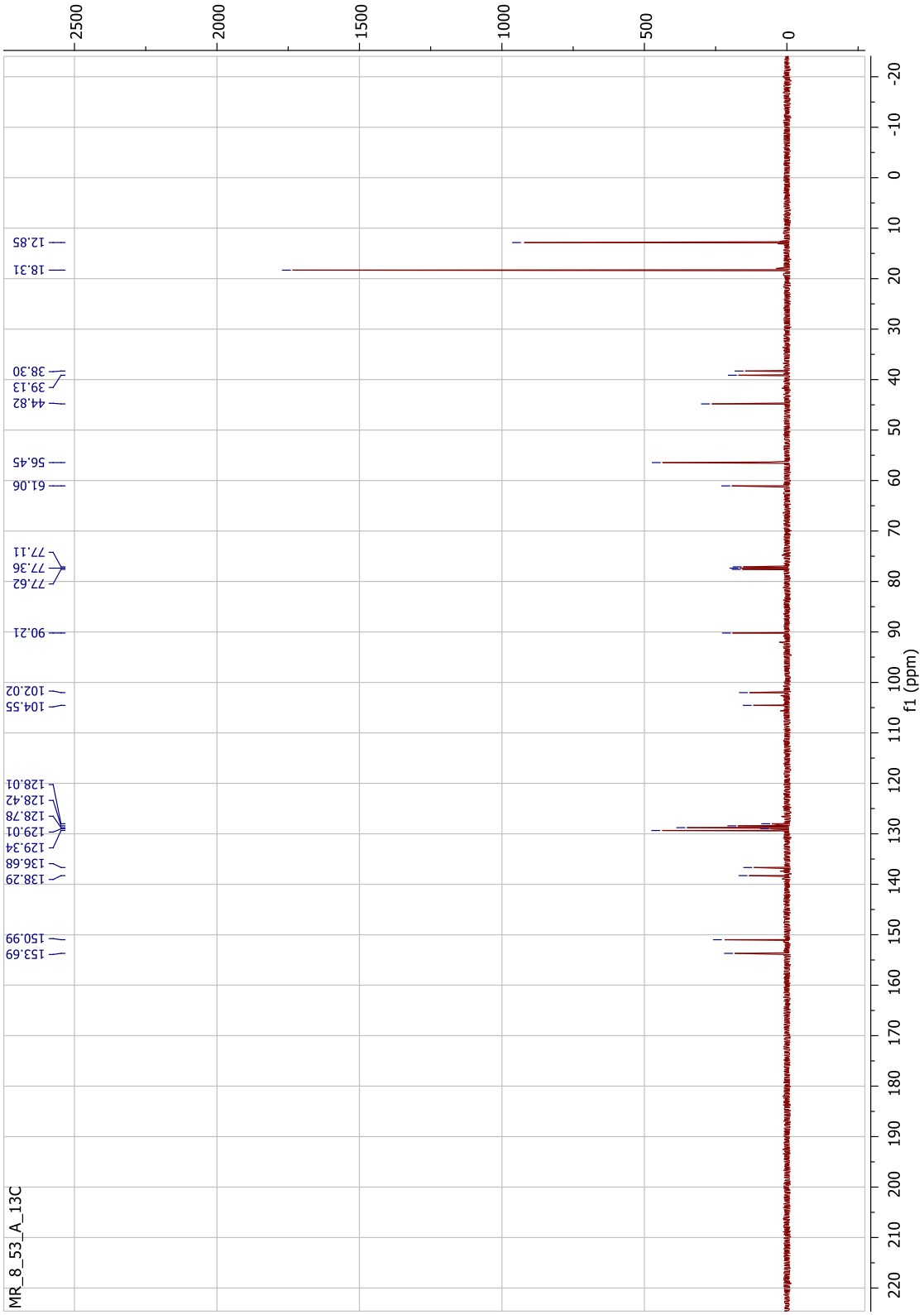

Figure 153. ^{13}C NMR spectrum of **206** (125 MHz, $CDCl_3$).

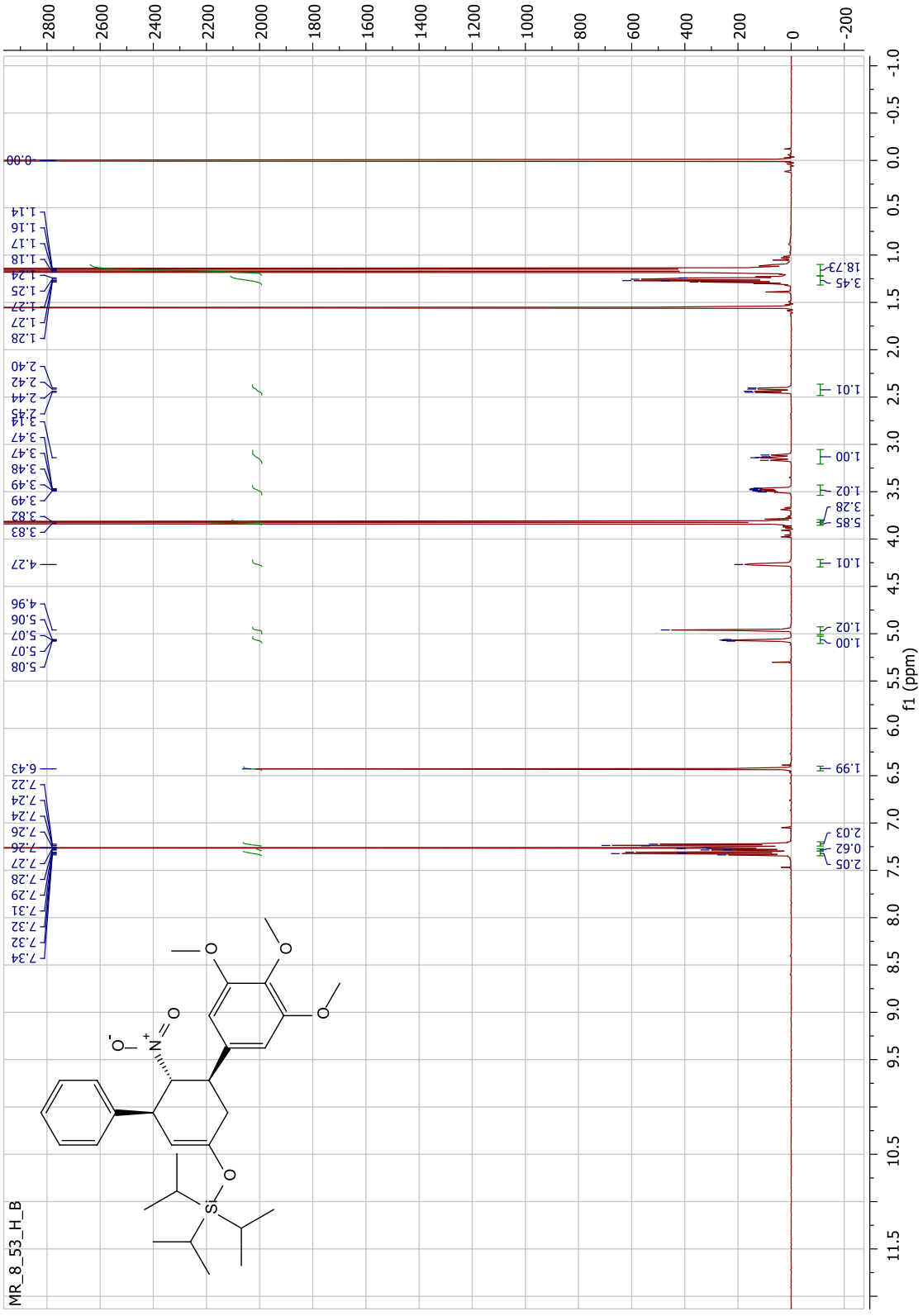

Figure 154. ^{1}H NMR spectrum of **305** (500 MHz, $CDCl_3$).

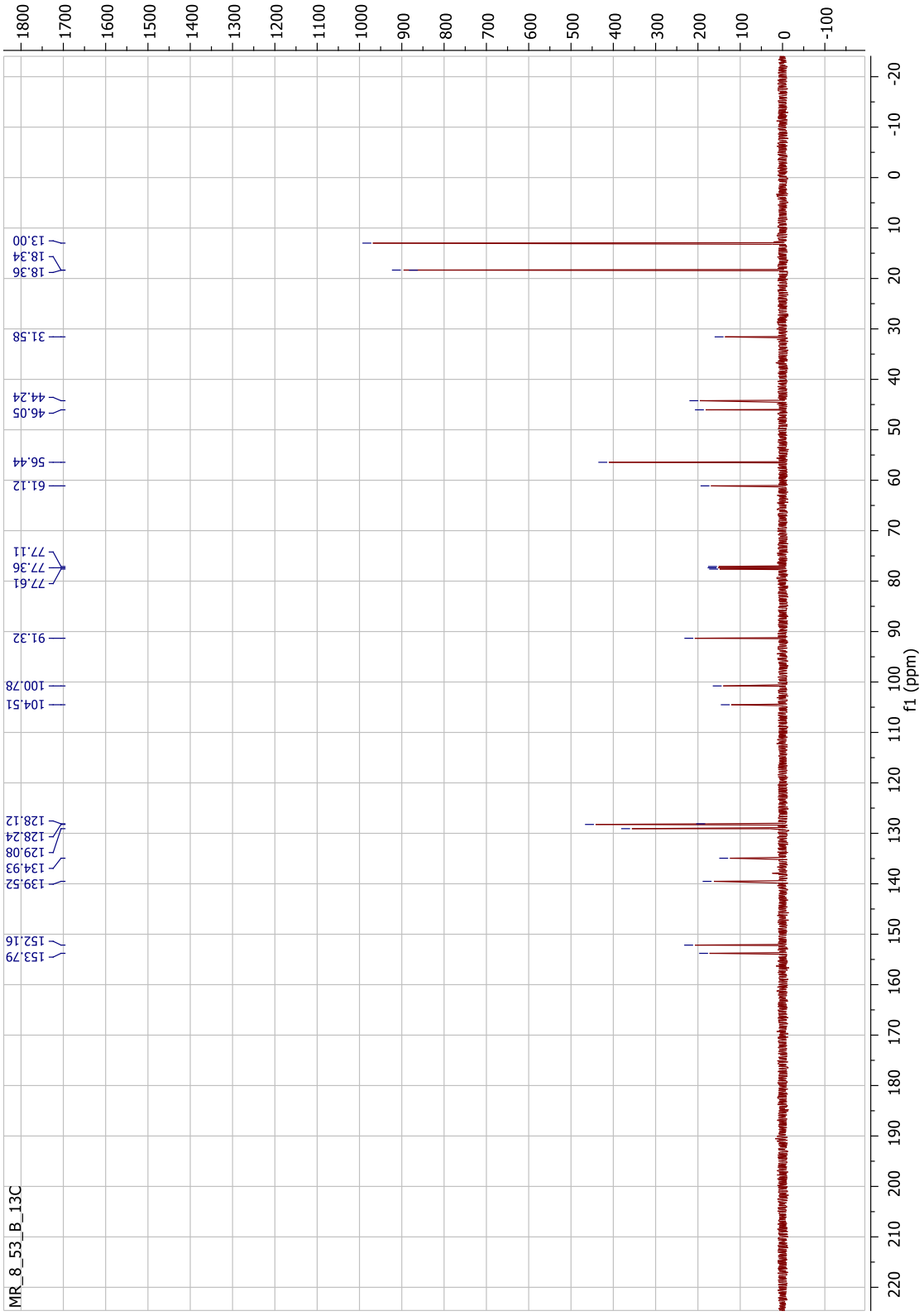

Figure 155. ^{13}C NMR spectrum of **305** (125 MHz, $CDCl_3$).

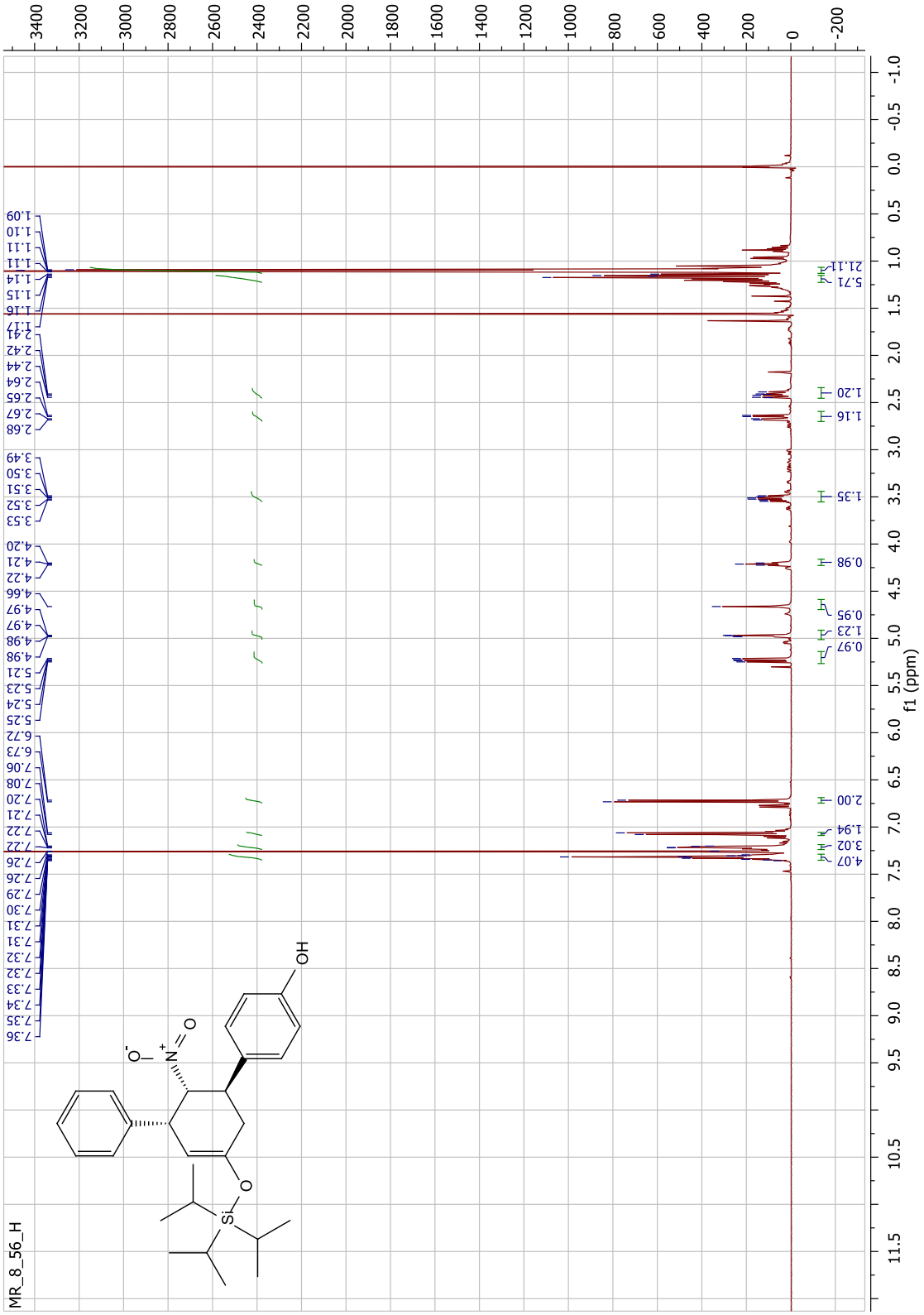

Figure 156. ^{1}H NMR spectrum of **207** (500 MHz, $CDCl_3$).

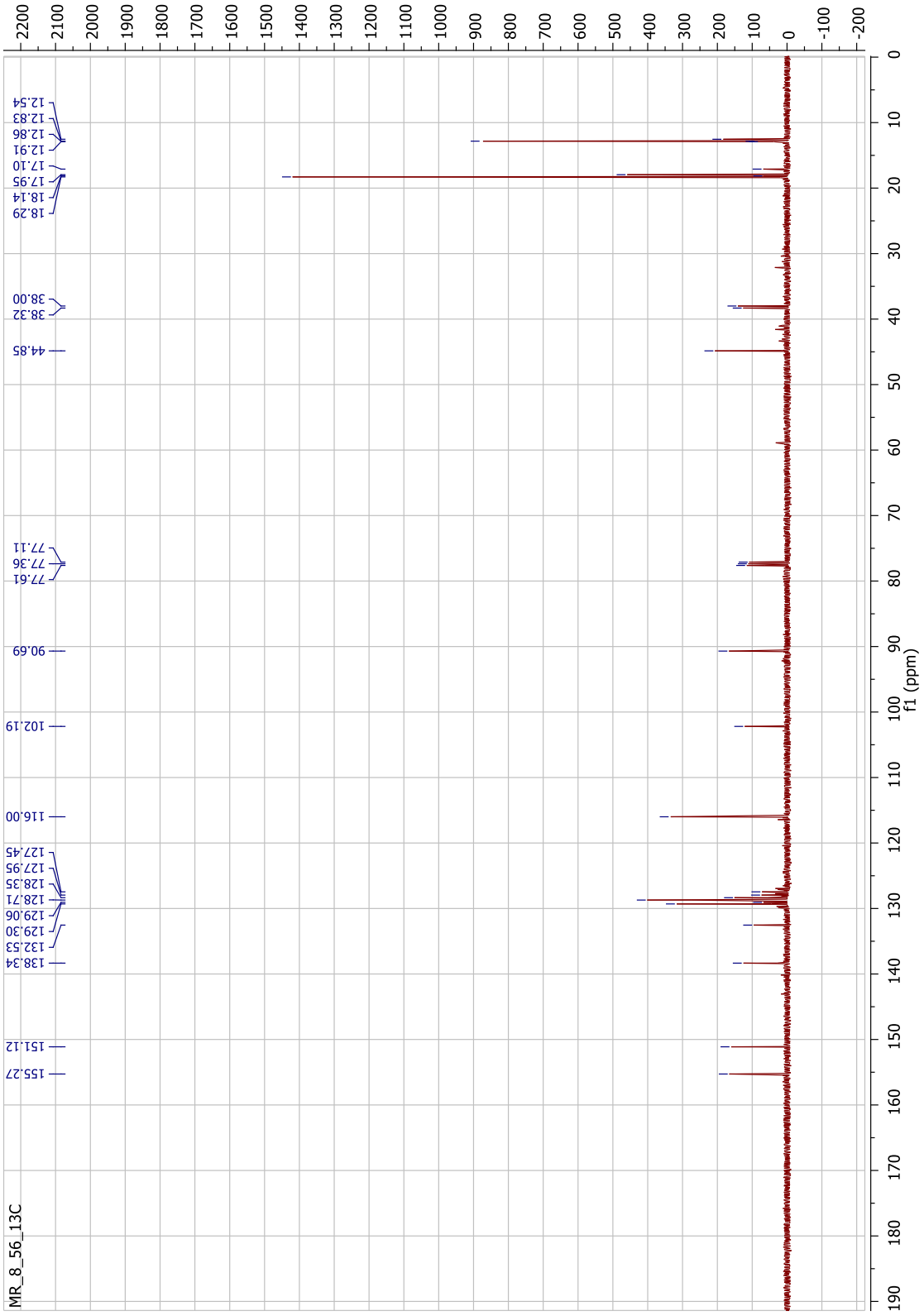

Figure 157. ^{13}C NMR spectrum of **207** (125 MHz, $CDCl_3$).

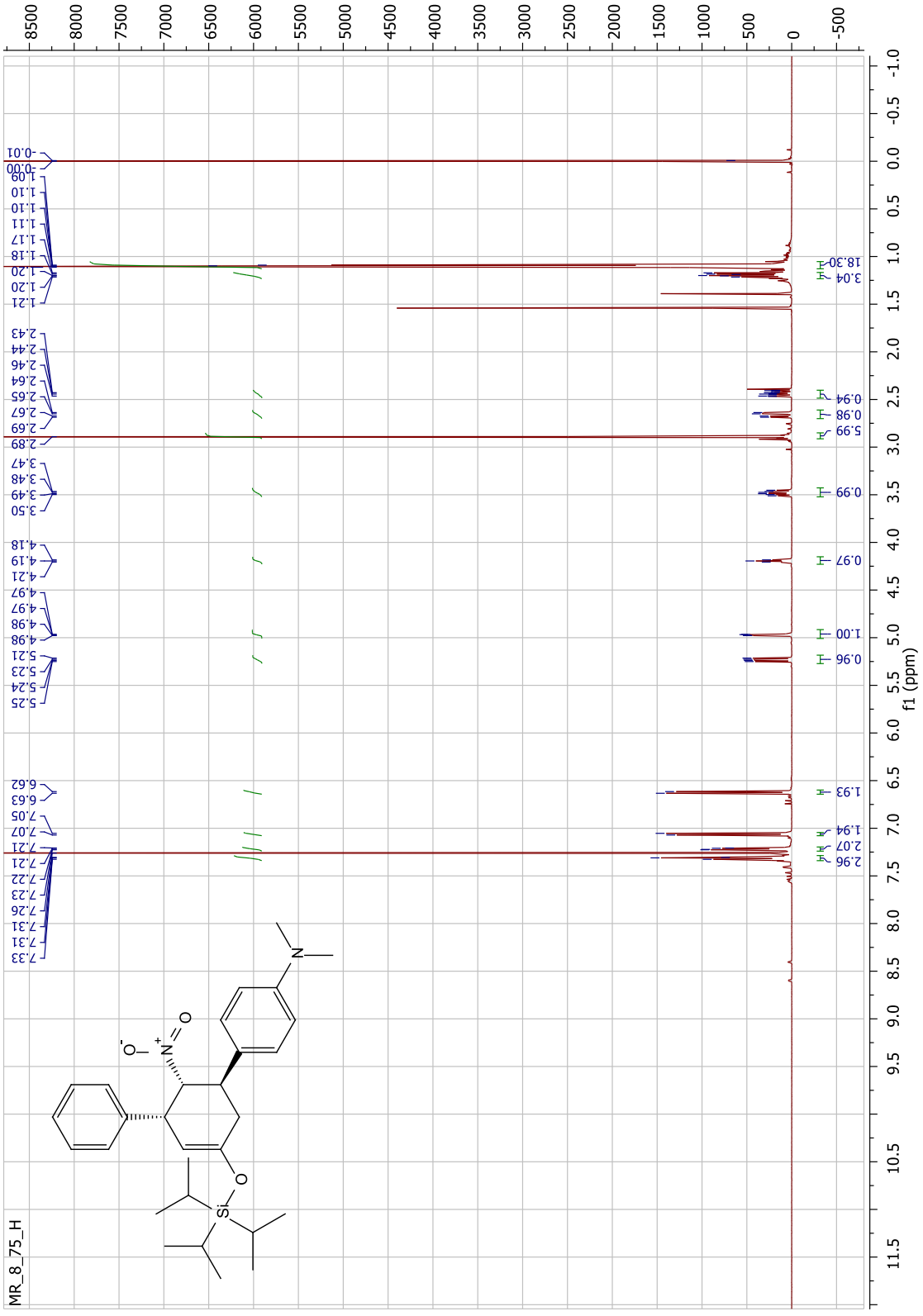

Figure 158. ^{1}H NMR spectrum of **208** (500 MHz, $CDCl_3$).

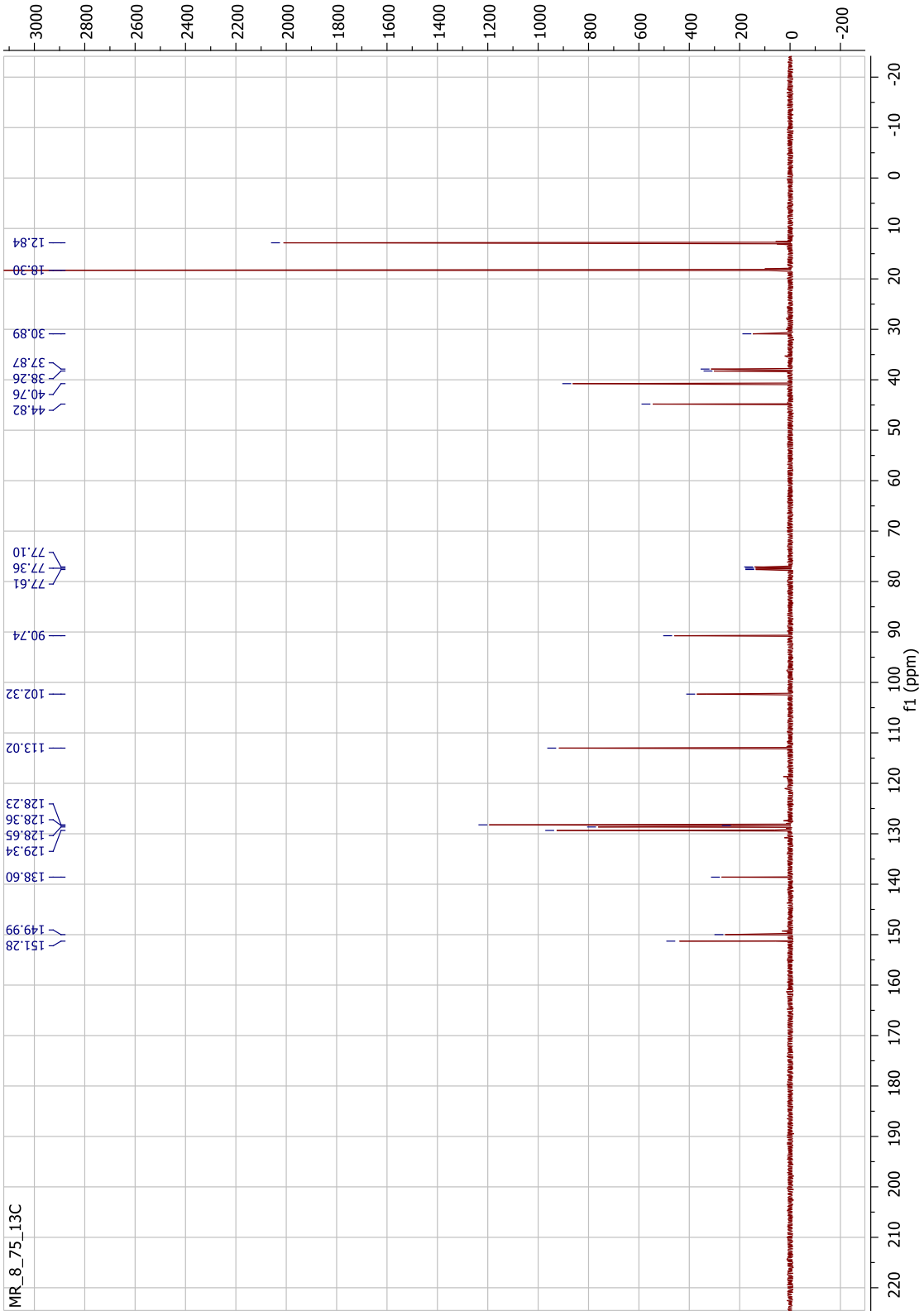

Figure 159. ^{13}C NMR spectrum of **208** (125 MHz, $CDCl_3$).

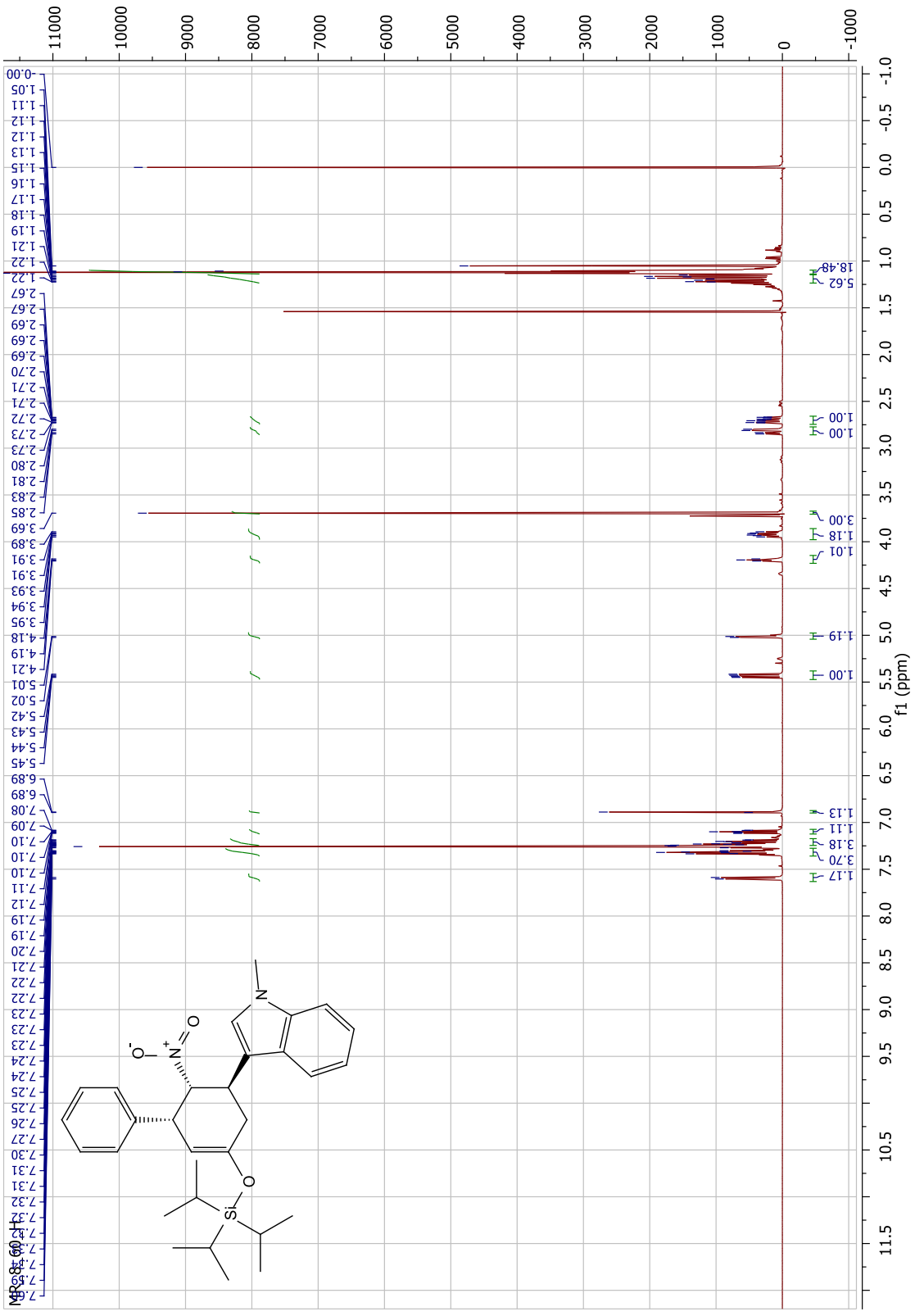

Figure 160. ^{1}H NMR spectrum of **209** (500 MHz, $CDCl_3$).

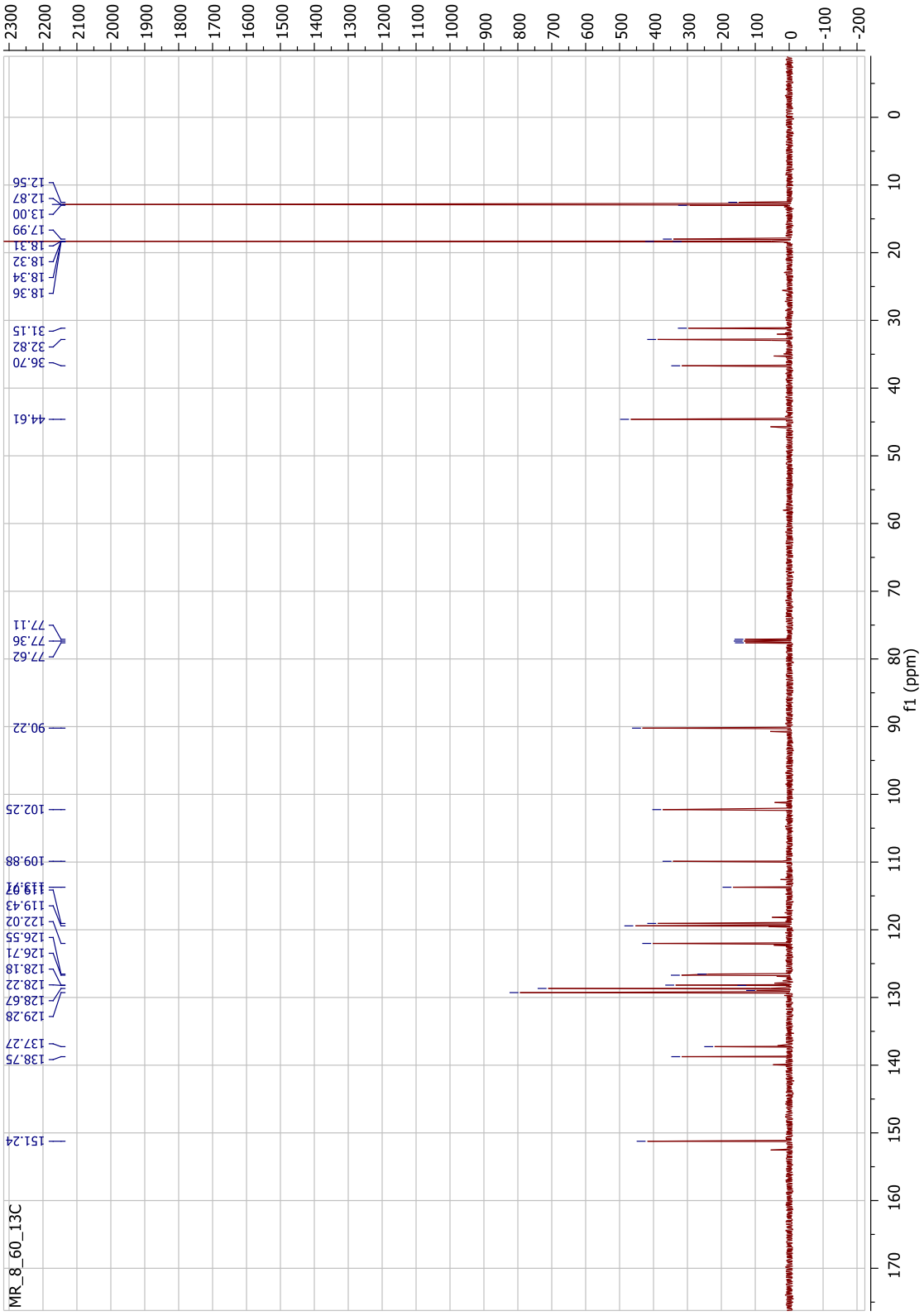

Figure 161. ^{13}C NMR spectrum of **209** (125 MHz, $CDCl_3$).

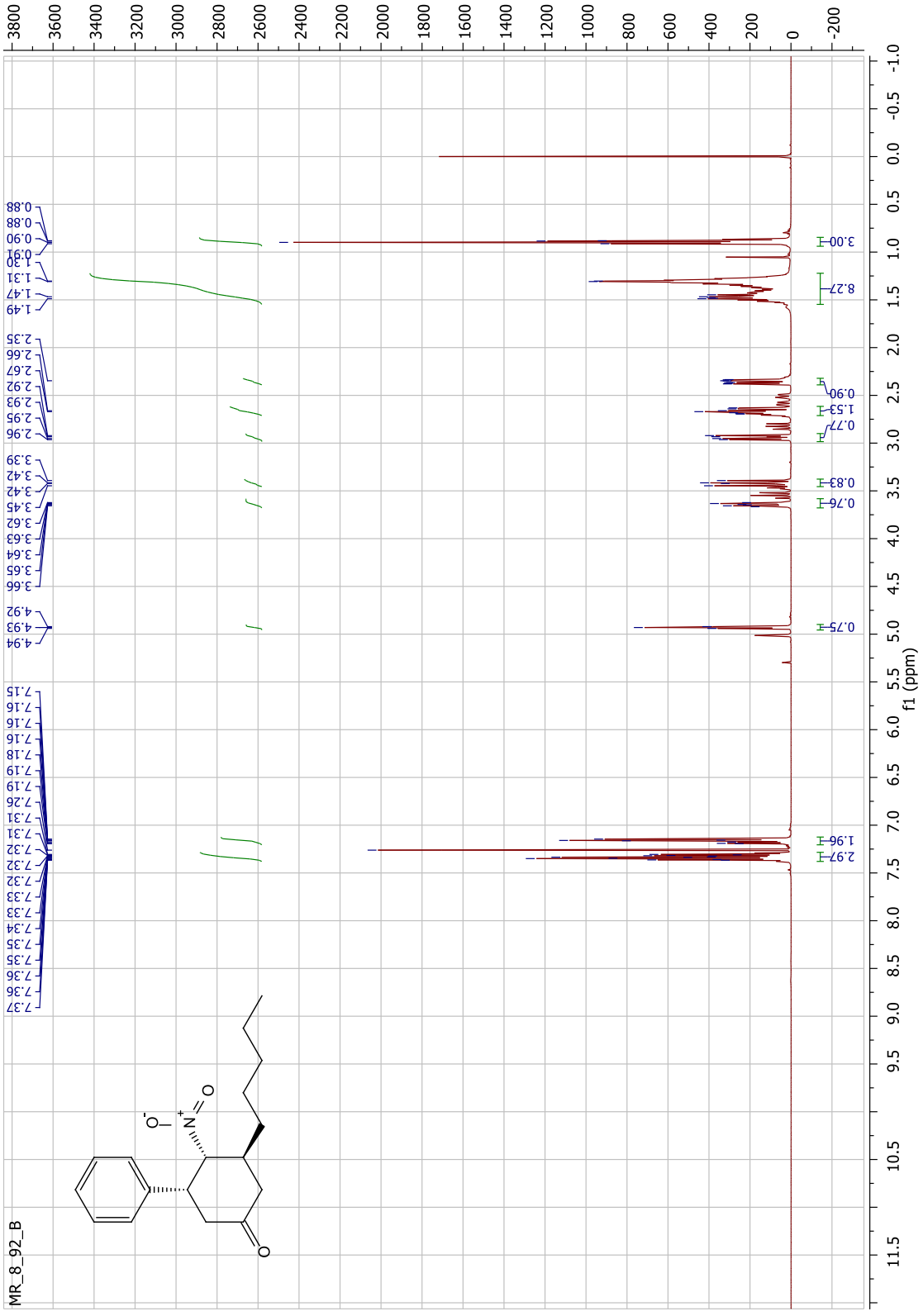

Figure 162. ^{1}H NMR spectrum of **210a** (500 MHz, $CDCl_3$).

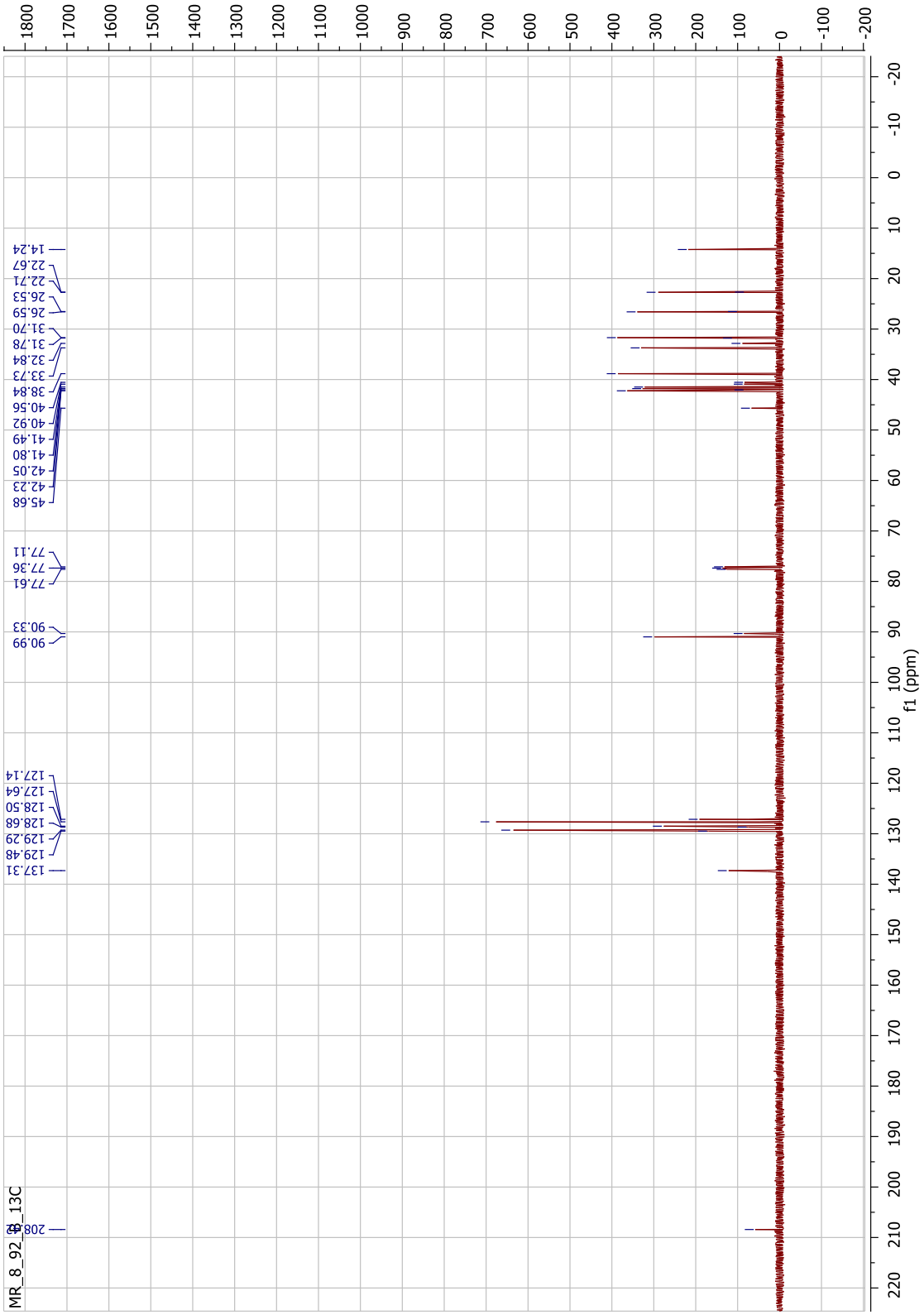

Figure 163. ^{13}C NMR spectrum of **210a** (125 MHz, $CDCl_3$).

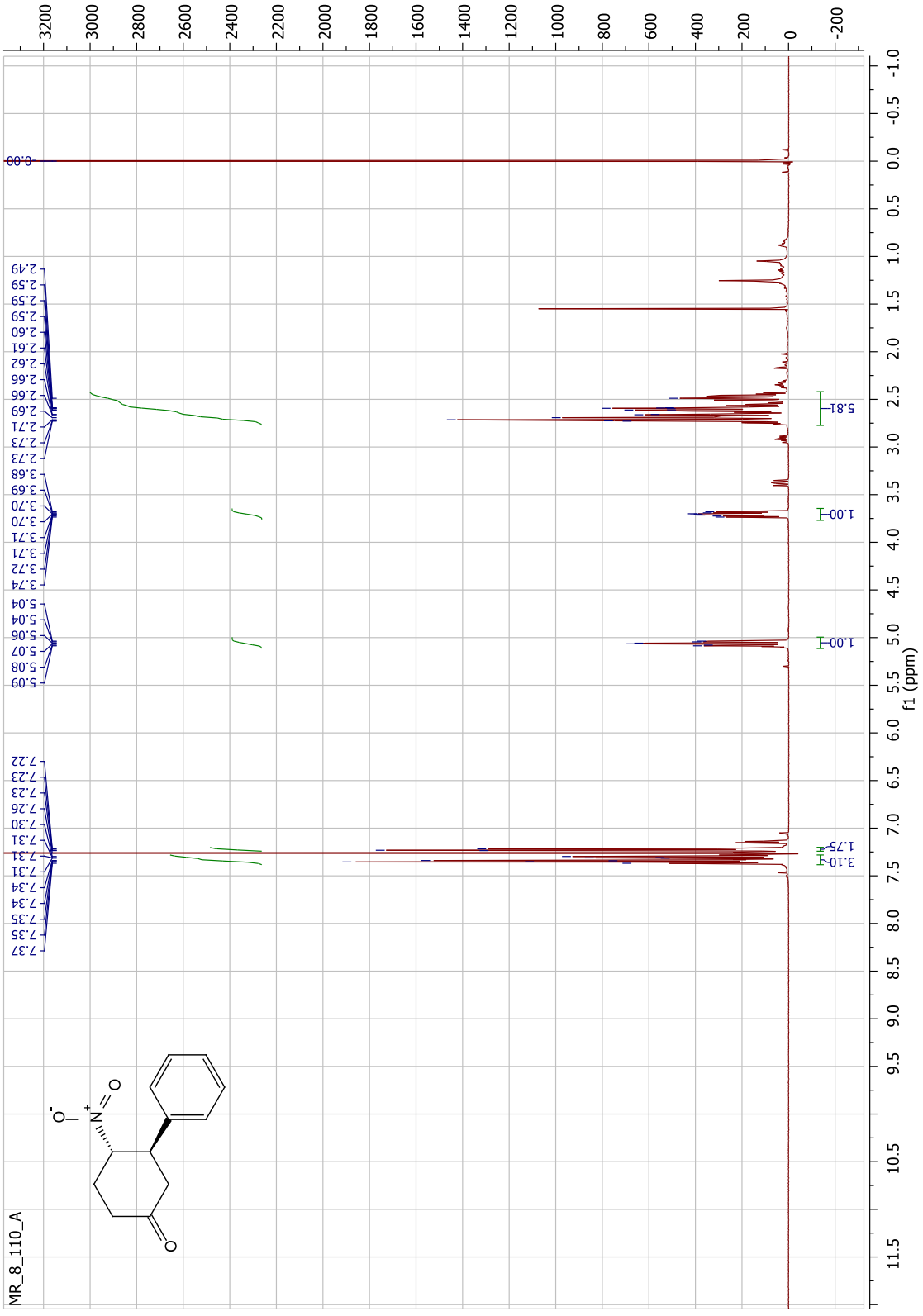

Figure 164. ^{1}H NMR spectrum of **211a** (500 MHz, $CDCl_3$).

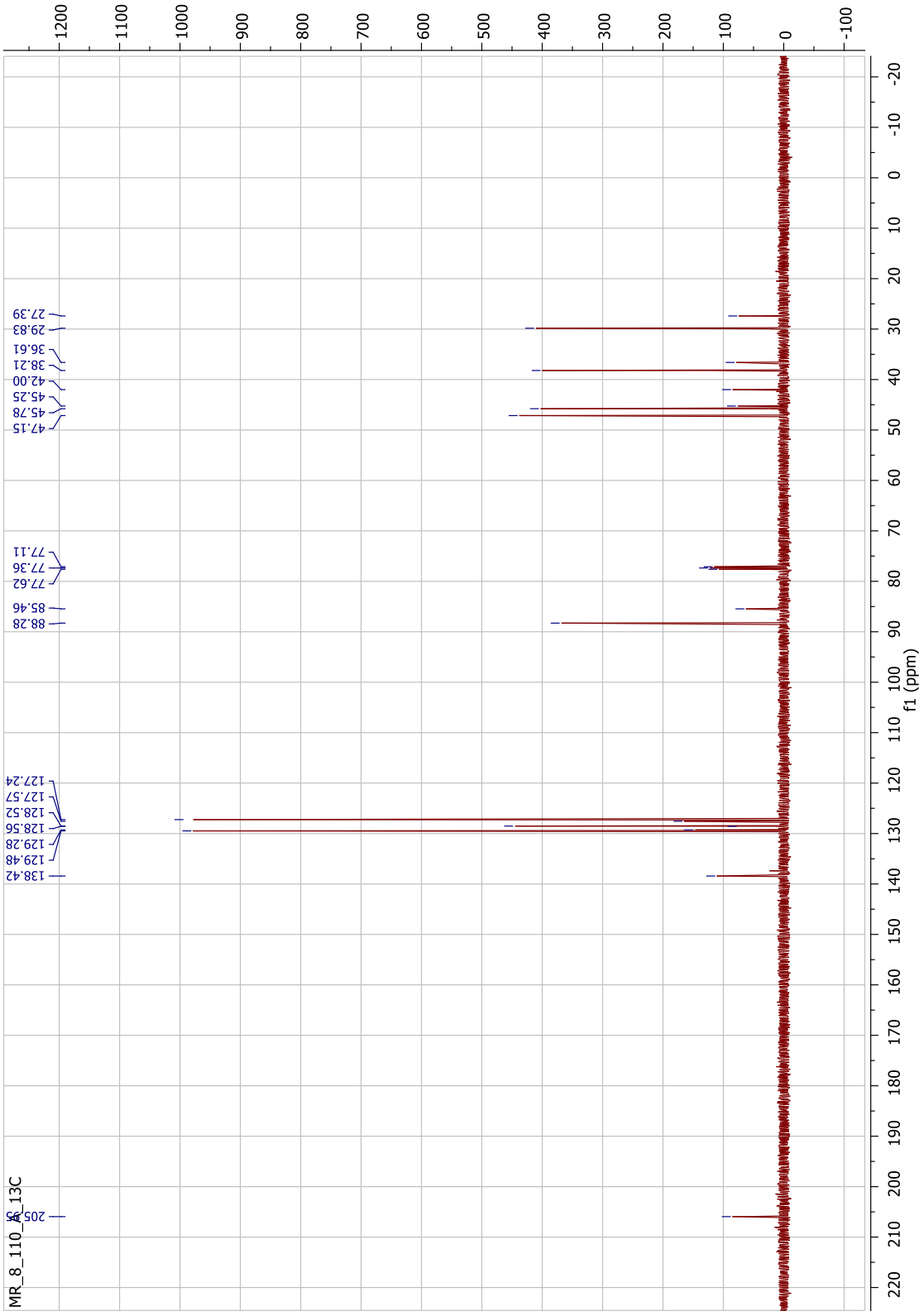

Figure 165. ^{13}C NMR spectrum of **211a** (125 MHz, $CDCl_3$).

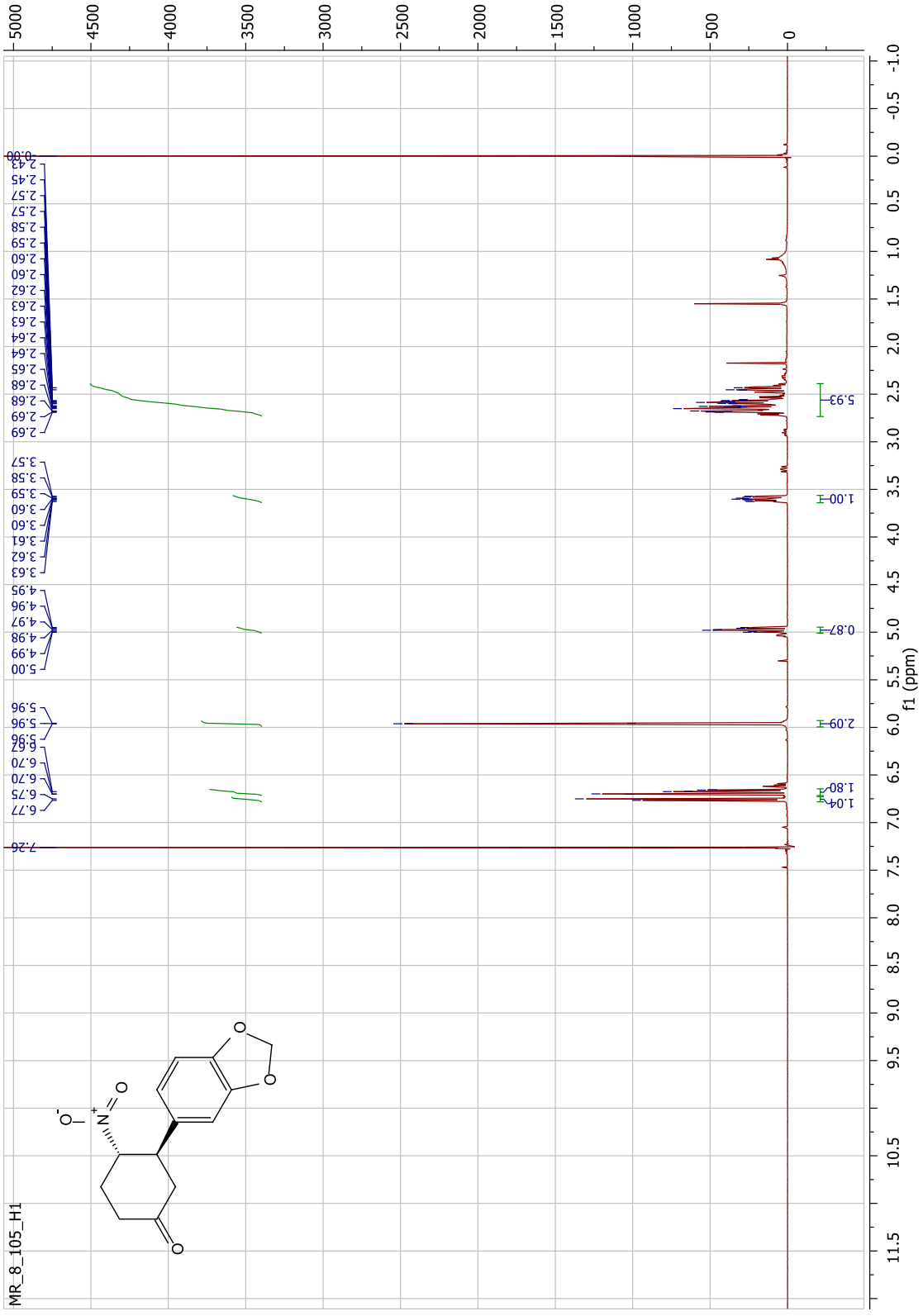

Figure 166. ^{1}H NMR spectrum of **212a** (500 MHz, $CDCl_3$).

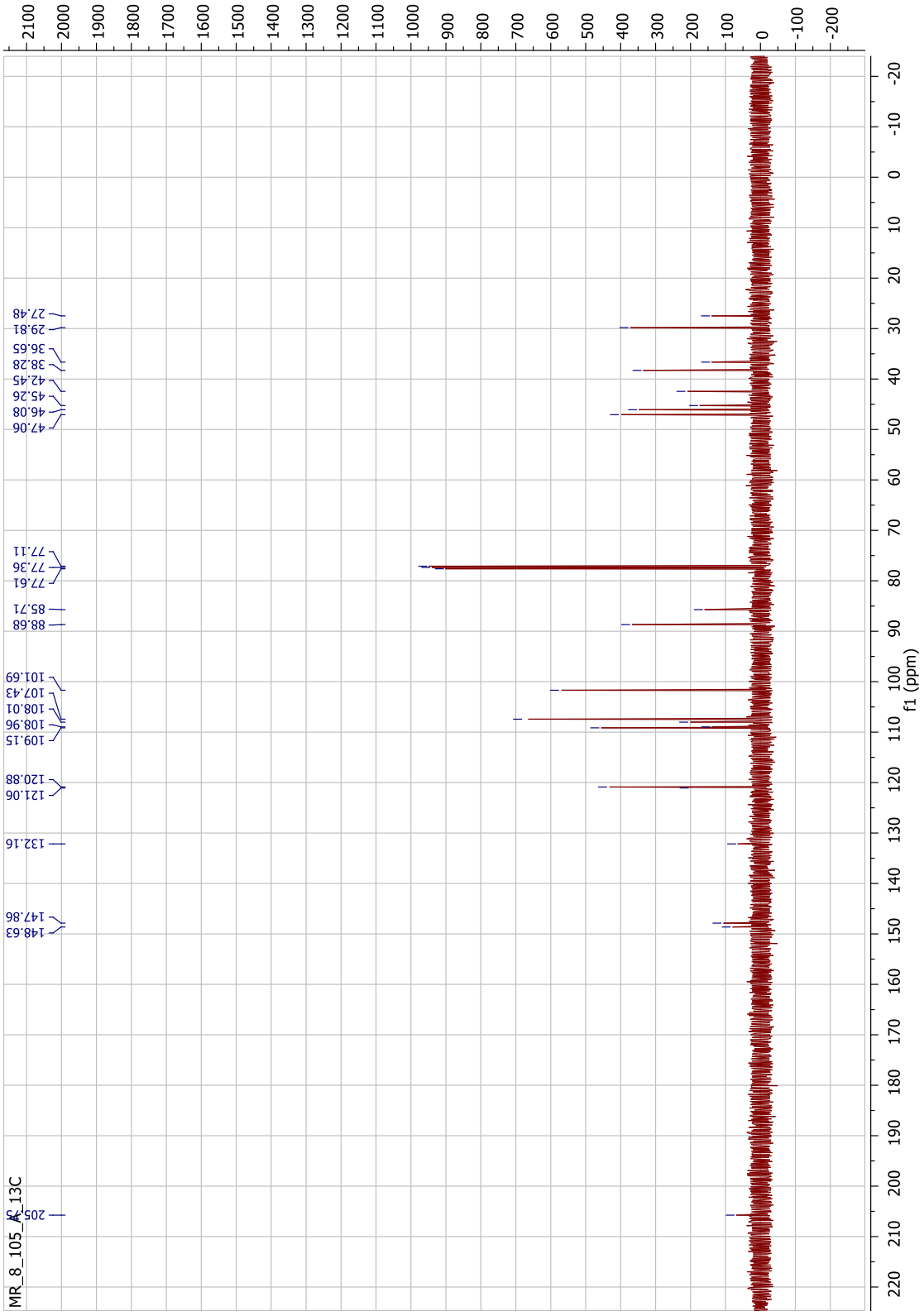

Figure 167. ^{13}C NMR spectrum of **212a** (125 MHz, $CDCl_3$).

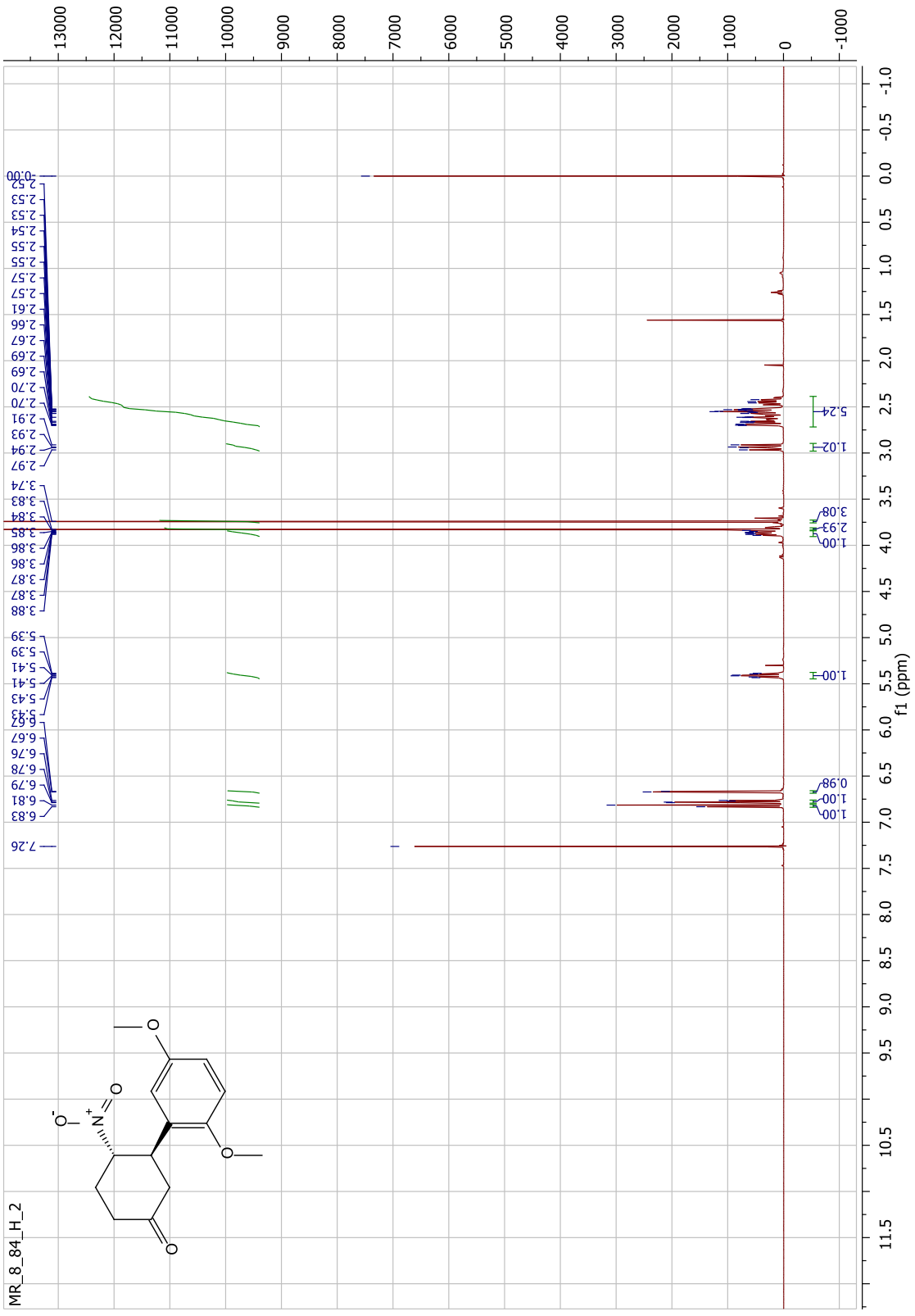

Figure 168. ^{1}H NMR spectrum of **213a** (500 MHz, $CDCl_3$).

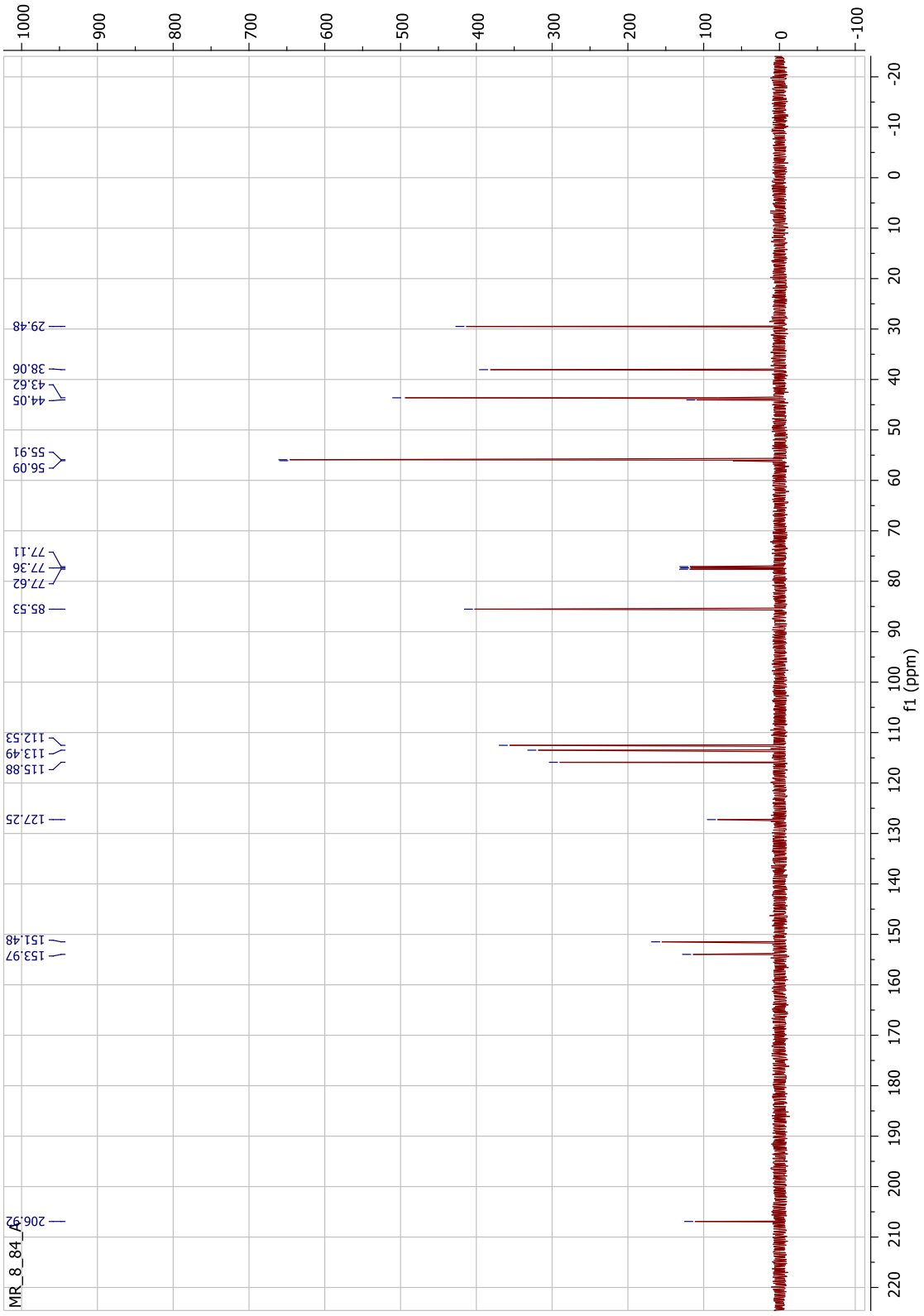

Figure 169. ^{13}C NMR spectrum of **213a** (125 MHz, $CDCl_3$).

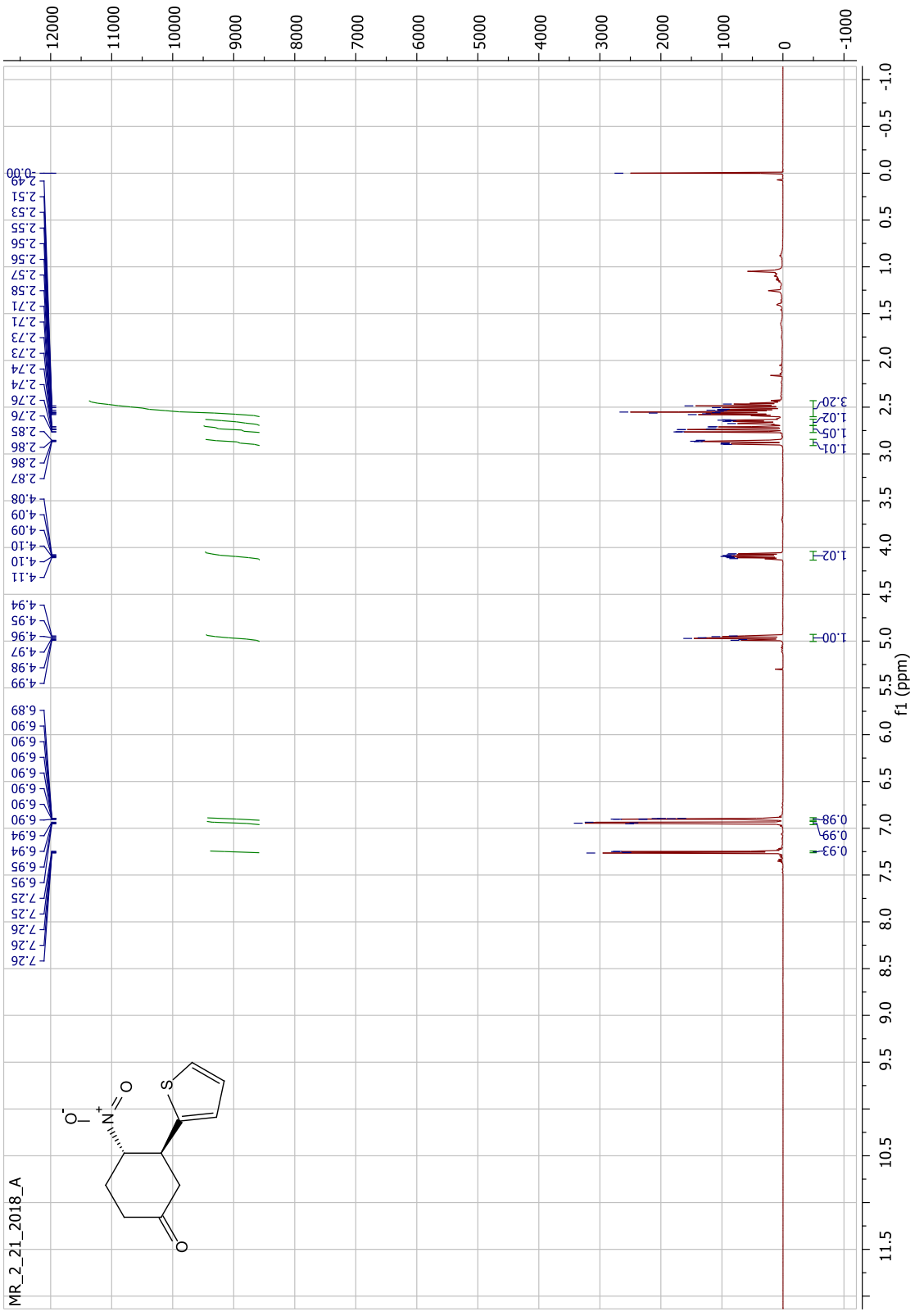

Figure 170. ^{1}H NMR spectrum of **215a** (500 MHz, $CDCl_3$).

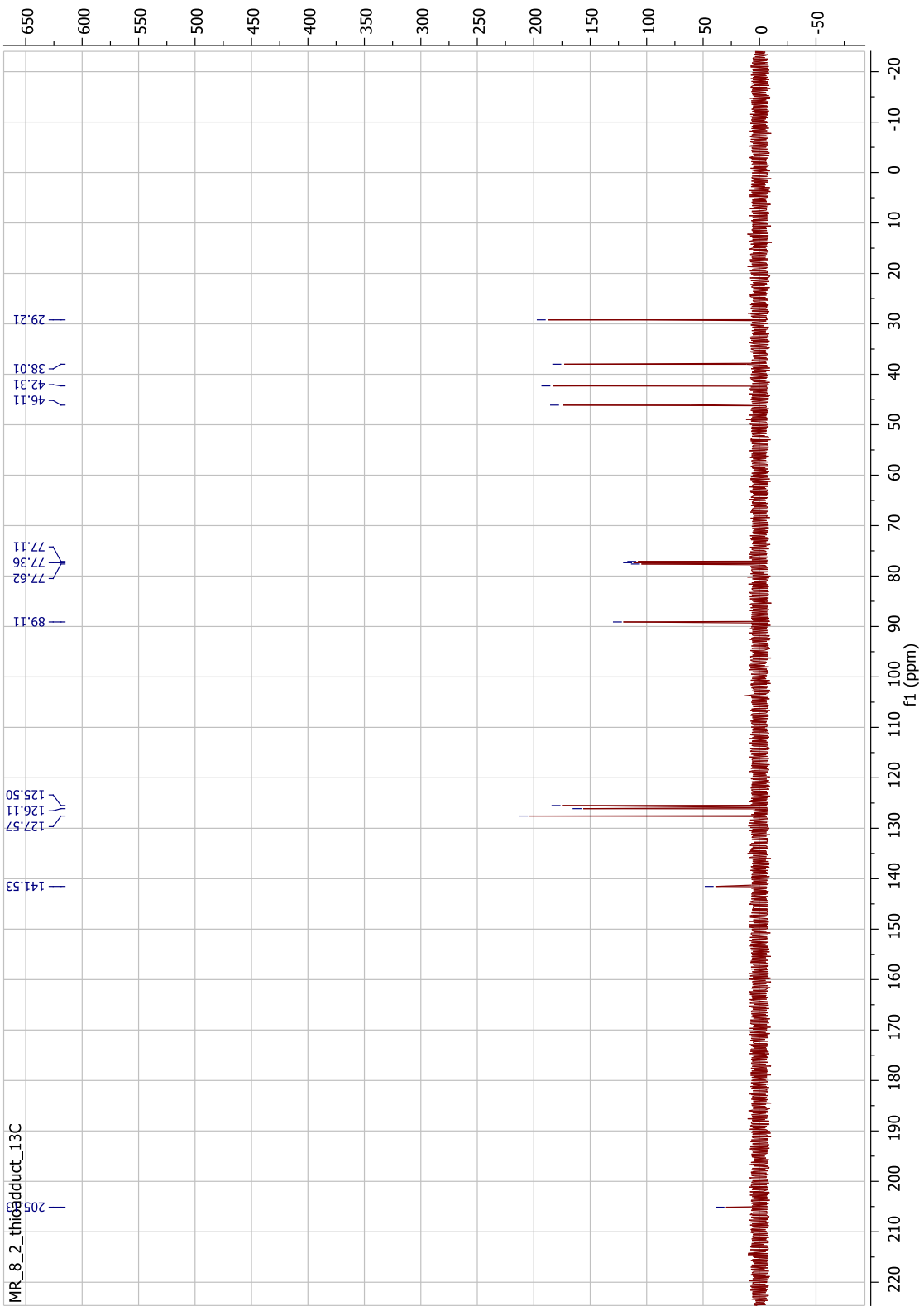

Figure 171. ^{13}C NMR spectrum of **215a** (125 MHz, $CDCl_3$).

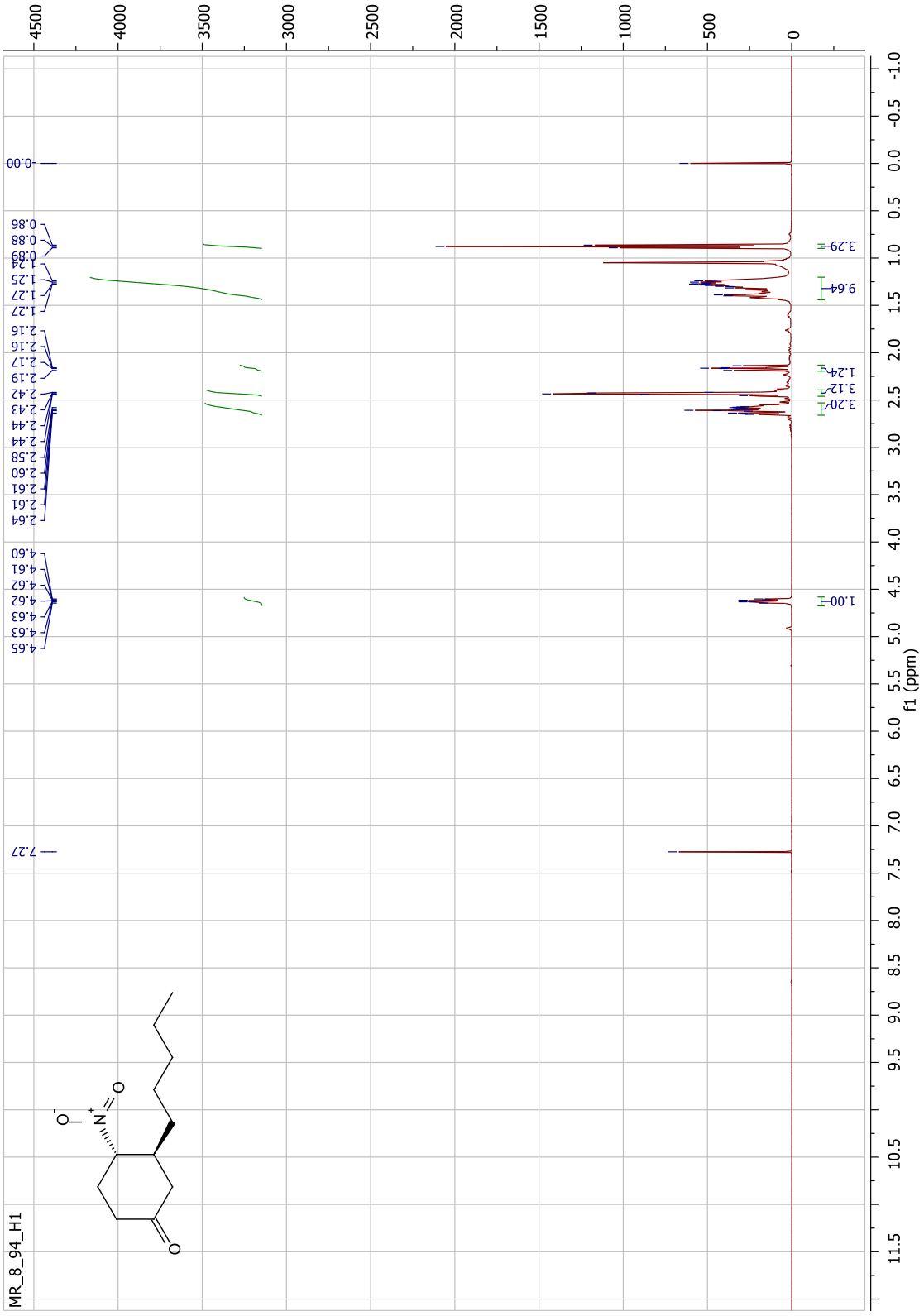

Figure 172. ^{1}H NMR spectrum of **216a** (500 MHz, $CDCl_3$).

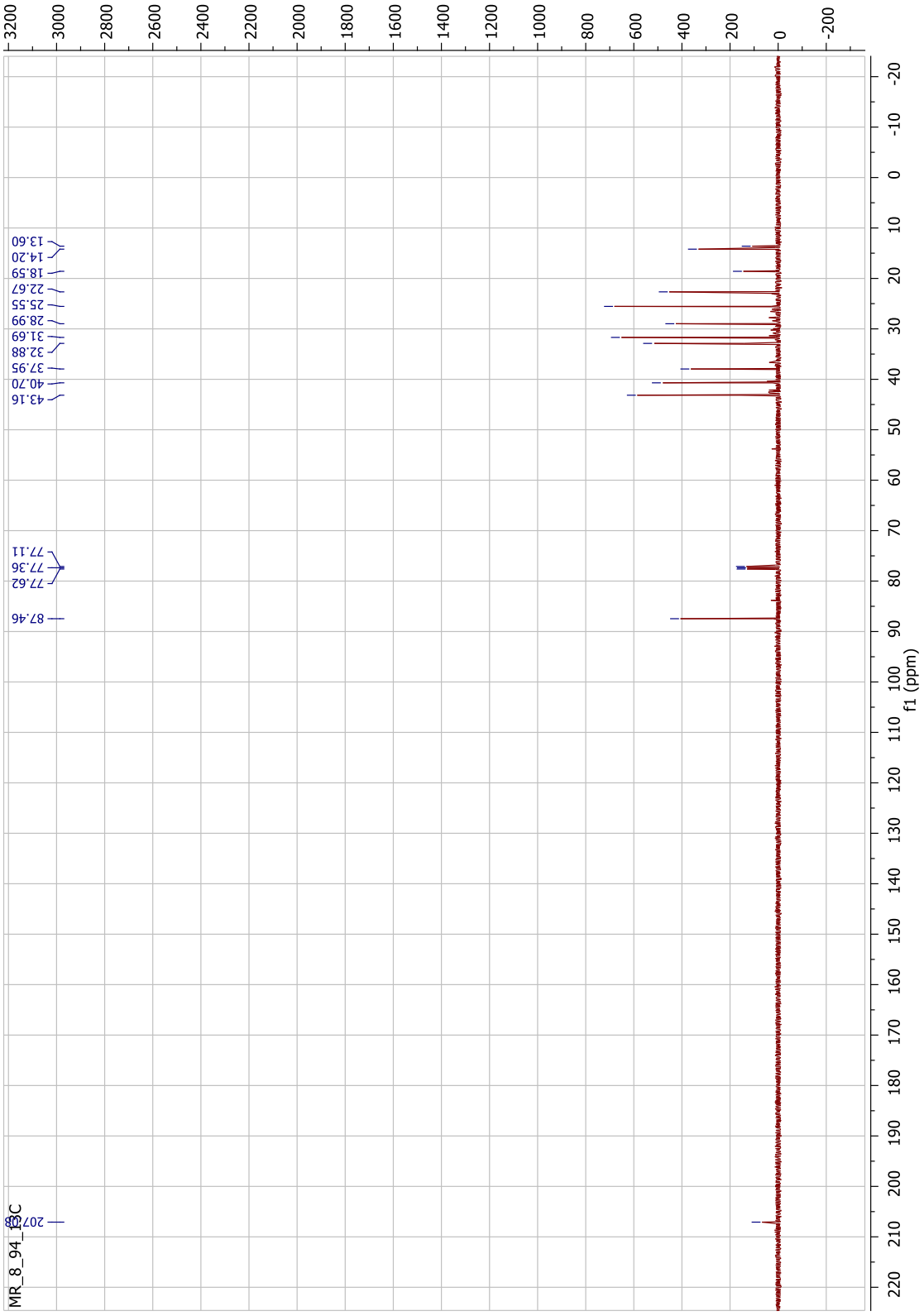

Figure 173. ^{13}C NMR spectrum of **216a** (125 MHz, $CDCl_3$).

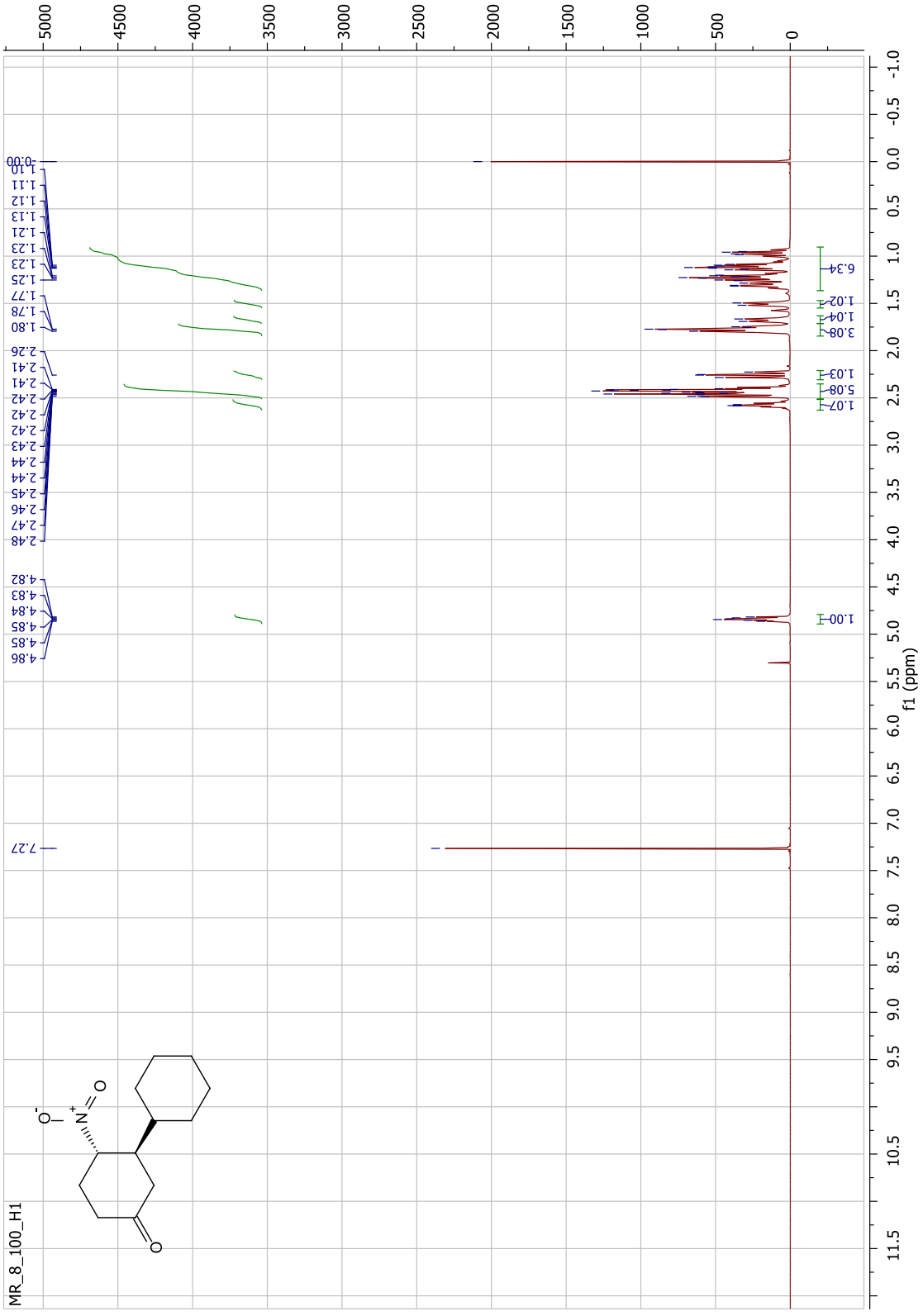

Figure 174. ^{1}H NMR spectrum of **217a** (500 MHz, $CDCl_3$).

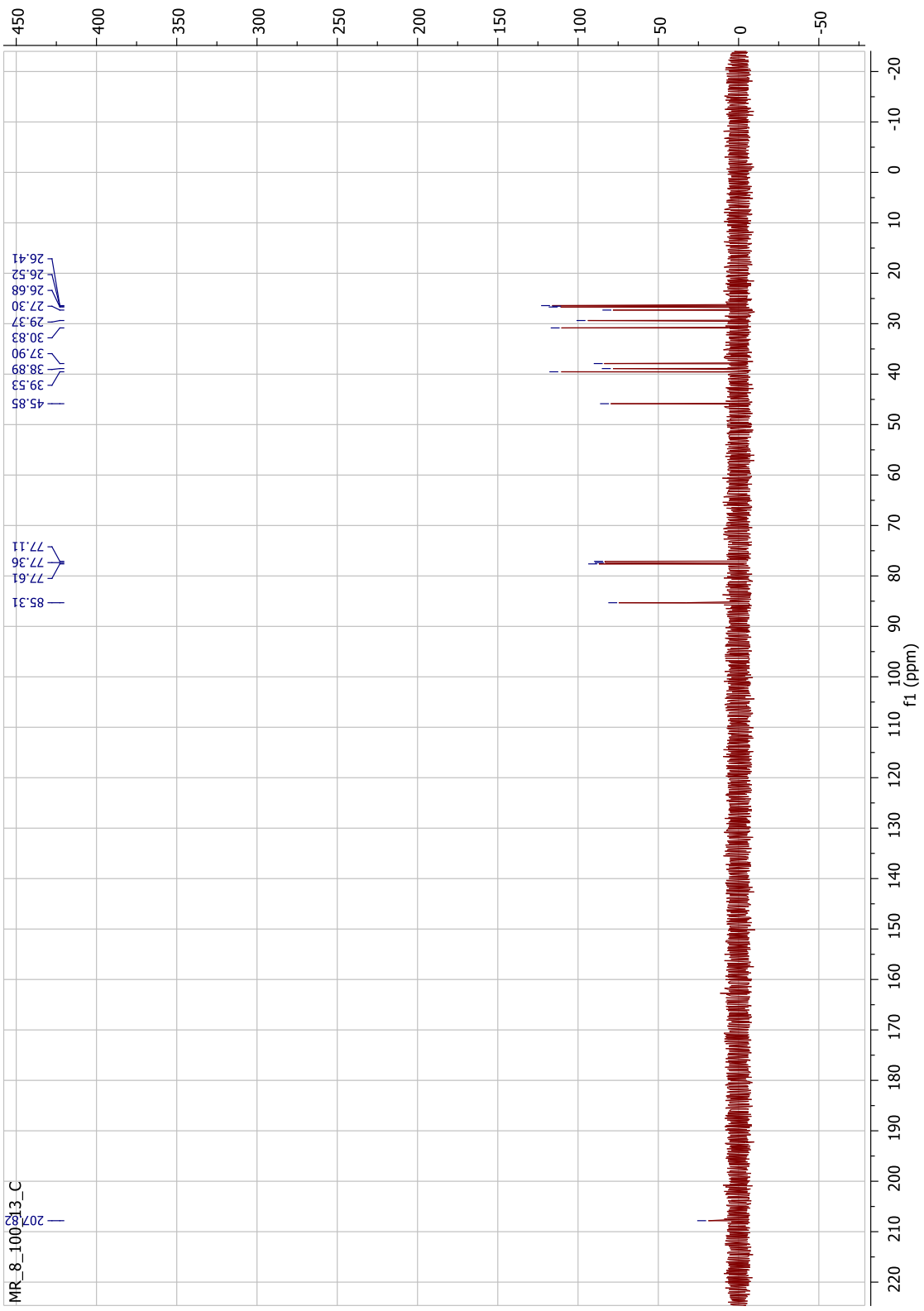

Figure 175. ^{13}C NMR spectrum of **217a** (125 MHz, $CDCl_3$).

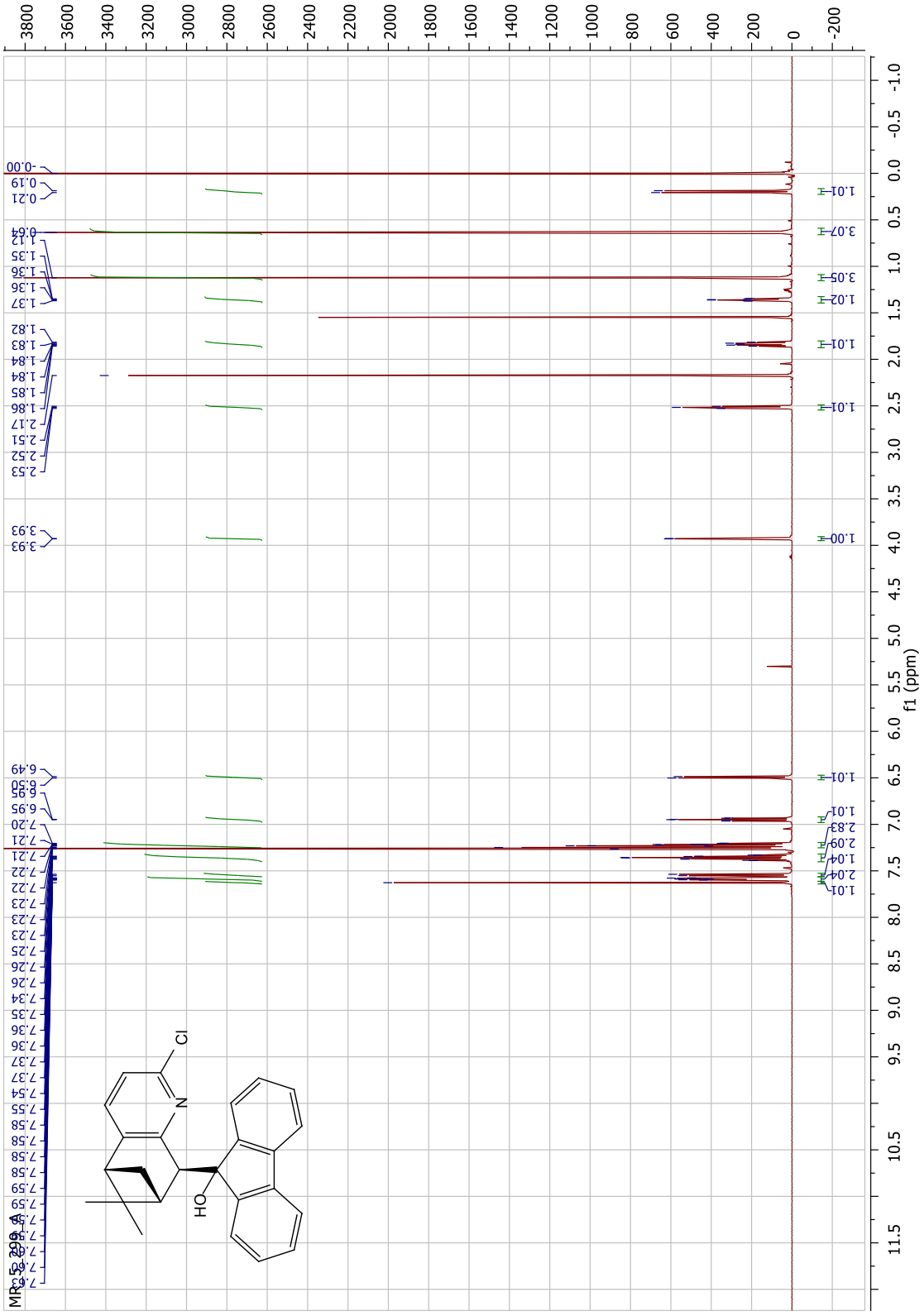

Figure 176. ^{1}H NMR spectrum of **250** (500 MHz, $CDCl_3$).

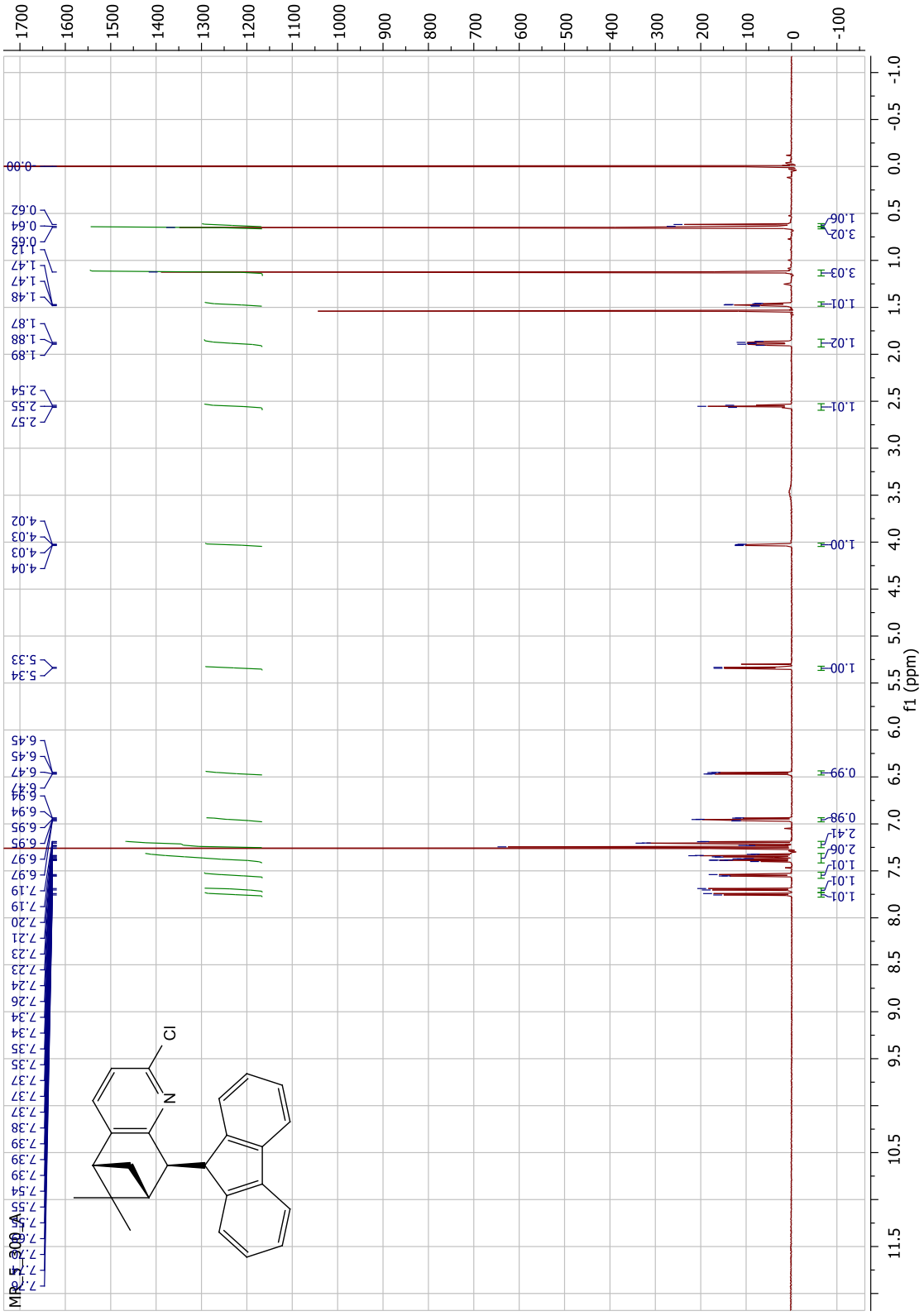

Figure 177. ^{1}H NMR spectrum of **251** (500 MHz, $CDCl_3$).

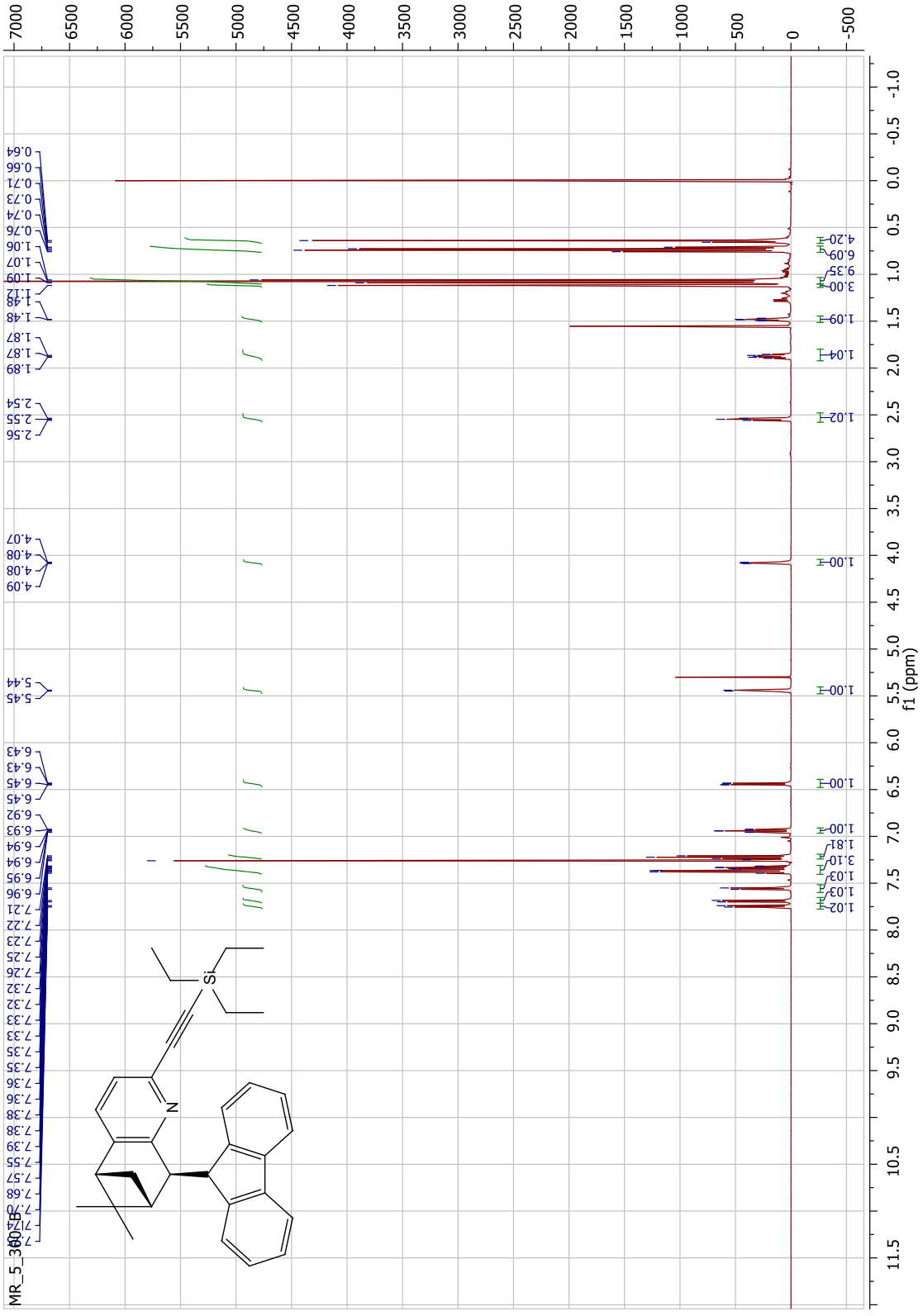

Figure 178. ^{1}H NMR spectrum of **252** (500 MHz, $CDCl_3$).

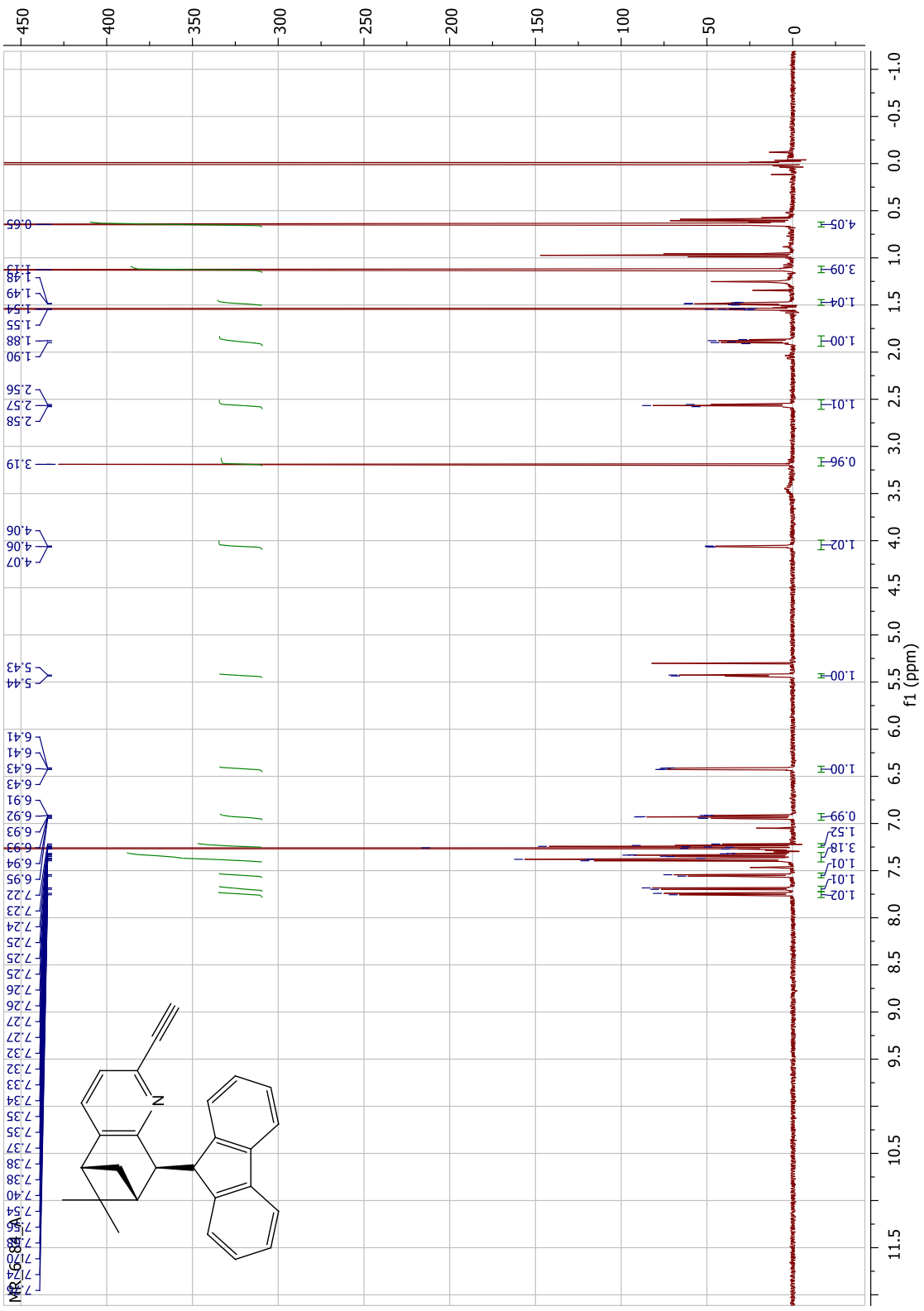

Figure 179. ^{1}H NMR spectrum of **253** (500 MHz, $CDCl_3$).

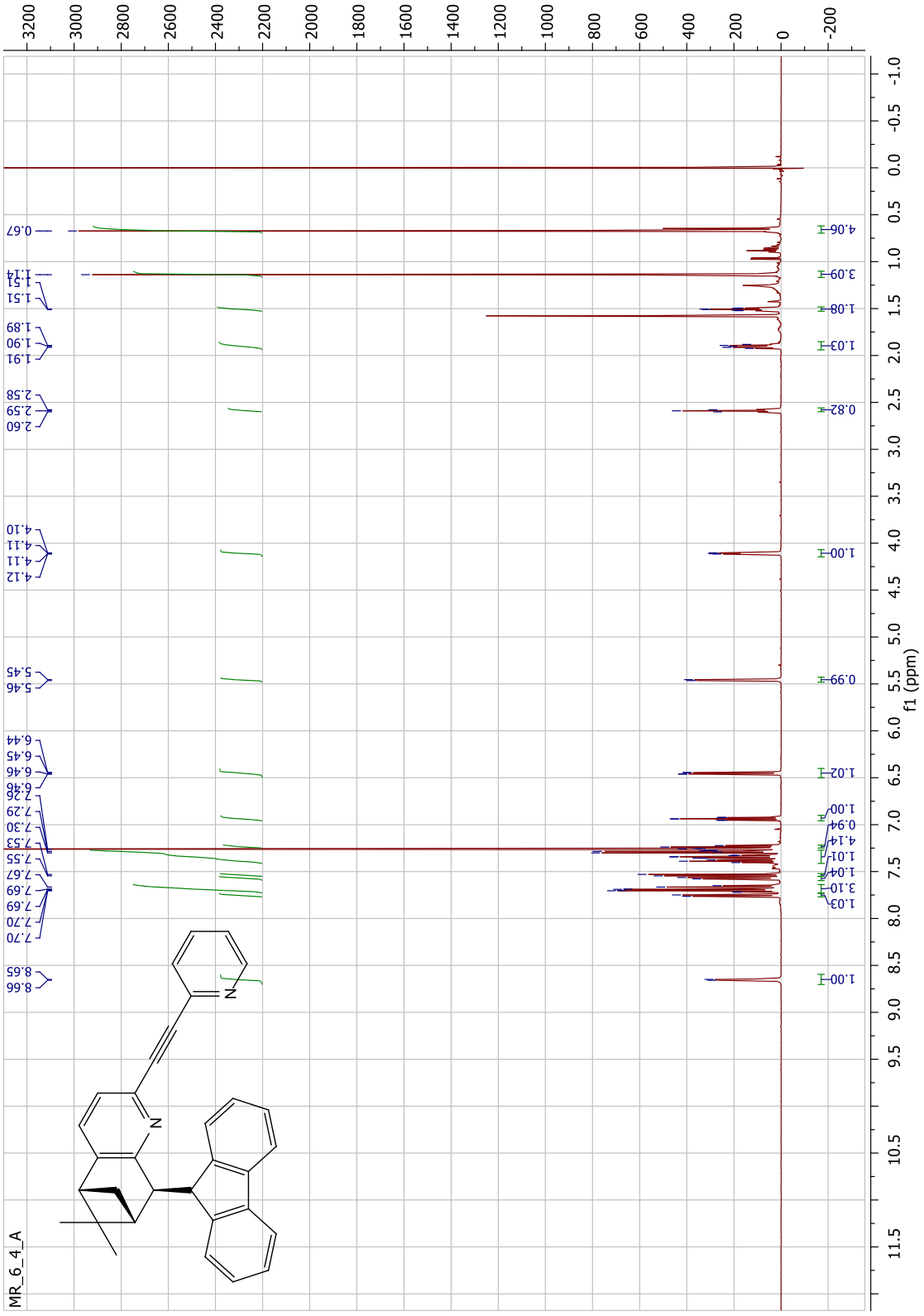

Figure 180. ^{1}H NMR spectrum of **254** (500 MHz, $CDCl_3$).

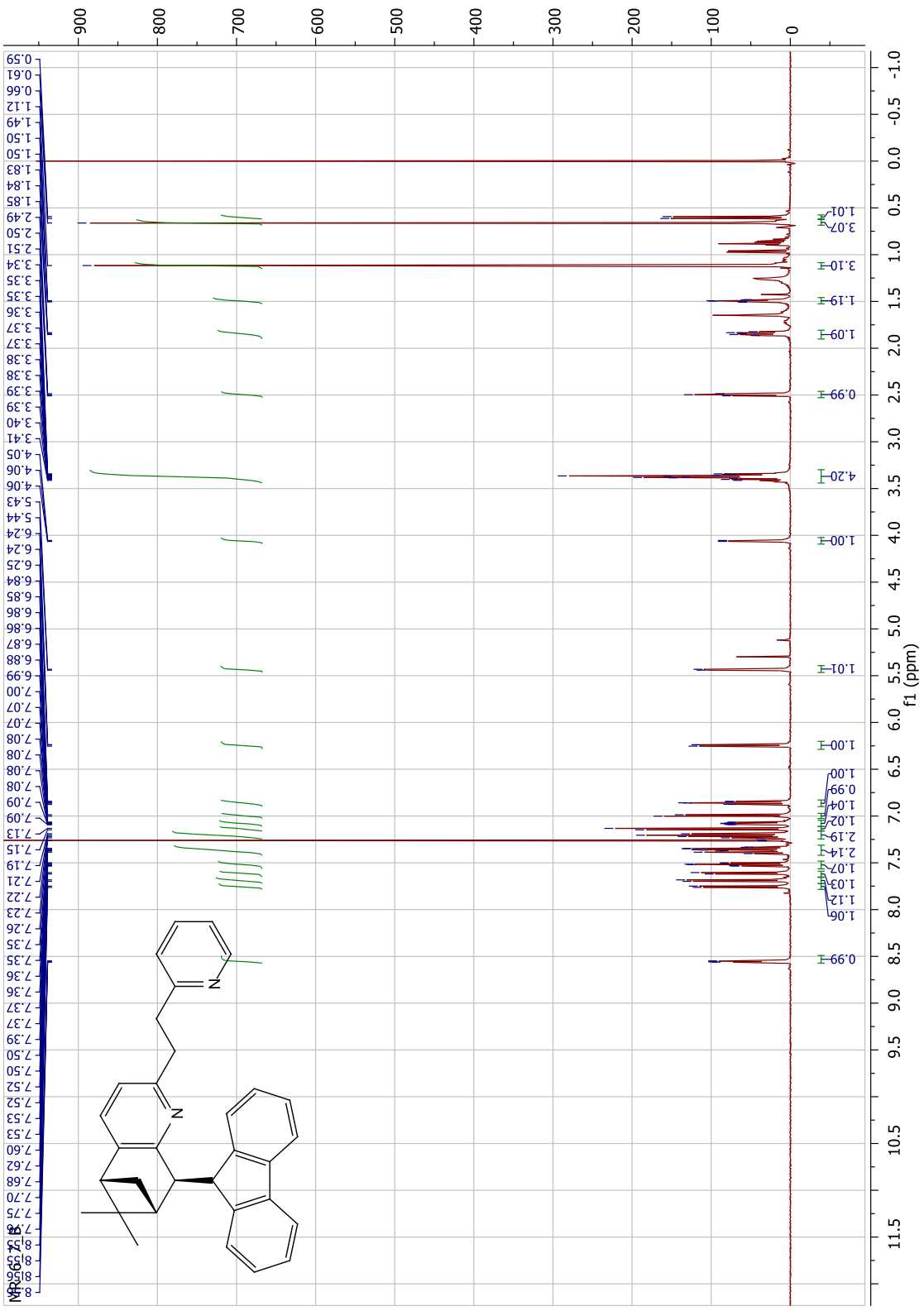

Figure 181. ^{1}H NMR spectrum of **306** (500 MHz, $CDCl_3$).

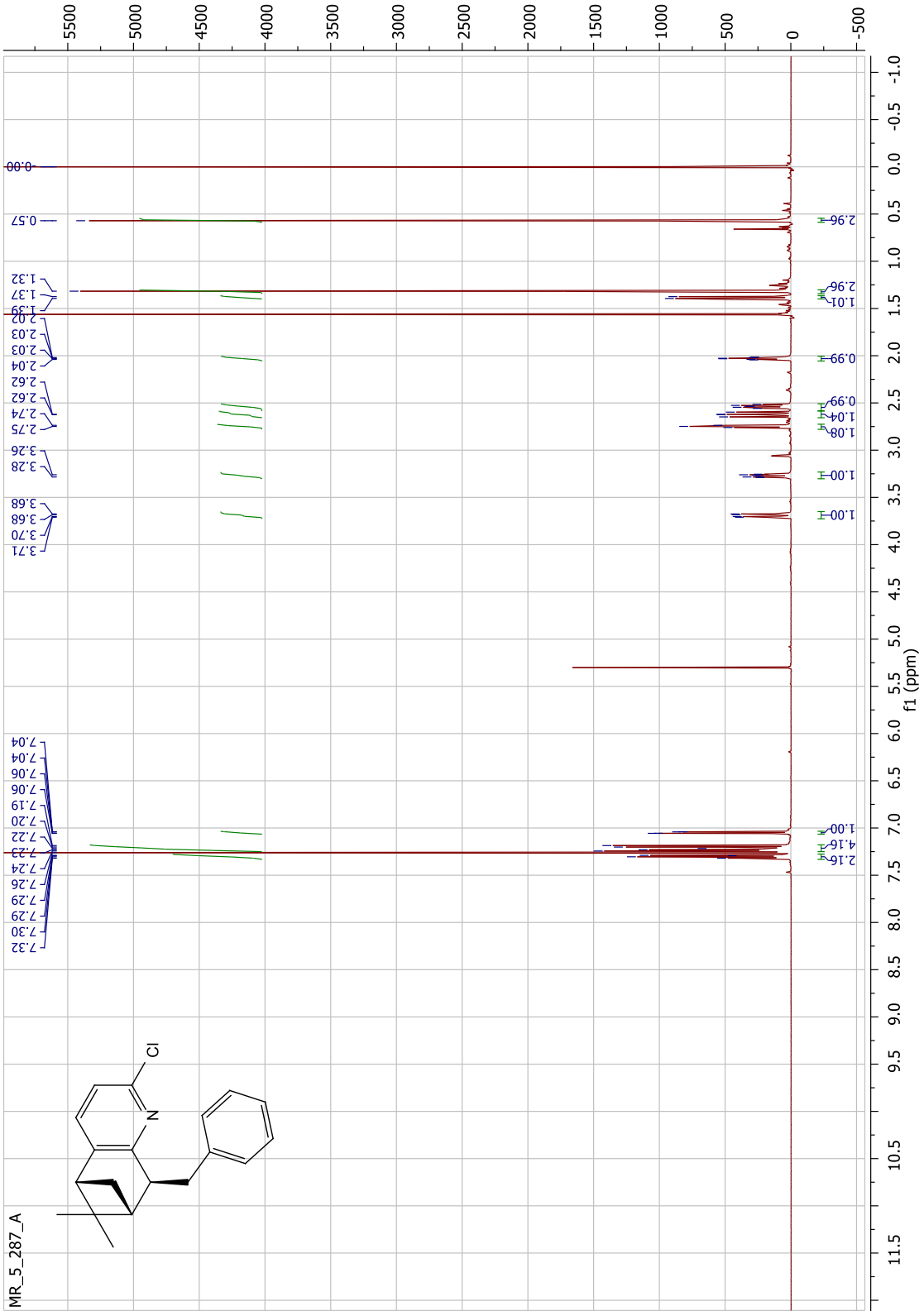

Figure 182. ^{1}H NMR spectrum of **307** (500 MHz, $CDCl_3$).

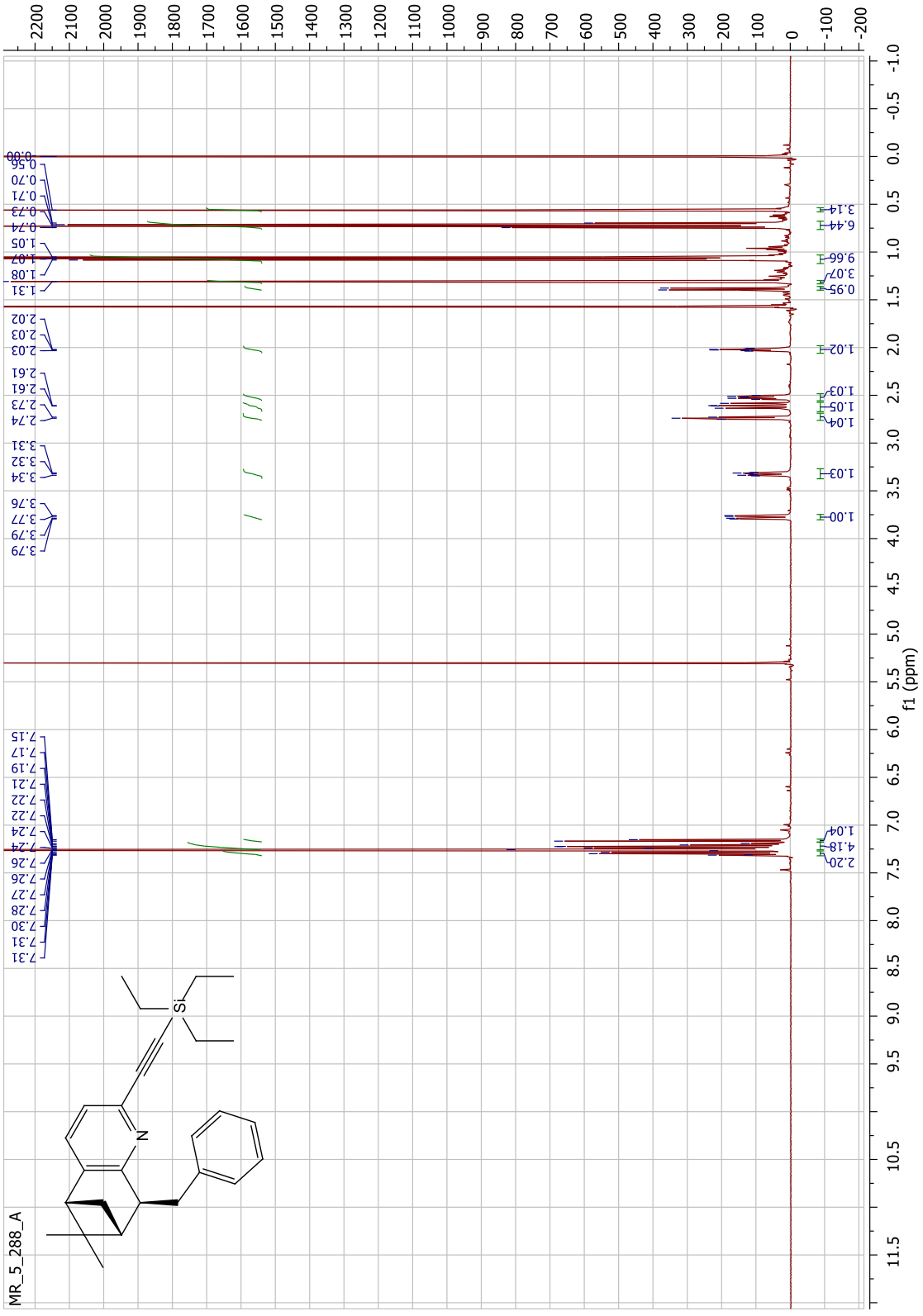

Figure 183. ^{1}H NMR spectrum of **308** (500 MHz, $CDCl_3$).

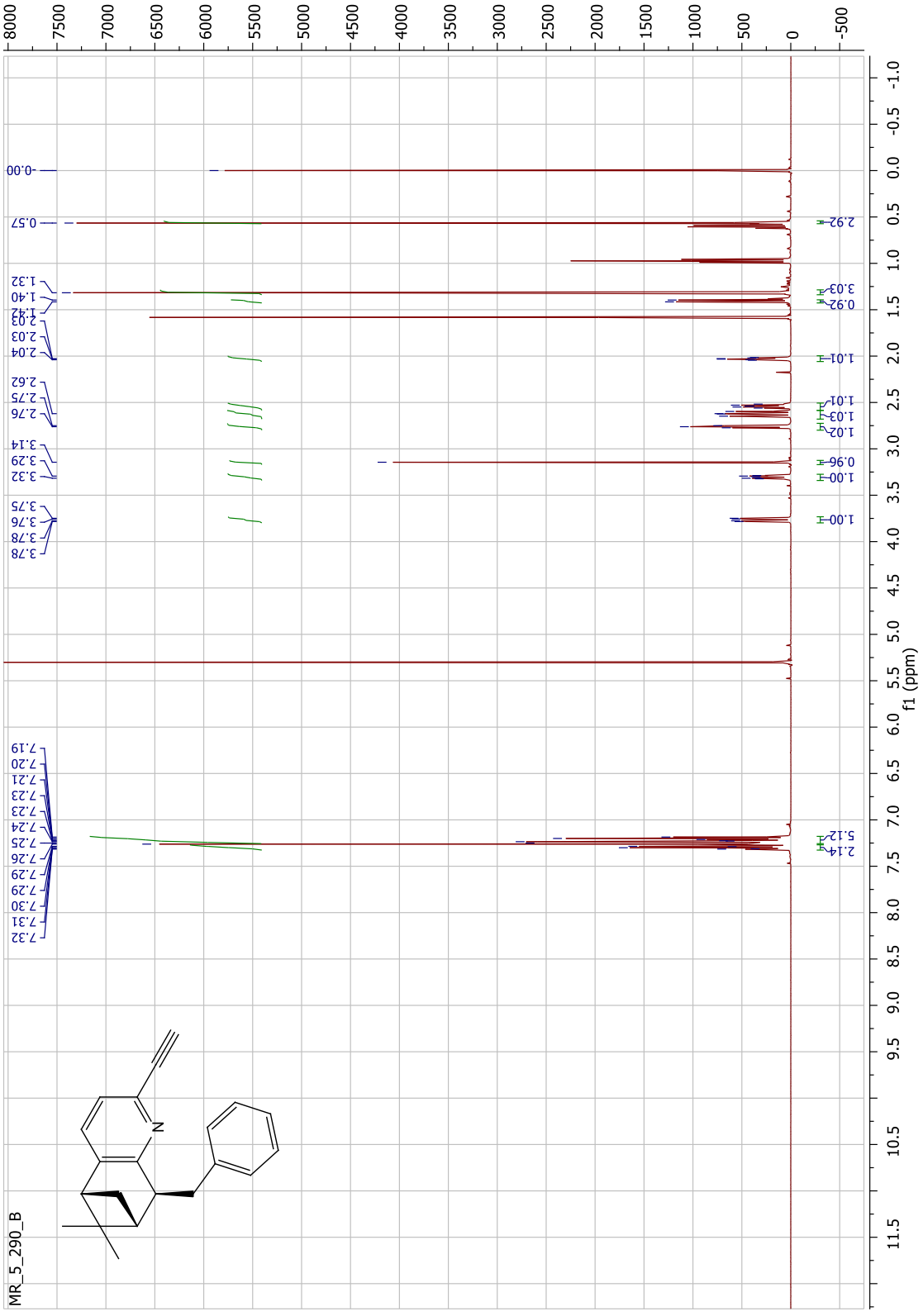

Figure 184. ^{1}H NMR spectrum of **309** (500 MHz, $CDCl_3$).

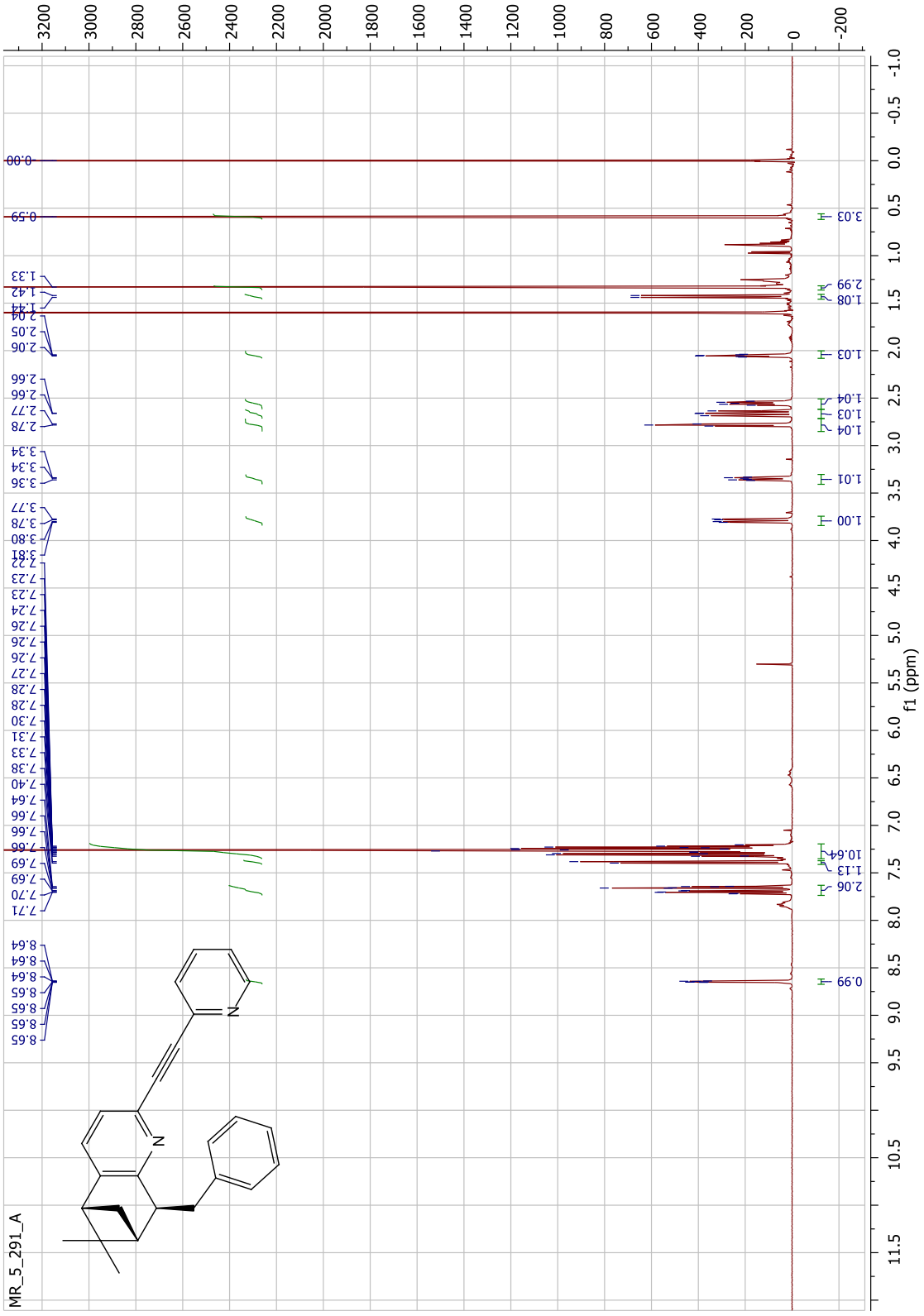

Figure 185. ^{1}H NMR spectrum of **310** (500 MHz, $CDCl_3$).

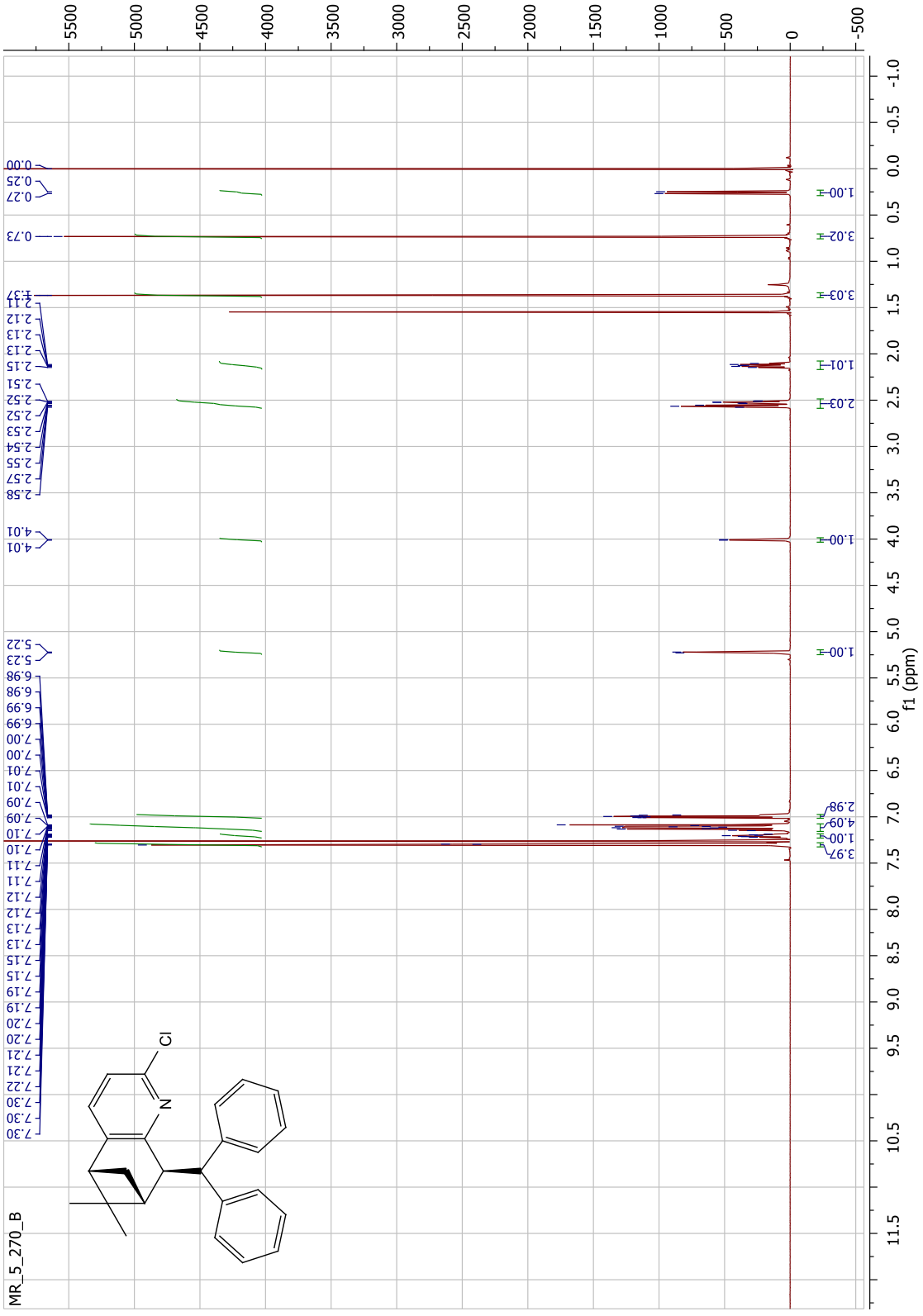

Figure 186. ^{1}H NMR spectrum of **311** (500 MHz, $CDCl_3$).

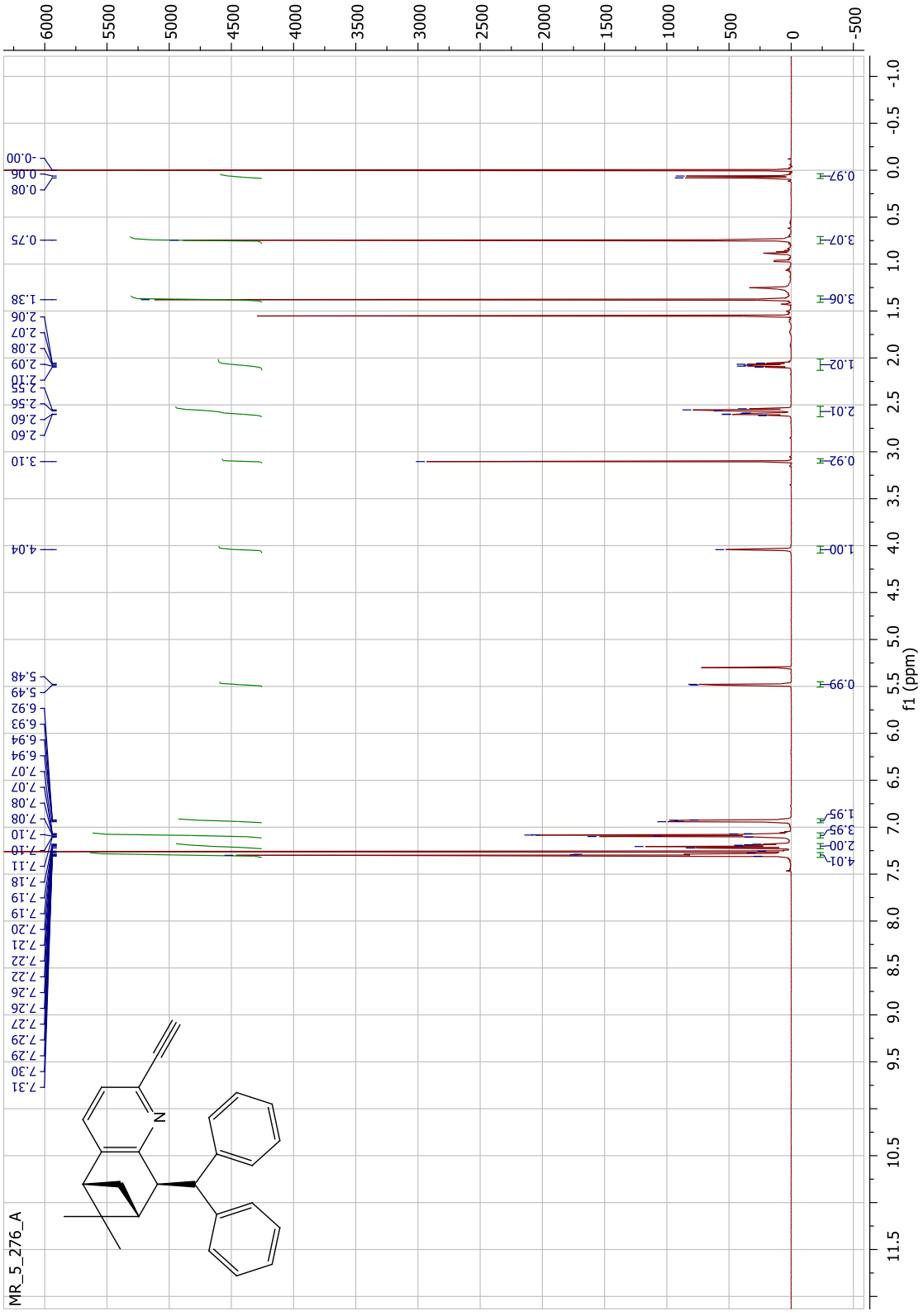

Figure 187. ^{1}H NMR spectrum of **312** (500 MHz, $CDCl_3$).

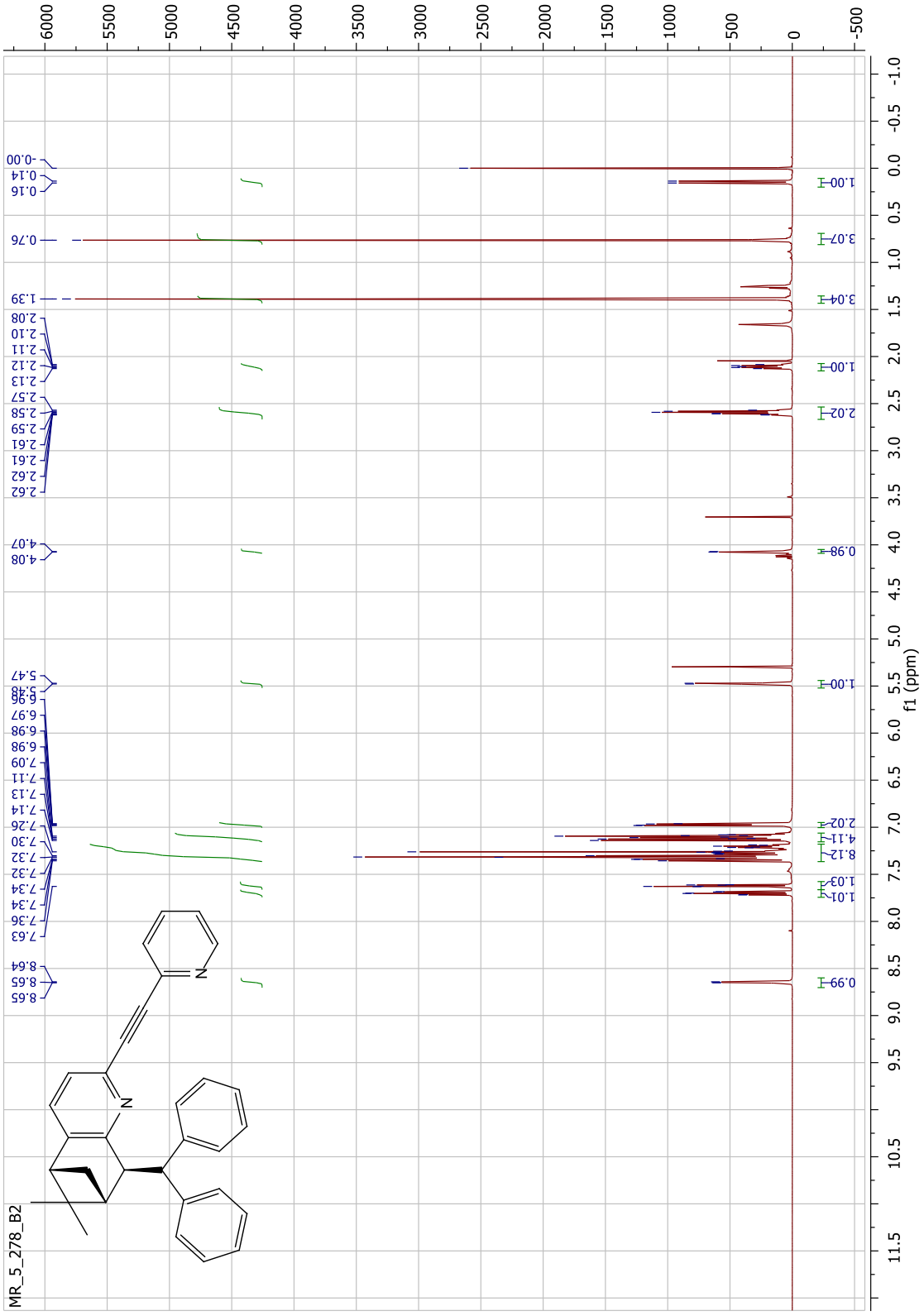

Figure 188. ^{1}H NMR spectrum of **313** (500 MHz, $CDCl_3$).

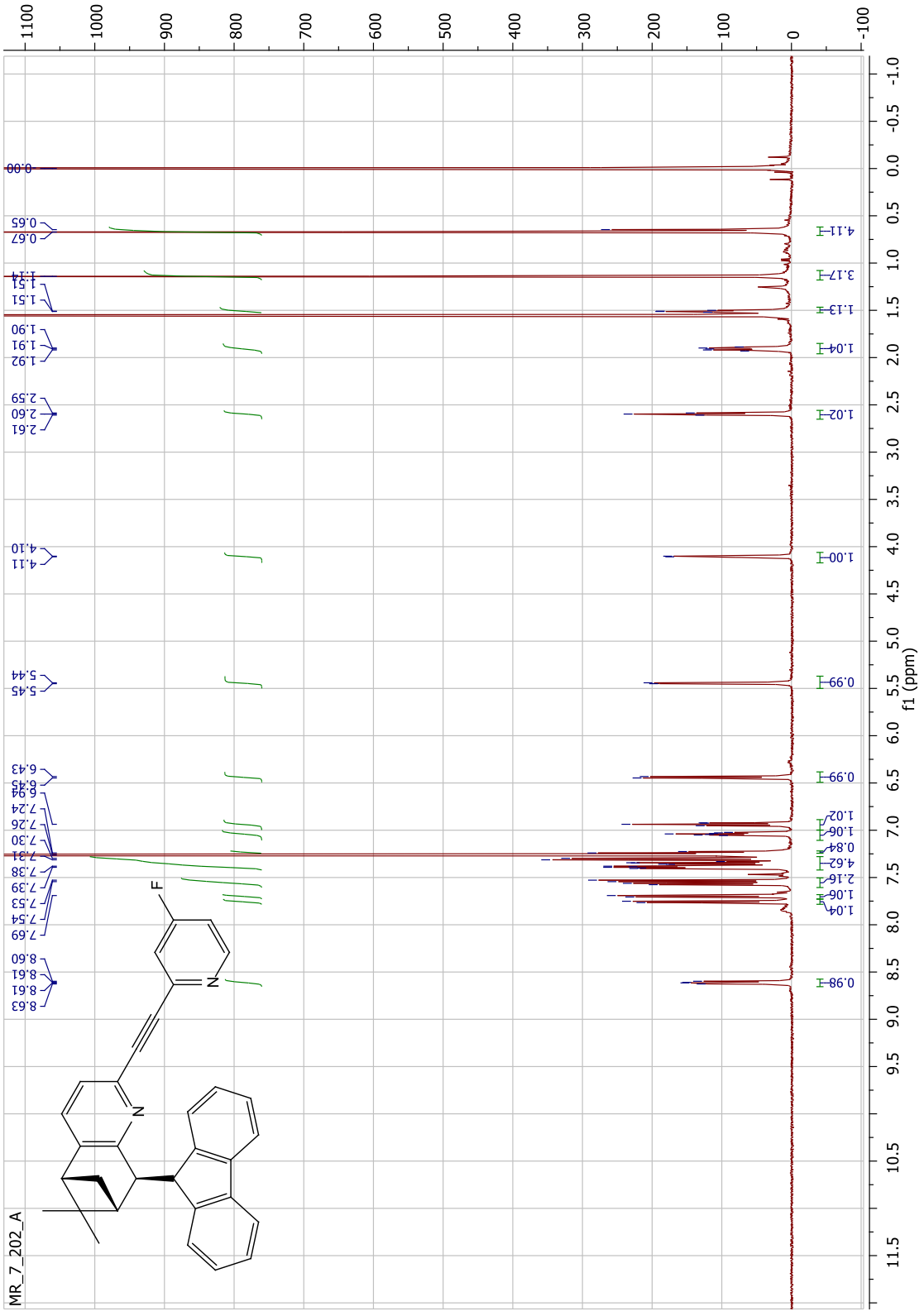

Figure 189. ^{1}H NMR spectrum of **319** (500 MHz, $CDCl_3$).

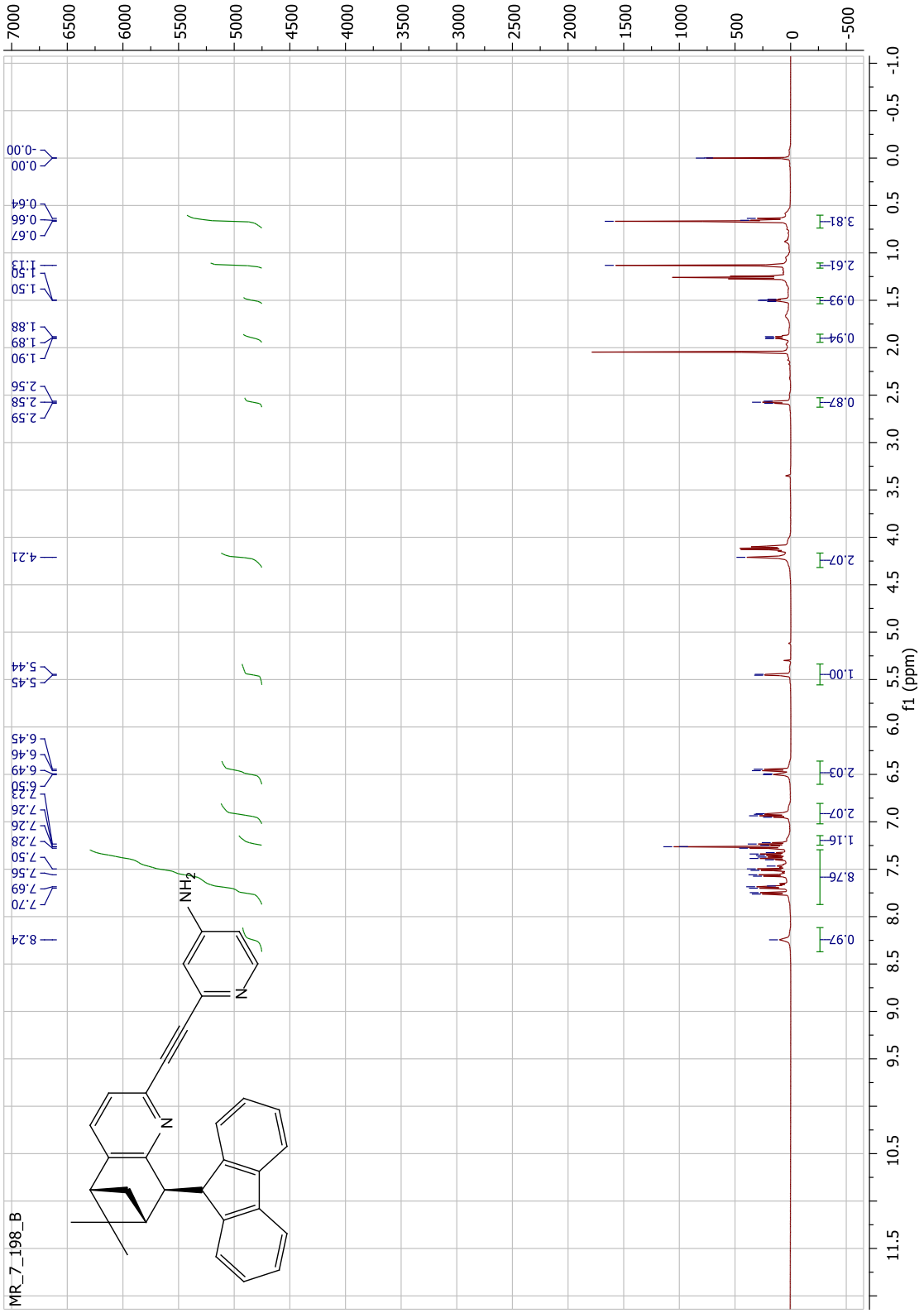

Figure 190. ^{1}H NMR spectrum of **320** (500 MHz, $CDCl_3$).

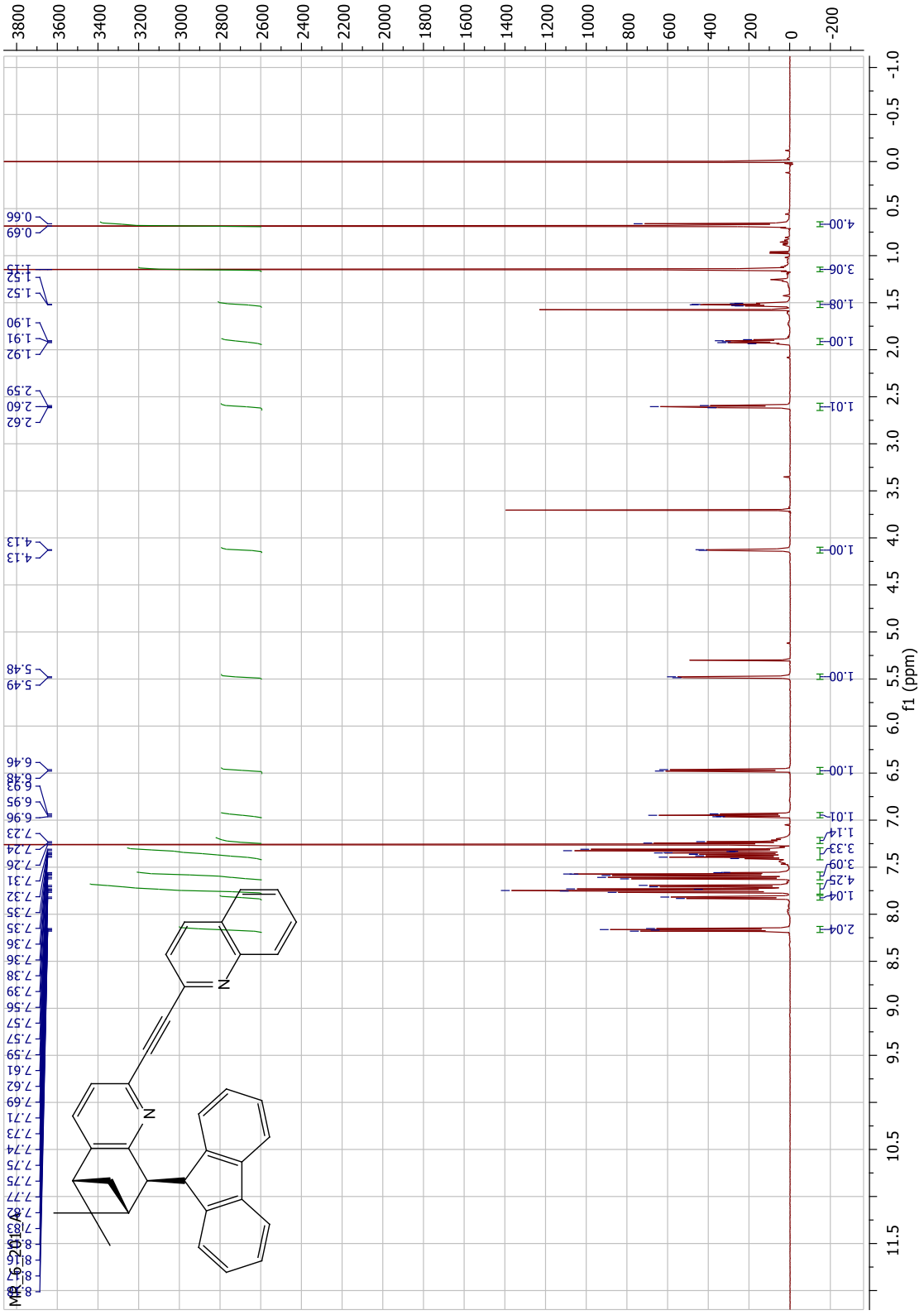

Figure 191. ^{1}H NMR spectrum of **321** (500 MHz, $CDCl_3$).

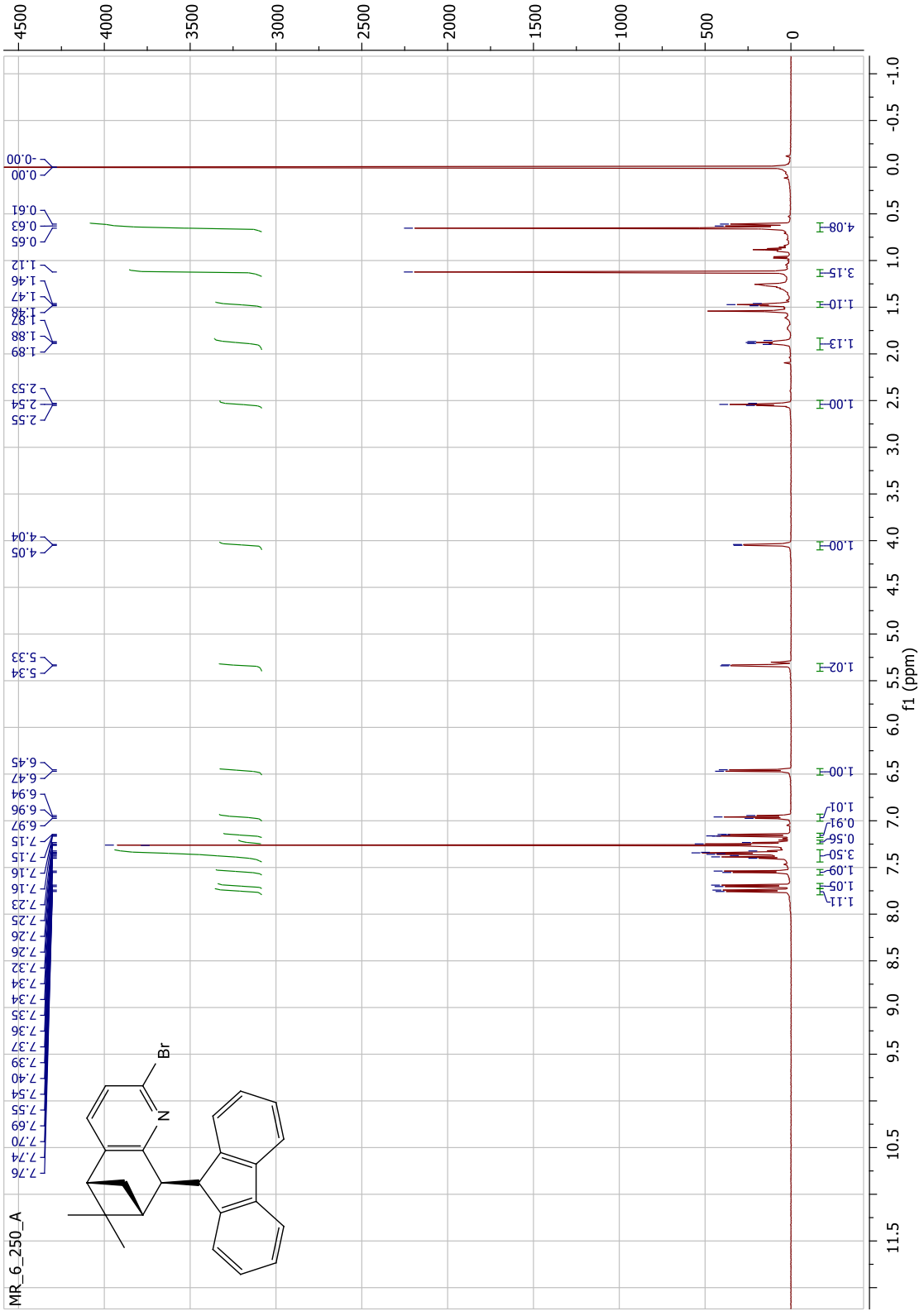

Figure 192. ^{1}H NMR spectrum of **270** (500 MHz, $CDCl_3$).

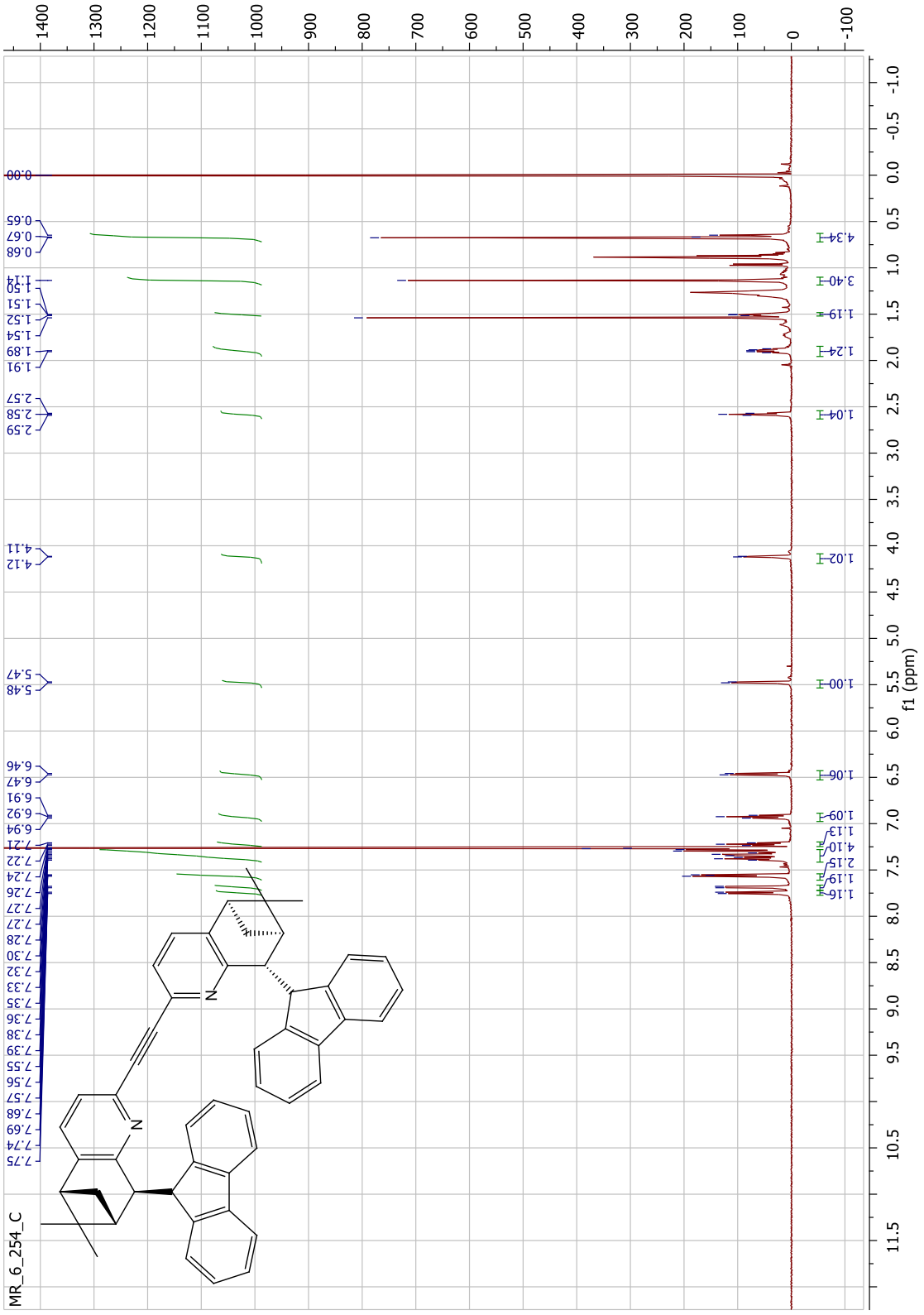

Figure 193. ^{1}H NMR spectrum of **322** (500 MHz, $CDCl_3$).

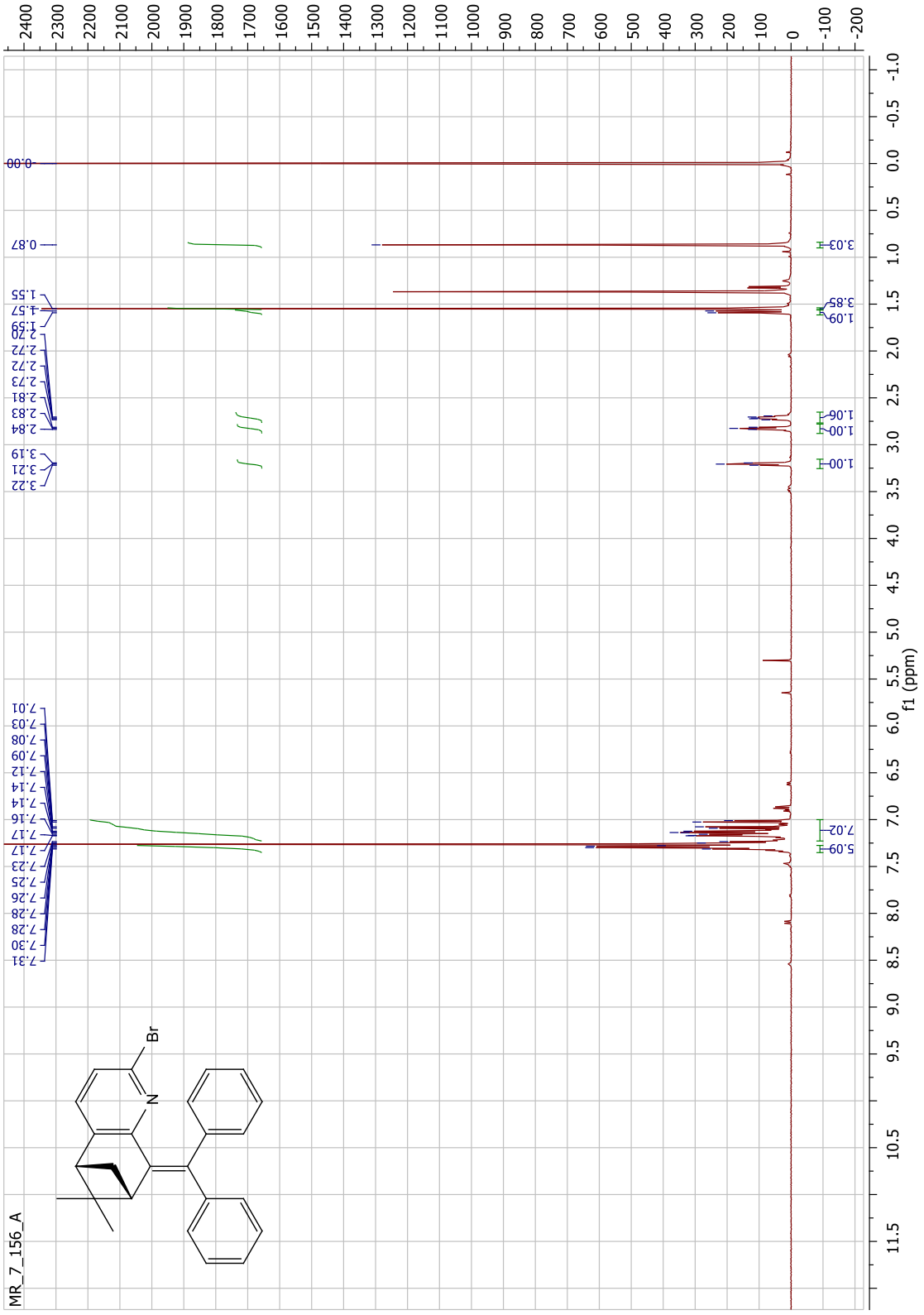

Figure 194. ^{1}H NMR spectrum of **269** (500 MHz, $CDCl_3$).

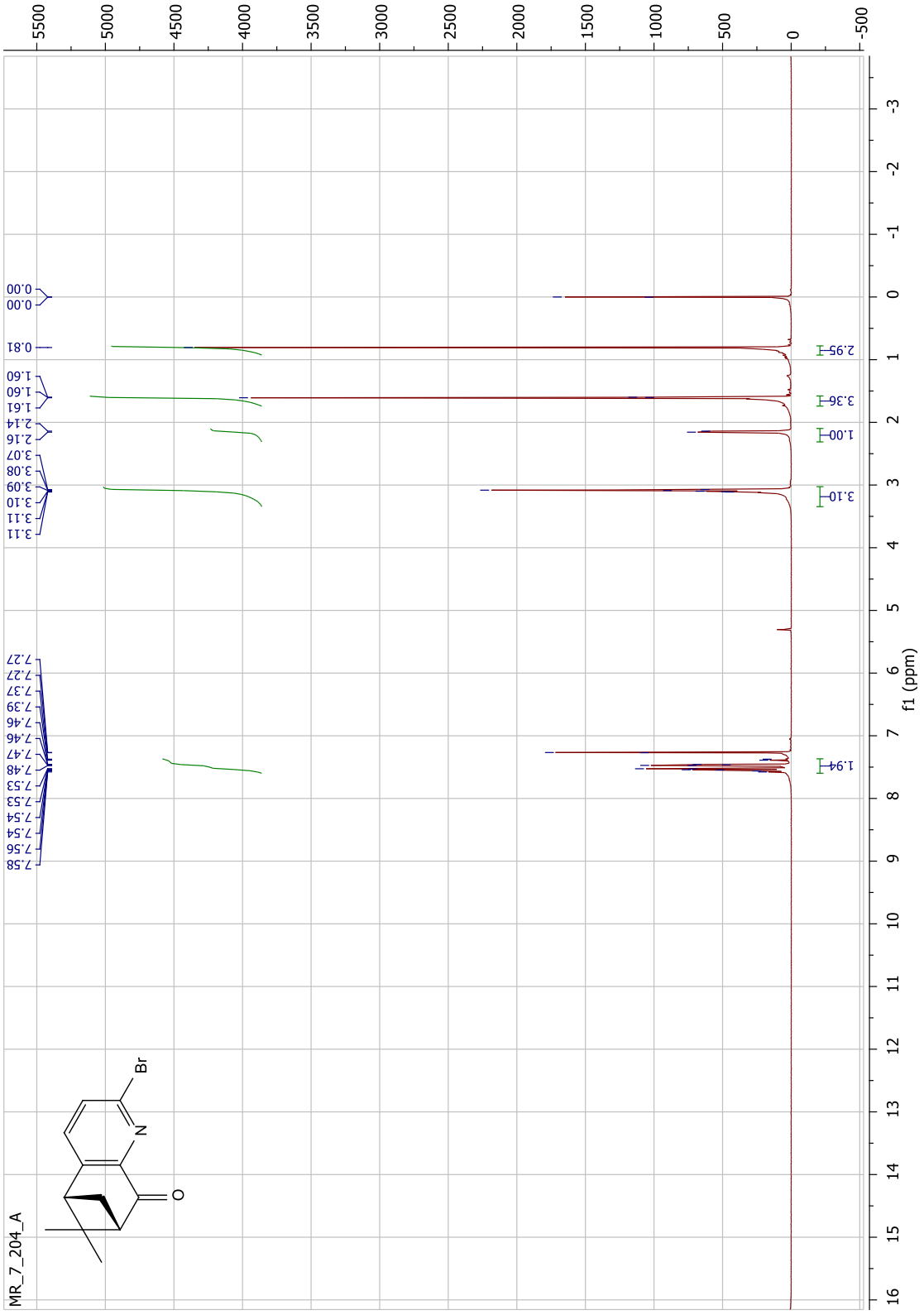

Figure 195. ^{1}H NMR spectrum of **274** (500 MHz, $CDCl_3$).

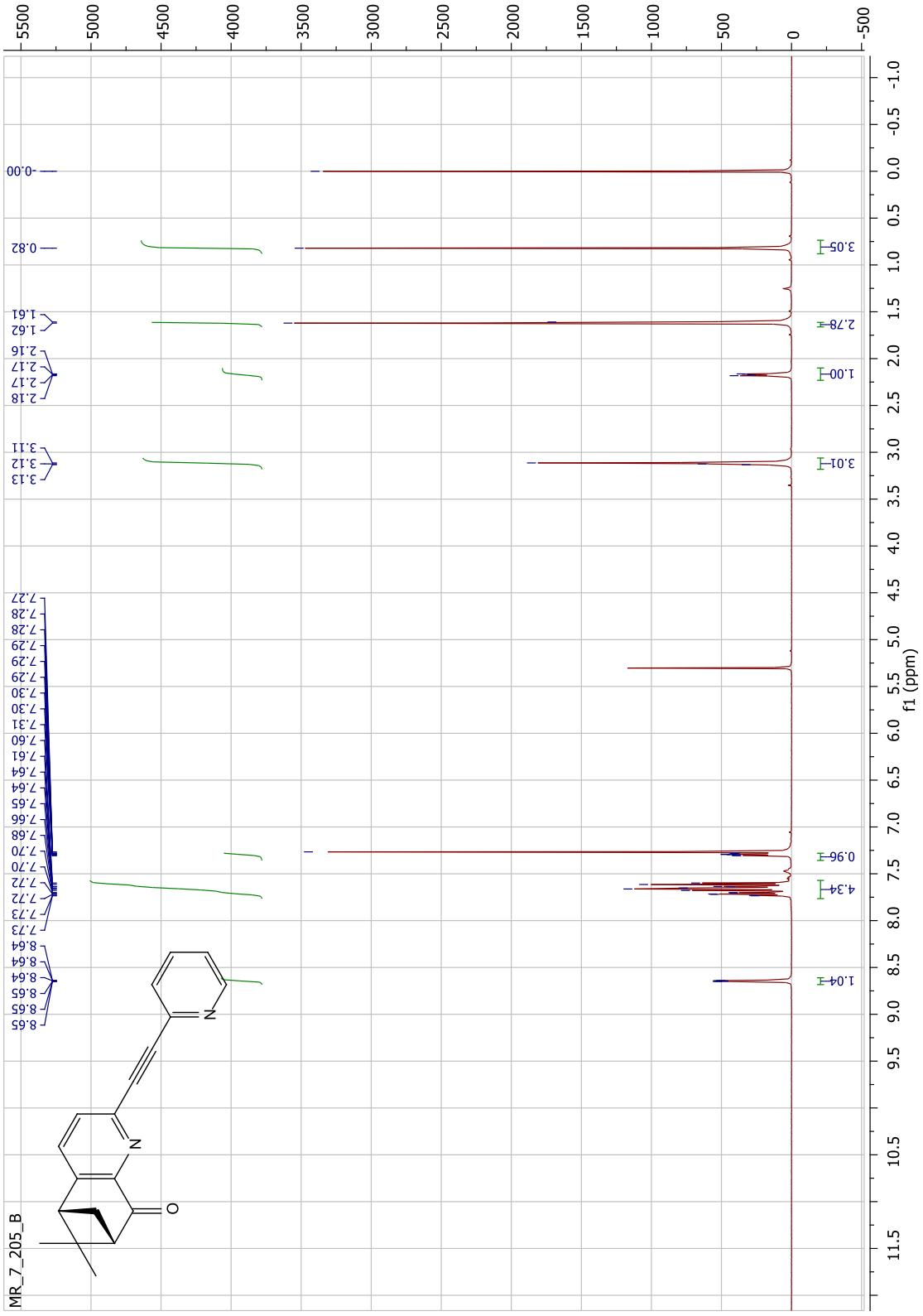

Figure 196. ^{1}H NMR spectrum of **267** (500 MHz, $CDCl_3$).

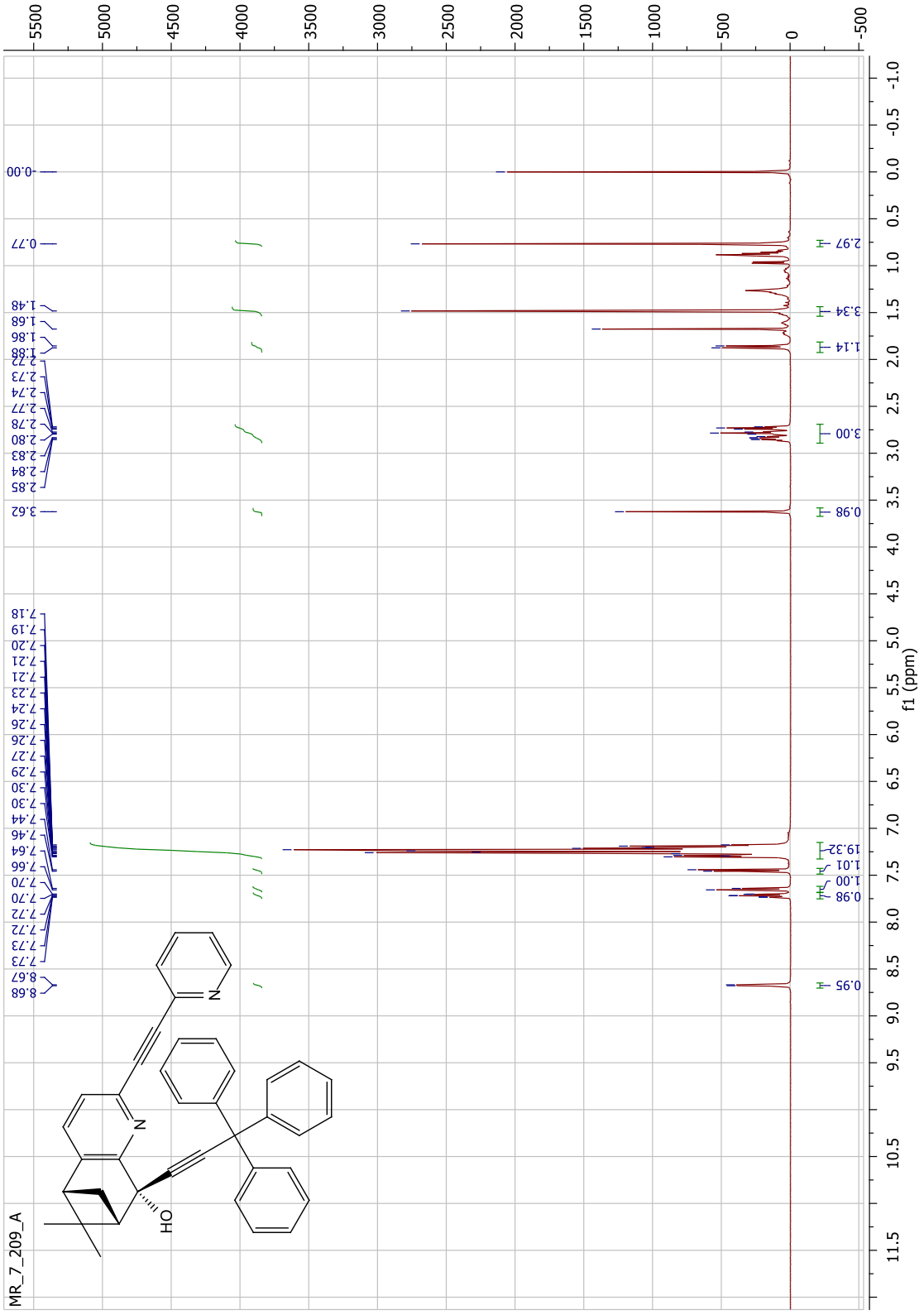

Figure 197. ^{1}H NMR spectrum of **324** (500 MHz, $CDCl_3$).

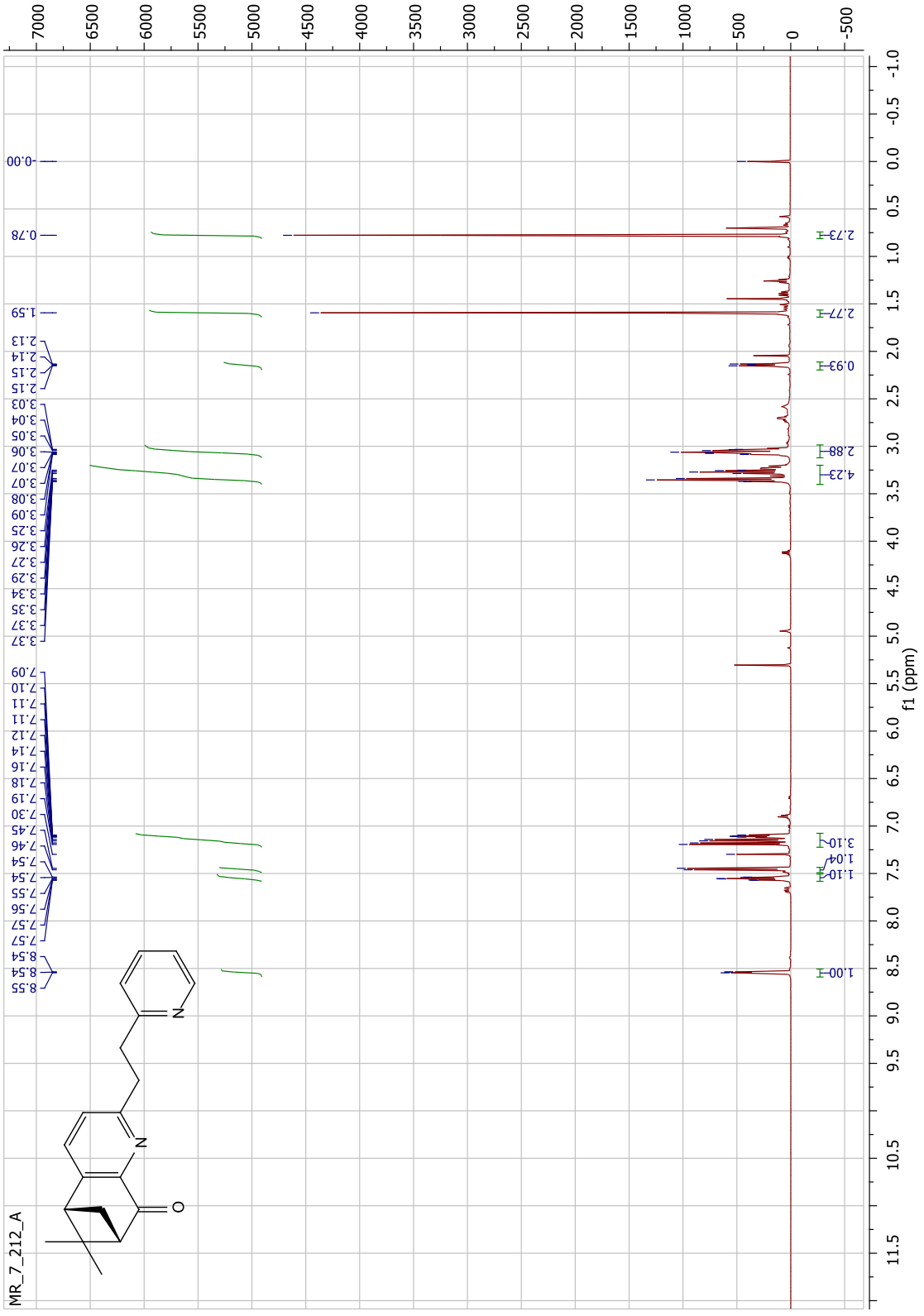

Figure 198. ^{1}H NMR spectrum of **280** (500 MHz, $CDCl_3$).

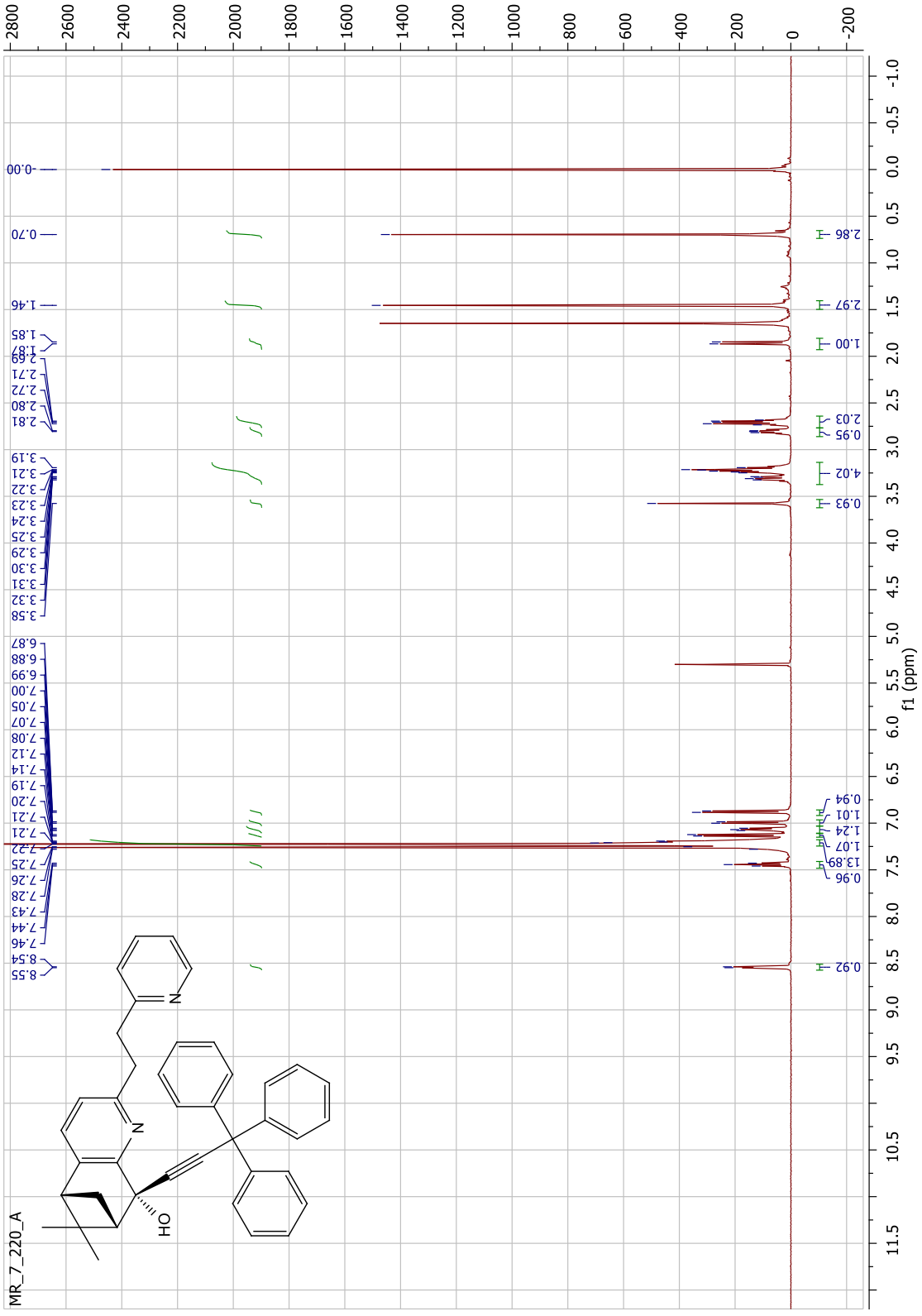

Figure 199. ^{1}H NMR spectrum of **325** (500 MHz, $CDCl_3$).

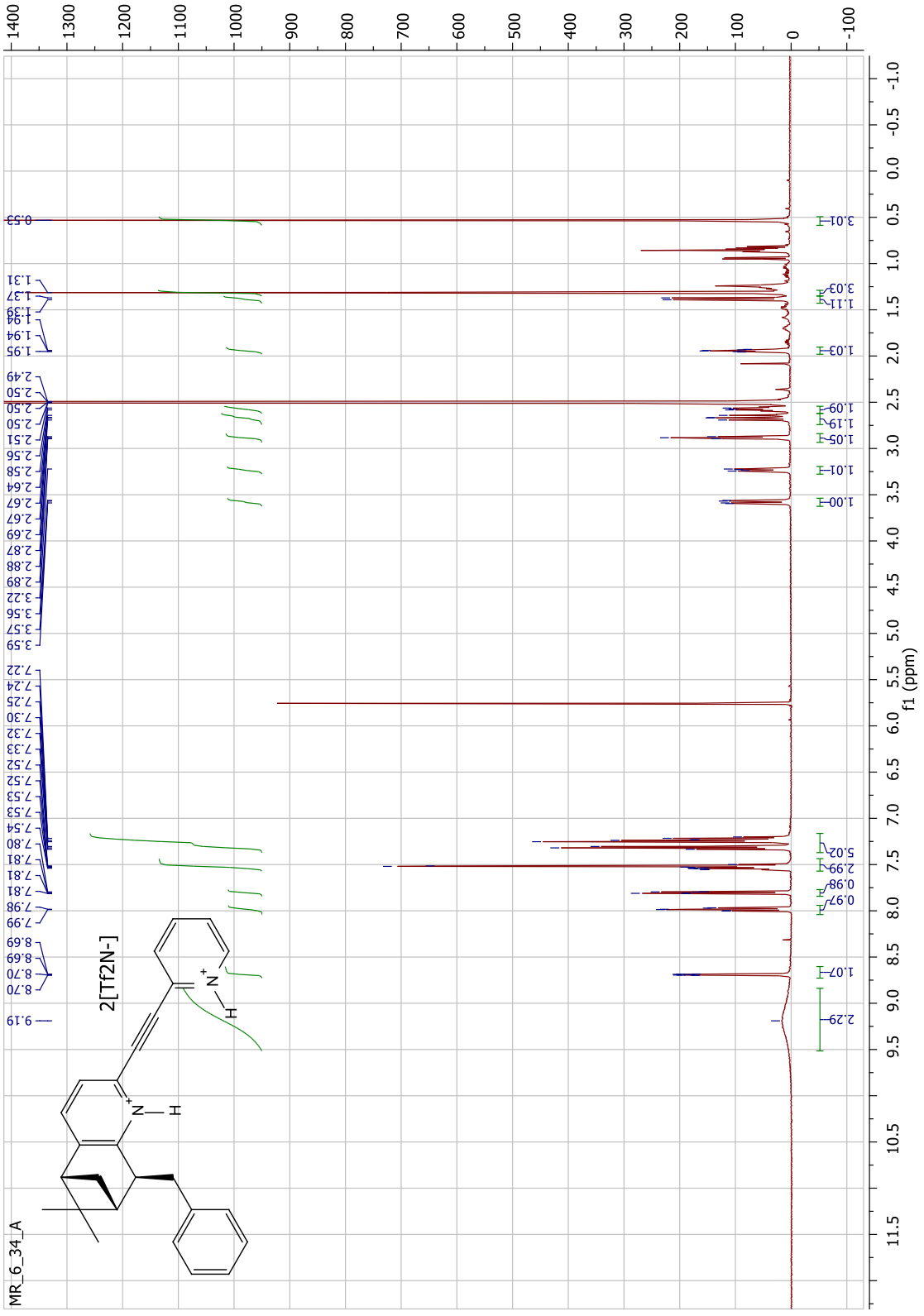

Figure 200. ^{1}H NMR spectrum of **255** (500 MHz, DMSO-d_6).

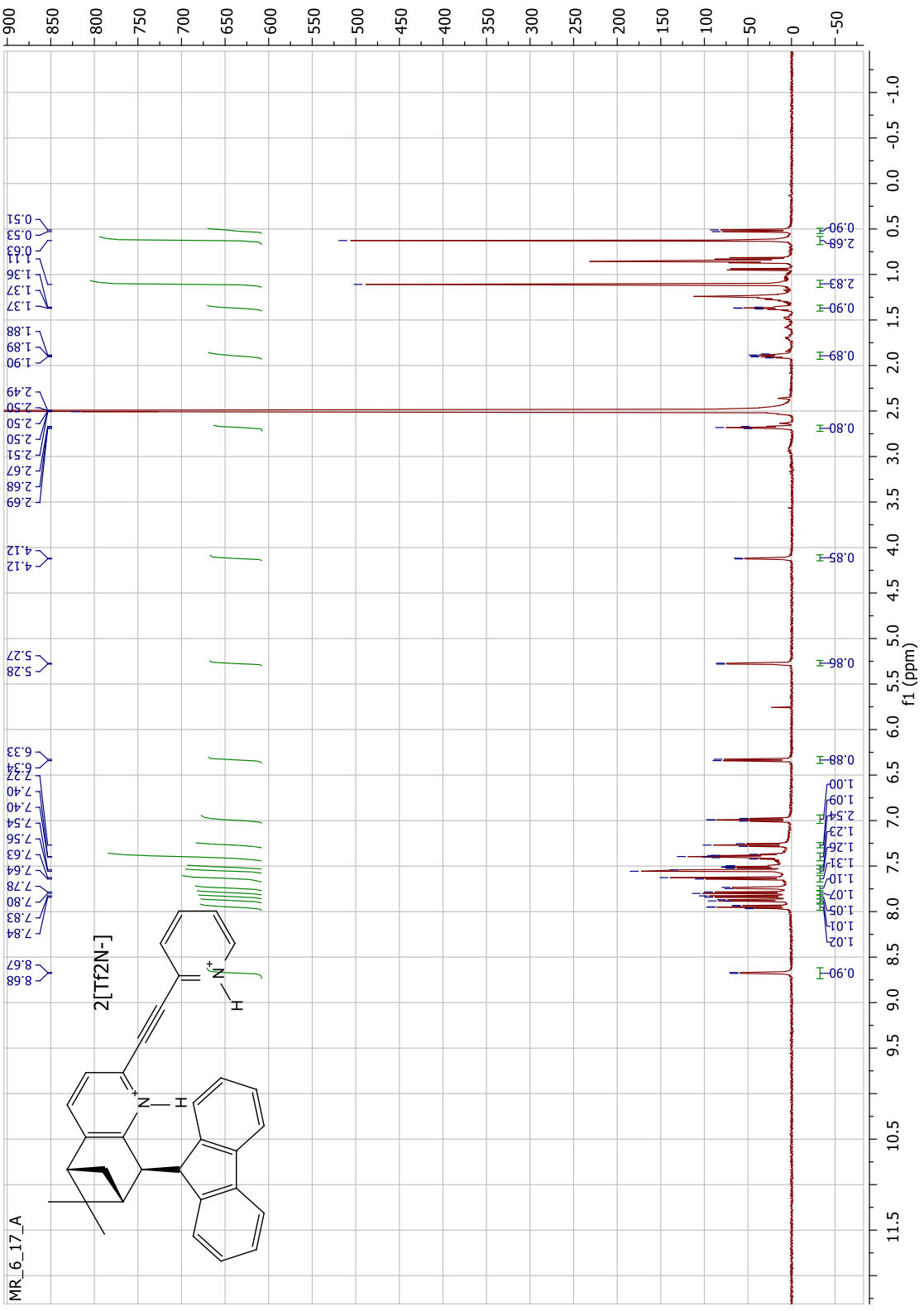

Figure 201. ^{1}H NMR spectrum of **257** (500 MHz, DMSO-d_6).

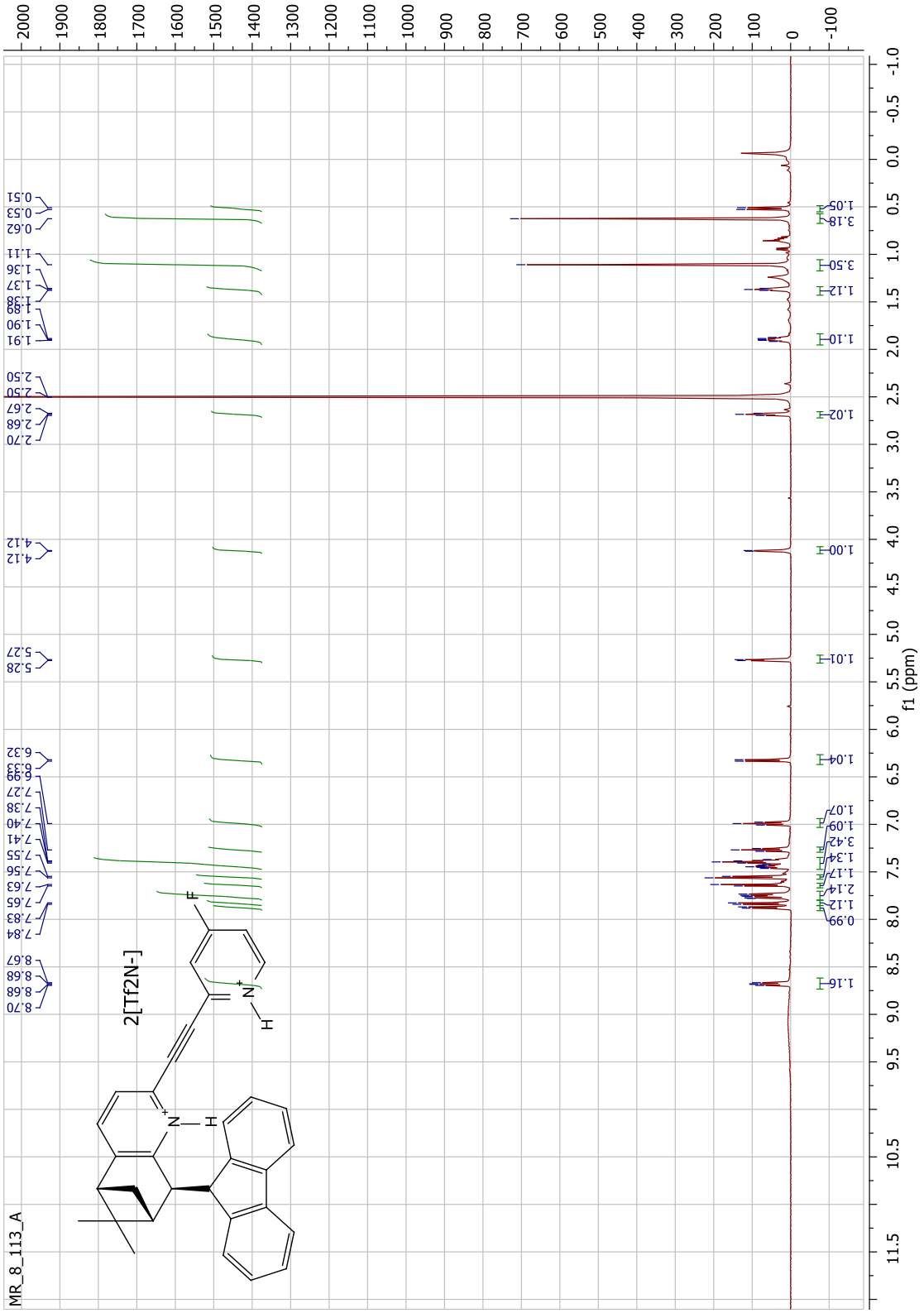

Figure 202. ^{1}H NMR spectrum of **259** (500 MHz, DMSO-d_6).

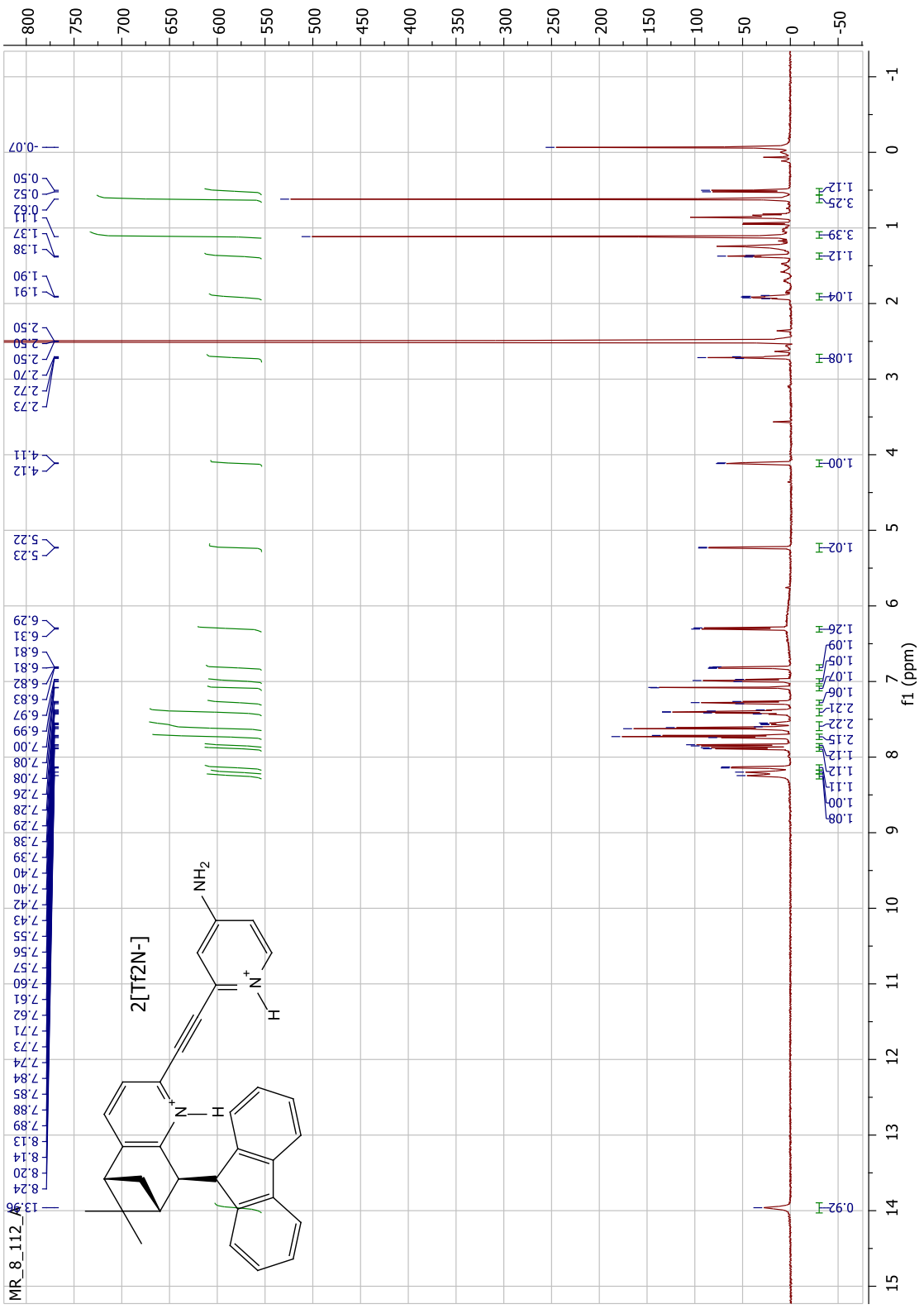

Figure 203. ^{1}H NMR spectrum of **260** (500 MHz, DMSO-d_6).

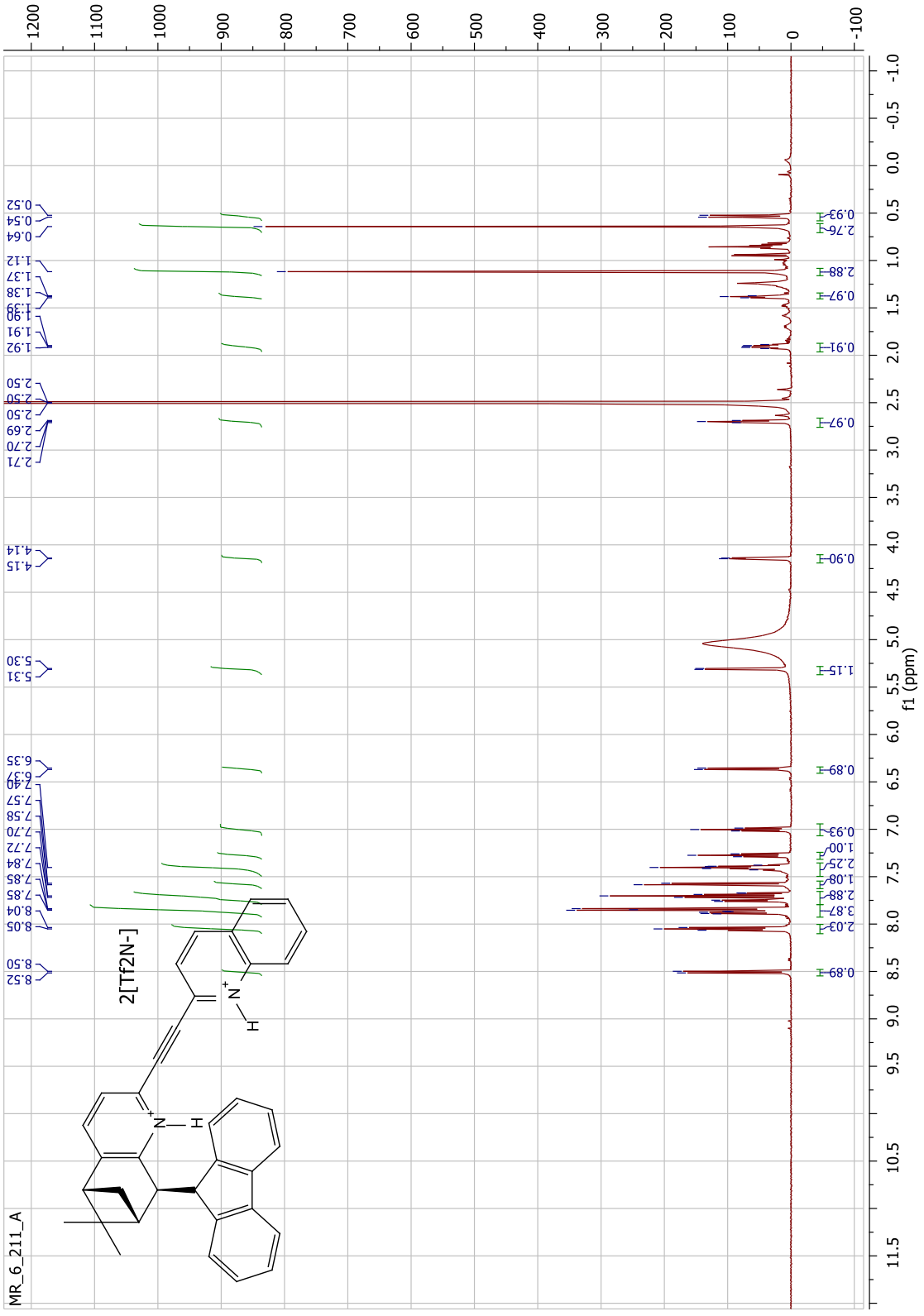

Figure 204. ^{1}H NMR spectrum of **261** (500 MHz, DMSO-d_6).

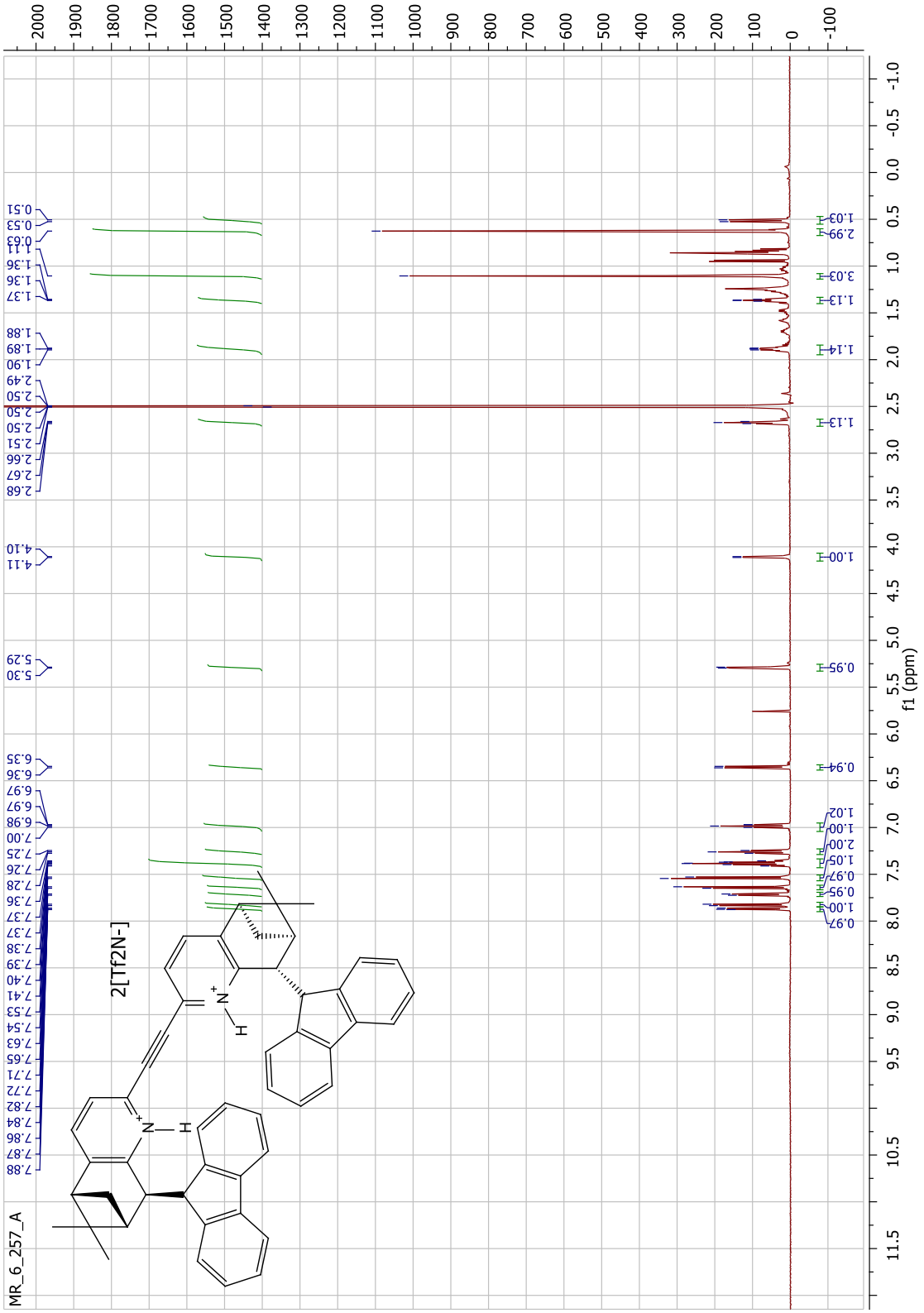

Figure 205. ^{1}H NMR spectrum of **262** (500 MHz, DMSO-d_6).

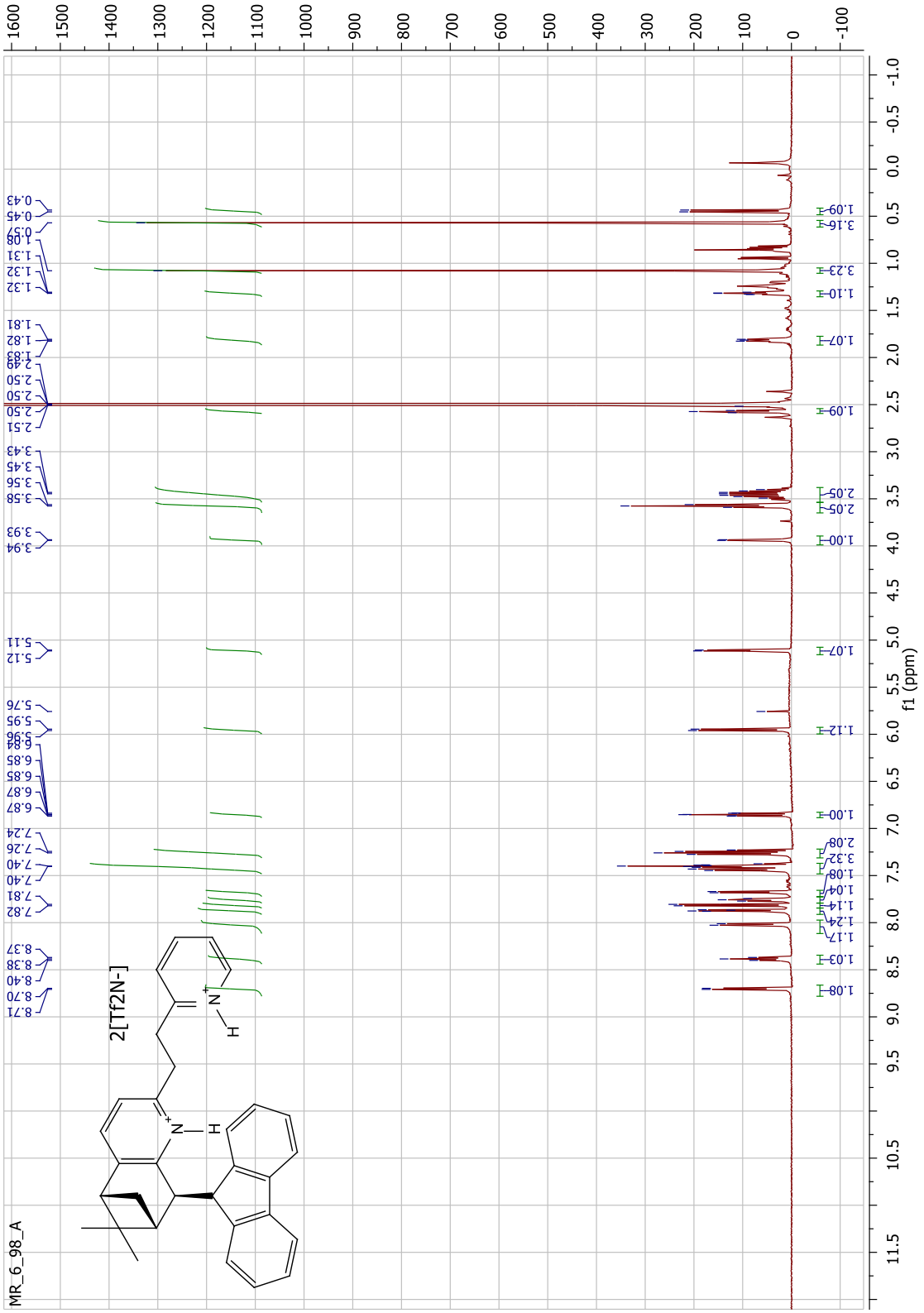

Figure 206. ^{1}H NMR spectrum of **263** (500 MHz, DMSO-d_6).

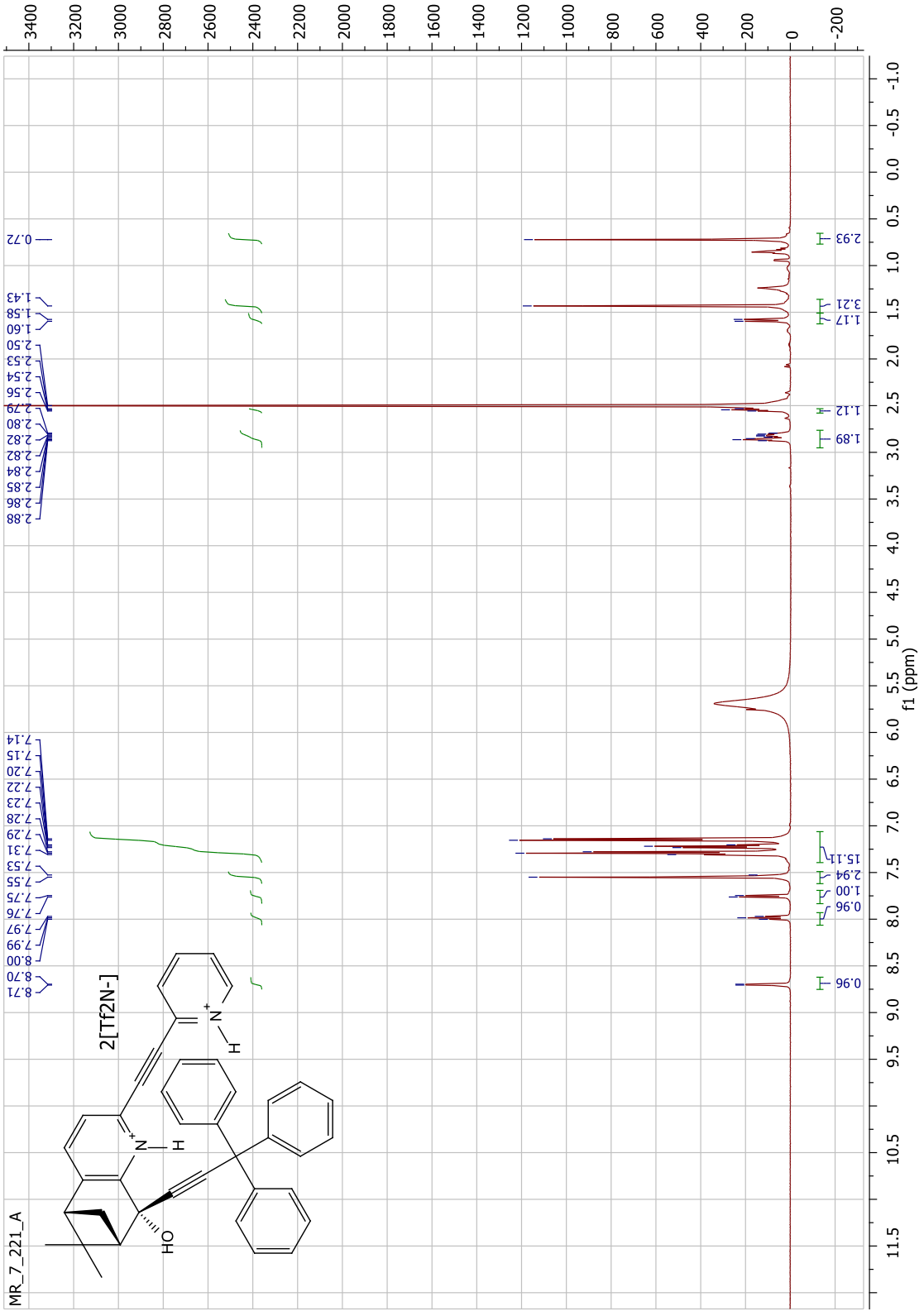

Figure 207. ^{1}H NMR spectrum of **279** (500 MHz, DMSO-d_6).

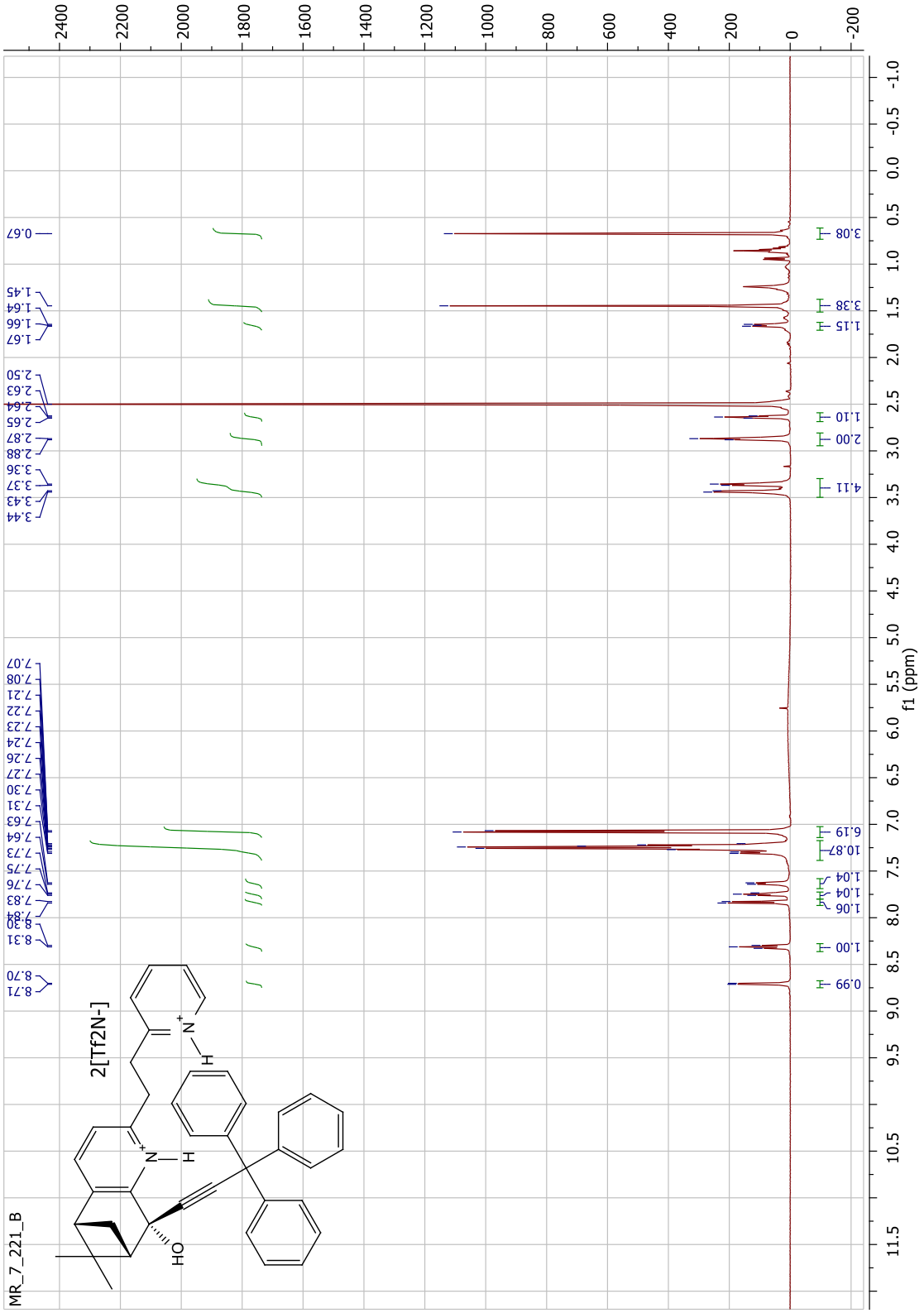

Figure 208. ^{1}H NMR spectrum of **326** (500 MHz, DMSO-d_6).

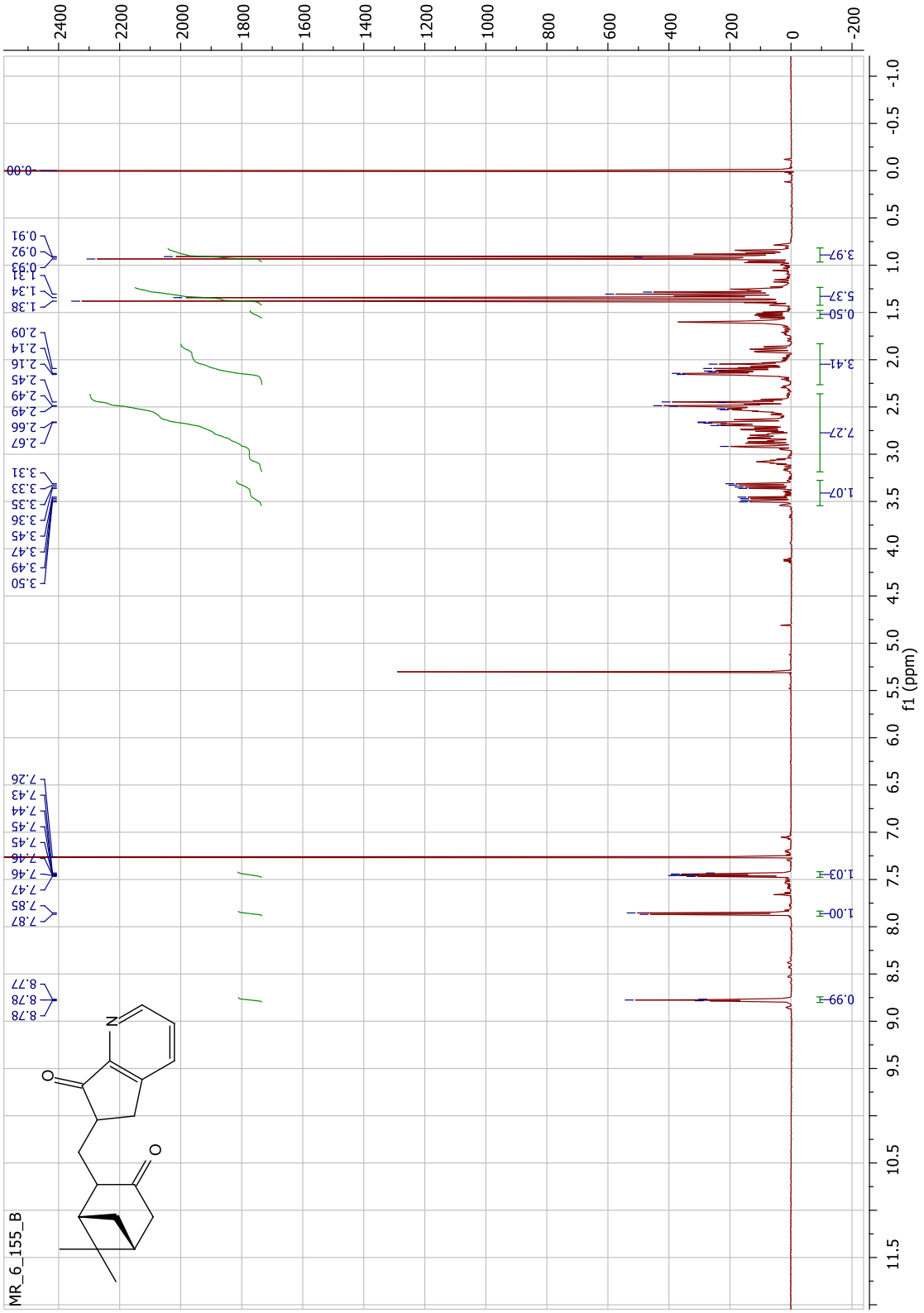

Figure 209. ^{1}H NMR spectrum of **283** (500 MHz, $CDCl_3$).

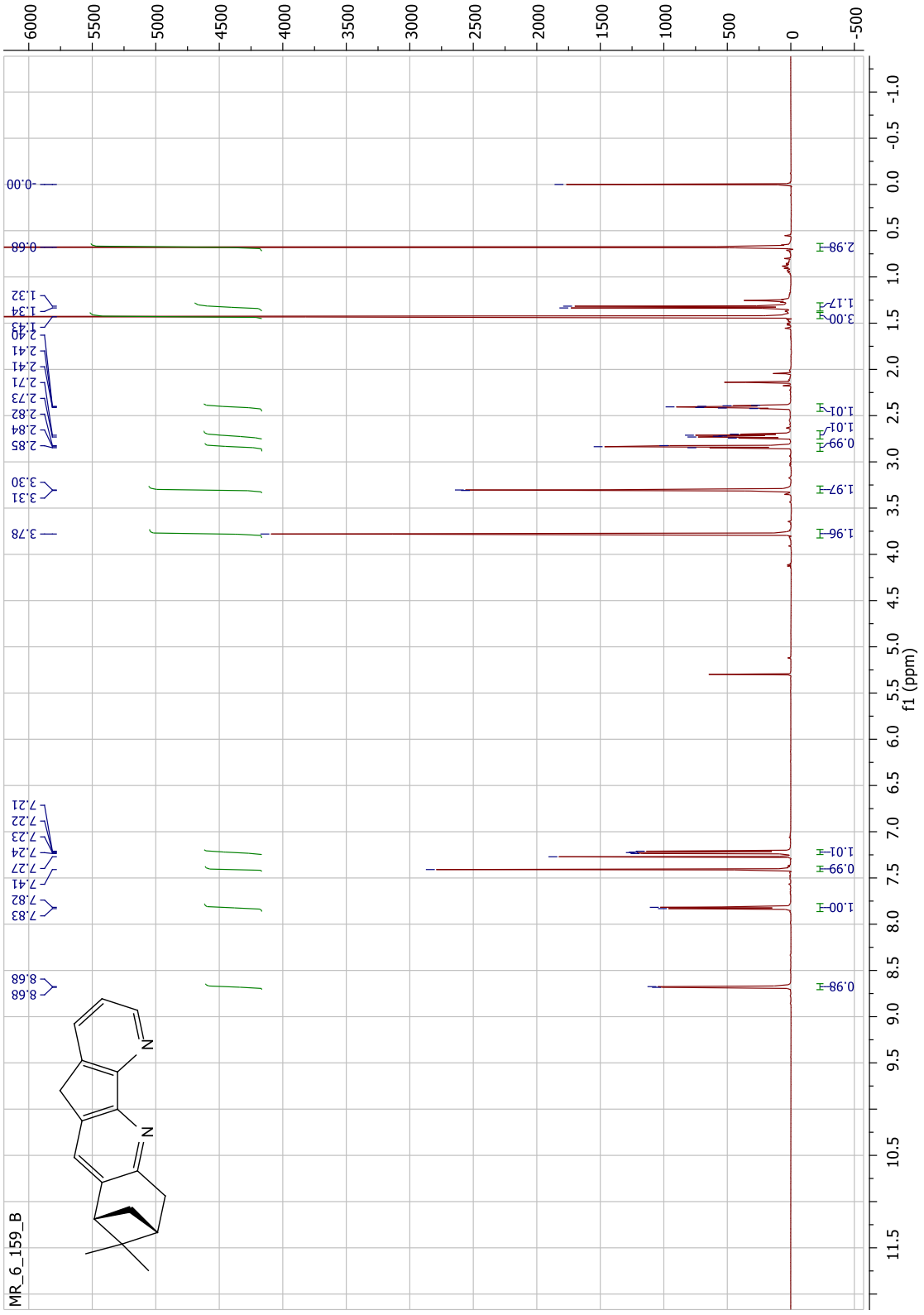

Figure 210. ^{1}H NMR spectrum of **284** (500 MHz, $CDCl_3$).

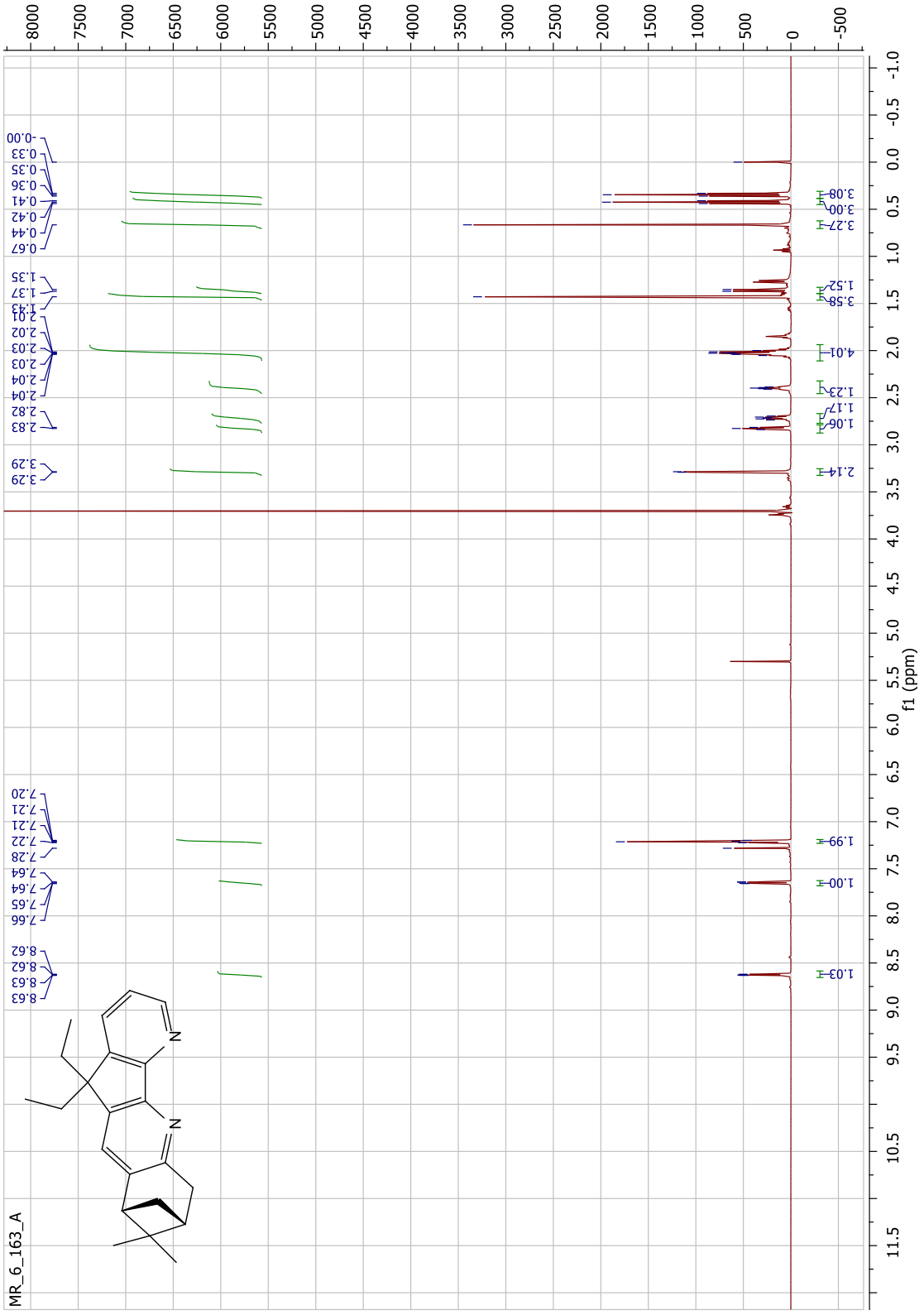

Figure 211. ^{1}H NMR spectrum of **285** (500 MHz, $CDCl_3$).